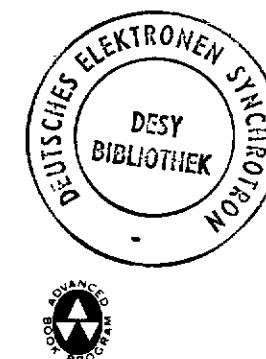


E  
File

# Applications of Perturbative QCD

**R. D. Field**  
*Department of Physics*  
*University of Florida*



12043 ✓  
(10982)

**ADDISON-WESLEY PUBLISHING COMPANY**  
*The Advanced Book Program*  
Redwood City, California • Menlo Park, California • Reading, Massachusetts  
New York • Don Mills, Ontario • Wokingham, United Kingdom • Amsterdam  
Bonn • Sydney • Singapore • Tokyo • Madrid • San Juan



*Publisher: Allan M. Wylde  
Production Manager: Jan Benes  
Editorial Coordinator: Aida Adams  
Promotions Manager: Laura Likely*

Copyright © 1989 by Addison-Wesley Publishing Company, Inc.

All rights reserved. No part of this publication may be reproduced, stored in a retrieval system, or transmitted in any form or by any means, electronic, mechanical, photocopying, recording, or otherwise, without the prior written permission of the publisher.  
Printed in the United States of America. Published simultaneously in Canada.

Library of Congress Cataloging-in-Publication Data

Field, Richard D.

Applications of perturbative QCD / Richard D. Field.  
p. cm.—(Frontiers in physics ; v. 77)

Includes index.

1. Quantum chromodynamics. 2. Perturbation (Quantum dynamics)  
3. Hadron interactions. I. Title. II. Series.  
QC793.3.Q35F54 1989 539.7'2—dc19  
ISBN 0-201-14295-3

89-138

ABCDEFGHIJK-AL-89

# Frontiers in Physics

David Pines/Editor

Volumes of the Series published from 1961 to 1973 are not officially numbered. The parenthetical numbers shown are designed to aid librarians and bibliographers to check the completeness of their holdings.

Titles published in this series prior to 1987 appear under either the W. A. Benjamin or the Benjamin/Cummings imprint; titles published since 1986 appear under the Addison-Wesley imprint.

- |  |  |
|--|--|
| (1) N. Bloembergen   | Nuclear Magnetic Relaxation: A Reprint Volume, 1961  |
| (2) G. F. Chew   | S-Matrix Theory of Strong Interactions: A Lecture Note and Reprint Volume, 1961                          |
| (3) R. P. Feynman  | Quantum Electrodynamics: A Lecture Note and Reprint Volume, 1961   |
| (4) R. P. Feynman  | The Theory of Fundamental Processes: A Lecture Note Volume, 1961   |
| (5) L. Van Hove,<br>N. M. Hugenholtz,<br>and L. P. Howland | Problem in Quantum Theory of Many-Particle Systems: A Lecture Note and Reprint Volume, 1961              |
| (6) D. Pines   | The Many-Body Problem: A Lecture Note and Reprint Volume, 1961   |
| (7) H. Frauenfelder  | The Mössbauer Effect: A Review—with a Collection of Reprints, 1962                                       |
| (8) L. P. Kadanoff<br>G. Baym                              | Quantum Statistical Mechanics: Green's Function Methods in Equilibrium and Nonequilibrium Problems, 1962 |
| (9) G. E. Pake   | Paramagnetic Resonance: An Introductory Monograph, 1962 [cr. (42)—2nd edition]                           |
| (10) P. W. Anderson  | Concepts in Solids: Lectures on the Theory of Solids, 1963   |

- |                                     |  |  |  |
|-------------------------------------|--|--|--|
| (11) S. C. Frautschi                | Regge Poles and S-Matrix Theory, 1963  | (37) R. P. Feynman                                       | Photo-Hadron Interactions, 1972  |
| (12) R. Hofstadter                  | Electron Scattering and Nuclear and Nucleon Structure: A Collection of Reprints with an Introduction, 1963                   | (38) E. R. Caianiello                                    | Combinatorics and Renormalization in Quantum Field Theory, 1973  |
| (13) A. M. Lane                     | Nuclear Theory: Pairing Force Correlations to Collective Motion, 1964  | (39) G. B. Field, H. Arp, and J. N. Bahcall              | The Redshift Controversy, 1973   |
| (14) R. Omnès                       | Mandelstam Theory and Regge Poles: An Introduction for Experimentalists, 1963  | (40) D. Horn   | Hadron Physics at Very High Energies, 1973   |
| M. Froissart                        | Complex Angular Momenta and Particle Physics: A Lecture Note and Reprint Volume, 1963  | (41) F. Zachariasen                                      |  |
| (15) E. J. Squires                  | The Equilibrium Theory of Classical Fluids: A Lecture Note and Reprint Volume, 1964  | (42) S. Ichimaru   | Basic Principles of Plasma Physics: A Statistical Approach, 1973 (2nd printing, with revisions, 1980)  |
| (16) H. L. Frisch                   | The Eightfold Way: (A Review—with a Collection of Reprints), 1964  | (43) G. E. Pake  | The Physical Principles of Electron Paramagnetic Resonance, 2nd Edition, completely revised, enlarged, and reset, 1973 [cf. (9)—1st edition] |
| J. L. Lebowitz                      | Strong-Interaction Physics: A Lecture Note Volume, 1964  | (44) T. L. Estle   |  |
| (17) M. Gell-Mann                   | Theory of Interacting Fermi Systems, 1964  |  | Volumes published from 1974 onward are being numbered as an integral part of the bibliography.   |
| Y. Ne'eman                          | Theory of Superconductivity, 1964 (revised 3rd printing, 1983)   | (45) R. C. Davidson                                      | Theory of Nonneutral Plasmas, 1974   |
| (18) M. Jacob                       | Nonlinear Optics: A Lecture Note and Reprint Volume, 1965  | (46) S. Doniach  | Green's Functions for Solid State Physicists, 1974   |
| G. F. Chew                          | Phase Transitions, 1965  | (47) E. H. Sondheimer                                    | Dual Resonance Models, 1974  |
| (19) P. Nozières                    | An Introduction to the Theory of Superfluidity, 1965   | (48) P. H. Frampton                                      | Modern Theory of Critical Phenomena, 1976  |
| (20) J. R. Schrieffer               | Superconductivity of Metals and Alloys, 1966   | (49) S. K. Ma  | Hydrodynamic Fluctuations, Broken Symmetry, and Correlation Functions, 1975  |
| (21) N. Bloembergen                 | Pseudopotentials in the Theory of Metals, 1966   | (50) D. Forster  | Qualitative Methods in Quantum Theory, 1977  |
| (22) R. Brout                       | Phenomenological Theories of High Energy Scattering: An Experimental Evaluation, 1967  | (51) A. B. Migdal  | Condensed Matter Physics: Dynamic Correlations, 1980   |
| (23) I. M. Khalatnikov              | The Anharmonic Crystal, 1967   | (52) S. W. Lovesey                                       | Gauge Fields: Introduction to Quantum Theory, 1980   |
| (24) P. G. deGennes                 | Augmented Plane Wave Method: A Guide to Performing Electronic Structure Calculations—A Lecture Note and Reprint Volume, 1967 | (53) L. D. Faddev  | Field Theory: A Modern Primer, 1981 [cf. 74—2nd edition]   |
| (25) W. A. Harrison                 | Algebraic Theory of Particle Physics: Hadron Dynamics in Terms of Unitary Spin Currents, 1967                                | (54) A. A. Slavnov                                       | Heavy Ion Reactions: Lecture Notes Vol. I: Elastic and Inelastic Reactions, 1981   |
| (26) V. Barger                      | Current Algebras and Applications to Particle Physics, 1968  | (55) P. Ramond   | Heavy Ion Reactions: Lecture Notes Vol. II, <i>in preparation</i>  |
| D. Cline                            | Nuclear Theory: The Quasiparticle Method, 1968   | (56) R. A. Broglia                                       | Lie Algebras in Particle Physics: From Isospin to Unified Theories, 1982   |
| (27) P. Choquard                    | The Quark Model, 1969  | (57) A. Winther  | Basic Notions of Condensed Matter Physics, 1983  |
| (28) T. Loucks                      | Approximation Methods in Quantum Mechanics, 1969   | (58) R. A. Broglia                                       | Gauge Theories of the Strong, Weak, and Electromagnetic Interactions, 1983   |
| (29) Y. Ne'eman                     | Nonlinear Plasma Theory, 1969  | (59) H. Georgi   | Crystal Optics and Additional Light Waves, 1983  |
| (30) S. L. Adler                    | Quantum Kinematics and Dynamics, 1970  | (60) P. W. Anderson                                      | Superspace or One Thousand and One Lessons in Supersymmetry, 1983  |
| R. F. Dashen                        | Statistical Mechanics: A Set of Lectures, 1972   | (61) C. Quigg  |  |
| (31) A. B. Migdal                   |  | (62) S. I. Pekar   |  |
| (32) J. J. J. Kokkedee              |  | (63) S. J. Gates, M. T. Grisaru, M. Roček, and W. Siegel |  |
| (33) A. B. Migdal                   |  |  |  |
| V. Krainov                          |  |  |  |
| (34) R. Z. Sagdeev and A. A. Galeev |  |  |  |
| (35) J. Schwinger                   |  |  |  |
| (36) R. P. Feynman                  |  |  |  |

- |    |   |   |
|----|---|---|
| 59 | R. N. Cahn  | Semi-Simple Lie Algebras and Their Representations, 1984                |
| 60 | G. G. Ross  | Grand Unified Theories, 1984  |
| 61 | S. W. Lovesey                                       | Condensed Matter Physics: Dynamic Correlations, 2nd Edition, 1986       |
| 62 | P. H. Frampton                                      | Gauge Field Theories, 1986  |
| 63 | J. I. Katz  | High Energy Astrophysics, 1987  |
| 64 | T. J. Ferbel  | Experimental Techniques in High Energy Physics, 1987                    |
| 65 | T. Applequist,<br>A. Chodos, and<br>P. G. O. Freund | Modern Kaluza-Klein Theories, 1987                                      |
| 66 | G. Parisi   | Statistical Field Theory, 1988  |
| 67 | R. C. Richardson                                    | Techniques in Low-Temperature Condensed Matter Physics, 1988            |
| 68 | E. N. Smith   | Quantum Many-Particle Systems, 1987                                     |
| 69 | J. W. Negele  | H. Orland   |
| 70 | E. Kolb   | The Early Universe, 1989  |
| 71 | M. Turner   |   |
| 72 | E. Kolb   | The Early Universe: Reprints, 1988                                      |
| 73 | M. Turner   |   |
| 74 | V. Barger   | Collider Physics, 1987  |
| 75 | R. J. N. Phillips                                   |   |
| 76 | T. Tajima   | Computational Plasma Physics, 1989                                      |
| 77 | W. Kruer  | The Physics of Laser Plasma Interactions, 1988                          |
|    | P. Ramond   | Field Theory: A Modern Primer 2nd edition, 1989<br>[cf. 51—1st edition] |
| 78 | B. F. Hatfield                                      | Quantum Field Theory of Point Particles and Strings, 1989               |
| 79 | P. Sokolsky   | Introduction to Ultrahigh Energy Cosmic Ray Physics, 1989               |
| 80 | R. Field  | Applications of Perturbative QCD, 1989                                  |

## Editor's Foreword

The problem of communicating in a coherent fashion recent developments in the most exciting and active fields of physics continues to be with us. The enormous growth in the number of physicists has tended to make the familiar channels of communication considerably less effective. It has become increasingly difficult for experts in a given field to keep up with the current literature; the novice can only be confused. What is needed is both a consistent account of a field and the presentation of a definite "point of view" concerning it. Formal monographs cannot meet such a need in a rapidly developing field, while the review article seems to have fallen into disfavor. Indeed, it would seem that the people most actively engaged in developing a given field are the people least likely to write at length about it.

FRONTIERS IN PHYSICS was conceived in 1961 in an effort to improve the situation in several ways. Leading physicists frequently give a series of lectures, a graduate seminar, or a graduate course in their special fields of interest. Such lectures serve to summarize the present status of a rapidly developing field and may well constitute the only coherent account available at the time. Often, notes on lectures exist (prepared by the lecturer himself, by graduate students, or by post-doctoral fellows) and are distributed in mimeographed form on a limited basis. One of the principal purposes of the FRONTIERS IN PHYSICS Series is to make such notes available to a wider audience of physicists.

It should be emphasized that lecture notes are necessarily rough and informal, both in style and content; and those in the series will prove no exception. This is as it should be. One point of the series is to offer new, rapid, more informal, and, it is hoped, more effective ways for physicists to teach one another. The point is lost if only elegant notes qualify.

As FRONTIERS IN PHYSICS has evolved, a third category of book, the informal text/monograph, an intermediate step between lecture notes and formal texts or monographs, has played an increasingly important role in the series. In an informal text or monograph an author has reworked his or her lecture notes to the point at which the manuscript represents a coherent summation of a newly-developed field, complete with references and problems, suitable for either classroom teaching or individual study.

During the past decade, perturbative quantum chromodynamics (QCD) has emerged as a major field of study for physicists working in elementary particle physics; it has significant applications in other sub-fields of physics, including heavy ion collisions, cosmology, and relativistic astrophysics. An introductory account of QCD is thus especially timely and Rick Field is unusually well-qualified to write such an account. Together with Richard Feynman at Caltech he developed many of the basic ideas of QCD, while during the past decade he has lectured on these and subsequent developments in summer schools and in one- and two-semester courses at both Caltech and the University of Florida. I share his hope that his book will benefit theorists and experimentalists at every level of experience, from the graduate student with a beginning understanding of Feynman diagrams to the experimentalist who wishes to carry out his own QCD calculations. As a sometime tennis pal, it is a special pleasure to welcome him to the ranks of FIP authors.

David Pines

Urbana, Illinois  
March, 1989

To Jimmie, Jason, Aimee, and Amanda

# Preface

I have attempted to provide a book at the level of the first volume of Bjorken and Drell but on perturbative quantum chromodynamics (QCD) rather than quantum electrodynamics. The book contains very little formal field theory. I start with the Feynman diagrams of QCD and attempt to teach QCD by doing calculations. In doing the calculations in this book the reader will not only develop calculational skills and learn mathematical techniques, but I hope gain an appreciation and understanding of the theory that might be missed in a formal field theory course. I believe that by working through this book a student with a rudimentary understanding of Feynman diagrams will develop the skills and understanding necessary to perform individual research and will be able to contribute to the field of perturbative QCD. Furthermore, I feel the book should be beneficial to both theorists and experimenters. Hopefully with this book students interested in experimental physics can learn to perform their own QCD calculations.

QCD is a precise and complete theory of quarks and gluons which purports to be an ultimate explanation of all strong interaction experiments at all energies, high and low. There are many reasons to hope and expect it to be right. The question is, is it indeed right? Mathematical complexity has, so far, prevented quantitatively testing its correctness. The primary obstruction is the fact that the fundamental quarks and gluons of QCD apparently cannot be isolated as free particles, but are always confined within hadrons by strong forces not amenable to treatment by perturbative methods. Nevertheless, because QCD is an asymptotically free theory, interaction forces become weak at small distances (large energies) and calculations using perturbation theory and Feynman diagrams are possible. Unfortunately, most processes involve both low and high energy aspects, and one must separate the low energy pieces, which are not calculable by perturbative methods, from the high energy perturbative parts. The nonperturbative (low energy) pieces are parameterized, taken from data, or a model is built to describe the regime.

It would take only one precise comparison with data to "prove" QCD correct. However, "true tests of perturbative QCD" often turn out merely as tests of the authors' cleverness in parameterizing the nonperturbative uncalculable part of the problem and not as actual tests of QCD. Great care must be taken in examining the sensitivity of predictions to the uncalculable parts of the problem. The belief that perturbative QCD is correct comes from the fact that the theory correctly predicts the approximate behavior of a wide class of experiments. It provides an understanding of why the "naive" parton model works so well (weak interaction forces at short distances) and predicts deviations from the parton model that are seen experimentally.

In Chapter 2 and 3 of this book the QCD perturbative predictions for electron-positron annihilations are examined. One can learn a great deal about perturbative QCD by studying electron-positron annihilations. Since this process involves no color in the initial state, it provides an excellent "theoretical laboratory" in which to develop the tools of perturbative QCD. Calculations will be performed using two different regularization schemes; the "massive gluon scheme" and dimensional regularization. There are lessons to be learned in both schemes and by comparing the results one can see clearly those quantities that are regularization scheme dependent and those that are not. Throughout the book we will always compare the "QCD" result with the "naive" parton model.

Deep inelastic lepton nucleon scattering will be covered in Chapter 4 and Chapter 5 covers the large-mass muon pair production in hadron-hadron collisions. Here we will use the techniques learned in Chapters 2 and 3 and again all calculations will be performed using the two regularization schemes. Chapter 6 is a bit more formal and will cover in more detail renormalization and the running coupling constant of QCD which is only briefly discussed in the introduction in Chapter 1.

Chapter 7 covers applications of perturbative QCD to the production of particles and "jets" in hadron-hadron collisions. Much has been learned about QCD by studying hadron-hadron collisions that involve large transverse momentum or result in the production of a large mass object.

In Chapter 8 I present several other applications of perturbative QCD. Here I do not go into quite as much detail as in the previous chapters. However, after working through Chapters 2-7 the reader should be able to perform the calculations presented in Chapter 8. At the end of each chapter I have provided a modest reading list and references. My list is not as extensive as, for example, the book by Quigg and I refer the reader to his book for a more complete reading list.

I have provided a set of appendices containing information that should be useful in working through this book. They contain formulas that I have collected through the years starting when I was a Ph.D. student of Professor J.D. Jackson at Berkeley in 1971.

This book is an outgrowth of the summer school lectures I gave at La Jolla (1978), Boulder (1979), and SLAC (1986) and a graduate course I gave at CALTECH (1980) and at the University of Florida (1984). The CALTECH course was two semesters in length and I was able to cover all the material in Chapters 1 through 6 of this book. The Florida course was one semester in length and I covered only selected topics throughout the book. The book is suitable for a one or two semester special topics course in high-energy physics or it can be used selectively to supplement a course on relativistic quantum mechanics. In addition the book can be used for reference and self-study by both theorists and experimenters.

I could not have written this book without the six years of collaborative work I did with Professor Richard Feynman at CALTECH. Many of the discussions I have presented here are an outgrowth of our work or are an outgrowth of things I learned from Professor Feynman. I am very thankful for the privilege and opportunity of working with Richard Feynman. I am also grateful to Geoffrey Fox and Stephan Wolfram both of whom taught me a lot while I was at CALTECH and both have made contributions to this book. I would like to thank the teaching assistants of the course I taught at CALTECH (1980), Rajan Gupta and Steve Otto. They provided solutions for all the homework problems I assigned throughout the course and thereby contributed greatly to this book.

I am grateful to the Aspen Center for Physics for the warm hospitality shown to me during the summer of 1987 where I wrote the first three chapters of this book. I also appreciate very much the hospitality shown to me by R. Schrieffer, S. Ellis, and A. Mueller at the Institute for Theoretical Physics at Santa Barbara where I attended a six months workshop on "QCD and its Applications" in Spring of 1988. I learned a lot at the workshop that helped me to write this book.

I would like to thank my tennis pals (Aimee, Amanda, Dee Dee, George, Howie, Jason, Jeff, Jimmie, Joyce, Lorna, Mike, Mike, Pierre, Rick, and Ron) for helping me keep my priorities straight.

Finally, I am grateful to my wife Jimmie for taking good care of me and our three children, Jason, Aimee, and Amanda, while I worked on this book.

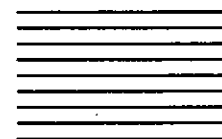
R.D. Field  
Florida, Fall 1988

# Contents

<b>Chapter 1 Introduction to QCD</b>	<b>1</b>
1.1 SU(3) of Color	2
1.2 Asymptotic Freedom	5
Problems	13
Further Reading	14
References	14
<b>Chapter 2 Electron-Positron Annihilations:</b>	
<b>Total Rate to Hadrons</b>	<b>15</b>
2.1 The Naive Parton Model	17
2.2 Summing over Polarization States	22
2.3 Real Gluon Emission	24
2.4 Virtual Gluon Corrections	31
2.5 Real Gluon Emission – MG Scheme	37
2.6 Virtual Gluon Corrections – MG Scheme	39
2.7 Order $\alpha_s$ Correction – MG Scheme	41
2.8 Real Gluon Emission – DR Scheme	42
2.9 Virtual Gluon Corrections – DR Scheme	47
2.10 Order $\alpha_s$ Corrections – DR Scheme	49
Problems	50
Further Reading	55
References	55
<b>Chapter 3 Electron-Positron Annihilations:</b>	
<b>Fragmentation Functions and Jets</b>	<b>56</b>
3.1 The Naive Parton Model	57
3.2 Parton Differential Cross Sections	64
3.3 Single Hadron Inclusive Cross Section	68
3.4 Summing Leading Logarithms	72

3.5 The Convolution Method	82	6.3 Vertex Corrections – $Z_1$	233
3.6 Jets – The Monte Carlo Method	87	6.4 The Running Coupling Constant	239
3.7 Jets – Analytic Results	93	6.5 The Beta Function	243
3.8 Summing Double Logarithms	97	6.6 The Renormalization Group Equation	246
Problems	101	Problems	252
Further Reading	105	Further Reading	258
References	105	References	258
<b>Chapter 4 Deep Inelastic Lepton Nucleon Scattering</b>	<b>107</b>	<b>Chapter 7 The Production of Particles and Jets in Hadron-Hadron Collisions</b>	<b>260</b>
4.1 The Naive Parton Model	108	7.1 Single and Double Photon Production	261
4.2 Cross Sections and Structure Functions	113	7.2 Large Transverse Momentum Mesons	270
4.3 Gluon Emission and Initial State Gluons	121	7.3 Jet Production	283
4.4 Order $\alpha_s$ , Corrections – MG Scheme	124	Problems	301
4.5 Order $\alpha_s$ , Corrections – DR Scheme	132	Further Reading	304
4.6 $Q^2$ Dependent Structure Functions	137	References	304
4.7 $Q^2$ Evolution – Moment Method	143	<b>Chapter 8 Other Applications of Perturbative QCD</b>	<b>306</b>
4.8 $Q^2$ Evolution – Convolution Method	148	8.1 Upsilon Decay	307
4.9 The Longitudinal Structure Function	150	8.2 The Pion Form Factor	312
4.10 Neutrino Nucleon Scattering	154	Problems	322
Problems	159	Further Reading	323
Further Reading	168	References	324
References	169	<b>Appendix A S-Matrix Formulas</b>	<b>325</b>
<b>Chapter 5 Large-Mass Muon-Pair Production in Hadron-Hadron Collisions</b>	<b>170</b>	A.1 Invariant Amplitude	326
5.1 The Naive Parton Model	171	A.2 Decay Process $\alpha \rightarrow (1, 2, \dots, n)$	326
5.2 Gluon Emission and Initial State Gluons	174	A.3 2-to-2 Differential Cross Section	326
5.3 Order $\alpha_s$ , Corrections – MG Scheme	177	References	329
5.4 Order $\alpha_s$ , Corrections – DR Scheme	184	<b>Appendix B Metric and Matrices</b>	<b>330</b>
5.5 The Drell-Yan “K-Factor”	186	B.1 Metric ( $N = 4$ dimensions)	331
5.6 Large Transverse Momentum Muon Pairs	195	B.2 Metric ( $N$ dimensions)	331
5.7 Small Transverse Momentum Muon Pairs	203	B.3 Dirac Algebra ( $N = 4$ dimensions)	332
5.8 Vector Boson Production	205	B.4 Dirac Matrices ( $N = 4$ dimensions)	332
Problems	213	B.5 Dirac Algebra ( $N$ dimensions)	333
Further Reading	223	B.6 Dirac Equation and Spinors	334
References	223	References	336
<b>Chapter 6 Renormalization and the Running Coupling Constant in QCD</b>	<b>225</b>		
6.1 The Gluon Propagator – $Z_3$	226		
6.2 Quark Self-Energy Corrections – $Z_2$	232		

# Introduction to QCD



<b>Appendix C Feynman Rules and Integrals</b>	<b>337</b>
C.1 Feynman Rules – General Discussion	338
C.2 Loop Integrations	340
C.3 Feynman Rules – QCD	341
C.4 Feynman Rules – Weinberg-Salam Model	344
References	347
<b>Appendix D SU(3) of Color</b>	<b>349</b>
D.1 Structure Constants and Color Matrices	350
D.2 Examples of Color Factors	353
References	353
<b>Appendix E Special Functions</b>	<b>354</b>
E.1 Gamma Function	355
E.2 Dilogarithm	357
E.3 “+ Functions”	358
E.4 Gegenbauer Polynomials	359
<b>Subject Index</b>	<b>361</b>

In 1954 Yang and Mills<sup>1</sup> constructed a theory analogous to Quantum Electrodynamics (QED) but for a system in which the particles carry more than one "charge." The generalization to two charges mediated by a vector particle results in a theory that is inconsistent with observations. However, with three charges mediated by vector particles obeying exact  $SU(3)$  symmetry one arrives at a theory that seems to describe the strong interactions. In this book we will learn about the nature of this theory by performing calculations. However, let us first qualitatively examine the behavior of a theory with three charges.

## 1.1 SU(3) of Color

In the theory of Quantum Chromodynamics (QCD) each quark carries a color charge that can take on three values;  $R$ =red,  $G$ =green,  $B$ =blue. When the field quantum (gluon) is emitted the quark color may or may not change giving nine ways of coupling a gluon between an initial and a final quark. Eight of the gluons form a "color"  $SU(3)$  octet,

$$\begin{aligned} g_1 &= R\bar{G} & g_2 &= R\bar{B} & g_3 &= G\bar{R} \\ g_4 &= G\bar{B} & g_5 &= B\bar{R} & g_6 &= B\bar{G} \\ g_7 &= \frac{1}{\sqrt{2}} (R\bar{R} - G\bar{G}) \\ g_8 &= \frac{1}{\sqrt{6}} (R\bar{R} + G\bar{G} - 2B\bar{B}) \end{aligned} \quad (1.1.1)$$

with one remaining as an  $SU(3)$  singlet,

$$g_0 = \frac{1}{\sqrt{3}} (R\bar{R} + G\bar{G} + B\bar{B}). \quad (1.1.2)$$

The singlet gluon couples equally to all quarks, and is independent of the octet. Since there is no good reason to include it, it is usually ignored. The octet of gluons and the three quark colors are assumed to form an exact  $SU(3)$  color symmetry.

In QED, the strength of the coupling between two quarks is given by

$$e_1 e_2 \alpha, \quad (1.1.3)$$

where  $e_1$  and  $e_2$  are the electric charges of the two quarks in units of  $e$  (*i.e.*,  $e_u = \frac{2}{3}$ ,  $e_d = -\frac{1}{3}$ , etc.) and  $\alpha$  is the fine structure constant,

$$\alpha = e^2/4\pi. \quad (1.1.4)$$

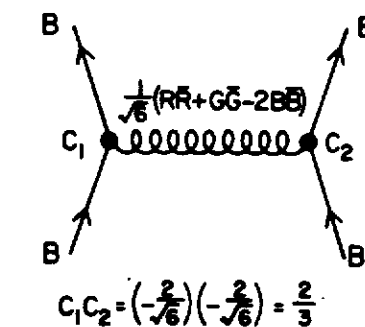


Figure 1.1 Color factors for the exchange of a single gluon between two *blue*,  $B$ , quarks. The overall color factor is the product of the factors for each vertex.

In QCD the situation is similar. The strength of the strong interaction coupling for the exchange of a single gluon between two colored quarks is

$$\left(\frac{c_1}{\sqrt{2}}\right) \left(\frac{c_2}{\sqrt{2}}\right) \alpha_s, \quad (1.1.5)$$

where  $c_1$  and  $c_2$  are the color coefficients that can be deduced from (1.1.1) and

$$\alpha_s = g_s^2/4\pi, \quad (1.1.6)$$

with  $g_s$  being the strong coupling constant. The extra  $1/\sqrt{2}$  at each vertex is historical.

Following the discussion in Chapter 2 of the book by Halzen and Martin<sup>2</sup> let us consider, for example, the color factor for the interaction between two quarks of the same color, say  $B$ , as shown in Fig. 1.1. Out of the eight gluons only the one containing  $B\bar{B}$  can contribute,  $g_8$  in (1.1.1). The color factor is thus

$$\frac{1}{2} \left(-\frac{2}{\sqrt{6}}\right) \left(-\frac{2}{\sqrt{6}}\right) = \frac{1}{3}, \quad (1.1.7)$$

where I have defined the color factor to be the coefficient of  $\alpha_s$  in (1.1.5). On the other hand, the interaction between the two  $R$  quarks shown in Fig. 1.2, can proceed by the exchange of two gluons  $g_7$  and  $g_8$  yielding the color factor

$$\frac{1}{2} \left(\frac{1}{\sqrt{6}}\right) \left(\frac{1}{\sqrt{6}}\right) + \frac{1}{2} \left(\frac{1}{\sqrt{2}}\right) \left(\frac{1}{\sqrt{2}}\right) = \frac{1}{3}, \quad (1.1.8)$$

which is the same as (1.1.7), as it must be from color symmetry.

An important color factor is the one arising from single gluon exchange

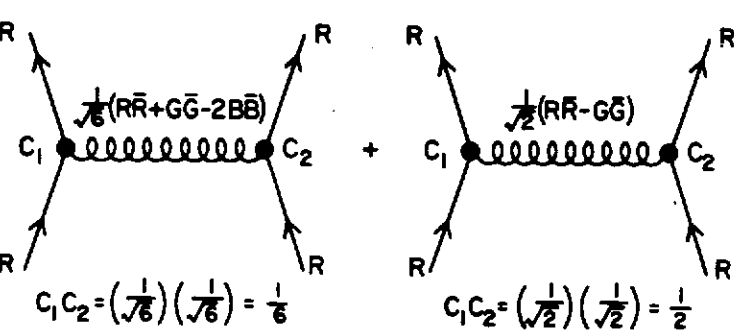


Figure 1.2 Color factors for the exchange of a single gluon between two red, R, quarks. The overall color factor is the sum of the factors for each diagram.

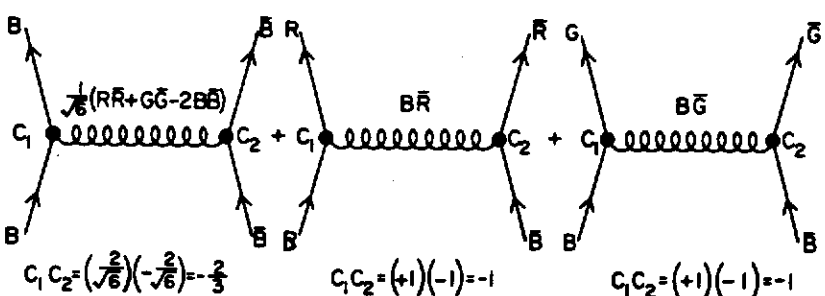


Figure 1.3 Color factors for the exchange of a single gluon between a blue, B, and a blue-bar, B-bar, quark. The overall color factor is the sum of the color factors for each diagram.

between a quark and antiquark in the color singlet state,

$$(q\bar{q})_{[1]} = \frac{1}{\sqrt{3}} (R\bar{R} + G\bar{G} + B\bar{B}). \quad (1.1.9)$$

Here all the colors occur equally so it is sufficient to consider just one, for example  $B\bar{B}$  interactions as in Fig. 1.3, and then multiply by three. For  $B\bar{B}$  interactions there are three possible gluon exchanges,  $g_8, g_5$  and  $g_6$ , yielding

the color factor

$$3 \left(\frac{1}{2}\right) \frac{1}{\sqrt{3}} \frac{1}{\sqrt{3}} \left(-\frac{2}{3} - 1 - 1\right) = -\frac{4}{3}. \quad (1.1.10)$$

The minus signs come from the antiparticle vertices. Just as is the case in QED, antiquarks have opposite charge to quarks.

As can be seen from (1.1.7) and (1.1.10) the color force can be both repulsive and attractive, respectively. Presumably, states with the largest (*negative*) color factors are the most tightly bound. For a color octet  $q\bar{q}$  state single gluon exchange is repulsive with the color factor

$$+\frac{1}{6}. \quad (1.1.11)$$

Of all the two body channels, the color singlet  $q\bar{q}$  state is the most attractive. Similarly, single gluon exchange in the color singlet three quark state is strongly attractive with the color factor

$$-2. \quad (1.1.12)$$

Since this analysis is based on single gluon exchange it cannot be taken too seriously. Multiple gluon exchange and the triple-gluon vertex have been ignored in a regime where lowest-order perturbation theory is surely not applicable. Nevertheless, on the basis of this naive single gluon exchange analysis, one might think it plausible that  $q\bar{q}$  and  $qqq$  states only exist as color singlets.

Color factors are generally not computed explicitly from the gluons in (1.1.1). It is easier to manipulate the  $SU(3)$  color matrices,  $T_a$ , which satisfy

$$[T_a, T_b] = if_{abc} T_c, \quad (1.1.13)$$

where  $f_{abc}$  are the antisymmetric structure constants of  $SU(3)$  given in Appendix D. The quark-gluon vertex in Fig. C.3 is given by

$$-ig_s T_{ij}^a \gamma_\mu, \quad (1.1.14)$$

where the indices  $i$  and  $j$  correspond to the quark colors and take on values from 1 to 3 while "a" corresponds to the gluon color states and takes on values from 1 to 8. The eight  $3 \times 3$   $SU(3)$  matrices,  $T_a$ , are given in (D.1.3). The color factors in (1.1.7) and (1.1.8) are given by

$$\sum_a (T_{ii}^a)^2 = \frac{1}{3}, \quad (1.1.15)$$

where I have used (D.1.6). Other examples are given in Appendix D.

## 1.2 Asymptotic Freedom

The starting point of this book will be the Feynman rules for QCD given in

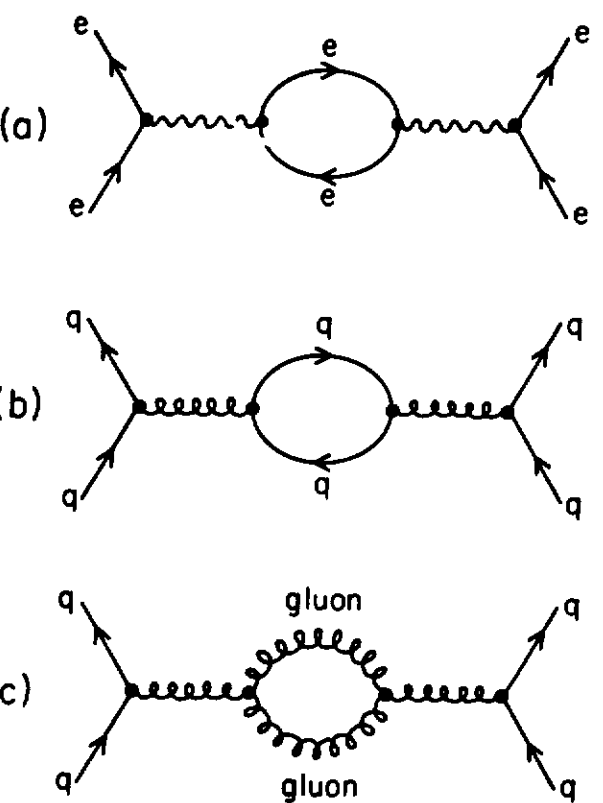


Figure 1.4 (a) Lowest order vacuum polarization correction to the electric charge. (b) Lowest order correction to the strong coupling due to a virtual quark-antiquark pair. (c) Lowest order correction to the strong coupling due to a pair of virtual gluons.

Appendix C. Given these rules we will perform many calculations and learn about perturbative QCD by *doing* perturbative QCD. We will encounter both infrared and ultraviolet divergences and develop schemes for handling them. We will begin in Chapter 2 by studying the perturbative QCD corrections to  $e^+e^-$  annihilations. Pedagogically this is a good place to start. It is a good “theoretical laboratory” to develop the tools necessary in analyzing other processes. We will not examine in detail the ultraviolet divergences whose renormalization results in the running coupling constant of QCD,  $\alpha_s(Q^2)$ , until Chapter 6. For now I will simply outline the behavior of the effective coupling in QCD and contrast it with the QED case.

In QED the strength of the coupling must be determined experimentally. Suppose that we decide to experimentally measure the strength of electromagnetic interactions by scattering an electron off an electron and comparing the result with a theoretical calculation. The rate for electron-electron scattering is affected by the presence of vacuum polarization diagrams like that shown in Fig. 1.4. One immediately runs into trouble, however, since the one electron loop correction to the photon propagator diverges like  $\log(\lambda)$ , where  $\lambda$  is some ultraviolet cutoff that can be arbitrarily large. In particular, the leading order bubble contribution is

$$\alpha_0 B(Q^2) = -\frac{\alpha_0}{3\pi} \left\{ \log(\lambda^2/Q^2) + \frac{5}{3} \right\} \quad \text{for } Q^2/m_e^2 \gg 1, \quad (1.2.1)$$

and

$$\alpha_0 B(Q^2) = -\frac{\alpha_0}{3\pi} \left\{ \log(\lambda^2/m_e^2) - \frac{1}{5} \frac{Q^2}{m_e^2} \right\} \quad \text{for } Q^2/m_e^2 \ll 1, \quad (1.2.2)$$

where  $q^2 = -Q^2$  is the 4-momentum squared of the virtual (spacelike) photon and  $m_e$  is the electron mass. The coupling  $\alpha_0$  is the “bare” electric charge ( $\alpha_0 = e_0^2/4\pi$ ). It is convenient to define an effective coupling,  $\alpha_{\text{eff}}(Q^2)$ , that incorporates all the vacuum polarization bubbles. Namely,

$$\alpha_{\text{eff}}(Q^2) = \alpha_0 (1 + \alpha_0 B(q^2) + \alpha_0 B(q^2)\alpha_0 B(q^2) + \dots), \quad (1.2.3)$$

yielding

$$\alpha_{\text{eff}}(Q^2) = \frac{\alpha_0}{1 - \alpha_0 B(q^2)}, \quad (1.2.4)$$

or

$$\frac{1}{\alpha_{\text{eff}}(Q^2)} = \frac{1}{\alpha_0} - B(q^2). \quad (1.2.5)$$

The procedure for handling the ultraviolet divergences like those appearing in  $B(q^2)$  in (1.2.1) is called renormalization. One defines an experimental electric charge,  $\alpha$ , by the large distance behavior of the electric potential (Thompson limit)

$$\alpha \equiv \alpha_{\text{eff}}(Q^2 = 0), \quad (1.2.6)$$

which experimentally is about 1/137. All results of calculations are now expressed in terms of the experimental coupling,  $\alpha$ , rather than the unobservable bare coupling,  $\alpha_0$ . In terms of  $\alpha$ , the effective coupling is given by

$$\frac{1}{\alpha_{\text{eff}}(Q^2)} = \frac{1}{\alpha} - (B(q^2) - B(0)), \quad (1.2.7)$$

where the quantity  $(B(Q^2) - B(0))$  is now independent of the artificial ultraviolet cutoff  $\lambda$ . The cutoff  $\lambda$  is now sent to infinity while holding  $\alpha$  constant. From (1.2.1) and (1.2.7) we see that the large  $q^2$  behavior of the effective

coupling is given by

$$\alpha_{QED}(Q^2) \equiv \alpha_{\text{eff}}(Q^2) = \frac{\alpha}{1 - (\alpha/3\pi) \log(Q^2/m_e^2)}. \quad (1.2.8)$$

In QED as  $Q^2$  increases,  $\alpha_{\text{eff}}(Q^2)$  increases. No matter how small  $\alpha$  is, one can always increase  $Q^2$  to a point where  $\alpha_{\text{eff}}(Q^2)$  becomes infinite. This means that perturbation theory breaks down at high  $Q^2$  in QED. One needs to include higher and higher orders in  $\alpha_{\text{eff}}$  as  $Q^2$  increases. At low  $Q^2$ , on the other hand,  $\alpha_{\text{eff}}(Q^2)$  is small ( $\alpha \approx 1/137$ ) and perturbation theory works well.

The physical reason for the rising effective charge with the increased  $Q^2$  of the probing photon is illustrated in Fig. 1.5. If  $Q^2$  is small then the photon cannot resolve small distances and “sees” a “point” charge shielded by the vacuum polarization of the infinite sea of electron-positron pairs. As  $Q^2$  increases, the photon “sees” a smaller and smaller spatial area and the shielding effect is less.

In QCD the behavior of the effective coupling constant is strikingly different. The reason for this difference is the feature of QCD, that the gluons carry charge (color) and interact with each other. The amount of the contributions of the various diagrams is gauge dependent. However, the situation is most clear in the Coulomb gauge. In this gauge, the lowest order bubble contribution to the gluon propagator is given for large  $Q^2$  by

$$\alpha_0 B_{QCD}(Q^2) = -\alpha_0 \tilde{a} \log(\lambda^2/Q^2), \quad (1.2.9)$$

where  $\lambda$  is the ultraviolet cutoff and  $\alpha_0$  is the bare quark-gluon coupling and where

$$\tilde{a} = -\beta_0/4\pi, \quad (1.2.10)$$

with

$$\beta_0 = -\left(\frac{2}{3}n_f + 5 - 16\right), \quad (1.2.11)$$

where  $n_f$  is the number of quark flavors. The  $+\frac{2}{3}n_f$  and the  $+5$  come from the quark loop and the transverse gluon loop in Fig. 1.4, respectively, and are of the same sign as the QED case. These contributions must be positive since the diagrams can be cut across the bubble and represent contributions to the physical rate for producing quark pairs or transverse gluon pairs which must be positive. The  $-16$  in (1.2.11) comes from the diagram with one transverse and one “Coulomb” gluon in the bubble. This contribution need not be positive since the instantaneous “Coulomb” gluon is not physical. If  $\frac{2}{3}n_f < 11$  then  $\beta_0$  is positive and  $\tilde{a}$  is negative in contrast to the QED case (1.2.1). As for the QED case, the ultraviolet divergences are handled by renormalization. Here, however, we cannot define the “experimental charge” by the  $Q^2 \rightarrow 0$  limit of  $\alpha_{\text{eff}}(Q^2)$  as we did in (1.2.6). We instead choose some  $Q^2$ , say  $Q^2 = \mu^2$ , to define the coupling and express all predictions in terms of the coupling at this point (called the renormalization point or subtraction point). The effective

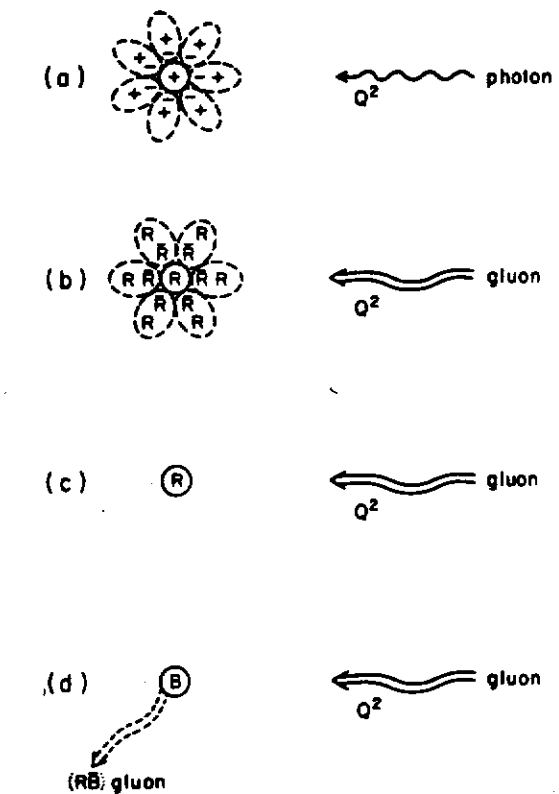


**Figure 1.5** (a) Illustration of how vacuum polarization in QED will shield a positive bare charge. (b) The same shielding as in (a) but for a red charge in QCD. (c) Shows how in QCD a red charge can radiate away its color via a RB gluon and become blue.

coupling is then given by

$$\frac{1}{\alpha_{\text{eff}}(Q^2)} = \frac{1}{\alpha(\mu^2)} - (B(Q^2) - B(\mu^2)). \quad (1.2.12)$$

As before, the quantity  $(B(Q^2) - B(\mu^2))$  is independent of the arbitrary cutoff  $\lambda$ . By the use of (1.2.9), we see that the leading order behavior of the coupling in QCD is

$$\alpha_s(Q^2) \equiv \alpha_{\text{eff}}(Q^2) = \frac{\alpha(\mu^2)}{1 + \alpha(\mu^2) \frac{\beta_0}{4\pi} \log(Q^2/\mu^2)}, \quad (1.2.13)$$

which approaches zero as  $Q^2 \rightarrow \infty$  (asymptotic freedom) as illustrated in

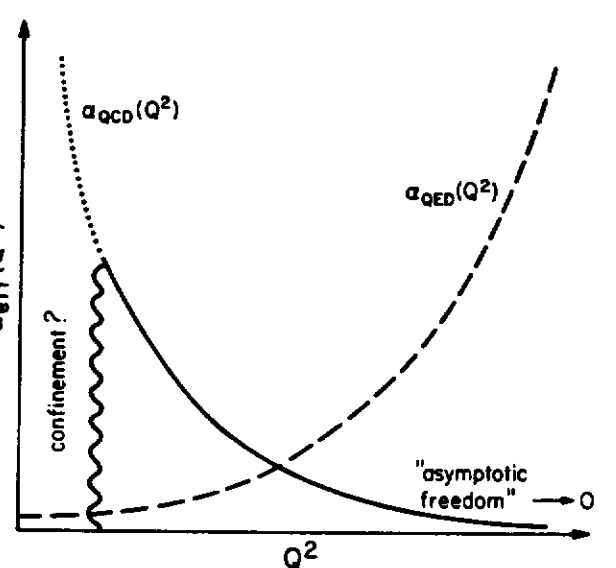


**Figure 1.6** Illustration of the behavior of the QED and QCD effective coupling constants as a function of the energy scale,  $Q^2$ . In QED the effective coupling,  $\alpha_{QED}(Q^2)$ , is small at small  $Q^2$ , but becomes large at large  $Q^2$  (i.e., short distances). In QCD the effective coupling is large at small  $Q^2$  (i.e., large distances) where confinement occurs, but decreases to zero at large  $Q^2$  (*asymptotic freedom*).

Fig. 1.6. This means that for QCD, perturbation theory should work well at high  $Q^2$  (short distances) but break down at small  $Q^2$  (large distances) where  $\alpha_s(Q^2)$  becomes large and presumably confines quarks within hadrons.

The nature of the QCD coupling constant  $\alpha_s(Q^2)$  takes a bit of getting used to. In QED it is easy to define what one means by the charge of an electron  $e$ . It is related to the large distance behavior of the electric potential (Thomson limit). One cannot do this for QCD since the  $Q^2 \rightarrow 0$  limit of  $\alpha_s(Q^2)$  cannot be calculated by perturbation theory. Instead we had to choose an arbitrary point  $\mu$  and define  $\alpha_s$  to be the effective coupling at that point,

$$\alpha_s \equiv \alpha_s(\mu^2). \quad (1.2.14)$$

It, however, does not matter which point  $\mu$  one chooses. If one chooses instead the point  $\bar{\mu}$  then the two couplings are related (to lowest order) by

$$\frac{1}{\alpha_s(\mu^2)} - \tilde{a} \log(Q^2/\mu^2) = \frac{1}{\alpha_s(\bar{\mu}^2)} - \tilde{a} \log(Q^2/\bar{\mu}^2), \quad (1.2.15)$$

or

$$\frac{1}{\alpha_s(\mu^2)} + \tilde{a} \log(\mu^2) = \frac{1}{\alpha_s(\bar{\mu}^2)} + \tilde{a} \log(\bar{\mu}^2). \quad (1.2.16)$$

Thus, the “real” parameter in the theory is not  $\alpha(\mu^2)$  or  $\mu^2$  but rather a mass scale,  $\Lambda$ , that is independent of  $\mu^2$  and is given to this order by

$$\log(\Lambda^2) = \frac{1}{\tilde{a}\alpha(\mu^2)} + \log(\mu^2). \quad (1.2.17)$$

In terms of the parameter  $\Lambda$ , the effective coupling is given by

$$\alpha_s(Q^2) \equiv \frac{g_s^2(Q^2)}{4\pi} = \frac{4\pi}{\beta_0 \log(Q^2/\Lambda^2)} \quad (1.2.18)$$

with

$$\beta_0 = 11 - \frac{2}{3}n_f. \quad (1.2.19)$$

It is interesting to notice that (1.2.18) becomes infinite at  $Q^2 = \Lambda^2$  which corresponds to a distance of about 0.5 Fermi for  $\Lambda \approx 500$  MeV. (This is extremely crude, however, since (1.2.18) is not applicable when  $\alpha_s(Q^2)$  becomes large.)

The physical reason for the behavior of  $\alpha_s(Q^2)$  is illustrated in Fig. 1.5. Quark-antiquark vacuum polarization shields the color charge as was the case in QED. However, now since the source can radiate charge (*i.e.*, change from red to blue by emitting a red-blue-bar gluon), the charge is no longer located at a definite place in space. It is diffusely spread out due to gluon emission and absorption. As one increases the  $Q^2$  of the incoming gluon probe, thereby looking at smaller and smaller spatial distances, it becomes less likely to find the “charge” (red in Fig. 1.5). This latter effect is stronger than the former and the effective charge thus appears weaker and weaker as the  $Q^2$  of the probe increases.

In Chapter 6 we will see that once we have calculated an observable using Feynman diagram techniques with a coupling  $g_s$  defined according to

$$\alpha_s = \alpha_s(\mu^2) = g_s^2/4\pi, \quad (1.2.20)$$

then the correct procedure is to simply replace  $\alpha_s$  by the effective coupling  $\alpha_s(Q^2)$  in (1.2.18). By this procedure one automatically incorporates an appropriate infinite set of diagrams into each calculation. It should be realized, however, that in leading order the perturbative parameter  $\Lambda$  is arbitrary. Changing the parameter  $\Lambda$  corresponds to adding a constant  $C$  as follows:

$$\begin{aligned} \alpha_s(Q^2) &= \frac{4\pi}{\beta_0 [\log(Q^2/\Lambda^2) + C]} \\ &= \frac{4\pi}{\beta_0 \log(Q^2/\Lambda^2)} - \frac{4\pi C}{\beta_0 \log^2(Q^2/\Lambda^2)} + \dots, \end{aligned} \quad (1.2.21)$$

The constant  $C$  produces changes at order  $\alpha_s^2(Q^2)$ . To leading order (1.2.18) and (1.2.21) are equivalent. In a similar manner changing ones definition of

**Table 1.1.** Value of the leading order QCD effective coupling,  $\alpha_{\text{LO}}$ , and the order  $\alpha_{\text{LO}}^2$  effective coupling in (1.2.23) versus  $Q$  for  $\Lambda = 200$  MeV and  $n_f = 4$ .

$Q$	$Q^2$	$\alpha_{\text{LO}}$	$\alpha_s$
2	4	0.327	0.247
4	16	0.252	0.196
10	100	0.193	0.155
31.6	1,000	0.149	0.124
50	2,500	0.137	0.115
100	10,000	0.121	0.103
500	250,000	0.096	0.084

$Q^2$  in (1.2.21) produces effects that are beyond leading order.

We will see in Chapter 6 that the effective coupling in QCD can be expanded in powers of the leading order coupling in (1.2.18),

$$\alpha_{\text{LO}}(Q^2) = \frac{12\pi}{(33 - 2n_f)\log(Q^2/\Lambda^2)}. \quad (1.2.22)$$

To order  $\alpha_{\text{LO}}^2$ ,

$$\alpha_s(Q^2) = \alpha_{\text{LO}}(Q^2) \left[ 1 - \frac{1}{4\pi} \frac{306 - 38n_f}{33 - 2n_f} \alpha_{\text{LO}}(Q^2) \log \log(Q^2/\Lambda^2) \right]. \quad (1.2.23)$$

By comparing observables that have been computed to one order beyond leading order with experiment one can in principle determine the QCD perturbative parameter  $\Lambda$  (provided, of course, that the higher orders are small!). However, the precise definition of  $\Lambda$  is still a matter of convention. Experimental observations indicate that

$$\Lambda_{\overline{MS}} \approx 200 \text{ MeV}, \quad (1.2.24)$$

with a large uncertainty of about 100 MeV,<sup>3,4</sup> and where  $(\overline{MS})$  corresponds to the modified minimal subtraction scheme (*convention*) discussed in Chapter 6.

In practice it has proved quite difficult to determine precisely the value of the perturbative parameter  $\Lambda$ . There are two reasons for this. First, since the effective coupling is not exceedingly small, calculations to a given order of perturbation theory do not always give an accurate result thereby introducing an error in the determination of  $\Lambda$ . Secondly, so called “higher twist” contributions are often important and difficult to estimate. These are correction terms that

die off like a power (*i.e.*,  $M^2/Q^2$ ) relative to the logarithmic correction of perturbative QCD. There is no systematic way to compute these “higher twist” corrections and they introduce a further uncertainty in determining  $\Lambda$ . The situation is best summarized by the limits<sup>4</sup>

$$0.10 \leq \alpha_s(Q^2 = 1000 \text{ GeV}^2) \leq 0.16, \quad (1.2.25)$$

with  $\alpha_s$  given in (1.2.23). Table 1.1 lists the value of the leading order QCD effective coupling,  $\alpha_{\text{LO}}$ , and the order  $\alpha_{\text{LO}}^2$  effective coupling in (1.2.23) versus  $Q$  for  $\Lambda = 200$  MeV and  $n_f = 4$ .

### Problems

- 1.1. Using the gluons in (1.1.1) show that the color factor

$$V_{q_i q_j} = \frac{1}{2} (P_{EX} - \frac{1}{3}),$$

where  $P_{EX}$  is a color exchange operator with the property that  $P_{EX} = +1$  for states symmetric in color exchange and  $P_{EX} = -1$  for states antisymmetric in color exchange.

- 1.2. Using the gluons in (1.1.1) or the color matrices in Appendix D compute the color factors for the following quark-antiquark, quark-quark, and three quark states:  $(q\bar{q})_{[1]}$ ,  $(q\bar{q})_{[8]}$ ,  $(qq)_{[3^*]}$ ,  $(qq)_{[6]}$ ,  $(qqq)_{[1]}$ , and  $(qqq)_{[8]}$ .

- 1.3. Using the commutation and anticommutation relations for the color matrices in Appendix D,

$$[T_a, T_b] = if_{abc} T_c, \\ \{T_a, T_b\} = \frac{1}{3} \delta_{ab} + d_{abc} T_c,$$

verify that

$$T_a T_b = \frac{1}{2} [\frac{1}{3} \delta_{ab} + (d_{abc} + if_{abc}) T_c], \\ \text{tr}(T_a T_b) = \frac{1}{2} \delta_{ab},$$

and

$$\text{tr}(T_a T_b T_c) = \frac{1}{4} (d_{abc} + if_{abc}).$$

- 1.4. Compute the color factors illustrated in Fig. D.1.

- 1.5. Show that a change in the perturbative parameter  $\Lambda$  in the expression for the effective QCD coupling,  $\alpha_s(Q^2)$ , in (1.2.18) corresponds to an effect of order  $\alpha_s^2$ .

- 1.6. Using  $n_f = 4$  and  $\Lambda = 200$  MeV, compute the value of  $Q$  where the leading order effective QCD coupling is equal to the leading order effective QED coupling in (1.2.8).

**Further Reading**

F.E. Close, *An Introduction to Quarks and Partons*, Academic Press, New York, 1979.

R.P. Feynman, "Gauge Theories," Les Houches, Session 29, North-Holland Publishing Company, 1977.

S. Gasiorowicz and J.L. Rosner, "Hadron Spectra and Quarks," *Am. J. Phys.* **49** (10), 954 (1981).

F. Halzen and A.D. Martin, *Quarks and Leptons: An Introductory Course in Modern Particle Physics*, John Wiley and Sons, Inc., 1984.

Chris Quigg, *Gauge Theories of the Strong, Weak, and Electromagnetic Interactions*, Frontiers in Physics, The Benjamin-Cummings Publishing Company, Inc., 1983.

P. Ramond, *Field Theory: A Modern Primer*, Frontiers in Physics, The Benjamin-Cummings Publishing Company, Inc., 1981.

---

**References**

---

1. C.N. Yang and R.L. Mill, *Phys. Rev.* **96**, 191 (1954).
2. F. Halzen and A.D. Martin, *Quarks and Leptons: An Introductory Course in Modern Particle Physics*, John Wiley and Sons, Inc., 1984.
3. D.W. Duke and R.G. Roberts, *Physics Reports* **120**, 275 (1985).
4. W. De Boer, SLAC-PUB-4428, invited talk at the X<sup>th</sup> Warsaw Symposium on Elementary Particle Physics, Kazimierz, Poland, May 25-29, 1987.

---

**CHAPTER 2**

---

**Electron-Positron Annihilations:  
Total Rate to Hadrons**

The vacuum in QCD is an extremely complicated object. Virtual pairs of all existing elementary particles are constantly being created and then die after living the time allowed them by the uncertainty principle. The timelike virtual photon that is produced when a high energy electron and positron annihilate provides an excellent probe of the vacuum. This virtual photon will couple to any elementary particle that carries electric charge and if its invariant mass,  $Q$ , is greater than the mass of the particle-antiparticle pair it can transform the pair from virtual to real. When the pair are leptons (*e.g.*,  $\mu^+\mu^-$ ) they fly out and can be detected experimentally. When the pair consists of, for example, a red quark-antiquark pair a remarkable phenomena occurs. At early times after the quark and antiquark are created short distance QCD dynamics dominates and the  $R$  quark and  $\bar{R}$  antiquark interact only weakly with each other since the strong coupling  $\alpha_s$  is small (*i.e.*, *asymptotic freedom*). In the center-of-mass frame the quark and antiquark begin to separate each carrying momentum  $\approx Q/2$ . At later times the distance between the  $R$  and  $\bar{R}$  color charges becomes large and the color forces between them increases. The color force between the separating color charges becomes larger and larger as time and distance increases until the vacuum breaks down and additional  $R\bar{R}$  quark pairs are created as illustrated in Fig. 2.1. These new quark-antiquark pairs then combine with each other and with the original quark and antiquark producing only color neutral (actually color *singlet*) hadrons in the final state. Experimentally the original quark and antiquark can not be directly detected. What is detected is the multitude of outgoing hadrons whose energies sum to give  $Q$ . By examining and studying these outgoing hadrons we learn about the quark and antiquark that initiated the process. Clearly from the point of view of perturbative QCD we are only going to be able to describe the early time (short distance) part of the phenomena where the QCD coupling is small. Perturbative QCD can tell us little about the later time (long distance) aspects of the phenomena. We will describe this long time, large distance, behavior in terms of a simple parton “fragmentation” model.

One can learn a great deal about QCD perturbation theory by studying electron-positron annihilations. This process provides an excellent “theoretical laboratory” in which to develop “tools” that can be used in performing other QCD calculations. In this chapter we will study the maximum inclusive process  $e^+e^- \rightarrow$  hadrons and compare it with the purely electromagnetic reaction  $e^+e^- \rightarrow \mu^+\mu^-$ . The annihilation of an electron and a positron into hadrons contains no color in the initial state and we know from a theorem due to Kinoshita<sup>1</sup>, Lee, and Nauenberg<sup>2</sup> that, at any order of perturbation theory, if we sum (*i.e.*, integrate) over all quark and gluon final states the result is finite even for massless quarks and gluons. However, the total cross section, for example, for the emission of a single real gluon,  $e^+e^- \rightarrow q\bar{q}g$ , is infinite. This infinity is canceled by virtual gluon corrections leaving a finite total cross section. To compute the finite corrections it is necessary to develop a regularization procedure that will control the infinities that occur in the individual real and virtual contributions. The two contributions are then added together

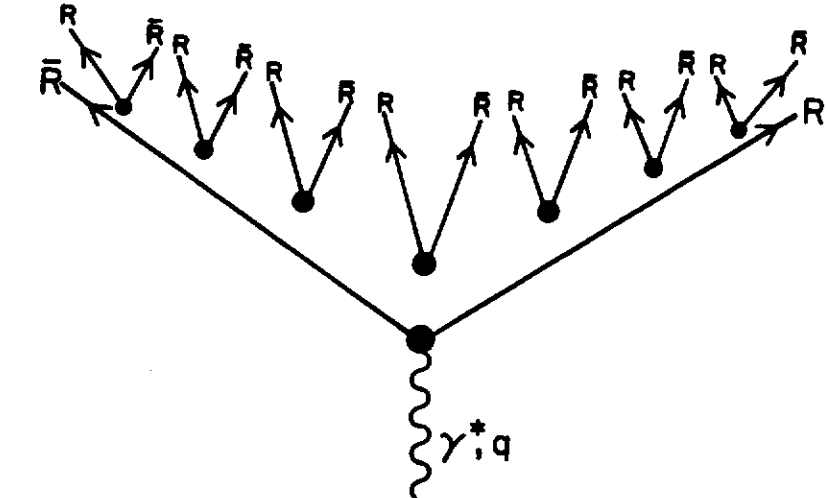


**Figure 2.1** Illustration of the phenomena that occurs when a red quark-antiquark pair is produced by a large invariant mass virtual photon in electron-positron annihilations. As time increases and the color charges begin to separate and the color force between them increases. Eventually new quark-antiquark pairs are “pulled” out of the vacuum and combine with each other and with the initial quark and antiquark to form color neutral (*i.e.*, color singlet) hadrons in the final state.

and the sum is finite and independent of the regularization scheme. Before we proceed with regularization schemes let us examine the naive parton model expectations for  $e^+e^- \rightarrow$  hadrons.

## 2.1 The Naive Parton Parton Model

The amplitude for a virtual photon to “decay” into a  $\mu^+\mu^-$  pair as shown in Fig. 2.2a is given by

$$A_\mu(p_2, s_2; p_1, s_1) = -ie\bar{u}(p_2, s_2)\gamma_\mu v(p_1, s_1), \quad (2.1.1)$$

where  $p_i$  and  $s_i$  are the momenta and spins, respectively, of the outgoing spin  $1/2$  fermions and where I have used the Feynman rules given in Appendix C. If we take the absolute value squared of this amplitude and sum over final state

spins we arrive at

$$\begin{aligned} L_{\mu\nu}(p_2; p_1) &= \sum_{s_1, s_2} A_\mu(p_2, s_2; p_1, s_1) A_\nu^\dagger(p_2, s_2; p_1, s_1) \\ &= e^2 \text{tr}(\not{p}_2 \gamma_\mu \not{p}_1 \gamma_\nu) \\ &= 4e^2 [(p_1)_\mu (p_2)_\nu + (p_1)_\nu (p_2)_\mu - g_{\mu\nu} p_1 \cdot p_2], \end{aligned} \quad (2.1.2)$$

where the masses of the particles have been neglected. The differential cross section for the electromagnetic process  $e^+e^- \rightarrow \mu^+\mu^-$  shown in Fig. 2.2b is, from Appendix A, given by

$$\frac{d\sigma}{d\Omega_{cm}} = \frac{1}{64\pi^2 E_{cm}^2} |\bar{\mathcal{M}}(e^+e^- \rightarrow \mu^+\mu^-)|^2, \quad (2.1.3)$$

where  $|\bar{\mathcal{M}}|^2$  is the spin averaged matrix element squared,

$$\begin{aligned} |\bar{\mathcal{M}}|^2 &= \frac{1}{4} L_{\mu\nu}(p_2; p_1) \frac{1}{q^4} L_{\mu\nu}^\dagger(p_2; p_1) \\ &= \frac{1}{4} \frac{e^4}{q^4} 32 [p_a \cdot p_1 p_b \cdot p_2 + p_a \cdot p_2 p_b \cdot p_1]. \end{aligned} \quad (2.1.4)$$

The invariants are defined by

$$s = (p_a + p_b)^2 = (p_1 + p_2)^2 = E_{cm}^2 = q^2 = Q^2, \quad (2.1.5)$$

$$t = (p_1 - p_a)^2 = -2p_1 \cdot p_a = -\frac{s}{2}(1 - \cos \theta_{cm}), \quad (2.1.6)$$

$$u = (p_2 - p_b)^2 = -2p_2 \cdot p_b = -\frac{s}{2}(1 - \cos \theta_{cm}), \quad (2.1.7)$$

$$u = (p_1 - p_2)^2 = -2p_1 \cdot p_2 = -\frac{s}{2}(1 + \cos \theta_{cm}), \quad (2.1.8)$$

$$u = (p_a - p_b)^2 = -2p_a \cdot p_b = -\frac{s}{2}(1 + \cos \theta_{cm}), \quad (2.1.9)$$

and energy and momentum conservation implies

$$p_a + p_b = p_1 + p_2, \quad (2.1.10)$$

where again masses have been neglected. Using these relationships we see that

$$\begin{aligned} p_a \cdot p_1 p_b \cdot p_2 + p_a \cdot p_2 p_b \cdot p_1 &= \frac{1}{4}(t^2 + u^2) \\ &= \frac{1}{8}s^2(1 + \cos^2 \theta_{cm}), \end{aligned} \quad (2.1.11)$$

and we arrive at

$$\frac{d\sigma}{d\Omega_{cm}} = \frac{1}{4} \frac{\alpha^2}{Q^2} (1 + \cos^2 \theta_{cm}), \quad (2.1.12)$$

where the QED coupling is taken as

$$\alpha = e^2/4\pi, \quad (2.1.13)$$

and  $Q$  is the center-of-mass energy,  $E_{cm} = Q$ . The solid angle is given by,

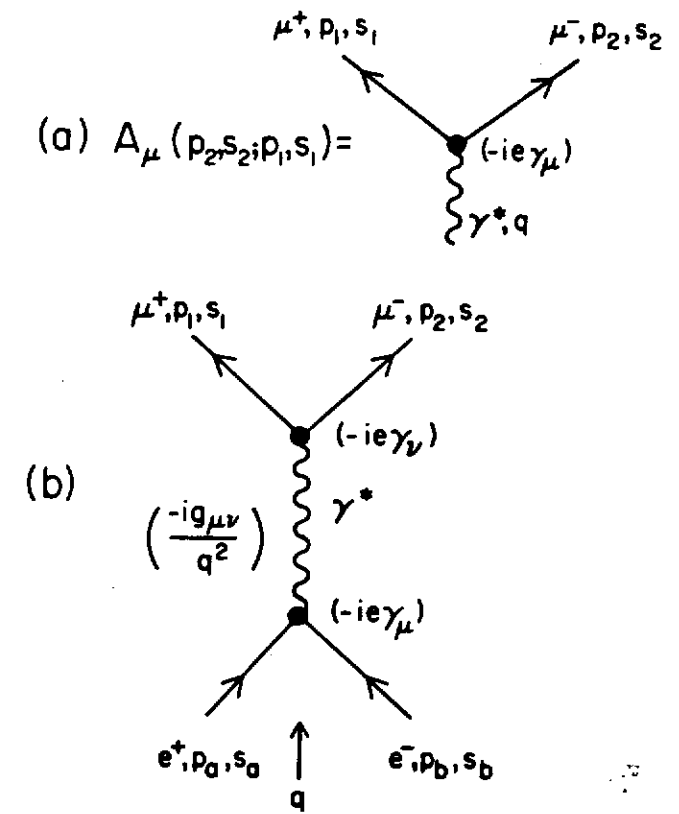


Figure 2.2 (a) Amplitude for the "decay" of a virtual photon into a  $\mu^+\mu^-$  pair.  
(b) Amplitude for an  $e^+e^-$  pair to annihilate and produce a  $\mu^+\mu^-$  pair by the production and "decay" of a single virtual photon.

$d\Omega_{cm} = d\cos \theta_{cm} d\phi_{cm}$ , where  $\theta_{cm}$  is the scattering angle between the outgoing  $\mu^+$  and the incoming  $e^+$ . Integrating over the angles  $\theta_{cm}$  and  $\phi_{cm}$  gives the total cross section

$$\sigma(e^+e^- \rightarrow \mu^+\mu^-) = \frac{4\pi}{3} \frac{\alpha^2}{Q^2}. \quad (2.1.14)$$

Replacing the  $\mu^+\mu^-$  pair with a quark-antiquark pair as in Fig. 2.3 gives

$$\sigma(e^+e^- \rightarrow q\bar{q}) = (3) \frac{4\pi}{3} \frac{\alpha^2}{Q^2} e_q^2, \quad (2.1.15)$$

which is identical to  $\sigma(e^+e^- \rightarrow \mu^+\mu^-)$  except for the factor of 3 which comes

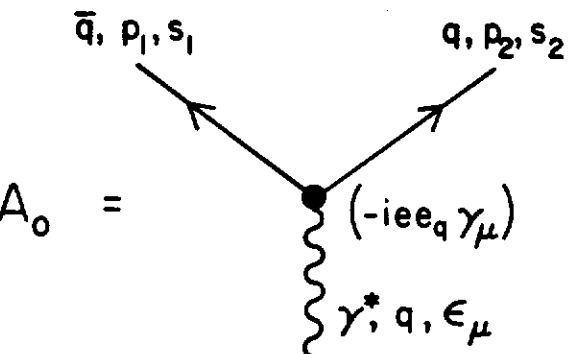


Figure 2.3 Born amplitude for the “decay” of a virtual photon into a quark-antiquark pair.

from the sum over the three quark colors and the factor  $e_q^2$ , where  $e_q$  is the charge of the quark  $q$  in units of the electric charge  $e$ . Assuming that quarks turn into hadrons with unit probability one arrives at the famous parton model prediction for the ratio of the total cross section  $e^+e^- \rightarrow$  hadrons to the total cross section for  $e^+e^- \rightarrow \mu^+\mu^-$ . Namely,

$$R_{e^+e^-} \equiv \sigma(e^+e^- \rightarrow \text{hadrons})/\sigma(e^+e^- \rightarrow \mu^+\mu^-) = 3 \sum_{i=1}^{n_f} e_{qi}^2, \quad (2.1.16)$$

where the sum is over all quark pairs that can be produced at the given center-of-mass energy of  $Q$ .

It is convenient to visualize this process as an  $e^+e^-$  pair which annihilates producing a virtual photon,  $\gamma^*$  which then “decays” into either a muon pair or a quark-antiquark pair (Fig. 2.2a or Fig. 2.3, respectively). From this point of view we arrive at (2.1.16) by considering the two-body differential decay rate,

$$dW = \frac{1}{2E_{cm}} |\bar{\mathcal{M}}|^2 d^6R_2, \quad (2.1.17)$$

where  $d^6R_2$  is the two-body phase-space factor,

$$d^6R_2 = \frac{d^3p_1}{(2\pi)^3(2E_1)} \frac{d^3p_2}{(2\pi)^3(2E_2)} (2\pi)^4 \delta^4(q - p_1 - p_2). \quad (2.1.18)$$

The total decay is deduced by integrating  $dW$  in (2.1.17) over the 4-momenta

of the decay products  $p_1$  and  $p_2$  subject to the constraint that  $p_1 + p_2 = q$ , where  $q$  is the 4-momentum of the virtual photon,  $\gamma^*$ . Integrating over the 3-momentum of particle 2 yields

$$\int d^3p_2 \delta^4(q - p_1 - p_2) = \delta(Q - E_1 - E_2). \quad (2.1.19)$$

Next we integrate over the direction of particle 1 using

$$\frac{d^3p_1}{2E_1} = \frac{1}{2} E_1 \sin \theta_1 d\theta_1 d\phi_1 dE_1, \quad (2.1.20)$$

where particles 1 and 2 have been taken to be massless and  $\theta_1$  and  $\phi_1$  are angles with respect to an arbitrary choice of axis. Integrating over  $\theta_1$  and  $\phi_1$  yields

$$\int \frac{d^3p_1}{2E_1} = \frac{4\pi}{2} E_1 dE_1. \quad (2.1.21)$$

The final integration over  $E_1$  is accomplished using the conservation of energy  $\delta$ -function,

$$\frac{\delta(Q - E_1 - E_2)}{2E_2} = \delta[(q - p_1 - p_2)^2] = \delta(Q^2 - 2E_1 Q), \quad (2.1.22)$$

giving

$$\int \frac{E_1 dE_1}{2E_2} \delta(Q - E_1 - E_2) = \frac{E_1}{2Q} = \frac{1}{4}, \quad (2.1.23)$$

since for massless particles  $E_1 = Q/2$ . Hence,

$$R_2 = \int d^6R_2 = \frac{1}{8\pi}, \quad (2.1.24)$$

and since the matrix element does not depend on any of the variables of integration the total decay rate is

$$W = \frac{1}{2Q} |\bar{\mathcal{M}}|^2 R_2 = \frac{1}{16\pi Q} |\bar{\mathcal{M}}|^2, \quad (2.1.25)$$

where  $|\bar{\mathcal{M}}|^2$  is the appropriate spin averaged matrix element squared. For the “decay” of a virtual photon into a muon pair as shown in Fig. 2.2a we have

$$|\bar{\mathcal{M}}(\gamma^* \rightarrow \mu^+\mu^-)|^2 = \sum_{\lambda} \sum_{s_1, s_2} A_{\mu}(p_2, s_2; p_1, s_1) A_{\nu}^{\dagger}(p_2, s_2; p_1, s_1) \epsilon_{\mu}(\lambda) \epsilon_{\nu}^*(\lambda) \\ = \sum_{\lambda} L_{\mu\nu}(p_2; p_1) \epsilon_{\mu}(\lambda) \epsilon_{\nu}^*(\lambda), \quad (2.1.26)$$

where  $L_{\mu\nu}$  is given in (2.1.2) and  $\epsilon_{\mu}(\lambda)$  is the polarization 4-vector of the virtual photon (see Appendix C). For simplicity we will use the replacement

$$\sum_{\lambda} \epsilon_{\mu}(\lambda) \epsilon_{\nu}^*(\lambda) \rightarrow -g_{\mu\nu}, \quad (2.1.27)$$

where  $g_{\mu\nu}$  is the metric defined in Appendix B. As I will explain in the next

section for a real photon the replacement in (2.1.27) is equivalent to summing over the physical (*i.e.*, *transverse*) polarization states. For a virtual photon the replacement in (2.1.27) results in a combination of the transverse and longitudinal cross sections which I will label by the subscript  $\Sigma$ . Namely,

$$|\mathcal{M}|_\Sigma^2 = -L_{\mu\mu}(p_2; p_1) = 8e^2 p_1 \cdot p_2. \quad (2.1.28)$$

Combining (2.1.25) and (2.1.28) and using (2.1.5) gives

$$W(\gamma_\Sigma^* \rightarrow \mu^+ \mu^-) = \alpha Q. \quad (2.1.29)$$

Similarly,

$$W(\gamma_\Sigma^* \rightarrow q\bar{q}) = \sigma_0 = 3\alpha e_q^2 Q, \quad (2.1.30)$$

and the ratio  $R = W(\gamma_\Sigma^* \rightarrow q\bar{q})/W(\gamma_\Sigma^* \rightarrow \mu^+ \mu^-)$  is the same as that arrived at in (2.1.16). I will call the rate the Born term,  $\sigma_0$ , and the amplitude

$$A_0 = -iee_q \bar{u}(p_2, s_2) \gamma_\mu v(p_1, s_1) \epsilon_\mu(\lambda), \quad (2.1.31)$$

shown in Fig. 2.3 the Born amplitude.

## 2.2 Summing Over Polarization States

Before proceeding to calculate the QCD corrections to the Born cross section in (2.1.30) I would like to discuss techniques for summing over photon and gluon polarization states. For the case of a real massless photon (or gluon) propagating along the  $\hat{z}$ -axis with 4-momentum  $k_\mu$  given by

$$k_\mu = \begin{pmatrix} k_0 \\ 0 \\ 0 \\ k_3 \end{pmatrix}, \quad (2.2.1)$$

the polarization 4-vector is given by

$$\epsilon_\mu(\lambda = \pm 1) = \frac{1}{\sqrt{2}} \begin{pmatrix} 0 \\ 1 \\ \pm i \\ 0 \end{pmatrix} \quad (2.2.2)$$

for helicity  $\lambda = \pm 1$ . The polarization 4-vector satisfies

$$k \cdot \epsilon = 0 \quad (2.2.3)$$

and

$$\epsilon^2 = -1. \quad (2.2.4)$$

The matrix element squared for any process with one real external photon

can be written as (2.1.26). Namely,

$$|\mathcal{M}|^2 = \sum_\lambda L_{\mu\nu} \epsilon_\mu(\lambda) \epsilon_\nu^*(\lambda), \quad (2.2.5)$$

and summing over the two helicity states in (2.2.2) gives

$$|\mathcal{M}|^2 = L_{11} + L_{22}. \quad (2.2.6)$$

On the other hand, if we make the replacement

$$\sum_\lambda \epsilon_\mu(\lambda) \epsilon_\nu^*(\lambda) \rightarrow -g_{\mu\nu}, \quad (2.2.7)$$

we arrive at

$$|\mathcal{M}|^2 = L_{11} + L_{22} + L_{33} - L_{00}, \quad (2.2.8)$$

which agrees with (2.2.6) provided

$$L_{00} = L_{33}. \quad (2.2.9)$$

Gauge invariance insures that this is indeed the case. From gauge invariance we have

$$k_\mu L_{\mu\nu} = 0, \quad (2.2.10)$$

and

$$k_\nu L_{\mu\nu} = 0, \quad (2.2.11)$$

since (in momentum space) the substitution

$$A_\mu(x) \rightarrow A_\mu(x) + k_\mu \Phi(x), \quad (2.2.12)$$

where  $A_\mu(x)$  is the electromagnetic current and  $\Phi(x)$  is an arbitrary function must leave the results invariant. From (2.2.1) and (2.2.10) we see that

$$k_0 L_{0\nu} - k_3 L_{3\nu} = 0 \quad (2.2.13)$$

or since  $k_0 = k_3$  (massless photons),

$$L_{0\nu} = L_{3\nu}. \quad (2.2.14)$$

Similarly,

$$L_{\mu 0} = L_{\mu 3}, \quad (2.2.15)$$

and these two conditions insure that (2.2.9) is satisfied. Thus, for real (massless) photons the substitution in (2.2.7) is equivalent to summing the two allowed helicity states.

Because of the gauge invariance conditions in (2.2.10) and (2.2.11) the substitution

$$\sum_\lambda \epsilon_\mu(\lambda) \epsilon_\nu^*(\lambda) \rightarrow - \left( g_{\mu\nu} + \eta \frac{k_\mu k_\nu}{k^2} \right) \quad (2.2.16)$$

will work equally well, where  $\eta$  is an arbitrary gauge parameter ( $\eta = 0$  is Feynman gauge,  $\eta = -1$  is Landau gauge).

The replacement in (2.2.16) works for an arbitrary number of external real massless photons. It also works for the case of *one* real external massless gluon. However, it does not work for processes with two or more external gluons in which the triple gluon vertex is present. In this case the replacement in (2.2.16) leaves extraneous unphysical spin states which can be removed by including diagrams with a fictitious “ghost” particle (see Appendix C). The couplings of this ghost particle are adjusted to precisely remove the unphysical spin states which arise from the replacement in (2.2.16). We will see an example of this when we study the process  $g + q \rightarrow g + q$  in Chapter 7.

For a massive boson with 4-momentum given by (2.2.1) (in this case  $k_0^2 = k_3^2 + M^2$ ) one also has the longitudinal polarization state

$$\epsilon_\mu(\lambda = 0) = \frac{1}{M} \begin{pmatrix} k_3 \\ 0 \\ 0 \\ k_0 \end{pmatrix}. \quad (2.2.17)$$

It is easy to show that the three polarization states of a massive boson are correctly summed over by the replacement

$$\sum_{\lambda} \epsilon_\mu(\lambda) \epsilon_{\nu}^{*}(\lambda) \rightarrow - \left( g_{\mu\nu} - \frac{k_{\mu}k_{\nu}}{M^2} \right). \quad (2.2.18)$$

For the case of a virtual photon as in (2.1.26), the replacement in (2.2.7) produces a combination of transverse and longitudinal cross sections which can be untangled if desired.

### 2.3 Real Gluon Emission

We now consider the three-body “decay” of a virtual photon,  $\gamma^*$ , into a quark-antiquark pair and a real gluon. The two amplitudes for this process are shown in Fig. 2.4 and are given by

$$A_R = \bar{u}(p_2, s_2) (-ig_s \gamma_\nu T_{ij}^a) \left( \frac{i p_a'}{p_a^2} \right) (-ie e_q \gamma_\mu) v(p_1, s_1) \epsilon_\mu \epsilon'_\nu, \quad (2.3.1)$$

and

$$B_R = \bar{u}(p_2, s_2) (-ie e_q \gamma_\mu) \left( \frac{i p_b'}{p_b^2} \right) (-ig_s \gamma_\nu T_{ij}^a) v(p_1, s_1) \epsilon_\mu \epsilon'_\nu, \quad (2.3.2)$$

where I have used the Feynman rules from Appendix C and where

$$p_a = p_2 + p_3, \quad (2.3.3)$$

$$p_b = p_1 + p_3, \quad (2.3.4)$$

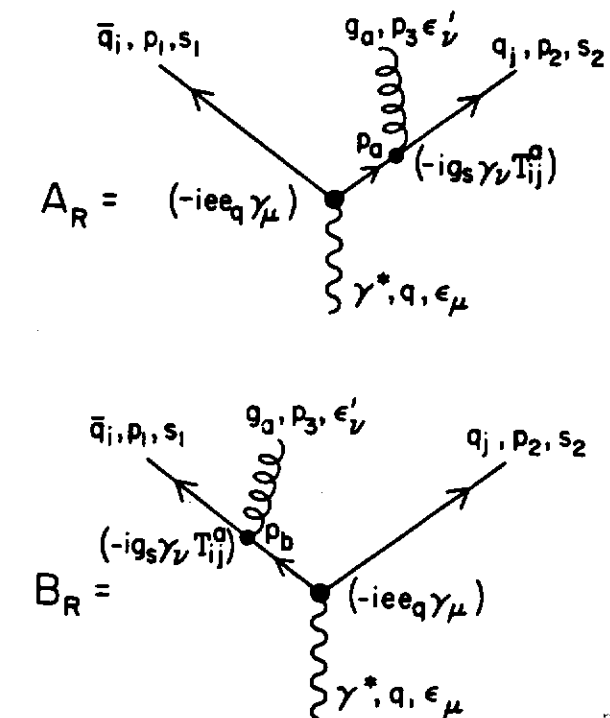


Figure 2.4 Amplitudes for the three-body “decay” of a virtual photon into a quark-antiquark pair and a gluon.

and the virtual photon 4-momentum is

$$q = p_1 + p_2 + p_3, \quad (2.3.5)$$

with

$$E_{cm} = Q = \sqrt{q^2}. \quad (2.3.6)$$

The three-body differential decay rate is

$$dW = \frac{1}{2E_{cm}} |\mathcal{M}|^2 d^3 R_3, \quad (2.3.7)$$

and the three-body phase-space factor is given by

$$d^3 R_3 = \frac{d^3 p_1}{(2\pi)^3 (2E_1)} \frac{d^3 p_2}{(2\pi)^3 (2E_2)} \frac{d^3 p_3}{(2\pi)^3 (2E_3)} (2\pi)^4 \delta^4(q - p_1 - p_2 - p_3). \quad (2.3.8)$$

Equations (2.3.7) and (2.3.8) replace the two-body formulas (2.1.17) and (2.1.18) and to arrive at a total rate we must integrate over the momentums of three decay particles (1 = antiquark, 2 = quark, 3 = gluon).

It is convenient to define the dimensionless energy fractions

$$x_i = 2E_i/Q \quad (i = 1, 2, 3). \quad (2.3.9)$$

If we neglect the masses of the decay products then

$$p_i \cdot p_j = \frac{1}{2}Q^2(1 - x_k), \quad (2.3.10)$$

and the Lorentz invariants become

$$s \equiv (p_1 + p_3)^2 = 2p_1 \cdot p_3 = Q^2(1 - x_2), \quad (2.3.11)$$

$$t \equiv (p_2 + p_3)^2 = 2p_2 \cdot p_3 = Q^2(1 - x_1), \quad (2.3.12)$$

$$u \equiv (p_1 + p_2)^2 = 2p_1 \cdot p_2 = Q^2(1 - x_3). \quad (2.3.13)$$

In analogy with (2.1.19) integrating over the 3-momentum of particle 3 gives

$$\int d^3 p_3 \delta^4(q - p_1 - p_2 - p_3) = \delta(Q - E_1 - E_2 - E_3). \quad (2.3.14)$$

The remaining energy conservation  $\delta$ -function implies that  $Q = E_1 + E_2 + E_3$  or from (2.3.9)

$$x_1 + x_2 + x_3 = 2, \quad (2.3.15)$$

and

$$s + t + u = Q^2. \quad (2.3.16)$$

We must now integrate (2.3.8) over the directions of particles 1 and 2 similar to (2.1.21). The result is

$$\int \int \frac{d^3 p_1}{2E_1} \frac{d^3 p_2}{2E_2} = \frac{(4\pi)(2\pi)}{4} E_1 dE_1 E_2 dE_2 \int_{-1}^1 dz, \quad (2.3.17)$$

where  $z = \cos \theta_{12}$  is the relative angle between particle 1 and particle 2 (we can pick the  $\hat{z}$ -axes in the direction of particle 1). The integration over  $z$  can be carried out using

$$\begin{aligned} \frac{\delta(Q - E_1 - E_2 - E_3)}{2E_3} &= \delta[(q - p_1 - p_2 - p_3)^2] \\ &= \delta[Q^2(1 - x_1 - x_2 + \frac{1}{2}x_1 x_2 (1 - z))] \end{aligned} \quad (2.3.18)$$

resulting in

$$\int_{-1}^1 dz \frac{\delta(Q - E_1 - E_2 - E_3)}{2E_3} = \frac{2}{x_1 x_2 Q^2}, \quad (2.3.19)$$

so that

$$d^2 R_3 = \frac{Q^2}{16(2\pi)^3} dx_1 dx_2. \quad (2.3.20)$$

At this point we cannot integrate the phase-space factor  $d^2 R_3$  any further since

the matrix element in (2.3.7) will depend in general on  $x_1$  and  $x_2$ . Combining (2.3.7) and (2.3.20) gives the differential decay rate

$$dW = \frac{Q}{32(2\pi)^3} |\bar{\mathcal{M}}|^2 dx_1 dx_2, \quad (2.3.21)$$

which when written as a differential cross section becomes

$$\frac{d\sigma}{dx_1 dx_2} = \frac{Q}{32(2\pi)^3} |\bar{\mathcal{M}}|^2. \quad (2.3.22)$$

The spin averaged matrix element squared for the decay of a virtual photon into a quark, antiquark, and a gluon is given by

$$|\bar{\mathcal{M}}(\gamma_\Sigma^* \rightarrow q\bar{q}g)|^2 = S_{22} + S_{11} + S_{12}, \quad (2.3.23)$$

where the subscript  $\Sigma$  refers to the fact that virtual photon polarization states have been summed by using the replacement in (2.1.27). The first term in (2.3.23) is given by

$$\begin{aligned} S_{22} &= |A_R|_\Sigma^2 = \frac{g_s^2 e^2 e_q^2}{p_a^4} \text{tr}(\mathbf{T}_a \mathbf{T}_a) \text{tr}(\not{p}_2 \gamma_\nu \not{p}_a \gamma_\mu \not{p}_1 \gamma_\mu \not{p}_a \gamma_\nu) \\ &= \frac{g_s^2 e^2 e_q^2}{p_a^4} (4)16 (2p_1 \cdot p_a p_2 \cdot p_a - p_1 \cdot p_2 p_a \cdot p_a) \\ &= 32e^2 e_q^2 g_s^2 \left( \frac{st}{t^2} \right) \\ &= 32e^2 e_q^2 g_s^2 \frac{(1-x_2)}{(1-x_1)}, \end{aligned} \quad (2.3.24)$$

where I have used

$$p_a^2 = t, \quad (2.3.25)$$

$$p_a \cdot p_1 = \frac{1}{2}(u+s), \quad (2.3.26)$$

$$p_a \cdot p_2 = \frac{1}{2}t, \quad (2.3.27)$$

and where the color factor

$$\text{tr}(\mathbf{T}_a \mathbf{T}_a) = \frac{1}{2}\delta_{aa} = 4 \quad (2.3.28)$$

is discussed in Appendix D. Similarly,

$$\begin{aligned} S_{11} &= |B_R|_\Sigma^2 = 32e^2 e_q^2 g_s^2 \left( \frac{st}{s^2} \right) \\ &= 32e^2 e_q^2 g_s^2 \frac{(1-x_1)}{(1-x_2)}, \end{aligned} \quad (2.3.29)$$

and

$$S_{12} = (2A_R B_R^*)_\Sigma = 32e^2 e_q^2 g_s^2 \left( \frac{2uQ^2}{st} \right)$$

$$= 32e^2 e_q^2 g_s^2 \left( \frac{2}{(1-x_1)(1-x_2)} - \frac{2}{(1-x_1)} - \frac{2}{(1-x_2)} \right). \quad (2.3.30)$$

The three pieces  $S_{11}$ ,  $S_{22}$  and  $S_{12}$  are gauge dependent with the results above holding only for the Feynman gauge (which is implemented by using (2.1.27) to sum the gluon polarization states). The sum

$$\begin{aligned} S_{11} + S_{22} + S_{12} &= |A_R + B_R|^2 \\ &= 32e^2 e_q^2 g_s^2 \frac{x_1^2 + x_2^2}{(1-x_1)(1-x_2)}, \end{aligned} \quad (2.3.31)$$

is, of course, gauge invariant. Combining (2.3.22) with (2.3.23) and (2.3.31) yields

$$\frac{1}{\sigma_0} \frac{d\sigma_\Sigma}{dx_1 dx_2} = \frac{2\alpha_s}{3\pi} \frac{x_1^2 + x_2^2}{(1-x_1)(1-x_2)}, \quad (2.3.32)$$

where the Born term  $\sigma_0$  is given in (2.1.30) and the strong coupling is

$$\alpha_s = g_s^2/4\pi. \quad (2.3.33)$$

The order  $\alpha_s$  correction to the Born term total cross section,  $\sigma_0$ , in (2.1.30) from the emission of a real gluon,  $\sigma(\text{real})$ , is arrived at by integrating (2.3.32) over the kinematically allowed range of  $x_1$  and  $x_2$ . The boundary of the allowed phase-space region for massless quarks and gluons is given by the implicit solution of

$$stu = 0, \quad (2.3.34)$$

or in terms of  $x_i$ :

$$(1-x_1)(1-x_2)(1-x_3) = 0. \quad (2.3.35)$$

The resulting triangular region

$$0 \leq x_1 \leq 1, \quad (2.3.36)$$

$$1-x_1 \leq x_2 \leq 1, \quad (2.3.37)$$

is shown in Fig. 2.5. The integral of (2.3.32) becomes

$$\sigma_\Sigma(\text{real}) = \frac{2\alpha_s}{3\pi} \sigma_0 \int_0^1 dx_1 \int_{1-x_1}^1 dx_2 \frac{x_1^2 + x_2^2}{(1-x_1)(1-x_2)}, \quad (2.3.38)$$

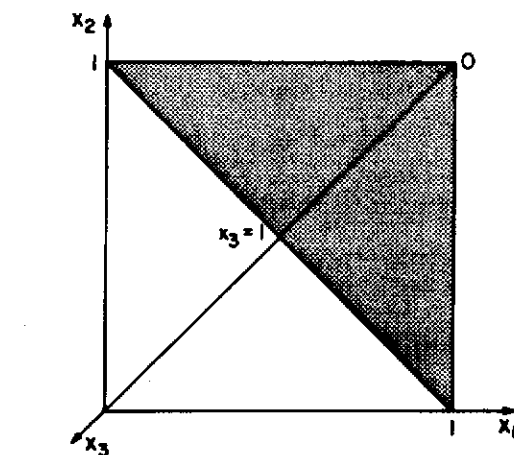
and we are left with a problem that will occur over and over as we perform perturbative QCD calculations. The differential cross section in (2.3.32) diverges as  $x_1$  or  $x_2$  goes to 1 and  $\sigma(\text{real})$  is infinite. The origin of this divergence is clear. Consider, for example, the invariant  $t$  in (2.3.12) and (2.3.24). In the massless limit we have

$$t = 2p_2 \cdot p_3 = 2E_2 \omega (1 - \cos \theta_{23}), \quad (2.3.39)$$

where  $\theta_{23}$  is the angle between  $\vec{p}_2$  and  $\vec{p}_3$  and  $E_2$  and  $\omega$  are the energy of the outgoing quark and gluon, respectively. The amplitude squared in (2.3.24) and hence the differential cross section diverges as  $t \rightarrow 0$  which occurs when

DALITZ PLOT FOR 3 PARTICLE FINAL STATE

(a) Massless Particles



(b) Massive Gluon:  $\beta = m_g^2/Q^2$

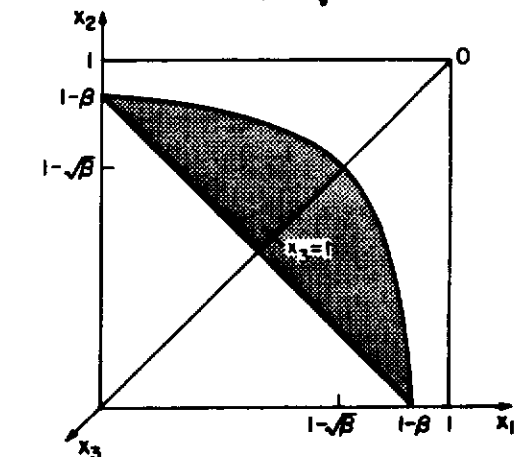


Figure 2.5 (a) Dalitz plot for the “decay” of a virtual photon with invariant mass  $Q$  into a massless quark, antiquark, and gluon each carrying fractional energy  $x_i = 2E_i/Q$ . The shaded area is the allowed kinematic region. (b) Same as (a) except now the gluon is given a fictitious mass,  $m_g$ , and  $\beta = m_g^2/Q^2$ .

the energy of the gluon goes to zero ( $\omega \rightarrow 0$ , “soft divergence”) or when the outgoing quark and gluon become parallel ( $\cos \theta_{23} \rightarrow 1$ , “parallel divergence”). The first type of divergence is referred to as an infrared divergence (it occurs

in the limit  $m_g \rightarrow 0$  and  $m_q \neq 0$ , where  $m_g$  and  $m_q$  are the gluon and quark masses, respectively), while the second is referred to as a mass singularity (it occurs as  $m_q \rightarrow 0$  with  $m_g = 0$ ).

In order to proceed we must decide on some way of regularizing the infrared and mass singularities. In addition, it better be true that no experimental observables depend on the manner in which we perform the regularization. Before we proceed to examine regularization schemes it is instructive to integrate (2.3.32) over the region

$$s \geq m^2, \quad (2.3.40)$$

$$t \geq m^2, \quad (2.3.41)$$

where  $m$  is an arbitrary mass (for example a pion mass). The result is the total cross section for producing a real gluon whose invariant mass with both the quark and antiquark is always greater than  $m^2$ ,

$$\sigma_m(\gamma_\Sigma^* \rightarrow q\bar{q}g) = \int_\beta^{1-\beta} dx_1 \int_{1-x_1}^{1-\beta} dx_2 \left( \frac{d\sigma_\Sigma}{dx_1 dx_2} \right), \quad (2.3.42)$$

where  $\beta = m^2/Q^2$ . The integrations in (2.3.42) are straightforward but not easy. This illustrates how quickly one runs into complicated math even though (2.3.32) appears to be a simple looking formula. It helps to rewrite the expression using

$$\frac{x_1^2 + x_2^2}{(1-x_1)(1-x_2)} = \frac{2}{(1-x_1)(1-x_2)} - \frac{(1+x_1)}{(1-x_2)} - \frac{(1+x_2)}{(1-x_1)}. \quad (2.3.43)$$

The second and third terms are easy to integrate,

$$\begin{aligned} \int_\beta^{1-\beta} dx_1 \int_{1-x_1}^{1-\beta} dx_2 \frac{(1+x_1)}{(1-x_2)} &= \int_\beta^{1-\beta} dx_1 \int_{1-x_1}^{1-\beta} dx_2 \frac{(1+x_2)}{(1-x_1)} \\ &= -\frac{3}{2} \log(\beta) - \frac{5}{4}, \end{aligned} \quad (2.3.44)$$

where terms which vanish in the limit  $\beta \rightarrow 0$  have been dropped. The  $\log(\beta)$  term arises from the integral

$$\int_{1-x_1}^{1-\beta} \frac{1}{1-x_2} dx_2 = \log(x_1/\beta). \quad (2.3.45)$$

Integrating the first term in (2.3.43) is tough. The results is

$$\begin{aligned} \int_\beta^{1-\beta} dx_1 \int_{1-x_1}^{1-\beta} dx_2 \frac{1}{(1-x_1)(1-x_2)} &= \log^2(\beta) - \log(\beta) \log(1-\beta) \\ &\quad + \text{Li}_2(1-\beta) - \text{Li}_2(\beta), \end{aligned} \quad (2.3.46)$$

where again I have dropped terms that vanish in the limit  $\beta \rightarrow 0$  and I have used

$$\int_\beta^{1-\beta} \frac{\log(x_1)}{1-x_1} dx_1 = \int_\beta^1 \frac{\log(x_1)}{1-x_1} dx_1 - \int_{1-\beta}^1 \frac{\log(x_1)}{1-x_1} dx_1$$

$$= \text{Li}_2(1-\beta) - \text{Li}_2(\beta), \quad (2.3.47)$$

where the dilogarithm function,  $\text{Li}_2(x)$ , is defined in Appendix E. Combining terms and using (E.2.12),

$$\text{Li}_2(\beta) + \text{Li}_2(1-\beta) = \frac{\pi^2}{6} - \log(\beta) \log(1-\beta), \quad (2.3.48)$$

and (E.2.7),

$$\text{Li}_2(1) = \frac{\pi^2}{6}, \quad (2.3.49)$$

gives

$$\sigma_m(\gamma_\Sigma^* \rightarrow q\bar{q}g) = \frac{2\alpha_s}{3\pi} \sigma_0 \left\{ 2 \log^2(\beta) + 3 \log(\beta) + \frac{\pi^2}{3} + \frac{5}{2} \right\}, \quad (2.3.50)$$

where again terms that vanish in the limit  $\beta \rightarrow 0$  have been dropped.

The cross section in (2.3.50) has a term that diverges like  $\log^2(\beta)$  as  $\beta \rightarrow 0$  which comes from the region in which both  $x_1$  and  $x_2$  approach 1. In addition, there is a term that diverges like  $\log(\beta)$  and there are terms that are finite as  $\beta \rightarrow 0$ . As  $Q$  increases this cross section increases like  $\log(Q)$ . The  $\log^2(\beta)$  term behaves like  $\log^2(Q)$  at large  $Q$ , but the coupling constant in (1.2.18) behaves like  $1/\log(Q)$  resulting in a net  $\log(Q)$  dependence of (2.3.50) as  $Q$  becomes large.

## 2.4 Virtual Gluon Corrections

The virtual corrections in Fig. 2.6 and Fig. 2.7 have the same final state as does the Born term in Fig. 2.3. These amplitudes must be added and then squared as follows

$$\begin{aligned} |A_0 + A_v + B_v + C_v|^2 &= |A_0|^2 + 2\text{Re}(A_0 A_v^*) \\ &\quad + 2\text{Re}(A_0 B_v^* + A_0 C_v^*) + |A_v + B_v + C_v|^2. \end{aligned} \quad (2.4.1)$$

The second and third terms are the same order (order  $\alpha_s$ ) as the real gluon correction in (2.3.38). The fourth term is order  $\alpha_s^2$  and will be neglected. The virtual amplitude,  $A_v$ , in Fig. 2.6 is given by

$$\begin{aligned} A_v &= \bar{u}(p_2, s_2) (-ig_s \gamma_\beta T_{i\ell}^a) \left( \frac{i\gamma_b}{p_b^2} \right) (-ie e_q \gamma_\mu) \left( \frac{-i\gamma_a}{p_a^2} \right) \\ &\quad (-ig_s \gamma_\alpha T_{j\ell}^a) \left[ \frac{-i(g_{\beta\alpha} + \eta k_\beta k_\alpha/k^2)}{k^2} \right] v(p_1, s_1), \end{aligned} \quad (2.4.2)$$

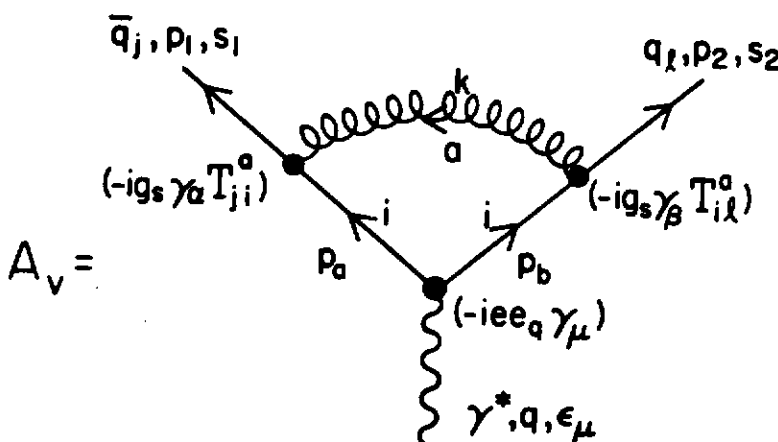


Figure 2.6 Virtual gluon corrections to the Born amplitude in Fig. 2.3.

where

$$p_a = p_1 - k, \quad (2.4.3)$$

$$p_b = p_2 + k, \quad (2.4.4)$$

and

$$q = p_a + p_b. \quad (2.4.5)$$

Combining this with the  $A_0$  amplitude in (2.1.31) and integrating over the 4-momentum,  $k$ , of the virtual gluon gives

$$\begin{aligned} \sigma_v(\text{virtual}) &= \int \frac{d^4k}{(2\pi)^4} (2A_0 A_v^*) \\ &= \frac{4}{3} \sigma_0 2g_s^2 (-i) \int \frac{d^4k}{(2\pi)^4} \frac{N(p_1, p_2, k, q)}{(p_1 - k)^2 (p_2 + k)^2 k^2}, \end{aligned} \quad (2.4.6)$$

where the numerator  $N(p_1, p_2, k, q)$  is given by

$$\begin{aligned} N(p_1, p_2, k, q) &= -2q^2 + \frac{8 p_1 \cdot k p_2 \cdot k}{q^2} + (4 + 2\eta)(p_2 \cdot k - p_1 \cdot k) \\ &\quad + \eta k^2 - 4\eta \frac{p_1 \cdot k p_2 \cdot k}{k^2}, \end{aligned} \quad (2.4.7)$$

and where  $\sigma_v(\text{virtual})$  refers to the order  $\alpha_s$  virtual contribution arising from

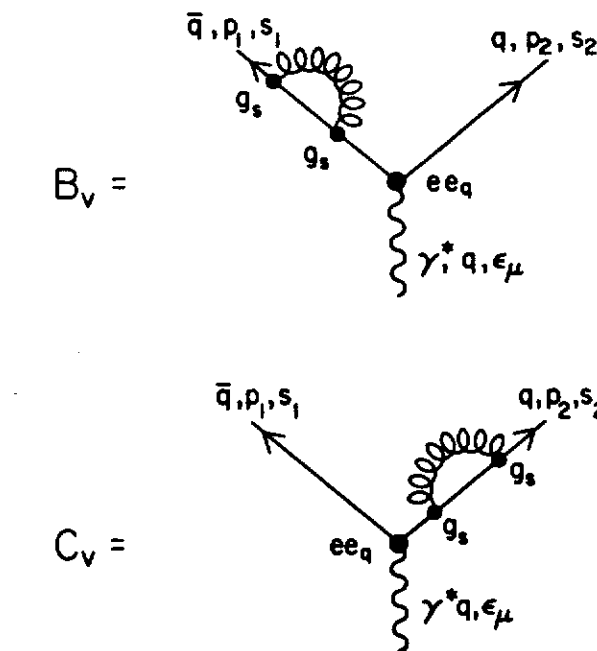


Figure 2.7 Virtual gluon corrections to the Born amplitude in Fig. 2.3.

the vertex correction. The color factor  $\text{tr}(T_a T_a) = 4$  has been included. Furthermore,  $\eta$  in (2.4.7) is a gauge parameter and comes from using

$$-\frac{i}{k^2} \left[ g_{\mu\nu} + \eta \frac{k_\mu k_\nu}{k^2} \right] \quad (2.4.8)$$

for the gluon propagator ( $\eta = 0$  is the Feynman gauge,  $\eta = -1$  is the Landau gauge, see Appendix C).

To evaluate  $\sigma_v(\text{virtual})$  we make use of the Feynman parameterizations given in Appendix C. In particular we use

$$\frac{1}{ab} = \int_0^1 dy \frac{1}{[ay + b(1-y)]^2}, \quad (2.4.9)$$

and set

$$a = (p_1 - k)^2 = k^2 - 2p_1 \cdot k, \quad (2.4.10)$$

$$b = (p_2 + k)^2 = k^2 + 2p_2 \cdot k, \quad (2.4.11)$$

so that

$$ay + b(1-y) = k^2 - 2k \cdot p_y, \quad (2.4.12)$$

with

$$p_y = yp_1 - (1-y)p_2. \quad (2.4.13)$$

This yields

$$\sigma_v(\text{virtual}) = \frac{4}{3}\sigma_0 2g_s^2(-i) \int \frac{d^4k}{(2\pi)^4} \int_0^1 dy \frac{N(p_1, p_2, k, q)}{(k^2 - 2p_y \cdot k)^2 k^2}. \quad (2.4.14)$$

The integration over  $k$  involves a  $1/k^2$  and a  $1/k^4$  piece. Namely,

$$\frac{1}{k^2} N(p_1, p_2, k, q) = \frac{q^2}{k^2} N_1(p_1, p_2, k, q) + \frac{q^2}{k^4} N_2(p_1, p_2, k, q), \quad (2.4.15)$$

with

$$N_1(p_1, p_2, k, q) = -2 + \frac{8 p_1 \cdot k p_2 \cdot k}{q^4} + (4 + 2\eta) \frac{p_2 \cdot k - p_1 \cdot k}{q^2} + \eta \frac{k^2}{q^2}, \quad (2.4.16)$$

and

$$N_2(p_1, p_2, k, q) = -4\eta \frac{p_1 \cdot k p_2 \cdot k}{q^2}. \quad (2.4.17)$$

We now use

$$\frac{1}{c^2 d} = \int_0^1 dx \frac{2x}{[cx + d(1-x)]^3}, \quad (2.4.18)$$

and

$$\frac{1}{c^2 d^2} = \int_0^1 dx \frac{6x(1-x)}{[cx + d(1-x)]^4}, \quad (2.4.19)$$

with

$$c = k^2 - 2p_y \cdot k, \quad (2.4.20)$$

$$d = k^2, \quad (2.4.21)$$

so that

$$\begin{aligned} cx + d(1-x) &= k^2 - 2xp_y \cdot k = (k - xp_y)^2 - x^2 p_y^2 \\ &= K^2 - C, \end{aligned} \quad (2.4.22)$$

where

$$K = k - xp_y, \quad (2.4.23)$$

and

$$C = x^2 p_y^2. \quad (2.4.24)$$

Shifting from an integral over  $k$  to one over  $K$  using  $k = K + xp_y$  yields

$$\sigma_v(\text{virtual}) = \frac{4}{3}\sigma_0 2g_s^2(-i) \int \frac{d^4K}{(2\pi)^4} \int_0^1 dy \int_0^1 dx$$

$$\left\{ \frac{2xq^2 N_1(k \rightarrow K + xp_y)}{[K^2 - C]^3} + \frac{6x(1-x)q^2 N_2(k \rightarrow K + xp_y)}{[K^2 - C]^4} \right\}. \quad (2.4.25)$$

The shifted numerator  $N_1$  is evaluated using the fact that

$$\frac{p_1 \cdot k p_2 \cdot k}{q^4} \rightarrow \frac{1}{8} \frac{K^2}{q^2} - \frac{1}{4} x^2 y(1-y), \quad (2.4.26)$$

$$\frac{p_2 \cdot k - p_1 \cdot k}{q^2} \rightarrow \frac{1}{2} x, \quad (2.4.27)$$

$$\frac{k^2}{q^2} \rightarrow \frac{K^2}{q^2} - x^2 y(1-y), \quad (2.4.28)$$

where terms odd in  $K$  are dropped since they contribute nothing to the integral over  $K$ . Symmetric integration requires an average over the directions of  $K_\mu$ , which is equivalent to the substitution

$$K_\mu K_\nu \rightarrow \frac{1}{4} K^2 g_{\mu\nu}. \quad (2.4.29)$$

In addition,

$$p_y^2 = -y(1-y)q^2, \quad (2.4.30)$$

and

$$C = -y(1-y)x^2 q^2, \quad (2.4.31)$$

so that the shifted numerators become

$$N_1(k \rightarrow K + xp_y) \rightarrow -2 - (2+\eta)x^2 y(1-y) + (2+\eta)x + (1+\eta) \frac{K^2}{q^2}, \quad (2.4.32)$$

and

$$N_2(k \rightarrow K + xp_y) \rightarrow -\eta \left( \frac{1}{2} K^2 - x^2 y(1-y)q^2 \right), \quad (2.4.33)$$

where I have rearranged several of the terms in  $N_1$ .

The integral over the momentum  $K$  is performed using (C.2.5),

$$\int \frac{d^4K}{(2\pi)^4} \frac{(K^2)^R}{[K^2 - C]^M} = \frac{i(-1)^{R+M}}{16\pi^2} C^{R-M+2} \frac{\Gamma(R+2)\Gamma(M-R-2)}{\Gamma(M)}, \quad (2.4.34)$$

yielding

$$\begin{aligned} \sigma_v(\text{virtual}) &= \frac{2\alpha_s}{3\pi} \sigma_0 \left\{ -\frac{1}{2}(2+\eta) + \int_0^1 dx \int_0^1 dy \frac{(-2 + (2+\eta)x)}{y(1-y)x} \right\} \\ &\quad + \frac{4}{3}\sigma_0 2g_s^2(-i) \int_0^1 dy \int_0^1 dx \int \frac{d^4K}{(2\pi)^4} \frac{2x(1+\eta)K^2}{[K^2 - C]^3}. \end{aligned} \quad (2.4.35)$$

The second term comes from last term of  $N_1$  in (2.4.32) and is ultraviolet divergent like  $\log(K)$  as  $K \rightarrow \infty$ . In the Landau gauge (*i.e.*,  $\eta = -1$ ) this term is absent but one is still left with the infrared divergences that occur in the  $x$  and  $y$  interactions of the first term.

This vertex correction is not only infinite, it is gauge dependent. To get

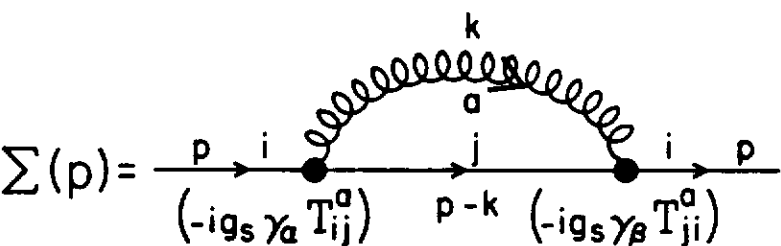


Figure 2.8 Leading order contribution to the quark self-energy.

a gauge independent result one must add the other order  $\alpha_s$  corrections in (2.4.1). The self-energy correction shown in Fig. 2.8 is given by

$$\Sigma(p) = (-g_s^2) \int \frac{d^4 k}{(2\pi)^4} \gamma_\alpha \frac{\not{p} - \not{k}}{(p - k)^2} \gamma_\beta \left( \frac{g_{\alpha\beta}}{k^2} + \eta \frac{k_\alpha k_\beta}{k^4} \right), \quad (2.4.36)$$

where again I have used the gluon propagator in (2.4.8), but I have not yet included the color factor. It will turn out that  $\Sigma(p)$  is proportional to  $\not{p}$  so that one can write

$$\Sigma(p) = -i\not{p}\bar{\Sigma}. \quad (2.4.37)$$

The contribution to the total  $\gamma^* \rightarrow q\bar{q}$  rate from the virtual self-energy amplitudes in Fig. 2.7 is then

$$\begin{aligned} \sigma_v(\text{virtual}) &= \int \frac{d^4 k}{(2\pi)^4} \frac{1}{2} (2A_0 B_v^* + 2A_0 C_v^*) \\ &= \frac{4}{3} \sigma_0 \frac{1}{2} \{2\bar{\Sigma} + 2\bar{\Sigma}\} = \frac{4}{3} \sigma_0 2\bar{\Sigma}, \end{aligned} \quad (2.4.38)$$

where the factor of 4 arises from the sum over color states. The factor of  $1/2$  comes from the usual convention of putting one-half of this correction into self-energy and one-half in the wave function renormalization. To evaluate  $\Sigma(p)$  in (2.4.36) we use both

$$\frac{1}{ab} = \int dx \frac{1}{[ax + b(1-x)]^2}, \quad (2.4.39)$$

and

$$\frac{1}{ab^2} = \int dx \frac{2(1-x)}{[ax + b(1-x)]^3}, \quad (2.4.40)$$

from (C.2.3) with

$$a = (p - k)^2 = k^2 - 2p \cdot k + p^2, \quad (2.4.41)$$

$$b = k^2, \quad (2.4.42)$$

$$ax + b(1-x) = K^2 - C, \quad (2.4.43)$$

with

$$K = k - xp, \quad (2.4.44)$$

and

$$C = -p^2 x(1-x). \quad (2.4.45)$$

The factors in (2.4.36) become

$$\gamma_\alpha (\not{p} - \not{k}) \gamma_\alpha = -2(\not{p} - \not{k}) \rightarrow -2\not{p}(1-x), \quad (2.4.46)$$

$$\begin{aligned} \frac{\not{k}(\not{p} - \not{k})\not{k}}{k^4} &= -\frac{1}{k^2}(\not{p} + \not{k}) + \frac{1}{k^4} 2p \cdot k \not{k} \\ &\rightarrow -\frac{1}{k^2} \not{p} (1+x) + \frac{2\not{p}}{k^4} \left( \frac{1}{4} K^2 + x^2 p^2 \right). \end{aligned} \quad (2.4.47)$$

After shifting  $k$  to  $K + xp$  and dropping terms odd in  $K$  we have

$$\begin{aligned} \bar{\Sigma} &= (-ig_s^2) \left\{ \int_0^1 dx \int \frac{d^4 K}{(2\pi)^4} \frac{[-2(1-x) - \eta(1+x)]}{[K^2 - C]^2} \right. \\ &\quad \left. + \int_0^1 dx \int \frac{d^4 K}{(2\pi)^4} \frac{\eta(1-x)[K^2 + 4x^2 p^2]}{[K^2 - C]^3} \right\}. \end{aligned} \quad (2.4.48)$$

As was the case with the vertex corrections  $\sigma_v(\text{virtual})$ , the self-energy corrections are gauge dependent and in general, contain both infrared and ultraviolet divergences.

At this point we cannot proceed without a procedure for regularizing the ultraviolet divergences in  $\sigma_v(\text{virtual})$  and  $\sigma_s(\text{virtual})$ . If we handle these divergences correctly we will find that these ultraviolet divergences cancel and that the sum

$$\sigma(\text{virtual}) = \sigma_v(\text{virtual}) + \sigma_s(\text{virtual}), \quad (2.4.49)$$

is gauge invariant and contains only infrared divergences. If we then regularize these infrared divergences together with the infrared divergences in  $\sigma(\text{real})$  we will find that the sum  $\sigma(\text{real}) + \sigma(\text{virtual})$  is finite and contains no divergences of any kind.

## 2.5 Real Gluon Emission – MG Scheme

We will consider two regularization schemes in this book, the “massive gluon scheme”<sup>3,4</sup> and dimensional regularization<sup>5,6</sup>. In the “massive gluon scheme” (MG) one regularizes the real and virtual corrections by giving the gluon a fictitious mass,  $m_g$ . This scheme breaks gauge invariance and is applicable only if the triple-gluon vertex does not play a role in the process. For the

process being considered the triple-gluon vertex is not present so this method is acceptable.

For the case of a massive gluon, the differential cross section in (2.3.32) becomes

$$\frac{d\sigma}{dx_1 dx_2} = \frac{2\alpha_s}{3\pi} \sigma_0 \frac{1}{(1-x_1)(1-x_2)} \left\{ x_1^2 + x_2^2 + \beta \left[ 2(x_1 + x_2) - \frac{(1-x_1)^2 + (1-x_2)^2}{(1-x_1)(1-x_2)} \right] + 2\beta^2 \right\}, \quad (2.5.1)$$

where  $\beta = m_g^2/Q^2$ . In addition, the region of integration is now given by

$$\begin{aligned} 0 &\leq x_1 \leq 1-\beta, \\ 1-\beta-x_1 &\leq x_2 \leq \frac{1-x_1-\beta}{1-x_1}, \end{aligned} \quad (2.5.2)$$

as shown in Fig. 2.5b. Integrating over  $x_2$  results in

$$\begin{aligned} \frac{d\sigma}{dx_1} = \frac{2\alpha_s}{3\pi} \sigma_0 & \left\{ \frac{1+x_1^2}{1-x_1} \log\left(\frac{x_1(1-x_1)}{\beta}\right) - \frac{3}{2} \frac{1}{1-x_1} \right. \\ & \left. + \frac{1}{2}x_1 + \frac{1}{2} + \frac{\beta(2-x_1)}{(1-x_1)^2} + \frac{1}{2} \frac{\beta^2}{(1-x_1)^3} \right\}, \end{aligned} \quad (2.5.3)$$

where I have dropped some terms that vanish in the limit  $\beta \rightarrow 0$ . The first term in (2.5.3) comes from

$$\int_{x_2^{\min}}^{x_2^{\max}} \frac{1}{1-x_2} dx_2 = \log\left(\frac{(x_1+\beta)(1-x_1)}{\beta}\right) \rightarrow \log\left(\frac{x_1(1-x_1)}{\beta}\right). \quad (2.5.4)$$

Care must be taken in not dropping the  $\beta$  and  $\beta^2$  terms in (2.5.3) for these terms give finite contributions when integrating over  $x_1$ . For example,

$$\int_0^{1-\beta} \frac{\beta}{(1-x_1)^2} dx_1 = 1, \quad \int_0^{1-\beta} \frac{\beta^2}{(1-x_1)^3} dx_1 = \frac{1}{2}. \quad (2.5.5)$$

We can replace the  $\beta$  and  $\beta^2$  terms by a  $\delta$ -function and arrive at

$$\begin{aligned} \frac{d\sigma}{dx_1} = \frac{2\alpha_s}{3\pi} \sigma_0 & \left\{ \frac{1+x_1^2}{1-x_1} \log\left(\frac{x_1(1-x_1)}{\beta}\right) - \frac{3}{2} \frac{1}{1-x_1} \right. \\ & \left. + \frac{1}{2}x_1 + \frac{1}{2} + \frac{5}{4}\delta(1-x_1) \right\}. \end{aligned} \quad (2.5.6)$$

Integrating over  $x_1$  using

$$\int_0^{1-\beta} \frac{1}{1-x_1} dx_1 = -\log(\beta), \quad (2.5.7)$$

$$\int_0^{1-\beta} \frac{1}{1-x_1} \log(1-x_1) dx_1 = -\frac{1}{2} \log^2(\beta), \quad (2.5.8)$$

$$\int_0^{1-\beta} \frac{1+x_1^2}{1-x_1} \log(x_1) dx_1 = -\frac{\pi^2}{3} + \frac{5}{4}, \quad (2.5.9)$$

$$\int_0^{1-\beta} \frac{1+x_1^2}{1-x_1} \log(1-x_1) dx_1 = -\log^2(\beta) + \frac{7}{4}, \quad (2.5.10)$$

yields

$$\sigma_{MG}(\text{real}) = \frac{2\alpha_s}{3\pi} \sigma_0 \left\{ \log^2(\beta) + 3\log(\beta) - \frac{\pi^2}{3} + 5 \right\}, \quad (2.5.11)$$

which, as expected from (2.3.50), contains a  $\log^2(\beta)$  and a  $\log(\beta)$  divergence as  $\beta \rightarrow 0$ .

## 2.6 Virtual Gluon Corrections – MG Scheme

The ultraviolet divergences in  $\sigma_v(\text{virtual})$  and  $\sigma_s(\text{virtual})$  in (2.4.35) and (2.4.48) can be regularized by multiplying the gluon propagator by a convergence factor

$$\frac{1}{k^2} \rightarrow \frac{1}{k^2} C(k), \quad (2.6.1)$$

where

$$C(k) = \frac{L}{L-k^2}, \quad (2.6.2)$$

and where  $L$  is large. For small  $k$ ,  $C(k)$  is approximately equal to one, but at large  $k$  it behaves like  $1/k^2$  causing the integrals to converge.

In the massive gluon scheme the infrared divergences are handled by replacing  $1/k^2$  by  $1/(k^2 - m_g^2)$  in the gluon propagator. Both the infrared and ultraviolet divergences can be treated simultaneously by the replacement

$$\frac{1}{k^2} \rightarrow - \int_{m_g^2}^L \frac{d\ell}{(k^2 - \ell)^2}, \quad (2.6.3)$$

for the gluon propagator. With this replacement the self-energy correction in (2.4.48) becomes

$$\bar{\Sigma}(p) = (ig_s^2) \int_{m_g^2}^L d\ell \int_0^1 dx \int \frac{d^4 K}{(2\pi)^4} \frac{2(1-x)[-2(1-x)]}{[K^2 - C]^3}, \quad (2.6.4)$$

where  $C$  in (2.4.45) is now given by

$$C = -p^2 x(1-x) + \ell(1-x), \quad (2.6.5)$$

and where for simplicity I have set  $\eta = 0$  (Feynman gauge). Integrating over

$\ell$  and  $K$  gives

$$\begin{aligned}\bar{\Sigma}_{MG}(p) &= (-g_s^2) \frac{1}{16\pi^2} \int_0^1 dx \ 2(1-x) \log\left(\frac{-p^2x + L}{-p^2x + m_g^2}\right) \\ &= (-g_s^2) \frac{1}{16\pi^2} \log(L/m_g^2),\end{aligned}\quad (2.6.6)$$

where terms that vanish in the limit  $m_g^2/L \rightarrow 0$  have been dropped. From (2.4.38) we arrive at

$$\sigma_s(\text{virtual}) = -\frac{2\alpha_s}{3\pi} \sigma_0 \log(L/m_g^2), \quad (2.6.7)$$

for the Feynman gauge. Similarly, the replacement (2.6.3) and setting  $\eta = 0$  gives

$$\begin{aligned}\sigma_v(\text{virtual}) &= \frac{4}{3} \sigma_0 2g_s^2 (-i) \int_{m_g^2}^L d\ell \int \frac{d^4 K}{(2\pi)^4} \int_0^1 dy \int_0^1 dx \\ &\frac{6x(1-x)q^2 [2 + 2x^2y(1-y) - 2x - K^2/q^2]}{[K^2 - C]^4},\end{aligned}\quad (2.6.8)$$

instead of (2.4.25), where  $C$  has changed from (2.4.31) to

$$C = -y(1-y)x^2q^2 + \ell(1-x). \quad (2.6.9)$$

Integrating over  $K$  yields

$$\begin{aligned}\sigma_v(\text{virtual}) &= \frac{2\alpha_s}{3\pi} \sigma_0 \int_{m_g^2}^L d\ell \int_0^1 dy \int_0^1 dx \\ &\left\{ \frac{x(1-x)q^2 [2 + 2x^2y(1-y) - 2x]}{[-y(1-y)x^2q^2 + \ell(1-x)]^2} + \frac{2x(1-x)}{[-y(1-y)x^2q^2 + \ell(1-x)]} \right\},\end{aligned}\quad (2.6.10)$$

and integrating over  $\ell$  gives

$$\begin{aligned}\sigma_v(\text{virtual}) &= \frac{2\alpha_s}{3\pi} \sigma_0 \int_0^1 dy \int_0^1 dx \\ &\left\{ \frac{xq^2 [2 + 2x^2y(1-y) - 2x]}{[-y(1-y)x^2q^2 + m_g^2(1-x)]} - \frac{xq^2 [2 + 2x^2y(1-y) - 2x]}{[-y(1-y)x^2q^2 + L(1-x)]} \right. \\ &\left. + 2x \log\left(\frac{-y(1-y)x^2q^2 + L(1-x)}{-y(1-y)x^2q^2 + m_g^2(1-x)}\right) \right\}.\end{aligned}\quad (2.6.11)$$

With  $q^2 > 0$  the denominators in (2.6.11) can vanish over the range of the  $x$  and  $y$  integrations. We can avoid this difficulty by requiring that  $q^2$  be spacelike

$$\bar{Q}^2 = -q^2 > 0, \quad (2.6.12)$$

and after we have performed the integrals we can analytically continue to the

$q^2 > 0$  (timelike) region. The integrals are tedious but straightforward. The result is

$$\sigma_v(\text{virtual}) = \frac{2\alpha_s}{3\pi} \sigma_0 \left\{ -\log^2(\bar{\beta}) - 3\log(\bar{\beta}) - \frac{7}{2} - \frac{2\pi^2}{3} + \log(L/m_g^2) \right\}, \quad (2.6.13)$$

where

$$\bar{\beta} = m_g^2/\bar{Q}^2, \quad (2.6.14)$$

with  $\bar{Q}$  given by (2.6.12). Combining this with  $\sigma_s(\text{virtual})$  in (2.6.7) gives

$$\begin{aligned}\sigma_{MG}(\text{virtual}) &= \sigma_v(\text{virtual}) + \sigma_s(\text{virtual}) \\ &= \frac{2\alpha_s}{3\pi} \sigma_0 \left\{ -\log^2(\bar{\beta}) - 3\log(\bar{\beta}) - \frac{7}{2} - \frac{2\pi^2}{3} \right\},\end{aligned}\quad (2.6.15)$$

which contains only infrared divergences. The dependence on the ultraviolet cutoff  $L$  has dropped out.

## 2.7 Order $\alpha_s$ Correction – MG Scheme

In the massive gluon scheme the order  $\alpha_s$  virtual corrections are given by (2.6.15). Namely,

$$\sigma_{MG}(\text{virtual}) = \frac{2\alpha_s}{3\pi} \sigma_0 \left\{ -\log^2(\bar{\beta}) - 3\log(\bar{\beta}) - \frac{7}{2} - \frac{2\pi^2}{3} \right\}_{\text{spacelike}}, \quad (2.7.1)$$

with  $\bar{\beta}$  given in (2.6.14) and  $\bar{Q}^2 = -q^2 > 0$  (*i.e.*,  $q^2$  is spacelike). For  $q^2$  timelike we analytically continue using

$$\log(-q^2) = \log(q^2) - i\pi, \quad (2.7.2)$$

$$\log^2(-q^2) = \log(q^2) - 2i\pi \log(q^2) - \pi^2, \quad (2.7.3)$$

and arrive at

$$\sigma_{MG}(\text{virtual}) = \frac{2\alpha_s}{3\pi} \sigma_0 \left\{ -\log^2(\beta) - 3\log(\beta) - \frac{7}{2} - \frac{2\pi^2}{3} + \pi^2 \right\}_{\text{timelike}}, \quad (2.7.4)$$

with

$$\beta = m_g^2/Q^2 \quad (2.7.5)$$

and  $Q^2 = q^2 > 0$  (*i.e.*,  $q^2$  timelike). Furthermore, because of (2.4.1) I need only keep the real part. The  $\pi^2$  in (2.7.4) comes from the analytic continuation from the spacelike to the timelike region of  $q^2$ . Combining this with the result in (2.5.11) for the real gluon corrections, we arrive at

$$\sigma_{MG}(\text{real}) + \sigma_{MG}(\text{virtual}) = \frac{2\alpha_s}{3\pi} \sigma_0 \left\{ -\frac{\pi^2}{3} + 5 - \frac{7}{2} - \frac{2\pi^2}{3} + \pi^2 \right\}$$

$$= \frac{2\alpha_s}{3\pi} \sigma_0 \left( \frac{3}{2} \right) = \frac{\alpha_s}{\pi} \sigma_0. \quad (2.7.6)$$

Both the  $\log^2(\beta)$  and  $\log(\beta)$  terms cancel out in the sum leaving a finite result in the limit  $m_g \rightarrow 0$ . Thus, the total rate for a virtual photon to decay into partons has the following perturbation series

$$\sigma_{\text{tot}}^{e^+e^-} = \sigma_0 \left( 1 + \frac{\alpha_s}{\pi} + \dots \right). \quad (2.7.7)$$

As discussed in the Chapter 1, higher order ultraviolet divergences can be absorbed into the definition of the coupling constant giving

$$\sigma_{\text{tot}}^{e^+e^-} = \sigma_0 \left( 1 + \frac{1}{\pi} \alpha_s(Q^2) + \dots \right), \quad (2.7.8)$$

where  $\alpha_s(Q^2) = 4\pi/(\beta_0 \log(Q^2/\Lambda^2))$  is the familiar running coupling constant in (1.2.18) and  $\Lambda$  is the QCD perturbative parameter that sets the scale.

## 2.8 Real Gluon Emission – DR Scheme

An elegant way to simultaneously regularize *both* infrared and ultraviolet divergences is to use dimensional regularization. Calculations are performed in  $N$  rather than four spacetime dimensions and in the end *after* adding together the real and virtual corrections one sets  $N = 4$ . Before proceeding with the three-body decay  $\gamma^* \rightarrow q\bar{q}g$  in  $N$  spacetime dimensions, we must recalculate the Born term  $\gamma^* \rightarrow q\bar{q}$  in (2.1.30) in  $N$  dimensions. The two-body differential decay rate in  $N$  dimensions is

$$dW = \frac{1}{2E_{cm}} |\mathcal{M}|^2 d^{2N-2}R_2, \quad (2.8.1)$$

where the two-body phase-space factor

$$d^{2N-2}R_2 = \frac{d^{N-1}p_1}{(2\pi)^{N-1}(2E_1)} \frac{d^{N-1}p_2}{(2\pi)^{N-1}(2E_2)} (2\pi)^N \delta^N(q - p_1 - p_2), \quad (2.8.2)$$

replaces (2.1.18). As in (2.1.19) integrating over  $p_2$  yields

$$\int d^{N-1}p_2 \delta^N(q - p_1 - p_2) = \delta(Q - E_1 - E_2), \quad (2.8.3)$$

however,

$$\begin{aligned} \frac{d^{N-1}p_1}{2E_1} &= \frac{1}{2} E_1^{N-3} \sin^{N-3} \theta_1 \sin^{N-4} \theta_2 \dots \\ &\dots \sin \theta_{N-3} d\theta_1 d\theta_2 \dots d\theta_{N-2} dE_1, \end{aligned} \quad (2.8.4)$$

replaces (2.1.20). Here the angles  $\theta_1, \dots, \theta_{N-2}$  are angles with respect to the axes in  $N-1$  dimensions. If  $N = 4$  (2.8.4) reduces to (2.1.20) with  $\theta_2$  in (2.8.4)

being the phi angle,  $\phi_1$ . The matrix element in (2.8.1) does not depend on these angles and they can be integrated out by repeated use of the formula

$$\int_0^\pi \sin^n \theta d\theta = \sqrt{\pi} \frac{\Gamma(\frac{n}{2} + \frac{1}{2})}{\Gamma(\frac{n}{2} + 1)}, \quad (2.8.5)$$

where the properties of the  $\Gamma$  function are reviewed in Appendix E. We arrive at

$$\int \frac{d^{N-1}p_1}{2E_1} = 2^{N-3} \pi^{(N-2)/2} \frac{\Gamma(\frac{N}{2} - 1)}{\Gamma(N-2)} E_1^{N-3} dE_1, \quad (2.8.6)$$

which replaces (2.1.21). The final integration over  $E_1$  is again accomplished using (2.1.22) which gives (for massless partons)

$$\int \frac{E_1^{N-3} dE_1}{2E_2} \delta(Q - E_1 - E_2) = \frac{E_1^{N-3}}{2Q} = \frac{Q^{N-4}}{2^{N-2}}. \quad (2.8.7)$$

Combining (2.8.2), (2.8.6) and (2.8.7) yields

$$R_2 = \int d^{2N-2}R_2 = \frac{1}{2^{N-1} \pi^{N/2-1}} \frac{\Gamma(\frac{N}{2} - 1)}{\Gamma(N-2)} Q^{N-4}, \quad (2.8.8)$$

which reduces to (2.1.24) when  $N = 4$ .

In  $N$  dimensions the matrix element squared for a virtual photon to decay into a quark-antiquark pair is given by

$$|\mathcal{M}(\gamma^* \rightarrow q\bar{q})|^2 = (3) 2(N-2) e_q^2 e_N^2 Q^2, \quad (2.8.9)$$

where I have used the  $N$  dimensional Dirac algebra from Appendix B and the factor of 3 comes from summing over color. In  $N \neq 4$  spacetime dimensions the gauge coupling,  $e_N$ , carries dimensions. It is useful to define a dimensionless coupling,  $e$ , and a mass,  $m_D$ , as follows

$$e_N = \frac{e}{(m_D)^{N/2-2}}, \quad (2.8.10)$$

and

$$\alpha_N^{\text{QED}} = e_N^2 / 4\pi = \frac{\alpha}{(m_D^2)^{N/2-2}}, \quad (2.8.11)$$

with

$$\alpha = e^2 / 4\pi, \quad (2.8.12)$$

being dimensionless. The “dimensional regularization mass”,  $m_D$ , plays an analogous role to the gluon mass,  $m_g$ , in the massive gluon regularization scheme. Combining (2.8.9) and (2.8.10) with (2.8.8) gives

$$\sigma(\gamma^* \rightarrow q\bar{q}) \equiv \sigma_0 = 3\alpha e_q^2 Q \frac{\Gamma(\frac{N}{2})}{\Gamma(N-2)} \left( \frac{Q^2}{4\pi m_D^2} \right)^{N/2-2} \quad (2.8.13)$$

or

$$\sigma_0 = 3\alpha e_q^2 Q \frac{\Gamma(2 + \frac{\epsilon}{2})}{\Gamma(2 + \epsilon)} \left( \frac{Q^2}{4\pi m_D^2} \right)^{\epsilon/2}, \quad (2.8.14)$$

where

$$N = 4 + \epsilon. \quad (2.8.15)$$

Of course, (2.8.14) reduces to (2.1.30) when  $\epsilon = 0$ .

To evaluate the three-body decay of a virtual photon into a quark, antiquark, and a gluon we proceed in an analogous manner. The three-body differential decay rate in  $N$  dimensions is

$$dW = \frac{1}{2E_{cm}} |\bar{\mathcal{M}}|^2 d^{3N-3}R_3, \quad (2.8.16)$$

where

$$\begin{aligned} d^{3N-3}R_3 = & \frac{d^{N-1}p_1}{(2\pi)^{N-1}(2E_1)} \frac{d^{N-1}p_2}{(2\pi)^{N-1}(2E_2)} \\ & \frac{d^{N-1}p_3}{(2\pi)^{N-1}(2E_3)} (2\pi)^N \delta^N(q - p_1 - p_2 - p_3). \end{aligned} \quad (2.8.17)$$

As in (2.3.14) integrating over  $p_3$  gives

$$\int d^{N-1}p_3 \delta^N(q - p_1 - p_2 - p_3) = \delta(Q - E_1 - E_2 - E_3). \quad (2.8.18)$$

To integrate over the directions of  $p_1$  and  $p_2$  one makes use of (2.8.4) and (2.8.6) which results in

$$\int \int \frac{d^{N-1}p_1}{2E_1} \frac{d^{N-1}p_2}{2E_2} = \frac{2^{N-3} \pi^{N-2}}{\Gamma(N-2)} E_1^{N-3} dE_1 E_2^{N-3} dE_2 \int_{-1}^1 dz (1-z^2)^{N/2-2}, \quad (2.8.19)$$

where as in (2.3.17) I have chosen the axis to be in the direction of particle 1 with  $z = \cos \theta_{12}$ , where  $\theta_{12}$  is the relative angle between particle 1 and particle 2, and all decay particles have been taken to be massless. Changing to the  $x_i$  variables in (2.3.9) and using (2.3.18) gives

$$\int_{-1}^1 dz (1-z^2)^{N/2-2} \frac{\delta(Q - E_1 - E_2 - E_3)}{2E_3} = \frac{2(1-z^2)^{N/2-2}}{x_1 x_2 Q^2}, \quad (2.8.20)$$

so that

$$d^2R_3 = \frac{Q^2}{16(2\pi)^3} \left(\frac{Q^2}{4\pi}\right)^\epsilon \frac{1}{\Gamma(2+\epsilon)} \left(\frac{1-z^2}{4}\right)^{\epsilon/2} x_1^\epsilon dx_1 x_2^\epsilon dx_2, \quad (2.8.21)$$

where

$$z = 1 + 2(1 - x_1 - x_2)/(x_1 x_2). \quad (2.8.22)$$

Equation (2.8.21) reduces to (2.3.20) when  $N = 4$  and as before we cannot integrate  $d^2R_3$  any further without knowing the matrix element since, in general, it will depend on  $x_1$  and  $x_2$ .

In  $N = 4 + \epsilon$  dimensions the matrix element squared for the process

$\gamma_\Sigma^* \rightarrow q\bar{q}g$  is given by

$$|\bar{\mathcal{M}}|_\Sigma^2 = 32 e_N^2 e_q^2 g_N^2 F(x_1, x_2), \quad (2.8.23)$$

where

$$\begin{aligned} F(x_1, x_2) = & \left(1 + \frac{\epsilon}{2}\right)^2 \left\{ \frac{x_1^2 + x_2^2}{(1-x_1)(1-x_2)} \right\} \\ & + \epsilon \left(1 + \frac{\epsilon}{2}\right) \left\{ \frac{2 - 2x_1 - 2x_2 + x_1 x_2}{(1-x_1)(1-x_2)} \right\}. \end{aligned} \quad (2.8.24)$$

In analogy with the QED case in (2.8.10) we define a dimensionless strong coupling,  $g_s$ , in terms of the  $N$  dimensional coupling,  $g_N$ , and the mass,  $m_D$ , as follows

$$g_N = \frac{g_s}{m_D^{\epsilon/2}}, \quad (2.8.25)$$

or

$$\alpha_N^{\text{QCD}} \equiv \frac{g_N^2}{4\pi} = \frac{\alpha_s}{(m_D^2)^{\epsilon/2}}, \quad (2.8.26)$$

where  $\alpha_s = g_s^2/4\pi$  is dimensionless. Combining (2.8.16), (2.8.21), and (2.8.23) gives

$$\frac{d\sigma_\Sigma}{dx_1 dx_2} = \frac{2\alpha_s}{\pi} \alpha e_q^2 Q \left(\frac{Q^2}{4\pi m_D^2}\right)^\epsilon \frac{F(x_1, x_2)}{\Gamma(2+\epsilon)} x_1^\epsilon x_2^\epsilon \left(\frac{1-z^2}{4}\right)^{\epsilon/2}, \quad (2.8.27)$$

where  $\alpha$  and  $\alpha_s$  are dimensionless. Dividing by  $\sigma_0$  in (2.8.14) yields

$$\frac{1}{\sigma_0} \frac{d\sigma_\Sigma}{dx_1 dx_2} = \frac{2\alpha_s}{3\pi} \left(\frac{Q^2}{4\pi m_D^2}\right)^{\epsilon/2} \frac{F(x_1, x_2)}{\Gamma(2+\frac{\epsilon}{2})} x_1^\epsilon x_2^\epsilon \left(\frac{1-z^2}{4}\right)^{\epsilon/2}. \quad (2.8.28)$$

The order  $\alpha_s$  contribution to the total rate is arrived at by integrating over the allowed region of  $x_1$  and  $x_2$ . Namely,

$$\begin{aligned} \sigma_{DR}(\text{real}) = & \frac{2\alpha_s}{3\pi} \sigma_0 \left(\frac{Q^2}{4\pi m_D^2}\right)^{\epsilon/2} \frac{1}{\Gamma(2+\frac{\epsilon}{2})} \\ & \int_0^1 dx_1 x_1^\epsilon \int_{1-x_1}^1 dx_2 x_2^\epsilon \left(\frac{1-z^2}{4}\right)^{\epsilon/2} F(x_1, x_2), \end{aligned} \quad (2.8.29)$$

where  $z$  is defined in (2.8.22) and where "DR" denotes the dimensional regularization scheme and "real" implies the production of a real gluon by in process  $\gamma^* \rightarrow q\bar{q}g$ . The nested integrals in (2.8.29) are painful to evaluate. It is easier to "decouple" the integrals by defining a variable  $v$  such that

$$x_2 = 1 - vx_1, \quad (2.8.30)$$

and to express everything in terms of  $x_1$  and  $v$  since both run from 0 to 1.

Using the fact that

$$\left(\frac{1-z^2}{4}\right)^{\epsilon/2} = v^{\epsilon/2} (1-v)^{\epsilon/2} (1-x_1)^{\epsilon/2} x_2^{-\epsilon}, \quad (2.8.31)$$

and  $dx_1 dx_2 = x_1 dx_1 dv$  we arrive at

$$\begin{aligned} \sigma_{DR}(\text{real}) &= \frac{2\alpha_s}{3\pi} \sigma_0 \left(\frac{Q^2}{4\pi m_D^2}\right)^{\epsilon/2} \frac{1}{\Gamma(2+\frac{\epsilon}{2})} \\ &\int_0^1 dx_1 x_1^\epsilon (1-x_1)^{\epsilon/2} \int_0^1 dv v^{\epsilon/2} (1-v)^{\epsilon/2} x_1 F(x_1, v), \end{aligned} \quad (2.8.32)$$

where (2.8.24) and (2.8.30) imply that

$$\begin{aligned} F(x_1, v) &= \frac{[(v^2 + 1)x_1^2 - 2vx_1 + 1]}{v(1-x_1)} + \frac{[(v^2 - v + 1)x_1^2 - x_1 + 1]}{v(1-x_1)} \epsilon \\ &+ \frac{1}{4} \frac{[(v^2 - 2v + 1)x_1^2 + 2(v-1)x_1 + 1]}{v(1-x_1)} \epsilon^2. \end{aligned} \quad (2.8.33)$$

It is necessary to keep both the  $\epsilon$  and  $\epsilon^2$  term in (2.8.33) since the integrations in (2.8.29) will produce  $1/\epsilon$  and  $1/\epsilon^2$  factors. With the use of (E.1.12),

$$\int_0^1 dx x^{R-1} (1-x)^{M-1} = \frac{\Gamma(R)\Gamma(M)}{\Gamma(R+M)}, \quad (2.8.34)$$

it is straightforward but tedious to insert (2.8.33) into (2.8.32) and perform the integrations. The result is

$$\sigma_{DR}(\text{real}) = \frac{2\alpha_s}{3\pi} \sigma_0 \left(\frac{Q^2}{4\pi m_D^2}\right)^{\epsilon/2} \frac{\Gamma^2(1+\frac{\epsilon}{2})}{\Gamma(1+\frac{3}{2}\epsilon)} \left\{ \frac{8}{\epsilon^2} - \frac{6}{\epsilon} + \frac{19}{2} + \dots \right\}, \quad (2.8.35)$$

where some terms that vanish in the limit  $\epsilon \rightarrow 0$  have been dropped. Equation (2.8.33) can now be expanded in a power series in  $\epsilon$ . To do so one uses

$$\frac{\Gamma^2(1+\frac{\epsilon}{2})}{\Gamma(1+\frac{3}{2}\epsilon)} = 1 + \frac{1}{2}\gamma_E \epsilon + \frac{1}{48}(6\gamma_E^2 - 7\pi^2)\epsilon^2 + \dots, \quad (2.8.36)$$

where  $\gamma_E$  is Euler's constant ( $\gamma_E = 0.5772157$ , see Appendix E) and

$$\begin{aligned} \left(\frac{Q^2}{4\pi m_D^2}\right)^{\epsilon/2} &= \exp\left\{\frac{\epsilon}{2} \log\left(\frac{Q^2}{4\pi m_D^2}\right)\right\} = 1 + \frac{1}{2} \log\left(\frac{Q^2}{4\pi m_D^2}\right) \epsilon \\ &+ \frac{1}{8} \log^2\left(\frac{Q^2}{4\pi m_D^2}\right) \epsilon^2 + \dots. \end{aligned} \quad (2.8.37)$$

Inserting (2.8.36) and (2.8.37) into (2.8.35) and dropping terms that vanish when  $\epsilon \rightarrow 0$  gives

$$\sigma_{DR}(\text{real}) = \frac{2\alpha_s}{3\pi} \sigma_0 \left\{ \frac{8}{\epsilon^2} + \frac{1}{\epsilon} \left[ 4 \log\left(\frac{Q^2}{4\pi m_D^2}\right) + 4\gamma_E - 6 \right] \right\}$$

$$\begin{aligned} &+ \log^2\left(\frac{Q^2}{4\pi m_D^2}\right) + (2\gamma_E - 3) \log\left(\frac{Q^2}{4\pi m_D^2}\right) \\ &+ \gamma_E^2 - \frac{3\gamma_E}{2} - \frac{7\pi^2}{6} + \frac{57}{6} + \dots \} \end{aligned} \quad (2.8.38)$$

In analogy with the massive gluon scheme  $\sigma_{DR}(\text{real})$  contains both a log squared and a log divergence as  $m_D \rightarrow 0$ .

## 2.9 Virtual Gluon Corrections – DR Scheme

In  $N$  spacetime dimensions the self-energy correction in (2.4.48) becomes

$$\begin{aligned} \bar{\Sigma} &= (-g_N^2)i \left\{ \int_0^1 \frac{d^N K}{(2\pi)^N} \frac{[(2-N)(1-x) - \eta(1+x)]}{[K^2 - C]^2} \right. \\ &\left. + \int_0^1 dx \int \frac{d^N K}{(2\pi)^N} \frac{\eta(1-x) [4K^2/N + 4x^2 p^2]}{[K^2 - C]^3} \right\}, \end{aligned} \quad (2.9.1)$$

where  $C$  is given by (2.4.45) and where (2.4.46) and (2.4.47) are replaced by

$$\gamma_\alpha(p - k) \gamma_\alpha \rightarrow (2-N)p(1-x), \quad (2.9.2)$$

$$\frac{k(p-k)k}{k^4} \rightarrow -\frac{1}{k^2} p(1-x) + \frac{2p}{k^4} \left( \frac{K^2}{N} + x^2 p^2 \right), \quad (2.9.3)$$

and, as before, terms odd in  $K = k - xp$  give no contribution and (2.4.29) becomes

$$K_\mu K_\nu \rightarrow \frac{1}{N} K^2 g_{\mu\nu}. \quad (2.9.4)$$

The integration over  $K$  is performed using (C.2.6),

$$\begin{aligned} \int \frac{d^N K}{(2\pi)^N} \frac{(K^2)^R}{[K^2 - C]^M} &= \frac{i(-1)^{R-M}}{(16\pi^2)^{N/4}} \\ &C^{R-M+N/2} \frac{\Gamma(R+\frac{N}{2}) \Gamma(M-R-\frac{N}{2})}{\Gamma(\frac{N}{2}) \Gamma(M)}, \end{aligned} \quad (2.9.5)$$

which replaces (2.4.34). The integrals over  $x$  are done with the aid of (2.8.34) with the result

$$\bar{\Sigma}_{DR} = \frac{g_s^2}{(16\pi^2)^{N/4}} \left( \frac{-p^2}{m_D^2} \right)^{N/2-2} (1 - \frac{N}{2})(1+\eta) \frac{\Gamma(2-\frac{N}{2}) \Gamma^2(\frac{N}{2}-1)}{\Gamma(N-2)}, \quad (2.9.6)$$

or

$$\bar{\Sigma}_{DR} = \frac{g_s^2}{16\pi^2} \left( \frac{-p^2}{4\pi m_D^2} \right)^{\epsilon/2} \frac{\Gamma(1-\frac{\epsilon}{2}) \Gamma^2(1+\frac{\epsilon}{2})}{\Gamma(1+\epsilon)} (1+\eta) \frac{(2+\epsilon)}{\epsilon(1+\epsilon)}, \quad (2.9.7)$$

where  $N = 4 + \epsilon$  and  $g_s$  is the dimensionless coupling in (2.8.25). In the dimensional regularization scheme the self-energy corrections vanish when  $\eta = -1$  (Landau gauge). Therefore when working in this scheme one usually chooses the Landau gauge and ignores self-energy corrections. Namely,

$$\bar{\Sigma}_{DR}(\text{Landau gauge}) = 0. \quad (2.9.8)$$

Furthermore  $\bar{\Sigma}_{DR}$  in (2.9.7) is zero for any value of  $\eta$  provided  $p^2 = 0$  (on the shell) and  $\epsilon > 0$ . This is a subtle point, but one can show that with the dimensional regularization scheme it is consistent to set  $\bar{\Sigma}_{DR} = 0$  for any  $\eta$  and any  $\epsilon$  provided  $p^2 = 0$  (*i.e.*, on shell).

In  $N$  dimensions the vertex correction in (2.4.6) becomes

$$\sigma_v(\text{virtual}) = \frac{4}{3}\sigma_0 2g_N^2(-i) \int \frac{d^N k}{(2\pi)^N} \frac{N(p_1, p_2, k, q)}{(p_1 - k)^2(p_2 + k)^2 k^2}, \quad (2.9.9)$$

with

$$\begin{aligned} N(p_1, p_2, k, q) = & -2q^2 + \frac{8 p_1 \cdot k p_2 \cdot k}{q^2} + (4 + 2\eta)(p_2 \cdot k - p_1 \cdot k) \\ & + \eta k^2 - 4\eta \frac{p_1 \cdot k p_2 \cdot k}{k^2} + (N - 4)k^2. \end{aligned} \quad (2.9.10)$$

Equation (2.4.25) becomes

$$\begin{aligned} \sigma_v(\text{virtual}) = & \frac{4}{3}\sigma_0 2g_N^2(-i) \int \frac{d^N K}{(2\pi)^N} \int_0^1 dy \int_0^1 dx \\ & \left\{ \frac{2xq^2 N_1(k \rightarrow K + xp_y)}{[K^2 - C]^3} + \frac{6x(1-x)q^2 N_2(k \rightarrow K + xp_y)}{[K^2 - C]^4} \right\}, \end{aligned} \quad (2.9.11)$$

with the shifted numerators ( $k \rightarrow K + xp_y$ ) in (2.4.32) and (2.4.33) becoming

$$\begin{aligned} N_1(k \rightarrow K + xp_y) \rightarrow & -2 - (2 + \eta)x^2y(1 - y) + (2 + \eta)x \\ & + (\eta + 1 + \epsilon) \frac{4}{N} \frac{K^2}{q^2}, \end{aligned} \quad (2.9.12)$$

$$N_2(k \rightarrow K + xp_y) \rightarrow -\eta \left( \frac{2}{N} K^2 - x^2 y(1 - y) q^2 \right), \quad (2.9.13)$$

where  $N = 4 + \epsilon$  and  $p_y$  and  $C$  are given by (2.4.30) and (2.4.31), respectively. The integrals over  $K$ ,  $x$ , and  $y$  are performed using (2.9.4), (2.9.5) and (2.8.34) with the result

$$\begin{aligned} \sigma_{DR}(\text{virtual}) = & \frac{2\alpha_s}{3\pi} \sigma_0 \left( \frac{\bar{Q}^2}{4\pi m_D^2} \right)^{\epsilon/2} \frac{\Gamma(1 - \frac{\epsilon}{2}) \Gamma^2(1 + \frac{\epsilon}{2})}{\Gamma(1 + \epsilon)} \\ & \left( -\frac{8}{\epsilon^2} + \frac{6}{\epsilon} - \frac{(8 + 4\epsilon)}{(1 + \epsilon)} \right), \end{aligned} \quad (2.9.14)$$

where  $\sigma_0$  is given by (2.8.14) and where  $m_D$  is the dimensional regularization

mass that arises from (2.8.26) and (as was the case in the massive gluon scheme) I have taken

$$\bar{Q}^2 = -q^2 > 0 \quad (2.9.15)$$

(*i.e.*,  $q^2$  spacelike) in order to avoid singularities within the regions of integration. Expanding in powers of  $\epsilon$  gives

$$\frac{\Gamma(1 - \frac{\epsilon}{2}) \Gamma^2(1 + \frac{\epsilon}{2})}{\Gamma(1 + \epsilon)} = 1 + \frac{1}{2}\gamma_E \epsilon + \frac{1}{48}(6\gamma_E^2 - \pi^2) \epsilon^2 + \dots, \quad (2.9.16)$$

and using (2.8.37) we arrive at

$$\begin{aligned} \sigma_{DR}(\text{virtual}) = & \frac{2\alpha_s}{3\pi} \sigma_0 \left\{ -\frac{8}{\epsilon^2} + \frac{1}{\epsilon} \left[ -4 \log \left( \frac{\bar{Q}^2}{4\pi m_D^2} \right) - 4\gamma_E + 6 \right] \right. \\ & - \log^2 \left( \frac{\bar{Q}^2}{4\pi m_D^2} \right) - (2\gamma_E - 3) \log \left( \frac{\bar{Q}^2}{4\pi m_D^2} \right) \\ & \left. - \gamma_E^2 + 3\gamma_E + \frac{\pi^2}{6} - 8 + \dots \right\}_{\text{spacelike}}, \end{aligned} \quad (2.9.17)$$

which is valid for  $q^2$  spacelike as defined in (2.9.15).

## 2.10 Order $\alpha_s$ Corrections – DR Scheme

In the dimensional regularization scheme the order  $\alpha_s$  virtual corrections are from (2.9.17),

$$\begin{aligned} \sigma_{DR}(\text{virtual}) = & \frac{2\alpha_s}{3\pi} \sigma_0 \left\{ -\frac{8}{\epsilon^2} + \frac{1}{\epsilon} \left[ -4 \log \left( \frac{\bar{Q}^2}{4\pi m_D^2} \right) - 4\gamma_E + 6 \right] \right. \\ & - \log^2 \left( \frac{\bar{Q}^2}{4\pi m_D^2} \right) - (2\gamma_E - 3) \log \left( \frac{\bar{Q}^2}{4\pi m_D^2} \right) \\ & \left. - \gamma_E^2 + 3\gamma_E + \frac{\pi^2}{6} - 8 \right\}_{\text{spacelike}}, \end{aligned} \quad (2.10.1)$$

where  $\bar{Q}^2 = -q^2 > 0$  (*i.e.*,  $q^2$  spacelike). For  $q^2$  timelike we analytically continue using (2.7.2) and (2.7.3) and arrive at

$$\begin{aligned} \sigma_{DR}(\text{virtual}) = & \frac{2\alpha_s}{3\pi} \sigma_0 \left\{ -\frac{8}{\epsilon^2} + \frac{1}{\epsilon} \left[ -4 \log \left( \frac{Q^2}{4\pi m_D^2} \right) - 4\gamma_E + 6 \right] \right. \\ & - \log^2 \left( \frac{Q^2}{4\pi m_D^2} \right) - (2\gamma_E - 3) \log \left( \frac{Q^2}{4\pi m_D^2} \right) \end{aligned}$$

$$-\gamma_E^2 + 3\gamma_E + \frac{\pi^2}{6} - 8 + \pi^2 \Big\}_{\text{timelike}}, \quad (2.10.2)$$

where now  $Q^2 = q^2 > 0$  (i.e.,  $q^2$  timelike) and where I have only kept the terms that are real.

Combining this with the result in (2.8.38) for the real gluon corrections,

$$\begin{aligned} \sigma_{DR}(\text{real}) &= \frac{2\alpha_s}{3\pi} \sigma_0 \left\{ \frac{8}{\epsilon^2} + \frac{1}{\epsilon} \left[ 4 \log \left( \frac{Q^2}{4\pi m_D^2} \right) + 4\gamma_E - 6 \right] \right. \\ &\quad + \log^2 \left( \frac{Q^2}{4\pi m_D^2} \right) + (2\gamma_E - 3) \log \left( \frac{Q^2}{4\pi m_D^2} \right) \\ &\quad \left. + \gamma_E^2 - 3\gamma_E - \frac{7\pi^2}{6} + \frac{57}{6} \right\}, \end{aligned} \quad (2.10.3)$$

gives

$$\begin{aligned} \sigma_{DR}(\text{real}) + \sigma_{DR}(\text{virtual}) &= \frac{2\alpha_s}{3\pi} \sigma_0 \left\{ -\frac{7\pi^2}{6} + \frac{57}{6} + \frac{\pi^2}{6} - 8 + \pi^2 \right\} \\ &= \frac{2\alpha_s}{3\pi} \sigma_0 \left( \frac{3}{2} \right) = \frac{\alpha_s}{\pi} \sigma_0, \end{aligned} \quad (2.10.4)$$

which is finite in the limit  $\epsilon \rightarrow 0$  and is precisely the same as the result obtained in (2.7.6) using the massive gluon scheme.

### Problems

- 2.1. Use  $\gamma_\mu \gamma_\nu + \gamma_\nu \gamma_\mu = 2g_{\mu\nu}$  and the cyclic property of traces to show that

$$\begin{aligned} \text{tr}[\not{a}\not{b}] &= 4a_\mu \\ \text{tr}[\not{a}\not{b}\not{c}\not{d}] &= 4(a_\mu b_\nu + a_\nu b_\mu - a \cdot b g_{\mu\nu}), \end{aligned}$$

where  $a$  and  $b$  are arbitrary 4-vectors.

- 2.2. Calculate the differential cross section,  $d\sigma/d\Omega_{cm}$ , and the total cross section,  $\sigma_{tot}$ , to order  $\alpha^2$  for the electromagnetic process  $e^+e^- \rightarrow \gamma^* \rightarrow \mu^+\mu^-$ . Neglect the masses of the electrons and muons.

- 2.3. Calculate the differential cross section,  $d\sigma/d\Omega_{cm}$ , and the total cross section,  $\sigma_{tot}$ , for the fictitious process  $e^+e^- \rightarrow S_0^* \rightarrow \mu^+\mu^-$ , where  $S_0$  is a massless scalar boson (spin 0). Neglect the masses of the electrons and muons. Compare the answer with the results from problem 2.2.

- 2.4. Integrate the two-body phase-space factor in (2.1.18),

$$d^6R_2 = \frac{d^3p_1}{(2\pi)^3(2E_1)} \frac{d^3p_2}{(2\pi)^3(2E_2)} (2\pi)^4 \delta^4(q - p_1 - p_2),$$

over  $p_1$  and  $p_2$  (assuming massless particles) and show that

$$R_2 = \int d^6R_2 = \frac{1}{8\pi}.$$

- 2.5. Consider the matrix element squared for a process with one real external photon which can be written in the form

$$|\mathcal{M}|^2 = \sum_\lambda L_{\mu\nu} \epsilon_\mu(\lambda) \epsilon_\nu^*(\lambda),$$

where  $\epsilon_\mu(\lambda)$  is the polarization 4-vector of the photon with helicity  $\lambda = \pm 1$ . Show that the replacement

$$\sum_\lambda \epsilon_\mu(\lambda) \epsilon_\nu^*(\lambda) \rightarrow - \left( g_{\mu\nu} + \eta \frac{k_\mu k_\nu}{k^2} \right),$$

where  $k_\mu$  is the photon 4-momentum is equivalent to summing over the physically allowed photon helicity states.

- 2.6. Assuming massless particles, integrate the three-body phase-space factor in (2.3.8),

$$\begin{aligned} d^9R_3 &= \frac{d^3p_1}{(2\pi)^3(2E_1)} \frac{d^3p_2}{(2\pi)^3(2E_2)} \\ &\quad \frac{d^3p_3}{(2\pi)^3(2E_3)} (2\pi)^4 \delta^4(q - p_1 - p_2 - p_3), \end{aligned}$$

over  $p_1$ ,  $p_2$ , and  $p_3$ ,

$$d^2R_3 = \int d^9R_3,$$

and show that

$$\begin{aligned} d^2R_3 &= \frac{1}{(2\pi)^5} \pi^2 dE_1 dE_2 = \frac{1}{(2\pi)^5} \frac{\pi^2}{4E_{cm}^2} ds dt \\ &= \frac{1}{(2\pi)^5} \frac{\pi^2}{4E_{cm}^2} ds du = \frac{1}{(2\pi)^5} \frac{\pi^2}{4E_{cm}^2} dt du, \\ &= \frac{1}{(2\pi)^5} \frac{\pi^2 E_{cm}^2}{4} dx_1 dx_2 = \frac{1}{(2\pi)^5} \frac{\pi^2 Q^2}{4} dx_1 dx_2, \end{aligned}$$

where  $E_{cm} = Q$  and

$$\begin{aligned} s &\equiv (p_1 + p_3)^2 = 2p_1 \cdot p_3 = Q^2(1 - x_2), \\ t &\equiv (p_2 + p_3)^2 = 2p_2 \cdot p_3 = Q^2(1 - x_1), \\ u &\equiv (p_1 + p_2)^2 = 2p_1 \cdot p_2 = Q^2(1 - x_3). \end{aligned}$$

- 2.7. Show that the differential cross section for the process  $\gamma_\Sigma^* \rightarrow q\bar{q}g$  in Fig. 2.4

can be written in the form

$$\frac{1}{\sigma_0} \frac{d\sigma_\Sigma}{dx_1 dx_2} = \frac{2\alpha_s}{3\pi} \frac{x_1^2 + x_2^2}{(1-x_1)(1-x_2)},$$

where  $\sigma_0$  is the Born term in (2.1.30) and  $x_i = 2E_i/Q$ , with  $E_{cm} = Q = E_1 + E_2 + E_3$ .

- 2.8. Suppose that in the “decay” of a virtual photon into a quark, antiquark, and a gluon we are only interested in the case where the gluon-quark and gluon-antiquark invariant mass is larger than the mass of a pion,  $m_\pi$ . Perform the integral

$$\sigma_m(\gamma^* \rightarrow q\bar{q}g) = \int_\beta^{1-\beta} dx_1 \int_{1-x_1}^{1-\beta} dx_2 \left( \frac{d\sigma_\Sigma}{dx_1 dx_2} \right),$$

where  $\beta = m_\pi^2/Q^2$  and where the differential cross is calculated to order  $\alpha_s$ . Keep the exact result and show that it reduces to (2.3.50) in the limit  $\beta \rightarrow 0$ .

- 2.9. Show that the cross section

$$S_{11} + S_{22} + S_{12} = |A_R + B_R|^2,$$

in (2.3.31) is gauge invariant by setting the gluon polarization 4-vector,  $\epsilon'_\nu$ , in Fig. 2.4 equal to  $(p_3)_\nu$  and verifying that the result is zero.

- 2.10. Verify (2.4.7) by showing that

$$\begin{aligned} \text{tr}(\not{p}_2 \gamma_\mu \not{p}_1 \gamma_\alpha \not{p}_a \gamma_\mu \not{p}_b \gamma_\alpha) + \frac{\eta}{k^2} \text{tr}(\not{p}_2 \gamma_\mu \not{p}_1 \not{k} \not{p}_a \gamma_\mu \not{p}_b \not{k}) = \\ -2q^2 + 8 \frac{\not{p}_1 \cdot \not{k} \not{p}_2 \cdot \not{k}}{q^2} + (4+2\eta)(\not{p}_2 \cdot \not{k} - \not{p}_1 \cdot \not{k}) \\ + \eta k^2 - 4\eta \frac{\not{p}_1 \cdot \not{k} \not{p}_2 \cdot \not{k}}{k^2}, \end{aligned}$$

where

$$\begin{aligned} p_a &= p_1 - k, \\ p_b &= p_2 + k, \end{aligned}$$

and

$$q = p_2 + p_b = p_1 + p_2.$$

- 2.11. Verify (2.4.35) and (2.4.48).

- 2.12. Integrate

$$\begin{aligned} \frac{d\sigma}{dx_1 dx_2} = \frac{2\alpha_s}{3\pi} \sigma_0 \frac{1}{(1-x_1)(1-x_2)} \left\{ x_1^2 + x_2^2 \right. \\ \left. + \beta \left[ 2(x_1 + x_2) - \frac{(1-x_1)^2 + (1-x_2)^2}{(1-x_1)(1-x_2)} \right] + 2\beta^2 \right\}, \end{aligned}$$

over the range

$$\begin{aligned} 0 \leq x_1 \leq 1 - \beta, \\ 1 - \beta - x_1 \leq x_2 \leq \frac{1 - x_1 - \beta}{1 - x_1}, \end{aligned}$$

where  $x_i = 2E_i/Q$  and  $\beta = m_g^2/Q^2$  and verify that

$$\begin{aligned} \sigma_{MG}(\text{real}) = \frac{2\alpha_s}{3\pi} \sigma_0 \left\{ (1+\beta)^2 \log^2(\beta) \right. \\ \left. - 2(1+\beta)^2 \log(1+\beta) \log(\beta) + 5 - 5\beta^2 \right. \\ \left. + 2(1+\beta)^2 \left[ \text{Li}_2\left(\frac{\beta}{1+\beta}\right) - \text{Li}_2\left(\frac{1}{1+\beta}\right) \right] \right\}. \end{aligned}$$

Show that this reduces to (2.5.11) in the limit  $\beta \rightarrow 0$ .

- 2.13. Show that in the massive gluon scheme the order  $\alpha_s$  virtual gluon correction to the process  $\gamma^* \rightarrow q\bar{q}$  is given by

$$\sigma_{MG}(\text{virtual}) = \frac{2\alpha_s}{3\pi} \sigma_0 \left\{ -\log^2(\bar{\beta}) - 3\log(\bar{\beta}) - \frac{7}{2} - \frac{2\pi^2}{3} \right\},$$

where  $\bar{\beta} = m_g^2/\bar{Q}^2$  and  $\bar{Q}^2 = -q^2 > 0$  (spacelike).

- 2.14. Integrate the two-body phase-space factor for massless particles in  $N$  spacetime dimensions,

$$d^{2N-2}R_2 = \frac{d^{N-1}p_1}{(2\pi)^{N-1}(2E_1)} \frac{d^{N-1}p_2}{(2\pi)^{N-1}(2E_2)} (2\pi)^N \delta^N(q - p_1 - p_2),$$

over  $p_1$  and  $p_2$  and show that

$$R_2 = \int d^{2N-2}R_2 = \frac{1}{8\pi} \frac{\Gamma(1+\frac{\epsilon}{2})}{\Gamma(1+\epsilon)} \left( \frac{Q^2}{4\pi} \right)^{\epsilon/2},$$

where  $N = 4 + \epsilon$  and  $Q = E_{cm}$ .

- 2.15. Show that the leading order (Born term) decay rate for the process  $\gamma^* \rightarrow q\bar{q}$  for massless particles in  $N$  spacetime dimensions is given by

$$\sigma_0 = 3\alpha e_q^2 Q \frac{\Gamma(2+\frac{\epsilon}{2})}{\Gamma(2+\epsilon)} \left( \frac{Q^2}{4\pi m_D^2} \right)^{\epsilon/2},$$

where  $N = 4 + \epsilon$  and  $\alpha$  is the dimensionless electromagnetic coupling in (2.8.11).

- 2.16. Integrate the three-body phase-space factor for massless particles in  $N$  spacetime dimensions,

$$d^{3N-3}R_3 = \frac{d^{N-1}p_1}{(2\pi)^{N-1}(2E_1)} \frac{d^{N-1}p_2}{(2\pi)^{N-1}(2E_2)} \frac{d^{N-1}p_3}{(2\pi)^{N-1}(2E_3)} (2\pi)^N \delta^N(q - p_1 - p_2 - p_3),$$

over  $p_1$ ,  $p_2$ , and  $p_3$ ,

$$d^2R_3 = \int d^{3N-3}R_3,$$

and show that

$$d^2R_3 = \frac{Q^2}{16(2\pi)^3} \frac{1}{\Gamma(2+\epsilon)} \left(\frac{Q^2}{4\pi}\right)^\epsilon \left(\frac{1-z^2}{4}\right)^{\epsilon/2} x_1^\epsilon dx_1 x_2^\epsilon dx_2,$$

where  $x_i = 2E_i/Q$  and

$$z = 1 - 2(1 - x_1 - x_2)/(x_1 x_2).$$

- 2.17. Using

$$\Gamma(1+\epsilon) = 1 - \gamma_E \epsilon + \frac{1}{2}(\gamma_E^2 + \frac{\pi^2}{6}) \epsilon^2 + \dots,$$

in (E.1.18) show that

$$\frac{\Gamma^2(1+\frac{\epsilon}{2})}{\Gamma(1+\frac{3}{2}\epsilon)} = 1 + \frac{1}{2}\gamma_E \epsilon + \frac{1}{48}(6\gamma_E^2 - 7\pi^2) \epsilon^2 + \dots,$$

and

$$\frac{\Gamma(1-\frac{\epsilon}{2})\Gamma^2(1+\frac{\epsilon}{2})}{\Gamma(1+\epsilon)} = 1 + \frac{1}{2}\gamma_E \epsilon + \frac{1}{48}(6\gamma_E^2 - \pi^2) \epsilon^2 + \dots.$$

- 2.18. Show that in  $N$  spacetime dimensions that the differential cross section for the process  $\gamma_\Sigma^* \rightarrow q\bar{q}g$  is given by

$$\frac{d\sigma_\Sigma}{dx_1 dx_2} = \frac{2\alpha_s}{\pi} \alpha e_q^2 Q \left(\frac{Q^2}{4\pi m_D^2}\right)^\epsilon \frac{F(x_1, x_2)}{\Gamma(2+\epsilon)} x_1^\epsilon x_2^\epsilon \left(\frac{1-z^2}{4}\right)^{\epsilon/2},$$

where  $F(x_1, x_2)$  is given in (2.8.24) and  $z = 1 - 2(1 - x_1 - x_2)/(x_1 x_2)$ . Perform the integral

$$\sigma_{DR}(\text{real}) = \int_0^1 dx_1 \int_{1-x_1}^1 dx_2 \frac{d\sigma_\Sigma}{dx_1 dx_2},$$

and verify that

$$\sigma_{DR}(\text{real}) = \frac{2\alpha_s}{3\pi} \sigma_0 \left(\frac{Q^2}{4\pi m_D^2}\right)^{\epsilon/2} \frac{\Gamma^2(1+\frac{\epsilon}{2})}{\Gamma(1+\frac{3}{2}\epsilon)} \left\{ \frac{8}{\epsilon^2} - \frac{6}{\epsilon} + \frac{19}{2} + \dots \right\}.$$

- 2.19. Show that in  $N$  spacetime dimensions that the order  $\alpha_s$  virtual gluon corrections to the  $\gamma^* \rightarrow q\bar{q}$  decay rate are given by

$$\sigma_{DR}(\text{virtual}) = \frac{2\alpha_s}{3\pi} \sigma_0 \left(\frac{\bar{Q}^2}{4\pi m_D^2}\right)^{\epsilon/2} \frac{\Gamma(1-\frac{\epsilon}{2})\Gamma^2(1+\frac{\epsilon}{2})}{\Gamma(1+\epsilon)} \left(-\frac{8}{\epsilon^2} + \frac{6}{\epsilon} - \frac{(8+4\epsilon)}{(1+\epsilon)}\right),$$

where  $\bar{Q}^2 = -q^2 > 0$  (spacelike).

#### Further Reading

J.D. Bjorken and S.D. Drell, *Relativistic Quantum Mechanics*, McGraw-Hill, New York, 1965.

R.P. Feynman, *Photon-Hadron Interactions*, Benjamin-Cummings Publishing Company, Reading, MA, 1972.

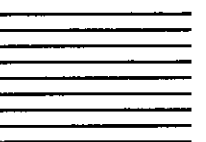
A. H. Mueller, *Physics Reports* 73, 237 (1981).

#### References

1. T. Kinoshita, *J. Math. Phys.* 3, 650 (1962).
2. T. D. Lee and M. Nauenberg, *Phys. Rev.* B133, 1547 (1964).
3. C.L. Basham, L.S. Brown, S.D. Ellis, and S.T. Love, *Phys. Rev.* D17, 2298 (1978). C.L. Basham, L.S. Brown, S.D. Ellis, and S.T. Love, *Phys. Rev. Lett.* 41, 1585 (1978).
4. G.C. Fox and S. Wolfram, *Nucl. Phys.* B149, 413 (1979).
5. G. 't Hooft and M. Veltman, *Nucl. Phys.* B44, 189 (1972).
6. W.J. Marciano, *Phys. Rev.* D12, 3861 (1975).

## CHAPTER 3

# Electron-Positron Annihilations: Fragmentation Functions and Jets



In the previous chapter we studied the total cross section for the annihilation of an electron and a positron into hadrons,  $e^+e^- \rightarrow \text{hadrons}$ . We were not concerned about the details of the final state so long as it was hadronic. However, there are many interesting questions about the configuration of final state hadrons. For example, before data became available some physicists believed that the final hadrons in  $e^+e^-$  annihilations would emerge spherically symmetric. Others argued that the final hadrons would “remember” the direction for the initial quark and antiquark in Fig. 2.1 that initiated the process. They conjectured that the final state would consist of a collection of hadrons called a “jet” moving in the direction of the initial quark and a jet of hadrons moving in the direction of the initial antiquark. We now know that jets exist and are a result of the asymptotic freedom property of QCD. The hadrons in a jet have small transverse momentum relative to their parent quarks direction and the sum of their longitudinal momentum roughly gives the parent quark momentum. The precise definition of a jet is arbitrary and depends on the experiment, but jets are the manifestation of quarks (and gluons) in the real world. Jets are as close as we can get experimentally to “seeing” quarks and gluons. We study jets to learn about the underlying quarks and gluons.

The maximum inclusive process  $e^+e^- \rightarrow \text{hadrons}$  examined in the previous chapter is an example of an observable where the infrared singularities that arise when one integrates over the final state partons are completely canceled by the virtual corrections. As  $Q^2$  increases  $\alpha_s(Q^2)$  becomes small and the QCD result approaches the naive parton model prediction. One might get the impression that since  $\alpha_s(Q^2)$  becomes small at large  $Q^2$  (*i.e.*, asymptotic freedom) that all QCD perturbative calculations approach the naive parton model predictions as  $Q^2 \rightarrow \infty$ . As we shall see in this chapter this is definitely not the case. In the previous chapter we integrated over all the phase space of the final state partons. In this chapter we will ask questions about the nature of final state. We will see that, for example, all the infrared singularities do not cancel when computing the quark inclusive cross section,  $e^+e^- \rightarrow q + X$ . As a consequence of this the QCD results for the single hadron inclusive cross section,  $e^+e^- \rightarrow h + X$ , differs more and more from the naive parton model expectations as  $Q^2$  becomes large even though  $\alpha_s(Q^2)$  becomes small. Before proceeding to compute parton differential cross sections in perturbative QCD we examine the expectations of the naive parton model.

## 3.1 The Naive Parton Model

In the naive parton model it is assumed, for example, that when the quark in Fig. 2.1 separates from the antiquark that each fragments or cascades into a collection (or “jet”) of hadrons, each having small transverse momentum relative to the parent quarks direction. The number of hadrons of type  $h$  with

energy fraction

$$z = 2E_h/Q, \quad (3.1.1)$$

per  $dz$  is described by the "fragmentation function"  $D_q^h(z, Q^2)$ , where  $q$  is the initiating quark. Energy conservation implies that

$$\sum_{\text{All } h} \int_0^1 dz z D_q^h(z, Q^2) = 1. \quad (3.1.2)$$

The single particle inclusive cross section is given by

$$\begin{aligned} \frac{d\sigma}{dz}(e^+ e^- \rightarrow h + X) &\equiv \frac{d\sigma^h}{dz}(Q^2) \\ &= 3\sigma(\mu\mu) \sum_{i=1}^{n_f} e_{q_i}^2 (D_{q_i}^h(z, Q^2) + D_{\bar{q}_i}^h(z, Q^2)) \end{aligned} \quad (3.1.3)$$

where

$$\sigma(\mu\mu) \equiv \sigma(e^+ e^- \rightarrow \mu^+ \mu^-) = \frac{4\pi \alpha^2}{3 Q^2}, \quad (3.1.4)$$

as in (2.1.14). The inclusive cross section is normalized according to

$$\sum_{\text{All } h} \int_0^1 \frac{1}{2} z \frac{d\sigma^h}{dz}(Q^2) dz = \sigma_{tot}^{e^+ e^-}, \quad (3.1.5)$$

where  $\sigma_{tot}^{e^+ e^-}$  is the total  $e^+ e^- \rightarrow$  hadrons cross section and the ratio  $R$  in (2.1.16) is

$$R^{e^+ e^-} = \frac{\sigma(e^+ e^- \rightarrow \text{hadrons})}{\sigma(\mu\mu)} = 3 \sum_{i=1}^{n_f} e_{q_i}^2. \quad (3.1.6)$$

In general the inclusive cross section can be a function of the center-of-mass energy  $Q$ , but in the naive parton model the fragmentations functions are assumed to scale (*i.e.*, depend only on the scaling variable  $z$ ),

$$D_q^h(z, Q^2) = D_q^h(z) \quad (\text{Parton model}). \quad (3.1.7)$$

Neglecting mass effects, the probability of finding, for example, a 10 GeV pion in a 20 GeV jet is assumed to be the same as the probability of finding a 20 GeV pion in a 40 GeV jet. Furthermore,  $z D_q^h(z)$  is assumed to approach a constant as  $z \rightarrow 0$ . This implies that the mean multiplicity of particles of type  $h$  emerging from the parent quark  $q$ ,

$$\int_{z_{min}}^1 D_q^h(z) dz, \quad (3.1.8)$$

rises logarithmically with the quark momentum,  $p_q = Q/2$ , since  $z_{min} = 2m_h/Q$ , where  $m_h$  is the mass of the hadron.

The fragmentation of quarks into hadrons is a non-perturbative phenomena and cannot at present be calculated from QCD. A simple mathematical

### Hierarchy of Final Mesons

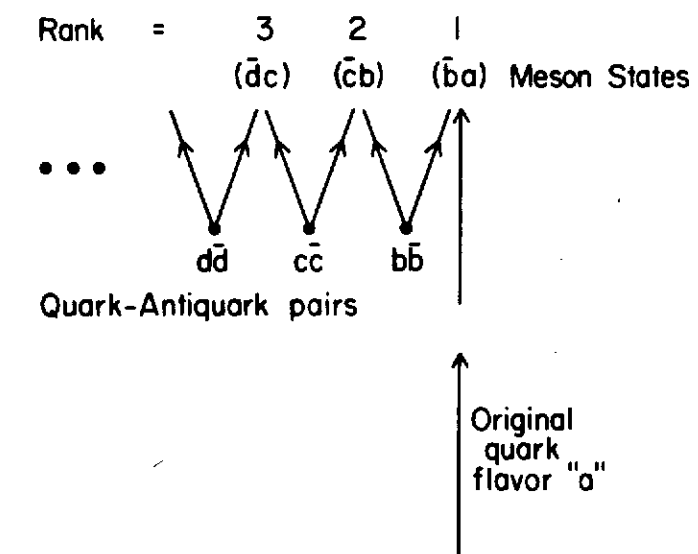


**Figure 3.1** Hierarchy of mesons formed when an initial quark of flavor "a" combines with an antiquark from a produced quark-antiquark pair, " $b\bar{b}$ ", forming the meson of rank 1. The resulting quark of flavor "b" then combines with an antiquark from another produced quark-antiquark pair forming the meson of rank 2 and so on.

model due to R.P. Feynman and myself<sup>1</sup> (called the FF parameterization) can be used to parameterize the non-perturbative aspects of quark jets. It is not meant to be a theory. It is simply a parameterization that incorporates many of the expected features of fragmentation. The model assumes that quark jets can be analyzed on the basis of a recursive principle. The ansatz is based on the idea that a quark of flavor "a" separating from an antiquark and having some momentum  $P_0$  in the  $\hat{z}$ -direction creates a color field in which new quark-antiquark pairs are produced. Quark "a" then combines with an antiquark, say "b", from the new pair  $b\bar{b}$  to form a meson of flavor  $a\bar{b}$  leaving the remaining "b" flavor quark to combine with further antiquarks. A "hierarchy" of mesons is thus formed of which  $a\bar{b}$  is first in "rank",  $b\bar{c}$  is second in rank,  $c\bar{d}$  is third in rank, *etc.*, as illustrated in Fig. 3.1. The "chain decay" ansatz assumes that, if the rank 1 meson carries away momentum  $\xi$ , from a quark jet of flavor "a" and momentum  $P_0$ , the remaining cascade starts with a quark of flavor "b" and momentum  $P_1 = P_0 - \xi$ , and the remaining hadrons are

distributed in precisely the same way as the hadrons which come from a jet originated by a quark of flavor "b" with momentum  $P_1$ . It is further assumed, as in the naive parton model, that all distributions scale. The complete jet can then be described by the function  $f(\eta)$  defined by,

$$\begin{aligned} f(\eta)d\eta = & \text{the probability that the first hierarchy (rank 1) meson leaves fractional momentum } \eta \text{ to the remaining cascade,} \\ & \quad (3.1.9) \end{aligned}$$

and is normalized so that

$$\int_0^1 f(\eta)d\eta = 1. \quad (3.1.10)$$

The probability of having hierarchy sequence with the  $n$ -th meson having momentum  $\xi_n$  is

$$\text{Prob}(\xi_1, \xi_2, \dots, \xi_n, \dots) d\xi_1 d\xi_2 \dots d\xi_n \dots = \prod_{i=1}^{\infty} f(\eta_i) d\eta_i, \quad (3.1.11)$$

where  $\eta_i = P_i/P_{i-1}$  and  $\xi_i = P_{i-1} - P_i$ .

If we now define the single particle distribution,  $F(z)$ , as

$$\begin{aligned} F(z)dz = & \text{the probability of finding a meson (independent} \\ & \text{of hierarchy) with fractional momentum } z \\ & \text{within } dz \text{ in a jet,} \quad (3.1.12) \end{aligned}$$

then  $F(z)$  must satisfy the integral equation

$$F(z) = f(1-z) + \int_z^1 \frac{d\eta}{\eta} f(\eta)F(z/\eta). \quad (3.1.13)$$

This equation arises because the meson might be first in rank (with probability  $f(1-z)dz$ ) or if not, then the first rank meson has left a momentum fraction  $\eta$  with probability  $f(\eta)d\eta$ , and in this remaining cascade the probability to find  $z$  in  $dz$  is  $F(z/\eta)dz/\eta$ .

The integral equation for  $F(z)$  in (3.1.13) can easily be solved by taking Fourier transforms. If we define

$$M(r) = \int_0^1 z^r F(z) dz, \quad (3.1.14)$$

and

$$C(r) = \int_0^1 \eta^r f(\eta) d\eta, \quad (3.1.15)$$

then (3.1.13) becomes

$$M(r) = A(r) + C(r)M(r), \quad (3.1.16)$$

or

$$M(r) = A(r)/(1 - C(r)), \quad (3.1.17)$$

where

$$A(r) = \int_0^1 z^r f(1-z) dz. \quad (3.1.18)$$

The integral kernel in (3.1.13) can be inverted algebraically in moment space. In particular,

$$1/(1 - C(r)) = 1 + C(r)/(1 - C(r)). \quad (3.1.19)$$

Thus, an equation of the form

$$\phi(z) = a(z) + \int \frac{d\eta}{\eta} f(\eta)\phi(z/\eta), \quad (3.1.20)$$

can be inverted to give

$$\phi(z) = a(z) + \int \frac{d\eta}{\eta} g(\eta)a(z/\eta), \quad (3.1.21)$$

where

$$\int_0^1 \eta^r g(\eta) d\eta = C(r)/(1 - C(r)). \quad (3.1.22)$$

Therefore (3.1.13) is solved by

$$F(z) = f(1-z) + \int_z^1 \frac{d\eta}{\eta} g(\eta)f(1-z/\eta). \quad (3.1.23)$$

The function  $g(\eta)d\eta$  can be interpreted as the probability that all mesons of lower rank than the given particle have left momentum fraction  $\eta$  of the original jet.

A nice consequence of this parameterization is (3.1.10) insures that

$$\int_0^1 zF(z) dz = 1. \quad (3.1.24)$$

In addition, (3.1.13) implies that

$$F(z) \underset{z \rightarrow 0}{\sim} R/z, \quad (3.1.25)$$

where  $R$  is a constant.

The functional form for  $f(\eta)$  is selected by examining  $e^+e^- \rightarrow h + X$  data. A simple form is

$$f(\eta) = (d+1)\eta^d, \quad (3.1.26)$$

which results in

$$zF(z) = f(1-z) = (d+1)(1-z)^d. \quad (3.1.27)$$

The power  $d = 2$  gives a qualitative description of the data, but as we shall see QCD perturbative corrections break the scaling assumptions of this naive mathematical model.

Additional parameters can be included to handle the flavor dependence of the fragmentation function. Suppose that we assume that new  $q\bar{q}$  pairs are

$u\bar{u}$  with probability  $\beta_u$ ,  $d\bar{d}$  with probability  $\beta_d$ ,  $s\bar{s}$  with probability  $\beta_s$ , etc. These probabilities must be normalized by

$$1 = \sum_{n=1}^{n_f} \beta_n, \quad (3.1.28)$$

and isospin symmetry implies

$$\beta_u = \beta_d = \beta. \quad (3.1.29)$$

Furthermore, data indicate that  $\beta_s \approx \frac{1}{2}\beta_u$  and that  $\beta_c$  and  $\beta_b$  are small.

For a quark of flavor  $q$ , the mean number of meson states of flavor "a $\bar{b}$ " at  $z$  is, in analogy to (3.1.13), given by

$$P_q^{a\bar{b}}(z) = \delta_{qa}\beta_b f(1-z) + \int \frac{d\eta}{\eta} f(\eta) \sum_c \beta_c P_c^{a\bar{b}}(z/\eta). \quad (3.1.30)$$

The first term arises because the a $\bar{b}$  meson state might be of first rank (but only if  $a = q$ , hence the delta function  $\delta_{qa}$ ) with probability  $f(1-z)$  times the chance,  $\beta_b$ , that the first new pair is of the required type. The second term occurs if the a $\bar{b}$  meson is not of first rank. In this case, the first pair might be c $\bar{c}$  (with probability  $\beta_c$ ) and leave a momentum fraction  $\eta$  to the cascade of quark c (with probability  $f(\eta)$ ) in which we find the state with probability  $P_c^{a\bar{b}}(z/\eta)dz/\eta$ .

If we now define an "average quark flavor" by

$$\langle q \rangle = \sum_{i=1}^{n_f} \beta_i q_i, \quad (3.1.31)$$

that is equal to  $u$  with probability  $\beta_u$ , equal to  $d$  with probability  $\beta_d$ , etc., and

$$P_{\langle q \rangle}^{a\bar{b}}(z) = \sum_c \beta_c P_c^{a\bar{b}}(z), \quad (3.1.32)$$

then from (3.1.30) we have

$$P_{\langle q \rangle}^{a\bar{b}}(z) = \beta_a \beta_b f(1-z) + \int \frac{d\eta}{\eta} f(\eta) P_{\langle q \rangle}^{a\bar{b}}(z/\eta). \quad (3.1.33)$$

Comparing with (3.1.13) yields

$$P_{\langle q \rangle}^{a\bar{b}}(z) = \beta_a \beta_b F(z). \quad (3.1.34)$$

Thus, if we know the distribution of mesons,  $F(z)$ , from quarks disregarding flavor, then those of flavor a $\bar{b}$  occur in the "average quark" jet with probabilities,  $\beta_a \beta_b$ . Only the contribution of the first rank quark differs from the average. Comparing (3.1.30) and (3.1.33) and using (3.1.34) gives

$$P_q^{a\bar{b}}(z) = \delta_{qa}\beta_b f(1-z) + \beta_a \beta_b \bar{F}(z), \quad (3.1.35)$$

where

$$\bar{F}(z) = F(z) - f(1-z), \quad (3.1.36)$$

is the probability of finding a meson of rank higher than one at  $z$ . For the choice of  $f(\eta)$  in (3.1.26)

$$z\bar{F}(z) = (d+1)(1-z)^{d+1}. \quad (3.1.37)$$

The probabilities,  $P_q^{a\bar{b}}(z)$ , are related to the fragmentation functions,  $D_q^h(z)$ , by

$$D_q^h(z) = \sum_{a,b} \Gamma_{ab}^h P_q^{a\bar{b}}(z), \quad (3.1.38)$$

where  $\Gamma_{ab}^h$  is the probability that the hadron  $h$  contains the quark-antiquark state a $\bar{b}$ . For example,  $\Gamma_{ud}^{\pi^+} = 1$  and  $\Gamma_{uu}^{\pi^0} = \Gamma_{dd}^{\pi^0} = \frac{1}{2}$ . Inserting (3.1.35) into (3.1.38) gives

$$D_q^h(z) = A_q^h f(1-z) + B^h \bar{F}(z), \quad (3.1.39)$$

where

$$A_q^h = \sum_b \Gamma_{qb}^h \beta_b, \quad (3.1.40)$$

and

$$B^h = \sum_q \beta_q A_q^h. \quad (3.1.41)$$

For example,

$$\begin{array}{lll} A_u^{\pi^+} = \beta & A_u^{\pi^0} = \frac{1}{2}\beta & A_u^{\pi^-} = 0 \\ A_d^{\pi^+} = 0 & A_u^{\pi^0} = \frac{1}{2}\beta & A_u^{\pi^-} = \beta \\ A_s^{\pi^+} = 0 & A_s^{\pi^0} = 0 & A_s^{\pi^-} = 0 \\ B^{\pi^+} = \beta^2 & B^{\pi^0} = \beta^2 & B^{\pi^-} = \beta^2 \end{array} \quad (3.1.42)$$

yielding

$$\begin{aligned} D_u^{\pi^+}(z) &= \beta f(1-z) + \beta^2 \bar{F}(z), \\ D_u^{\pi^0}(z) &= \frac{1}{2}\beta f(1-z) + \beta^2 \bar{F}(z), \\ D_u^{\pi^-}(z) &= \beta^2 \bar{F}(z), \end{aligned} \quad (3.1.43)$$

where I have used (3.1.29) and set  $\beta_c = \beta_b = 0$ .

It is interesting to investigate how the charges of the mesons are distributed along the direction of the initial quark. Suppose we have some additive quantum number,  $Q$ , like electric charge, or the third component of isospin, or hypercharge. Then if we weigh each "meson", a $\bar{b}$ , by its charge  $e_a - e_b$ , we obtain the net average charge distribution of the jet. Namely,

$$\langle Q_q(z) \rangle = \sum_{a,b} (e_a - e_b) P_q^{a\bar{b}}(z) = (e_q - e_{\langle q \rangle}) f(1-z), \quad (3.1.44)$$

where

$$e_{(q)} = \sum_a \beta_a e_a, \quad (3.1.45)$$

is the “mean quark” charge. The hadrons in the jet carry an average total charge,  $e_q - e_{(q)}$ , equal to the charge of the quark *plus* a correction,  $-e_{(q)}$ , proportional to the deviation of the probability of production of new pairs from the  $SU(N)$  value of  $1/N$ . For the case of electric charge we have

$$\begin{aligned} e_{(q)} &= \left(\frac{2}{3}\right) \beta_u + \left(-\frac{1}{3}\right) \beta_d + \left(-\frac{1}{3}\right) \beta_s \\ &= \frac{1}{3}\beta - \frac{1}{3}\beta_s = \beta - \frac{1}{3}, \end{aligned} \quad (3.1.46)$$

where I have, for the sake of this discussion used (3.1.29) and assumed  $\beta_c = \beta_b = 0$ . In this case, the average of the total electric charge of a  $u, d$ , and  $s$  quark jet is

$$\begin{aligned} \langle Q_u \rangle &= 1 - \beta = 0.6, \\ \langle Q_d \rangle &= -\beta = -0.4, \\ \langle Q_s \rangle &= -\beta = -0.4, \end{aligned} \quad (3.1.47)$$

where I have taken  $\beta = 0.4$ . The hadrons do “remember” something about the electric charge of the quark from which they originated, although the knowledge is not precisely the charge of the quark.

They are, of course, QCD perturbative corrections that modify this simple parton model picture. For example, the diagrams in Fig. 2.3 give rise to gluon jets and break the scaling assumption in (3.1.7). We now proceed to examine some of these corrections.

### 3.2 Parton Differential Cross Sections

Equation (2.5.6) gives the differential cross section (in the massive gluon scheme) for producing a quark in the process  $\gamma^* \rightarrow q\bar{q}g$  carrying fractional energy  $x$ ,

$$\begin{aligned} \frac{1}{\sigma_0} \frac{d\sigma_{MG}^q}{dx} &= \frac{2\alpha_s}{3\pi} \left\{ \frac{1+x^2}{1-x} \log\left(\frac{x(1-x)Q^2}{m_g^2}\right) \right. \\ &\quad \left. - \frac{3}{2} \frac{1}{1-x} + \frac{1}{2} x + \frac{1}{2} \right\}_{x<1}. \end{aligned} \quad (3.2.1)$$

This differential cross section diverges as  $x \rightarrow 1$ , but we know from Chapter 2 that if we integrate over  $x$  and add the virtual corrections the result is finite. In particular,

$$\sigma_{MG}(\text{virtual}) + \int_0^1 \frac{d\sigma_{MG}^q}{dx} dx = \frac{\alpha_s}{\pi} \sigma_0 \quad (3.2.2)$$

or

$$\int_0^1 \left\{ \frac{d\sigma_{MG}^q}{dx} + \left( \sigma_{MG}(\text{virtual}) - \frac{\alpha_s}{\pi} \sigma_0 \right) \delta(1-x) \right\} dx = 0. \quad (3.2.3)$$

It is very useful to define “+ functions”<sup>2</sup> that allow us to include the virtual corrections in the differential cross section,  $d\sigma_{MG}^q/dx$ . We first turn  $d\sigma_{MG}^q/dx$  into a pure “+ function” whose integral over  $x$  vanishes as in (3.2.3). Namely,

$$\int_0^1 \left( \frac{d\sigma_{MG}^q}{dx} \right)_+ dx = 0. \quad (3.2.4)$$

Then we write a new differential cross section according to

$$\frac{1}{\sigma_0} \frac{d\sigma^q}{dx} = \frac{1}{\sigma_0} \left( \frac{d\sigma^q}{dx} \right)_+ + \alpha_s I_q^{e^+ e^-} \delta(1-x), \quad (3.2.5)$$

where

$$\sigma_{tot}^{e^+ e^-} = \sigma_0 \left( 1 + \alpha_s I_q^{e^+ e^-} + \dots \right), \quad (3.2.6)$$

and from (2.7.7)

$$\alpha_s I_q^{e^+ e^-} = \frac{\alpha_s}{\pi}. \quad (3.2.7)$$

Once  $d\sigma^q/dx$  for  $x < 1$  and the complete (real *plus* virtual) integral over  $x$  are known, then it is easy to construct the distribution in (3.2.5). The “+ function” is constructed by adding an appropriate  $\delta$ -function contribution so that (3.2.4) is satisfied. Then to get the complete (real *plus* virtual) distribution one simply adds the  $\delta$ -function that gives the correct total integral. Several “+ functions” are discussed in Appendix E. In general, they are defined according to

$$(F(x))_+ \equiv \lim_{\beta \rightarrow 0} \left\{ F(x) \theta(1-x-\beta) - \delta(1-x-\beta) \int_0^{1-\beta} F(y) dy \right\}. \quad (3.2.8)$$

For  $x < 1 - \beta$ ,  $(F(x))_+ = F(x)$ , but the integral over  $x$  of  $(F(x))_+$  vanishes. From (3.2.1) it is easy to see that

$$\frac{1}{\sigma_0} \left( \frac{d\sigma_{MG}^q}{dx} \right)_+ = \frac{\alpha_s}{2\pi} P_{q \rightarrow qg}(x) \log(Q^2/m_g^2) + \alpha_s f_{MG,q}^{e^+ e^-}(x), \quad (3.2.9)$$

where

$$P_{q \rightarrow qg}(x) = \frac{4}{3} \left( \frac{1+x^2}{1-x} \right)_+ = \frac{4}{3} \left\{ \frac{1+x^2}{(1-x)_+} + \frac{3}{2} \delta(1-x) \right\}, \quad (3.2.10)$$

and

$$\alpha_s f_{MG,q}^{e^+ e^-}(x) = \frac{2\alpha_s}{3\pi} \left\{ (1+x^2) \left( \frac{\log(1-x)}{1-x} \right)_+ + \frac{1+x^2}{1-x} \log(x) \right\}$$

$$-\frac{3}{2} \frac{1}{(1-x)_+} + \frac{1}{2}(1+x)_+ + \left( \frac{\pi^2}{3} - \frac{15}{4} \right) \delta(1-x) \Big\}. \quad (3.2.11)$$

Since  $P_{q \rightarrow qg}(x)$  is a pure “+” function”:

$$\int_0^1 P_{q \rightarrow qg}(x) dx = 0. \quad (3.2.12)$$

Furthermore, by the use of

$$\int_0^1 (1+x^2) \left( \frac{\log(1-x)}{1-x} \right)_+ dx = \frac{7}{4}, \quad (3.2.13)$$

and

$$\int_0^1 \frac{1+x^2}{1-x} \log(x) dx = -\frac{\pi^2}{3} + \frac{5}{4}, \quad (3.2.14)$$

it is easy to see that

$$\int_0^1 \alpha_s f_{MG,q}^{e+\epsilon^-}(x) dx = 0. \quad (3.2.15)$$

The quark differential cross section in (3.2.5) with  $(d\sigma^q/dx)_+$  given by (3.2.9) contains both real and virtual corrections.

From the definition (3.2.8) we see that the two “+ functions” appearing in (3.2.11) are given by

$$\frac{1}{(1-x)_+} = \frac{1}{1-x} \theta(1-x-\beta) + \log(\beta) \delta(1-x-\beta), \quad (3.2.16)$$

and

$$\left( \frac{\log(1-x)}{1-x} \right)_+ = \frac{\log(1-x)}{1-x} \theta(1-x-\beta) + \frac{1}{2} \log^2(\beta) \delta(1-x-\beta), \quad (3.2.17)$$

in the limit  $\beta \rightarrow 0$ . These two “+ functions” are plotted in Appendix E.

To arrive at the quark differential cross section in the dimensional regularization scheme we integrate (2.8.28) only over  $x_2$  (or equivalently  $v$ ). In particular,

$$\frac{1}{\sigma_0} \frac{d\sigma_{DR}^q}{dx} = \frac{2\alpha_s}{3\pi} \left( \frac{x^2(1-x)Q^2}{4\pi m_D^2} \right)^{\epsilon/2} \frac{1}{\Gamma(2+\frac{\epsilon}{2})} \int_0^1 dv v^{\frac{\epsilon}{2}} (1-v)^{\frac{1}{2}} x F(x, v), \quad (3.2.18)$$

where  $x F(x, v)$  is given by (2.8.33) with  $x_1 = x$  and  $N = 4 + \epsilon$ . Integrating over  $v$  yields

$$\begin{aligned} \frac{1}{\sigma_0} \frac{d\sigma_{DR}^q}{dx} &= \frac{2\alpha_s}{3\pi} \left( \frac{x^2(1-x)Q^2}{4\pi m_D^2} \right)^{\epsilon/2} \frac{\Gamma(1+\frac{\epsilon}{2})}{\Gamma(1+\epsilon)} \left\{ \frac{1+x^2}{1-x} \frac{2}{\epsilon} \right. \\ &\quad \left. - \frac{3}{2} \frac{1}{1-x} - \frac{3}{2} x + \frac{5}{2} + \dots \right\}, \end{aligned} \quad (3.2.19)$$

where I have dropped some of the terms that vanish as  $\epsilon \rightarrow 0$ . Using the

expansion

$$\frac{\Gamma(1+\frac{\epsilon}{2})}{\Gamma(1+\epsilon)} = 1 + \frac{1}{2}\gamma_E \epsilon + \frac{1}{16} (2\gamma_E^2 - \pi^2) \epsilon^2 + \dots, \quad (3.2.20)$$

we arrive at

$$\begin{aligned} \frac{1}{\sigma_0} \frac{d\sigma_{DR}^q}{dx} &= \frac{2\alpha_s}{3\pi} \left\{ \frac{1+x^2}{1-x} \frac{2}{\epsilon} + \frac{1+x^2}{1-x} \left[ \log \left( \frac{x^2(1-x)Q^2}{4\pi m_D^2} \right) + \gamma_E \right] \right. \\ &\quad \left. - \frac{3}{2} \frac{1}{1-x} - \frac{3}{2} x + \frac{5}{2} \right\}, \end{aligned} \quad (3.2.21)$$

so that

$$\frac{1}{\sigma_0} \left( \frac{d\sigma_{DR}^q}{dx} \right)_+ = \frac{\alpha_s}{2\pi} P_{q \rightarrow qg}(x) \log(Q^2/m_D^2) + \alpha_s f_{DR,q}^{e+\epsilon^-}(x), \quad (3.2.22)$$

where  $P_{q \rightarrow qg}(x)$  is the same function that appears in (3.2.9) and

$$\begin{aligned} \alpha_s f_{DR,q}^{e+\epsilon^-}(x) &= \frac{2\alpha_s}{3\pi} \left\{ (1+x^2) \left( \frac{\log(1-x)}{1-x} \right)_+ + \frac{2(1+x^2)}{1-x} \log(x) \right. \\ &\quad \left. - \frac{3}{2} \frac{1}{(1-x)_+} - \frac{3}{2} x + \frac{5}{2} + \left( \frac{2\pi^2}{3} - 6 \right) \delta(1-x) \right\} \\ &\quad + \frac{\alpha_s}{2\pi} P_{q \rightarrow qg}(x) \left\{ \frac{2}{\epsilon} + \gamma_E - \log(4\pi) \right\}. \end{aligned} \quad (3.2.23)$$

Equations (3.2.1) and (3.2.21) illustrate a feature in common with many of the calculations we will be performing in this book. The quark cross sections are regularization scheme dependent. The coefficient of the  $\log(Q^2)$  term is universal (scheme independent) but the “little  $f$ ” functions in (3.2.9) and (3.2.22) are different and depend on the scheme. Nevertheless these “little  $f$ ” functions have a unique integral. By construction,

$$\int_0^1 f_{DR,q}^{e+\epsilon^-}(x) dx = \int_0^1 f_{MG,q}^{e+\epsilon^-}(x) dx = 0. \quad (3.2.24)$$

Furthermore, equations (3.2.9) and (3.2.22) contain explicitly the gluon mass and the dimensional regularization mass, respectively. These masses are an artifact of method we choose to regularize the calculation and we believe that QCD should give a finite result for experimental observables in limit that  $m_g$  or  $m_D$  goes to zero. We also believe that experimental observables cannot depend on the regularization scheme chosen. This means that  $(d\sigma/dx)_+$  better not be a direct experimental observable or we are in serious trouble. Finally, from the point of view of a perturbation series in  $\alpha_s$  the first term in (3.2.9) or (3.2.22) does not become small as  $Q$  increases. Terms of the form  $[\alpha_s(Q^2) \log(Q^2)]^n$  are of order one for any  $n$  since  $\alpha_s(Q^2) \sim 1/\log(Q^2)$ . All terms of this form must be summed in order to arrive at a valid perturbation expansion.

In a similar manner one can construct the differential cross section for

producing a gluon in the process  $\gamma^* \rightarrow q\bar{q}g$  carrying fractional energy  $x$ . In this case

$$\frac{1}{\sigma_0} \frac{d\sigma^g}{dx} = \frac{1}{\sigma_0} \left( \frac{d\sigma^g}{dx} \right)_+ + \alpha_s I_g^{e^+ e^-} \delta(x), \quad (3.2.25)$$

where  $\alpha_s I_g^{e^+ e^-} = \alpha_s I_q^{e^+ e^-} = \alpha_s/\pi$ . In the massive gluon scheme one gets

$$\frac{1}{\sigma_0} \left( \frac{d\sigma_{MG}}{dx} \right)_+ = 2 \left( \frac{\alpha_s}{2\pi} \right) P_{q \rightarrow gg}(x) \log(Q^2/m_g^2) + 2\alpha_s f_{MG,g}^{e^+ e^-}(x), \quad (3.2.26)$$

where

$$P_{q \rightarrow gg}(x) = P_{q \rightarrow gg}(1-x), \quad (3.2.27)$$

or

$$P_{q \rightarrow gg}(x) = \frac{4}{3} \left\{ \frac{1 + (1-x)^2}{(x)_+} + \frac{3}{2} \delta(x) \right\}, \quad (3.2.28)$$

and

$$\alpha_s f_{MG,g}^{e^+ e^-}(x) = \frac{2\alpha_s}{3\pi} \left\{ 2(1 + (1-x)^2) \left( \frac{\log(x)}{x} \right)_+ - 2x - \frac{7}{4} \delta(x) \right\}. \quad (3.2.29)$$

Here the “+” functions are defined with respect to the point  $x = 0$ . In addition, it is easy to show that

$$\int_0^1 x [P_{q \rightarrow gg}(x) + P_{q \rightarrow gg}(x)] dx = 0. \quad (3.2.30)$$

The factors of 2 in (3.2.26) are important since later we will associate  $1/2$  of  $d\sigma^g/dx$  with the produced quark and  $1/2$  of it with the produced antiquark.

In general the “little  $f$ ” functions must be labeled by the process and the regularization scheme since they depend on both. However, in addition to (3.2.24)

$$\int_0^1 x [f_q^{e^+ e^-}(x) + f_g^{e^+ e^-}(x)] dx = 0, \quad (3.2.31)$$

regardless of the scheme.

### 3.3 Single Hadron Inclusive Cross Section

The next step is to embed the parton cross sections within the desired hadronic process. What is measured experimentally in  $e^+ e^-$  annihilations is the probability of observing an outgoing hadron from the process  $e^+ e^- \rightarrow \gamma^* \rightarrow$  hadrons carrying a certain fraction  $z$  of the available energy,

$$z = 2E_h/Q. \quad (3.3.1)$$

This inclusive single hadron cross section is related to the parton differential cross sections according to

$$\begin{aligned} d\sigma^h(z, Q^2) &= \left( \frac{d\sigma^q}{dy} \right) dy D_{0,q}^h(x) dx \\ &+ \left( \frac{d\sigma^g}{dy} \right) dy D_{0,g}^h(x) dx \\ &+ \left( \frac{d\sigma^q}{dy} \right) dy D_{0,q}^h(x) dx, \end{aligned} \quad (3.3.2)$$

where  $(d\sigma^q/dy)dy$  is the probability of finding a quark with energy

$$E_q = \frac{1}{2}yQ, \quad (3.3.3)$$

and  $D_{0,q}^h(x)dx$  is the probability that a quark of energy  $E_q$  fragments into a hadron carrying fractional energy,

$$x = E_h/E_q. \quad (3.3.4)$$

Similarly  $(d\sigma^g/dy)dy$  is the probability of finding a gluon with energy  $E_g = yQ/2$  and  $D_{0,g}^h(x)dx$  is the gluon fragmentation function. The “outside” experimental variable  $z$  is related to the two “inside” parton variables  $x$  and  $y$  as follows,

$$x = z/y, \quad (3.3.5)$$

and  $0 \leq x \leq 1$  implies that  $z \leq y \leq 1$ . Thus,

$$\begin{aligned} \frac{d\sigma^h}{dz}(Q^2) &= 3\sigma(\mu\mu) \int_z^1 \frac{dy}{y} \left\{ \sum_{i=1}^{n_f} e_i^2 [D_{0,q_i}^h(z/y) + D_{0,\bar{q}_i}^h(z/y)] \right. \\ &\quad \left[ \left( 1 + \frac{\alpha_s}{\pi} \right) \delta(1-y) + \frac{\alpha_s}{2\pi} P_{q \rightarrow gg}(y) \log(Q^2/m^2) + \alpha_s f_q^{e^+ e^-}(y) \right] \\ &\quad \left. + 2 \sum_{i=1}^{n_f} e_i^2 D_{0,g}^h(z/y) \left[ \frac{\alpha_s}{2\pi} P_{q \rightarrow gg}(y) \log(Q^2/m^2) + \alpha_s f_g^{e^+ e^-}(y) \right] \right\}, \end{aligned} \quad (3.3.6)$$

where I have summed over  $n_f$  quark flavors and three quark colors and where  $P_{q \rightarrow gg}(y)$  and  $P_{q \rightarrow gg}(y)$  are given by (3.2.10) and (3.2.28), respectively, and where  $\sigma(\mu\mu)$  is the  $\gamma^* \rightarrow \mu^+ \mu^-$  rate in (3.1.4). The “little  $f$ ” functions are the scheme dependent functions in (3.2.11), (3.2.23) and (3.2.29) and  $m = m_g$  or  $m_D$  depending on the scheme. The fragmentation functions  $D_{0,q}^h$  and  $D_{0,g}^h$  contain the non-perturbative information on how the quarks and gluons turn into the outgoing hadrons. At this stage all we know is that energy is conserved so that (3.1.2) holds. Namely,

$$\sum_{\text{All } h} \int_0^1 x D_{0,q_i}^h(x) dx = 1, \quad (3.3.7)$$

$$\sum_{\text{All } h} \int_0^1 x D_{0,g}^h(x) dx = 1. \quad (3.3.8)$$

This together with (3.2.30) and (3.2.31) insures that the normalization condition in (3.1.5) holds,

$$\sum_{\text{All } h} \int_0^1 \frac{1}{2} z \frac{d\sigma^h}{dz}(Q^2) dz = \sigma_{tot}^{e^+ e^-}, \quad (3.3.9)$$

where,  $\sigma_{tot}^{e^+ e^-}$  is given by (2.7.8).

We now define experimentally observable fragmentation functions according to (3.1.3) so that to order  $\alpha_s$  (in the massive gluon scheme)

$$\begin{aligned} D_q^h(z, Q^2) &= \int_z^1 \frac{dy}{y} \left\{ D_{0,q}^h(z/y) \right. \\ &\quad \left[ \delta(1-y) + \frac{\alpha_s}{\pi} P_{q \rightarrow qq}(y) \log(Q^2/m_g^2) + \alpha_s f_{MG,q}^{e^+ e^-}(y) \right] \\ &\quad \left. + D_{0,g}^h(z/y) \left[ \frac{\alpha_s}{2\pi} P_{q \rightarrow gg}(y) \log(Q^2/m_g^2) + \alpha_s f_{MG,g}^{e^+ e^-}(y) \right] \right\}. \end{aligned} \quad (3.3.10)$$

We cannot calculate  $D_q^h(z, Q^2)$  at a given  $Q^2$  since the “bare” fragmentation functions  $D_{0,q}^h(x)$  and  $D_{0,g}^h(x)$  are unknown. Because of this the “little  $f$ ” functions  $f_q^{e^+ e^-}$  and  $f_g^{e^+ e^-}$  are not directly experimentally observable, which is fortunate since they are regularization scheme dependent.

At this point it is convenient to define “convolution notation” as follows:

$$C(z) = A * B \equiv \int_z^1 \frac{dy}{y} A(z/y) B(y) = \int_z^1 \frac{dy}{y} A(y) B(z/y), \quad (3.3.11)$$

whereupon (3.3.10) becomes

$$\begin{aligned} D_q^h(z, Q^2) &= D_{0,q}^h * \left( 1 + \frac{\alpha_s}{2\pi} P_{q \rightarrow qq} \log(Q^2/m_g^2) + \alpha_s f_{MG,q}^{e^+ e^-} \right) \\ &\quad + D_{0,g}^h * \left( \frac{\alpha_s}{2\pi} P_{q \rightarrow gg} \log(Q^2/m_g^2) + \alpha_s f_{MG,g}^{e^+ e^-} \right), \end{aligned} \quad (3.3.12)$$

and

$$D_{NS}^h(z, Q^2) = D_{0,NS}^h * \left( 1 + \frac{\alpha_s}{2\pi} P_{q \rightarrow qq} \log(Q^2/m_g^2) + \alpha_s f_{MG,q}^{e^+ e^-} \right), \quad (3.3.13)$$

where the “non-singlet” fragmentation functions are defined by

$$D_{NS}^h(z, Q^2) \equiv D_q^h(z, Q^2) - D_{\bar{q}}^h(z, Q^2). \quad (3.3.14)$$

The non-singlet functions are somewhat easier to analyze because the gluon term,  $D_{0,g}^h$ , drops out since it contributes equally to both  $D_q^h(z, Q^2)$  and  $D_{\bar{q}}^h(z, Q^2)$ .

The fragmentation functions in (3.3.12) and (3.3.13) still appear to diverge like  $\log(m_g)$  in the limit  $m_g \rightarrow 0$ . Since we believe that all observable quantities should be well behaved in the limit of zero gluon mass (or in the

limit in which the dimensional regularization mass goes to zero), this divergence must be an artifact of the way we have done the calculation. For example, we have divided the observable  $D_{NS}^h(z, Q^2)$  into two terms,  $D_{0,NS}^h(z)$  and  $P_{q \rightarrow qq}(y) \log(Q^2/m_g^2)$ . This latter term diverges as  $m_g \rightarrow 0$  but  $D_{0,NS}^h(z, Q^2)$  must remain finite. This means that  $D_{0,NS}^h(z)$  must also diverge as  $m_g \rightarrow 0$  in such a way that the product is finite. The function  $D_{0,NS}^h(z)$  must, therefore, have the form

$$D_{0,NS}^h(z) = \overline{D}_{0,NS}^h * \left( 1 + \frac{\alpha_s}{2\pi} P_{q \rightarrow qq} \log(m_g^2/\Lambda^2) + \dots \right), \quad (3.3.15)$$

or

$$\overline{D}_{0,NS}^h(z) = D_{0,NS}^h * \left( 1 + \frac{\alpha_s}{2\pi} P_{q \rightarrow qq} \log(\Lambda^2/m_g^2) + \dots \right), \quad (3.3.16)$$

where  $\Lambda$  is a mass scale that is related to the size of hadrons and where  $\overline{D}_{0,NS}^h$  is finite in the limit  $m_g \rightarrow 0$ . The mass singularities are “factored” off into  $D_{0,NS}^h$  as follows

$$\begin{aligned} D_{NS}^h(z, Q^2) &= D_{0,NS}^h * \left( 1 + \frac{\alpha_s}{2\pi} P_{q \rightarrow qq} [\log(Q^2/\Lambda^2) + \log(\Lambda^2/m_g^2)] \right) \\ &= D_{0,NS}^h * \left( 1 + \frac{\alpha_s}{2\pi} P_{q \rightarrow qq} \log(\Lambda^2/m_g^2) \right) \\ &\quad * \left( 1 + \frac{\alpha_s}{2\pi} P_{q \rightarrow qq} \log(Q^2/\Lambda^2) \right) + \dots \\ &= \overline{D}_{0,NS}^h * \left( 1 + \frac{\alpha_s}{2\pi} P_{q \rightarrow qq} \log(Q^2/\Lambda^2) \right) + O(\alpha_s^2). \end{aligned} \quad (3.3.17)$$

The mass singularity  $\log(m_g^2)$  has been absorbed into the unknown function  $\overline{D}_{0,NS}^h$  which is assumed to be well behaved in the limit  $m_g \rightarrow 0$ . The scale  $\Lambda$  can be taken to be the perturbative parameter in (1.2.18) which sets the value of  $\alpha_s(Q^2)$  at a given scale  $Q$ . At this order the “factorization of the mass singularities” is a trivial property of logarithms. It has been shown, however, that to all orders of perturbation theory, one can factor out and absorb these singularities into the functions  $\overline{D}_{0,q}$  and  $\overline{D}_{0,g}$ .<sup>3-6</sup>

Alternatively we can write

$$\begin{aligned} D_{NS}^h(z, Q^2) &= D_{0,NS}^h * \left( 1 + \frac{\alpha_s}{2\pi} P_{q \rightarrow qq} [\log(Q^2/\mu^2) + \log(\mu^2/m_g^2)] \right) \\ &= \overline{D}_{0,NS}^h * \left( 1 + \frac{\alpha_s}{2\pi} P_{q \rightarrow qq} \log(Q^2/\mu^2) \right) + \dots, \end{aligned} \quad (3.3.18)$$

where

$$\overline{D}_{0,NS}^h(z) = D_{0,NS}^h * \left( 1 + \frac{\alpha_s}{2\pi} P_{q \rightarrow qq} \log(\mu^2/m_g^2) + \dots \right), \quad (3.3.19)$$

and where  $\mu$  is the “renormalization point” used to define the strong coupling,  $\alpha_s \equiv \alpha_s(\mu^2)$ , as discussed in Chapter 6. The scale  $\mu$  is available to us and can be used to “factor off” the mass singularities. From this point of view (3.3.16) can be thought of as simply setting  $\mu = \Lambda$  for convenience, since the scale  $\mu$  is arbitrary in any case. On the other hand, we will see in Chapter

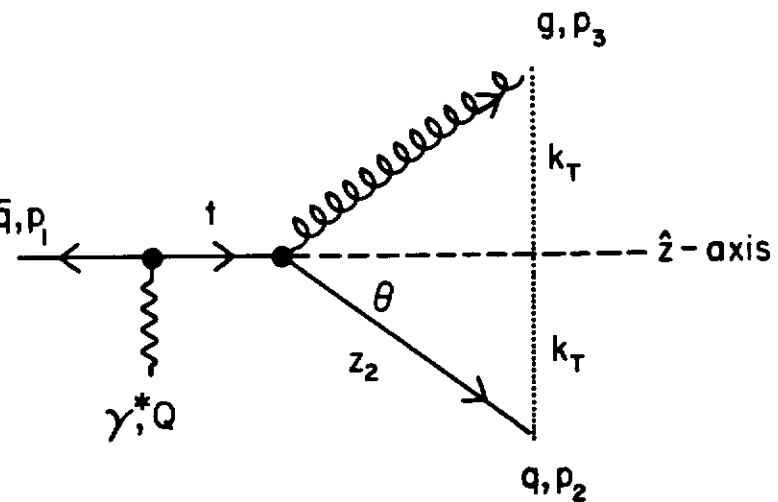


**Figure 3.2** Illustration of the “decay” of a quark,  $q$ , with invariant mass  $\sqrt{t}$  into a gluon,  $g$ , and another quark carrying a fraction  $z_2$  of the parent quark’s  $E + p_z$ . The outgoing quark has transverse momentum,  $k_T$ , relative to the  $\hat{z}$ -axis defined along the direction of the initial quark.

that choosing the renormalization point  $\mu$  as the “separation mass” will allow us to compute the  $Q^2$  dependence of the fragmentation functions using “renormalization group equations” (RGE).

Since  $\bar{D}_{0,NS}(z)$  in (3.3.16) is unknown we still cannot calculate the observable  $D_{NS}^h(z, Q^2)$  from perturbation theory. These functions contain information on the way in which partons turn into hadrons which is clearly a non-perturbative phenomena. We will, however, be able to calculate the change in  $D_{NS}^h(z, Q^2)$  as we change  $Q^2$ . Since  $\alpha_s(Q^2) \log Q^2$  is of order one, we must first sum all terms of the form  $[\alpha_s(Q^2) \log Q^2]^n$ .

### 3.4 Summing Leading Logarithms

There are two ways to sum the leading log contributions. In Chapter 6 we will sum them using “renormalization group equations” (RGE). Here we use brute force and explicitly sum the leading log contributions. Let us begin by

examining the  $\gamma^* \rightarrow \bar{q}qg$  double differential cross section

$$\frac{1}{\sigma_0} \frac{d\sigma}{dx_1 dx_2} = \frac{2\alpha_s}{3\pi} \frac{x_1^2 + x_2^2}{(1-x_1)(1-x_2)}, \quad (3.4.1)$$

from yet another point of view. This time we introduce the light cone variables

$$(E + p_z)_i = z_i Q, \quad (3.4.2)$$

$$(E - p_z)_i = y_i Q, \quad (3.4.3)$$

where as shown in Fig. 3.2, the  $\hat{z}$ -axis is defined in the direction  $\vec{p}_2 + \vec{p}_3$ . The light cone variables for parton 2 (quark) and parton 3 (gluon) satisfy

$$z_2 + z_3 = 1, \quad (3.4.4)$$

$$y_2 + y_3 = \hat{t} = (1-x_1), \quad (3.4.5)$$

$$z_2 y_2 = z_3 y_3 = z_2 (1-z_2) \hat{t} = k_T^2 / Q^2, \quad (3.4.6)$$

$$z_2 = x_2 - \hat{t}(1-x_2)/(1-\hat{t}), \quad (3.4.7)$$

where

$$\hat{t} = t/Q^2, \quad (3.4.8)$$

with  $t$  is defined in (2.3.12) and where  $k_T$  is the transverse momentum relative to the  $\hat{z}$ -axis (*i.e.*, relative to  $\vec{p}_2 + \vec{p}_3$ ). The differential cross section (3.4.1) when written in terms of  $z = z_2$  and the invariant mass squared,  $t$ , of parton 2 and 3 becomes

$$\frac{1}{\sigma_0} \frac{d\sigma}{dz d\hat{t}} = \frac{2\alpha_s}{3\pi} \left\{ \frac{1+z^2}{\hat{t}(1-z)} - \frac{2(1-z(1-z))}{(1-z)} + \frac{\hat{t}(1+(1-z)^2)}{(1-z)} \right\}. \quad (3.4.9)$$

In the region where  $k_T^2/Q^2 = z(1-z)\hat{t}$  is small this cross section can be approximated by the first term. The approximation

$$\frac{1}{\sigma_0} \left( \frac{d\sigma}{dz d\hat{t}} \right)_{LPA} = \frac{2\alpha_s}{3\pi} \frac{1+z^2}{(1-z)\hat{t}}, \quad (3.4.10)$$

is known as the “leading pole” approximation (LPA)<sup>7–11</sup> and when integrated over  $\hat{t}$  produces the leading log singularity. The virtual corrections can be included by writing (3.4.10) in terms of a “+” function as follows

$$\frac{1}{\sigma_0} \left( \frac{d\sigma}{dz d\hat{t}} \right)_{LPA} = \frac{\alpha_s(t)}{2\pi\hat{t}} P_{q \rightarrow gg}(z), \quad (3.4.11)$$

where  $P_{q \rightarrow gg}(z)$  is the same as (3.2.10). Namely,

$$P_{q \rightarrow gg}(z) = \frac{4}{3} \left( \frac{1+z^2}{1-z} \right)_+. \quad (3.4.12)$$

Integrating the leading pole (3.4.11) over  $\hat{t}$  gives the leading log (LL) piece of

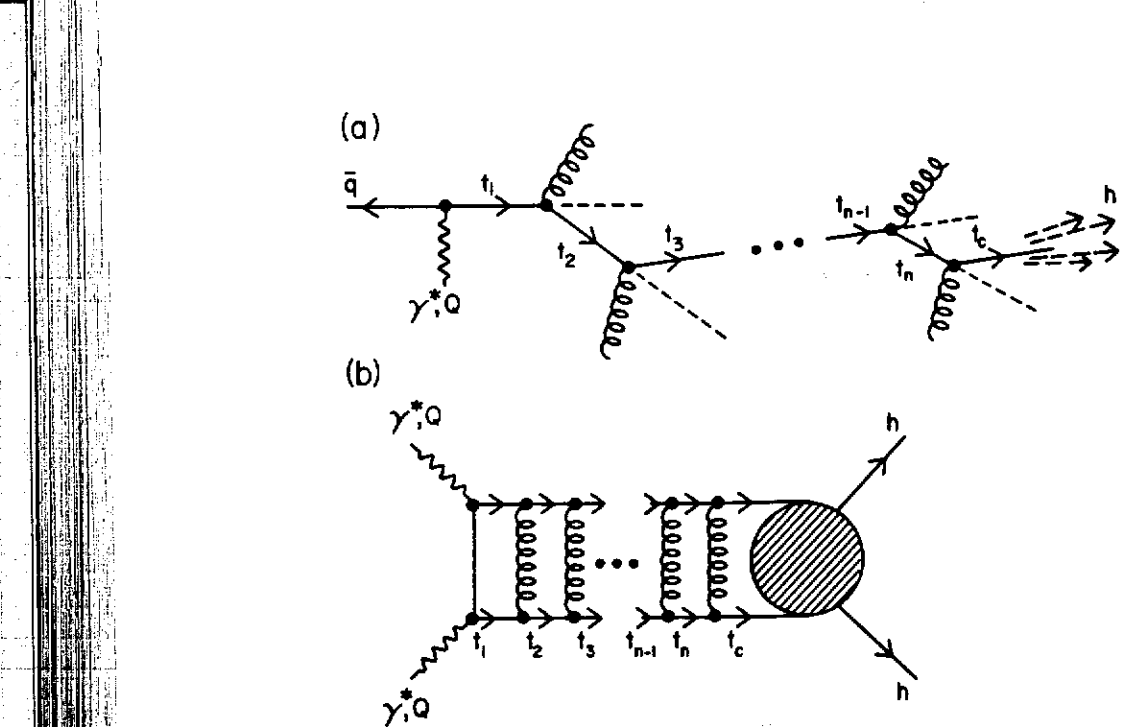


Figure 3.3 (a) Illustration of the case where an initial quark produced by the “decay” of a virtual photon of invariant mass,  $Q$ , emits  $n$  gluons and has its invariant mass degraded from  $t_1$  to  $t_c$  ( $Q^2 \geq t_1 \geq t_2 \geq \dots \geq t_n \geq t_c$ ) whereby it subsequently “fragments” into hadron,  $h$ . (b) Square of the amplitude for the process in (a) in the “leading pole” approximation. In an axial gauge interference terms do not contribute to leading order and the cross section takes on a simple ladder form.

(3.2.9). For example,

$$\frac{1}{\sigma_0} \left( \frac{d\sigma}{dz} \right)_{LL} = \int_{\beta}^1 \frac{1}{\sigma_0} \left( \frac{d\sigma}{dz dt} \right)_{LPA} dt = \frac{\alpha_s}{2\pi} P_{q \rightarrow qg}(z) \log(Q^2/m_g^2), \quad (3.4.13)$$

where I have taken  $\beta = m_g^2/Q^2$  and where, for the moment, I have ignored the  $t$  dependence of  $\alpha_s$ .

We will interpret (3.4.11) as the probability that a quark of invariant mass  $\sqrt{t}$  propagates and “decays” into a quark and gluon carrying  $z$  and  $(1-z)$ , respectively, of its  $(E + p_z)$ . We would like to construct final states with, for example,  $n$  gluons by multiplying the LPA probability by itself  $n$  times (i.e., independent emission) as illustrated in Fig. 3.3. Unfortunately, if we examine the contributions to the LPA probability from the three terms in (2.3.23) we

find

$$S_{11} = |B_R|^2 = 8C(1-x_1)/(1-x_2) \xrightarrow{LPA} 8C(1-z)/\hat{t}, \quad (3.4.14)$$

$$S_{22} = |A_R|^2 = 8C(1-x_2)/(1-x_1) \xrightarrow{LPA} 0, \quad (3.4.15)$$

$$\begin{aligned} S_{12} &= 2A_R B_R^* \\ &= 8C \left( \frac{2}{(1-x_1)(1-x_2)} - \frac{2}{(1-x_1)} - \frac{2}{(1-x_2)} \right) \\ &\xrightarrow{LPA} 8C \frac{2z}{(1-z)\hat{t}}, \end{aligned} \quad (3.4.16)$$

where

$$C = 4e^2 e_q^2 g_s^2, \quad (3.4.17)$$

and where the terms were calculated using the Feynman gauge. The sum of the three terms, of course, reproduces the LPA result in (3.4.10). However, since the interference term (3.4.16) contributes to the result, it appears as if we cannot simply multiply the probabilities of successive emissions. If interference terms are present then we must add the amplitudes and then square. It does not seem as if we have “independent” emission. These interference terms would correspond to diagrams in which the gluons in the ladder in Fig. 3.3b are crossed.

However, each of the three terms,  $S_{11}$ ,  $S_{22}$ , and  $S_{12}$  are gauge dependent. Only the sum is gauge independent. We can move the contributions around so that, for example,  $S_{11}$  alone contains the complete LPA approximation and the interference term does not contribute at leading order. In an axial gauge, the sum over gluon polarization states is replaced by

$$\sum_{\lambda} \epsilon_{\mu}(\lambda) \epsilon_{\nu}^*(\lambda) = -g_{\mu\nu} + \frac{n_{\mu} k_{\nu} + n_{\nu} k_{\mu}}{(n \cdot k)} - \frac{n^2 k_{\mu} k_{\nu}}{(n \cdot k)^2}, \quad (3.4.18)$$

where  $k$  is the gluon momentum and  $n_{\mu}$  is an arbitrary 4-vector satisfying

$$n \cdot n = 0, \quad (3.4.19)$$

(usually one takes  $n^2 = 0$  as well). With the choice, for example, of

$$n = q - p_2/x_2, \quad (3.4.20)$$

we have

$$S_{11} = 8C \frac{1+x_2^2}{(1-x_1)(1-x_2)} \xrightarrow{LPA} 8C \frac{1+z^2}{(1-z)\hat{t}}, \quad (3.4.21)$$

$$S_{22} = 8C \frac{1-x_1}{(1-x_2)} \xrightarrow{LPA} 0, \quad (3.4.22)$$

$$S_{12} = 8C \frac{-2}{(1-x_2)} \xrightarrow{LPA} 0, \quad (3.4.23)$$

where  $C$  is given by (3.4.17). In this gauge (and in any axial gauge) the cross

section for the emissions of  $n$  gluons in the LPA approximation has the simple ladder structure shown in Fig. 3.3b and the probability of emitting  $n$  gluons becomes the product of each emission,

$$\left( \frac{d\sigma/\sigma_0}{dz_1 \dots dz_n dt_1 \dots dt_n} \right)_{\text{LPA}} = \left[ \frac{\alpha_s(t_1)}{2\pi t_1} P_{q \rightarrow qg}(z_1) \right] \left[ \frac{\alpha_s(t_2)}{2\pi t_2} P_{q \rightarrow qg}(z_2) \right] \dots \left[ \frac{\alpha_s(t_n)}{2\pi t_n} P_{q \rightarrow qg}(z_n) \right], \quad (3.4.24)$$

where  $P_{q \rightarrow qg}(z)$  is given by (3.4.12) and where the invariant masses are ordered according to

$$Q^2 \geq t_1 \geq t_2 \geq \dots \geq t_{n-1} \geq t_n, \quad (3.4.25)$$

or

$$1 \geq \hat{t}_1 \geq \hat{t}_2 \geq \dots \geq \hat{t}_{n-1} \geq \hat{t}_n. \quad (3.4.26)$$

The interference terms are non-leading.

It is easy to generalize the LPA cross section in (3.4.24) to include all possibilities. The LPA probability for a parton of type  $j$  (quark, antiquark, or gluon) with invariant mass  $\sqrt{t}$  to propagate and “decay” into partons of type  $j_1$  and  $j_2$  carrying fractions  $z$  and  $(1-z)$ , respectively, of its  $(E + p_z)$  is given by

$$\frac{\alpha_s(t)}{2\pi t} P_{j \rightarrow j_1 j_2}(z), \quad (3.4.27)$$

where the “splitting function”  $P_{q \rightarrow qg}(z)$  is given by (3.4.12) and

$$P_{q \rightarrow qg}(z) = P_{q \rightarrow qg}(1-z), \quad (3.4.28)$$

$$P_{q \rightarrow q\bar{q}}(z) = \frac{1}{2}(z^2 + (1-z)^2), \quad (3.4.29)$$

$$P_{g \rightarrow gg}(z) = \frac{6(1-z+z^2)^2}{z(1-z)}. \quad (3.4.30)$$

The “splitting function”  $P_{g \rightarrow gg}(z)$  will be derived in Chapter 4 but the calculation of  $P_{q \rightarrow q\bar{q}}(z)$  will be left as an exercise for the reader. The LPA cross section (or probability) of any final state configuration of quarks, antiquarks, and gluons is given by the product of the probabilities for each individual emission. Thus

$$\left( \frac{d\sigma/\sigma_0}{dz_1 \dots dz_n dt_1 \dots dt_n} \right)_{\text{LPA}} = \left[ \frac{\alpha_s(t_1)}{2\pi t_1} P_1(z_1) \right] \left[ \frac{\alpha_s(t_2)}{2\pi t_2} P_2(z_2) \right] \dots \left[ \frac{\alpha_s(t_n)}{2\pi t_n} P_n(z_n) \right], \quad (3.4.31)$$

where  $P_j(z)$  are the appropriate  $P_{j \rightarrow j_1 j_2}(z)$  functions and where the invariant masses are ordered according to (3.4.25).

It is now easy to obtain the precise form of the leading log terms in the perturbation series and to sum these terms to all orders. For simplicity I will take the non-singlet fragmentation function in (3.3.14) which corresponds to

the LPA cross section in (3.4.24) and I will include in the sum all subprocess in which the final quark in Fig. 3.3 has an invariant mass squared greater than some cut-off,  $t_c$ . The first term in the series is simply

$$D_{NS}^h(z, Q^2) = D_{NS}^h(z, t_c) + \dots, \quad (3.4.32)$$

and corresponds to no emitted gluons. The next term involves one gluon emission

$$\frac{1}{\sigma_0} \frac{d\sigma}{dz} = P_{q \rightarrow qg}(z) \int_{t_c}^1 \frac{\alpha_s(t)}{2\pi t} dt, \quad (3.4.33)$$

where

$$\alpha_s(t) = \frac{4\pi}{\beta_0 \log(t/\Lambda^2)}, \quad (3.4.34)$$

with  $\beta_0$  given by (1.2.19). To integrate (3.4.33) we change variables to

$$\kappa = \frac{2}{\beta_0} \log\{\alpha_s(t_c)/\alpha_s(t)\}, \quad (3.4.35)$$

so that

$$\frac{d\kappa}{dt} = \frac{\alpha_s(t)}{2\pi t}, \quad (3.4.36)$$

and the integral becomes

$$\int_0^\kappa d\kappa = \kappa. \quad (3.4.37)$$

The series now becomes

$$D_{NS}^h(z, Q^2) = D_{0,NS}^h + \kappa P_{q \rightarrow qg} * D_{0,NS}^h + \dots, \quad (3.4.38)$$

where I am using the convolution notation defined in (3.3.11) and where

$$D_{0,NS}^h = D_{NS}^h(z, t_c). \quad (3.4.39)$$

The next term arises from the emission of two gluons

$$\frac{1}{\sigma_0} \frac{d\sigma}{dz_1 dz_2} = P_{q \rightarrow qg}(z_1) P_{q \rightarrow qg}(z_2) \int_{t_c}^1 \frac{\alpha(t_1)}{2\pi t_1} dt_1 \int_{t_c}^{t_1} \frac{\alpha(t_2)}{2\pi t_2} dt_2. \quad (3.4.40)$$

After changing variables to  $\kappa$  we are left with the “nested” integral

$$\int_0^\kappa d\kappa_1 \int_0^{\kappa_1} d\kappa_2 = \frac{1}{2}\kappa^2. \quad (3.4.41)$$

The factor of  $1/2$  is crucial and arises because of the way the integrals are “nested” (the area of the triangle formed by dividing a square along its diagonal is  $1/2$  the area of the square). The series now becomes

$$D_{NS}^h(z, Q^2) = D_{0,NS}^h + \kappa P_{q \rightarrow qg} * D_{0,NS}^h + \frac{1}{2}\kappa^2 P_{q \rightarrow qg} * P_{q \rightarrow qg} * D_{0,NS}^h + \dots. \quad (3.4.42)$$

It is easy to see that the series is that of an exponential. The  $n$ -th term involves

the nested integral

$$\int_0^\kappa dk_1 \int_0^{k_1} dk_2 \dots \int_0^{k_{n-1}} dk_n = \frac{\kappa^n}{n!}, \quad (3.4.43)$$

and the infinite sum becomes

$$D_{NS}^h(z, Q^2) = \exp(\kappa P_{q \rightarrow gg} * D_{NS}^h(t_c)), \quad (3.4.44)$$

where

$$\exp(\kappa P_{q \rightarrow gg} *) \equiv e^{\kappa P_{q \rightarrow gg} *} = \sum_{n=0}^{\infty} \frac{(\kappa P_{q \rightarrow gg} *)^n}{n!}. \quad (3.4.45)$$

Equation (3.4.44) allows us to calculate  $D_{NS}^h(z, Q^2)$  in terms of its value at the reference point  $t_c = Q_0^2$  (provided  $Q > Q_0$ ) and is accurate so long as the cut-off,  $t_c$ , is large enough so that  $\alpha_s(t_c)$  is small and hence perturbation theory is valid. If we differentiate (3.4.44) with respect to  $\kappa$  we get

$$\frac{dD_{NS}^h(z, Q^2)}{d\kappa} = P_{q \rightarrow gg} * D_{NS}^h(Q^2), \quad (3.4.46)$$

or

$$\begin{aligned} \frac{dD_{NS}^h(z, Q^2)}{d\tau} &= \frac{\alpha_s(Q^2)}{2\pi} P_{q \rightarrow gg} * D_{NS}^h(Q^2) \\ &= \frac{\alpha_s(Q^2)}{2\pi} \int_z^1 \frac{dy}{y} P_{q \rightarrow gg}(y) D_{NS}^h(z/y, Q^2), \end{aligned} \quad (3.4.47)$$

where

$$\tau = \log(Q^2/\Lambda^2), \quad (3.4.48)$$

and

$$\frac{d\kappa}{d\tau} = \frac{\alpha_s}{2\pi}. \quad (3.4.49)$$

Equation (3.4.47) is the usual Altarelli-Parisi<sup>12</sup> form of the equation that govern the  $Q^2$  evolution of the non-singlet fragmentation function  $D_{NS}^h(z, Q^2)$ .<sup>13</sup> The solution of (3.4.47) is (3.4.44). At leading log order the “little  $f$ ” functions do not contribute.

In (3.4.44) we have succeeded in separating the perturbative part,  $e^{\kappa P_{q \rightarrow gg} *}$ , (i.e., the gluon ladder in Fig. 3.3b) from the non-perturbative part,  $D_{NS}^h(z, t_c)$ , which described the shaded blob in Fig. 3.3b. The fragmentation function  $D_{NS}^h(z, t_c)$  involves momenta scales less than the cut-off  $t_c$ . Previously we called this function  $\overline{D}_{0,NS}^h(z)$  or  $D_{0,NS}^h(z)$  and we were not careful in its definition. The parton model fragmentation functions in (3.1.42) can be used to parameterize the uncalculable  $D_{NS}^h(z, t_c)$  functions.

It is not difficult to deduce the equations that govern the  $Q^2$  dependence of the individual quark and gluon fragmentation functions. From (3.3.12) we have

$$D_q^h(z, Q^2) = \overline{D}_{0,q}^h * \left( 1 + \frac{\alpha_s}{2\pi} P_{q \rightarrow gg} \log(Q^2/\Lambda^2) \right)$$

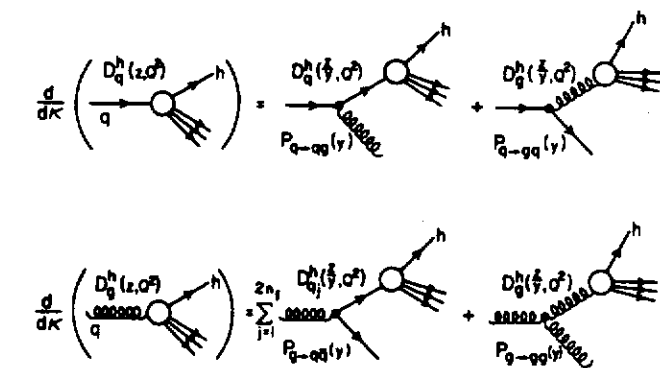


**Figure 3.4** Illustrates that the leading order rate of change of the quark fragmentation function,  $D_q^h(z, Q^2)$ , with respect to  $\kappa$  is generated by the two terms that arise when the quark radiates a gluon. The observed hadron can originate from the resulting quark jet or the resulting gluon jet. Similarly the leading order rate of change of the gluon fragmentation function,  $D_g^h(z, Q^2)$ , with respect to  $\kappa$  is generated by two terms. The incident gluon can produce a quark-antiquark pair that fragment into the observed hadron or it can radiate a gluon which fragments into the observed hadron.

$$+ \overline{D}_{0,g}^h * \left( \frac{\alpha_s}{2\pi} P_{g \rightarrow gg} \log(Q^2/\Lambda^2) \right) \quad (3.4.50)$$

and similarly

$$\begin{aligned} D_g^h(z, Q^2) &= \overline{D}_0^h * \left( 1 + \frac{\alpha_s}{2\pi} P_{g \rightarrow gg} \log(Q^2/\Lambda^2) \right) \\ &+ \sum_{j=1}^{2n_f} \overline{D}_{0,gj}^h * \left( \frac{\alpha_s}{2\pi} P_{g \rightarrow gg} \log(Q^2/\Lambda^2) \right), \end{aligned} \quad (3.4.51)$$

where the mass singularities have been absorbed into the unknown  $\overline{D}_0^h$  functions and the “little  $f$ ” functions have been dropped since they produce corrections beyond leading order. The summation runs from 1 to  $2n_f$  since it includes both quarks and antiquarks.

Differentiating (3.4.50) and (3.4.51) with respect to  $\tau$  defined in (3.4.48) and keeping only leading order gives

$$\frac{dD_q^h(z, Q^2)}{d\tau} = \frac{\alpha_s(Q^2)}{2\pi} \{ P_{q \rightarrow gg} * D_q^h(Q^2) + P_{g \rightarrow gg} * D_g^h(Q^2) \}, \quad (3.4.52)$$

$$\frac{dD_g^h(z, Q^2)}{d\tau} = \frac{\alpha_s(Q^2)}{2\pi} \left\{ \sum_{j=1}^{2n_f} P_{g \rightarrow q\bar{q}} * D_{qj}^h(Q^2) + P_{g \rightarrow gg} * D_g^h(Q^2) \right\}, \quad (3.4.53)$$

which because of (3.4.49) can be written as

$$\frac{dD_q^h(z, Q^2)}{d\kappa} = P_{q \rightarrow gg} * D_q^h(Q^2) + P_{q \rightarrow gg} * D_g^h(Q^2), \quad (3.4.54)$$

$$\frac{dD_g^h(z, Q^2)}{d\kappa} = \sum_{j=1}^{2n_f} P_{g \rightarrow q\bar{q}} * D_{qj}^h(Q^2) + P_{g \rightarrow gg} * D_g^h(Q^2), \quad (3.4.55)$$

and is illustrated in Fig. 3.4. These coupled differential equations are solved by defining a “singlet” fragmentation function

$$D_s^h(z, Q^2) = \sum_{i=1}^{n_f} [D_{qi}^h(z, Q^2) + D_{q\bar{q}}^h(z, Q^2)], \quad (3.4.56)$$

in addition to the “non-singlet” distribution already defined by (3.3.14). The singlet and gluon equations can be written in matrix form as

$$\frac{d\mathbf{D}^h(z, Q^2)}{d\kappa} = \mathbf{P} * \mathbf{D}^h(Q^2), \quad (3.4.57)$$

where

$$\mathbf{D}^h(z, Q^2) = \begin{pmatrix} D_s^h(z, Q^2) \\ D_g^h(z, Q^2) \end{pmatrix}, \quad (3.4.58)$$

and

$$\mathbf{P}(y) = \begin{pmatrix} P_{q \rightarrow gg}(y) & 2n_f P_{q \rightarrow gg}(y) \\ P_{g \rightarrow q\bar{q}}(y) & P_{g \rightarrow gg}(y) \end{pmatrix}. \quad (3.4.59)$$

The non-singlet satisfies the equation,

$$\frac{dD_{NS}^h(z, Q^2)}{d\kappa} = P_{q \rightarrow gg} * D_{NS}^h(Q^2). \quad (3.4.60)$$

The formal solutions of these equations are

$$\mathbf{D}^h(z, Q^2) = \exp(\kappa \mathbf{P} *) \mathbf{D}^h(t_c), \quad (3.4.61)$$

and

$$D_{NS}^h(z, Q^2) = \exp(\kappa P_{q \rightarrow gg} *) D_{NS}^h(t_c), \quad (3.4.62)$$

respectively. These equations relate the fragmentation functions at  $Q^2$  to those at the reference point  $t_c = Q_0^2$ .

The leading order  $Q^2$  evolution formulas do not depend on the “little  $f$ ” functions  $f_q(y)$  and  $f_g(y)$ . However, as we will see in more detail in Chapter 6 these terms do play a role in next order. Combining (3.3.13) and (3.3.15)

gives

$$D_{NS}^h(z, Q^2) = \overline{D}_{0,NS}^h + \frac{\alpha_s}{2\pi} \log(Q^2/\Lambda^2) \overline{D}_{0,NS}^h * P_{q \rightarrow gg} + \alpha_s \overline{D}_{0,NS}^h * f_q, \quad (3.4.63)$$

for the non-singlet fragmentation function, where  $f_q = f_q^{e^+ e^-}$  is process and scheme dependent. The change of  $D_{NS}^h(z, Q^2)$  with respect to  $\alpha_s$  is given by

$$\frac{dD_{NS}^h(z, Q^2)}{d\alpha_s} = \frac{1}{2\pi} \log(Q^2/\Lambda^2) D_{NS}^h * P_{q \rightarrow gg} + D_{NS}^h * f_q, \quad (3.4.64)$$

and in higher orders one has

$$\frac{dD_{NS}^h(z, Q^2)}{d\alpha_s} = [\tau(P/2\pi + \alpha_s R + \dots) + (f + \alpha_s g + \dots)] * D_{NS}^h, \quad (3.4.65)$$

where  $P = P_{q \rightarrow gg}$ ,  $f = f_q$ , and  $\tau = \log(Q^2/\Lambda^2)$ . The terms in (3.4.65) containing a factor of  $\tau$  are process independent but may depend on the regularization scheme. They arise from the mass singularities. The “constant terms” (i.e.,  $f(y)$ ,  $g(y)$ , etc.) are, in general, process and regularization scheme dependent. To compute the rate of change of  $D_{NS}^h$  with respect to  $\log(Q^2)$  we use perturbation theory (in  $\alpha_s$ ) to deduce how  $D_{NS}^h$  changes with  $\alpha_s$  but then we must include the fact that  $\alpha_s$  itself depends on  $\log(Q^2)$  according to

$$-\frac{d\alpha_s}{d\tau} = b_0 \alpha_s^2 + b_1 \alpha_s^3 + \dots, \quad (3.4.66)$$

where  $b_0 = \beta_0/(4\pi)$  with  $\beta_0$  given in (1.2.19) and where  $b_1$  will be given in Chapter 6. Since QCD is a renormalizable theory a change in the ultraviolet cut-off,  $M_{cut}$ , is related to a change in the coupling  $\alpha_s$ . If one neglects quark masses then the lagrangian in QCD is scale invariant so that changing  $Q$  and  $M_{cut}$  together makes no change. Therefore, a change in  $Q$  can be related to a certain change in  $\alpha_s$  and one arrives at a type of “renormalization group” equation,

$$\frac{dD_{NS}^h(z, Q^2)}{d\tau} = \frac{dD_{NS}^h(z, Q^2)}{d\alpha_s} \left( \frac{d\alpha_s}{d\tau} \right). \quad (3.4.67)$$

Inserting (3.4.65) and (3.4.66) into (3.4.67) and keeping terms to order  $\alpha_s^2$  gives

$$\begin{aligned} \frac{dD_{NS}^h(z, Q^2)}{d\tau} &= \frac{\alpha_s}{2\pi} b_0 (\tau \alpha_s) P * D_{NS}^h(Q^2) \\ &+ b_0 \alpha_s^2 \left[ (\tau \alpha_s) R + f + \left( \frac{b_1}{2\pi b_0} \right) (\tau \alpha_s) P \right] * D_{NS}^h(Q^2), \end{aligned} \quad (3.4.68)$$

where  $(\tau \alpha_s)$  is of order 1. Since the  $Q^2$  dependence of the fragmentation function is an observable, it must be that the right hand side of (3.4.68) is regularization scheme independent. This is true since even though  $f$  and  $R$  are scheme dependent, the combination of  $R$  and  $f$  that appears in (3.4.68)

is not. In leading order  $\tau\alpha_s = 1/b_0$  and (3.4.68) becomes

$$\frac{dD_{NS}^h(z, Q^2)}{d\tau} = \frac{\alpha_s}{2\pi} P * D_{NS}^h(Q^2), \quad (3.4.69)$$

which is the same as (3.4.47).

### 3.5 The Convolution Method

Equations (3.4.52) and (3.4.53) can be solved numerically by a variety of methods. One method involves taking the moments of the fragmentation functions. The convolutions then become a product of moments and the solution is then straightforward. This method will be discussed in Chapter 4 for the parton distribution functions and can be applied equally well for the fragmentation functions.

Alternatively one can attempt to evaluate (3.4.62) directly. Namely,

$$\begin{aligned} D_{NS}^h(z, Q^2) &= \exp(\kappa P_{q \rightarrow gg} * D_{NS}^h(Q_0^2)) \\ &= D_{NS}^h(Q_0^2) + \kappa P_{q \rightarrow gg} * D_{NS}^h(Q_0^2) \\ &\quad + \frac{1}{2}\kappa^2 P_{q \rightarrow gg} * P_{q \rightarrow gg} * D_{NS}^h(Q_0^2) + \dots, \end{aligned} \quad (3.5.1)$$

Table 3.1 shows that  $\kappa$  is quite small provided  $Q^2$  is not too large so one might think that summing the full series in (3.5.1) is unnecessary and that the first two terms would provide a sufficiently accurate result. Unfortunately, due to the behavior of  $P_{q \rightarrow gg}(y)$  this is not the case and one must sum the complete series.

Table 3.1. Values of  $\alpha_s$  and  $\kappa$  versus  $Q$  with  $\Lambda = 0.2 \text{ GeV}$ ,  $Q_0 = 2 \text{ GeV}$  and  $n_f = 4$ .

$Q(\text{GeV})$	$Q^2(\text{GeV}^2)$	$\alpha_s$	$\kappa$
2	4	0.327	0
4	16	0.252	0.063
10	100	0.193	0.127
50	2,500	0.137	0.210
100	10,000	0.121	0.238
500	250,000	0.096	0.314

Suppose we keep only the first two terms in (3.5.1), then from (E.3.7) we

see that as  $z \rightarrow 1$ ,

$$\frac{D_{NS}^h(z, Q^2)}{D_{NS}^h(z, Q_0^2)} \underset{z \rightarrow 1}{\approx} 1 + \kappa \log(1 - z). \quad (3.5.2)$$

No matter how small  $\kappa$  is,  $\log(1 - z)$  becomes large as  $z \rightarrow 1$  so that one must include higher and higher terms in  $\kappa$ . This behavior arises because of the  $1/(1-y)_+$  term in  $P_{q \rightarrow gg}(y)$ . Perhaps we can find another function,  $P_A(y)$  with the same singularity structure as  $y \rightarrow 1$ , but which we can explicitly do the sum

$$\exp(\kappa P_A * D_{NS}^h) \equiv R * D_{NS}^h. \quad (3.5.3)$$

It is not hard to find such a function. Consider the function

$$P_A(y) = \frac{4}{3} \left( \frac{2}{-\log(y)} \right)_+. \quad (3.5.4)$$

This function has the property that its moments are

$$A_n = \int_0^1 dy y^{n-1} P_A(y) = -\frac{8}{3} \log(n), \quad (3.5.5)$$

so that

$$R_n = \int_0^1 dy y^{n-1} R(y) = \exp[-\frac{8}{3} \kappa \log(n)] = n^{-\frac{8}{3} \kappa}. \quad (3.5.6)$$

All we need to do is to solve (3.5.6) for  $R(y)$ . Using

$$\int_0^1 dy y^{n-1} (-\log(y))^P = \frac{\Gamma(P+1)}{n^{P+1}}, \quad (3.5.7)$$

we arrive at

$$R(y) = \frac{(-\log(y))^{\frac{8}{3} \kappa - 1}}{\Gamma(\frac{8}{3} \kappa)},$$

where  $R$  is defined in (3.5.3). Equation (3.5.1) can now be written

$$\begin{aligned} D_{NS}^h(z, Q^2) &= \exp(\kappa P_{q \rightarrow gg} * D_{NS}^h(Q_0^2)) \\ &= \exp(\kappa P_A * \exp(\kappa P_\Delta * D_{NS}^h(Q_0^2))) \\ &= R * \exp(\kappa P_\Delta * D_{NS}^h(Q_0^2)), \end{aligned} \quad (3.5.8)$$

where

$$P_\Delta(y) = P_{q \rightarrow gg}(y) - P_A(y) = \frac{4}{3} \left[ \left( \frac{1+y^2}{1-y} \right)_+ - \frac{2}{(-\log(y))_+} \right]. \quad (3.5.9)$$

Since  $P_A(y)$  and  $P_{q \rightarrow gg}(y)$  have the same singularity structure as  $y \rightarrow 1$  (i.e.,  $-\log(y) \sim 1-y$ ),  $P_\Delta(y)$  is well behaved and one can remove the “+” functions”

leaving

$$P_\Delta(y) = \frac{4}{3} \left[ \frac{1+y^2}{1-y} + \frac{2}{\log(y)} + (\frac{3}{2} - 2\gamma_E) \delta(1-y) \right], \quad (3.5.10)$$

where  $\gamma_E$  is Eulers constant (see Appendix E). We can now expand  $\exp(\kappa P_\Delta)$  in (3.5.8) and keep only the first two terms. This gives

$$D_{NS}^h(z, Q^2) = R * D_{NS}^h(Q_0^2) + \kappa R * P_\Delta * D_{NS}^h(Q_0^2) + O(\kappa^2). \quad (3.5.11)$$

Defining

$$\begin{aligned} \tilde{D}_{NS}^h(z, Q^2) &\equiv R * D_{NS}^h(z, Q_0^2) \\ &= \int_z^1 \frac{dy}{y} D_{NS}^h(z/y, Q_0^2) \frac{(-\log(y))^{\frac{8}{3}\kappa-1}}{\Gamma(\frac{8}{3}\kappa)}, \end{aligned} \quad (3.5.12)$$

we arrive at

$$D_{NS}^h(z, Q^2) = \tilde{D}_{NS}^h(z, Q^2) + \kappa \int_z^1 \frac{dy}{y} \tilde{D}_{NS}^h(z/y, Q^2) P_\Delta(y) + O(\kappa^2), \quad (3.5.13)$$

where  $P_\Delta(y)$  is given by (3.5.10) and  $\kappa$  is defined in (3.4.35). Using this equation one can calculate  $D_{NS}^h(z, Q^2)$  from a main term,  $\tilde{D}_{NS}^h$ , and a correction term that is proportional to  $\kappa$ . Equation (3.5.13) is not exact but is very accurate even for  $\kappa$  as big as  $1/3$  (see Table 3.1). Of course, if the first correction term is not small then one can calculate the order  $\kappa^2$  correction term as well.

We see that in order to compute  $D_{NS}^h(z, Q^2)$  we need to know the fragmentation function at a reference momentum  $Q_0^2$ ,  $D_{NS}^h(z', Q_0^2)$ , for values of  $z'$  in the range  $z \leq z' \leq 1$ . In addition, we need to know  $\kappa$  which is calculated from the knowledge of  $\alpha_s(Q^2)$  which in turn depends on the QCD parameter  $\Lambda$ . Thus, given  $D_{NS}^h(z, Q_0^2)$  the one parameter  $\Lambda$  governs the  $Q^2$  evolution.

The  $Q^2$  evolution of the singlet and gluon fragmentation functions is a bit more complicated. As can be seen from (3.4.61)  $D_s^h(z, Q^2)$  depends on both  $D_s^h(z, Q_0^2)$  and  $D_g^h(z, Q_0^2)$ . Similarly  $D_g^h(z, Q^2)$  depends on both  $D_g^h(z, Q_0^2)$  and  $D_s^h(z, Q_0^2)$ . The manner in which this mixing occurs is governed by the matrix  $P(y)$  in (3.4.59). Equation (3.5.8) is not valid in this case since the matrices  $P_A$  and  $P_\Delta$  do not commute. In this case we write (3.4.57) as

$$\frac{dD^h(x, Q^2)}{d\kappa} = (P_A + P_\Delta) * D^h(Q^2), \quad (3.5.14)$$

where

$$P_A = \begin{pmatrix} a_q P_0 & 0 \\ 0 & a_g P_0 \end{pmatrix}, \quad (3.5.15)$$

with

$$P_0(y) = \frac{1}{(-\log(y))_+} \quad (3.5.16)$$

and

$$a_q = \frac{8}{3}, \quad a_g = 6. \quad (3.5.17)$$

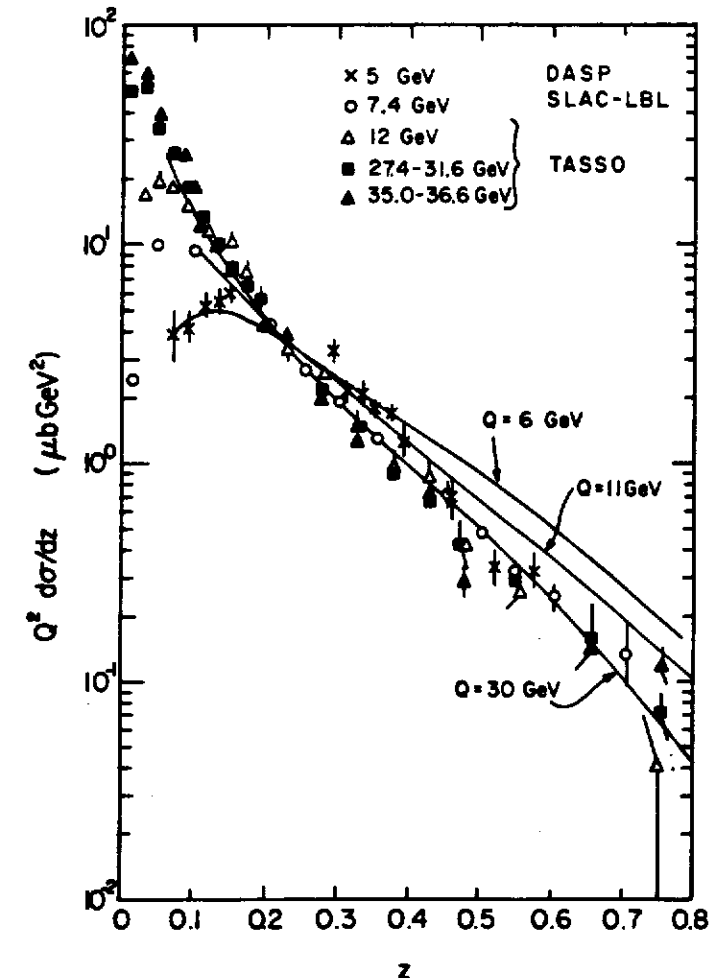


Figure 3.5 Data on the  $Q^2$  dependence of the charged pion fragmentation function compared with QCD predictions (taken from Ref. 14).

With this choice,

$$P_\Delta = P - P_A = \begin{pmatrix} P_{\Delta q}(y) & 2n_f P_{q \rightarrow gq}(y) \\ P_{g \rightarrow qq}(y) & P_{\Delta g}(y) \end{pmatrix}, \quad (3.5.18)$$

where

$$P_{\Delta q}(y) = P_{q \rightarrow q}(y) - a_q P_0(y) = P_\Delta(y), \quad (3.5.19)$$

with  $P_\Delta(y)$  given in (3.5.9) and

$$\begin{aligned} P_{\Delta g}(y) &= P_{g \rightarrow gg}(y) - a_g P_0(y) \\ &= 6 \left\{ \frac{y}{1-y} + \frac{1}{\log(y)} + \frac{1-y}{y} + y(1-y) \right. \\ &\quad \left. + \left( \frac{11}{12} - \frac{1}{18} n_f - \gamma_E \right) \delta(1-y) \right\}. \end{aligned} \quad (3.5.20)$$

To order  $\kappa$  the solution of (3.5.14) is given by

$$\begin{aligned} D^h(z, Q^2) &= \exp(\kappa P_A*) D^h(Q_0^2) \\ &\quad + \kappa \int d\rho \exp[\rho \kappa P_A*] P_\Delta \exp[(1-\rho)\kappa P_A*] D^h(Q_0^2), \end{aligned} \quad (3.5.21)$$

which can easily be seen to yield

$$\begin{aligned} D_{q_i}^h(z, Q^2) &= \tilde{D}_{q_i}^h(a_q, z, Q^2) + \kappa \int_z^1 \frac{dy}{y} \tilde{D}_{q_i}^h(a_q, z/y, Q^2) P_{g \rightarrow gg}(y) \\ &\quad + \kappa \int_z^1 \frac{dy}{y} \tilde{D}_g^h(z/y, Q^2) P_{g \rightarrow gg}(y), \end{aligned} \quad (3.5.22)$$

$$\begin{aligned} D_g^h(z, Q^2) &= \tilde{D}_g^h(a_g, z, Q^2) + \kappa \int_z^1 \frac{dy}{y} \tilde{D}_g^h(a_g, z/y, Q^2) P_{\Delta g}(y) \\ &\quad + \kappa \sum_{j=1}^{2n_f} \int_z^1 \frac{dy}{y} \tilde{D}_{q_j}^h(z/y, Q^2) P_{g \rightarrow q\bar{q}}(y), \end{aligned} \quad (3.5.23)$$

where

$$\tilde{D}_i^h(a, z, Q^2) = \int_z^1 \frac{dy}{y} D_i^h(z/y, Q_0^2) \frac{(-\log(y))^{\alpha\kappa-1}}{\Gamma(\alpha\kappa)}. \quad (3.5.24)$$

The function  $\tilde{D}_i^h$  is new and is computed by averaging  $\tilde{D}_i^h(a, z, Q^2)$  over  $a$ . Namely,

$$\tilde{D}_i^h(z, Q^2) = \frac{1}{(a_g - a_q)} \int_{a_q}^{a_g} \tilde{D}_i^h(a, z, Q^2) da. \quad (3.5.25)$$

Equations (3.5.22) and (3.5.23) express the fragmentation functions at  $Q^2$  directly in terms of those at  $Q_0^2$ . The equations are not exact since terms of order  $\kappa^2$  have been neglected. They are, however, quite accurate in the range  $0.05 \leq z \leq 1$  for  $\kappa \lesssim 0.3$ . One loses accuracy at small  $z$  due to the  $1/y$  terms in  $P_{g \rightarrow gg}(y)$  and  $P_{g \rightarrow gg}(y)$ . Figure 3.5 shows an example of the  $Q^2$  evolution of the fragmentation functions in  $e^+e^-$  annihilations.

From (3.5.22) and (3.5.23) it is easy to deduce the large  $z$  behavior of fragmentation functions since as  $z \rightarrow 1$   $D_i^h(z, Q^2)$  approaches  $\tilde{D}_i^h(a, z, Q^2)$ .

Suppose at  $Q_0^2$  we have

$$D_i^h(z, Q_0^2) = A(1-z)^P \underset{z \rightarrow 1}{\approx} A(-\log(z))^P. \quad (3.5.26)$$

In this case  $\tilde{D}_i^h(a, z, Q^2)$  can be calculated analytically yielding

$$\tilde{D}_i^h(a, z, Q^2) = A \frac{\Gamma(P+1)}{\Gamma(P+1+\alpha\kappa)} (-\log(z))^{P+\alpha\kappa} \underset{z \rightarrow 1}{\sim} C(1-z)^{P+\xi_a(Q^2)}, \quad (3.5.27)$$

where

$$\xi_a(Q^2) = \alpha\kappa. \quad (3.5.28)$$

For quarks,

$$\xi_q(Q^2) = \frac{8}{3} \frac{2}{\beta_0} \log\{\log(Q^2/\Lambda^2)/\log(Q_0^2/\Lambda^2)\}, \quad (3.5.29)$$

and for gluons,

$$\xi_g(Q^2) = 6 \frac{2}{\beta_0} \log\{\log(Q^2/\Lambda^2)/\log(Q_0^2/\Lambda^2)\}, \quad (3.5.30)$$

with  $\beta_0 = 11 - 2\gamma_F/3$ . The fragmentation functions become steeper as  $Q^2$  increases (*i.e.*, they fall off with a higher power of  $(1-z)$ ) with the gluon fragmentation function changing more rapidly since

$$\frac{\xi_g(Q^2)}{\xi_q(Q^2)} = 6 \frac{\frac{2}{3}}{\frac{2}{3}} = \frac{9}{4}. \quad (3.5.31)$$

For example, if  $D_q^h(z, Q_0^2) = D_g^h(z, Q_0^2)$  then at higher values of  $Q^2$  the gluon fragmentation function would fall off with a higher power of  $(1-z)$  as  $z \rightarrow 1$ . The difference in the power would be given by

$$\xi_g(Q^2) - \xi_q(Q^2) = (6 - \frac{8}{3})\kappa = \frac{10}{3}\kappa. \quad (3.5.32)$$

At large  $Q^2$ , gluon fragmentation functions are softer than the corresponding quark fragmentation function.

### 3.6 Jets – The Monte Carlo Method

It is relatively easy to generate Monte-Carlo events in which quarks, antiquarks, and gluons are distributed according to the leading pole formula in (3.4.31). Let us consider first the case in which quarks are allowed to radiate gluons but where the gluons do not radiate additional partons (*i.e.*, the non-singlet equation (3.4.24)).

First we must decide on a cut-off procedure. Otherwise, the Monte Carlo will produce final states containing an infinite number of partons. A massless quark given enough time will radiate an infinite number of massless gluons.

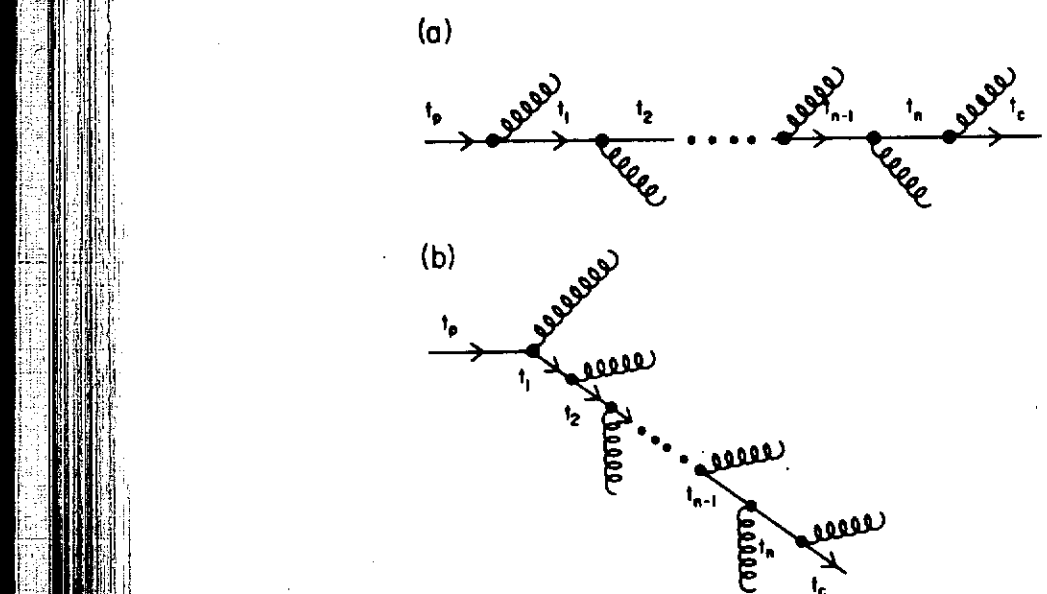


Figure 3.6 (a) Illustrates the case where an initial quark of invariant mass  $\sqrt{t_p}$  emits  $n$  unresolvably soft gluons until its invariant mass has been degraded to  $\sqrt{t_c}$ . This configuration of a quark and its accompanying soft gluons is defined as an outgoing “final state” quark. (b) Illustration of the case where one hard gluon is emitted followed by the emission of unresolvably soft gluons.

In the real world, on the other hand, quarks do not have an infinite amount of time to radiate because at some stage non-perturbative effects take over and hadrons are formed. We will use both an invariant mass cut-off,  $t_c = \mu_c^2$ , and a cut-off in  $z$ . Partons with an invariant mass less than  $\mu_c$  are allowed to propagate freely to the final state with no additional radiation. Also, we will consider partons with  $z < z_c$  as unresolvably soft.

Given a quark with a maximum possible invariant mass of  $\sqrt{t_p}$ , we must decide whether it will emit a resolvable gluon or not. Let  $\pi_q(t_p, t_c)$  be the probability that a quark of maximum invariant mass  $\sqrt{t_p}$  emits only unresolvably soft gluons (i.e.,  $z > 1 - z_c$ ) until its invariant mass has been degraded to  $\sqrt{t_c}$ . This situation is illustrated in Fig. 3.6a. To compute  $\pi_q(t_p, t_c)$  we must integrate (3.4.24) over the appropriate regions and sum over all possible gluon emissions. Namely,

$$\pi_q(t_p, t_c) = \sum_{n=0}^{\infty} \left\{ \int_{t_c}^{t_p} \frac{\alpha_s(t_1)}{2\pi t_1} dt_1 \int_{t_2}^{t_1} \frac{\alpha_s(t_2)}{2\pi t_2} dt_2 \dots \int_{t_n}^{t_{n-1}} \frac{\alpha_s(t_n)}{2\pi t_n} dt_n \right\}$$

$$\int_{z_1 > 1 - z_c} P_{q \rightarrow qg}(z_1) dz_1 \int_{z_2 > 1 - z_c} P_{q \rightarrow qg}(z_2) dz_2 \dots \int_{z_n > 1 - z_c} P_{q \rightarrow qg}(z_n) dz_n \}, \quad (3.6.1)$$

where the invariant masses are ordered according to (3.4.25) and

$$z_i = (E + p_z)_i / (E + p_z)_{i-1}. \quad (3.6.2)$$

The nested integrals over the invariant masses are the same as in (3.4.43),

$$\int_0^{\kappa_p} d\kappa_1 \int_0^{\kappa_1} d\kappa_2 \dots \int_0^{\kappa_{n-1}} d\kappa_n = \frac{\kappa_p^n}{n!}, \quad (3.6.3)$$

where  $\kappa$  is defined in (3.4.35) and

$$\kappa_p = \frac{2}{\beta_0} \log\{\alpha_s(t_c)/\alpha_s(t_p)\}. \quad (3.6.4)$$

Furthermore we know that

$$\int_0^1 P_{q \rightarrow qg}(z) dz = 0, \quad (3.6.5)$$

which means that the integration over the soft gluon region can be arrived at as follows

$$\int_{1-z_c}^1 P_{q \rightarrow qg}(z) dz = - \int_0^{1-z_c} P_{q \rightarrow qg}(z) dz \equiv -\gamma_{NS}(z_c), \quad (3.6.6)$$

with

$$\gamma_{NS}(0) = 0. \quad (3.6.7)$$

We now have

$$\pi_q(t_p, t_c) = \sum_{n=0}^{\infty} \frac{\kappa_p^n}{n!} (-\gamma_{NS}(z_c))^n = \exp[-\kappa_p \gamma_{NS}(z_c)], \quad (3.6.8)$$

or

$$\pi_q(t_p, t_c) = [\alpha_s(t_p)/\alpha_s(t_c)]^{d_{NS}}, \quad (3.6.9)$$

with

$$d_{NS} = 2\gamma_{NS}(z_c)/\beta_0. \quad (3.6.10)$$

Given that a quark does decide to produce resolvable radiation then we must produce correctly its invariant mass. Its invariant mass is given by (3.4.24) modified by possible subsequent emissions. We must calculate the invariant mass distribution for the situation shown in Fig. 3.6b in which one gluon is “hard” and all the rest are soft. We will label this distribution by  $\Xi_q(t)$ . Actually we already know this distribution because we know that if we integrate  $\Xi_q(t)$  over  $t$  from  $t_c$  to  $t_p$  we must get  $1 - \pi_q(t_p, t_c)$ . Namely,

$$\int_{t_c}^{t_p} \Xi_q(t) dt = 1 - \pi_q(t_p, t_c), \quad (3.6.11)$$

or

$$\Xi_q(t) = -\frac{d\pi_q(t, t_c)}{dt}, \quad (3.6.12)$$

which from (3.6.9) implies

$$\Xi_q(t) = \frac{\alpha_s(t)}{2\pi t} \gamma_{NS}(z_c) \pi_q(t, t_c). \quad (3.6.13)$$

The Monte-Carlo scheme proceeds as follows:

- (i) Starting with quark 1 in Fig. 3.7a we decide whether it will radiate any "resolvable" radiation. This is done by generating a random number  $r$  from 0 to 1. If  $r < \pi_q(t_p = Q^2, t_c)$  then this "quark" with its accompanying soft radiation is allowed to propagate freely and appears in the final state. If  $r > \pi_q(t_p = Q^2, t_c)$  then it is allowed to radiate and we proceed to the next step.
- (ii) If the quark does decide to radiate then its invariant mass is generated according to (3.6.13). This is done by generating another random number  $r$  from 0 to 1 and solving the following equation for  $t$ :

$$r = \frac{\int_{t_c}^t \Xi_q(t) dt}{\int_{t_c}^{t_p} \Xi_q(t) dt} = \frac{1 - \pi_q(t, t_c)}{1 - \pi_q(t_p, t_c)}. \quad (3.6.14)$$

The solution is

$$t/\Lambda^2 = (t_c/\Lambda^2)^b, \quad (3.6.15)$$

with

$$b = [(1 - r) + r\pi_q(t_p, t_c)]^{1/d_{NS}}, \quad (3.6.16)$$

and  $d_{NS}$  given in (3.6.10).

- (iii) The value of  $z$  for the decay is chosen according to the  $P_{q \rightarrow qg}(z)$  distribution in (3.4.12).
- (iv) Now quark 2 in Fig. 3.7b is examined. Its maximum invariant mass  $\sqrt{t_p}$  is equal to the previous quarks chosen invariant mass  $\sqrt{t_1}$ . Again  $\pi_q(t_p = t_1, t_c)$  is examined to decide whether or not further resolvable radiation is to be emitted. If not, then this "quark" along with its accompanying soft radiation is allowed to propagate to the final state. If radiation is to occur then the invariant mass of quark 2 is generated as in (ii).
- (v) This process is continued until all quarks have decided to generate no further resolvable radiation with  $t > t_c$ .

It is easy to generalize the prescription to include the case where gluons "decay" as well. The probability that a parton of type  $j$  (quark or gluon) and maximum invariant mass  $\sqrt{t_p}$  should evolve until it has  $\sqrt{t} < \mu_c$  emitting only unresolvably soft ( $z < z_c$  or  $z < 1 - z_c$ ) partons is given by

$$\pi_j(t_p, t_c) = \sum_{n=0}^{\infty} \left\{ \int_{t_c}^{t_p} \frac{\alpha_s(t_1)}{2\pi t_1} dt_1 \int_{t_c}^{t_1} \frac{\alpha_s(t_2)}{2\pi t_2} dt_2 \dots \right.$$

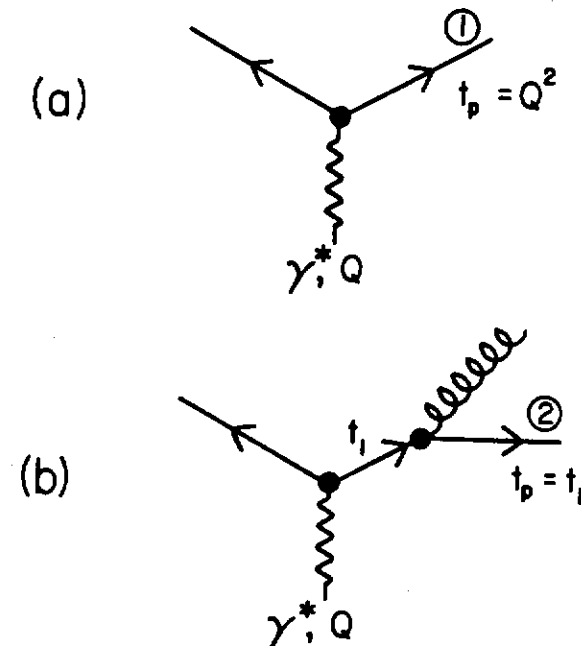


**Figure 3.7** (a) Illustration of the "decay" of a virtual photon of invariant mass  $Q$  into a quark with maximum possible invariant mass  $\sqrt{t_p} = Q$  and an antiquark. (b) Quark 1 in (a) subsequently "decays" into a gluon and quark 2 of maximum invariant mass  $\sqrt{t_p} = \sqrt{t_1}$ , where  $t_1$  is the invariant mass squared of the gluon and quark 2.

$$\int_{t_c}^{t_{n-1}} \frac{\alpha_s(t_n)}{2\pi t_n} dt_n \int_{\substack{z_2 < 1-z_c \\ z_2 > z_c}} P_{j_1 \rightarrow \text{All}}(z_1) dz_1 \quad (3.6.17)$$

$$\left. \int_{\substack{z_2 < 1-z_c \\ z_2 > z_c}} P_{j_2 \rightarrow \text{All}}(z_2) dz_2 \dots \int_{\substack{z_n < 1-z_c \\ z_n > z_c}} P_{j_n \rightarrow \text{All}}(z_n) dz_n \right\},$$

or

$$\pi_j(t_p, t_c) = [\alpha_s(t_p)/\alpha_s(t_c)]^{d_j}, \quad (3.6.18)$$

with

$$d_j = 2\gamma_j(z_c)/\beta_0, \quad (3.6.19)$$

and

$$\gamma_j(z_c) = \int_{z_c}^{1-z_c} P_{j \rightarrow \text{All}}(z) dz \quad (3.6.20)$$

$$\gamma_j(0) = 0. \quad (3.6.21)$$

Step (i) proceeds as before but using (3.6.18). Step (ii) is also the same except now the  $t$ -distribution is given by

$$\Xi_j(t) = -\frac{d\pi_j(t, t_c)}{dt}. \quad (3.6.22)$$

Having determined that parton  $j$  is to radiate, and selected its invariant mass  $t$  step (iii) is modified slightly. It becomes

(iii') The decay products  $j_1$  and  $j_2$  ( $j \rightarrow j_1 + j_2$ ) and the value of  $z$  is determined according to (3.4.27).

The partons  $j_1$  and  $j_2$  are allowed to evolve as was parton  $j$ , and the cascade continues until all partons have chosen to generate no further resolvable radiation with  $t > t_c$ .

Parton showers generated in this manner can be viewed almost classically. “Virtual” partons will live for a time,  $\Delta\tau$ , determined by the degree to which they are off-shell,

$$\Delta\tau \sim 1/\Delta E \sim (E + |\vec{p}|)/t \sim p/t, \quad (3.6.23)$$

and then “decay”, where  $p$  and  $t$  are the magnitude of the momentum and invariant mass squared, respectively, of the parton. The time for the emission of a gluon is roughly  $1/p$ , so as long as

$$1/p \ll p/t \quad (3.6.24)$$

the independent emission (LPA) assumption is accurate. Equation (3.6.24) is satisfied except perhaps at early times where  $t \sim Q^2$ . The development of a parton shower is illustrated in Fig. 3.8. At early times (short distances) invariant masses are large (on the order of  $Q$ ). Here interferences are important and gluons may be emitted at large angles where the LPA formula is not accurate. One can correct for this by using (at this stage) the complete order  $\alpha_s$  formula in (3.4.9). At later times the invariant masses of the partons are smaller (because they are ordered as in (3.4.25)) and the angles of emission are small. In this region one is justified in assuming independent emission, interferences are not important and the LPA approach correctly describes the development. At even longer times the invariant masses become small and comparable to  $\Lambda$ . Here  $\alpha_s(t)$  is large, non-perturbative effects dominate, and the hadrons are formed. Presumably in this region interference effects are also important. Fig. 3.9 shows an  $e^+e^-$  event at  $Q = 100$  GeV generated from a QCD parton-shower Monte Carlo Model.

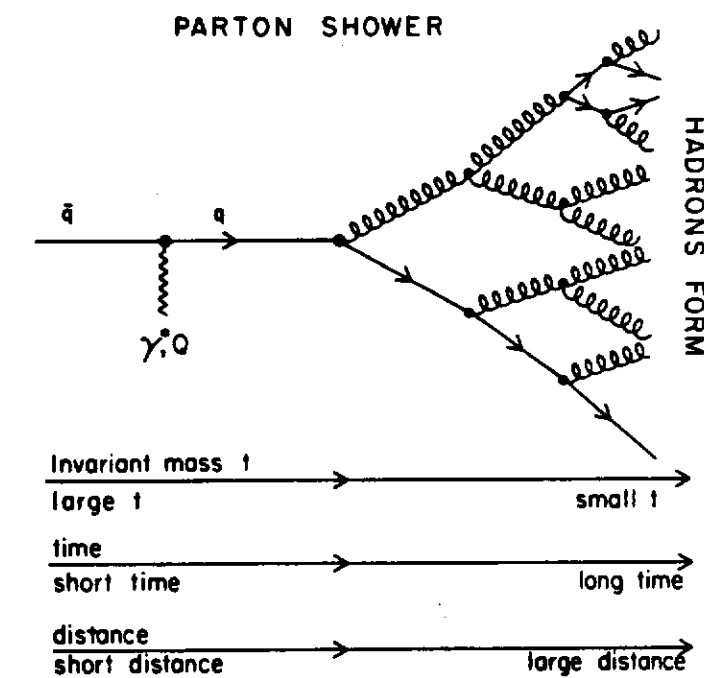


**Figure 3.8** Illustration of the development of a “parton shower” initiated by the “decay” of a virtual photon of invariant mass,  $Q$ , into a quark-antiquark pair. From left to right time and distance increase while the invariant masses of the partons decrease. Finally, when the invariant masses of the partons become comparable to the perturbative parameter  $\Lambda$  hadrons are formed.

### 3.7 Jets – Analytic Results

In addition to the Monte Carlo methods discussed in the previous section, one can perform analytic calculations using the leading pole formula in (3.4.31). For example, suppose we are interested in the small  $z$  behavior of quark and gluon jets. Let us define

$P_n^q(t_p, t_c, z_0) =$  the probability that quark with maximum invariant mass,  $\sqrt{t_p}$ , emits  $n$  gluons (as in Fig. 3.6) each of which has its  $(k_0 + k_z) \geq z_0 Q/2$  while the quark invariant mass is degraded to  $\sqrt{t_c}$ . (3.7.1)

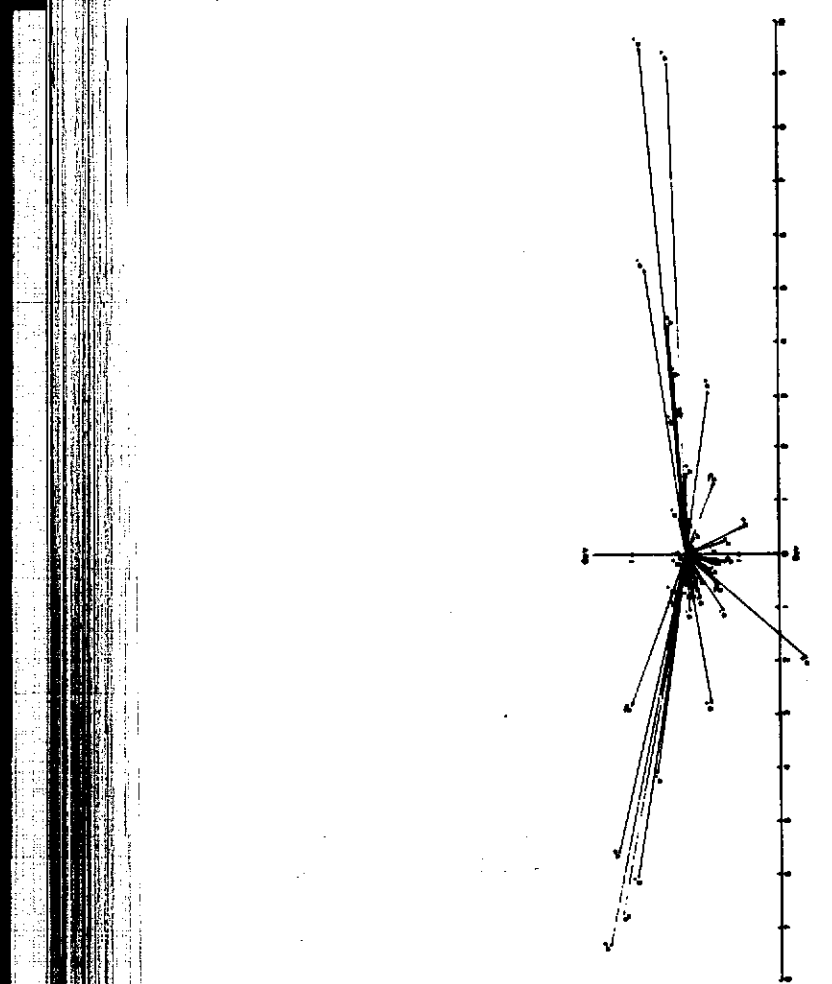


**Figure 3.9** An event at  $Q = 100$  GeV generated from a QCD parton-shower Monte Carlo model. The event contains a  $c\bar{c}$ ,  $d\bar{d}$ , and  $s\bar{s}$  quark pair together with 14 gluons resulting in 47 particles with 32 charged ( $\pi^0 = 7$ ,  $\pi^+ = 10$ ,  $\pi^- = 12$ ,  $K^+ = 6$ ,  $K^0 = 2$ ,  $K^- = 3$ ,  $\bar{K}^0 = 5$ ,  $\nu_\mu = 1$ ,  $\mu^- = 1$ ).

Similarly  $P_n^g(t_p, t_c, z_0)$  is the probability that a gluon emits  $n$  gluons each of which has  $(k_0 + k_i) \geq z_0 Q/2$ . We will consider only the case where  $z_0 \ll 1$  so that we can approximate (3.4.12) and (3.4.30) by

$$P_{g \rightarrow gg}(z) \underset{z \rightarrow 0}{\approx} \left(\frac{8}{3}\right) \frac{1}{z} = a_g \frac{1}{z}, \quad (3.7.2)$$

$$P_{g \rightarrow gg}(z) \underset{z \rightarrow 0}{\approx} (6) \frac{1}{z} = a_g \frac{1}{z}, \quad (3.7.3)$$

respectively, where  $a_q$  and  $a_g$  are the same as in (3.5.17). Using the LPA cross section we have

$$\begin{aligned} P_n(t_p, t_c, z_0) &= a^n \int_{t_c}^{t_p} \frac{\alpha(t_1)}{2\pi t_1} dt_1 \int_{t_c}^{t_1} \frac{\alpha(t_2)}{2\pi t_2} dt_2 \dots \int_{t_c}^{t_{n-1}} \frac{\alpha(t_n)}{2\pi t_n} dt_n \\ &\quad \int_{z_0}^1 \frac{dz_1}{z_1} \int_{z_0/z_1}^1 \frac{dz_2}{z_2} \dots \int_{z_0/(z_1 z_2 \dots z_{n-1})}^1 \frac{dz_n}{z_n}, \end{aligned} \quad (3.7.4)$$

where the invariant masses are ordered according to (3.4.25) and where  $a = a_q$  and  $a = a_g$  for a quark and gluon jet, respectively. The range of the  $z$  integrals is deduced from relationship

$$\begin{aligned} z_0 &\leq \frac{(k_0 + k_s)_i}{(\frac{1}{2}Q)} = \frac{(k_0 + k_s)_i}{(k_0 + k_s)_{i-1}} \frac{(k_0 + k_s)_{i-1}}{(k_0 + k_s)_{i-2}} \dots \frac{(k_0 + k_s)_2}{(k_0 + k_s)_1} \frac{(k_0 + k_s)_1}{(\frac{1}{2}Q)} \\ &= z_i z_{i-1} \dots z_2 z_1, \end{aligned} \quad (3.7.5)$$

so that

$$z_i \geq z_0 / (z_1 z_2 \dots z_{i-1}). \quad (3.7.6)$$

The nested integrals over the invariant masses are the same as (3.6.3),

$$\begin{aligned} &\int_{t_c}^{t_p} \frac{\alpha(t_1)}{2\pi t_1} dt_1 \int_{t_c}^{t_1} \frac{\alpha(t_2)}{2\pi t_2} dt_2 \dots \int_{t_c}^{t_{n-1}} \frac{\alpha(t_n)}{2\pi t_n} dt_n \\ &= \int_0^{\kappa_p} d\kappa_1 \int_0^{\kappa_1} d\kappa_2 \dots \int_0^{\kappa_{n-1}} d\kappa_n = \frac{\kappa_p^n}{n!}, \end{aligned} \quad (3.7.7)$$

where  $\kappa_p$  is defined by (3.6.4). Namely,

$$\kappa_p = \frac{2}{\beta_0} \log\{\alpha_s(t_c)/\alpha_s(t_p)\}. \quad (3.7.8)$$

The  $z$  integrations are done by changing variables to

$$Y_i = \log(z_i), \quad (3.7.9)$$

so that

$$dY_i = dz_i/z_i, \quad (3.7.10)$$

and

$$\log[z_0 / (z_1 z_2 \dots z_n)] = Y_0 - Y_1 - Y_2 - \dots - Y_n. \quad (3.7.11)$$

With this change of variables,

$$\begin{aligned} I_n &= \int_{z_0}^1 \frac{dz_1}{z_1} \int_{z_0/z_1}^1 \frac{dz_2}{z_2} \dots \int_{z_0/(z_1 z_2 \dots z_{n-1})}^1 \frac{dz_n}{z_n} \\ &= \int_{Y_0}^0 dY_1 \int_{Y_0-Y_1}^0 dY_2 \dots \int_{Y_0-Y_1-\dots-Y_{n-1}}^0 dY_n, \end{aligned} \quad (3.7.12)$$

which for  $n = 2$  is

$$I_2 = \int_{Y_0}^0 dY_1 (Y_1 - Y_0) = \frac{1}{2} Y_0^2, \quad (3.7.13)$$

and for  $n = 3$  is

$$\begin{aligned} I_3 &= \int_{Y_0}^0 dY_1 \int_{Y_0-Y_1}^0 dY_2 (Y_0 - Y_1 - Y_2) \\ &= \int_{Y_0}^0 dY_1 \frac{1}{2}(Y_0 - Y_1)^2 = -\frac{1}{2} \frac{1}{3} Y_0^3. \end{aligned} \quad (3.7.14)$$

It is easy to see that

$$I_n = \frac{(-Y_0)^n}{n!} = \frac{\log^n(1/z_0)}{n!}. \quad (3.7.15)$$

Combining (3.7.7) and (3.7.15) yields

$$P_n(t_p, t_c, z_0) = \frac{a^n \kappa_p^n \log^n(1/z_0)}{n! n!}, \quad (3.7.16)$$

where  $a = a_q$  or  $a = a_g$  for a quark and gluon jet, respectively. The probability of emitting *any* number of gluons each with  $(k_0 + k_z) \geq z_0 Q/2$  is the sum

$$P(t_p, t_c, z_0) = \sum_{n=0}^{\infty} P_n(t_p, t_c, z_0), \quad (3.7.17)$$

which we can perform with the aid of

$$I_k(\rho) = \sum_{n=0}^{\infty} \frac{1}{n!(n+k)!} \left(\frac{\rho}{2}\right)^{k+2n}, \quad (3.7.18)$$

where  $I_k(\rho)$  are the modified Bessel functions of the first kind. Thus,

$$P(t_p, t_c, z_0) = I_0(\rho) = \sum_{n=0}^{\infty} \frac{1}{n! n!} \left(\frac{\rho}{2}\right)^{2n}, \quad (3.7.19)$$

where  $\rho$  is identified as

$$\rho = 2\sqrt{a\kappa_p \log(1/z_0)}. \quad (3.7.20)$$

Since we are considering the case where  $z_0 \ll 1$  this means that  $\rho \gg 1$  and we can approximate the Bessel function  $I_0(\rho)$  with its asymptotic form

$$I_0(\rho) \xrightarrow[\rho \rightarrow \infty]{} \frac{e^\rho}{\sqrt{2\pi\rho}}, \quad (3.7.21)$$

so that

$$P(t_p, t_c, z_0) \xrightarrow[z_0 \rightarrow 0]{} \frac{\exp(2\sqrt{a\kappa_p \log(1/z_0)})}{\sqrt{4\pi\sqrt{a\kappa_p \log(1/z_0)}}}. \quad (3.7.22)$$

The average number of gluons with  $(k_0 + k_z) \geq z_0 Q/2$  emitted by the jet

is given by

$$\langle N \rangle = \frac{\sum_{n=0}^{\infty} n P_n(t_p, t_c, z_0)}{P(t_p, t_c, z_0)}. \quad (3.7.23)$$

The numerator can be written

$$\sum_{n=0}^{\infty} \frac{n}{n! n!} \left(\frac{\rho}{2}\right)^{2n} = \left(\frac{\rho}{2}\right) \frac{d}{d\rho} \left\{ \sum_{n=0}^{\infty} \frac{1}{n! n!} \left(\frac{\rho}{2}\right)^{2n} \right\}, \quad (3.7.24)$$

which means that

$$\langle N \rangle = \frac{\left(\frac{\rho}{2}\right) \frac{d}{d\rho} \{I_0(\rho)\}}{I_0(\rho)} = \left(\frac{\rho}{2}\right) \frac{I_1(\rho)}{I_0(\rho)}, \quad (3.7.25)$$

where  $\rho$  is given by (3.7.20). The asymptotic form in (3.7.21) yields

$$\langle N \rangle \approx_{z_0 \rightarrow 0} \frac{\rho}{2} = \sqrt{a\kappa_p \log(1/z_0)}, \quad (3.7.26)$$

where  $a = a_q$  and  $a = a_g$  for a quark and gluon jet, respectively. The ratio of the average number of gluons with  $(k_0 + k_z) \geq z_0 Q/2$  emitted by a gluon initiated jet to the average number emitted by a quark initiated jet is thus

$$\frac{\langle N_g \rangle}{\langle N_q \rangle} \approx_{z_0 \rightarrow 0} \sqrt{a_g/a_q} = \frac{3}{2}. \quad (3.7.27)$$

Gluon jets are expected to have, on the average, a higher multiplicity and a “softer” (*i.e.*, less high momentum) distribution of particles than quark jets.

### 3.8 Summing Double Logarithms

We have seen an example of an observable, such as  $\sigma_{tot}^{e^+ e^-}$  in (2.7.8), that contains no infrared divergences. Both the log squared and the single log canceled out when real and virtual corrections were added. We have also seen an example of a cross section, such as  $d\sigma^h/dz$  in (3.3.6) that contains a single logarithmic divergence of the form  $\alpha_s(Q^2) \log(Q^2)$ . Since this term is of order 1, all terms of the form  $[\alpha_s(Q^2) \log(Q^2)]^n$  were summed to arrive at a meaningful result. There are also observables, like  $\sigma_m$  in (2.3.50) that contain double logarithmic divergences of the form  $\alpha_s \log^2(Q^2)$ . Here again one must sum all terms of the form  $[\alpha_s \log^2(Q^2)]^n$  in order to obtain a meaningful result.

An interesting observable of this type is  $S(\theta)$  which is illustrated in Fig. 3.10 and defined by

$S(\theta) =$  the probability that the quark created in the decay  $\gamma^* \rightarrow q\bar{q}$  is diverted from its initial direction (opposite the antiquark) by an angle  $\theta$  by successive

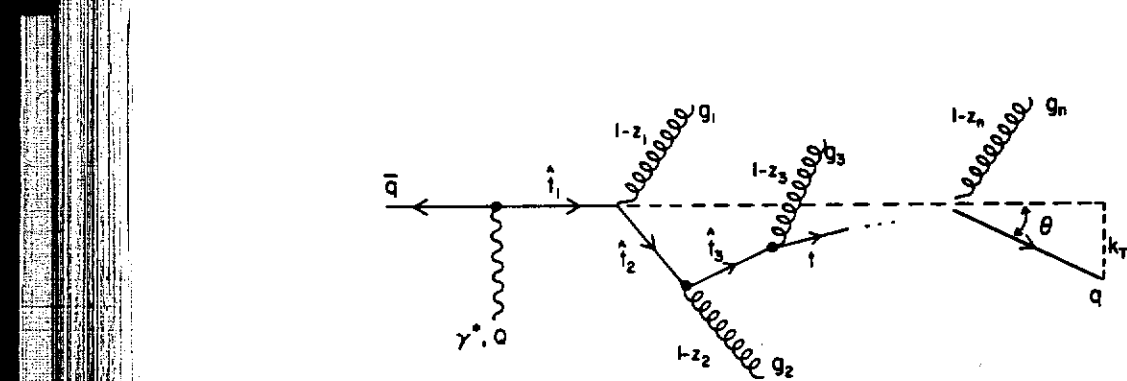


Figure 3.10 Illustrates the case where the quark created by the “decay” of a virtual photon of invariant mass  $Q$  is diverted by an angle  $\theta$  from its initial direction (opposite the antiquark) by the emission of  $n$  gluons.

$$\text{gluon emissions.} \quad (3.8.1)$$

The situation is simplified by making the small angle approximation

$$\tan(\theta) \approx \theta \approx \frac{k_T}{k_L} \approx \frac{2k_T}{Q}. \quad (3.8.2)$$

Conservation of probability insures that

$$S(\theta) + T(\theta) = 1, \quad (3.8.3)$$

where

$T(\theta)$  = the probability that the quark created in the decay  $\gamma^* \rightarrow q\bar{q}$  is diverted from its initial direction (opposite the antiquark) by an angle greater than  $\theta$  by successive gluon emissions.  $(3.8.4)$

The function  $T(\theta)$  is the integral of the transverse momentum distribution of the quark in Fig. 3.10. Namely,

$$T(\theta) = T(k_T^2) = \int_{k_T^2}^{Q^2/4} \frac{1}{\sigma_0} \frac{d\sigma_q}{dk_T^2}(Q^2, k_T^2) dk_T^2, \quad (3.8.5)$$

where from (3.8.2)

$$k_T^2 = \frac{1}{4}\theta^2 Q^2. \quad (3.8.6)$$

The single gluon contribution to  $S(\theta)$  comes from the  $\gamma^* \rightarrow q\bar{q}g$  diagram in

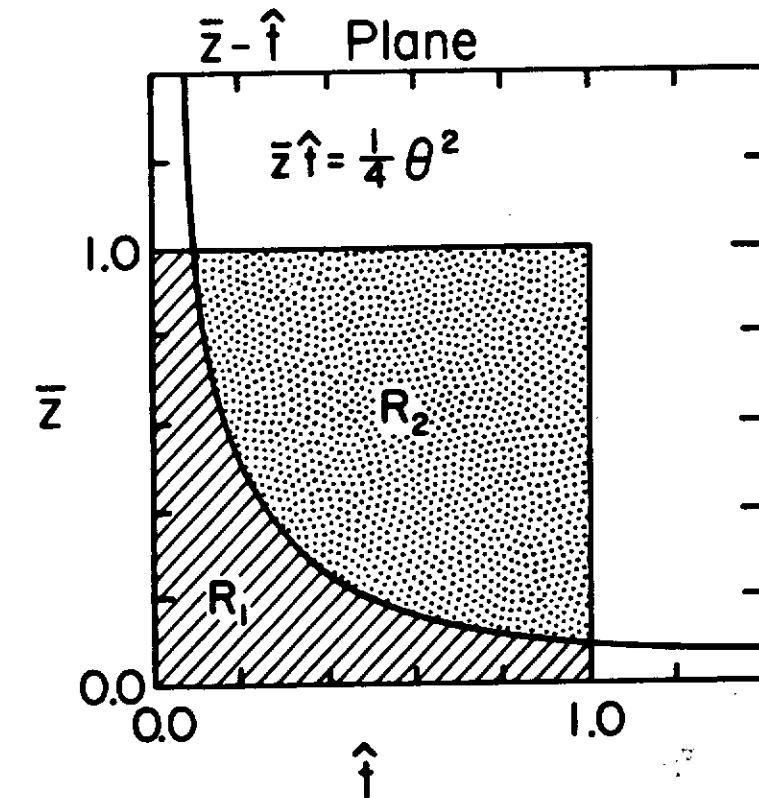


Figure 3.11 Shows the  $\tilde{z} - \hat{i}$  plane, where  $\tilde{z} = 1 - z$ . The solid curve is  $\tilde{z}\hat{i} = \theta^2/4$  and  $R_1$  is the region of integration for  $S(\theta)$ . The complementary region  $R_2$  is the range of integration for  $T(\theta)$  and  $S(\theta) + T(\theta) = 1$ .

Fig. 3.2 and to arrive at what will turn out to be the leading double logarithm we can use the LPA approximation in (3.4.10),

$$\frac{1}{\sigma_0} \left( \frac{d\sigma}{dzdi} \right)_{\text{LPA}} = \frac{2\alpha_s}{3\pi} \frac{1+z^2}{(1-z)\hat{i}}. \quad (3.8.7)$$

This term dominates since the range of integration for  $S(\theta)$  is from (3.4.6) given by

$$\frac{k_T^2}{Q^2} = z(1-z)\hat{i} \leq \frac{\theta^2}{4}, \quad (3.8.8)$$

where  $\theta \ll 1$ . This can be simplified further by defining

$$\bar{z} = 1 - z, \quad (3.8.9)$$

and noting that (3.8.8) implies that both  $\hat{t}$  and  $\bar{z}$  are small so that the range can be approximated by the condition

$$\bar{z}\hat{t} \leq \frac{\theta^2}{4}, \quad (3.8.10)$$

with  $0 \leq \bar{z} \leq 1$  and  $0 \leq \hat{t} \leq 1$ . This corresponds to the region  $R_1$  in Fig. 3.11. Namely,

$$0 \leq \hat{t} \leq 1, \quad (3.8.11)$$

$$0 \leq \bar{z} \leq \frac{\theta^2}{4\hat{t}}, \quad (3.8.12)$$

and includes the points  $\hat{t} = 0$  and  $\bar{z} = 0$  ( $z = 1$ ) where (3.8.7) diverges. We know from our study of  $\sigma_{tot}^{e^+e^-}$  in Chapter 2 that these divergences are canceled by virtual corrections but rather than going through this again it is simpler to compute  $T(\theta)$  by integrating over the complementary range  $R_2$  in Fig. 3.11,

$$\frac{1}{4}\theta^2 \leq \hat{t} \leq 1 \quad (3.8.13)$$

$$\frac{\theta^2}{4\hat{t}} \leq \bar{z} \leq 1, \quad (3.8.14)$$

and then to use (3.8.3) to deduce  $S(\theta)$ . From (3.8.7) we have

$$\begin{aligned} (T_1(\theta))_{LDLA} &= \frac{2\alpha_s}{3\pi} \int_{\frac{1}{4}\theta^2}^1 \frac{d\hat{t}}{\hat{t}} \int_{\frac{\theta^2}{4\hat{t}}}^1 \frac{2d\bar{z}}{\bar{z}} \\ &= -\frac{2\alpha_s}{3\pi} 2 \int_{\frac{1}{4}\theta^2}^1 \frac{d\hat{t}}{\hat{t}} \log\left(\frac{\theta^2}{4\hat{t}}\right) \\ &= \frac{2\alpha_s}{3\pi} \log^2(\theta^2/4) \end{aligned} \quad (3.8.15)$$

and from (3.8.3),

$$(S_1(\theta))_{LDLA} = 1 - \frac{2\alpha_s}{3\pi} \log^2(\theta^2/4), \quad (3.8.16)$$

where the subscript LDLA refers to the leading double log approximations that we have made and the subscript 1 means that we have computed only the single gluon emission contribution.

The quark transverse momentum spectrum can be computed easily since from (3.8.5)

$$\frac{1}{\sigma_0} \frac{d\sigma_q}{dk_T^2}(Q, k_T^2) = \frac{dS(k_T^2)}{dk_T^2} = -\frac{dT(k_T^2)}{dk_T^2}. \quad (3.8.17)$$

Using (3.8.16) we arrive at

$$\frac{1}{\sigma_0} \frac{d\sigma_q}{dk_T^2}(Q, k_T^2) = -\frac{4\alpha_s}{3\pi} \frac{1}{k_T^2} \log(k_T^2/Q^2), \quad (3.8.18)$$

which is valid provided  $k_T^2/Q^2 \ll 1$  and which becomes infinitely large as  $k_T^2 \rightarrow 0$ . The single gluon emission result in (3.8.18) does *not* give a good approximation to the correct answer obtained by summing over all possible gluon emissions.

The leading double logarithm summation is a bit more difficult to deduce than the leading log summation. The LDLA result for  $n$  gluon emissions is given by

$$(S_n(\theta))_{LDLA} = \frac{1}{n!} \left[ -\frac{2\alpha_s}{3\pi} \log^2(\theta^2/4) \right]^n, \quad (3.8.19)$$

and the sum over all possible gluon emissions,

$$S_{LDLA}(\theta) = \sum_{n=0}^{\infty} S_n(\theta), \quad (3.8.20)$$

becomes

$$S_{LDLA}(\theta) = \exp\left\{-\frac{2\alpha_s}{3\pi} \log^2(\theta^2/4)\right\}. \quad (3.8.21)$$

Equation (3.8.16) was just the first two terms in the exponential series.<sup>15,16</sup>

The  $k_T$  distribution in (3.8.18) which diverged at  $k_T = 0$  becomes

$$\frac{1}{\sigma_0} \left( \frac{d\sigma}{dk_T^2} \right)_{LDLA} = -\frac{4\alpha_s}{3\pi} \frac{1}{k_T^2} \log(k_T^2/Q^2) \exp\left\{-\frac{2\alpha_s}{3\pi} \log^2(k_T^2/Q^2)\right\}, \quad (3.8.22)$$

which now vanishes at  $k_T = 0$ . The exponential factor,

$$F(k_T^2) = \exp\left\{-\frac{2\alpha_s}{3\pi} \log^2(k_T^2/Q^2)\right\}, \quad (3.8.23)$$

converts the single gluon result in (3.8.18) to the correct answer in (3.8.22) is sometimes referred to as the “Sudakov form factor”.<sup>17</sup> When properly included the  $k_T$  distribution vanishes as  $k_T \rightarrow 0$ . Once one allows for an infinite amount of gluon emission, it becomes very unlikely (in fact, infinitely unlikely) that the quark in Fig. 3.10 remains at  $k_T = 0$  and is not deflected. The situation becomes more complicated when effects due to the running coupling constant  $\alpha_s(k_T)$  are included. I refer the interested reader to the literature.<sup>18–25</sup>

### Problems

- 3.1. Show that (3.1.23) together with the normalization condition on  $f(\eta)$  given by (3.1.10) guarantees that  $\int_0^1 zF(z)dz = 1$  as stated in (3.1.24).
- 3.2. Show that for the choice of  $f(\eta)$  given in (3.1.26), namely,  $f(\eta) = (d+1)\eta^d$ ,

that the generating function in (3.1.23) becomes  $g(\eta) = (d+1)/\eta$  and  $zF(z) = (d+1)(1-z)^d$  as claimed in (3.1.27).

- 3.3. Show that the integral equation (3.1.23) guarantees that  $zF(z) \underset{z \rightarrow 0}{\sim} R$  as claimed in (3.1.25) and that  $1/R = - \int_0^1 f(\eta) \log(\eta) d\eta$ . Evaluate  $R$  for the choice of  $f(\eta) = (d+1)\eta^d$ .
- 3.4. Show that a fragmentation function of the form  $F(z) = R/z$  produces a logarithmic growth in particle multiplicity and a uniform distribution in  $Y_z = -\log(z)$ .
- 3.5. Show that the probability of finding a meson state of flavor “ $a\bar{b}$ ” carrying energy fraction  $z$  of an “average quark”,  $P_{(q)}^{a\bar{b}}(z)$ , defined in (3.1.32) satisfies the integral equation (3.1.33) and that  $P_{(q)}^{a\bar{b}}(z) = \beta_a \beta_b F(z)$ , where  $F(z)$  satisfies (3.1.13).
- 3.6. Show that  $P_q^{a\bar{b}}(z)$  given by (3.1.30) satisfies (3.1.35) provided  $\bar{F}(z) = F(z) - f(1-z)$ .
- 3.7. Show that as  $z \rightarrow 1$  the fragmentation function  $F(z)$  in (3.1.23) approaches  $f(1-z)$  and hence,  $D_q^h(z) \underset{z \rightarrow 1}{\sim} A_q^h f(1-z)$ .
- 3.8. What are the fragmentation functions  $D_u^{K^+}(z)$ ,  $D_u^{K^-}(z)$ ,  $D_s^{K^+}(z)$ , and  $D_s^{K^-}(z)$  in the FF parameterization? (Assume that  $\beta_c = \beta_b = 0$ .) Using the result from problem 6 show that  $D_u^{K^+}(z)/D_u^{\pi^+}(z) \rightarrow (1-\beta)/\beta$  as  $z \rightarrow 1$ . Data on the production of  $K^+$  and  $\pi^+$  mesons in proton-proton collisions at large transverse momentum,  $p_T$ , show that as  $p_T$  becomes large the  $K^+/\pi^+$  ratio approaches  $1/2$ . What does this tell us about  $\beta$ ?
- 3.9. Using the FF parameterization with  $\beta_u = \beta_d = \beta$ ,  $\beta_s = 1 - 2\beta$ ,  $\beta_c = \beta_b = 0$ , and  $\beta = 0.4$ , compute the average hypercharge,  $Y$ , and average third component of isospin,  $I_z$ , for a high energy jet initiated by a  $u$ ,  $d$ , and  $s$  quark.
- 3.10. Show that
$$\left( \frac{1+x^2}{1-x} \right)_+ = \left\{ \frac{1+x^2}{(1-x)_+} + \frac{3}{2}\delta(1-x) \right\}.$$
- 3.11. Using (3.2.11) and (3.2.23) verify that
$$\int_0^1 f_{MG,q}^{e^+e^-}(x) dx = \int_0^1 f_{DR,q}^{e^+e^-}(x) dx = 0.$$
- 3.12. Verify (3.2.12) and (3.2.13).
- 3.13. Using the definition of “+ functions” in (3.2.8) verify (3.2.16) and (3.2.17).

- 3.14. Use the Taylor expansion

$$\Gamma(1+\epsilon) = 1 - \gamma_E \epsilon + \frac{1}{2} \left( \gamma_E^2 + \frac{\pi^2}{6} \right) \epsilon^2 + \dots,$$

from (E.1.18) to verify the expansion in (3.2.20).

- 3.15. Let

$$I = \int_0^1 dv v^{\frac{\epsilon}{2}} (1-v)^{\frac{\epsilon}{2}} xF(x,v),$$

where  $xF(x,v)$  is given by (2.8.33) with  $x_1 = x$ . Show that

$$I = \frac{\Gamma^2(1+\frac{\epsilon}{2})}{\Gamma(1+\epsilon)} \left\{ \frac{1+x^2}{1-x} \frac{2}{\epsilon} + \frac{1}{2} \frac{1}{1-x} - \frac{5}{2}x + \frac{3}{2} + \dots \right\},$$

where some terms that vanish as  $\epsilon \rightarrow 0$  have been dropped. Is it necessary to include the terms of order  $\epsilon^2$  in the expression for  $xF(x,v)$ ? Use this result to verify (3.2.19). Also, verify (3.2.21), (3.2.22), and (3.2.23).

- 3.16. Derive the expression for  $f_{MG,q}^{e^+e^-}(x)$  given in (3.2.29).

- 3.17. Verify (3.2.30).

- 3.18. Verify that (3.2.31) holds in the massive gluon scheme.

- 3.19. Using the dimensional regularization scheme, DR, show that the differential cross section for producing a gluon in the process  $\gamma^* \rightarrow q\bar{q}g$  carrying fractional energy  $x$  is given by

$$\frac{d\sigma_{DR}^g}{dx} = \frac{2\alpha_s}{3\pi} \sigma_0 \left( \frac{x^2(1-x)Q^2}{4\pi m_D^2} \right)^{\frac{\epsilon}{2}} \frac{1}{\Gamma(2+\frac{\epsilon}{2})} \int_0^1 dv v^{\frac{\epsilon}{2}} (1-v)^{\frac{\epsilon}{2}} x \bar{F}(x,v),$$

where  $\bar{F}(x,v)$  is arrived at from (2.8.24) by making the replacements  $x_1 = 1-x+xv$  and  $x_2 = 1-vx$ . Perform the integral and verify that

$$\frac{1}{\sigma_0} \left( \frac{d\sigma_{DR}^g}{dx} \right)_+ = 2 \left( \frac{\alpha_s}{2\pi} \right) P_{q \rightarrow gq}(x) \log(Q^2/m_D^2) + 2\alpha_s f_{DR,q}^{e^+e^-}(x),$$

where  $P_{q \rightarrow gq}(x)$  is the same as (3.2.27) and

$$\begin{aligned} \alpha_s f_{DR,q}^{e^+e^-}(x) = & \frac{2\alpha_s}{3\pi} \left\{ 2(1+(1-x)^2) \left( \frac{\log(x)}{x} \right)_+ \right. \\ & + (1+(1-x)^2) \frac{\log(1-x)}{x} + \left( \frac{\pi^2}{3} - 4 \right) \delta(x) \Big\} \\ & + \frac{\alpha_s}{2\pi} P_{q \rightarrow gq}(x) \left\{ \frac{2}{\epsilon} + \gamma_E - \log(4\pi) \right\}. \end{aligned}$$

Verify that (3.2.31) holds in the dimensional regularization scheme.

- 3.20. Verify (E.3.7) and (E.3.8).
- 3.21. Show that (3.2.30) and (3.2.31) together with (3.2.12) insures that the normalization condition in (3.3.9) holds at leading order and at order  $\alpha_s$ .
- 3.22. Verify (3.4.4), (3.4.5), (3.4.6), and (3.4.7). Derive (3.4.9) from (3.4.1) using  $z = z_2$  defined in (3.4.7) and  $\hat{t}$  defined in (3.4.8).
- 3.23. Using the axial gauge defined in (3.4.18) choose  $n = q - p_2/x_2$  and derive (3.4.21), (3.4.22), and (3.4.23).
- 3.24. Derive the gluon "splitting function",  $P_{g \rightarrow gg}(z)$ , in (3.4.30).
- 3.25. Compute the order  $\kappa^3$  term in the series in (3.4.42) and convince yourself that the series exponentiates as stated in (3.4.44).
- 3.26. Show that, if instead of behaving as given in (3.4.34)  $\alpha_s$  were constant, then the series for  $D_{NS}^h(z, Q^2)$  in (3.4.44) would be

$$D_{NS}^h(z, Q^2) = \exp\left(\frac{\alpha_s}{2\pi} \log(Q^2/t_c) P_{q \rightarrow gg}^*\right) D_{NS}^h(t_c).$$

Differentiate this result with respect to  $\tau = \log(Q^2/\Lambda^2)$  and show that the result is the same as (3.4.47). Explain.

- 3.27. Show that  $P_\Delta(y)$  in (3.5.9) is equivalent to (3.5.10), where  $\gamma_E$  is Eulers constant,

$$\int_0^\infty e^{-x} \log(x) dx = -\gamma_E.$$

*Hint:* change variables to  $x = -\log(y)$  and integrate by parts.

- 3.28. Write a computer program to evaluate the integrals in (3.5.12) and (3.5.13) numerically. Start at  $Q_0 = 2$  GeV (and  $\Lambda = 200$  MeV) with a non-singlet  $\pi^+$  fragmentation function for a  $u$  quark that is parameterized according the FF prescription,

$$D_{NS,u}^{*\pi^+}(z, Q_0^2) = D_u^{*\pi^+}(z) - D_u^{*\pi^+}(z) = \beta f(1-z).$$

Choose  $\beta = 0.4$  and  $f(1-z) = 3(1-z)^2$  and plot  $D_{NS,u}^{*\pi^+}(z, Q^2)$  at  $Q=10$ , 100, and 1000 GeV using the convolution method to order  $\kappa$ . Is it necessary to evaluate order  $\kappa^2$  terms at these values of  $Q$ ?

- 3.29. Suppose that at  $Q_0 = 2$  GeV that the quark and gluon fragmentation functions are equal and given by,

$$D_q^h(z, Q_0^2) = D_g^h(z, Q_0^2) = A(1-z)^2.$$

Show that

$$\frac{D_g^h(z, Q^2)}{D_q^h(z, Q^2)} \underset{z \rightarrow 1}{\sim} (1-z)^{10\kappa/3},$$

where

$$\kappa = \frac{2}{11 - 2n_f/3} \log\{\log(Q^2/\Lambda^2)/\log(Q_0^2/\Lambda^2)\}.$$

What is  $D_g^h(z, Q^2)/D_q^h(z, Q^2)$  at  $Q = 1000$  GeV,  $z = 0.9$ , if  $\Lambda = 200$  MeV and  $n_f = 4$ ? What does this imply about gluon jets compared to quark jets?

- 3.30. Calculate the explicit form of  $\gamma_{NS}(z_c)$  in (3.6.6). What is the numerical value of  $\gamma_{NS}(z_c)$  for  $z_c = 0.01$ ? In the LPA what is the numerical value of the probability that a quark produced by a virtual photon in an  $e^+e^-$  annihilation at a center-of-mass energy of  $Q = 10$  GeV emits only unresolvably soft gluons until its invariant mass has been degraded to  $\sqrt{t_c}$ , if  $\sqrt{t_c} = 2$  GeV,  $z_c = 0.01$ ,  $\Lambda = 200$  MeV, and  $n_f = 4$  (consider only the non-singlet probability  $\pi_q(t_p = Q^2, t_c)$  in (3.6.9))? What if  $Q = 100$  GeV?

#### Further Reading

S.D. Ellis, "Jets and Quantum Chromodynamics," Lectures presented at the NATO Advanced Study Institute on Quantum Flavordynamics, Quantum Chromodynamics, and Unified Theories, Boulder, 1979, ed. by K.T. Mahanthappa and J. Randa, (Plenum Press, 1980).

A. H. Mueller, *Physics Reports* 73, 237 (1981).

#### References

1. R.D. Field and R.P. Feynman, *Nucl. Phys.* **B136**, 1 (1978).
2. G. Altarelli, R.K. Ellis, G. Martinelli, and S.Y. Pi, *Nucl. Phys.* **B160**, 301 (1979).
3. R.K. Ellis, H. Georgi, M. Machacek, H.D. Politzer and G.G. Ross, *Phys. Lett.* **78B**, 281 (1978). *ibid* *Nucl. Phys.* **B152**, 285 (1979).
4. D. Amati, R. Petronzio and G. Veneziano, *Nucl. Phys.* **B146**, 29 (1978).
5. S. Libby and G. Sterman, *Phys. Rev.* **D18**, 3252 (1978).
6. A.H. Mueller, *Phys. Rev.* **D18**, 3705 (1978).
7. G.C. Fox and S. Wolfram, *Nucl. Phys.* **B168**, 285 (1980).
8. Stephan Wolfram, "Jet Development in Leading Log QCD," CALT-68-740 (1979) unpublished.
9. G.C. Fox and S. Wolfram, "A Gallimaufry of  $e^+e^-$  Annihilation Event Shapes," CALT-68-723 (1979) unpublished.

10. R. Odorico, *Nucl. Phys.* **B199**, 189 (1982). *ibid Phys. Lett.* **118B**, 151 (1982). *ibid Nucl. Phys.* **B228**, 381 (1983).
11. K. Konishi, A. Ukawa and G. Veneziano, *Nucl. Phys.* **B157**, 45 (1979). *ibid Phys. Lett.* **80B**, 259 (1979).
12. G. Altarelli and G. Parisi, *Nucl. Phys.* **B126**, 298 (1977).
13. J.F. Owens, *Phys. Lett.* **76B**, 85 (1978).
14. R. D. Field and S. Wolfram, *Nucl. Phys.* **B213**, 65 (1983).
15. T. Kinoshita and A. Ukawa, *Phys. Rev.* **D13**, 1573 (1976). *ibid Phys. Rev.* **D15**, 1596 (1977). *ibid Phys. Rev.* **D16**, 332 (1977).
16. J. Frenkel and J.C. Taylor, *Nucl. Phys.* **B109**, 439 (1976). *ibid Nucl. Phys.* **B116**, 185 (1976).
17. V. Sudakov, *Sov. Phys. JEPT* **3**, 65 (1956).
18. Yu. L. Domshitzer, D.L. Dyakonov, and S.I. Troyan, *Phys. Lett.* **78B**, 290 (1978).
19. W.J. Stirling, *Nucl. Phys.* **B145**, 477 (1978).
20. G. Parisi and R. Petronzio, *Nucl. Phys.* **B154**, 427 (1979).
21. C.Y. Lo and J.D. Sullivan, *Phys. Lett.* **86B**, 327 (1979).
22. A.H. Mueller, *Phys. Rev.* **D20**, 2037 (1979).
23. J.C. Collins, *Phys. Rev.* **D22**, 1478 (1980).
24. H.F. Jones and J. Wyndham, *Nucl. Phys.* **B176**, 466 (1980).
25. S.D. Ellis and W.J. Stirling, *Phys. Rev.* **D23**, 214 (1981).

## Deep Inelastic Lepton Nucleon Scattering



The first evidence that the proton has substructure came from deep inelastic electron proton scattering ( $e + p \rightarrow e + X$ ). It is probably the most studied QCD process. Not only does this process allow for tests of perturbative QCD but also provides us with knowledge on the distribution of partons (quarks and gluons) within the proton. It is important to understand the precise definition of these distributions for they will be used in later chapters to make predictions of other experiments.

## 4.1 The Naive Parton Model

In the naive parton model, one defines parton distributions,  $G_{N \rightarrow q}(x)$ , as the number of quarks  $q$  with fractional of momentum between  $x$  and  $x + dx$  within a nucleon of high momentum. In particular, some of the functions that describe the quark distributions in a proton are:

$$\begin{aligned} u(x) &\equiv G_{p \rightarrow u}(x), & \bar{u}(x) &\equiv G_{p \rightarrow \bar{u}}(x), \\ d(x) &\equiv G_{p \rightarrow d}(x), & \bar{d}(x) &\equiv G_{p \rightarrow \bar{d}}(x), \\ s(x) &\equiv G_{p \rightarrow s}(x), & \bar{s}(x) &\equiv G_{p \rightarrow \bar{s}}(x), \\ c(x) &\equiv G_{p \rightarrow c}(x), & \bar{c}(x) &\equiv G_{p \rightarrow \bar{c}}(x), \end{aligned} \quad (4.1.1)$$

where  $u$ ,  $d$ ,  $s$ , and  $c$  refer to up, down, strange, and charm quarks, respectively, and  $\bar{u}$ ,  $\bar{d}$ ,  $\bar{s}$ , and  $\bar{c}$  to their antiquarks. The distribution of gluons within a proton is defined by

$$g(x) \equiv G_{p \rightarrow g}(x), \quad (4.1.2)$$

where  $g$  stands for gluon. These distributions satisfy the following sum rules:

$$\int_0^1 [u(x) - \bar{u}(x)]dx = 2, \quad (4.1.3)$$

$$\int_0^1 [d(x) - \bar{d}(x)]dx = 1, \quad (4.1.4)$$

$$\int_0^1 [s(x) - \bar{s}(x)]dx = \int_0^1 [c(x) - \bar{c}(x)]dx = 0. \quad (4.1.5)$$

That is, the net number of each kind of quark is just the number one arrives at in the simple non-relativistic quark model.

If we define

$$U \equiv \int_0^1 xu(x)dx, \quad (4.1.6)$$

$$D \equiv \int_0^1 xd(x)dx, \quad (4.1.7)$$

etc., as the total fraction of momentum carried by  $u$ ,  $d$ , ..., etc., quarks

within the proton and

$$G \equiv \int_0^1 xg(x)dx, \quad (4.1.8)$$

as the total fraction of the proton momentum carried by gluons, then presumably

$$Q + \bar{Q} + G = 1, \quad (4.1.9)$$

where

$$Q = U + D + S + C + \dots, \quad (4.1.10)$$

is the total fraction of momentum carried by quarks and

$$\bar{Q} = \bar{U} + \bar{D} + \bar{S} + \bar{C} + \dots, \quad (4.1.11)$$

is the total fraction carried by antiquarks. The distributions of partons within a neutron are arrived at using isospin symmetry, which implies that

$$G_{n \rightarrow u}(x) = G_{p \rightarrow d}(x) = d(x), \quad (4.1.12)$$

$$G_{n \rightarrow d}(x) = G_{p \rightarrow u}(x) = u(x), \quad (4.1.13)$$

$$G_{n \rightarrow s}(x) = G_{p \rightarrow s}(x) = s(x), \quad (4.1.14)$$

$$G_{n \rightarrow g}(x) = G_{p \rightarrow g}(x) = g(x), \quad (4.1.15)$$

etc.

In the naive parton model, knowledge of the deep inelastic structure functions for electron, neutrino, and antineutrino scattering constrains the  $u(x)$ ,  $d(x)$ ,  $\bar{u}(x)$ ,  $\bar{d}(x)$ ,  $s(x)$ ,  $\bar{s}(x)$ ,  $c(x)$  and  $\bar{c}(x)$  distributions. For example,

$$\begin{aligned} F_2^{ep}(x) &= \frac{4}{9}x[u(x) + \bar{u}(x) + c(x) + \bar{c}(x)] \\ &+ \frac{1}{9}x[d(x) + \bar{d}(x) + s(x) + \bar{s}(x)], \end{aligned} \quad (4.1.16)$$

$$\begin{aligned} F_2^{en}(x) &= \frac{4}{9}x[d(x) + \bar{d}(x) + c(x) + \bar{c}(x)] \\ &+ \frac{1}{9}x[u(x) + \bar{u}(x) + s(x) + \bar{s}(x)], \end{aligned} \quad (4.1.17)$$

$$F_2^{\nu p}(x) = 2x[d(x) + s(x) + \bar{u}(x) + \bar{c}(x)], \quad (4.1.18)$$

$$F_2^{\nu n}(x) = 2x[u(x) + s(x) + \bar{d}(x) + \bar{c}(x)], \quad (4.1.19)$$

$$F_2^{\bar{\nu} p}(x) = 2x[u(x) + c(x) + \bar{d}(x) + \bar{s}(x)], \quad (4.1.20)$$

$$F_2^{\bar{\nu} n}(x) = 2x[d(x) + c(x) + \bar{u}(x) + \bar{s}(x)], \quad (4.1.21)$$

$$xF_3^{\nu p}(x) = 2x[d(x) + s(x) - \bar{u}(x) - \bar{c}(x)], \quad (4.1.22)$$

$$xF_3^{\nu n}(x) = 2x[u(x) + s(x) - \bar{d}(x) - \bar{c}(x)], \quad (4.1.23)$$

$$xF_3^{\bar{\nu} p}(x) = 2x[u(x) + c(x) - \bar{d}(x) - \bar{s}(x)], \quad (4.1.24)$$

$$xF_3^{\bar{\nu} n}(x) = 2x[d(x) + c(x) - \bar{u}(x) - \bar{s}(x)], \quad (4.1.25)$$

where the approximation  $\cos \theta_c = 1$  ( $\theta_c$  = Cabibbo angle) has been made. The structure functions  $F_2(x)$  and  $F_3(x)$  will be defined later. Since fermions

and antifermions contribute with an opposite sign to  $xF_3(x)$ <sup>1</sup> it is useful to define

$$F_Q(x) = \frac{1}{2}(F_2(x) + xF_3(x)), \quad (4.1.26)$$

$$F_A(x) = \frac{1}{2}(F_2(x) - xF_3(x)), \quad (4.1.27)$$

which measure quark and antiquark distributions, respectively. For example,

$$F_Q^{\nu p}(x) = 2x[d(x) + s(x)], \quad (4.1.28)$$

$$F_A^{\nu p}(x) = 2x[\bar{u}(x) + \bar{c}(x)], \quad (4.1.29)$$

$$F_Q^{\nu n}(x) = 2x[u(x) + s(x)], \quad (4.1.30)$$

$$F_A^{\nu n}(x) = 2x[\bar{d}(x) + \bar{c}(x)], \quad (4.1.31)$$

$$F_Q^{\nu p}(x) = 2x[u(x) + c(x)], \quad (4.1.32)$$

$$F_A^{\nu p}(x) = 2x[\bar{d}(x) + \bar{s}(x)], \quad (4.1.33)$$

$$F_Q^{\nu n}(x) = 2x[d(x) + c(x)], \quad (4.1.34)$$

$$F_A^{\nu n}(x) = 2x[\bar{u}(x) + \bar{s}(x)]. \quad (4.1.35)$$

For an isoscalar target,

$$N = \frac{1}{2}(p + n), \quad (4.1.36)$$

and we have

$$\begin{aligned} F_2^{eN}(x) &= \frac{5}{18}x[u(x) + d(x) + \bar{u}(x) + \bar{d}(x)] \\ &\quad + \frac{8}{18}x[c(x) + \bar{c}(x)] + \frac{2}{18}x[s(x) + \bar{s}(x)], \end{aligned} \quad (4.1.37)$$

$$F_Q^{\nu N}(x) = 2x[u(x) + d(x) + 2s(x)], \quad (4.1.38)$$

$$F_A^{\nu N}(x) = 2x[\bar{u}(x) + \bar{d}(x) + 2\bar{c}(x)], \quad (4.1.39)$$

$$F_Q^{\nu N}(x) = 2x[u(x) + d(x) + 2c(x)], \quad (4.1.40)$$

$$F_A^{\nu N}(x) = 2x[\bar{u}(x) + \bar{d}(x) + 2\bar{s}(x)]. \quad (4.1.41)$$

In the naive parton model the structure functions depend only on scaling variable<sup>2</sup>,

$$x = Q^2/(2M\nu), \quad (4.1.42)$$

whereas in general they could depend on both the energy loss of the leptons,  $\nu = E' - E$  and the four momentum transfer,  $q^2 = -Q^2$ . This is because the basic subprocess is assumed to be a virtual photon of 4-momentum  $q_\mu$  interacting with a quark of 4-momentum  $p_\mu$  ( $p_\mu = \xi P_\mu$ ) with limited transverse momentum producing a quark with 4-momentum,  $p'_\mu = p_\mu + q_\mu$ , as shown in Fig. 4.1. The condition

$$(p')^2 = m_q^2, \quad (4.1.43)$$

where  $m_q$  is the quark mass, implies

$$(\xi P + q)^2 = \xi^2 M^2 + 2\xi(P \cdot q) + q^2 = m_q^2, \quad (4.1.44)$$

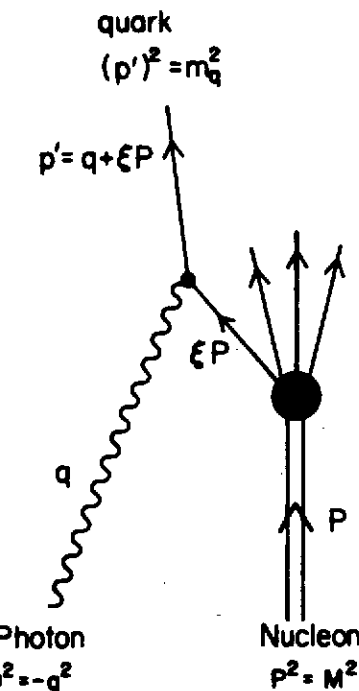


Figure 4.1 Collision of a virtual photon,  $\gamma^*$ , and a nucleon,  $N$ , in the parton model. The photon interacts with a parton carrying momentum fraction,  $\xi$ , of the nucleon.

which as  $-q^2 = Q^2 \rightarrow \infty$  and  $P \cdot q = M\nu \rightarrow \infty$  gives

$$\xi = \frac{-q^2}{2P \cdot q} = \frac{Q^2}{2M\nu} = x, \quad (4.1.45)$$

where  $M$  is the nucleon mass.

If we neglect the strange and charm content within the proton, then the quark number sum rules (4.1.3) and (4.1.4) imply

$$\int_0^1 (F_3^{\nu p}(x) + F_3^{\nu n}(x)) dx = 6, \quad (4.1.46)$$

and

$$\frac{F_2^{ep}(x) + F_2^{en}(x)}{xF_2^{\nu p}(x) + xF_2^{\nu n}(x)} = \frac{5}{18}. \quad (4.1.47)$$

Both (4.1.46) and (4.1.47) are in accordance with data<sup>3</sup>. Furthermore, the low

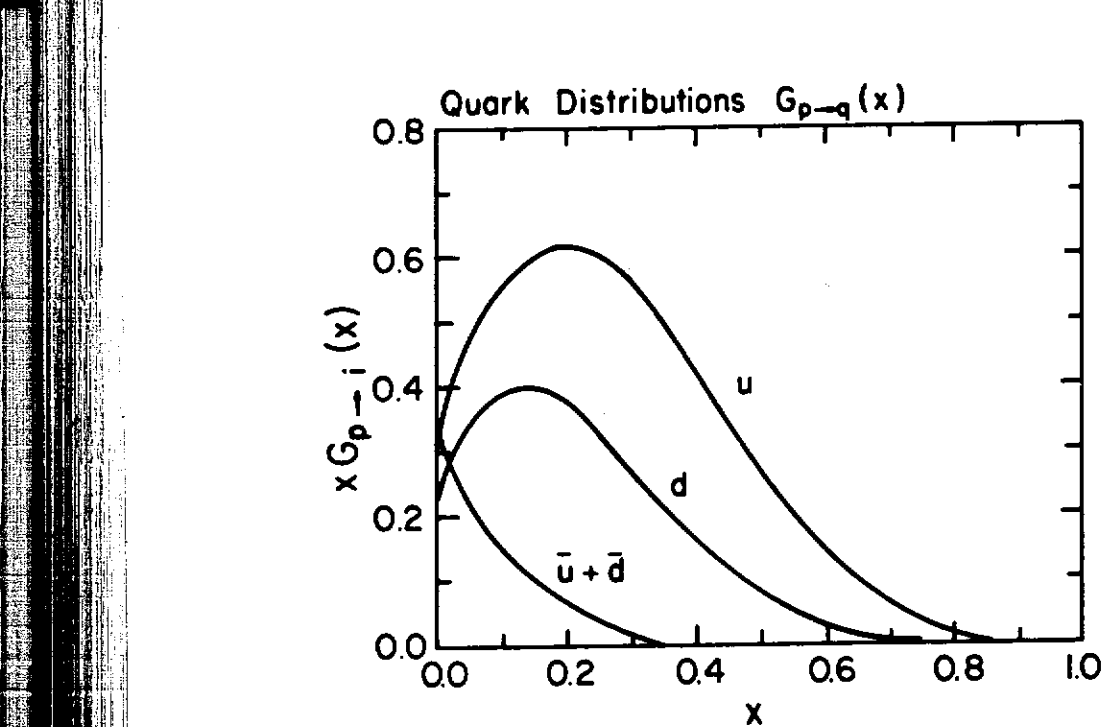


Figure 4.2 Quark distributions within the proton (taken from Ref. 4).

$Q^2$  electron data indicate that

$$\frac{g}{\pi} \int_0^1 (F_2^{ep}(x) + F_2^{en}(x)) dx \approx Q + \bar{Q} \approx 0.45, \quad (4.1.48)$$

indicating that about 50% of the proton momentum is carried by gluons. A fit to the low  $Q^2$  lepton-nucleon data gives the quark distributions shown in Fig. 4.2<sup>4</sup> and yields

$$\begin{aligned} U &= 0.28, \\ D &= 0.15, \\ S &= 0.02, \\ \bar{Q} &= 0.05, \\ G &= 0.50. \end{aligned} \quad (4.1.49)$$

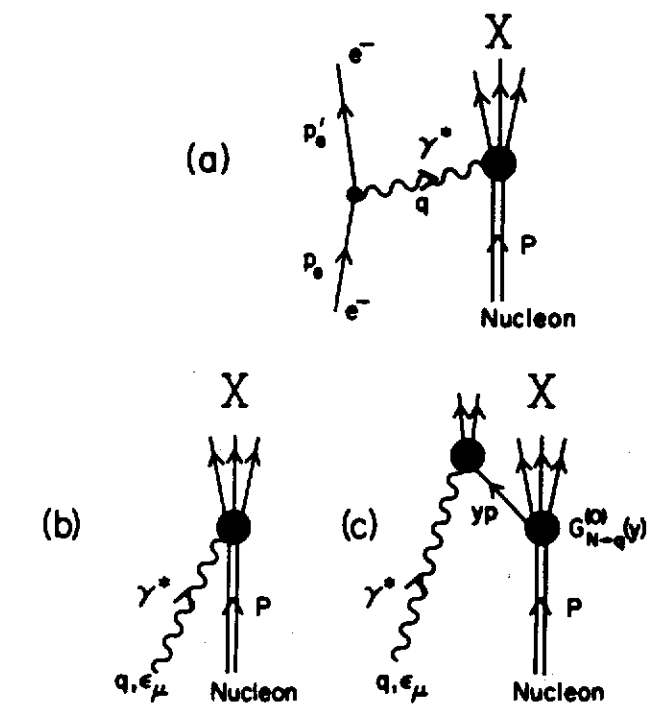


Figure 4.3 (a) Deep inelastic electron nucleon scattering,  $e^- + p \rightarrow e^- + X$ , is related to the (b) virtual photon nucleon total cross section,  $\gamma^* p \rightarrow X$ , which can be expressed in terms of the (c) virtual photon quark total cross section,  $\gamma^* q \rightarrow X$ .

## 4.2 Cross Sections and Structure Functions

The square of the invariant amplitude for the inelastic scattering of an electron off a nucleon shown in Fig. 4.3a is given by

$$|\overline{\mathcal{M}}|^2 = \frac{e^4}{Q^4} L_{\mu\nu} W_{\mu\nu}, \quad (4.2.1)$$

where

$$Q^2 = -q^2, \quad (4.2.2)$$

is the square of the virtual photon 4-momentum and where the spin averaging factors have been absorbed into the tensors  $L_{\mu\nu}$  and  $W_{\mu\nu}$ , which describe the structure of the leptonic and hadronic vertices, respectively. The leptonic

tensor is identical to (2.1.2) and is given by

$$\begin{aligned} L_{\mu\nu} &= \frac{1}{2} \text{tr}(p'_e \gamma_\mu p_e \gamma_\nu) \\ &= \frac{1}{2} 4[(p_e)_\mu (p'_e)_\nu + (p'_e)_\mu (p_e)_\nu - g_{\mu\nu} p_e \cdot p'_e], \end{aligned} \quad (4.2.3)$$

where  $p_e$  and  $p'_e$  are the 4-momenta of the initial and scattered electrons, respectively, and where the electron mass has been neglected and the factor of  $1/2$  arises from the initial state spin averaging. The most general form for the hadronic tensor  $W_{\mu\nu}$  consistent with current conservation which requires

$$q_\mu W_{\mu\nu} = 0, \quad (4.2.4)$$

$$q_\nu W_{\mu\nu} = 0, \quad (4.2.5)$$

is

$$W_{\mu\nu} = -W_1 \left( g_{\mu\nu} - \frac{q_\mu q_\nu}{q^2} \right) + \frac{W_2}{M^2} \left[ P_\mu - \frac{(P \cdot q) q_\mu}{q^2} \right] \left[ P_\nu - \frac{(P \cdot q) q_\nu}{q^2} \right], \quad (4.2.6)$$

where  $P_\mu$  is the nucleon 4-momentum. The structure functions  $W_1$  and  $W_2$  are in general a function of both  $Q^2$  and  $\nu$ , where

$$q = p'_e - p_e, \quad (4.2.7)$$

is the 4-momentum transfer and

$$\nu = E' - E, \quad (4.2.8)$$

is the energy loss of the electrons.

In the laboratory frame the initial and final electron 4-vectors are given by

$$p_e = \begin{pmatrix} E \\ 0 \\ 0 \\ E \end{pmatrix}, \quad (4.2.9)$$

$$p'_e = \begin{pmatrix} E' \\ E' \sin(\theta_{lab}) \\ 0 \\ E' \cos(\theta_{lab}) \end{pmatrix}, \quad (4.2.10)$$

and the nucleon 4-vector is given by

$$P_\mu = \begin{pmatrix} M \\ 0 \\ 0 \\ 0 \end{pmatrix}, \quad (4.2.11)$$

and

$$P \cdot q = M\nu, \quad (4.2.12)$$

where  $M$  is the nucleon mass. The differential cross section in the laboratory

frame is thus

$$\begin{aligned} \frac{d^2\sigma}{dE'd\Omega'} &= \frac{1}{16\pi^2} \frac{E'}{E} |\bar{\mathcal{M}}|^2 = \frac{e^4}{16\pi^2 Q^4} \frac{E'}{E} L_{\mu\nu} W_{\mu\nu} \\ &= \frac{4\alpha^2(E')^2}{Q^4} \left\{ 2W_1(\nu, Q^2) \sin^2\left(\frac{\theta_{lab}}{2}\right) \right. \\ &\quad \left. + W_2(\nu, Q^2) \cos^2\left(\frac{\theta_{lab}}{2}\right) \right\}. \end{aligned} \quad (4.2.13)$$

The structure functions  $W_1$  and  $W_2$  are related to the virtual photon nucleon total cross section shown in Fig. 4.3b. The cross section for the absorption of a virtual photon with helicity  $\lambda$  is given by

$$\sigma_\lambda(\gamma^* N) = \frac{4\pi^2\alpha}{q_{lab}} \epsilon_\mu(\lambda) \epsilon_\nu^*(\lambda) W_{\mu\nu}, \quad (4.2.14)$$

where  $\epsilon_\mu(\lambda)$  is the polarization 4-vector of the virtual photon with helicity  $\lambda$  and  $q_{lab}$  is the magnitude of the 3-momentum of the virtual photon in the laboratory frame. To write this in an invariant form we notice that the flux factor in (A.3.15) implies

$$M q_{lab} = [(P \cdot q)^2 + Q^2 M^2]^{\frac{1}{2}}, \quad (4.2.15)$$

which gives

$$\sigma_\lambda(\gamma^* N) = \frac{4\pi^2\alpha}{\sqrt{\nu^2 + Q^2}} \epsilon_\mu(\lambda) \epsilon_\nu^*(\lambda) W_{\mu\nu}. \quad (4.2.16)$$

We will also write this in the form

$$\sigma_\lambda(\gamma^* N) = \epsilon_\mu(\lambda) \epsilon_\nu^*(\lambda) \sigma_{\mu\nu}(\gamma^* N), \quad (4.2.17)$$

where

$$\sigma_{\mu\nu}(\gamma^* N) = \frac{4\pi^2\alpha}{\sqrt{\nu^2 + Q^2}} W_{\mu\nu}. \quad (4.2.18)$$

If we sum the virtual photon polarization states by the replacement

$$\sum_\lambda \epsilon_\mu(\lambda) \epsilon_\nu^*(\lambda) \rightarrow -g_{\mu\nu}, \quad (4.2.19)$$

we arrive at

$$\begin{aligned} \sigma_\Sigma(\gamma^* N) &= -g_{\mu\nu} \sigma_{\mu\nu}(\gamma^* N) = \\ &= \frac{4\pi^2\alpha}{\sqrt{\nu^2 + Q^2}} \left\{ 3W_1 - \left( 1 + \frac{\nu^2}{Q^2} \right) W_2 \right\}, \end{aligned} \quad (4.2.20)$$

where I have labeled this cross section with the subscript  $\Sigma$  to denote that (4.2.19) has been used. This cross section is a combination of the transverse and longitudinal cross sections.

The cross section for absorption of transverse photons ( $\lambda = \pm 1$ ) propagating along the  $\hat{z}$ -axis with 4-momentum given by

$$q_\mu = \begin{pmatrix} q_0 \\ 0 \\ 0 \\ q_3 \end{pmatrix} = \begin{pmatrix} \nu \\ 0 \\ 0 \\ \sqrt{\nu^2 + Q^2} \end{pmatrix}, \quad (4.2.21)$$

is arrived at by using

$$\epsilon_\mu(\lambda = \pm 1) = \frac{1}{\sqrt{2}} \begin{pmatrix} 0 \\ 1 \\ \pm i \\ 0 \end{pmatrix}, \quad (4.2.22)$$

and computing

$$\sigma_T(\gamma^* N) = \frac{1}{2} [\sigma_{\lambda=+1}(\gamma^* N) + \sigma_{\lambda=-1}(\gamma^* N)]. \quad (4.2.23)$$

The result is

$$\sigma_T(\gamma^* N) = \frac{4\pi^2\alpha}{\sqrt{\nu^2 + Q^2}} W_1. \quad (4.2.24)$$

The cross section for absorption of longitudinal (or scalar) photons can be arrived at by using

$$\epsilon_\mu(\lambda = 0) = \frac{1}{\sqrt{-q^2}} \begin{pmatrix} q_3 \\ 0 \\ 0 \\ q_0 \end{pmatrix} = \frac{1}{Q} \begin{pmatrix} \sqrt{\nu^2 + Q^2} \\ 0 \\ 0 \\ \nu \end{pmatrix}, \quad (4.2.25)$$

which is analogous to (C.1.5), with

$$q \cdot \epsilon = 0, \quad (4.2.26)$$

but in this case (i.e.,  $q^2$  spacelike)

$$\epsilon^2 = +1. \quad (4.2.27)$$

Inserting (4.2.25) into (4.2.14) yields

$$\sigma_L(\gamma^* N) = \frac{4\pi^2\alpha}{\sqrt{\nu^2 + Q^2}} \left\{ -W_1 + \left( 1 + \frac{\nu^2}{Q^2} \right) W_2 \right\}. \quad (4.2.28)$$

A more convenient way of computing the longitudinal cross section is by projection. One writes the polarization vector in (4.2.25) as a linear combination of the 4-vectors  $P_\mu$  and  $q_\mu$ . Namely

$$\epsilon_\mu(\lambda = 0) = aP_\mu + bq_\mu. \quad (4.2.29)$$

The condition  $q \cdot \epsilon = 0$  implies

$$b = -a(P \cdot q)/q^2, \quad (4.2.30)$$

and the normalization  $\epsilon^2 = 1$  gives

$$a = \left( P^2 - \frac{(P \cdot q)^2}{q^2} \right)^{-\frac{1}{2}}, \quad (4.2.31)$$

or

$$a = \frac{Q}{M\sqrt{\nu^2 + Q^2}}. \quad (4.2.32)$$

Using

$$\epsilon_\mu(\lambda = 0) = a \left( P_\mu - \frac{P \cdot q}{q^2} q_\mu \right), \quad (4.2.33)$$

with  $a$  given above the projection in (4.2.16) becomes

$$\begin{aligned} \epsilon_\mu(\lambda = 0)\epsilon_\nu^*(\lambda = 0)W_{\mu\nu} &= a^2 \left( P_\mu - \frac{P \cdot q}{q^2} q_\mu \right) \left( P_\nu - \frac{P \cdot q}{q^2} q_\nu \right) W_{\mu\nu} \\ &= a^2 P_\mu P_\nu W_{\mu\nu}, \end{aligned} \quad (4.2.34)$$

since  $W_{\mu\nu}$  satisfies (4.2.4) and (4.2.5). It is easy to see that

$$a^2 P_\mu P_\nu W_{\mu\nu} = -W_1 + \left( 1 + \frac{\nu^2}{Q^2} \right) W_2, \quad (4.2.35)$$

where  $a$  is given by (4.2.32). Thus,

$$\begin{aligned} \sigma_L(\gamma^* N) &= \frac{Q^2}{M^2(\nu^2 + Q^2)} P_\mu P_\nu \sigma_{\mu\nu}(\gamma^* N) = \\ &= \frac{4\pi^2\alpha}{\sqrt{\nu^2 + Q^2}} \left\{ -W_1 + \left( 1 + \frac{\nu^2}{Q^2} \right) W_2 \right\}, \end{aligned} \quad (4.2.36)$$

which is the same result as obtained in (4.2.28).

We can now solve for the structure functions  $W_1$  and  $W_2$  in terms of the virtual photon total cross section  $\sigma_{\mu\nu}(\gamma^* N)$  in (4.2.17). From (4.2.36) and (4.2.20) we arrive at

$$2MW_1 = \frac{M\sqrt{\nu^2 + Q^2}}{4\pi^2\alpha} (\sigma_\Sigma(\gamma^* N) + \sigma_L(\gamma^* N)), \quad (4.2.37)$$

$$2M \left( 1 + \frac{\nu^2}{Q^2} \right) W_2 = \frac{M\sqrt{\nu^2 + Q^2}}{4\pi^2\alpha} (\sigma_\Sigma(\gamma^* N) + 3\sigma_L(\gamma^* N)), \quad (4.2.38)$$

where

$$\sigma_\Sigma(\gamma^* N) = -g_{\mu\nu} \sigma_{\mu\nu}(\gamma^* N) \quad (4.2.39)$$

and

$$\sigma_L(\gamma^* N) = \frac{Q^2}{M^2(\nu^2 + Q^2)} P_\mu P_\nu \sigma_{\mu\nu}(\gamma^* N). \quad (4.2.40)$$

We are going to be interested in the region  $Q^2$  large and  $x$  fixed, where  $x$  is

the scaling variable in (4.1.45). Namely,

$$x = \frac{Q^2}{2P \cdot q} = \frac{Q^2}{2M\nu}, \quad (4.2.41)$$

so that

$$1 + \frac{\nu^2}{Q^2} \xrightarrow[\substack{Q^2 \text{ large} \\ x \text{ fixed}}} \frac{\nu}{2Mx}, \quad (4.2.42)$$

and

$$M\sqrt{\nu^2 + Q^2} \xrightarrow[\substack{Q^2 \text{ large} \\ x \text{ fixed}}} \frac{Q^2}{2x}. \quad (4.2.43)$$

These approximations give

$$\begin{aligned} 2MW_1(x, Q^2) &\equiv 2F_1(x, Q^2) \equiv \mathcal{F}_1(x, Q^2) = \\ &= \frac{Q^2}{8\pi^2\alpha x} [\sigma_\Sigma(\gamma^* N) + \sigma_L(\gamma^* N)], \end{aligned} \quad (4.2.44)$$

$$\begin{aligned} \frac{\nu W_2(x, Q^2)}{x} &\equiv \frac{1}{x} F_2(x, Q^2) \equiv \mathcal{F}_2(x, Q^2) = \\ &= \frac{Q^2}{8\pi^2\alpha x} [\sigma_\Sigma(\gamma^* N) + 3\sigma_L(\gamma^* N)], \end{aligned} \quad (4.2.45)$$

where  $\sigma_\Sigma(\gamma^* N)$  is given by (4.2.39) and

$$\sigma_L(\gamma^* N) = \frac{4x^2}{Q^2} P_\mu P_\nu \sigma_{\mu\nu}(\gamma^* N). \quad (4.2.46)$$

The structure functions  $F_1$  and  $F_2$  are related to  $W_1$  and  $\nu W_2$  according to

$$F_1(x, Q^2) \equiv MW_1(x, Q^2), \quad (4.2.47)$$

$$F_2(x, Q^2) \equiv \nu W_2(x, Q^2), \quad (4.2.48)$$

and it is convenient to define

$$\mathcal{F}_1(x, Q^2) = 2F_1(x, Q^2), \quad (4.2.49)$$

and

$$\mathcal{F}_2(x, Q^2) = \frac{1}{x} F_2(x, Q^2). \quad (4.2.50)$$

The longitudinal and transverse structure functions are defined by

$$F_L(x, Q^2) = F_2(x, Q^2) - 2xF_1(x, Q^2), \quad (4.2.51)$$

$$F_T(x, Q^2) = 2F_1(x, Q^2), \quad (4.2.52)$$

respectively, which can be written as

$$\mathcal{F}_L(x, Q^2) = \mathcal{F}_2(x, Q^2) - \mathcal{F}_1(x, Q^2), \quad (4.2.53)$$

$$\mathcal{F}_T(x, Q^2) = \mathcal{F}_1(x, Q^2), \quad (4.2.54)$$

where

$$\mathcal{F}_L(x, Q^2) = \frac{1}{x} F_L(x, Q^2). \quad (4.2.55)$$

From (4.2.44) and (4.2.45) we see that

$$\begin{aligned} \mathcal{F}_L(x, Q^2) &= 2 \left( \frac{Q^2}{8\pi^2\alpha x} \right) \sigma_L(\gamma^* N) \\ &= \left( \frac{x}{\pi^2\alpha} \right) P_\mu P_\nu \sigma_{\mu\nu}(\gamma^* N) \end{aligned} \quad , (4.2.56)$$

and from (4.2.24) and (4.2.44) we see that

$$\mathcal{F}_1(x, Q^2) = 2 \left( \frac{Q^2}{8\pi^2\alpha x} \right) \sigma_T(\gamma^* N), \quad (4.2.57)$$

so that

$$R^{DIS}(x, Q^2) \equiv \frac{\mathcal{F}_L(x, Q^2)}{\mathcal{F}_1(x, Q^2)} = \frac{\sigma_L(\gamma^* N)}{\sigma_T(\gamma^* N)}, \quad (4.2.58)$$

measures the ratio of the longitudinal to the transverse virtual photon nucleon total cross section. It is also useful to define

$$R_2^{DIS}(x, Q^2) \equiv \frac{\mathcal{F}_L(x, Q^2)}{\mathcal{F}_2(x, Q^2)} = \frac{\sigma_L(\gamma^* p)}{\sigma_T(\gamma^* N) + \sigma_L(\gamma^* p)}, \quad (4.2.59)$$

with

$$\mathcal{F}_2(x, Q^2) = 2 \left( \frac{Q^2}{8\pi^2\alpha x} \right) (\sigma_T(\gamma^* N) + \sigma_L(\gamma^* N)). \quad (4.2.60)$$

Furthermore, if we define a structure function  $\mathcal{F}_\Sigma(x, Q^2)$  by

$$\mathcal{F}_\Sigma(x, Q^2) = \left( \frac{Q^2}{8\pi^2\alpha x} \right) \sigma_\Sigma(\gamma^* N), \quad (4.2.61)$$

then

$$\mathcal{F}_\Sigma(x, Q^2) = \frac{3}{2} \mathcal{F}_1(x, Q^2) - \frac{1}{2} \mathcal{F}_2(x, Q^2), \quad (4.2.62)$$

$$\mathcal{F}_2(x, Q^2) = \mathcal{F}_\Sigma(x, Q^2) + \frac{3}{2} \mathcal{F}_L(x, Q^2), \quad (4.2.63)$$

$$\mathcal{F}_1(x, Q^2) = \mathcal{F}_\Sigma(x, Q^2) + \frac{1}{2} \mathcal{F}_L(x, Q^2), \quad (4.2.64)$$

and

$$\sigma_\Sigma(\gamma^* N) = 2\sigma_T(\gamma^* N) - \sigma_L(\gamma^* N). \quad (4.2.65)$$

We can now express the virtual photon nucleon total cross section in terms of the virtual photon parton total cross section as shown in Fig. 4.3c. For example, the structure function  $\mathcal{F}(x, Q^2)$  can be decomposed as follows

$$\mathcal{F}(x, Q^2) dx = G_{p \rightarrow q}^{(0)}(y) dy \hat{\mathcal{F}}(z, Q^2) dz, \quad (4.2.66)$$

where  $G_{p \rightarrow q}^{(0)}(y) dy$  is the probability of finding a quark with 4-momentum

$$p = yP, \quad (4.2.67)$$

and  $\hat{F}(z, Q^2)$  is the structure function corresponding to the virtual photon parton total cross section where

$$z = \frac{Q^2}{2p \cdot q}, \quad (4.2.68)$$

which is from (4.2.67) related to  $x$  by

$$z = x/y. \quad (4.2.69)$$

In particular,

$$\begin{aligned} \mathcal{F}_\Sigma(x, Q^2) &= \int_x^1 \frac{dy}{y} G_{p \rightarrow q}^{(0)}(y) \hat{F}_\Sigma(z, Q^2) \\ &= \int_x^1 \frac{dy}{y} G_{p \rightarrow q}^{(0)}(y) \left( \frac{Q^2}{8\pi^2 \alpha z} \right) \hat{\sigma}_\Sigma(\gamma^* q), \end{aligned} \quad (4.2.70)$$

and

$$\mathcal{F}_L(x, Q^2) = \int_x^1 \frac{dy}{y} G_{p \rightarrow q}^{(0)}(y) \left( \frac{Q^2}{8\pi^2 \alpha z} \right) 2\hat{\sigma}_L(\gamma^* q), \quad (4.2.71)$$

with

$$\hat{\sigma}_L(\gamma^* N) = \frac{4z^2}{Q^2} p_\mu p_\nu \hat{\sigma}_{\mu\nu}(\gamma^* q), \quad (4.2.72)$$

where the virtual photon quark total cross section is defined in analogy to (4.2.17),

$$\hat{\sigma}_\lambda(\gamma^* q) = \epsilon_\mu(\lambda) \epsilon_\nu^*(\lambda) \hat{\sigma}_{\mu\nu}(\gamma^* q). \quad (4.2.73)$$

The factor of 2 in (4.2.71) is due to the fact that in (4.2.23) we defined  $\hat{\sigma}_L$  as the *average* of the two longitudinal helicities rather than the sum of the two.

In the naive parton model one only considers the Born term  $\gamma^* q \rightarrow q$  in Fig. 4.1 when computing the virtual photon parton total cross section. This Born term gives

$$\hat{\sigma}_\Sigma(\gamma^* q \rightarrow q) = \frac{8\pi^2 \alpha e_q^2 z}{Q^2} \delta(1-z), \quad (4.2.74)$$

and

$$\hat{\sigma}_L(\gamma^* q \rightarrow q) = \frac{4z^2}{Q^2} p_\mu p_\nu \hat{\sigma}_{\mu\nu}(\gamma^* q \rightarrow q) = 0, \quad (4.2.75)$$

provided that one neglects quark masses. This implies from (4.2.70) that

$$\mathcal{F}_\Sigma(x, Q^2) = e_q^2 G_{p \rightarrow q}^{(0)}(x), \quad (4.2.76)$$

and from (4.2.71) that

$$\mathcal{F}_L(x, Q^2) = 0, \quad (4.2.77)$$

so that

$$\mathcal{F}_2(x, Q^2) = \mathcal{F}_2(x) = e_q^2 G_{p \rightarrow q}^{(0)}(x), \quad (4.2.78)$$

$$\mathcal{F}_1(x, Q^2) = \mathcal{F}_1(x) = e_q^2 G_{p \rightarrow q}^{(0)}(x), \quad (4.2.79)$$

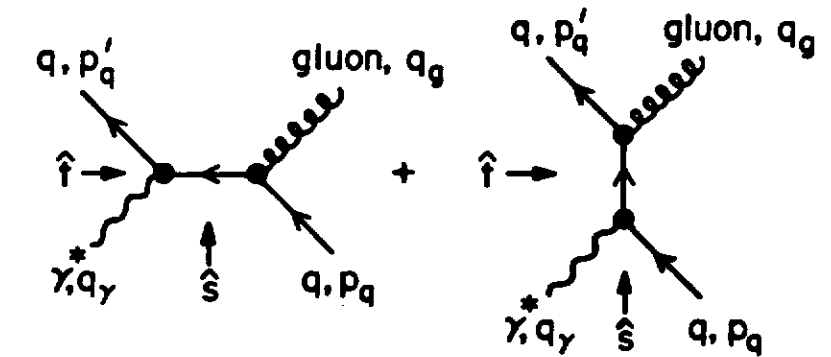


**Figure 4.4.** Leading order diagrams for gluon production via the “Compton” process  $\gamma^* + q \rightarrow q + g$ , where  $p_\gamma$  and  $p_q$  are the 4-momenta of the initial virtual photon and quark, respectively, and  $p_{q'}$  and  $p_g$  are the 4-momenta of the outgoing quark and gluon, respectively.

and

$$R_1^{DIS}(x, Q^2) = R_2^{DIS}(x, Q^2) = 0. \quad (4.2.80)$$

In the naive parton model  $\mathcal{F}_1(x)$  and  $\mathcal{F}_2(x)$  are equal and measure the quark distributions as given in (4.1.16) and (4.1.17). The longitudinal structure function vanishes provided  $Q^2$  is large enough to neglect “higher twist” terms that behave like  $M^2/Q^2$ .

### 4.3 Gluon Emission and Initial State Gluons

We now consider, as we did for  $e^+e^-$  annihilations in Chapter 2, the possibility that a quark can radiate a gluon before or after its interaction with the virtual photon,  $\gamma^*$ , as in Fig. 4.4. The differential cross section for the subprocess  $\gamma^* + q \rightarrow q + g$  is given by

$$\begin{aligned} \frac{d\hat{\sigma}_\Sigma^q}{dt}(\hat{s}, \hat{t}) &= \frac{1}{64\pi\hat{s}\hat{p}_{cm}^2} |\overline{\mathcal{M}}(\gamma_\Sigma^* + q \rightarrow q + g)|^2 \\ &= \frac{z^2}{16\pi Q^4} |\overline{\mathcal{M}}(\gamma_\Sigma^* + q \rightarrow q + g)|^2, \end{aligned} \quad (4.3.1)$$

where I have used (A.3.17) and in this case (A.3.11) becomes

$$\hat{s}p_{cm}^2 = \frac{(\hat{s} + Q^2)^2}{4} = \frac{Q^4}{4z^2}, \quad (4.3.2)$$

where  $z$  is defined as in (4.2.68),

$$z = \frac{Q^2}{2p_q \cdot q_\gamma} = \frac{Q^2}{\hat{s} + Q^2}. \quad (4.3.3)$$

The invariants are given by

$$\hat{s} = (q_\gamma + p_q)^2 = (p'_q + q_g)^2 = -Q^2 + 2q_\gamma \cdot p_q, \quad (4.3.4)$$

$$\hat{t} = (p'_q - q_\gamma)^2 = (p_q - q_g)^2 = -2q_\gamma \cdot p'_q, \quad (4.3.5)$$

$$\hat{u} = (q_g - q_\gamma)^2 = (p_q - p'_q)^2 = -2q_\gamma \cdot q_g, \quad (4.3.6)$$

with momentum conservation giving

$$q_\gamma + p_q = p'_q + q_g, \quad (4.3.7)$$

so that

$$\hat{s} + \hat{t} + \hat{u} + Q^2 = 0, \quad (4.3.8)$$

where

$$Q^2 = -q_\gamma^2, \quad (4.3.9)$$

where the 4-momentum of the initial quark,  $p_q$ , final quark,  $p'_q$ , gluon,  $q_g$  and virtual photon,  $q_\gamma$ , are shown in Fig. 4.4.

The subscript  $\Sigma$  in (4.3.1) is to signify that (4.2.19) has been used to sum the incoming virtual photon polarization states, and the superscript  $q$  labels the subprocess  $\gamma^* + q \rightarrow q + g$ . The amplitude squared is given by

$$|\bar{\mathcal{M}}(\gamma_\Sigma^* + q \rightarrow q + g)|^2 = e^2 e_q^2 g_s^2 \frac{4}{3} \frac{1}{2} \\ 8 \left\{ -\frac{\hat{t}}{\hat{s}} - \frac{\hat{s}}{\hat{t}} - \frac{2Q^2(\hat{s} + \hat{t} + Q^2)}{\hat{s}\hat{t}} \right\}, \quad (4.3.10)$$

where the factor of  $4/3$  is the color factor  $\text{tr}(T_a T_a)/3$  as discussed in Appendix D and the factor  $1/2$  is to average over initial state quark spins. The differential cross section is thus given by

$$\frac{d\hat{\sigma}_\Sigma^q}{dt}(\hat{s}, \hat{t}) = \frac{\pi \alpha \alpha_s e_q^2 z^2}{Q^4} \frac{16}{3} \left\{ -\frac{\hat{t}}{\hat{s}} - \frac{\hat{s}}{\hat{t}} - \frac{2Q^2(\hat{s} + \hat{t} + Q^2)}{\hat{s}\hat{t}} \right\}. \quad (4.3.11)$$

The total virtual photon quark cross section is arrived at by integrating (4.3.11) over  $\hat{t}$ . Namely,

$$\hat{\sigma}_\Sigma^q(\hat{s}) = \int_{\hat{t}_{\min}}^{\hat{t}_{\max}} \frac{d\hat{\sigma}_\Sigma^q}{dt}(\hat{s}, \hat{t}) d\hat{t}, \quad (4.3.12)$$

where

$$\hat{t}_{\min} = 0, \quad (4.3.13)$$

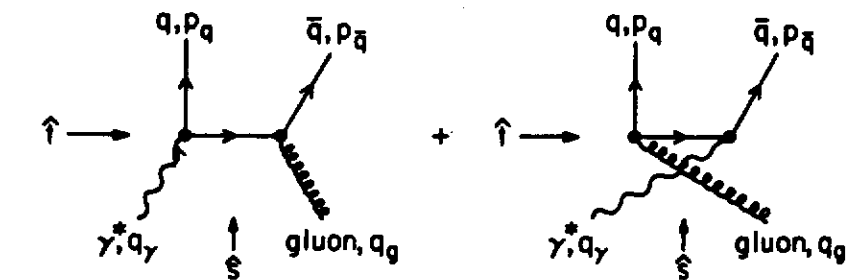


**Figure 4.5** Leading order diagrams for photon-gluon “annihilation” via the process  $\gamma^* + g \rightarrow q + \bar{q}$ , where  $q_\gamma$  and  $q_g$  are the 4-momenta of the initial virtual photon and gluon, respectively, and  $p_q$  and  $p_{\bar{q}}$  are the 4-momenta of the outgoing quark and antiquark, respectively.

and

$$\hat{t}_{\max} = -(\hat{s} + Q^2) = -Q^2/z. \quad (4.3.14)$$

As was the case for  $e^+e^-$  annihilations in (2.3.37) this integral is divergent and we cannot proceed without choosing a regularization scheme. The differential cross section in (4.3.11) becomes infinite as  $\hat{t} \rightarrow 0$  and this vanishing of  $\hat{t}$  occurs for the same reasons as shown in (2.3.39) (i.e.,  $\omega \rightarrow 0$  or  $\theta_{23} \rightarrow 0$ ).

One must also correct the naive parton model by including the possibility that a gluon in the initial proton can produce a quark-antiquark pair which the virtual photon then couples to as shown in Fig. 4.5. The differential cross section for the subprocess  $\gamma^* + g \rightarrow q + \bar{q}$  is given by

$$\frac{d\hat{\sigma}_\Sigma^q}{dt}(\hat{s}, \hat{t}) = \frac{1}{64\pi \hat{s} p_{cm}^2} |\bar{\mathcal{M}}(\gamma_\Sigma^* + g \rightarrow q + \bar{q})|^2 \\ = \frac{z^2}{16\pi Q^4} |\bar{\mathcal{M}}(\gamma_\Sigma^* + g \rightarrow q + \bar{q})|^2, \quad (4.3.15)$$

where in this case

$$z = \frac{Q^2}{2q_g \cdot q_\gamma} = \frac{Q^2}{\hat{s} + Q^2}, \quad (4.3.16)$$

and

$$\hat{s} = (q_\gamma + q_g)^2, \quad (4.3.17)$$

$$\hat{t} = (p_q - q_\gamma)^2, \quad (4.3.18)$$

$$\hat{u} = (p_{\bar{q}} - q_{\gamma})^2, \quad (4.3.19)$$

with (4.3.8) and (4.3.9) also holding. As in (4.3.1) the subscript  $\Sigma$  is to signify that the polarization states of the incoming virtual photon have been summed using (4.2.19). The superscript  $g$  labels the subprocess  $\gamma^* + g \rightarrow q + \bar{q}$ . The amplitude in Fig. 4.5 squared is given by

$$|\overline{\mathcal{M}}(\gamma^* + g \rightarrow q + \bar{q})|^2 = e^2 e_q^2 g_s^2 \frac{4}{8} \frac{1}{2} \\ 8 \left\{ \frac{\hat{u}}{\hat{t}} + \frac{\hat{t}}{\hat{u}} + \frac{2Q^2(\hat{u} + \hat{t} + Q^2)}{\hat{t}\hat{u}} \right\}, \quad (4.3.20)$$

where the factor of  $4/8$  is the color factor  $\text{tr}(T_a T_a)/8$  as discussed in Appendix D and  $1/2$  is to average over the two spin states of the initial state gluon (considered as massless). The differential cross section in (4.3.15) is thus

$$\frac{d\hat{\sigma}_{\Sigma}^g}{dt}(\hat{s}, \hat{t}) = \frac{\pi \alpha \alpha_s e_q^2 z^2}{Q^4} 2 \left\{ \frac{\hat{u}}{\hat{t}} + \frac{\hat{t}}{\hat{u}} + \frac{2Q^2(\hat{t} + \hat{u} + Q^2)}{\hat{t}\hat{u}} \right\}, \quad (4.3.21)$$

which diverges as  $\hat{t} \rightarrow 0$  or  $\hat{u} \rightarrow 0$ . The total cross section arrived at by integrating over  $\hat{t}$  is

$$\hat{\sigma}_{\Sigma}^g(\hat{s}) = \int_{\hat{t}_{\min}}^{\hat{t}_{\max}} \frac{d\hat{\sigma}_{\Sigma}^g}{dt}(\hat{s}, \hat{t}) d\hat{t}, \quad (4.3.22)$$

and is infinite since  $\hat{t}_{\min} = 0$ . Again the origin of these divergences are the same as in (2.3.39) and we cannot proceed without choosing some scheme for regularizing the infrared singularities.

## 4.4 Order $\alpha_s$ Corrections – MG Scheme

We can regulate the divergences in the subprocess  $\gamma^* + q \rightarrow q + g$  by giving the gluon a fictitious mass  $q_g^2 = m_g^2$  as we did in the  $e^+e^-$  case in Chapter 2. The differential cross section in (4.3.11) becomes

$$\frac{d\hat{\sigma}_{\Sigma}^g}{dt}(\hat{s}, \hat{t}) = \frac{\pi \alpha \alpha_s e_q^2 z^2}{Q^4} \frac{16}{3} \left\{ -\frac{\hat{t}}{\hat{s}} - \frac{\hat{s}}{\hat{t}} - \frac{2(Q^2 - m_g^2)(\hat{s} + \hat{t} + Q^2 - m_g^2)}{\hat{s}\hat{t}} \right. \\ \left. - m_g^2 Q^2 \left( \frac{1}{\hat{t}^2} + \frac{1}{\hat{s}^2} \right) \right\}. \quad (4.4.1)$$

Integrating over  $\hat{t}$  with

$$\hat{t}_{\min} = -\frac{\beta z Q^2}{1-z}, \quad (4.4.2)$$

$$\hat{t}_{\max} = -\frac{Q^2}{z} + \beta Q^2, \quad (4.4.3)$$

gives

$$\hat{\sigma}_{MG, \Sigma}^g(z, Q^2) = \frac{\pi \alpha \alpha_s e_q^2}{Q^2} \frac{16}{3} z \left\{ \frac{(1+z^2)}{1-z} \log \left( \frac{Q^2(1-z)}{m_g^2 z^2} \right) \right. \\ \left. - \frac{3}{2} \frac{1}{1-z} + z + 1 + \beta \frac{2z^3 - z^2}{(1-z)^2} + \frac{1}{2} \beta^2 \frac{2z^3 - z^4}{(1-z)^3} \right\}, \quad (4.4.4)$$

where the label “MG” refers to the massive gluon scheme and

$$\beta = m_g^2/Q^2, \quad (4.4.5)$$

and  $z$  is defined by (4.3.3). Terms that give no contribution to the integral over  $z$  in the limit  $\beta \rightarrow 0$  have been dropped. The logarithmic term in the total cross section comes from the integral

$$\left( \frac{\hat{s}^2 + 2Q^2(\hat{s} + Q^2)}{\hat{s}} \right) \int_{-Q^2/z}^{-\beta z Q^2/(1-z)} \left( -\frac{d\hat{t}}{\hat{t}} \right) = \\ \frac{Q^2(1+z^2)}{z(1-z)} \log \left( \frac{(1-z)}{\beta z^2} \right), \quad (4.4.6)$$

while the  $1/(1-z)$  term originates from

$$-\frac{1}{\hat{s}} \int_{-Q^2/z}^0 (\hat{t} + 2Q^2) d\hat{t} = \frac{1}{2} \frac{Q^2}{z(1-z)} - 2 \frac{Q^2}{(1-z)} \\ = -\frac{3}{2} \frac{Q^2}{z(1-z)} + 2 \frac{Q^2}{z}, \quad (4.4.7)$$

and

$$-m_g^2 Q^2 \int_{-Q^2/z}^{-\beta z Q^2/(1-z)} \frac{d\hat{t}}{\hat{t}^2} = -\frac{(1-z)}{z} Q^2. \quad (4.4.8)$$

This parton subprocess must be “embedded” in the experimentally observed reaction  $\gamma^* + N \rightarrow X$  as shown in Fig. 4.3c. For example,

$$d\sigma = G_{p \rightarrow q}^{(0)}(y) dy \left( \frac{d\hat{\sigma}^q}{dz} \right) dz, \quad (4.4.9)$$

where  $G_{p \rightarrow q}^{(0)}(y)$  is the probability of finding a quark with momentum

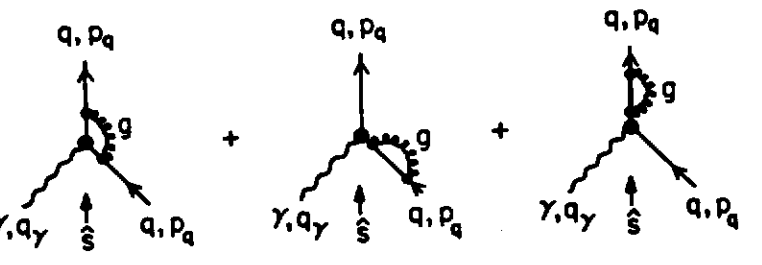
$$p_q = y P, \quad (4.4.10)$$

and  $(d\hat{\sigma}^q/dz)dz$  is the cross section for scattering with a value of  $z$  given by (4.3.3). Defining the parton model scaling variable  $x$  as in (4.1.45),

$$x = \frac{Q^2}{2P \cdot q_{\gamma}}, \quad (4.4.11)$$

gives

$$z = x/y, \quad (4.4.12)$$

Figure 4.6 Virtual gluon corrections to the Born term,  $\gamma^* + q \rightarrow q$ .

so that

$$\frac{1}{\sigma_0} \frac{d\sigma}{dx} = \int_z^1 \frac{dy}{y} G_{p \rightarrow q}^{(0)}(y) \left( \frac{1}{\sigma_0} \frac{d\hat{\sigma}^q}{dz} \right), \quad (4.4.13)$$

with the limits of integration coming from the condition that  $z \leq 1$ .Equation (4.2.70) shows that the structure function  $F_\Sigma(x, Q^2)$  is related to the total  $\gamma^* q$  cross section by

$$F_\Sigma(x, Q^2) = \int_z^1 \frac{dy}{y} G_{p \rightarrow q}^{(0)}(y) \left( \frac{Q^2}{8\pi^2 \alpha z} \right) \hat{\sigma}_\Sigma^q(z, Q^2), \quad (4.4.14)$$

and comparing this with (4.4.13) gives

$$\frac{1}{\sigma_0} \frac{d\hat{\sigma}_\Sigma^q}{dz} = \left( \frac{Q^2}{8\pi^2 \alpha e_q^2 z} \right) \hat{\sigma}_\Sigma^q(z, Q^2), \quad (4.4.15)$$

where  $\sigma_0$  is given by (2.1.30). Substituting (4.4.4) into this equation yields

$$\left( \frac{1}{\sigma_0} \frac{d\hat{\sigma}_{MG,\Sigma}^q}{dz} \right)_{DIS} = \frac{2\alpha_s}{3\pi} \left\{ \frac{1+z^2}{1-z} \log \left( \frac{(1-z)Q^2}{z^2 m_g^2} \right) - \frac{3}{2} \frac{1}{1-z} + z + 1 + \frac{5}{4} \delta(1-z) \right\}, \quad (4.4.16)$$

where  $DIS$  refers to deep inelastic scattering and where the  $\beta$  and  $\beta^2$  terms in (4.4.4) have been replaced by a  $\delta$ -function contribution similar to what we did in (2.5.6).It is interesting to compare this with the  $e^+e^-$  result from (2.5.6),

$$\left( \frac{1}{\sigma_0} \frac{d\hat{\sigma}_{MG}^q}{dz} \right)_{e^+e^-} = \frac{2\alpha_s}{3\pi} \left\{ \frac{1+z^2}{1-z} \log \left( \frac{x(1-x)Q^2}{m_g^2} \right) \right.$$

$$\left. - \frac{3}{2} \frac{1}{1-x} + \frac{1}{2}x + \frac{1}{2} + \frac{5}{4} \delta(1-x) \right\}. \quad (4.4.17)$$

Equations (4.4.16) and (4.4.17) are very similar but not quite the same. The integral over  $x$  of (4.4.17) was accomplished using (2.5.7) - (2.5.10) with the result in (2.5.11) that

$$(\hat{\sigma}_{MG}(\text{real}))_{e^+e^-} = \frac{2\alpha_s}{3\pi} \sigma_0 \left\{ \log^2(\beta) + 3 \log(\beta) - \frac{\pi^2}{3} + 5 \right\}. \quad (4.4.18)$$

The integration of (4.4.16) can also be performed using (2.5.7) - (2.5.10) and yields the slightly different result,

$$(\hat{\sigma}_{MG}(\text{real}))_{DIS} = \frac{2\alpha_s}{3\pi} \sigma_0 \left\{ \log^2(\beta) + 3 \log(\beta) + \frac{2\pi^2}{3} + 2 \right\}, \quad (4.4.19)$$

with  $\beta$  given by (4.4.5) and  $Q^2 = -q^2 > 0$  (i.e., spacelike). The virtual gluon contributions in Fig. 4.6 are given by (2.7.1). Namely,

$$(\hat{\sigma}_{MG}(\text{virtual}))_{DIS} = \frac{2\alpha_s}{3\pi} \sigma_0 \left\{ -\log^2(\beta) - 3 \log(\beta) - \frac{7}{2} - \frac{2\pi^2}{3} \right\}_{\text{spacelike}}, \quad (4.4.20)$$

and, as was the  $e^+e^-$  case, the total

$$\begin{aligned} (\hat{\sigma}_{MG}(\text{real}) + \hat{\sigma}_{MG}(\text{virtual}))_{DIS} &= \frac{2\alpha_s}{3\pi} \sigma_0 \left\{ \frac{2\pi^2}{3} + 2 - \frac{7}{2} - \frac{2\pi^2}{3} \right\}, \\ &= \frac{2\alpha_s}{3\pi} \sigma_0 \left( -\frac{3}{2} \right) = -\frac{\alpha_s}{\pi} \sigma_0, \end{aligned} \quad (4.4.21)$$

is finite and independent of  $\beta$  as  $\beta \rightarrow 0$ . Equation (4.4.21), however, has the opposite sign from the  $e^+e^-$  case in (2.7.6). In this case the perturbation series has the form

$$\sigma_{\text{tot}}^{DIS} = \sigma_0 \left( 1 - \frac{\alpha_s}{\pi} + \dots \right), \quad (4.4.22)$$

compared with

$$\sigma_{\text{tot}}^{e^+e^-} = \sigma_0 \left( 1 + \frac{\alpha_s}{\pi} + \dots \right), \quad (4.4.23)$$

for  $e^+e^-$  annihilations. In  $e^+e^-$  annihilations the final state gluon interactions are attractive (color singlet) causing the total cross section to increase. In deep inelastic scattering this is not the case and the order  $\alpha_s$  corrections reduce the total cross section.

Now that we know from (4.4.21) that

$$\hat{\sigma}_{MG}^q(\text{virtual}) + \int_0^1 \frac{d\hat{\sigma}_{MG,\Sigma}^q}{dz} dz = -\frac{\alpha_s}{\pi} \sigma_0, \quad (4.4.24)$$

we write

$$\int_0^1 \left\{ \frac{d\hat{\sigma}_{MG,\Sigma}^q}{dz} + \left( \hat{\sigma}_{MG}^q(\text{virtual}) + \frac{\alpha_s}{\pi} \sigma_0 \right) \delta(1-z) \right\} dz = 0, \quad (4.4.25)$$

and define “+ functions” just as we did in (3.2.4) and (3.2.5). Namely,

$$\int_0^1 \left( \frac{d\sigma_{MG}^q}{dz} \right)_+ dz = 0, \quad (4.4.26)$$

and the new differential cross section is written as

$$\frac{1}{\sigma_0} \frac{d\sigma^q}{dz} = \frac{1}{\sigma_0} \left( \frac{d\sigma^q}{dz} \right)_+ + \alpha_s I_q^{DIS} \delta(1-z), \quad (4.4.27)$$

with

$$\sigma_{tot}^{DIS} = \sigma_0 (1 + \alpha_s I_q^{DIS} + \dots), \quad (4.4.28)$$

and

$$\alpha_s I_q^{DIS} = -\frac{\alpha_s}{\pi}. \quad (4.4.29)$$

In this case

$$\frac{1}{\sigma_0} \left( \frac{d\hat{\sigma}_{MG,\Sigma}^q}{dz} \right)_+ = \frac{\alpha_s}{2\pi} P_{q \rightarrow qg}(z) \log(Q^2/m_g^2) + \alpha_s f_{MG,\Sigma}^{q,DIS}(z), \quad (4.4.30)$$

where

$$P_{q \rightarrow qg}(z) = \frac{4}{3} \left( \frac{1+z^2}{1-z} \right)_+ \quad (4.4.31)$$

is the same function as (3.2.8) and

$$\begin{aligned} \alpha_s f_{MG,\Sigma}^{q,DIS}(z) = & \frac{2\alpha_s}{3\pi} \left\{ (1+z^2) \left( \frac{\log(1-z)}{1-z} \right)_+ + \frac{1+z^2}{1-z} (-2\log(z)) \right. \\ & \left. - \frac{3}{2} \frac{1}{(1-z)_+} + z + 1 - \left( \frac{2\pi^2}{3} + \frac{9}{4} \right) \delta(1-z) \right\}. \end{aligned} \quad (4.4.32)$$

As before the “little  $f$ ” function in (4.4.30) depends on the process and the regularization scheme chosen. However since (4.4.28) must hold in any regularization scheme, the integral

$$\int_0^1 f_{\Sigma}^{q,DIS}(z) dz = 0, \quad (4.4.33)$$

is valid regardless of scheme. Using (4.4.14) and (4.4.15) the  $\mathcal{F}_{\Sigma}$  structure function becomes

$$\begin{aligned} \mathcal{F}_{\Sigma}^q(x, Q^2) = & e_q^2 \int_0^1 \frac{dy}{y} G_{p \rightarrow q}^{(0)}(y) \left\{ \left( 1 - \frac{\alpha_s}{\pi} \right) \delta(1-z) \right. \\ & \left. + \frac{\alpha_s}{2\pi} P_{q \rightarrow qg}(z) \log(Q^2/m_g^2) + \alpha_s f_{MG,\Sigma}^{q,DIS}(z) \right\}, \end{aligned} \quad (4.4.34)$$

where  $z = x/y$  and where the superscript  $q$  signifies that this is the contribution to  $\mathcal{F}_{\Sigma}$  from the subprocess  $\gamma^* + q \rightarrow q + g$ .

The differential cross section for scattering longitudinal photons via the subprocess  $\gamma_L^* + q \rightarrow q + g$  can be calculated using the projection technique

in (4.2.72),

$$\begin{aligned} \frac{d\hat{\sigma}_L^q}{dt}(\hat{s}, \hat{t}) = & \frac{1}{64\pi\hat{s}\hat{p}_{cm}^2} \left( \frac{4z^2}{Q^2} \right) (p_q)_\mu(p_q)_\nu |\bar{\mathcal{M}}(\gamma^* + q \rightarrow q + g)|_{\mu\nu}^2 \\ = & \frac{z^2}{16\pi Q^4} \left( \frac{4z^2}{Q^2} \right) (p_q)_\mu(p_q)_\nu |\bar{\mathcal{M}}(\gamma^* + q \rightarrow q + g)|_{\mu\nu}^2, \end{aligned} \quad (4.4.35)$$

where  $p_q$  is the initial quark 4-momentum. It is easy to see that

$$(p_q)_\mu(p_q)_\nu |\bar{\mathcal{M}}|_{\mu\nu}^2 = e^2 e_q^2 g_s^2 \frac{4}{3} \frac{1}{2} 4(Q^2 + \hat{t} + \hat{s}), \quad (4.4.36)$$

so that

$$\frac{d\hat{\sigma}_L^q}{dt}(\hat{s}, \hat{t}) = \frac{\pi\alpha_s e_q^2 z^2}{Q^4} \left( \frac{4z^2}{Q^2} \right) \frac{8}{3} (Q^2 + \hat{t} + \hat{s}). \quad (4.4.37)$$

This cross section is finite when integrated over  $\hat{t}$  and is given by

$$\hat{\sigma}_L^q(x, Q^2) = \pi\alpha_s e_q^2 \left( \frac{4z^2}{Q^2} \right) \left( \frac{4}{3} \right). \quad (4.4.38)$$

Here there is no need to label it by a regularization scheme since no divergences are encountered.

The longitudinal structure function  $\mathcal{F}_L(x, Q^2)$  is related to the total  $\gamma_L^* q$  cross section in (4.4.38) as given in (4.2.71). Namely,

$$\mathcal{F}_L(x, Q^2) = \int_x^1 \frac{dy}{y} G_{p \rightarrow q}(y) \left( \frac{Q^2}{8\pi^2\alpha z} \right) 2\hat{\sigma}_L(z, Q^2), \quad (4.4.39)$$

so that

$$\mathcal{F}_L^q(x, Q^2) = e_q^2 \int_x^1 \frac{dy}{y} G_{p \rightarrow q}^{(0)}(y) [\alpha_s f_L^{q,DIS}(z)], \quad (4.4.40)$$

where  $z = x/y$  and

$$\alpha_s f_L^{q,DIS}(z) = \frac{2\alpha_s}{3\pi} 2z, \quad (4.4.41)$$

where the superscript  $q$  on  $\mathcal{F}_L$  indicates that this is the contribution to the longitudinal structure function from the subprocess,  $\gamma^* + q \rightarrow q + g$ . Unlike (4.4.26) this “little  $f$ ” function does not depend on the regularization scheme. Integrating (4.4.41) over  $z$  gives

$$\int_0^1 \alpha_s f_L^{q,DIS}(z) dz = \frac{2\alpha_s}{3\pi}. \quad (4.4.42)$$

From (4.2.63) we have

$$\mathcal{F}_2(x, Q^2) = \mathcal{F}_{\Sigma}(x, Q^2) + \frac{3}{2} \mathcal{F}_L(x, Q^2), \quad (4.4.43)$$

so that the contribution to the structure function  $\mathcal{F}_2$  from the subprocesses

$\gamma^* + q \rightarrow q$  and  $\gamma^* + q \rightarrow q + g$  is

$$\mathcal{F}_2^g(x, Q^2) = e_q^2 \int_0^1 \frac{dy}{y} G_{p \rightarrow q}^{(0)}(y) \left\{ \delta(1-z) + \frac{\alpha_s}{2\pi} p_{q \rightarrow qg}(z) \log(Q^2/m_g^2) + \alpha_s f_{MG,2}^{g,DIS}(z) \right\}, \quad (4.4.44)$$

where  $z = x/y$  and

$$\alpha_s f_{MG,2}^{g,DIS}(z) = \frac{2\alpha_s}{3\pi} \left\{ (1+z^2) \left( \frac{\log(1-z)}{1-z} \right)_+ + \frac{1+z^2}{1-z} (-2\log(z)) - \frac{3}{2} \frac{1}{(1-z)_+} + 4z + 1 - \left( \frac{2\pi^2}{3} + \frac{9}{4} \right) \delta(1-z) \right\}. \quad (4.4.45)$$

The factor  $-(\alpha_s/\pi)\delta(1-z)$  in (4.4.34) has been placed in the function  $f_2^g(z)$ . This “little  $f$ ” function is scheme dependent but the integral

$$\begin{aligned} \int_0^1 \alpha_s f_2^{g,DIS}(z) dz &= \\ &= -\frac{\alpha_s}{\pi} + \int_0^1 \alpha_s f_\Sigma^{g,DIS}(z) dz + \frac{3}{2} \int_0^1 \alpha_s f_L^{g,DIS}(z) dz = 0, \end{aligned} \quad (4.4.46)$$

is not.

For the initial state gluon subprocess  $\gamma^* + g \rightarrow q + \bar{q}$  in Fig. 4.5 we cannot regularize by taking  $q_g^2 = m_g^2$  because then the incoming gluon could actually decay into a massless quark-antiquark pair. To regulate this process we take the incoming gluon slightly off-shell and spacelike,  $q_g^2 = -m_g^2$ . In this case the differential cross section in (4.3.21) becomes

$$\begin{aligned} \frac{d\hat{\sigma}_\Sigma^g}{d\hat{t}} &= \frac{\pi\alpha\alpha_s e_q^2 z^2}{Q^4} 2 \left\{ \frac{\hat{u}}{\hat{t}} + \frac{\hat{t}}{\hat{u}} + \frac{2Q^2}{\hat{t}\hat{u}} (\hat{t} + \hat{u} + Q^2) \right. \\ &\quad \left. + \frac{2m_g^2}{\hat{t}\hat{u}} (\hat{t} + \hat{u} + m_g^2) - Q^2 m_g^2 \left( \frac{1}{\hat{u}^2} + \frac{1}{\hat{t}^2} - \frac{4}{\hat{t}\hat{u}} \right) \right\}, \end{aligned} \quad (4.4.47)$$

and  $\hat{t}_{\min}$  and  $\hat{t}_{\max}$  become

$$\hat{t}_{\min} = \hat{u}_{\min} = -m_g^2 z, \quad (4.4.48)$$

$$\hat{t}_{\max} = \hat{u}_{\max} = -Q^2/z, \quad (4.4.49)$$

with  $z$  is defined in (4.3.16). Integrating (4.4.47) over  $\hat{t}$  gives

$$\hat{\sigma}_{MG,\Sigma}^g(z, Q^2) = \frac{\pi\alpha\alpha_s e_q^2 z}{Q^2} 4 \left\{ (z^2 + (1-z)^2) \log\left(\frac{Q^2}{z^2 m_g^2}\right) - 2 \right\}, \quad (4.4.50)$$

where some terms that vanish as  $m_g^2 \rightarrow 0$  have been dropped. From (4.4.15) we arrive at

$$\left( \frac{1}{\sigma_0} \frac{d\hat{\sigma}_{MG}^g}{dz} \right)_{DIS} = 2 \frac{\alpha_s}{2\pi} P_{g \rightarrow q\bar{q}}(z) \log(Q^2/m_g^2) + 2\alpha_s f_{MG,\Sigma}^{g,DIS}(z), \quad (4.4.51)$$

with

$$P_{g \rightarrow q\bar{q}}(z) = \frac{1}{2}(z^2 + (1-z)^2), \quad (4.4.52)$$

and

$$\alpha_s f_{MG,\Sigma}^{g,DIS}(z) = -\frac{\alpha_s}{2\pi} [(z^2 + (1-z)^2) \log(z) + 1]. \quad (4.4.53)$$

In evaluating the integral of (4.4.47) over  $\hat{t}$  it is convenient to use

$$\frac{1}{\hat{t}\hat{u}} = -\frac{z}{Q^2} \left( \frac{1}{\hat{t}} + \frac{1}{\hat{u}} \right), \quad (4.4.54)$$

so that

$$\begin{aligned} \frac{\hat{u}}{\hat{t}} + \frac{\hat{t}}{\hat{u}} + \frac{2Q^2}{\hat{t}\hat{u}} (\hat{t} + \hat{u} + Q^2) &= \left( -\frac{Q^2}{\hat{t}z} (z^2 + (1-z)^2) - 1 \right) \\ &\quad + \left( -\frac{Q^2}{\hat{u}z} (z^2 + (1-z)^2) - 1 \right). \end{aligned} \quad (4.4.55)$$

Integrating the first term over  $\hat{t}$  and the second over  $\hat{u}$  gives

$$\begin{aligned} 2 \int_{-Q^2/z}^{-m_g^2 z} \left( -\frac{Q^2}{\hat{t}z} (z^2 + (1-z)^2) - 1 \right) d\hat{t} &= \\ \frac{2Q^2}{z} \left[ (z^2 + (1-z)^2) \log\left(\frac{Q^2}{m_g^2 z^2}\right) - 1 \right]. \end{aligned} \quad (4.4.56)$$

The contribution to the structure function  $\mathcal{F}_\Sigma$  from the subprocess  $\gamma^* + g \rightarrow q + \bar{q}$  is thus

$$\mathcal{F}_\Sigma^g(x, Q^2) = 2e_q^2 \int_x^1 \frac{dy}{y} G_{p \rightarrow q}^{(0)}(y) \left\{ \frac{\alpha_s}{2\pi} P_{g \rightarrow q\bar{q}}(z) \log(Q^2/m_g^2) + \alpha_s f_{MG,\Sigma}^{g,DIS}(z) \right\}, \quad (4.4.57)$$

where  $z = x/y$ .

The differential cross section for the scattering of longitudinal photons via the subprocess  $\gamma_L^* + g \rightarrow q + \bar{q}$  is

$$\frac{d\hat{\sigma}_L^g}{d\hat{t}}(\hat{s}, \hat{t}) = \frac{z^2}{16\pi Q^4} \left( \frac{4z^2}{Q^2} \right) (q_g)_\mu(q_g)_\nu |\overline{\mathcal{M}}(\gamma_L^* + g \rightarrow q + \bar{q})|_{\mu\nu}^2, \quad (4.4.58)$$

where

$$(q_g)_\mu(q_g)_\nu |\overline{\mathcal{M}}|_{\mu\nu}^2 = e^2 e_q^2 j_s^2 \frac{1}{8} 8\hat{s}, \quad (4.4.59)$$

giving

$$\frac{d\hat{\sigma}_L^g}{d\hat{t}}(\hat{s}, \hat{t}) = \frac{\pi\alpha\alpha_s e_q^2 z}{Q^2} \left( \frac{4z^2}{Q^2} \right) 2(1-z), \quad (4.4.60)$$

since

$$\hat{s} = \frac{(1-z)}{z} Q^2. \quad (4.4.61)$$

Equation (4.4.60) contains no divergent terms and can easily be integrated over  $\hat{t}$  giving

$$\hat{\sigma}_L^g(z, Q^2) = \pi \alpha \alpha_s e_q^2 \left( \frac{4z^2}{Q^2} \right) 2(1-z), \quad (4.4.62)$$

which from (4.4.15) gives a contribution to the longitudinal structure function of

$$\mathcal{F}_L^g(x, Q^2) = 2e_q^2 \int_x^1 \frac{dy}{y} G_{p \rightarrow g}^{(0)}(y) \left[ \alpha_s f_L^{g, DIS}(z) \right], \quad (4.4.63)$$

with  $z = x/y$  and

$$\alpha_s f_L^{g, DIS}(z) = \frac{\alpha_s}{2\pi} 2z(1-z), \quad (4.4.64)$$

and the gluon contribution to the structure function  $\mathcal{F}_2$  in (4.4.43) becomes

$$\begin{aligned} \mathcal{F}_2^g(x, Q^2) &= 2e_q^2 \int_x^1 \frac{dy}{y} G_{p \rightarrow g}^{(0)}(y) \\ &\quad \left\{ \frac{\alpha_s}{2\pi} P_{g \rightarrow q\bar{q}}(z) \log(Q^2/m_g^2) + \alpha_s f_{MG,2}^{g, DIS}(z) \right\}, \end{aligned} \quad (4.4.65)$$

where  $P_{g \rightarrow q\bar{q}}(z)$  is given by (4.4.52) and

$$\alpha_s f_{MG,2}^{g, DIS}(z) = \frac{\alpha_s}{2\pi} [-(z^2 + (1-z)^2) \log(z) - 1 + 3z - 3z^2]. \quad (4.4.66)$$

If we combine (4.4.44) with (4.4.65) we get the contribution to the  $\mathcal{F}_2$  structure function from the subprocesses  $\gamma^* + q \rightarrow q$ ,  $\gamma^* + q \rightarrow q + g$ ,  $\gamma^* + \bar{q} \rightarrow \bar{q} + g$ , and  $\gamma^* + g \rightarrow q + \bar{q}$ . Namely,

$$\begin{aligned} \mathcal{F}_2(x, Q^2) &= e_q^2 \int_x^1 \frac{dy}{y} \left( G_{p \rightarrow q}^{(0)}(y) + G_{p \rightarrow \bar{q}}^{(0)}(y) \right) \\ &\quad \left\{ \delta(1-z) + \frac{\alpha_s}{2\pi} P_{q \rightarrow gg}(z) \log(Q^2/m_g^2) + \alpha_s f_{MG,2}^{g, DIS}(z) \right\} \\ &\quad + 2e_q^2 \int_x^1 \frac{dy}{y} G_{p \rightarrow g}^{(0)}(y) \left\{ \frac{\alpha_s}{2\pi} P_{g \rightarrow q\bar{q}}(z) \log(Q^2/m_g^2) + \alpha_s f_{MG,2}^{g, DIS}(z) \right\}, \end{aligned} \quad (4.4.67)$$

where  $z = x/y$ .

## 4.5 Order $\alpha_s$ Corrections – DR Scheme

We can regulate the divergences in the 2-to-2 scattering subprocess  $\gamma^* + q \rightarrow q + g$  and  $\gamma^* + g \rightarrow q + \bar{q}$  by considering the scattering to occur in  $N$  rather than 4 spacetime dimensions. In  $N$  spacetime dimensions the 2-to-2 cross section has the form

$$d\hat{\sigma} = \frac{1}{4(p_1 \cdot p_2)} |\mathcal{M}|^2 d^{2N-2}R_2, \quad (4.5.1)$$

where the two-body phase-space factor  $d^{2N-2}R_2$  is similar to (2.8.2). Namely

$$d^{2N-2}R_2 = \frac{d^{N-1}p_3}{(2\pi)^{N-1}(2E_3)} \frac{d^{N-1}p_4}{(2\pi)^{N-1}(2E_4)} (2\pi)^N \delta^N(p_3 + p_4 - p_1 - p_2). \quad (4.5.2)$$

Integrating over  $p_4$  yields

$$\int d^{N-1}p_4 \delta^N(p_3 + p_4 - p_1 - p_2) = \delta(E_3 + E_4 - E_1 - E_2). \quad (4.5.3)$$

Now if we let  $y = \cos \theta_{13}$ , where  $\theta_{13}$  is the scattering angle between particles 1 and 3 then

$$d^{N-1}p_3 = \frac{2\pi^{(N-2)/2}}{\Gamma(N/2-1)} p_3^{N-2} dp_3 (1-y^2)^{N/2-2} dy. \quad (4.5.4)$$

Integrating over the magnitude of  $p_3$  gives

$$\int dp_3 \frac{1}{4E_3 E_4} p_3^{N-2} \delta(E_3 + E_4 - E_{cm}) = \frac{(\hat{p}_{cm}')^{N-3}}{4\sqrt{\hat{s}}}, \quad (4.5.5)$$

where

$$(\hat{p}_{cm}')^2 = [\hat{s} - (m_3 + m_4)^2][\hat{s} - (m_3 - m_4)^2]/(4\hat{s}), \quad (4.5.6)$$

and

$$p_1 \cdot p_2 = \sqrt{\hat{s}} \hat{p}_{cm}, \quad (4.5.7)$$

with

$$\hat{p}_{cm}^2 = [\hat{s} - (m_1 + m_2)^2][\hat{s} - (m_1 - m_2)^2]/(4\hat{s}). \quad (4.5.8)$$

Combining (4.5.4) and (4.5.1) yields

$$\frac{d\hat{\sigma}}{dy}(\hat{s}, \hat{t}) = \frac{1}{32\pi\hat{s}} \frac{(\hat{p}_{cm}')^{N-3}}{\hat{p}_{cm}} |\mathcal{M}|^2 \frac{(1-y^2)^{N/2-2}}{2^{N-4}\pi^{N/2-2}\Gamma(N/2-1)}. \quad (4.5.9)$$

For the subprocess  $\gamma^* + q \rightarrow q + g$  we have the following:

$$\hat{p}_{cm} = \frac{(\hat{s} + Q^2)}{2\sqrt{\hat{s}}}, \quad (4.5.10)$$

$$\hat{p}_{cm}' = \frac{1}{2}\sqrt{\hat{s}}, \quad (4.5.11)$$

$$\hat{t} = -\frac{Q^2}{2z}(1-y), \quad (4.5.12)$$

$$z = \frac{Q^2}{\hat{s} + Q^2}, \quad (4.5.13)$$

$$\hat{s} = (1-z)Q^2/z, \quad (4.5.14)$$

where  $Q^2 = -q_\gamma^2$ . The integral of (4.5.9) over  $y$  is given by

$$\hat{\sigma}_{DR}^g(z, Q^2) = \frac{z}{32\pi Q^2} \left( \frac{(1-z)Q^2}{4\pi z} \right)^{\epsilon/2} \frac{1}{2^\epsilon \Gamma(1+\epsilon/2)}, \quad (4.5.15)$$

where

$$I = \int_{-1}^1 dy (1-y^2)^{\epsilon/2} |\bar{M}(\gamma^* + q \rightarrow g + q)|^2, \quad (4.5.16)$$

with  $N = 4 + \epsilon$ .

In  $N = 4 + \epsilon$  dimensions the matrix element squared is given by

$$\begin{aligned} |\bar{M}(\gamma_\Sigma^* + q \rightarrow q + g)|^2 &= 16\pi^2 \alpha_N^{QED} \alpha_N^{QCD} e_q^2 \frac{4}{3} \frac{1}{2} \\ &\left\{ \frac{4(4z^2 + 4yz - 4z + y^2 - 2y + 5)}{(1-y)(1-z)} + \frac{4(4z^2 - 4z + y^2 + 3)}{(1-y)(1-z)} \epsilon \right. \\ &\left. + \frac{4z^2 + (-4y - 4)z + y^2 + 2y + 1}{(1-y)(1-z)} \epsilon^2 \right\}, \end{aligned} \quad (4.5.17)$$

where  $\alpha_N^{QED}$  and  $\alpha_N^{QCD}$  are the  $N$ -dimensional couplings in (2.8.11) and (2.8.26), respectively. To evaluate the integral  $I$  in (4.5.16) we use

$$\begin{aligned} \int_{-1}^1 (1-y^2)^A \frac{y^B}{1-y} dy &= \frac{\Gamma(A) \Gamma(\frac{1}{2}B+1)}{\Gamma(A+\frac{1}{2}B+1)} \quad (B \text{ odd}) \\ &= \frac{\Gamma(A) \Gamma(\frac{1}{2}B+\frac{1}{2})}{\Gamma(A+\frac{1}{2}B+\frac{1}{2})} \quad (B \text{ even}). \end{aligned} \quad (4.5.18)$$

The integrated cross section (4.5.15) becomes

$$\hat{\sigma}_{DR,\Sigma}^q(z, Q^2) = \frac{16\pi \alpha_N^{QED} \alpha_s e_q^2 z}{3Q^2} \left( \frac{Q^2(1-z)}{z4\pi m_D^2} \right)^{\epsilon/2} \frac{\Gamma(1+\frac{\epsilon}{2})}{\Gamma(1+\epsilon)} \left\{ \frac{1+z^2}{1-z} \frac{2}{\epsilon} + \frac{4z^2 - 8z + 5}{2(1-z)} + \frac{z^2 + 2z - 1}{2(1-z)} \epsilon + \dots \right\}, \quad (4.5.19)$$

where the mass  $m_D$  comes from using (2.8.26) and  $\alpha_s$  is now dimensionless. Using the  $N$ -dimensional analogue of (4.4.15),

$$\frac{1}{\sigma_0} \frac{d\sigma}{dz} = \frac{Q^2}{8\pi^2 \alpha_N^{QED} e_q^2 z (1+\frac{\epsilon}{2})} \hat{\sigma}^q, \quad (4.5.20)$$

where the factor of  $(1+\frac{\epsilon}{2})$  comes from the Born term matrix element evaluated in  $N$  spacetime dimensions

$$|\bar{M}(\gamma_\Sigma^* + q \rightarrow q)|^2 = 4 \left(1 + \frac{\epsilon}{2}\right) e_N^2 Q^2. \quad (4.5.21)$$

From (4.5.19) and (4.5.20) we arrive at

$$\begin{aligned} \left( \frac{1}{\sigma_0} \frac{d\hat{\sigma}_{DR}^q}{dz} \right)_{DIS} &= \frac{2\alpha_s}{3\pi} \left( \frac{(1-z)Q^2}{z4\pi m_D^2} \right)^{\epsilon/2} \frac{\Gamma(1+\frac{\epsilon}{2})}{\Gamma(1+\epsilon)} \\ &\left\{ \frac{1+z^2}{1-z} \frac{2}{\epsilon} - \frac{3}{2} \frac{1}{1-z} - z + 3 + \dots \right\}. \end{aligned} \quad (4.5.22)$$

This can be compared with the  $e^+e^-$  result in (3.2.19),

$$\begin{aligned} \left( \frac{1}{\sigma_0} \frac{d\hat{\sigma}_{DR}}{dx} \right)_{e^+e^-} &= \frac{2\alpha_s}{3\pi} \left( \frac{x^2(1-x)Q^2}{4\pi m_D^2} \right)^{\epsilon/2} \frac{\Gamma(1+\frac{\epsilon}{2})}{\Gamma(1+\epsilon)} \\ &\left\{ \frac{1+x^2}{1-x} \frac{2}{\epsilon} - \frac{3}{2} \frac{1}{1-x} - \frac{3}{2} x + \frac{5}{2} + \dots \right\}, \end{aligned} \quad (4.5.23)$$

which again is similar but not the same. If we expand the  $\Gamma$  functions in (4.5.22) according to

$$\frac{\Gamma(1+\frac{1}{2}\epsilon)}{\Gamma(1+\epsilon)} = 1 + \frac{1}{2}\gamma_E \epsilon + \frac{1}{16}(2\gamma_E^2 - \pi^2) \epsilon^2 + \dots, \quad (4.5.24)$$

and use (2.8.37) we arrive at

$$\begin{aligned} \left( \frac{1}{\sigma_0} \frac{d\hat{\sigma}_{DR,\Sigma}^q}{dz} \right)_{DIS} &= \frac{2\alpha_s}{3\pi} \left\{ \frac{1+z^2}{1-z} \left[ \log \left( \frac{Q^2(1-z)}{z4\pi m_D^2} \right) + \gamma_E \right] \right. \\ &\left. + \frac{1+z^2}{1-z} \frac{2}{\epsilon} - \frac{3}{2} \frac{1}{1-z} - z + 3 + \dots \right\}, \end{aligned} \quad (4.5.25)$$

where terms that vanish as  $\epsilon \rightarrow 0$  have been dropped.

Integrating (4.5.22) over  $z$  yields

$$\begin{aligned} (\hat{\sigma}_{DR}(\text{real}))_{DIS} &= \frac{2\alpha_s}{3\pi} \sigma_0 \left( \frac{Q^2}{4\pi m_D^2} \right)^{\epsilon/2} \frac{\Gamma(1-\frac{\epsilon}{2}) \Gamma^2(1+\frac{\epsilon}{2})}{\Gamma(1+\epsilon)} \\ &\left\{ \frac{8}{\epsilon^2} - \frac{6}{\epsilon} + \frac{13}{2} \right\}. \end{aligned} \quad (4.5.26)$$

The virtual gluon contributions in Fig. 4.6 are given by (2.9.14). Namely,

$$\begin{aligned} (\hat{\sigma}_{DR}(\text{virtual}))_{DIS} &= \frac{2\alpha_s}{3\pi} \sigma_0 \left( \frac{Q^2}{4\pi m_D^2} \right)^{\epsilon/2} \frac{\Gamma(1-\frac{\epsilon}{2}) \Gamma^2(1+\frac{\epsilon}{2})}{\Gamma(1+\epsilon)} \\ &\left\{ -\frac{8}{\epsilon^2} + \frac{6}{\epsilon} - 8 \right\}_{\text{spacelike}}, \end{aligned} \quad (4.5.27)$$

so that

$$\begin{aligned} (\hat{\sigma}_{DR}(\text{real}) + \hat{\sigma}_{DR}(\text{virtual}))_{DIS} &= \frac{2\alpha_s}{3\pi} \sigma_0 \left\{ \frac{13}{2} - 8 \right\} \\ &= \frac{2\alpha_s}{3\pi} \sigma_0 \left( -\frac{3}{2} \right) = -\frac{\alpha_s}{\pi} \sigma_0. \end{aligned} \quad (4.5.28)$$

This is the same result arrived at for the massive gluon scheme in (4.4.21). If we define “+ functions” as in (4.4.30) we get from (4.5.25) and (4.5.28)

$$\frac{1}{\sigma_0} \left( \frac{d\hat{\sigma}_{DR,\Sigma}^q}{dz} \right)_+ = \frac{\alpha_s}{2\pi} P_{q \rightarrow gg}(z) \log(Q^2/m_D^2) + \alpha_s f_{DR,\Sigma}^{q,DIS}(z), \quad (4.5.29)$$

where  $P_{q \rightarrow gg}(z)$  is given by (4.4.31) and

$$\begin{aligned} \alpha_s f_{DR,\Sigma}^{q,DIS}(z) = & \frac{2\alpha_s}{2\pi} \left\{ (1+z^2) \left( \frac{\log(1-z)}{1-z} \right)_+ - \frac{1+z^2}{1-z} \log(z) \right. \\ & - \frac{3}{2} \frac{1}{(1-z)_+} - z + 3 - \left( \frac{\pi^2}{3} + 3 \right) \delta(1-z) \Big\} \\ & + \frac{\alpha_s}{2\pi} P_{q \rightarrow gg}(z) \left\{ \frac{2}{\epsilon} + \gamma_\epsilon - \log(4\pi) \right\}, \end{aligned} \quad (4.5.30)$$

with the integral of (4.5.30) giving zero as in (4.4.33). The regularization scheme dependence of this “little  $f$ ” function can again be clearly seen by comparing (4.5.30) with (4.4.32). In the dimensional regularization scheme the  $\mathcal{F}_\Sigma$  structure function in (4.4.34) becomes

$$\begin{aligned} \mathcal{F}_\Sigma^q(x, Q^2) = & e_q^2 \int_x^1 \frac{dy}{y} G_{p \rightarrow q}^{(0)}(y) \left\{ \left( 1 - \frac{\alpha_s}{\pi} \right) \delta(1-z) \right. \\ & \left. + \frac{\alpha_s}{2\pi} P_{q \rightarrow gg}(z) \log(Q^2/m_D^2) + \alpha_s f_{DR,\Sigma}^{q,DIS}(z) \right\}, \end{aligned} \quad (4.5.31)$$

where  $z = x/y$ . The longitudinal structure function in (4.4.40) is scheme independent so

$$\begin{aligned} \mathcal{F}_2^q(x, Q^2) = & e_q^2 \int_x^1 \frac{dy}{y} G_{p \rightarrow q}^{(0)}(y) \left\{ \delta(1-z) \right. \\ & \left. + \frac{\alpha_s}{2\pi} P_{q \rightarrow gg}(z) \log(Q^2/m_D^2) + \alpha_s f_{DR,2}^{q,DIS}(z) \right\}, \end{aligned} \quad (4.5.32)$$

where  $z = x/y$  and

$$\begin{aligned} \alpha_s f_{DR,2}^{q,DIS}(z) = & \frac{2\alpha_s}{3\pi} \left\{ (1+z^2) \left( \frac{\log(1-z)}{1-z} \right)_+ - \frac{1+z^2}{1-z} \log(z) \right. \\ & - \frac{3}{2} \frac{1}{(1-z)_+} + 2z + 3 - \left( \frac{\pi^2}{3} + \frac{9}{2} \right) \delta(1-z) \Big\} \\ & + \frac{\alpha_s}{2\pi} P_{q \rightarrow gg}(z) \left\{ \frac{2}{\epsilon} + \gamma_\epsilon - \log(4\pi) \right\}. \end{aligned} \quad (4.5.33)$$

The subprocess  $\gamma^* + g \rightarrow q + \bar{q}$  is handled in a similar manner<sup>5</sup> and the contribution to the  $\mathcal{F}_\Sigma$  structure function is given by

$$\begin{aligned} \mathcal{F}_\Sigma^g(x, Q^2) = & 2e_q^2 \int_x^1 \frac{dy}{y} G_{p \rightarrow g}^{(0)}(y) \\ & \left\{ \frac{\alpha_s}{2\pi} P_{g \rightarrow q\bar{q}}(z) \log(Q^2/m_D^2) + \alpha_s f_{DR,\Sigma}^{g,DIS}(z) \right\}, \end{aligned} \quad (4.5.34)$$

where  $z = x/y$  and

$$\alpha_s f_{DR,\Sigma}^{g,DIS}(z) = \frac{\alpha_s}{2\pi} \left\{ \frac{1}{2} (z^2 + (1-z)^2) \log \left( \frac{1-z}{z} \right) \right\}$$

$$+ \frac{\alpha_s}{2\pi} P_{g \rightarrow q\bar{q}}(z) \left\{ \frac{2}{\epsilon} + \gamma_\epsilon - \log(4\pi) \right\}. \quad (4.5.35)$$

The contribution to the longitudinal structure function in (4.5.63) is the same since no divergences are encountered, therefore (4.4.65) becomes

$$\begin{aligned} \mathcal{F}_2^g(x, Q^2) = & 2e_q^2 \int_x^1 \frac{dy}{y} G_{p \rightarrow g}^{(0)}(y) \\ & \left\{ \frac{\alpha_s}{2\pi} P_{g \rightarrow q\bar{q}}(z) \log(Q^2/m_D^2) + \alpha_s f_{DR,2}^{g,DIS}(z) \right\}, \end{aligned} \quad (4.5.36)$$

with

$$\begin{aligned} \alpha_s f_{DR,2}^{g,DIS}(z) = & \frac{\alpha_s}{2\pi} \left\{ \frac{1}{2} (z^2 + (1-z)^2) \log \left( \frac{1-z}{z} \right) + 3z - 3z^2 \right\} \\ & + \frac{\alpha_s}{2\pi} P_{g \rightarrow q\bar{q}}(z) \left\{ \frac{2}{\epsilon} + \gamma_\epsilon - \log(4\pi) \right\}, \end{aligned} \quad (4.5.37)$$

and (4.4.67) becomes

$$\begin{aligned} \mathcal{F}_2(x, Q^2) = & e_q^2 \int_x^1 \frac{dy}{y} \left( G_{p \rightarrow q}^{(0)}(y) + G_{p \rightarrow \bar{q}}^{(0)}(y) \right) \\ & \left\{ \delta(1-z) + \frac{\alpha_s}{2\pi} P_{q \rightarrow gg}(z) \log(Q^2/m_D^2) + \alpha_s f_{DR,2}^{q,DIS}(z) \right\} \\ & + 2e_q^2 \int_0^1 \frac{dy}{y} G_{p \rightarrow g}^{(0)}(y) \\ & \left\{ \frac{\alpha_s}{2\pi} P_{g \rightarrow q\bar{q}}(z) \log(Q^2/m_D^2) + \alpha_s f_{DR,2}^{g,DIS}(z) \right\}, \end{aligned} \quad (4.5.38)$$

where  $z = x/y$ .

## 4.6 $Q^2$ Dependent Structure Functions

The quark distribution are defined from the  $\mathcal{F}_2$  structure function as in (4.1.16). Namely,

$$\mathcal{F}_2(x, Q^2) \equiv \sum_{i=1}^{n_f} e_{q_i}^2 \left( G_{p \rightarrow q_i}^{(2)}(x, Q^2) + G_{p \rightarrow \bar{q}_i}^{(2)}(x, Q^2) \right), \quad (4.6.1)$$

where the superscript (2) refers to the  $\mathcal{F}_2$  structure function and where  $n_f$  is the number of quark flavors. From (4.4.67) or (4.5.38) we see that

$$\begin{aligned} G_{p \rightarrow q}^{(2)}(x, Q^2) = & \int_x^1 \frac{dy}{y} G_{p \rightarrow q}^{(0)}(y) \left\{ \delta(1-z) \right. \\ & \left. + \frac{\alpha_s}{2\pi} P_{q \rightarrow gg}(z) \log(Q^2/m^2) + \alpha_s f_2^{q,DIS}(z) \right\} \end{aligned}$$

$$+ \int_x^1 \frac{dy}{y} G_{p \rightarrow g}^{(0)}(y) \\ \left\{ \frac{\alpha_s}{2\pi} P_{g \rightarrow q\bar{q}}(z) \log(Q^2/m^2) + \alpha_s f_2^{g,DIS}(z) \right\}, \quad (4.6.2)$$

where  $z = x/y$  and where the mass  $m$  is the dimensional regularization mass  $m_D$  or the gluon mass  $m_g$  depending on the scheme. The “little  $f$ ” functions are regularization scheme dependent and are given by (4.4.45) and (4.4.66) in the massive glue scheme and by (4.5.33) and (4.5.37) in the dimensional regularization scheme. If we define the convolution notations as in (3.3.11) then (4.6.2) becomes

$$G_{p \rightarrow q}^{(2)}(x, Q^2) = G_{p \rightarrow q}^{(0)} * \left( 1 + \frac{\alpha_s}{2\pi} P_{q \rightarrow gg} \log(Q^2/m^2) + \alpha_s f_2^{q,DIS} \right) \\ + G_{p \rightarrow g}^{(0)} * \left( \frac{\alpha_s}{2\pi} P_{g \rightarrow q\bar{q}} \log(Q^2/m^2) + \alpha_s f_2^{g,DIS} \right). \quad (4.6.3)$$

As explained in (3.3.17) the  $\log(m^2)$  divergences are absorbed into the unknown distributions  $G^{(0)}$  leaving

$$G_{p \rightarrow q}^{(2)}(x, Q^2) = \overline{G}_{p \rightarrow q}^{(0)} * \left( 1 + \frac{\alpha_s}{2\pi} P_{q \rightarrow gg} \log(Q^2/\Lambda^2) + \alpha_s f_2^{q,DIS} \right) \\ + \overline{G}_{p \rightarrow g}^{(0)} * \left( \frac{\alpha_s}{2\pi} P_{g \rightarrow q\bar{q}} \log(Q^2/\Lambda^2) + \alpha_s f_2^{g,DIS} \right), \quad (4.6.4)$$

which is analogous to (3.4.50) for the fragmentation functions. All leading log terms of the form  $[\alpha_s(Q^2) \log(Q^2)]^n$  are then summed in precisely the same way we did in Chapter 3<sup>6</sup>. The result for the “non-singlet” distribution

$$G_{NS}(x, Q^2) = G_{p \rightarrow q}(x, Q^2) - G_{p \rightarrow \bar{q}}(x, Q^2), \quad (4.6.5)$$

is the same as (3.4.44). Namely,

$$G_{NS}(x, Q^2) = \exp(\kappa P_{q \rightarrow gg} * G_{NS}(t_c)), \quad (4.6.6)$$

where  $\kappa$  is as defined in (3.4.35),

$$\kappa = \frac{2}{\beta_0} \log\{\alpha_s(t_c)/\alpha_s(t)\}, \quad (4.6.7)$$

and where  $t_c = Q_0^2$  is the reference momentum squared. Differentiating (4.6.6) with respect to  $\kappa$  gives

$$\frac{dG_{NS}(x, Q^2)}{d\kappa} = G_{NS}(Q^2) * P_{q \rightarrow gg}, \quad (4.6.8)$$

or

$$\frac{dG_{NS}(x, Q^2)}{d\tau} = \frac{\alpha_s(Q^2)}{2\pi} G_{NS}(Q^2) * P_{q \rightarrow gg}, \quad (4.6.9)$$

since

$$\frac{d\kappa}{d\tau} = \frac{\alpha_s(Q^2)}{2\pi} \quad (4.6.10)$$

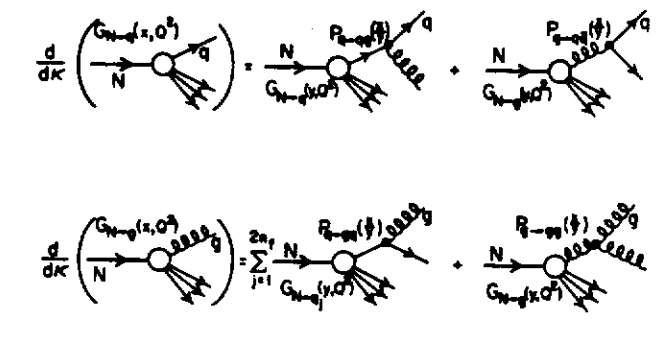


**Figure 4.7** Illustrates that the leading order rate of change of the quark distribution,  $G_{N \rightarrow q}(x, Q^2)$ , with respect to  $\kappa$  is generated by two terms. Quarks can lose momentum by radiating a gluon and additional quarks are generated when a gluon splits into a quark-antiquark pair. Similarly, the leading order rate of change of the gluon distribution,  $G_{N \rightarrow g}(x, Q^2)$ , with respect to  $\kappa$  is generated by two terms. Gluons can lose momentum by radiating a gluon and additional gluons are produced by Bremsstrahlung off of quarks and antiquarks.

with

$$\tau = \log(Q^2/\Lambda^2). \quad (4.6.11)$$

Here I have dropped the superscript (2) since the “little  $f$ ” functions in (4.6.4) do not contribute to the leading order  $Q^2$  evolution of the distribution functions.

As illustrated in Fig. 4.7 it is easy to see that the evolution of the quark and gluon distributions are governed by<sup>7</sup>

$$\frac{dG_{p \rightarrow q}(x, Q^2)}{d\kappa} = G_{p \rightarrow q}(Q^2) * P_{q \rightarrow gg} + G_{p \rightarrow g}(Q^2) * P_{g \rightarrow q\bar{q}}, \quad (4.6.12)$$

$$\frac{dG_{p \rightarrow g}(x, Q^2)}{d\kappa} = \sum_{j=1}^{2n_f} G_{p \rightarrow q_j}(Q^2) * P_{q \rightarrow gg} + G_{p \rightarrow g}(Q^2) * P_{g \rightarrow gg}, \quad (4.6.13)$$

where  $P_{g \rightarrow gg}(z)$  is given in (4.4.52) and

$$P_{q \rightarrow gg}(z) = P_{q \rightarrow gg}(1-z) = \frac{4}{3} \frac{1+(1-z)^2}{z}, \quad (4.6.14)$$

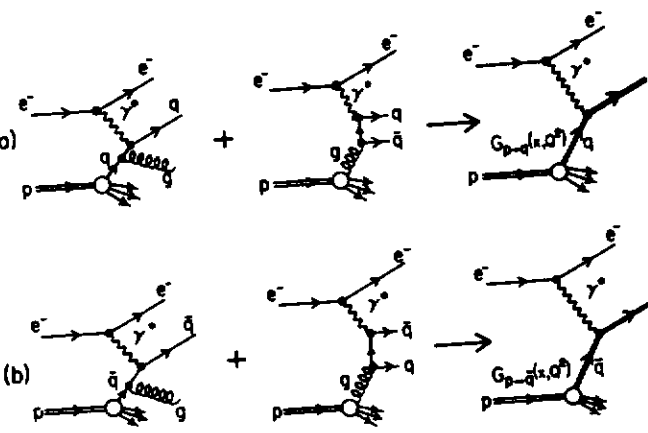


Figure 4.8 Illustrates how in deep inelastic electron proton scattering the leading log contributions from the subprocess  $\gamma^* + q \rightarrow q + g$  and  $\gamma^* + g \rightarrow q + \bar{q}$  are summed to form the  $Q^2$  dependent quark distribution,  $G_{p-q}(x, Q^2)$ . Similarly, the leading log contributions from the subprocess  $\gamma^* + \bar{q} \rightarrow \bar{q} + g$  and  $\gamma^* + g \rightarrow \bar{q} + q$  are summed to form the  $Q^2$  dependent antiquark distribution,  $G_{p-\bar{q}}(x, Q^2)$ .

and

$$P_{g-gg}(z) = 6 \left[ \frac{z}{(1-z)_+} + \frac{1-z}{z} + z(1-z) + \frac{(11 - \frac{2}{3}n_f)}{12} \delta(1-z) \right]. \quad (4.6.15)$$

Fig. 4.8 shows how the leading logarithm contributions from the subprocesses  $\gamma^* + q \rightarrow q + g$  and  $\gamma^* + g \rightarrow q + \bar{q}$  sum to form  $G_{p-q}(x, Q^2)$  and similarly the leading logarithm contributions from  $\gamma^* + \bar{q} \rightarrow \bar{q} + g$  and  $\gamma^* + g \rightarrow \bar{q} + q$  sum to form  $G_{p-\bar{q}}(x, Q^2)$ .

The coupled equations in (4.6.12) and (4.6.13) are solved in a manner similar to the fragmentation function evolution equations in (3.4.52) and (3.4.53). One defines a “singlet” distribution,

$$G_S(x, Q^2) = \sum_{i=1}^{n_f} [G_{p-q_i}(x, Q^2) + G_{p-\bar{q}_i}(x, Q^2)], \quad (4.6.16)$$

which together with the gluon distribution satisfies a matrix equation similar to (3.4.59),

$$\frac{d\mathbf{G}(x, Q^2)}{d\kappa} = \mathbf{P} * \mathbf{G}(Q^2), \quad (4.6.17)$$

with the formal solution given by

$$\mathbf{G}(x, Q^2) = \exp(\kappa \mathbf{P} * ) \mathbf{G}(Q_0^2), \quad (4.6.18)$$

where

$$\mathbf{G}(x, Q^2) \equiv \begin{pmatrix} G_S(x, Q^2) \\ G_{p-q}(x, Q^2) \\ G_{p-\bar{q}}(x, Q^2) \end{pmatrix}, \quad (4.6.19)$$

but where in this case the matrix  $\mathbf{P}$  is given by

$$\mathbf{P}(z) = \begin{pmatrix} P_{q-qg}(z) & 2n_f P_{g-q\bar{q}}(z) \\ P_{q-gg}(z) & P_{g-gg}(z) \end{pmatrix}. \quad (4.6.20)$$

This  $\mathbf{P}(z)$  function differs from the fragmentation function case in (3.4.59) by the interchange of  $P_{q-gg}$  and  $P_{g-q\bar{q}}$ . This means that the evolution of the singlet and gluon distributions functions differ from the evolution of the singlet and gluon fragmentation functions.

The net number of quarks,  $N_q$  of flavor  $q$  within the proton is given by

$$N_q = \int_0^1 (G_{p-q}(x, Q^2) - G_{p-\bar{q}}(x, Q^2)) dx, \quad (4.6.21)$$

and the condition (3.2.12) that

$$\int_0^1 P_{q-qg}(z) dz = 0, \quad (4.6.22)$$

insures that

$$\frac{dN_q}{d\tau} = 0. \quad (4.6.23)$$

This is important and means that  $N_q$  does not depend on  $Q^2$ . If, for example, we set  $N_u = 2$  as in (4.1.3) it will remain fixed at higher values of  $Q^2$ . Furthermore, the conditions

$$\int_0^1 z(P_{q-qg}(z) + P_{q-gg}(z)) dz = 0, \quad (4.6.24)$$

$$\int_0^1 z(2n_f P_{g-q\bar{q}}(z) + P_{g-gg}(z)) dz = 0, \quad (4.6.25)$$

guarantee that

$$\begin{aligned} \frac{d}{d\tau} \left\{ \int_0^1 x \left[ \sum_{n=1}^{n_f} (G_{p-q_n}(x, Q^2) + G_{p-\bar{q}_n}(x, Q^2)) + G_{p-g}(x, Q^2) \right] dx \right\} = \\ \frac{d}{d\tau} \left\{ \int_0^1 x (G_S(x, Q^2) + G_{p-g}(x, Q^2)) dx \right\} = 0, \end{aligned} \quad (4.6.26)$$

so that the total momentum of all the partons with the proton is independent of  $Q^2$ . If we normalize

$$Q + \bar{Q} + G = 1, \quad (4.6.27)$$

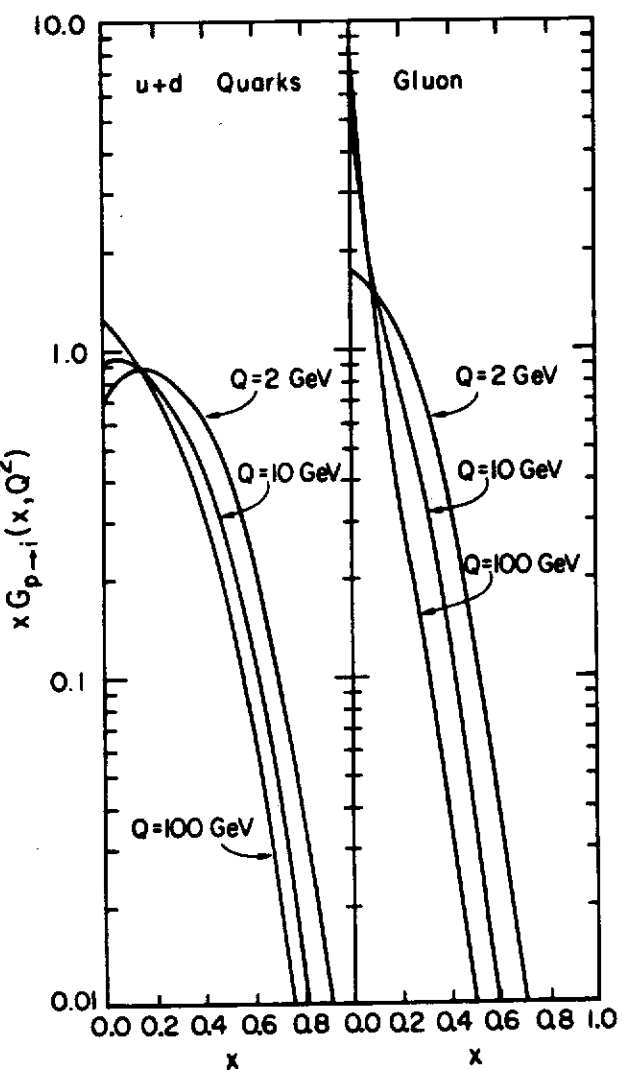


**Figure 4.9** Shows the  $Q^2$  dependence of the quark,  $xG_{p \rightarrow u+d}(x, Q^2)$ , and the gluon distribution,  $xG_{p \rightarrow g}(x, Q^2)$ , within the proton.

as in (4.1.9), then it will remain equal to 1 at all other  $Q^2$  values. Figure 4.9 shows the  $Q^2$  dependence of the quark and gluon distributions from a recent fit by Duke and Owens<sup>8</sup> with  $\Lambda = 0.2$  GeV.

## 4.7 $Q^2$ Evolution – Moment Method

Equation (4.6.8) and (4.6.17) can be written in terms of the moments of the parton distribution as follows:

$$\frac{dM_n^{NS}(Q^2)}{d\kappa} = A_n^{NS} M_n^{NS}(Q^2), \quad (4.7.1)$$

and

$$\frac{dM_n(Q^2)}{d\kappa} = \mathbf{A}_n \mathbf{M}_n(Q^2), \quad (4.7.2)$$

where

$$M_n(Q^2) = \int_0^1 dx x^{n-1} G(x, Q^2), \quad (4.7.3)$$

$$\mathbf{M}_n(Q^2) = \begin{pmatrix} M_n^s(Q^2) \\ M_n^g(Q^2) \end{pmatrix} \quad (4.7.4)$$

and

$$\mathbf{A}_n = \begin{pmatrix} A_n^{NS} & 2n_f A_n^{q\bar{q}} \\ A_n^{gg} & A_n^{gg} \end{pmatrix}, \quad (4.7.5)$$

where  $M_n^{NS}$ ,  $M_n^s$  and  $M_n^g$  are the moments of the non-singlet, singlet and gluon distributions, respectively. The “anomalous dimensions”  $A_n$  are given by

$$A_n^{NS} = \int_0^1 z^{n-1} P_{q \rightarrow qg}(z) dz = \frac{4}{3} \left[ -\frac{1}{2} + \frac{1}{n(n+1)} - 2 \sum_{j=2}^n \frac{1}{j} \right], \quad (4.7.6)$$

$$A_n^{gg} = \int_0^1 z^{n-1} P_{g \rightarrow gg}(z) dz = \frac{4}{3} \frac{2+n+n^2}{n(n^2-1)}, \quad (4.7.7)$$

$$A_n^{q\bar{q}} = \int_0^1 z^{n-1} P_{g \rightarrow q\bar{q}}(z) dz = \frac{1}{2} \frac{2+n+n^2}{n(n+1)(n+2)}, \quad (4.7.8)$$

and

$$A_n^{gg} = \int_0^1 z^{n-1} P_{g \rightarrow gg}(z) dz = 3 \left[ -\frac{1}{6} + \frac{2}{n(n-1)} + \frac{2}{(n+1)(n+2)} - 2 \sum_{j=2}^n \frac{1}{j} - \frac{1}{9} n_f \right]. \quad (4.7.9)$$

Equations (4.7.1) and (4.7.4) give three independent  $Q^2$  evolution equations

for the moments. Namely,

$$\begin{aligned} M_n^{NS}(Q^2) &= \exp(\kappa A_n^{NS}) M_n^{NS}(Q_0^2) \\ &= [\alpha_s(Q_0^2)/\alpha_s(Q^2)]^{2A_n^{NS}/\beta_0} M_n^{NS}(Q_0^2), \end{aligned} \quad (4.7.10)$$

and

$$M^+(Q^2) = \exp(\kappa A_n^+) M_n^+(Q_0^2), \quad (4.7.11)$$

$$M^-(Q^2) = \exp(\kappa A_n^-) M_n^-(Q_0^2), \quad (4.7.12)$$

where  $A_n^\pm$  are the eigenvalues obtained upon diagonalizing the matrix in (4.7.5),

$$\begin{pmatrix} A_n^+ & 0 \\ 0 & A_n^- \end{pmatrix} = \mathbf{R} \mathbf{A}_n \mathbf{R}^{-1}. \quad (4.7.13)$$

The moments  $M_n^\pm$  are combinations of  $M_n^s$  and  $M_n^g$  obtained from

$$\begin{pmatrix} M_n^+ \\ M_n^- \end{pmatrix} = \mathbf{R} \mathbf{M}_n, \quad (4.7.14)$$

where  $\mathbf{M}_n$  is given in (4.7.2) and  $\mathbf{R}$  is the matrix that diagonalizes  $\mathbf{A}_n$  as in (4.7.13).

For example, let us examine the  $n = 2$  moments. These moments are important since they correspond to total momentum fractions. The matrix  $\mathbf{A}_n$  for the  $n = 2$  moments is

$$\mathbf{A}_2 = \begin{pmatrix} -16/9 & n_f/3 \\ 16/9 & -n_f/3 \end{pmatrix}, \quad (4.7.15)$$

with eigenvalues

$$A_2^+ = -(16 + 3n_f)/9, \quad (4.7.16)$$

and

$$A_2^- = 0. \quad (4.7.17)$$

The matrix  $\mathbf{R}$  and its inverse are

$$\mathbf{R} = \frac{3}{\sqrt{16 + 3n_f}} \begin{pmatrix} 16/9 & -n_f/3 \\ 1 & 1 \end{pmatrix}, \quad (4.7.18)$$

$$\mathbf{R}^{-1} = \frac{3}{\sqrt{16 + 3n_f}} \begin{pmatrix} 1 & n_f/3 \\ -1 & 16/9 \end{pmatrix}, \quad (4.7.19)$$

which gives

$$M_2^+ = \frac{3}{\sqrt{16 + 3n_f}} \left( \frac{16}{9} M_2^s - \frac{n_f}{3} M_2^g \right), \quad (4.7.20)$$

$$M_2^- = \frac{3}{\sqrt{16 + 3n_f}} (M_2^s + M_2^g). \quad (4.7.21)$$

From (4.7.11) and (4.7.12) we see that

$$\begin{aligned} \left[ \frac{16}{9} M_2^s(Q^2) - \frac{n_f}{3} M_2^g(Q^2) \right] &= \\ [\log(Q_0^2/\Lambda^2)/\log(Q^2/\Lambda^2)]^{d_2^+} \left[ \frac{16}{9} M_2^s(Q_0^2) - \frac{n_f}{3} M_2^g(Q_0^2) \right], \end{aligned} \quad (4.7.22)$$

where

$$d_2^+ = -\frac{2}{\beta_0} A_2^+ = \frac{2(16 + 3n_f)}{3(33 - 2n_f)}, \quad (4.7.23)$$

and

$$M_2^s(Q^2) + M_2^g(Q^2) = M_2^s(Q_0^2) + M_2^g(Q_0^2). \quad (4.7.24)$$

The non-singlet equation in (4.7.10) implies that

$$\begin{aligned} [M_2^s(Q^2) - M_2^g(Q^2)] &= \\ [\log(Q_0^2/\Lambda^2)/\log(Q^2/\Lambda^2)]^{d_2^{NS}} \left[ M_2^s(Q_0^2) - M_2^g(Q_0^2) \right], \end{aligned} \quad (4.7.25)$$

where

$$d_2^{NS} = -\frac{2}{\beta_0} A_2^{NS} = \frac{2}{\beta_0} \frac{16}{9} = \frac{32}{3(33 - 2n_f)}. \quad (4.7.26)$$

Using the notation defined in (4.1.6) – (4.1.11) for the total fraction of momentum carried by the various quarks and solving equations (4.7.22), (4.7.24) and (4.7.25) yields

$$Q(Q^2) = \frac{3}{2} \frac{n_f}{(16 + 3n_f)} + \frac{1}{2} A \zeta^{d_2^{NS}} + \frac{1}{2} B \zeta^{d_2^+}, \quad (4.7.27)$$

$$\bar{Q}(Q^2) = \frac{3}{2} \frac{n_f}{(16 + 3n_f)} - \frac{1}{2} A \zeta^{d_2^{NS}} + \frac{1}{2} B \zeta^{d_2^+}, \quad (4.7.28)$$

$$G(Q^2) = \frac{16}{(16 + 3n_f)} - B \zeta^{d_2^+}, \quad (4.7.29)$$

where

$$A = Q(Q_0^2) - \bar{Q}(Q_0^2), \quad (4.7.30)$$

$$B = \frac{1}{(16 + 3n_f)} (16Q(Q_0^2) + 16\bar{Q}(Q_0^2) - 3n_f G(Q_0^2)), \quad (4.7.31)$$

and

$$\zeta = \log(Q_0^2/\Lambda^2)/\log(Q^2/\Lambda^2). \quad (4.7.32)$$

Equation (4.7.24) is equivalent to (4.6.26) and I have taken

$$Q(Q^2) + \bar{Q}(Q^2) + G(Q^2) = Q(Q_0^2) + \bar{Q}(Q_0^2) + G(Q_0^2) = 1. \quad (4.7.33)$$

Since  $d_2^{NS}$  and  $d_2^+$  are positive (provided  $2n_f < 33$ ) (4.7.27), (4.7.28), and

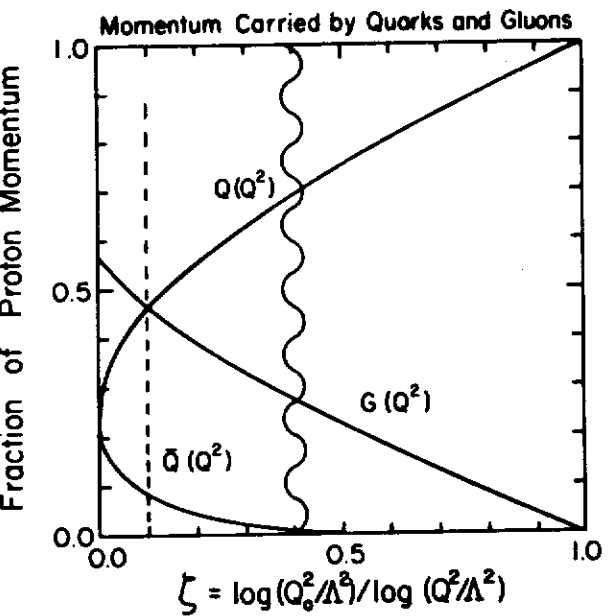


Figure 4.10 Shows the  $Q^2$  dependence of the total fraction of the proton's momentum carried by quarks,  $Q(Q^2)$ , antiquarks,  $\bar{Q}(Q^2)$ , and gluons,  $G(Q^2)$ , if  $Q(Q_0^2) = 1$  and  $\bar{Q}(Q_0^2) = G(Q_0^2) = 0$ . The momentum fractions are plotted versus  $\zeta = \log(Q_0^2/\Lambda^2)/\log(Q^2/\Lambda^2)$  which is equal to 1 when  $Q = Q_0$  and goes to 0 as  $Q \rightarrow \infty$ . The wavy line marks the boundary between the perturbative (left) and the non-perturbative (right) regions (for  $\Lambda = 200$  MeV). The dotted line corresponds to the point where  $Q = G = 0.47$  and  $\bar{Q} = 0.06$ .

(4.7.29) imply the following asymptotic momentum fractions:

$$Q(Q^2) \xrightarrow[Q^2 \rightarrow \infty]{} \frac{3}{2(16+3n_f)} \xrightarrow[n_f=4]{} \frac{1}{2} \left(\frac{3}{7}\right) \quad (4.7.34)$$

$$\bar{Q}(Q^2) \xrightarrow[Q^2 \rightarrow \infty]{} \frac{3}{2(16+3n_f)} \xrightarrow[n_f=4]{} \frac{1}{2} \left(\frac{3}{7}\right) \quad (4.7.35)$$

$$G(Q^2) \xrightarrow[Q^2 \rightarrow \infty]{} \frac{16}{(16+3n_f)} \xrightarrow[n_f=4]{} \frac{4}{7} \quad (4.7.36)$$

At  $Q^2 \rightarrow \infty$  quark and antiquark momentum fractions are equal and the gluon momentum fraction is  $16/(16+3n_f)$  regardless of the situation at the reference momentum  $Q_0$ .

It is amusing to look at the non-relativistic quark model case

$$Q(Q_0^2) = 1, \quad (4.7.37)$$

$$\bar{Q}(Q_0^2) = G(Q_0^2) = 0. \quad (4.7.38)$$

If all the momentum of the proton is carried by quarks at the reference momentum,  $Q_0$ , then

$$A = 1, \quad (4.7.39)$$

$$B = \frac{16}{(16+3n_f)} \xrightarrow[n_f=4]{} \frac{4}{7}, \quad (4.7.40)$$

and for  $n_f = 4$  (4.7.27), (4.7.28), and (4.7.29) become

$$Q(Q^2) = \frac{1}{2} \left( \frac{3}{7} + \zeta^{0.427} + \frac{4}{7} \zeta^{0.747} \right), \quad (4.7.41)$$

$$\bar{Q}(Q^2) = \frac{1}{2} \left( \frac{3}{7} - \zeta^{0.427} + \frac{4}{7} \zeta^{0.747} \right), \quad (4.7.42)$$

$$G(Q^2) = \frac{4}{7} \left( 1 - \zeta^{0.747} \right), \quad (4.7.43)$$

as plotted in Fig. 4.10. Present day fits to the data give<sup>8</sup>

$$Q(Q^2 = 16 \text{ GeV}^2) \approx 0.44, \quad (4.7.44)$$

$$\bar{Q}(Q^2 = 16 \text{ GeV}^2) \approx 0.08, \quad (4.7.45)$$

$$G(Q^2 = 16 \text{ GeV}^2) \approx 0.44, \quad (4.7.46)$$

which is roughly consistent with the evolution in Fig. 4.10 at the point

$$\zeta(Q^2 = 16 \text{ GeV}^2) \approx 0.1. \quad (4.7.47)$$

This implies

$$\left( \frac{Q_0}{\Lambda} \right) = \left( \frac{4 \text{ GeV}}{\Lambda} \right)^{1/10}, \quad (4.7.48)$$

or

$$Q_0 \approx 270 \text{ MeV}, \quad (4.7.49)$$

for  $\Lambda = 200$  MeV. All of this seems quite reasonable except for the fact that unfortunately this  $Q_0$  value corresponds to

$$\alpha_s(Q_0^2) \approx 2.5, \quad (4.7.50)$$

and thus the perturbative formulas are not valid. In fact, the point

$$\alpha_s(Q^2) = 1, \quad (4.7.51)$$

corresponds to the point

$$\zeta \approx 0.4, \quad (4.7.52)$$

with  $\Lambda = 200$  MeV and  $n_f = 4$ , so that the evolution in Fig. 4.10 for  $\zeta \gtrsim 0.4$  cannot be believed.

If we take the logarithm of both sides of the non-singlet moments in

(4.7.10), we arrive at

$$\log(M_n^{NS}(Q^2)) = \kappa A_n^{NS} + \log(M_n^{NS}(Q_0^2)), \quad (4.7.53)$$

where

$$\kappa = \frac{2}{\beta_0} \log\{\log(Q^2/\Lambda^2)/\log(Q_0^2/\Lambda^2)\}. \quad (4.7.54)$$

Thus,

$$\frac{1}{d_n^{NS}} \log(M_n^{NS}(Q^2)) = C(n) - \log(\log(Q^2/\Lambda^2)), \quad (4.7.55)$$

where

$$d_n^{NS} \equiv -\frac{2}{\beta_0} A_n^{NS}, \quad (4.7.56)$$

and

$$C(n) = \frac{1}{d_n^{NS}} \log(M_n^{NS}(Q_0^2)) + \log(\log(Q_0^2/\Lambda^2)), \quad (4.7.57)$$

is independent of  $Q^2$ . This means that

$$\frac{1}{d_n^{NS}} \log(M_n^{NS}(Q^2)) - \frac{1}{d_\ell^{NS}} \log(M_\ell^{NS}(Q^2)) = C(n) - C(\ell), \quad (4.7.58)$$

or

$$\log(M_n^{NS}(Q^2)) = \frac{d_n^{NS}}{d_\ell^{NS}} \log(M_\ell^{NS}(Q^2)) + d_n^{NS}(C(n) - C(\ell)). \quad (4.7.59)$$

At this order of perturbation theory this implies that a plot of  $\log(M_n^{NS}(Q^2))$  versus  $\log(M_\ell^{NS}(Q^2))$  is a straight line with a slope given by a ratio of the anomalous dimensions

$$\frac{d_n^{NS}}{d_\ell^{NS}} = \frac{A_n^{NS}}{A_\ell^{NS}}, \quad (4.7.60)$$

and is independent of the perturbative parameter,  $\Lambda$ , and the number of quark flavors,  $n_f$ .

## 4.8 $Q^2$ Evolution – Convolution Method

We can approximate the integral equations in (4.6.6) and (4.6.18) by using the convolution method presented in Chapter 3 for the fragmentation functions. In analogy to (3.5.13) the non-singlet structure function is given by

$$G_{NS}(x, Q^2) = \tilde{G}_{NS}(x, Q^2) + \kappa \int_x^1 \frac{dy}{y} \tilde{G}(x/y, Q^2) P_\Delta(y) + O(\kappa^2), \quad (4.8.1)$$

where

$$\tilde{G}_{NS}(x, Q^2) = \int_x^1 \frac{dy}{y} G_{NS}(x/y, Q_0^2) \frac{(-\log(y))^{\frac{2}{3}\kappa-1}}{\Gamma(\frac{2}{3}\kappa)}, \quad (4.8.2)$$

and

$$P_\Delta(y) = \frac{4}{3} \left[ \frac{1+y^2}{1-y} + \frac{2}{\log(y)} + \left( \frac{3}{2} - 2\gamma_E \right) \delta(1-y) \right], \quad (4.8.3)$$

where  $\kappa$  is defined in (4.6.7). The individual quark and gluon distributions are given by

$$G_{p \rightarrow q_i}(x, Q^2) = \tilde{G}_{p \rightarrow q_i}(a_q, x, Q^2) + \kappa \int_x^1 \frac{dy}{y} \tilde{G}_{p \rightarrow q_i}(a_q, y, Q^2) P_{\Delta q}(x/y) \\ + \kappa \int_x^1 \frac{dy}{y} \tilde{G}_{p \rightarrow g}(y, Q^2) P_{g \rightarrow q\bar{q}}(x/y), \quad (4.8.4)$$

$$G_{p \rightarrow g}(x, Q^2) = \tilde{G}_{p \rightarrow g}(a_g, x, Q^2) + \kappa \int_x^1 \frac{dy}{y} \tilde{G}_{p \rightarrow g}(a_g, y, Q^2) P_{\Delta g}(x/y) \\ + \kappa \sum_{j=1}^{2n_f} \int_x^1 \frac{dy}{y} \tilde{G}_{p \rightarrow q_j}(y, Q^2) P_{q_j \rightarrow g\bar{q}}(x/y), \quad (4.8.5)$$

where

$$\tilde{G}_{p \rightarrow i}(a, x, Q^2) = \int_x^1 \frac{dy}{y} G_{p \rightarrow i}(x/y, Q_0^2) \frac{(-\log(y))^{\alpha\kappa-1}}{\Gamma(\alpha K)}, \quad (4.8.6)$$

and

$$P_{\Delta q}(z) = P_\Delta(z), \quad (4.8.7)$$

with  $P_\Delta(z)$  given in (4.8.3) and

$$P_{\Delta g}(z) = 6 \left[ \frac{z}{1-z} + \frac{1}{\log(z)} + \frac{1-z}{z} + z(1-z) \right. \\ \left. + \left( \frac{11}{12} - \frac{2}{36} n_f - \gamma_E \right) \delta(1-z) \right]. \quad (4.8.8)$$

Furthermore  $a_q$  and  $a_g$  are given in (3.5.17). The quantity  $\tilde{G}(x, Q^2)$  is computed by averaging  $\tilde{G}(a, x, Q^2)$  over  $a$ . Namely,

$$\tilde{G}_{p \rightarrow i}(x, Q^2) = \frac{1}{(a_g - a_q)} \int_{a_q}^{a_g} \tilde{G}_{p \rightarrow i}(a, x, Q^2) da. \quad (4.8.9)$$

These equations express the distributions at  $Q^2$  directly in terms of those at  $Q_0^2$ . They are the same as the fragmentation function equations in (3.5.22) and (3.5.23) except for the interchange of  $P_{q \rightarrow g\bar{q}}$  and  $P_{g \rightarrow q\bar{q}}$ . The equations are not exact since terms of order  $\kappa^2$  and higher have been neglected. They are, however, very accurate in the range  $0.05 \leq x \leq 1$  for  $\kappa \leq 0.3$ .

As was the case for the fragmentation functions the convolution equations

in (4.8.4) and (4.8.5) allow an easy determination of the large  $x$  behavior of  $G(x, Q^2)$  since

$$G(x, Q^2) \xrightarrow{x \rightarrow 1} \tilde{G}(a, x, Q^2). \quad (4.8.10)$$

If at  $Q_0^2$  we have

$$G(x, Q_0^2) = A(1-x)^P \xrightarrow{x \rightarrow 1} A(-\log(x))^P, \quad (4.8.11)$$

then

$$\tilde{G}(a, x, Q^2) = A \frac{\Gamma(P+1)}{\Gamma(P+1+a\kappa)} (-\log(x))^{P+a\kappa} \xrightarrow{x \rightarrow 1} C(1-x)^{P+\xi_a(Q^2)}, \quad (4.8.12)$$

where

$$\xi_a(Q^2) = a\kappa. \quad (4.8.13)$$

For quarks

$$\xi_q(Q^2) = \frac{8}{3} \frac{2}{\beta_0} \log \left\{ \log(Q^2/\Lambda^2) / \log(Q_0^2/\Lambda^2) \right\}, \quad (4.8.14)$$

and for gluons

$$\xi_g(Q^2) = 6 \frac{2}{\beta_0} \log \left\{ \log(Q^2/\Lambda^2) / \log(Q_0^2/\Lambda^2) \right\}. \quad (4.8.15)$$

As in the fragmentation case, the gluon distribution becomes steeper than the quark distributions and the difference is governed by the ratio<sup>9</sup>

$$\frac{\xi_g(Q^2)}{\xi_q(Q^2)} = 6 \left(\frac{3}{8}\right) = \frac{9}{4}. \quad (4.8.16)$$

## 4.9 The Longitudinal Structure Function

After summing the leading logarithm terms in (4.6.3) we arrive at

$$G_{p \rightarrow q}^{(2)}(x, Q^2) = \bar{G}_{p \rightarrow q}(Q^2) * (1 + \alpha_s f_1^{q,DIS}) + \bar{G}_{p \rightarrow g}(Q^2) * (\alpha_s f_2^{q,DIS}), \quad (4.9.1)$$

where the superscript (2) refers to the fact that  $G^{(2)}(x, Q^2)$  is defined from  $\mathcal{F}_2(x, Q^2)$  structure function as in (4.6.1) and where the convolution notation defined in (3.3.11) is being used. To leading order both  $G_{p \rightarrow q}^{(2)}$  and  $\bar{G}_{p \rightarrow q}$  are solutions of the  $Q^2$  evolution equation (4.6.12) and  $\bar{G}_{p \rightarrow q}$  satisfies (4.6.13). The “little  $f$ ” functions in (4.9.1) are regularization scheme dependent which means that, at this stage, so is  $G_{p \rightarrow q}^{(2)}(x, Q^2)$ . However since

$$\int_0^1 \alpha_s f_2^{q,DIS}(z) dz = 0, \quad (4.9.2)$$

in any scheme, we have

$$\begin{aligned} \int_0^1 [G_{p \rightarrow q}^{(2)}(x, Q^2) - G_{p \rightarrow q}^{(2)}(x, Q^2)] dx = \\ \int_0^1 [\bar{G}_{p \rightarrow q}(x, Q^2) - \bar{G}_{p \rightarrow q}(x, Q^2)] dx. \end{aligned} \quad (4.9.3)$$

This means that the net number of quarks in the proton (4.6.19) is not affected by the higher order corrections that produced the “little  $f$ ” functions. This is a nice feature and it is one of the reasons that we use the  $\mathcal{F}_2(x, Q^2)$  observable to define the quark distributions.

However, we could define “quark distributions” from the  $\mathcal{F}_1(x, Q^2)$  structure. Namely,

$$\mathcal{F}_1(x, Q^2) \equiv \sum_{i=1}^{n_f} e_{q_i}^2 (G_{p \rightarrow q_i}^{(1)}(x, Q^2) + G_{p \rightarrow \bar{q}_i}^{(1)}(x, Q^2)), \quad (4.9.4)$$

where the superscript (1) refers to the  $\mathcal{F}_1$  structure function. In this case (4.9.1) becomes

$$G_{p \rightarrow q}^{(1)}(x, Q^2) = \bar{G}_{p \rightarrow q}(Q^2) * (1 + \alpha_s f_1^{q,DIS}) + \bar{G}_{p \rightarrow g}(Q^2) * (\alpha_s f_1^{g,DIS}), \quad (4.9.5)$$

where, to leading order,  $G_{p \rightarrow q}^{(1)}(x, Q^2)$  also satisfies (4.6.12). The “little  $f$ ” functions are again scheme dependent and are given by

$$\alpha_s f_1^{q,DIS}(z) = \alpha_s f_2^{q,DIS}(z) - \alpha_s f_L^{q,DIS}(z), \quad (4.9.6)$$

which means that  $G_{p \rightarrow q}^{(1)}(x, Q^2)$  is also scheme dependent. However, we cannot actually calculate  $G_{p \rightarrow q}^{(1)}$  or  $G_{p \rightarrow q}^{(2)}$ . If we are given  $G_{p \rightarrow q}^{(2)}$  or  $G_{p \rightarrow q}^{(1)}$  at one value of  $Q^2$ , say  $Q_0^2$ , we can calculate it at higher values of  $Q^2$  from the evolution equations which, at leading order, do not involve the “little  $f$ ” functions. We now define the observable  $\mathcal{F}_2(x, Q^2)$  in (4.6.1) to be our “reference distributions.” That is, we define quark distributions  $G_{p \rightarrow q}(x, Q^2)$  according to

$$G_{p \rightarrow q}(x, Q^2) \equiv G_{p \rightarrow q}^{(2)}(x, Q^2). \quad (4.9.7)$$

Given  $G_{p \rightarrow q}(x, Q_0^2)$  we can calculate  $G_{p \rightarrow q}(x, Q^2)$  from the  $Q^2$  evolution equations. With this definition equation (4.9.5) becomes

$$\begin{aligned} G_{p \rightarrow q}^{(1)}(x, Q^2) = & G_{p \rightarrow q}(Q^2) * (1 + \alpha_s \Delta f_1^{q,DIS}) \\ & + G_{p \rightarrow g}(Q^2) * (\alpha_s \Delta f_1^{g,DIS}), \end{aligned} \quad (4.9.8)$$

or

$$\begin{aligned} G_{p \rightarrow q}^{(1)}(x, Q^2) = & \int_x^1 \frac{dy}{y} \left\{ G_{p \rightarrow q}(y, Q^2) [\delta(1-z) + \alpha_s \Delta f_1^{q,DIS}(z)] \right. \\ & \left. + G_{p \rightarrow g}(y, Q^2) \alpha_s \Delta f_1^{g,DIS}(z) \right\}, \end{aligned} \quad (4.9.9)$$

where  $z = x/y$  and where

$$\begin{aligned}\alpha_s \Delta f_1^{q,DIS}(z) &= \alpha_s [f_1^{q,DIS}(z) - f_2^{q,DIS}(z)] \\ &= -\alpha_s f_L^{q,DIS}(z),\end{aligned}\quad (4.9.10)$$

and

$$\begin{aligned}\alpha_s \Delta f_1^{g,DIS}(z) &= \alpha_s [f_1^{g,DIS}(z) - f_2^{g,DIS}(z)] \\ &= -\alpha_s f_L^{g,DIS}(z).\end{aligned}\quad (4.9.11)$$

The  $\Delta f_1$  functions are related to the longitudinal function  $f_L$  given by (4.4.41) and (4.4.64). The  $\Delta f_1$  functions do not depend on the regularization scheme and tell us how much the  $G_{p \rightarrow q}^{(1)}(x, Q^2)$  distributions differ from the “reference distributions”  $G_{p \rightarrow q}(x, Q^2)$ . In the naive parton model equation (4.2.77) holds and there is no difference between  $G_{p \rightarrow q}^{(1)}$  and  $G_{p \rightarrow q}$ . In QCD they differ at order  $\alpha_s$ , and (4.9.9) tells us how to calculate  $G_{p \rightarrow q}^{(1)}(x, Q^2)$  in terms of  $G_{p \rightarrow q}(x, Q^2)$ .

The longitudinal structure function  $F_L(x, Q^2)$  is given by

$$\begin{aligned}F_L(x, Q^2) &= \alpha_s(Q^2) \int_x^1 \frac{dy}{y} \left\{ \sum_{i=1}^{n_f} e_{q_i}^2 (G_{p \rightarrow q_i}(y, Q^2) + G_{p \rightarrow \bar{q}_i}(y, Q^2)) f_L^{q,DIS}(z) \right. \\ &\quad \left. + \left( \sum_{i=1}^{2n_f} e_{q_i}^2 \right) G_{p \rightarrow g}(y, Q^2) f_L^{g,DIS}(z) \right\},\end{aligned}\quad (4.9.12)$$

where  $z = x/y$ . This can be written in the form<sup>10</sup>

$$\begin{aligned}F_L(x, Q^2) &= \frac{\alpha_s(Q^2)}{2\pi} x^2 \int_x^1 \frac{dy}{y^3} \left\{ \frac{8}{3} F_2(y, Q^2) \right. \\ &\quad \left. + 2a_e y G_{p \rightarrow g}(y, Q^2) \left( 1 - \frac{x}{y} \right) \right\},\end{aligned}\quad (4.9.13)$$

where  $F_L(x, Q^2) = x F_L(x, Q^2)$ ,  $F_2(x, Q^2) = x F_2(x, Q^2)$ , and

$$a_e = \sum_{i=1}^{2n_f} e_{q_i}^2 \stackrel{n_f=4}{=} \frac{20}{9}.\quad (4.9.14)$$

The sum runs from 1 to  $2n_f$  since it includes both quarks and antiquarks. Equation (4.9.13) allows us to calculate the longitudinal structure function  $F_L(x, Q^2)$  in terms of the structure function  $F_2(x, Q^2)$  and the gluon distribution  $G_{p \rightarrow g}(x, Q^2)$ .

The integral of the observable  $R^{DIS}(x, Q^2)$  defined in (4.2.58),

$$\begin{aligned}R^{DIS}(x, Q^2) &= F_L(x, Q^2)/(F_L(x, Q^2) + F_2(x, Q^2)) \\ &= R_2^{DIS}(x, Q^2)/(1 + R_2^{DIS}(x, Q^2)),\end{aligned}\quad (4.9.15)$$

and

$$R_2^{DIS}(x, Q^2) = F_L(x, Q^2)/F_2(x, Q^2),\quad (4.9.16)$$

are easy to estimate in QCD. In particular,

$$\bar{R}_2^{DIS}(Q^2) = \bar{F}_L(Q^2)/\bar{F}_2(Q^2).\quad (4.9.17)$$

where

$$\bar{F}_i(Q^2) = \int_0^1 F_i(x, Q^2) dx,\quad (4.9.18)$$

for  $i = 2, L$  and using (4.4.41) and (4.4.64) we see that

$$\alpha_s \int_0^1 z f_L^{q,DIS}(z) dz = \frac{\alpha_s}{2\pi} \frac{8}{9},\quad (4.9.19)$$

$$\alpha_s \int_0^1 z f_L^{g,DIS}(z) dz = \frac{\alpha_s}{2\pi} \frac{1}{6},\quad (4.9.20)$$

so that the integral over  $x$  of (4.9.13) becomes

$$\bar{F}_L(Q^2) = \frac{\alpha_s}{2\pi} \left[ \frac{8}{9} \bar{F}_2(Q^2) + \frac{1}{6} a_e G(Q^2) \right],\quad (4.9.21)$$

where  $G(Q^2)$  is the total momentum carried by gluons,

$$G(Q^2) = \int_0^1 x G_{p \rightarrow g}(x, Q^2) dx.\quad (4.9.22)$$

At  $Q^2 = 16$  GeV<sup>2</sup> the following is approximately true:

$$\bar{F}_2(Q^2 = 16 \text{ GeV}) \approx 0.164,\quad (4.9.23)$$

$$G(Q^2 = 16 \text{ GeV}) \approx 0.514,\quad (4.9.24)$$

so that

$$\bar{R}_2(Q^2 = 16 \text{ GeV}) \approx 0.107,\quad (4.9.25)$$

$$\bar{R}(Q^2 = 16 \text{ GeV}) \approx 0.12.\quad (4.9.26)$$

At this  $Q^2$ , about half of  $\bar{F}_L(Q^2)$  is due to the gluon term  $G(Q^2)$  and about half is due to the quark term  $\bar{F}_2(Q^2)$ .

In all of this discussion, we have neglected corrections of order  $M^2/Q^2$ . Such contributions cannot be calculated by perturbation theory. An estimate of the  $1/Q^2$  contribution to  $R$  is

$$R(\text{primordial}) = 4\langle k_T^2 \rangle_{\text{primordial}}/Q^2,\quad (4.9.27)$$

where  $k_T$  is the non-perturbative “primordial” component to the transverse momentum of quarks within hadrons. The perturbative contribution to  $R$  behaves roughly as  $\alpha_s(Q^2) \sim 1/\log(Q^2/\Lambda^2)$ , so that at sufficiently large  $Q^2$  this contribution dominates. However, at  $Q^2 = 16$  GeV<sup>2</sup>,  $R(\text{primordial}) \approx 0.06$  (using  $R(\text{primordial}) \approx 1/Q^2$ ) which is certainly not negligible compared to the value of 0.12 arrived at in (4.9.26) for  $R(\text{perturbative})$ .

## 4.10 Neutrino Nucleon Scattering

The cross section in (4.2.13) for electron nucleon scattering can be expressed as

$$\frac{d^2\sigma^{eN}}{dxdy} = \frac{4\pi\alpha^2}{Q^4} [F_2(x, Q^2)(1-y) + F_1(x, Q^2)xy^2], \quad (4.10.1)$$

where

$$y \equiv \nu/E, \quad (4.10.2)$$

is the inelasticity parameter satisfying

$$0 \leq y \leq 1, \quad (4.10.3)$$

and where

$$\mathcal{F}_1(x, Q^2) = 2F_1(x, Q^2), \quad (4.10.4)$$

$$\mathcal{F}_2(x, Q^2) = F_2(x, Q^2)/x. \quad (4.10.5)$$

In addition, a term proportional to  $M/E$  has been neglected in (4.10.1).

The corresponding cross section for neutrino and antineutrino nucleon scattering is given by

$$\begin{aligned} \frac{d^2\sigma^{(\nu,\bar{\nu})N}}{dxdy} = & \frac{G_F^2 ME}{\pi} \left[ F_2(x, Q^2)(1-y) + F_1(x, Q^2)xy^2 \right. \\ & \left. \pm F_3(x, Q^2)xy(1-\frac{1}{2}y) \right], \end{aligned} \quad (4.10.6)$$

where  $G_F$  is the Fermi constant and where

$$F_3(x, Q^2) \equiv \mathcal{F}_3(x, Q^2) \equiv \nu W_3(x, Q^2), \quad (4.10.7)$$

arises from the parity-violating  $\epsilon_{\mu\nu\alpha\beta} P_\alpha q_\beta$  term in the general expression for the hadronic vertex in (4.2.6). This third structure function is not present in the electron scattering case. As in the electron scattering case, we define quark distributions as follows:

$$\mathcal{F}_1(x, Q^2) = 2 \sum_i G_{N \rightarrow q_i}^{(1)}(x, Q^2) + 2 \sum_j G_{N \rightarrow \bar{q}_j}^{(1)}(x, Q^2), \quad (4.10.8)$$

$$\mathcal{F}_2(x, Q^2) = 2 \sum_i G_{N \rightarrow q_i}^{(2)}(x, Q^2) + 2 \sum_j G_{N \rightarrow \bar{q}_j}^{(2)}(x, Q^2), \quad (4.10.9)$$

$$\mathcal{F}_3(x, Q^2) = 2 \sum_i G_{N \rightarrow q_i}^{(3)}(x, Q^2) - 2 \sum_j G_{N \rightarrow \bar{q}_j}^{(3)}(x, Q^2). \quad (4.10.10)$$

where the sums are over the appropriate quark and antiquark flavors shown in (4.1.18) – (4.1.25). Fermions contribute to  $\mathcal{F}_3(x, Q^2)$  with a positive sign while antiquarks contribute with a negative sign. The distributions satisfy

(4.9.5) and (4.9.1),

$$\begin{aligned} G_{N \rightarrow q}^{(1)}(x, Q^2) = & \bar{G}_{N \rightarrow q}(Q^2) * \left( 1 + \alpha_s f_1^{q,DIS} \right) \\ & + \bar{G}_{N \rightarrow g}(Q^2) * \left( \alpha_s f_1^{g,DIS} \right), \end{aligned} \quad (4.10.11)$$

$$\begin{aligned} G_{N \rightarrow q}^{(2)}(x, Q^2) = & \bar{G}_{N \rightarrow q}(Q^2) * \left( 1 + \alpha_s f_2^{q,DIS} \right) \\ & + \bar{G}_{N \rightarrow g}(Q^2) * \left( \alpha_s f_2^{g,DIS} \right), \end{aligned} \quad (4.10.12)$$

and similarly

$$G_{N \rightarrow q}^{(3)}(x, Q^2) = \bar{G}_{N \rightarrow q}(Q^2) * \left( 1 + \alpha_s f_3^{q,DIS} \right), \quad (4.10.13)$$

where again convolution notation has been used. The “little  $f$ ” functions are regularization scheme dependent as usual and are calculated from the virtual  $W$ -boson subprocesses  $W^* + q \rightarrow q + g$  and  $W^* + g \rightarrow q + \bar{q}$ . The “little  $f$ ” functions in (4.10.11) and (4.10.12) are identical to those computed from the virtual photon subprocess  $\gamma^* + q \rightarrow q + g$  and  $\gamma^* + g \rightarrow q + \bar{q}$ . The  $f_3^q$  function is new and in the massive gluon scheme it is given by

$$\begin{aligned} \alpha_s f_{MG,3}^{q,DIS}(z) = & \frac{2\alpha_s}{3\pi} \left\{ (1+z^2) \left( \frac{\log(1-z)}{1-z} \right)_+ + \frac{1+z^2}{1-z} (-2\log(z)) \right. \\ & \left. - \frac{3}{2} \frac{1}{(1-z)_+} + 3z - \left( \frac{2\pi^2}{3} + \frac{9}{4} \right) \delta(1-z) \right\}. \end{aligned} \quad (4.10.14)$$

There is no gluon contribution to  $G_{N \rightarrow q}^{(3)}(x, Q^2)$ . If we now define  $G_{N \rightarrow q}^{(2)}(x, Q^2)$  to be our reference distribution then

$$\begin{aligned} G_{N \rightarrow q}^{(1)}(x, Q^2) = & G_{N \rightarrow q}(Q^2) * \left( 1 + \alpha_s \Delta f_1^{q,DIS} \right)^c \\ & + G_{N \rightarrow g}(Q^2) * \left( \alpha_s \Delta f_1^{g,DIS} \right), \end{aligned} \quad (4.10.15)$$

$$G_{N \rightarrow q}^{(2)}(x, Q^2) \equiv G_{N \rightarrow q}(x, Q^2), \quad (4.10.16)$$

$$G_{N \rightarrow q}^{(3)}(x, Q^2) = \bar{G}_{N \rightarrow q}(Q^2) * \left( 1 + \alpha_s \Delta f_3^{q,DIS} \right), \quad (4.10.17)$$

where

$$\begin{aligned} \alpha_s \Delta f_1^{q,DIS}(z) = & \alpha_s \left( f_1^{q,DIS}(z) - f_2^{q,DIS}(z) \right) = -\alpha_s f_L^{q,DIS}(z) \\ = & -\frac{\alpha_s}{2\pi} \frac{4}{3} 2z, \end{aligned} \quad (4.10.18)$$

$$\begin{aligned} \alpha_s \Delta f_1^{g,DIS}(z) = & \alpha_s \left( f_1^{g,DIS}(z) - f_2^{g,DIS}(z) \right) = -\alpha_s f_L^{g,DIS}(z) \\ = & -\frac{\alpha_s}{2\pi} 2z(1-z), \end{aligned} \quad (4.10.19)$$

$$\alpha_s \Delta f_3^{q,DIS}(z) = \alpha_s \left( f_3^{q,DIS}(z) - f_3^{g,DIS}(z) \right)$$

$$= -\frac{\alpha_s}{2\pi} \frac{4}{3}(1+z). \quad (4.10.20)$$

These ‘‘little  $\Delta f$ ’’ functions are unique and independent of the regularization scheme.

For neutrino nucleon scattering (4.10.9) becomes

$$\begin{aligned} \mathcal{F}_2^{\nu N}(x, Q^2) = & 2G_{N \rightarrow d}(x, Q^2) + 2G_{N \rightarrow s}(x, Q^2) \\ & + 2G_{N \rightarrow u}(x, Q^2) + 2G_{N \rightarrow \bar{e}}(x, Q^2), \end{aligned} \quad (4.10.21)$$

and (4.10.10) becomes

$$\begin{aligned} \mathcal{F}_3^{\nu N}(x, Q^2) = & 2G_{N \rightarrow d}(Q^2) * (1 + \alpha_s \Delta f_3^{q,DIS}) \\ & + 2G_{N \rightarrow s}(Q^2) * (1 + \alpha_s \Delta f_3^{q,DIS}) \\ & - 2G_{N \rightarrow u}(Q^2) * (1 + \alpha_s \Delta f_3^{q,DIS}) \\ & - 2G_{N \rightarrow \bar{e}}(Q^2) * (1 + \alpha_s \Delta f_3^{q,DIS}), \end{aligned} \quad (4.10.22)$$

where I am using convolution notation. The structure functions (4.1.26) and (4.1.27),

$$\mathcal{F}_Q(x, Q^2) \equiv \frac{1}{2}(\mathcal{F}_2(x, Q^2) + \mathcal{F}_3(x, Q^2)), \quad (4.10.23)$$

$$\mathcal{F}_A(x, Q^2) \equiv \frac{1}{2}(\mathcal{F}_2(x, Q^2) - \mathcal{F}_3(x, Q^2)), \quad (4.10.24)$$

which in the naive parton model project out the quark and antiquark distributions now give

$$\begin{aligned} \mathcal{F}_Q^{\nu N}(x, Q^2) = & G_{N \rightarrow d}(Q^2) * (2 + \alpha_s \Delta f_3^{q,DIS}) \\ & + G_{N \rightarrow s}(Q^2) * (2 + \alpha_s \Delta f_3^{q,DIS}) \\ & + G_{N \rightarrow u}(Q^2) * (-\alpha_s \Delta f_3^{q,DIS}) \\ & + G_{N \rightarrow \bar{e}}(Q^2) * (-\alpha_s \Delta f_3^{q,DIS}), \end{aligned} \quad (4.10.25)$$

or

$$\begin{aligned} \mathcal{F}_A^{\nu N}(x, Q^2) = & 2G_{N \rightarrow d}(x, Q^2) + 2G_{N \rightarrow s}(x, Q^2) \\ & + \int_x^1 \frac{dy}{y} [G_{N \rightarrow d}(y, Q^2) + G_{N \rightarrow s}(y, Q^2)] \alpha_s \Delta f_3^{q,DIS}(z) \\ & + \int_x^1 \frac{dy}{y} [G_{N \rightarrow u}(y, Q^2) + G_{N \rightarrow \bar{e}}(y, Q^2)] \alpha_s \Delta f_3^{q,DIS}(z), \end{aligned} \quad (4.10.26)$$

where  $z = x/y$ . Similarly,

$$\begin{aligned} \mathcal{F}_A^{\nu N}(x, Q^2) = & G_{N \rightarrow u}(Q^2) * (2 + \alpha_s \Delta f_3^{q,DIS}) \\ & + G_{N \rightarrow \bar{e}}(Q^2) * (2 + \alpha_s \Delta f_3^{q,DIS}) \\ & + G_{N \rightarrow d}(Q^2) * (-\alpha_s \Delta f_3^{q,DIS}) \\ & + G_{N \rightarrow s}(Q^2) * (-\alpha_s \Delta f_3^{q,DIS}), \end{aligned} \quad (4.10.27)$$

or

$$\begin{aligned} \mathcal{F}_A^{\nu N}(x, Q^2) = & 2G_{N \rightarrow d}(x, Q^2) + 2G_{N \rightarrow s}(x, Q^2) \\ & + \int_x^1 \frac{dy}{y} [G_{N \rightarrow d}(y, Q^2) + G_{N \rightarrow s}(y, Q^2)] \alpha_s \Delta f_3^{q,DIS}(z) \\ & - \int_x^1 \frac{dy}{y} [G_{N \rightarrow u}(y, Q^2) + G_{N \rightarrow \bar{e}}(y, Q^2)] \alpha_s \Delta f_3^{q,DIS}(z), \end{aligned} \quad (4.10.28)$$

where  $z = x/y$ . At order  $\alpha_s$ ,  $\mathcal{F}_Q(x, Q^2)$  receives a contribution from antiquarks and  $\mathcal{F}_A(x, Q^2)$  receives a contribution from quarks. If we multiply (4.10.25) and (4.10.27) by  $x$  and integrate we see that

$$\begin{aligned} \overline{\mathcal{F}}_Q^{\nu N}(Q^2) = & (U + D + 2S)(1 - 0.0885\alpha_s(Q^2)) \\ & + (\overline{U} + \overline{D} + 2\overline{S})(0.0885\alpha_s(Q^2)), \end{aligned} \quad (4.10.29)$$

and

$$\begin{aligned} \overline{\mathcal{F}}_A^{\nu N}(Q^2) = & (\overline{U} + \overline{D} + 2\overline{S})(1 - 0.0885\alpha_s(Q^2)) \\ & + (U + D + 2S)(0.0885\alpha_s(Q^2)), \end{aligned} \quad (4.10.30)$$

where I have taken an isoscalar target

$$N = \frac{1}{2}(p + n), \quad (4.10.31)$$

and defined

$$\overline{\mathcal{F}}_i(x, Q^2) = \int_0^1 x \mathcal{F}_i(x, Q^2) dx. \quad (4.10.32)$$

The quantities  $U, D, S, \dots$  are the total fraction of momentum carried by  $u, d, s, \dots$  quarks respectively, as defined in (4.1.6)–(4.1.8) and I have used

$$\alpha_s \int_0^1 z \Delta f_3^{q,DIS}(z) dz = -\frac{10}{9} \frac{\alpha_s}{2\pi} = -0.177 \alpha_s. \quad (4.10.33)$$

At order  $\alpha_s$ ,  $\overline{\mathcal{F}}_Q$  receives a contribution from antiquarks and  $\overline{\mathcal{F}}_A$  receives a contribution from quarks.

The longitudinal structure function for neutrino nucleon scattering is given by

$$\mathcal{F}_L^{\nu N}(x, Q^2) = \mathcal{F}_2^{\nu N}(x, Q^2) - \mathcal{F}_1^{\nu N}(x, Q^2), \quad (4.10.34)$$

and, in particular, since

$$\begin{aligned} \mathcal{F}_1^{\nu N}(x, Q^2) = & 2G_{N \rightarrow d}(Q^2) * (1 + \alpha_s \Delta f_1^{q,DIS}) \\ & + 2G_{N \rightarrow s}(Q^2) * (1 + \alpha_s \Delta f_1^{q,DIS}) \\ & + 2G_{N \rightarrow u}(Q^2) * (1 + \alpha_s \Delta f_1^{q,DIS}) \\ & + 2G_{N \rightarrow \bar{e}}(Q^2) * (1 + \alpha_s \Delta f_1^{q,DIS}) \\ & + 8G_{N \rightarrow g}(Q^2) * (\alpha_s \Delta f_1^{q,DIS}), \end{aligned} \quad (4.10.35)$$

we have

$$\begin{aligned}\mathcal{F}_L^{\nu N}(x, Q^2) = & 2G_{N-d}(Q^2) * (\alpha_s \Delta f_L^{q, DIS}) \\ & + 2G_{N-s}(Q^2) * (\alpha_s \Delta f_L^{q, DIS}) \\ & + 2G_{N-g}(Q^2) * (\alpha_s \Delta f_L^{q, DIS}) \\ & + 2G_{N-\bar{g}}(Q^2) * (\alpha_s \Delta f_L^{q, DIS}) \\ & + 8G_{N-g}(Q^2) * (\alpha_s \Delta f_L^{q, DIS}),\end{aligned}\quad (4.10.36)$$

where again convolution notation is being used. Comparing with (4.10.21) shows that

$$\begin{aligned}\mathcal{F}_L^{\nu N}(x, Q^2) = & \mathcal{F}_2^{\nu N}(Q^2) * (\alpha_s f_L^{q, DIS}) \\ & + 8G_{N-g}(Q^2) * (\alpha_s f_L^{q, DIS}).\end{aligned}\quad (4.10.37)$$

If we substitute (4.4.41) and (4.4.64) for  $f_L^q$  and  $f_L^g$ , respectively, then we arrive at

$$\begin{aligned}F_L^{(\nu, p)}(x, Q^2) = & \frac{\alpha_s(Q^2)}{2\pi} x^2 \int_x^1 \frac{dy}{y^3} \left\{ \frac{8}{3} F_2^{(\nu, p)}(y, Q^2) \right. \\ & \left. + 2a_\nu y G_{N-g}(y, Q^2) \left( 1 - \frac{x}{y} \right) \right\},\end{aligned}\quad (4.10.38)$$

where  $F_L(x, Q^2) = x\mathcal{F}_L(x, Q^2)$  and  $F_2(x, Q^2) = x\mathcal{F}_2(x, Q^2)$ . This result is the same as the electron scattering case in (4.9.13) except now

$$a_\nu = 8.\quad (4.10.39)$$

Integrating over  $x$  as in (4.9.18) gives

$$\overline{F}_L^{(\nu, p)}(Q^2) = \frac{\alpha_s}{2\pi} \left[ \frac{8}{9} \overline{F}_2^{(\nu, p)}(Q^2) + \frac{1}{6} a_\nu G(Q^2) \right],\quad (4.10.40)$$

and

$$\begin{aligned}\overline{F}_L^{\nu N}(Q^2) = & 0.141 \alpha_s(Q^2) [U + D + 2S + \overline{U} + \overline{D} + 2\overline{C}] \\ & + 0.212 \alpha_s(Q^2) G,\end{aligned}\quad (4.10.41)$$

while (4.9.21) implies that

$$\begin{aligned}\overline{F}_L^{e N}(Q^2) = & 0.141 \alpha_s(Q^2) [\frac{5}{18}(U + D + \overline{U} + \overline{D}) + \frac{8}{18}(C + \overline{C}) + \frac{2}{18}(S + \overline{S})] \\ & + 0.059 \alpha_s(Q^2) G.\end{aligned}\quad (4.10.42)$$

It appears that gluons contribute more to the  $\nu N$  longitudinal structure function, however, if we multiply the  $eN$  structure function by the factor of  $18/5$  like in (4.1.47) we have

$$\begin{aligned}\frac{18}{5} \overline{F}_L^{e N}(Q^2) = & 0.141 \alpha_s(Q^2) [(U + D + \overline{U} + \overline{D}) + \frac{8}{5}(C + \overline{C}) + \frac{2}{5}(S + \overline{S})] \\ & + 0.212 \alpha_s(Q^2) G,\end{aligned}\quad (4.10.43)$$

and the gluon terms are now identical. If we neglect the strange and charm content within the nucleon then to order  $\alpha_s$  we have

$$\frac{\overline{F}_L^{e N}(Q^2)}{\overline{F}_L^{\nu N}(Q^2)} = \frac{5}{18},\quad (4.10.44)$$

and

$$\overline{R}_2^{e N}(Q^2) = \overline{R}_2^{\nu N}(Q^2),\quad (4.10.45)$$

where  $\overline{R}_2$  is defined in (4.9.17).

### Problems

4.1. Starting with the general form of the hadronic tensor given in (4.2.6),

$$\begin{aligned}W_{\mu\nu} = & -W_1 \left( g_{\mu\nu} - \frac{q_\mu q_\nu}{q^2} \right) \\ & + \frac{W_2}{M^2} \left[ P_\mu - \frac{(P \cdot q) q_\mu}{q^2} \right] \left[ P_\nu - \frac{(P \cdot q) q_\nu}{q^2} \right],\end{aligned}$$

with the total photon nucleon cross section given by

$$\sigma_\lambda(\gamma^* N) = \frac{4\pi^2 \alpha}{\sqrt{\nu^2 + Q^2}} \epsilon_\mu(\lambda) \epsilon_\nu^*(\lambda) W_{\mu\nu},$$

where  $\lambda$  is the photon helicity, show that the transverse cross section,

$$\sigma_T(\gamma^* N) = \frac{1}{2} [\sigma_{\lambda=+1}(\gamma^* N) + \sigma_{\lambda=-1}(\gamma^* N)],$$

is given by

$$\sigma_T(\gamma^* N) = \frac{4\pi^2 \alpha}{\sqrt{\nu^2 + Q^2}} W_1,$$

and the longitudinal cross section is given by

$$\sigma_L(\gamma^* N) = \frac{4\pi^2 \alpha}{\sqrt{\nu^2 + Q^2}} \left\{ -W_1 + \left( 1 + \frac{\nu^2}{Q^2} \right) W_2 \right\},$$

where  $Q^2 = -q^2 > 0$  and  $\nu = (P \cdot q)/M$ .

4.2. Verify that by setting

$$\epsilon_\mu(\lambda = 0) = \frac{Q}{M\sqrt{\nu^2 + Q^2}} \left( P_\mu - \frac{P \cdot q}{q^2} q_\mu \right),$$

and substituting into (4.2.16) one projects out the longitudinal cross section

$$\sigma_L(\gamma^* N) = \frac{4\pi^2 \alpha}{\sqrt{\nu^2 + Q^2}} \left\{ -W_1 + \left( 1 + \frac{\nu^2}{Q^2} \right) W_2 \right\}.$$

- 4.3. Using (4.2.3) for the leptonic tensor  $L_{\mu\nu}$  and (4.2.6) for the hadronic tensor  $W_{\mu\nu}$  compute  $L_{\mu\nu}W_{\mu\nu}$  and verify (4.2.13).

- 4.4. Show that for massless partons that the differential cross sections for the “Compton” subprocess  $\gamma_\Sigma^* + q \rightarrow q + g$  in Fig. 4.4 and the “annihilation” subprocess  $\gamma_\Sigma^* + g \rightarrow q + \bar{q}$  in Fig. 4.5 are given by

$$\frac{d\hat{\sigma}_\Sigma^q}{d\hat{t}}(\hat{s}, \hat{t}) = \frac{\pi\alpha\alpha_s e_q^2 z^2}{Q^4} \frac{16}{3} \left\{ \frac{\hat{s}^2 + \hat{t}^2 - 2Q^2\hat{u}}{-\hat{s}\hat{t}} \right\},$$

and

$$\frac{d\hat{\sigma}_\Sigma^g}{d\hat{t}}(\hat{s}, \hat{t}) = \frac{\pi\alpha\alpha_s e_q^2 z^2}{Q^4} 2 \left\{ \frac{\hat{t}^2 + \hat{u}^2 - 2Q^2\hat{s}}{\hat{t}\hat{u}} \right\},$$

respectively, where  $z = Q^2/(\hat{s} + Q^2)$ ,  $q_\gamma^2 = -Q^2$ , and  $\hat{s} + \hat{t} + \hat{u} = -Q^2$ .

- 4.5. Show that the differential cross sections for the “Compton” subprocess  $\gamma_\Sigma^* + q \rightarrow q + g$  in Fig. 4.4 is given by

$$\begin{aligned} \frac{d\hat{\sigma}_\Sigma^q}{d\hat{t}}(\hat{s}, \hat{t}) &= \frac{\pi\alpha\alpha_s e_q^2 z^2}{Q^4} \frac{16}{3} \left\{ \frac{\hat{s}^2 + \hat{t}^2 - 2(Q^2 - m_g^2)\hat{u}}{-\hat{s}\hat{t}} \right. \\ &\quad \left. - m_g^2 Q^2 \left( \frac{1}{\hat{t}^2} + \frac{1}{\hat{s}^2} \right) \right\}, \end{aligned}$$

where  $q_\gamma^2 = -Q^2$ ,  $q_g^2 = m_g^2$ , and  $\hat{s} + \hat{t} + \hat{u} = m_g^2 - Q^2$ . Show that in this case the minimum and maximum values of  $\hat{t}$  are given by

$$\begin{aligned} \hat{t}_{\min} &= -\beta z Q^2 / (1-z), \\ \hat{t}_{\max} &= \beta Q^2 - Q^2/z, \end{aligned}$$

where  $\beta = m_g^2/Q^2$ .

- 4.6. Integrate  $d\hat{\sigma}_\Sigma^q/d\hat{t}$  given in (4.4.1) over  $\hat{t}$  and show that

$$\begin{aligned} \hat{\sigma}_{MG,\Sigma}^q(z, Q^2) &= \int_{-Q^2/z}^{-m_g^2 z/(1-z)} \frac{d\hat{\sigma}_\Sigma^q}{d\hat{t}} d\hat{t} = \\ &= \frac{\pi\alpha\alpha_s e_q^2 z}{Q^2} \frac{16}{3} \left\{ \frac{1+z^2}{1-z} \log\left(\frac{(1-z)Q^2}{z^2 m_g^2}\right) \right. \\ &\quad \left. - \frac{3}{2} \frac{1}{1-z} + z + 1 + \frac{5}{4} \delta(1-z) \right\}, \end{aligned}$$

where some terms that vanish in the limit  $m_g \rightarrow 0$  have been dropped and  $z = Q^2/(\hat{s} + Q^2)$ .

- 4.7. Integrate  $d\hat{\sigma}_{MG,\Sigma}^q/dz$  given in (4.4.16) over  $z$ ,

$$\hat{\sigma}(\text{real}) = \int_0^{1/(1+\beta)} \frac{d\hat{\sigma}_\Sigma^q}{dz} dz,$$

and show that

$$(\hat{\sigma}_{MG}(\text{real}))_{DIS} = \frac{2\alpha_s}{3\pi} \sigma_0 \left\{ \log^2(\beta) + 3\log(\beta) + \frac{2\pi^2}{3} + 2 \right\}.$$

Add the virtual gluon cross section given in (4.4.20) and show that

$$\sigma_{\text{tot}}^{\text{DIS}} = \sigma_0 \left( 1 - \frac{\alpha_s}{\pi} + \dots \right).$$

- 4.8. Prove that in the limit of massless partons that the leading order longitudinal cross section  $\hat{\sigma}_L(\gamma^* q \rightarrow q)$  vanishes.

- 4.9. Show that

$$(p_q)_\mu (p_q)_\nu |\overline{\mathcal{M}}(\gamma^* + q \rightarrow q + g)|_{\mu\nu}^2 = 16\pi^2\alpha\alpha_s e_q^2 \frac{8}{3}(Q^2 + \hat{t} + \hat{s}),$$

and that

$$\begin{aligned} \sigma_L^q(z, Q^2) &= \frac{\pi\alpha\alpha_s e_q^2 z^2}{Q^4} \frac{4z^2}{Q^2} \frac{8}{3} \int_{-Q^2/z}^0 (Q^2 + \hat{t} + \hat{s}) d\hat{t} \\ &= \pi\alpha\alpha_s e_q^2 \left( \frac{4z^2}{Q^2} \right) \left( \frac{4}{3} \right), \end{aligned}$$

where  $z = Q^2/(\hat{s} + Q^2)$ . Verify that  $\mathcal{F}_L^q(x, Q^2)$  is given by (4.4.40) with

$$\alpha_s f_L^{q,DIS}(z) = \frac{2\alpha_s}{3\pi} 2z.$$

- 4.10. Show that the differential cross sections for the “annihilation” subprocess  $\gamma_\Sigma^* + g \rightarrow q + \bar{q}$  in Fig. 4.5 is given by

$$\begin{aligned} \frac{d\hat{\sigma}_\Sigma^g}{d\hat{t}}(\hat{s}, \hat{t}) &= \frac{\pi\alpha\alpha_s e_q^2 z^2}{Q^4} 2 \left\{ \frac{\hat{t}^2 + \hat{u}^2 - 2(Q^2 + m_g^2)\hat{s}}{\hat{t}\hat{u}} \right. \\ &\quad \left. - m_g^2 Q^2 \left( \frac{1}{\hat{t}^2} + \frac{1}{\hat{u}^2} \right) \right\}, \end{aligned}$$

where  $q_\gamma^2 = -Q^2$ ,  $q_g^2 = -m_g^2$ , and  $\hat{s} + \hat{t} + \hat{u} = -m_g^2 - Q^2$ . Show that in this case the minimum and maximum values of  $\hat{t}$  are given by

$$\begin{aligned} \hat{t}_{\min} &= -m_g^2 z, \\ \hat{t}_{\max} &= -Q^2/z. \end{aligned}$$

- 4.11. Integrate  $d\hat{\sigma}_\Sigma^g/d\hat{t}$  in (4.4.47) over  $\hat{t}$  and show that

$$\begin{aligned} \hat{\sigma}_{MG,\Sigma}^g(z, Q^2) &= \int_{-Q^2/z}^{-m_g^2 z} \frac{d\hat{\sigma}_\Sigma^g}{d\hat{t}} d\hat{t} \\ &= \frac{\pi\alpha\alpha_s e_q^2 z}{Q^2} 4 \left\{ (z^2 + (1-z)^2) \log\left(\frac{Q^2}{z^2 m_g^2}\right) - 2 \right\}, \end{aligned}$$

where some terms that vanish in the limit  $m_g \rightarrow 0$  have been dropped. Using (4.4.15) show that

$$\left( \frac{1}{\sigma_0} \frac{d\sigma_{MG}^g}{dz} \right)_{DIS} = 2 \frac{\alpha_s}{2\pi} P_{g \rightarrow q\bar{q}}(z) \log(Q^2/m_g^2) + 2\alpha_s f_{MG,\Sigma}^{g,DIS}(z),$$

where

$$P_{g \rightarrow q\bar{q}}(z) = \frac{1}{2}(z^2 + (1-z)^2),$$

and

$$\alpha_s f_{MG,\Sigma}^{g,DIS}(z) = -\frac{\alpha_s}{2\pi} [(z^2 + (1-z)^2) \log(z) + 1].$$

4.12. Show that

$$(p_g)_\mu (p_g)_\nu |\overline{\mathcal{M}}(\gamma^* + g \rightarrow q + \bar{q})|_{\mu\nu}^2 = 16\pi^2 \alpha \alpha_s e_q^2 2\hat{s},$$

and that

$$\begin{aligned} \sigma_L^g(z, Q^2) &= \frac{\pi \alpha \alpha_s e_q^2 z^2}{Q^4} \frac{4z^2}{Q^2} \int_{-Q^2/z}^0 2\hat{s} d\hat{t} \\ &= \pi \alpha \alpha_s e_q^2 \left( \frac{4z^2}{Q^2} \right) 2(1-z), \end{aligned}$$

where  $z = Q^2/(\hat{s} + Q^2)$ . Verify that  $\mathcal{F}_L^g(x, Q^2)$  is given by (4.4.63) with

$$\alpha_s f_L^{g,DIS}(z) = \frac{2\alpha_s}{3\pi} 2z(1-z).$$

4.13. Starting from the 2-to-2 cross section  $(1+2 \rightarrow 3+4)$  in  $N$  spacetime dimensions,

$$\begin{aligned} d^{2N-2}R_2 &= \frac{d^{N-1}p_3}{(2\pi)^{N-1}(2E_3)} \\ &\quad \frac{d^{N-1}p_4}{(2\pi)^{N-1}(2E_4)} (2\pi)^N \delta^N(p_3 + p_4 - p_1 - p_2), \end{aligned}$$

show that

$$\hat{\sigma} = \frac{1}{32\pi\hat{s}} \frac{(\hat{p}'_{cm})^{1+\epsilon}}{\hat{p}_{cm}} \frac{1}{(4\pi)^{\epsilon/2} \Gamma(1+\frac{\epsilon}{2})} \int_{-1}^1 dy (1-y^2)^{\epsilon/2} |\overline{\mathcal{M}}|^2,$$

where  $\hat{p}_{cm}$  and  $\hat{p}'_{cm}$  are the initial and final state center-of-mass momentum, respectively, and  $N = 4 + \epsilon$ ,  $y = \cos(\theta_{13})$ , and

$$\hat{\sigma} = \int_{-1}^1 \frac{d\hat{\sigma}}{dy} dy.$$

4.14. Show that for massless partons in  $N$  spacetime dimensions the matrix elements squared for the “Compton” subprocess in Fig. 4.4 and the “annihilation” subprocess in Fig. 4.5 are given by

$$\begin{aligned} |\overline{\mathcal{M}}(\gamma_\Sigma^* + q \rightarrow q + g)| &= e_N^2 g_N^2 e_q^2 \frac{16}{3} \left( 1 + \frac{\epsilon}{2} \right) \\ &\quad \left\{ \frac{\hat{s}^2 + \hat{t}^2 - 2Q^2\hat{u}}{-\hat{s}\hat{t}} + \frac{\epsilon}{2} \frac{(Q^2 + \hat{u})^2}{-\hat{s}\hat{t}} \right\}, \end{aligned}$$

and

$$\begin{aligned} |\overline{\mathcal{M}}(\gamma_\Sigma^* + g \rightarrow g + \bar{q})| &= e_N^2 g_N^2 e_q^2 2 \left( 1 + \frac{\epsilon}{2} \right) \\ &\quad \left\{ \frac{\hat{t}^2 + \hat{u}^2 - 2Q^2\hat{s}}{\hat{t}\hat{u}} + \frac{\epsilon}{2} \frac{(Q^2 + \hat{s})^2}{\hat{t}\hat{u}} \right\}, \end{aligned}$$

respectively, where  $N = 4 + \epsilon$ ,  $q_\gamma^2 = -Q^2$ , and  $\hat{s} + \hat{t} + \hat{u} = -Q^2$ .

4.15. Using (4.5.18) show that

$$\begin{aligned} \int_{-1}^1 (1-y^2)^{\epsilon/2} \frac{1}{1-y} dy &= \int_{-1}^1 (1-y^2)^{\epsilon/2} \frac{1}{1-y^2} dy = \frac{2}{\epsilon} f_y, \\ \int_{-1}^1 (1-y^2)^{\epsilon/2} \frac{y^2}{1-y} dy &= \int_{-1}^1 (1-y^2)^{\epsilon/2} \frac{y^2}{1-y^2} dy = \frac{2}{\epsilon(1+\epsilon)} f_y, \end{aligned}$$

and that

$$\begin{aligned} \int_{-1}^1 (1-y^2)^{\epsilon/2} \frac{y}{1-y} dy &= \frac{2}{\epsilon(1+\epsilon)} f_y, \\ \int_{-1}^1 (1-y^2)^{\epsilon/2} \frac{y}{1-y^2} dy &= 0, \end{aligned}$$

where

$$f_y = \frac{2^\epsilon \Gamma^2(1+\frac{\epsilon}{2})}{\Gamma(1+\epsilon)}.$$

4.16. Using (E.1.12) show that

$$\begin{aligned} \int_0^1 (1-z)^{\epsilon/2} z^{-\epsilon/2} \frac{1}{1-z} dz &= \frac{2}{\epsilon} f_z, \\ \int_0^1 (1-z)^{\epsilon/2} z^{-\epsilon/2} \frac{z}{1-z} dz &= \left( \frac{2}{\epsilon} - 1 \right) f_z, \\ \int_0^1 (1-z)^{\epsilon/2} z^{-\epsilon/2} \frac{z^2}{1-z} dz &= \left( \frac{2}{\epsilon} - \frac{3}{2} + \frac{1}{4}\epsilon \right) f_z, \end{aligned}$$

where

$$f_z = \Gamma\left(1 - \frac{\epsilon}{2}\right) \Gamma\left(1 + \frac{\epsilon}{2}\right).$$

- 4.17. Show that for massless partons in  $N$  spacetime dimensions the matrix elements squared for the “Compton” subprocess in Fig. 4.4 is given by

$$|\bar{\mathcal{M}}(\gamma_\Sigma^* + q \rightarrow q + g)| = 16\pi^2 \alpha_N^{QED} \alpha_N^{QCD} e_q^2 \frac{16}{3} \left(1 + \frac{\epsilon}{2}\right) \left\{ \frac{1}{2} \frac{4z^2 - 4z + 4yz + y^2 + 2y + 5}{(1-z)(1-y)} + \frac{\epsilon}{4} \frac{(2z-1+y)^2}{(1-z)(1-y)} \right\},$$

where  $N = 4 + \epsilon$ , and

$$\begin{aligned} \hat{s} &= (1-z)Q^2/z, \\ \hat{t} &= -\frac{Q^2}{2z}(1-y), \\ \hat{u} &= -\frac{Q^2}{2z}(1+y), \end{aligned}$$

with  $\hat{s} + \hat{t} + \hat{u} = -Q^2$ . Verify that

$$I = \int_{-1}^1 dy (1-y^2)^{\epsilon/2} |\bar{\mathcal{M}}|^2 = 16\pi^2 \alpha_N^{QED} \alpha_N^{QCD} e_q^2 \frac{16}{3} \left(1 + \frac{\epsilon}{2}\right) \frac{2^\epsilon \Gamma^2(1+\frac{\epsilon}{2})}{\Gamma(1+\epsilon)} \left\{ \frac{1+z^2}{1-z} \frac{4}{\epsilon} - \frac{3}{1-z} - 2z + 6 + \dots \right\}.$$

Using (4.4.15) and (4.5.15) show that

$$\left( \frac{1}{\sigma_0} \frac{d\hat{\sigma}_{DR}^q}{dz} \right)_{DIS} = \frac{2\alpha_s}{3\pi} \left( \frac{(1-z)Q^2}{z4\pi m_D^2} \right)^{\epsilon/2} \frac{\Gamma(1+\frac{\epsilon}{2})}{\Gamma(1+\epsilon)} \left\{ \frac{1+z^2}{1-z} \frac{2}{\epsilon} - \frac{3}{2} \frac{1}{1-z} - z + 3 + \dots \right\}.$$

Integrate this over  $z$  and show that

$$(\hat{\sigma}_{DR}(\text{real}))_{DIS} = \int_0^1 \left( \frac{d\hat{\sigma}_{DR}^q}{dz} \right)_{DIS} dz = \frac{2\alpha_s}{3\pi} \sigma_0 \left( \frac{Q^2}{4\pi m_D^2} \right)^{\epsilon/2} \frac{2^\epsilon \Gamma^2(1+\frac{\epsilon}{2})}{\Gamma(1+\epsilon)} \left\{ \frac{8}{\epsilon^2} - \frac{6}{\epsilon} + \frac{13}{2} + \dots \right\}.$$

Combine this with the virtual corrections in (4.5.27) and verify that

$$(\hat{\sigma}_{DR}(\text{real}) + \hat{\sigma}_{DR}(\text{virtual}))_{DIS} = -\frac{\alpha_s}{\pi} \sigma_0.$$

- 4.18. Using (4.5.22) show that

$$\frac{1}{\sigma_0} \left( \frac{d\hat{\sigma}_{DR,\Sigma}^q}{dz} \right)_+ = \frac{\alpha_s}{2\pi} P_{q \rightarrow gg}(z) \log(Q^2/m_D^2) + \alpha_s f_{DR,\Sigma}^{q,DIS}(z),$$

where

$$P_{q \rightarrow gg}(z) = \frac{4}{3} \left( \frac{1+z^2}{1-z} \right)_+,$$

and

$$\begin{aligned} \alpha_s f_{DR,\Sigma}^{q,DIS}(z) = & \frac{2\alpha_s}{2\pi} \left\{ (1+z^2) \left( \frac{\log(1-z)}{1-z} \right)_+ - \frac{1+z^2}{1-z} \log(z) \right. \\ & - \frac{3}{2} \frac{1}{(1-z)_+} - z + 3 - \left( \frac{\pi^2}{3} + 3 \right) \delta(1-z) \Big\} \\ & + \frac{\alpha_s}{2\pi} P_{q \rightarrow gg}(z) \left\{ \frac{2}{\epsilon} + \gamma_\epsilon - \log(4\pi) \right\}. \end{aligned}$$

Verify that

$$\int_0^1 \alpha_s f_{DR,\Sigma}^{q,DIS}(z) dz = 0.$$

- 4.19. Show that for massless partons in  $N$  spacetime dimensions the matrix elements squared for the “annihilation” subprocess in Fig. 4.5 is given by

$$|\bar{\mathcal{M}}(\gamma_\Sigma^* + g \rightarrow q + \bar{q})| = 16\pi^2 \alpha_N^{QED} \alpha_N^{QCD} e_q^2 2 \left(1 + \frac{\epsilon}{2}\right) \left\{ \frac{(1-y)^2 + (1+y)^2 - 8z(1-z)}{(1-y^2)} + \frac{\epsilon}{2} \frac{4}{(1-y^2)} \right\},$$

where  $N = 4 + \epsilon$ , and

$$\begin{aligned} \hat{s} &= (1-z)Q^2/z, \\ \hat{t} &= -\frac{Q^2}{2z}(1-y), \\ \hat{u} &= -\frac{Q^2}{2z}(1+y), \end{aligned}$$

with  $\hat{s} + \hat{t} + \hat{u} = -Q^2$ . Verify that

$$I = \int_{-1}^1 dy (1-y^2)^{\epsilon/2} |\bar{\mathcal{M}}|^2 = 16\pi^2 \alpha_N^{QED} \alpha_N^{QCD} e_q^2 2 \left(1 + \frac{\epsilon}{2}\right) \frac{2^\epsilon \Gamma^2(1+\frac{\epsilon}{2})}{\Gamma(1+\epsilon)} \left\{ 4(z^2 + (1-z)^2) \frac{2}{\epsilon} + \frac{4\epsilon}{1+\epsilon} \right\}.$$

Using (4.4.15) and (4.5.15) show that

$$\left( \frac{1}{\sigma_0} \frac{d\hat{\sigma}_{DR}^q}{dz} \right)_{DIS} = 2 \frac{2\alpha_s}{3\pi} \left( \frac{(1-z)Q^2}{z4\pi m_D^2} \right)^{\epsilon/2} \frac{\Gamma(1+\frac{\epsilon}{2})}{\Gamma(1+\epsilon)} \left\{ \frac{1}{2} (z^2 + (1-z)^2) \frac{2}{\epsilon} + \frac{1}{2} \frac{\epsilon}{1+\epsilon} \right\}.$$

Expand this in powers of  $\epsilon$  and show that

$$\left( \frac{1}{\sigma_0} \frac{d\hat{\sigma}_{DR}^g}{dz} \right)_{DIS} = 2 \frac{\alpha_s}{2\pi} P_{q \rightarrow gg}(z) \log(Q^2/m_D^2) + 2\alpha_s f_{DR,\Sigma}^{g,DIS}(z),$$

where

$$P_{q \rightarrow gg}(z) = \frac{1}{2}(z^2 + (1-z)^2),$$

and

$$\begin{aligned} \alpha_s f_{DR,\Sigma}^{g,DIS}(z) = & \frac{\alpha_s}{2\pi} \left\{ \frac{1}{2}(z^2 + (1-z)^2) \log\left(\frac{1-z}{z}\right) \right\} \\ & + \frac{\alpha_s}{2\pi} P_{g \rightarrow gg}(z) \left\{ \frac{2}{\epsilon} + \gamma_e - \log(4\pi) \right\}. \end{aligned}$$

4.20. Verify that

$$\int_0^1 P_{q \rightarrow gg}(z) dz = 0,$$

$$\int_0^1 z(P_{q \rightarrow gg}(z) + P_{g \rightarrow gg}(z)) dz = 0,$$

$$\int_0^1 z(2n_f P_{g \rightarrow q\bar{q}}(z) + P_{g \rightarrow gg}(z)) dz = 0,$$

and show that these relationships insure that

$$\frac{dN_q}{d\tau} = 0,$$

and

$$\frac{d}{d\tau}(Q + \bar{Q} + G) = 0,$$

where  $\tau = \log(Q^2/\Lambda^2)$  and

$$N_q = \int_0^1 (G_{p \rightarrow q}(x, Q^2) - G_{p \rightarrow \bar{q}}(x, Q^2)) dx,$$

is the net number of quarks of flavor  $q_i$  within the proton and  $Q$ ,  $\bar{Q}$ , and  $G$  are the total proton momentum fractions carried by quarks, antiquarks and gluons, respectively.

4.21. Verify that

$$A_n^{NS} = \int_0^1 z^{n-1} P_{q \rightarrow gg}(z) dz = \frac{4}{3} \left[ -\frac{1}{2} + \frac{1}{n(n+1)} - 2 \sum_{j=2}^n \frac{1}{j} \right],$$

$$A_n^{gq} = \int_0^1 z^{n-1} P_{q \rightarrow gg}(z) dz = \frac{4}{3} \frac{2+n+n^2}{n(n^2-1)},$$

$$A_n^{q\bar{q}} = \int_0^1 z^{n-1} P_{g \rightarrow q\bar{q}}(z) dz = \frac{1}{2} \frac{2+n+n^2}{n(n+1)(n+2)},$$

and

$$\begin{aligned} A_n^{gg} = & \int_0^1 z^{n-1} P_{g \rightarrow gg}(z) dz = \\ & 3 \left[ -\frac{1}{6} + \frac{2}{n(n-1)} + \frac{2}{(n+1)(n+2)} - 2 \sum_{j=2}^n \frac{1}{j} - \frac{1}{9} n_f \right]. \end{aligned}$$

4.22. Show that regardless of the total fraction of the protons momentum carried by quarks,  $Q(Q_0^2)$ , antiquarks,  $\bar{Q}(Q_0^2)$ , and gluons,  $G(Q_0^2)$ , at the reference momentum,  $Q_0$ , that the following is true asymptotically

$$Q(Q^2) \xrightarrow{Q^2 \rightarrow \infty} \frac{3}{2} \frac{n_f}{(16+3n_f)},$$

$$\bar{Q}(Q^2) \xrightarrow{Q^2 \rightarrow \infty} \frac{3}{2} \frac{n_f}{(16+3n_f)},$$

$$G(Q^2) \xrightarrow{Q^2 \rightarrow \infty} \frac{16}{(16+3n_f)},$$

where  $n_f$  is the number of quark flavors and the momentum fractions are normalized so that

$$Q(Q_0^2) + \bar{Q}(Q_0^2) + G(Q_0^2) = 1.$$

4.23. Using the leading order  $Q^2$  evolution equations plot  $\log(M_n^{NS}(Q^2))$  versus  $\log(M_\ell^{NS}(Q^2))$  for  $n = 2, 3, 4$  and  $\ell = 2, 3, 4$ . Also plot  $[M_n^{NS}(Q^2)]^{-1/\alpha_s^{NS}}$  versus  $\log(Q^2)$  for  $n = 2, 3, 4$  with  $\Lambda = 200$  MeV and  $Q_0 = 2$  GeV.

4.24. Verify that

$$\int_0^1 \alpha_s f_{2,MG}^{q,DIS}(z) dz = \int_0^1 \alpha_s f_{2,DR}^{q,DIS}(z) dz = 0,$$

where  $f_{2,MG}^{q,DIS}$  and  $f_{2,DR}^{q,DIS}$  are given by (4.4.45) and (4.5.33), respectively.

Show that this insures that

$$\int_0^1 [G_{p \rightarrow q}^{(2)}(x, Q^2) - G_{p \rightarrow \bar{q}}^{(2)}(x, Q^2)] dx = \\ \int_0^1 [\bar{G}_{p \rightarrow q}(x, Q^2) - \bar{G}_{p \rightarrow \bar{q}}(x, Q^2)] dx.$$

where

$$G_{p \rightarrow q}^{(2)}(x, Q^2) = \bar{G}_{p \rightarrow q}(Q^2) * (1 + \alpha_s f_2^{q, DIS}) \\ + \bar{G}_{p \rightarrow g}(Q^2) * (\alpha_s f_2^{g, DIS}),$$

and

$$G_{p \rightarrow \bar{q}}^{(2)}(x, Q^2) = \bar{G}_{p \rightarrow \bar{q}}(Q^2) * (1 + \alpha_s f_2^{q, DIS}) \\ + \bar{G}_{p \rightarrow g}(Q^2) * (\alpha_s f_2^{g, DIS}).$$

- 4.25. Show that to order  $\alpha_s$ , the longitudinal structure function is given in terms of  $F_2(x, Q^2)$  and the gluon distribution  $G_{p \rightarrow g}(x, Q^2)$  by

$$F_L(x, Q^2) = \frac{\alpha_s(Q^2)}{2\pi} x^2 \int_x^1 \frac{dy}{y^3} \left\{ \frac{8}{3} F_2(y, Q^2) + 2ay G_{p \rightarrow g}(y, Q^2) \left( 1 - \frac{x}{y} \right) \right\},$$

where

$$a = a_e = 2 \sum_{i=1}^{n_f} e_{q_i}^2,$$

for deep inelastic electron scattering and

$$a = a_\nu = 8,$$

for deep inelastic neutrino and antineutrino scattering. Verify that

$$\bar{F}_L(Q^2) = \frac{\alpha_s}{2\pi} \left[ \frac{8}{9} \bar{F}_2(Q^2) + \frac{1}{6} a G(Q^2) \right],$$

where

$$\bar{F}_i(Q^2) = \int_0^1 F_i(x, Q^2) dx,$$

for  $i = 2, L$  and  $G(Q^2)$  is the total momentum carried by gluons.

#### Further Reading

G. Altarelli, "Partons in Quantum Chromodynamics," *Physics Reports* **81**, 1 (1982).

A. H. Mueller, *Physics Reports* **73**, 237 (1981).

W.B. Atwood, J.D. Bjorken, S.J. Brodsky, and R. Stroynowuri, "Lectures on Lepton Nucleon Scattering and Quantum Chromodynamics," ed. B. A.

Jaffe and D. Rueller, Birkhauser Boston Publishers, 1982.

A.J. Buras, *Rev. Mod. Phys.* **52**, 199 (1980).

Chris Quigg, *Gauge Theories of the Strong, Weak, and Electromagnetic Interactions*, Frontiers in Physics, The Benjamin-Cummings Publishing Company, Inc., 1983.

#### References

1. See, for example, Chris Quigg, *Gauge Theories of the Strong, Weak, and Electromagnetic Interactions*, Frontiers in Physics, The Benjamin-Cummings Publishing Company, Inc., 1983.
2. R.P. Feynman, *Photon-Hadron Interactions*, Benjamin, Reading, MA, 1972.
3. J. Dress, in Proceedings of the 1981 International Symposium on Leptons and Photon Interactions at High Energies, edited by W. Pfeil, Physikaliches Institut Universität Bonn, Bonn, 1981.
4. R.D. Field and R.P. Feynman, *Phys. Rev.* **D15**, 2590 (1977).
5. G. Altarelli, R.K. Ellis, and G. Martinelli, *Nucl. Phys.* **B143**, 521 (1978). *Erratum* **B146**, 544 (1978).
6. A.B. Carter and C.H. Llewellyn-Smith, *Nucl. Phys.* **B162**, 397 (1980).
7. G. Altarelli and G. Parisi, *Nucl. Phys.* **B126**, 278 (1977).
8. D. Duke and J. Owens, *Phys. Rev.* **D30**, 49 (1984).
9. D.J. Gross, *Phys. Rev. Lett.* **32**, 1071 (1974).
10. G. Altarelli and G. Martinelli, *Phys. Lett.* **76B**, 89 (1978).

CHAPTER 5

# Large-Mass Muon Pair Production in Hadron-Hadron Collisions



In 1970 Drell and Yan<sup>1</sup> developed a model for the production of massive lepton pairs in hadron-hadron collisions. In the model a quark from one of the incident hadrons annihilates with an antiquark in the other incident hadron producing a virtual photon which in turn “decays” into a massive lepton pair. In the previous chapter a spacelike virtual photon served as a probe of the structure of the proton. Here we use as a probe the timelike virtual photon that is produced and subsequently “decays” into a  $\mu^+ \mu^-$  pair. Here the role of the 4-momentum transfer squared,  $Q^2$ , of the scattered electrons in deep inelastic scattering is played by the mass squared of the muon pair,  $M^2$ . Large-mass muon pair production in hadron-hadron collision provides many interesting tests of perturbative QCD. In particular, QCD predicts sizable deviations from the naive parton model predictions both in the rate for muon pair production and in their transverse momentum spectrum.

## 5.1 The Naive Parton Model

In the naive parton model large mass muon pairs are produced in proton-proton collisions via the subprocess  $q + \bar{q} \rightarrow \gamma^* \rightarrow \mu^+ + \mu^-$ . The experimental cross section is expressed in terms of the parton subprocess as follows

$$d\sigma = G_{p \rightarrow q}(x_a) dx_a G_{p \rightarrow \bar{q}}(x_b) dx_b \hat{\sigma}(q + \bar{q} \rightarrow \gamma^* \rightarrow \mu^+ + \mu^-), \quad (5.1.1)$$

where  $G_{p \rightarrow q}(x_a) dx_a$  is the probability of finding a quark with momentum

$$p_q = x_a P_A, \quad (5.1.2)$$

and  $G_{p \rightarrow \bar{q}}(x_b) dx_b$  is the probability of finding an antiquark with momentum

$$p_{\bar{q}} = x_b P_B, \quad (5.1.3)$$

where  $P_A$  and  $P_B$  are the momentum of the initial two protons as shown in Fig. 5.1. It is convenient to define the dimensionless variables

$$\tau = M^2/s, \quad (5.1.4)$$

and

$$\hat{s} = M^2/\hat{s}, \quad (5.1.5)$$

where  $M$  is the mass of the muon pair and where  $s$  is the external proton-proton center-of-mass energy squared

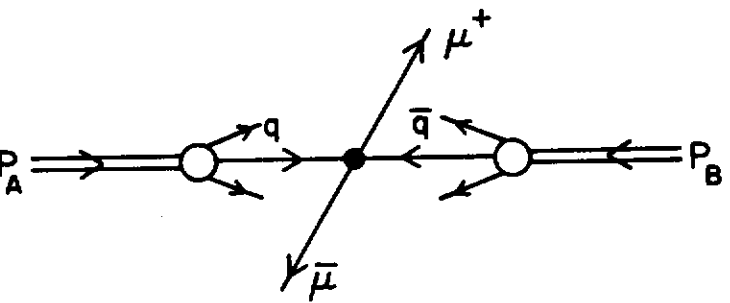
$$s = (P_A + P_B)^2 = 2P_{cm}^2, \quad (5.1.6)$$

$$P_{cm} = \frac{1}{2}\sqrt{s}, \quad (5.1.7)$$

and  $\hat{s}$  is the internal parton-parton center-of-mass energy squared

$$\hat{s} = (p_q + p_{\bar{q}})^2 = 2p_q \cdot p_{\bar{q}}. \quad (5.1.8)$$

$$(a) p + p \rightarrow \mu^+ \mu^- + X$$



$$(b) p + p \rightarrow \gamma^* + X$$

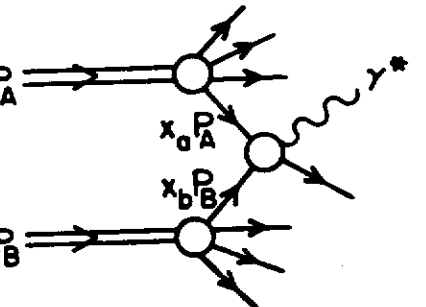


Figure 5.1 (a) Illustration of the collision of hadron A (momentum  $P_A$ ) with hadron B (momentum  $P_B$ ) producing a  $\mu^+ \mu^-$  pair via quark-antiquark annihilation. (b) The production of a virtual photon in proton-proton collisions,  $p + p \rightarrow \gamma^* + X$  is described in terms of a 2-to-2 parton subprocess in which one incoming parton has momentum  $x_a P_A$  and the other has momentum  $x_b P_B$ .

Equations (5.1.2) and (5.1.3) imply

$$\hat{s} = x_a x_b s, \quad (5.1.9)$$

or

$$\tau = x_a x_b \hat{\tau}. \quad (5.1.10)$$

The longitudinal momentum of the muon pair are

$$P_L = p_q - p_{\bar{q}}, \quad (5.1.11)$$

and, if we assume that the incoming partons are parallel to the incident protons then the total energy is

$$E^2 = P_L^2 + M^2, \quad (5.1.12)$$

since in this case the muon pair in Fig. 5.1a has no transverse momentum. Equation (5.1.11) implies

$$x_L = x_a - x_b, \quad (5.1.13)$$

where

$$x_L \equiv 2P_L/\sqrt{s}, \quad (5.1.14)$$

and (5.1.12) gives

$$x_E^2 = x_L^2 + 4\tau^2, \quad (5.1.15)$$

where

$$x_E \equiv 2E/\sqrt{s}. \quad (5.1.16)$$

The total cross section for a quark and anti-quark to annihilate into a muon pair,  $q + \bar{q} \rightarrow \mu^+ + \mu^-$  is given by

$$\hat{\sigma}(q + \bar{q} \rightarrow \mu^+ \mu^-) \equiv \sigma_0 = \frac{1}{3} \frac{4\pi\alpha^2 e_q^2}{3M^2}, \quad (5.1.17)$$

which is the same as the  $e^+ e^- \rightarrow \mu^+ \mu^-$  cross section computed in (2.1.14) except for the color factor  $1/3$  and the replacement  $Q^2 = M^2$ , where  $M$  is the virtual photon invariant mass with

$$\hat{s} = M^2, \quad (5.1.18)$$

or

$$\hat{\tau} = 1. \quad (5.1.19)$$

The color factor of  $1/3$  comes from our convention of averaging over initial state color. In this case there are three color states so the color factor is  $3(\frac{1}{3})(\frac{1}{3}) = \frac{1}{3}$ . From (5.1.10) and (5.1.13) we see that  $x_a$  and  $x_b$  are completely specified in terms of  $\tau$  and  $x_L$  according to

$$x_a x_b = \tau, \quad (5.1.20)$$

$$x_a - x_b = x_L, \quad (5.1.21)$$

and (5.1.1) gives

$$\frac{d\sigma_{DY}}{d\tau dx_L}(s, M^2, x_L) = \frac{4\pi\alpha^2}{9M^2} \frac{1}{(x_a + x_b)} P_{q\bar{q}}(x_a, x_b), \quad (5.1.22)$$

with the joint  $q\bar{q}$  probability function given by

$$P_{q\bar{q}}(x_a, x_b) = \sum_{i=1}^{n_f} e_{q_i}^2 [G_{p \rightarrow q_i}(x_a) G_{p \rightarrow \bar{q}_i}(x_b) + G_{p \rightarrow \bar{q}_i}(x_a) G_{p \rightarrow q_i}(x_b)], \quad (5.1.23)$$

where I have included  $n_f$  quark flavors and the interchanged term  $\bar{q}+q \rightarrow \mu^+ + \mu^-$ . The superscript  $DY$  refers to the "Drell-Yan" process  $p+p \rightarrow \mu^+ \mu^- + X$ . Equations (5.1.20) and (5.1.21) imply

$$x_a = \frac{1}{2}(x_E + x_L) = \sqrt{\tau} e^y, \quad (5.1.24)$$

$$x_b = \frac{1}{2}(x_E - x_L) = \sqrt{\tau} e^{-y}, \quad (5.1.25)$$

where  $x_E$  is given in (5.1.15) and  $y$  is the rapidity of the muon pair defined by

$$y \equiv \frac{1}{2} \log \left( \frac{E + p_L}{E - p_L} \right). \quad (5.1.26)$$

In this case,

$$y = \frac{1}{2} \log \left( \frac{x_a}{x_b} \right). \quad (5.1.27)$$

Furthermore, it is easy to verify that

$$\frac{d\sigma}{dy} = x_E \frac{d\sigma}{dx_E} = (x_a + x_b) \frac{d\sigma}{dx_L}, \quad (5.1.28)$$

so that, for example,

$$\frac{d\sigma_{DY}}{d\tau dy}(s, M^2, y) = \frac{4\pi\alpha^2}{9M^2} P_{q\bar{q}}(x_a, x_b). \quad (5.1.29)$$

Integrating (5.1.22) over  $x_L$  or (5.1.29) over  $y$  gives

$$\frac{d\sigma_{DY}}{d\tau}(s, M^2) = \frac{4\pi\alpha^2}{9M^2} \int_{\tau}^1 \frac{dx_a}{x_a} P_{q\bar{q}}(x_a, \tau/x_a), \quad (5.1.30)$$

where  $P_{q\bar{q}}(x_a, x_b)$  is given in (5.1.23). In general  $d\sigma_{DY}/d\tau$  is a function of both  $s$  and  $M^2$ , but (5.1.30) shows that in the naive parton model

$$M^2 \frac{d\sigma_{DY}}{d\tau}(s, M^2) = F(\tau), \quad (5.1.31)$$

is a function only of the dimensionless variable  $\tau = M^2/s$ .

## 5.2 Gluon Emission and Initial State Gluons

We now consider the possibility that the initial quark or antiquark can radiate

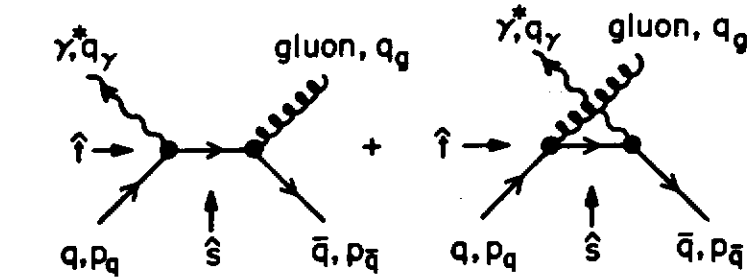


Figure 5.2 Leading order diagrams for the quark-antiquark "annihilation" subprocess  $q + \bar{q} \rightarrow \gamma^* + g$ .

a gluon before annihilating into a virtual photon as shown in Fig. 5.2. The differential cross section for the subprocess  $q + \bar{q} \rightarrow \gamma^* + g$  is

$$\begin{aligned} \frac{d\hat{\sigma}_{DY}^g}{dt}(\hat{s}, \hat{t}) &= \frac{1}{64\pi\hat{s}\hat{p}_{cm}^2} |\overline{\mathcal{M}}(q + \bar{q} \rightarrow \gamma^* + g)|^2 \\ &= \frac{1}{16\pi\hat{s}^2} |\overline{\mathcal{M}}(q + \bar{q} \rightarrow \gamma^* + g)|^2. \end{aligned} \quad (5.2.1)$$

In this case,

$$\hat{s} \hat{p}_{cm}^2 = \frac{1}{4}\hat{s}^2. \quad (5.2.2)$$

and the amplitude squared is given by

$$|\overline{\mathcal{M}}(q + \bar{q} \rightarrow \gamma^* + g)|^2 = e^2 e_g^2 g_s^2 \frac{4}{9} \frac{1}{4} \left[ \frac{\hat{u}}{\hat{t}} + \frac{\hat{t}}{\hat{u}} + \frac{2M^2(M^2 - \hat{t} - \hat{u})}{\hat{t}\hat{u}} \right], \quad (5.2.3)$$

where  $\frac{4}{9}$  is the color factor and  $\frac{1}{4}$  is the spin averaging factor. As before the subscript  $\Sigma$  refers to the use of (4.2.19) to sum the photon polarization states. Except for these color and spin factors this amplitude is the same as  $|\mathcal{M}(\gamma_\Sigma^* + g \rightarrow q + \bar{q})|^2$  in (4.3.21) with the replacement  $Q^2 \rightarrow -M^2$  since in this case the invariant mass of the virtual photon is timelike,

$$M^2 = q_\gamma^2, \quad (5.2.4)$$

rather than spacelike as in (4.3.9). In this case the invariants are given by

$$\hat{s} = (p_q + p_{\bar{q}})^2, \quad (5.2.5)$$

$$\hat{t} = (q_\gamma - p_q)^2, \quad (5.2.6)$$

$$\hat{u} = (p_{\bar{q}} - p_q)^2, \quad (5.2.7)$$

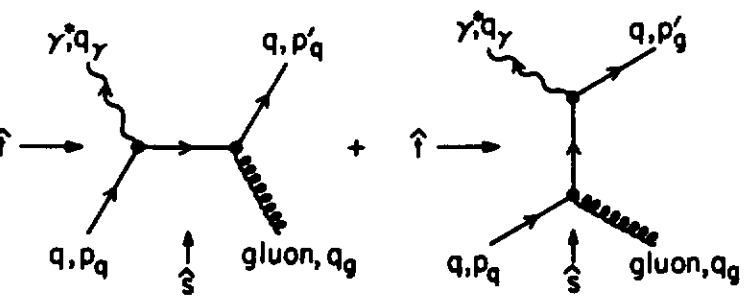


Figure 5.3 Leading order diagrams for the “Compton” subprocess  $q + g \rightarrow \gamma^* + q$ , where the 4-momenta are defined in Fig. 5.2 and where

$$\hat{s} + \hat{t} + \hat{u} = M^2. \quad (5.2.8)$$

Inserting (5.2.3) into (5.2.1) yields

$$\frac{d\hat{\sigma}_{DY}^q}{d\hat{t}}(\hat{s}, \hat{t}) = \frac{\pi\alpha\alpha_s e_q^2}{\hat{s}^2} \frac{8}{9} \left\{ \frac{\hat{u}}{\hat{t}} + \frac{\hat{t}}{\hat{u}} + \frac{2M^2(M^2 - \hat{t} - \hat{u})}{\hat{t}\hat{u}} \right\}, \quad (5.2.9)$$

where the superscript  $q$  refers to the “annihilation” process  $q + \bar{q} \rightarrow \gamma^* + g$  and the  $DY$  refers to the Drell-Yan production of muon pairs. The integral over  $\hat{t}$  is given by

$$\hat{\sigma}_{DY}^q(\hat{s}) = \int_{\hat{t}_{\min}}^{\hat{t}_{\max}} \frac{d\hat{\sigma}_{DY}^q}{d\hat{t}}(\hat{s}, \hat{t}) d\hat{t}, \quad (5.2.10)$$

where

$$\hat{t}_{\min} = 0, \quad (5.2.11)$$

and

$$\hat{t}_{\max} = M^2 - \hat{s} = -(1 - \hat{\tau})\hat{s}, \quad (5.2.12)$$

with  $\hat{\tau}$  defined in (5.1.5). This integral diverges for precisely the same reason as the deep inelastic scattering integral (4.3.22) and again we cannot proceed without a regularization scheme.

We must also correct the naive parton model by including the “Compton” subprocess  $q + g \rightarrow \gamma^* + q$  shown in Fig. 5.3. The differential cross section for this subprocess is

$$\frac{d\hat{\sigma}_{DY}^q}{d\hat{t}}(\hat{s}, \hat{t}) = \frac{1}{16\pi\hat{s}^2} |\overline{\mathcal{M}}(q + g \rightarrow \gamma^* + q)|^2, \quad (5.2.13)$$

with

$$|\overline{\mathcal{M}}(g + q \rightarrow \gamma^* + q)|^2 = e^2 e_q^2 g_s^2 \frac{4}{24} \frac{1}{4} \\ 8 \left\{ -\frac{\hat{t}}{\hat{s}} - \frac{\hat{s}}{\hat{t}} + \frac{2M^2(\hat{s} + \hat{t} - M^2)}{\hat{s}\hat{t}} \right\}, \quad (5.2.14)$$

which except for the color factor of  $4/24$  and the spin averaging factor  $1/4$  is the same as  $|\overline{\mathcal{M}}(\gamma_\Sigma^* + q \rightarrow q + g)|^2$  in (4.3.10) with the replacement  $Q^2 \rightarrow -M^2$ . The invariants in (5.2.14) are defined by

$$\hat{s} = (p_q + q_g)^2, \quad (5.2.15)$$

$$\hat{t} = (q_\gamma - p_q)^2, \quad (5.2.16)$$

$$\hat{u} = (q_\gamma - q_g)^2, \quad (5.2.17)$$

where  $M^2 = q_\gamma^2$  is the virtual photon mass squared. Substituting (5.2.14) into (5.2.13) gives

$$\frac{d\hat{\sigma}_{DY}^q}{d\hat{t}}(\hat{s}, \hat{t}) = \frac{\pi\alpha\alpha_s e_q^2}{\hat{s}^2} \frac{1}{3} \left\{ -\frac{\hat{t}}{\hat{s}} - \frac{\hat{s}}{\hat{t}} + \frac{2M^2(\hat{s} + \hat{t} - M^2)}{\hat{s}\hat{t}} \right\}, \quad (5.2.18)$$

and the integral

$$\hat{\sigma}_{DY}^q(\hat{s}) = \int_{\hat{t}_{\min}}^{\hat{t}_{\max}} \frac{d\hat{\sigma}_{DY}^q}{d\hat{t}}(\hat{s}, \hat{t}) d\hat{t}, \quad (5.2.19)$$

is again infinite with  $\hat{t}_{\min}$  given by (5.2.11) and we cannot proceed without a regularization scheme.

### 5.3 Order $\alpha_s$ Corrections – MG Scheme

We can regulate the divergences in the “annihilation” subprocess  $q + \bar{q} \rightarrow \gamma^* + g$  by giving the gluon a fictitious mass  $q_g^2 = m_g^2$  as we did for deep inelastic scattering in Chapter 4. The differential cross section in (5.2.9) becomes

$$\frac{d\hat{\sigma}_{DY}^q}{d\hat{t}}(\hat{s}, \hat{t}) = \frac{\pi\alpha\alpha_s e_q^2}{\hat{s}^2} \frac{8}{9} \left\{ \frac{\hat{u}}{\hat{t}} + \frac{\hat{t}}{\hat{u}} + \frac{2(M^2 + m_g^2)(M^2 + m_g^2 - \hat{u} - \hat{t})}{\hat{t}\hat{u}} \right. \\ \left. - M^2 m_g^2 \left( \frac{1}{\hat{t}^2} + \frac{1}{\hat{u}^2} \right) \right\}, \quad (5.3.1)$$

The integration of this over  $\hat{t}$  as defined in (5.2.10) is a bit more difficult than the other cases we have considered so far. One must be careful to keep the exact form for  $\hat{t}_{\min}$  and  $\hat{t}_{\max}$ . Namely,

$$\hat{t}_{\min,\max} = -\frac{M^2}{2\hat{\tau}} \left\{ (1 - \hat{\tau} - \beta\hat{\tau}) \mp [(1 - \hat{\tau})^2 + \beta\hat{\tau}(\beta\hat{\tau} - 2\hat{\tau} - 2)]^{\frac{1}{2}} \right\}, \quad (5.3.2)$$

with

$$\beta = m_g^2/M^2, \quad (5.3.3)$$

where  $\hat{\tau}$  is defined by (5.1.5). The result is

$$\hat{\sigma}_{DY}^q(\hat{\tau}) = \frac{\pi \alpha \alpha_s e_q^2}{\hat{s}} \frac{8}{9} \left\{ 2 \frac{1 + \hat{\tau}^2}{1 - \hat{\tau}} \log(\hat{t}_{\max}/\hat{t}_{\min}) - 4(1 - \hat{\tau}) \right\}, \quad (5.3.4)$$

where  $\hat{t}_{\max}$  and  $\hat{t}_{\min}$  are given by (5.3.2). In arriving at this result it is convenient to use the same trick as in (4.4.54). We write

$$\frac{1}{\hat{t}\hat{u}} = -\frac{1}{\hat{s}(1 - \hat{\tau})} \left( \frac{1}{\hat{t}} + \frac{1}{\hat{u}} \right), \quad (5.3.5)$$

so that

$$\frac{\hat{u}}{\hat{t}} + \frac{\hat{t}}{\hat{u}} + \frac{2M^2(M^2 - \hat{t} - \hat{u})}{\hat{t}\hat{u}} = \left( -\frac{\hat{s}}{\hat{t}} \frac{(1 + \hat{\tau}^2)}{(1 - \hat{\tau})} - 1 \right) + \left( -\frac{\hat{s}}{\hat{u}} \frac{(1 + \hat{\tau}^2)}{(1 - \hat{\tau})} - 1 \right). \quad (5.3.6)$$

Integrating the first term over  $\hat{t}$  and the second over  $\hat{u}$  gives

$$2 \int_{\hat{t}_{\min}}^{\hat{t}_{\max}} \left( -\frac{\hat{s}}{\hat{t}} \frac{(1 + \hat{\tau}^2)}{(1 - \hat{\tau})} - 1 \right) d\hat{t} = 2\hat{s} \left[ \frac{(1 + \hat{\tau}^2)}{(1 - \hat{\tau})} \log(\hat{t}_{\max}/\hat{t}_{\min}) - (1 - \hat{\tau}) \right]. \quad (5.3.7)$$

This parton subprocess must be “embedded” in the experimentally observed process  $p + p \rightarrow \mu^+ \mu^- + X$ , where  $M$  is the mass of the muon pair and  $s$  is the proton-proton center-of-mass energy squared as shown in Fig. 5.1b. Namely,

$$\sigma(s, M^2) = G_{p \rightarrow q}^{(0)}(x_a) dx_a G_{p \rightarrow \bar{q}}^{(0)}(x_b) dx_b \left( \frac{d\hat{\sigma}_{DY}^q}{d\hat{\tau}} \right) d\hat{\tau}, \quad (5.3.8)$$

where  $G_{p \rightarrow q}^{(0)}(x_a) dx_a$  is the probability of finding a quark with momentum

$$p_q = x_a P_A, \quad (5.3.9)$$

and  $G_{p \rightarrow \bar{q}}^{(0)}(x_b) dx_b$  is the probability of finding an antiquark with momentum

$$p_{\bar{q}} = x_b P_B, \quad (5.3.10)$$

with  $s$  and  $\hat{s}$  defined by (5.1.6) and (5.2.5), respectively, and as in (5.1.10)

$$\tau = M^2/s = x_a x_b \hat{\tau}. \quad (5.3.11)$$

The quantity  $(d\hat{\sigma}_{DY}^q/d\hat{\tau}) d\hat{\tau}$  is the probability that the two quarks will annihilate and produce a  $\mu^+ \mu^-$  pair with mass  $M$ . From (5.3.8) we have

$$\frac{d\sigma_{DY}^q}{d\tau}(s, M^2) = \int_{\tau}^1 \frac{dx_a}{x_a} \int_{\tau/x_a}^1 \frac{dx_b}{x_b} G_{p \rightarrow q}^{(0)}(x_a) G_{p \rightarrow \bar{q}}^{(0)}(x_b) \left( \frac{d\hat{\sigma}_{DY}^q}{d\hat{\tau}} \right), \quad (5.3.12)$$

where the  $q$  corresponds to the contribution from the “annihilation” subprocess and the limits of integration are determined from (5.3.11) using the fact that  $0 \leq \hat{\tau} \leq 1$ . The double differential cross section is related to  $d\hat{\sigma}/d\hat{\tau}$  by

$$\frac{d\hat{\sigma}_{DY}^q}{dM^2 d\hat{\tau}}(q + \bar{q} \rightarrow \mu^+ \mu^- + g) = \frac{\alpha}{3\pi M^2} \frac{d\hat{\sigma}_{DY}^q}{d\hat{\tau}}(q + \bar{q} \rightarrow \gamma^* + g), \quad (5.3.13)$$

where the factor of  $\alpha/(3\pi M^2)$  comes from integrating over the muon pair angular distribution. Integrating over  $\hat{\tau}$  yields

$$\frac{1}{\sigma_0} \frac{d\hat{\sigma}_{DY}^q}{d\hat{\tau}} = \left( \frac{3}{4\pi^2 \alpha e_q^2} \right) \hat{s} \hat{\sigma}_{DY}^q, \quad (5.3.14)$$

where  $\sigma_0$  is the parton model Born cross section given in (5.1.17). Comparing (5.3.13) and (5.3.4) we see that

$$\left( \frac{1}{\sigma_0} \frac{d\hat{\sigma}_{MG}^q}{d\hat{\tau}} \right)_{DY} = 2 \frac{2\alpha_s}{3\pi} \left\{ \frac{1 + \hat{\tau}^2}{1 - \hat{\tau}} \log \left( \frac{(1 - \hat{\tau})^2 M^2}{\hat{\tau}^2 m_g^2} \right) - 2(1 - \hat{\tau}) \right. \\ \left. + \left( 2 \log^2(2) - \frac{\pi^2}{6} \right) \delta(1 - \hat{\tau}) \right\}, \quad (5.3.15)$$

where the  $\delta$ -function term comes from the fact that

$$\int_0^{1-2\sqrt{\beta}} \frac{\log(\hat{t}_{\min}/\hat{t}_{\max})}{1 - \hat{\tau}} d\hat{\tau} = \frac{\pi^2}{12} - \log^2(2) \\ + \int_0^{1-2\sqrt{\beta}} \frac{\log(\beta \hat{\tau}^2/(1 - \hat{\tau})^2)}{1 - \hat{\tau}} d\hat{\tau}, \quad (5.3.16)$$

where  $\hat{t}_{\min}, \hat{t}_{\max}$  are given by (5.3.2). Integrating (5.3.15) over  $\hat{\tau}$  from  $\hat{t}_{\min} = 0$  to  $\hat{t}_{\max} = 1/(1 + \sqrt{\beta})^2 \approx 1 - 2\sqrt{\beta}$  gives

$$(\hat{\sigma}_{MG}(\text{real}))_{DY} = \frac{2\alpha_s}{3\pi} \sigma_0 \{ \log^2(\beta) + 3 \log(\beta) + \pi^2 \}. \quad (5.3.17)$$

The virtual corrections shown in Fig. 5.4 are the same as the  $e^+ e^-$  case in (2.7.3) but with  $Q^2 = q_\gamma^2 = M^2$  ( $q_\gamma^2$  timelike). Namely,

$$(\hat{\sigma}_{MG}(\text{virtual}))_{DY} = \frac{2\alpha_s}{3\pi} \sigma_0 \{ -\log^2(\beta) - 3 \log(\beta) \\ - \frac{7}{2} - \frac{2\pi^2}{3} + \pi^2 \}_{\text{timelike}}, \quad (5.3.18)$$

and as has been true in the other cases we have considered, the total

$$(\hat{\sigma}_{MG}(\text{real}) + \hat{\sigma}_{MG}(\text{virtual}))_{DY} \equiv \alpha_s I_q^{DY} \sigma_0 = \frac{2\alpha_s}{3\pi} \sigma_0 \left\{ \pi^2 - \frac{7}{2} - \frac{2\pi^2}{3} + \pi^2 \right\} \\ = \frac{2\sigma_0}{3\pi} \left\{ \frac{4\pi^2}{3} - \frac{7}{2} \right\}$$

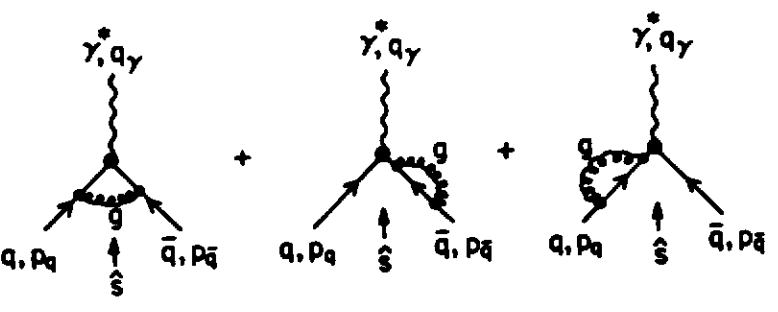


Figure 5.4 Virtual gluon corrections to the quark-antiquark annihilation Born term  $q + \bar{q} \rightarrow \gamma^*$ .

$$= \alpha_s \sigma_0 \left( \frac{8\pi}{9} - \frac{7}{3\pi} \right), \quad (5.3.19)$$

is finite and independent of  $\beta$  as  $\beta \rightarrow 0$ . This can be compared to the  $e^+e^-$  case in (2.7.6)

$$(\hat{\sigma}_{MG}(\text{real}) + \hat{\sigma}_{MG}(\text{virtual}))_{e^+e^-} \equiv \alpha_s I_q^{e^+e^-} \sigma_0 = \frac{\alpha_s}{\pi} \sigma_0, \quad (5.3.20)$$

and the deep inelastic scattering case in (4.4.21)

$$(\hat{\sigma}_{MG}(\text{real}) + \hat{\sigma}_{MG}(\text{virtual}))_{DIS} \equiv \alpha_s I_q^{DIS} \sigma_0 = -\frac{\alpha_s}{\pi} \sigma_0. \quad (5.3.21)$$

In the Drell-Yan case the perturbation series behaves like

$$\sigma_{\text{tot}}^{DY} = \sigma_0 (1 + \alpha_s I_q^{DY} + \dots), \quad (5.3.22)$$

with

$$\alpha_s I_q^{DY} = \alpha_s \left( \frac{8\pi}{9} - \frac{7}{3\pi} \right), \quad (5.3.23)$$

so that

$$\sigma_{\text{tot}}^{DY} = \sigma_0 \left\{ 1 + \left( \frac{8\pi}{9} - \frac{7}{3\pi} \right) \alpha_s + \dots \right\}, \quad (5.3.24)$$

or

$$\sigma_{\text{tot}}^{DY} = \sigma_0 (1 + 2.05 \alpha_s + \dots). \quad (5.3.25)$$

The order  $\alpha_s$  corrections to the Drell-Yan process are very large and positive<sup>2,3</sup>. The coefficient of the  $\alpha_s$  term is so large that one must worry about the contribution from the  $\alpha_s^2$  and higher order terms. Can we believe the first two terms in (5.3.24) adequately reproduces the sum for  $\alpha_s \approx 1/3$  or  $1/4$ ? For  $\alpha_s = 1/3$  the second term represents a 66% increase over the Born term!

Actually the situation is better than it looks. If we keep track of the  $\pi^2$  that comes from the analytic continuation from the spacelike (deep inelastic scattering) to the timelike (Drell-Yan) region of  $q^2$  we have

$$\begin{aligned} (\hat{\sigma}_{MG}(\text{real}) + \hat{\sigma}_{MG}(\text{virtual}))_{DY} &= \frac{2\alpha_s}{3\pi} \sigma_0 \left\{ \frac{\pi^2}{3} - \frac{7}{2} + \pi^2 \right\} \\ &= \alpha_s \sigma_0 \left\{ \frac{2\pi}{9} - \frac{7}{3\pi} + \frac{2\pi}{3} \right\}, \end{aligned} \quad (5.3.26)$$

where the third term comes from the analytic continuation of  $\log^2(q^2)$  in (2.7.4). The series is now

$$\sigma_{\text{tot}}^{DY} = \sigma_0 \left( 1 - 0.045 \alpha_s + \frac{2\pi}{3} \alpha_s + \dots \right), \quad (5.3.27)$$

and at least part of the series can be shown to exponentiate<sup>4,5</sup>. In Chapter 3 we saw that the leading double logarithms formed an exponential series as shown in (3.8.21). This means that the leading double logarithm in the expression for the virtual corrections in (5.3.18) exponentiates and hence the  $\pi^2$  term that come from the analytic continuation of  $\log^2(q^2)$  also exponentiates so that

$$\sigma_0 \left( 1 + \frac{2\pi}{3} \alpha_s + \dots \right) = \sigma_0 \exp \left( \frac{2\pi}{3} \alpha_s \right). \quad (5.3.28)$$

The series in (5.3.25) thus becomes

$$\begin{aligned} \sigma_{\text{tot}}^{DY} &= \sigma_0 \left\{ 1 + \left( \frac{2\pi}{9} - \frac{7}{3\pi} \right) \alpha_s + \frac{2\pi}{3} \alpha_s + \dots \right\} \\ &= \sigma_0 \exp \left( \frac{2\pi}{3} \alpha_s \right) \left\{ 1 + \left( \frac{2\pi}{9} - \frac{7}{3\pi} \right) \alpha_s + \dots \right\} \\ &= \sigma_0 \exp \left( \frac{2\pi}{3} \alpha_s \right) (1 - 0.045 \alpha_s + \dots), \end{aligned} \quad (5.3.29)$$

which appears to be a well behaved perturbation series. For  $\alpha_s = 1/3$  it becomes

$$\begin{aligned} \sigma_{\text{tot}}^{DY} &= \sigma_0 \exp(0.698) (1 - 0.015 + \dots) \\ &\approx 1.98 \sigma_0, \end{aligned} \quad (5.3.30)$$

and is about a factor of 2 greater than the parton model Born term.

Now that we have determined the integral over  $\hat{\tau}$  we know that at order  $\alpha_s$ ,

$$\int_0^1 \left\{ \frac{d\hat{\sigma}_{MG}^q}{d\hat{\tau}} + (\hat{\sigma}_{MG}(\text{virtual}) - \sigma_0 \alpha_s I_q^{DY}) \delta(1 - \hat{\tau}) \right\} d\hat{\tau} = 0, \quad (5.3.31)$$

where  $I_q^{DY}$  is given by (5.3.23) and we can now define “+ functions” just as we did in Chapter 3 and in Chapter 4. Namely,

$$\frac{1}{\sigma_0} \left( \frac{d\hat{\sigma}_{MG,DY}^q}{d\hat{t}} \right)_+ = 2 \frac{\alpha_s}{2\pi} P_{q \rightarrow qg}(\hat{t}) \log(M^2/m_g^2) + \alpha_s f_{MG}^{q,DY}(\hat{t}), \quad (5.3.32)$$

where

$$P_{q \rightarrow qg}(\hat{t}) = \frac{4}{3} \left( \frac{1+\hat{t}^2}{1-\hat{t}} \right)_+, \quad (5.3.33)$$

is the same function as (4.4.31) and

$$\begin{aligned} \alpha_s f_{MG}^{q,DY}(\hat{t}) &= \frac{2\alpha_s}{3\pi} \left\{ 2(1+\hat{t}^2) \left( \frac{\log(1-\hat{t})}{1-\hat{t}} \right)_+ \right. \\ &\quad \left. - 2 \left( \frac{1+\hat{t}^2}{1-\hat{t}} \right) \log(\hat{t}) - 2(1-\hat{t}) - \frac{2\pi^2}{3} \delta(1-\hat{t}) \right\}, \end{aligned} \quad (5.3.34)$$

where

$$\int_0^1 \alpha_s f_{MG}^{q,DY}(\hat{t}) d\hat{t} = 0, \quad (5.3.35)$$

is valid regardless of the scheme. We now write a new differential cross section that includes both real and virtual corrections

$$\frac{1}{\sigma_0} \frac{d\hat{\sigma}_{MG,DY}^q}{d\hat{t}} = \frac{1}{\sigma_0} \left( \frac{d\hat{\sigma}_{MG,DY}^q}{d\hat{t}} \right)_+ + \alpha_s I_q^{DY} \delta(1-\hat{t}), \quad (5.3.36)$$

and inserting this and the Born term into (5.3.12) yields

$$\begin{aligned} s \frac{d\sigma_{DY}^q}{dM^2}(s, M^2) &= \frac{4\pi \alpha^2 e_q^2}{9 M^2} \int_r^1 \frac{dx_a}{x_a} \int_{\tau/x_a}^1 \frac{dx_b}{x_b} G_{p \rightarrow q}^{(0)}(x_a) G_{p \rightarrow q}^{(0)}(x_b) \\ &\quad \left\{ (\sigma_{tot}^{DY}/\sigma_0) \delta(1-\hat{t}) + 2 \frac{\alpha_s}{2\pi} P_{q \rightarrow qg}(\hat{t}) \log(M^2/m_g^2) + 2\alpha_s f_{MG}^{q,DY}(\hat{t}) \right\}, \end{aligned} \quad (5.3.37)$$

where  $\hat{t} = \tau/(x_a x_b)$  and the superscript  $q$  refers to the contribution from the “annihilation” subprocess  $q + \bar{q} \rightarrow \gamma^* + g$ .

For the initial state gluon “Compton” subprocess,  $g + q \rightarrow \gamma^* + q$ , shown in Fig. 5.3 we regularize by taking the gluon off mass-shell  $q_g^2 = -m_g^2$  as we did in Chapter 4. The differential cross section in (5.2.18) becomes

$$\begin{aligned} \frac{d\hat{\sigma}_{DY}^g}{d\hat{t}}(\hat{s}, \hat{t}) &= \frac{\pi \alpha \alpha_s e_q^2}{\hat{s}^2} \frac{1}{3} \left\{ -\frac{\hat{t}}{\hat{s}} - \frac{\hat{s}}{\hat{t}} + \frac{2(M^2 - m_g^2)(\hat{s} + \hat{t} - M^2 + m_g^2)}{\hat{s}\hat{t}} \right. \\ &\quad \left. - M^2 m_g^2 \left( \frac{1}{\hat{s}^2} + \frac{1}{\hat{t}^2} \right) \right\}, \end{aligned} \quad (5.3.38)$$

In this case the limits of integration (5.2.19) become

$$\hat{t}_{min} = -\frac{M^2 m_g^2}{\hat{s}} = -m_g^2 \hat{t}, \quad (5.3.39)$$

$$\hat{t}_{max} = M^2 - \hat{s} = -M^2(1 - \hat{t})/\hat{t}, \quad (5.3.40)$$

and integration over  $\hat{t}$  yields,

$$\begin{aligned} \hat{\sigma}_{DY}^g(\hat{s}) &= \frac{\pi \alpha \alpha_s e_q^2}{\hat{s}^2} \frac{1}{3} \left\{ \left( \hat{s} + \frac{2M^4}{\hat{s}} - 2M^2 \right) \log \left( \frac{\hat{s}(\hat{s} - m^2)}{M^2 m_g^2} \right) \right. \\ &\quad \left. + \frac{1}{2} \frac{(\hat{s} - m^2)^2}{\hat{s}} + \frac{2M^2}{\hat{s}} (\hat{s} - m^2) - 1 \right\}, \end{aligned} \quad (5.3.41)$$

where I have used

$$\begin{aligned} \int_{\hat{t}_{max}}^{\hat{t}_{min}} d\hat{t} &= \hat{s} - M^2, & \int_{\hat{t}_{max}}^{\hat{t}_{min}} \hat{t} d\hat{t} &= -\frac{1}{2}(\hat{s} - m^2)^2, \\ \int_{\hat{t}_{max}}^{\hat{t}_{min}} \frac{d\hat{t}}{\hat{t}} &= \log(\hat{t}_{min}/\hat{t}_{max}) = -\log \left( \frac{(\hat{s} - M^2)\hat{t}}{M^2 m_g^2} \right), \\ m_g^2 \int_{\hat{t}_{max}}^{\hat{t}_{min}} \frac{dt}{\hat{t}^2} &= -\frac{\hat{s}}{M^2}. \end{aligned} \quad (5.3.42)$$

Changing variables to  $\hat{t} = M^2/\hat{s}$  and using the relationship in (5.3.14) gives

$$\left( \frac{1}{\sigma_0} \frac{d\hat{\sigma}_{MG}^q}{d\hat{t}} \right)_{DY} = \frac{\alpha_s}{2\pi} P_{g \rightarrow q\bar{q}}(\hat{t}) \log(M^2/m_g^2) + \alpha_s f_{MG}^{q,DY}(\hat{t}), \quad (5.3.43)$$

where

$$P_{g \rightarrow q\bar{q}}(\hat{t}) = \frac{1}{2}(\hat{t}^2 + (1-\hat{t})^2) \quad (5.3.44)$$

is the same function as in (4.4.52) and

$$\begin{aligned} \alpha_s f_{MG}^{q,DY}(\hat{t}) &= \frac{\alpha_s}{2\pi} \frac{1}{2} \left\{ (\hat{t}^2 + (1-\hat{t})^2) \log \left( \frac{1-\hat{t}}{\hat{t}^2} \right) \right. \\ &\quad \left. - \frac{1}{2} + \hat{t} - \frac{3}{2}\hat{t}^2 \right\}. \end{aligned} \quad (5.3.45)$$

Inserting (5.3.43) into (5.3.12) gives the gluon contribution to  $d\sigma/d\tau$ . Namely,

$$\begin{aligned} s \frac{d\sigma_{DY}^g}{dM^2}(s, M^2) &= \frac{4\pi \alpha^2 e_q^2}{9 M^2} \int_r^1 \frac{dx_a}{x_a} \int_{\tau/x_a}^1 \frac{dx_b}{x_b} G_{p \rightarrow g}^{(0)}(x_a) G_{p \rightarrow g}^{(0)}(x_b) \\ &\quad \left\{ \frac{\alpha_s}{2\pi} P_{g \rightarrow q\bar{q}}(\hat{t}) \log(M^2/m_g^2) + \alpha_s f_{MG}^{q,DY}(\hat{t}) \right\}, \end{aligned} \quad (5.3.46)$$

where  $\hat{t} = \tau/(x_a x_b)$ .

## 5.4 Order $\alpha_s$ Corrections – DR Scheme

We can regulate the divergences in the subprocesses  $q + \bar{q} \rightarrow \gamma^* + g$  and  $q + g \rightarrow \gamma^* + q$  using dimensional regularization. Starting with (4.5.9) and using the fact that, in this case,

$$\hat{p}_{cm} = \frac{1}{2}\sqrt{\hat{s}}, \quad (5.4.1)$$

$$\hat{p}'_{cm} = \frac{(\hat{s} - M^2)}{2\sqrt{\hat{s}}} = \frac{1}{2}(1 - \hat{\tau})\sqrt{\hat{s}}, \quad (5.4.2)$$

where  $\hat{\tau}$  is defined in (5.1.5), we arrive at

$$\hat{\sigma}_{DY}(\hat{\tau}) = \frac{(1 - \hat{\tau})}{32\pi\hat{s}} \left( \frac{M^2(1 - \hat{\tau})^2}{4\pi\hat{\tau}} \right)^{\epsilon/2} \frac{I}{2^\epsilon \Gamma(1 + \frac{\epsilon}{2})}, \quad (5.4.3)$$

where

$$I = \int_{-1}^1 dy (1 - y^2)^{\epsilon/2} |\mathcal{M}|^2, \quad (5.4.4)$$

with  $N = 4 + \epsilon$  and

$$\hat{t} = -\frac{1}{2}(\hat{s} - M^2)(1 - y) = -\frac{\hat{s}}{2}(1 - \hat{\tau})(1 - y), \quad (5.4.5)$$

$$\hat{u} = -\frac{1}{2}(\hat{s} - M^2)(1 + y) = -\frac{\hat{s}}{2}(1 - \hat{\tau})(1 + y). \quad (5.4.6)$$

In  $N = 4 + \epsilon$  dimensions the matrix element squared for the annihilation subprocess is given by

$$|\mathcal{M}(q + \bar{q} \rightarrow \gamma^* + g)|^2 = 16\pi^2 \alpha_N^{QED} \alpha_N^{QCD} e_q^2 \frac{8}{9} \left(1 + \frac{\epsilon}{2}\right) \left\{ \frac{2(\hat{\tau}^2 y^2 - 2\hat{\tau}y^2 + y^2 + \hat{\tau}^2 + 2\hat{\tau} + 1)}{(1 - \hat{\tau})^2(1 - y^2)} + \frac{2}{(1 - y^2)} \epsilon \right\}, \quad (5.4.7)$$

where  $\alpha_N^{QED}$  and  $\alpha_N^{QCD}$  are the  $N$ -dimensional couplings in (2.8.11) and (2.8.26), respectively. The integral  $I$  in (5.4.4) is evaluated using (4.5.18) with the result

$$\hat{\sigma}_{DY}^q(\hat{\tau}) = \frac{\pi \alpha_N^{QED} \alpha_s e_q^2}{\hat{s}} \frac{16}{9} \left( \frac{M^2(1 - \hat{\tau})^2}{\hat{\tau} 4\pi m_D^2} \right)^{\epsilon/2} \frac{\Gamma(1 + \frac{\epsilon}{2})}{\Gamma(1 + \epsilon)} \left(1 + \frac{\epsilon}{2}\right) \left\{ \frac{1 + \hat{\tau}^2}{1 - \hat{\tau}} \frac{2}{\epsilon} + \frac{\epsilon(1 - \hat{\tau})}{1 + \epsilon} \right\}, \quad (5.4.8)$$

where the mass  $m_D$  comes from using (2.8.26) and  $\alpha_s$  is now dimensionless. Using the  $N$ -dimensional analogue of (5.3.14),

$$\left( \frac{1}{\sigma_0} \frac{d\hat{\sigma}^q}{d\hat{\tau}} \right) = \frac{3}{4\pi^2 \alpha e_q^2 (1 + \frac{\epsilon}{2})} \hat{s} \hat{\sigma}_{DY}^q, \quad (5.4.9)$$

where the factor of  $(1 + \frac{\epsilon}{2})$  comes from evaluating the Born term in  $N$  dimensions,

$$|\mathcal{M}(q + \bar{q} \rightarrow \gamma^*)|^2 = 4 \left(1 + \frac{\epsilon}{2}\right) e^2 e_q^2 M^2, \quad (5.4.10)$$

yields the result

$$\left( \frac{1}{\sigma_0} \frac{d\hat{\sigma}_{DR}^q}{d\hat{\tau}} \right)_{DY} = 2 \frac{2\alpha_s}{3\pi} \left( \frac{(1 - \hat{\tau})^2 M^2}{\hat{\tau} 4\pi m_D^2} \right)^{\epsilon/2} \frac{\Gamma(1 + \frac{\epsilon}{2})}{\Gamma(1 + \epsilon)} \left\{ \frac{1 + \hat{\tau}^2}{1 - \hat{\tau}} \frac{2}{\epsilon} + \frac{\epsilon(1 - \hat{\tau})}{1 + \epsilon} \right\}, \quad (5.4.11)$$

where  $\sigma_0$  is  $N$ -dimensional Born cross section. Integrating over  $\hat{\tau}$  gives

$$(\hat{\sigma}_{DR}(\text{real}))_{DY} = \frac{2\alpha_s}{3\pi} \sigma_0 \left( \frac{M^2}{4\pi m_D^2} \right)^{\epsilon/2} \Gamma\left(1 - \frac{\epsilon}{2}\right) \left\{ \frac{8}{\epsilon^2} - \frac{6}{\epsilon} + \frac{9}{2} + \dots \right\}. \quad (5.4.12)$$

The virtual corrections in Fig. 5.4 are given in (2.10.2) by

$$(\hat{\sigma}_{DR}(\text{virtual}))_{DY} = \frac{2\alpha_s}{3\pi} \sigma_0 \left( \frac{M^2}{4\pi m_D^2} \right)^{\epsilon/2} \frac{\Gamma(1 - \frac{\epsilon}{2}) \Gamma^2(1 + \frac{\epsilon}{2})}{\Gamma(1 + \epsilon)} \left\{ -\frac{8}{\epsilon^2} + \frac{6}{\epsilon} - 8 + \pi^2 + \dots \right\}_{\text{timelike}}. \quad (5.4.13)$$

where  $q^2 = M^2$  is timelike. From the expansion in (2.9.16) and

$$\Gamma\left(1 - \frac{\epsilon}{2}\right) = 1 + \frac{1}{2}\gamma_E \epsilon + \frac{1}{8} \left( \frac{\pi^2}{6} + \gamma_E^2 \right) \epsilon^2 + \dots, \quad (5.4.14)$$

we see that the sum of (5.4.12) and (5.4.13) is given by

$$(\hat{\sigma}_{DR}(\text{real}) + \hat{\sigma}_{DR}(\text{virtual}))_{DY} \equiv \alpha_s I_q^{DY} \sigma_0 = \frac{2\alpha_s}{3\pi} \sigma_0 \left\{ \frac{4\pi^2}{3} - \frac{7}{2} \right\}, \quad (5.4.15)$$

in the limit  $\epsilon \rightarrow 0$ , which is the same result as in (5.3.19). We now define “+ functions” and arrive at

$$\frac{1}{\sigma_0} \left( \frac{d\hat{\sigma}_{DR,DY}^q}{d\hat{\tau}} \right)_+ = 2 \frac{\alpha_s}{2\pi} P_{q \rightarrow gg}(\hat{\tau}) \log(M^2/m_D^2) + 2\alpha_s f_{DR}^{q,DY}(\hat{\tau}), \quad (5.4.16)$$

where  $P_{q \rightarrow gg}(\hat{\tau})$  is the same as (5.3.33) and

$$\alpha_s f_{DR}^{q,DY}(\hat{\tau}) = \frac{2\alpha_s}{3\pi} \left\{ 2(1 + \hat{\tau}^2) \left( \frac{\log(1 - \hat{\tau})}{1 - \hat{\tau}} \right)_+ - \frac{1 + \hat{\tau}^2}{1 - \hat{\tau}} \log(\hat{\tau}) - \left( \frac{\pi^2}{3} + \frac{9}{4} \right) \delta(1 - \hat{\tau}) \right\}$$

$$+ \frac{\alpha_s}{2\pi} P_{q \rightarrow qg}(\hat{\tau}) \left\{ \frac{2}{\epsilon} + \gamma_E - \log(4\pi) \right\}. \quad (5.4.17)$$

The integral of  $f_{DR}^{q,DY}$  over  $\hat{\tau}$  vanishes as in (5.3.35).

The "Compton" subprocess  $q + g \rightarrow \gamma^* + q$  is treated in a similar fashion with the result<sup>3</sup>

$$\frac{1}{\sigma_0} \left( \frac{d\hat{\sigma}_{DR}^q}{d\hat{\tau}} \right)_{DY} = \frac{\alpha_s}{2\pi} P_{g \rightarrow q\bar{q}}(\hat{\tau}) \log(M^2/m_D^2) + \alpha_s f_{DR}^{g,DY}(\hat{\tau}), \quad (5.4.18)$$

where  $P_{g \rightarrow q\bar{q}}(\hat{\tau})$  is given by (5.3.44) and

$$\begin{aligned} \alpha_s f_{DR}^{g,DY}(\hat{\tau}) &= \frac{\alpha_s}{2\pi} \frac{1}{2} \left\{ (\hat{\tau}^2 + (1 - \hat{\tau})^2) \log \left( \frac{(1 - \hat{\tau})^2}{\hat{\tau}} \right) - \frac{3}{2} \hat{\tau}^2 + \hat{\tau} + \frac{3}{2} \right\} \\ &\quad + \frac{\alpha_s}{2\pi} P_{g \rightarrow q\bar{q}}(\hat{\tau}) \left\{ \frac{2}{\epsilon} + \gamma_E - \log(4\pi) \right\}. \end{aligned} \quad (5.4.19)$$

## 5.5 The Drell-Yan "K-Factor"

If we combine the "annihilation" term with the "Compton" term and also include terms with the initial two partons interchanged, then the muon pair (or "Drell-Yan") cross section becomes (for one quark flavor)

$$\begin{aligned} s \frac{d\sigma_{DY}}{dM^2}(s, M^2) &= \frac{4\pi \alpha^2 e_q^2}{9 M^2} \int_{\tau}^1 \frac{dx_a}{x_a} \int_{\tau/x_a}^1 \frac{dx_b}{x_b} \\ &\quad \left\{ \left( \overline{G}_{p \rightarrow q}^{(0)}(x_a) \overline{G}_{p \rightarrow q}^{(0)}(x_b) + \overline{G}_{p \rightarrow q}^{(0)}(x_a) \overline{G}_{p \rightarrow q}^{(0)}(x_b) \right) \right. \\ &\quad \left[ (\sigma_{tot}^{DY}/\sigma_0) \delta(1 - \hat{\tau}) + \frac{\alpha_s}{2\pi} 2P_{q \rightarrow qg}(\hat{\tau}) \log(M^2/\Lambda^2) + 2\alpha_s f^{q,DY}(\hat{\tau}) \right] \\ &\quad + \left( \overline{G}_{p \rightarrow q}^{(0)}(x_a) \overline{G}_{p \rightarrow g}^{(0)}(x_b) + \overline{G}_{p \rightarrow g}^{(0)}(x_a) \overline{G}_{p \rightarrow q}^{(0)}(x_b) \right) \\ &\quad \left[ \frac{\alpha_s}{2\pi} P_{g \rightarrow q\bar{q}}(\hat{\tau}) \log(M^2/\Lambda^2) + \alpha_s f_{DR}^{g,DY}(\hat{\tau}) \right] \\ &\quad \left. + \left( \overline{G}_{p \rightarrow q}^{(0)}(x_a) \overline{G}_{p \rightarrow g}^{(0)}(x_b) + \overline{G}_{p \rightarrow g}^{(0)}(x_a) \overline{G}_{p \rightarrow q}^{(0)}(x_b) \right) \right. \\ &\quad \left. \left[ \frac{\alpha_s}{2\pi} P_{g \rightarrow q\bar{q}}(\hat{\tau}) \log(M^2/\Lambda^2) + \alpha_s f_{DR}^{g,DY}(\hat{\tau}) \right] \right\}, \end{aligned} \quad (5.5.1)$$

where  $\hat{\tau} = \tau/(x_a x_b)$  and

$$\sigma_{tot}^{DY}/\sigma_0 = 1 + \alpha_s I_q^{DY} + \dots, \quad (5.5.2)$$

with  $I_q^{DY}$  given in (5.3.23). The "little  $f$ " functions are scheme dependent and are given by (5.3.34) and (5.3.45) in the massive gluon scheme and by (5.4.17) and (5.4.19) in dimensional regularization. The  $\log(m_g^2)$  or  $\log(m_D^2)$  divergences have been absorbed into the  $G_{p \rightarrow q}^{(0)}$  and  $G_{p \rightarrow g}^{(0)}$  structure functions as we did in (3.3.15) for the fragmentation functions.

If we now define "Drell-Yan" quark distributions by the parton model formula in (5.1.30) we have

$$s \frac{d\sigma_{DY}}{dM^2}(s, M^2) = \frac{4\pi\alpha^2}{9M^2} \int_{\tau}^1 \frac{dx_a}{x_a} P_{q\bar{q}}^{DY}(x_a, \tau/x_a, M^2), \quad (5.5.3)$$

where the probability joint "Drell-Yan"  $q\bar{q}$  probability function is given by

$$\begin{aligned} P_{q\bar{q}}^{DY}(x_a, x_b, M^2) &= \sum_{i=1}^{n_f} e_{q_i}^2 [G_{p \rightarrow q_i}^{DY}(x_a, M^2) G_{p \rightarrow \bar{q}_i}^{DY}(x_b, M^2) \\ &\quad + G_{p \rightarrow \bar{q}_i}^{DY}(x_a, M^2) G_{p \rightarrow q_i}^{DY}(x_b, M^2)], \end{aligned} \quad (5.5.4)$$

with (5.5.1) giving the "Drell-Yan" quark and antiquark probability distributions

$$\begin{aligned} G_{p \rightarrow q}^{DY}(x, M^2) &= \overline{G}_{p \rightarrow q}^{(0)} * \left[ 1 + \frac{\alpha_s}{2\pi} P_{q \rightarrow qg} \log(Q^2/\Lambda^2) \right. \\ &\quad \left. + \alpha_s f^{q,DY} + \frac{1}{2} \alpha_s \left( \frac{8\pi}{9} - \frac{7}{3\pi} \right) \right] \\ &\quad + \overline{G}_{p \rightarrow g}^{(0)} * \left[ \frac{\alpha_s}{2\pi} P_{g \rightarrow q\bar{q}} \log(Q^2/\Lambda^2) + \alpha_s f_{DR}^{g,DY} \right], \end{aligned} \quad (5.5.5)$$

and

$$\begin{aligned} G_{p \rightarrow \bar{q}}^{DY}(x, M^2) &= \overline{G}_{p \rightarrow \bar{q}}^{(0)} * \left[ 1 + \frac{\alpha_s}{2\pi} P_{q \rightarrow qg} \log(Q^2/\Lambda^2) \right. \\ &\quad \left. + \alpha_s f^{q,DY} + \frac{1}{2} \alpha_s \left( \frac{8\pi}{9} - \frac{7}{3\pi} \right) \right] \\ &\quad + \overline{G}_{p \rightarrow g}^{(0)} * \left[ \frac{\alpha_s}{2\pi} P_{g \rightarrow q\bar{q}} \log(Q^2/\Lambda^2) + \alpha_s f_{DR}^{g,DY} \right]. \end{aligned} \quad (5.5.6)$$

The "convolution notation" defined in (3.3.11) is being used and also I have used the unexponentiated form of  $\sigma_{tot}^{DY}$  in (5.3.24),

$$\frac{\sigma_{tot}^{DY}}{\sigma_0} = \left[ 1 + \frac{1}{2} \left( \frac{8\pi}{9} - \frac{7}{3\pi} \right) \alpha_s \right] \left[ 1 + \frac{1}{2} \left( \frac{8\pi}{9} - \frac{7}{3\pi} \right) \alpha_s \right] + O(\alpha_s^2). \quad (5.5.7)$$

These "Drell-Yan" parton distributions are scheme dependent since the "little  $f$ " functions are scheme dependent. We now express them in terms of our reference distributions from deep inelastic scattering

$$G_{p \rightarrow q}(x, Q^2) \equiv G_{p \rightarrow q}^{(2)}(x, Q^2), \quad (5.5.8)$$

as in (4.9.7), then from (4.9.1) we see that

$$\begin{aligned} G_{p \rightarrow q}^{DY}(x, M^2) &= G_{p \rightarrow q}(M^2) * \left[ 1 + \alpha_s \Delta f_q^{DY} + \frac{1}{2} \alpha_s \left( \frac{8\pi}{9} - \frac{7}{3\pi} \right) \right] \\ &\quad + G_{p \rightarrow g}(M^2) * [\alpha_s \Delta f_g^{DY}], \end{aligned} \quad (5.5.9)$$

and

$$G_{p \rightarrow \bar{q}}^{DY}(x, M^2) = G_{p \rightarrow \bar{q}}(M^2) * \left[ 1 + \alpha_s \Delta f_q^{DY} + \frac{1}{2} \alpha_s \left( \frac{8\pi}{9} - \frac{7}{3\pi} \right) \right] \\ + G_{p \rightarrow g}(M^2) * [\alpha_s \Delta f_g^{DY}], \quad (5.5.10)$$

where

$$\begin{aligned} \alpha_s \Delta f_q^{DY}(z) &= \alpha_s \left( f_{MG}^{q,DY}(z) - f_{MG,2}^{q,DIS}(z) \right) \\ &= \alpha_s \left( f_{DR}^{q,DY}(z) - f_{DR,2}^{q,DIS}(z) \right) \\ &= \frac{2\alpha_s}{3\pi} \left\{ (1+z^2) \left( \frac{\log(1-z)}{1-z} \right)_+ \right. \\ &\quad \left. + \frac{3}{2} \frac{1}{(1-z)_+} - 3 - 2z + \frac{9}{4} \delta(1-z) \right\}, \end{aligned} \quad (5.5.11)$$

and

$$\begin{aligned} \alpha_s \Delta f_g^{DY}(z) &= \alpha_s \left( f_{MG}^{g,DY}(z) - f_{MG,2}^{g,DIS}(z) \right) \\ &= \alpha_s \left( f_{DR}^{g,DY}(z) - f_{DR,2}^{g,DIS}(z) \right) \\ &= \frac{\alpha_s}{2\pi^2} \left\{ z^2 + (1-z)^2 \log(1-z) \right. \\ &\quad \left. + \frac{1}{2} (9z^2 - 10z + 3) \right\}. \end{aligned} \quad (5.5.12)$$

Equations (5.5.9) and (5.5.10) are not scheme dependent since the  $\Delta f^{DY}$  functions are the same regardless of the regularization scheme chosen. This means that we can predict the difference between quark distributions defined according to (5.5.13) and those defined in deep inelastic scattering by (4.6.1).

In leading order we neglect terms proportional to  $\alpha_s(Q^2)$  and we see that the "Drell-Yan" distributions are the same as the deep inelastic quark distributions<sup>6,7</sup> but with  $Q^2$  replaced by  $M^2$ . Namely,

$$G_{p \rightarrow q}^{DY}(x, M^2) = G_{p \rightarrow q}(x, M^2), \quad (\text{leading order}), \quad (5.5.13)$$

and

$$P_{q\bar{q}}^{DY}(x_a, x_b, M^2) = P_{q\bar{q}}^{DIS}(x_a, x_b, M^2), \quad (\text{leading order}), \quad (5.5.14)$$

where

$$P_{q\bar{q}}^{DIS}(x_a, x_b, Q^2) = \sum_{i=1}^{n_f} e_{q_i}^2 [G_{p \rightarrow q_i}(x_a, Q^2) G_{p \rightarrow \bar{q}_i}(x_b, Q^2) \\ + G_{p \rightarrow \bar{q}_i}(x_a, Q^2) G_{p \rightarrow q_i}(x_b, Q^2)]. \quad (5.5.15)$$

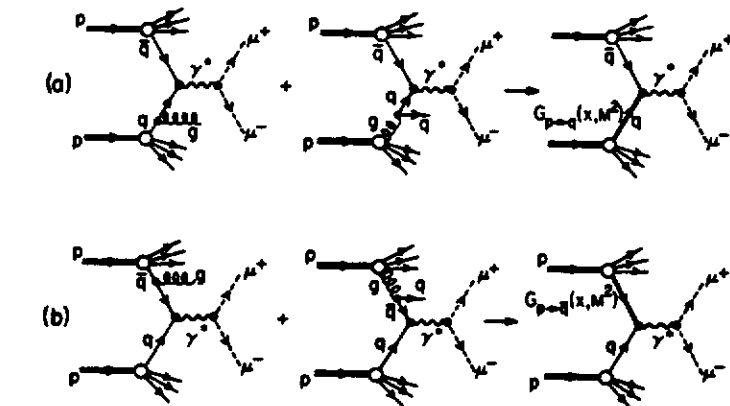


Figure 5.5 Illustrates how in the production of large-mass muon pairs in hadron-hadron collisions the leading log contributions from the subprocess  $\bar{q} + q \rightarrow \gamma^* + g$  and  $\bar{q} + g \rightarrow \gamma^* + \bar{q}$  are summed to form the  $M^2$  dependent quark distribution,  $G_{p \rightarrow q}(x, M^2)$ , where  $M$  is the mass of the muon pair. Similarly, the leading log contributions from the subprocess  $\bar{q} + q \rightarrow g + \gamma^*$  and  $g + g \rightarrow q + \gamma^*$  are summed to form the  $M^2$  dependent antiquark distribution,  $G_{p \rightarrow \bar{q}}(x, M^2)$ .

Thus, in leading order the Drell-Yan cross section in (5.5.3) becomes

$$\left( s \frac{d\sigma_{DY}}{dM^2}(x, M^2) \right)_{\text{leading order}} = \frac{4\pi\alpha^2}{9M^2} \int_\tau^1 \frac{dx_a}{x_a} P_{q\bar{q}}^{DIS}(x_a, \tau/x_a, M^2). \quad (5.5.16)$$

This is illustrated in Fig. 5.5 where the leading logarithm contributions from the subprocesses  $q + \bar{q} \rightarrow \gamma^* + g$  and  $q + g \rightarrow \gamma^* + \bar{q}$  sum to give  $G_{p \rightarrow q}(x, M^2)$  and  $G_{p \rightarrow \bar{q}}(x, M^2)$  just as they did in Fig. 4.8. However, at order  $\alpha_s$ , the Drell-Yan cross section becomes

$$\begin{aligned} \left( s \frac{d\sigma_{DY}}{dM^2}(s, M^2) \right)_{\text{order } \alpha_s} &= \frac{\sigma_{\text{tot}}^{DY}}{\sigma_0} \left( s \frac{d\sigma_{DY}}{dM^2}(s, M^2) \right)_{\text{leading order}} \\ &+ \frac{4\pi\alpha^2}{9M^2} \int_\tau^1 \frac{dx_a}{x_a} \int_{\tau/x_a}^1 \frac{dx_b}{x_b} P_{q\bar{q}}^{DIS}(x_a, x_b, M^2) 2\alpha_s \Delta f_q^{DY}(\hat{\tau}) \\ &+ \frac{4\pi\alpha^2}{9M^2} \int_\tau^1 \frac{dx_a}{x_a} \int_{\tau/x_a}^1 \frac{dx_b}{x_b} P_{q\bar{q}}^{DIS}(x_a, x_b, M^2) \alpha_s \Delta f_g^{DY}(\hat{\tau}) \end{aligned}$$

$$+ \frac{4\pi\alpha^2}{9M^2} \int_{\tau}^1 \frac{dx_a}{x_a} \int_{\tau/x_a}^1 \frac{dx_b}{x_b} P_{qg}^{DIS}(x_a, x_b, M^2) \alpha_s \Delta f_g^{DY}(\hat{\tau}), \quad (5.5.17)$$

where  $\hat{\tau} = \tau/(x_a x_b)$ , and where  $\Delta f_q^{DY}$  is given by (5.5.11) and  $\Delta f_g^{DY}$  by (5.5.12). The joint  $qg$  and  $\bar{q}g$  probabilities are given in terms of the deep inelastic scattering distributions as follows:

$$P_{qg}^{DIS}(x_a, x_b, Q^2) = \sum_{i=1}^{n_f} e_{qi}^2 [G_{p \rightarrow q_i}(x_a, Q^2) G_{p \rightarrow g}(x_b, Q^2) + G_{p \rightarrow g}(x_a, Q^2) G_{p \rightarrow q_i}(x_b, Q^2)], \quad (5.5.18)$$

and

$$P_{\bar{q}g}^{DIS}(x_a, x_b, Q^2) = \sum_{i=1}^{n_f} e_{qi}^2 [G_{p \rightarrow \bar{q}_i}(x_a, Q^2) G_{p \rightarrow g}(x_b, Q^2) + G_{p \rightarrow g}(x_a, Q^2) G_{p \rightarrow \bar{q}_i}(x_b, Q^2)], \quad (5.5.19)$$

respectively.

The Drell-Yan "K-factor" is a complicated function and is defined to be the ratio of the order  $\alpha_s$  result to the leading order result. Namely,

$$K_{DY}(s, M^2) = \frac{(s \frac{d\sigma_{DY}}{dM^2}(s, M^2))_{\text{order } \alpha_s}}{(s \frac{d\sigma_{DY}}{dM^2}(s, M^2))_{\text{leading order}}}. \quad (5.5.20)$$

Equation (5.5.17) shows that the "K-factor" consists of three terms,

$$K_{DY}(s, M^2) = K_{DY}^\delta(M^2) + K_{DY}^q(s, M^2) + K_{DY}^g(s, M^2). \quad (5.5.21)$$

The first term is a  $\delta$ -function contribution arising from the first term in (5.5.17) and the  $\delta$ -function piece of  $\Delta f_q^{DY}$  in (5.5.11),

$$\begin{aligned} K_{DY}^\delta(M^2) &= \frac{\sigma_{\text{tot}}^{DY}}{\sigma_0} + \frac{9}{3\pi} \alpha_s(M^2) \\ &= 1 + \alpha_s I_q^{DY} + \frac{9}{3\pi} \alpha_s. \end{aligned} \quad (5.5.22)$$

From (5.3.23) we have

$$\begin{aligned} K_{DY}^\delta(M^2) &= 1 + \left( \frac{8\pi}{9} - \frac{7}{3\pi} + \frac{9}{3\pi} \right) \alpha_s(M^2) + \dots \\ &\approx 1 + 3.0 \alpha_s(M^2) + \dots, \end{aligned} \quad (5.5.23)$$

which with  $\alpha_s(M^2) = 1/3$  looks like

$$K_{DY}^\delta(M^2) \approx 1 + 1 + \dots. \quad (5.5.24)$$

The second term in the perturbative expansion of  $K_{DY}^\delta$  is as big as the first and one has to doubt whether the first two terms give a good approximation to the complete series. On the other hand, part of the series exponentiates

and it is (5.3.29) that we should use for  $\sigma_{\text{tot}}^{DY}$ . In this case

$$\begin{aligned} K_{DY}^\delta(M^2) &= \exp\left(\frac{2\pi}{3}\alpha_s(M^2)\right) \left\{ 1 + \left( \frac{2\pi}{9} - \frac{7}{3\pi} + \frac{9}{3\pi} \right) \alpha_s(M^2) + \dots \right\} \\ &\approx \exp\left(\frac{2\pi}{3}\alpha_s(M^2)\right) \{ 1 + 0.91 \alpha_s(M^2) + \dots \}, \end{aligned} \quad (5.5.25)$$

which with  $\alpha_s(M^2) = 1/3$  looks like

$$K_{DY}^\delta(M^2) \approx \exp(0.698) (1 + 0.30 + \dots) = 2.61. \quad (5.5.26)$$

Here the second term is a 30% corrections to the first so it appears to be a well behaved perturbation series. Equation (5.5.26) is about 30% larger than the factor of 2 arising from the unexponentiated series in (5.5.24). The  $K_{DY}^\delta(M^2)$  factor is shown in Fig. 5.6 at  $\sqrt{s} = 27.4$  GeV for the exponentiated series and  $\Lambda = 0.2$  GeV.

The third term in (5.5.21) is the "gluon" contribution which is given by

$$\begin{aligned} K_{DY}^q(s, M^2) &= \left\{ \int_{\tau}^1 \frac{dx_a}{x_a} \int_{\tau/x_a}^1 \frac{dx_b}{x_b} P_{qg}^{DIS}(x_a, x_b, M^2) \alpha_s \Delta f_g^{DY}(\hat{\tau}) \right. \\ &\quad \left. + \int_{\tau}^1 \frac{dx_a}{x_a} \int_{\tau/x_a}^1 \frac{dx_b}{x_b} P_{\bar{q}g}^{DIS}(x_a, x_b, M^2) \alpha_s \Delta f_g^{DY}(\hat{\tau}) \right\} \\ &/ \left\{ \int_{\tau}^1 \frac{dx_a}{x_a} P_{q\bar{q}}^{DIS}(x_a, \tau/x_a, M^2) \right\}, \end{aligned} \quad (5.5.27)$$

where  $\hat{\tau} = \tau/(x_a x_b)$ . It is also shown in Fig. 5.6 at the CM energy of 27.4 GeV and is less than one since the order  $\alpha_s$  gluon corrections slightly reduce the overall muon pair rate.

The quark term in (5.5.21) is given by

$$\begin{aligned} K_{DY}^q(s, M^2) &= \left\{ \int_{\tau}^1 \frac{dx_a}{x_a} \int_{\tau/x_a}^1 \frac{dx_b}{x_b} P_{q\bar{q}}^{DIS}(x_a, x_b, M^2) 2\alpha_s \Delta \tilde{f}_q^{DY}(\hat{\tau}) \right\} \\ &/ \left\{ \int_{\tau}^1 \frac{dx_a}{x_a} P_{q\bar{q}}^{DIS}(x_a, \tau/x_a, M^2) \right\}, \end{aligned} \quad (5.5.28)$$

where  $\hat{\tau} = \tau/(x_a x_b)$  and where  $\Delta \tilde{f}_q^{DY}$  is the same as (5.5.11) but with the  $\delta$ -function contribution removed. In particular,

$$\alpha_s \Delta \tilde{f}_q^{DY}(\hat{\tau}) = \frac{2\alpha_s}{3\pi} \left\{ (1 + \hat{\tau}^2) \left( \frac{\log(1 - \hat{\tau})}{1 - \hat{\tau}} \right)_+ + \frac{3}{2} \frac{1}{(1 - \hat{\tau})_+} - 3 - 2\hat{\tau} \right\}. \quad (5.5.29)$$

As can be seen in Fig. 5.6 the term  $K_{DY}^q(s, M^2)$  is small except when  $\tau$  approaches one. The "+" function terms in (5.5.29) cause these corrections to be arbitrarily large near the kinematic boundary. This can be seen clearly in the "Drell-Yan" structure functions defined in (5.5.9) and (5.5.10). The

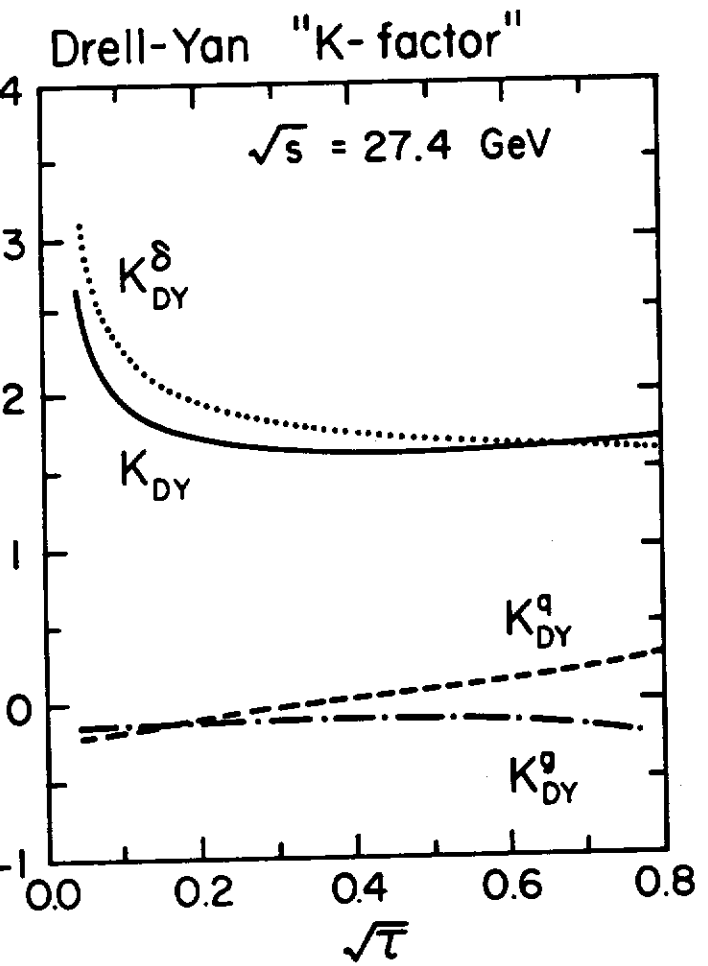


Figure 5.6 Drell-Yan "K-factor",  $K_{DY}$ , computed with  $\Lambda = 200$  MeV at  $\sqrt{s} = 27.4$  GeV plotted versus  $\sqrt{\tau}$ . The quark, gluon, and  $\delta$ -function contributions are shown separately with  $K_{DY} = K_{DY}^\delta + K_{DY}^q + K_{DY}^g$ .

$(\log(1 - \hat{\tau})/(1 - \hat{\tau}))_+$  term gives

$$\frac{G_{p \rightarrow q}^{DY}(x, Q^2)}{G_{p \rightarrow q}(x, Q^2)} \xrightarrow{x \rightarrow 1} 1 + \frac{\alpha_s(Q^2)}{3\pi} \log^2(1 - x), \quad (5.5.30)$$

which shows that the order  $\alpha_s(Q^2)$  correction becomes arbitrarily large as

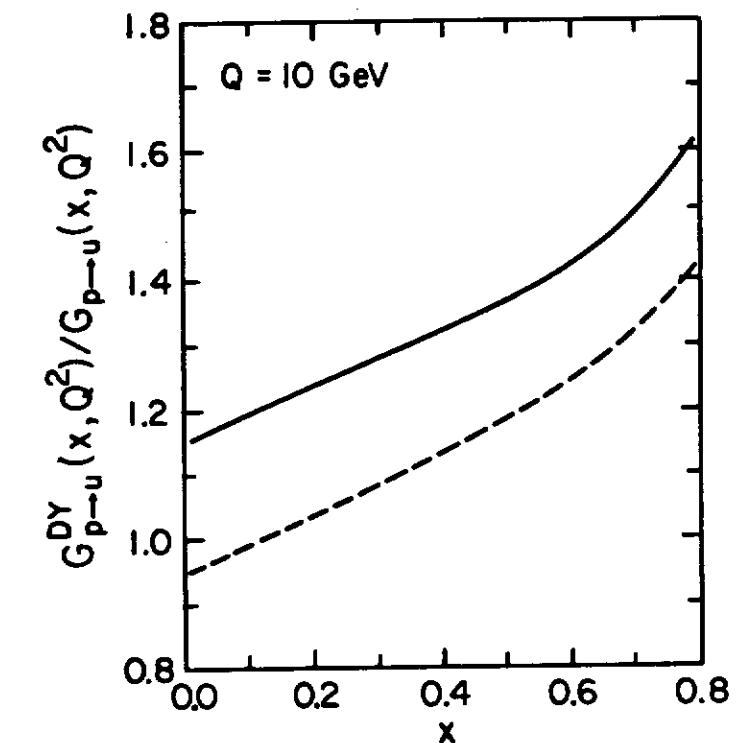


Figure 5.7 Ratio of  $u$ -quark probability distributions defined in the Drell-Yan process,  $G_{p \rightarrow u}^{DY}(x, Q^2)$ , to the "reference" distribution defined from the  $F_2$  structure function in deep inelastic lepton-hadron scattering,  $G_{p \rightarrow u}(x, Q^2)$ , at  $Q = 10$  GeV. The solid (dashed) curves correspond to defining the Drell-Yan quark distributions without (with) the total cross section  $\sigma_{tot}^{DY}$  explicitly removed.

$x \rightarrow 1$ . The solid curve in Fig. 5.7 shows the ratio  $G_{p \rightarrow u}^{DY}(x, Q^2)/G_{p \rightarrow u}(x, Q^2)$  at  $Q^2 = 100$  GeV $^2$ .

Instead of defining the "Drell-Yan" distribution functions according to (5.5.3), it is perhaps better to explicitly remove  $\sigma_{tot}^{DY}$ . Suppose we define the "Drell-Yan" structure distributions according to

$$s \frac{d\sigma_{DY}}{dM^2}(s, M^2) = \sigma_{tot}^{DY} \int_\tau^1 \frac{dx_a}{x_a} \hat{P}_{qq}^{DY}(x_a, \tau/x_a, M^2), \quad (5.5.31)$$

with

$$\hat{P}_{q\bar{q}}^{DY}(x_a, x_b, M^2) = \sum_{i=1}^{n_f} e_{q_i}^2 \left[ \hat{G}_{p\rightarrow q_i}^{DY}(x_a, M^2) \hat{G}_{p\rightarrow \bar{q}_i}^{DY}(x_b, M^2) \right. \\ \left. + \hat{G}_{p\rightarrow \bar{q}_i}^{DY}(x_a, M^2) \hat{G}_{p\rightarrow q_i}^{DY}(x_b, M^2) \right], \quad (5.5.32)$$

where  $\sigma_{tot}^{DY}$  is given by (5.3.24) or by (5.3.29). In terms of the deep inelastic scattering reference structure functions we now have

$$\hat{G}_{p\rightarrow q}^{DY}(x, M^2) = G_{p\rightarrow q}(M^2) * (1 + \alpha_s \Delta f_q^{DY}) \\ + G_{p\rightarrow g}(M^2) * (\alpha_s \Delta f_g^{DY}), \quad (5.5.33)$$

and

$$\hat{G}_{p\rightarrow \bar{q}}^{DY}(x, M^2) = G_{p\rightarrow \bar{q}}(M^2) * (1 + \alpha_s \Delta f_{\bar{q}}^{DY}) \\ + G_{p\rightarrow g}(M^2) * (\alpha_s \Delta f_g^{DY}). \quad (5.5.34)$$

With this definition

$$\int_0^1 \left( \hat{G}_{p\rightarrow q_i}^{DY}(x, M^2) - \hat{G}_{p\rightarrow \bar{q}_i}^{DY}(x, M^2) \right) dx = \\ \int_0^1 (G_{p\rightarrow q_i}(x, M^2) - G_{p\rightarrow \bar{q}_i}(x, M^2)) dx, \quad (5.5.35)$$

since

$$\int_0^1 \alpha_s \Delta f_q^{DY}(z) dz = 0, \quad (5.5.36)$$

With this definition (at least at this order of perturbation theory) the number of quarks in the proton is the same for the "Drell-Yan" as for the reference distributions.

The extraction of  $\sigma_{tot}^{DY}$  in (5.5.31) removes most of the  $\delta$ -function contribution ( $\Delta f_q^{DY}$  still has a small  $\delta$ -function term) and as long as one stays away from the  $x \rightarrow 1$  region the structure functions,  $\hat{G}^{DY}(x, Q^2)$  in (5.5.32) do not differ greatly from the deep inelastic scattering reference distributions  $G(x, Q^2)$  (dashed curve in Fig. 5.7). The major difference between the leading order and the order  $\alpha_s$ , Drell-Yan muon pair cross section lies in the multiplicative factor

$$\sigma_{tot}^{DY}/\sigma_0 = \exp\left(\frac{2\pi}{3}\alpha_s(M^2)\right)(1 - 0.045\alpha_s(M^2) + \dots), \quad (5.5.37)$$

which for  $\alpha_s(M^2) = 1/3$  is about a factor of 2 as shown in (5.3.30). This can be compared to the  $e^+e^-$  result in (2.7.8) of

$$\sigma_{tot}^{e^+e^-}/\sigma_0 = (1 + 0.318\alpha_s(Q^2) + \dots), \quad (5.5.38)$$

which for  $\alpha_s(Q^2) = 1/3$  is only a factor of 1.11 (i.e., about a 10% effect).

Experimentally the Drell-Yan "K-factor" is roughly a factor of 2 which

agrees well with the order  $\alpha_s$  prediction together with the exponentiated series in (5.5.37)<sup>8</sup>. This appears to be a great triumph for perturbative QCD. The experimental Drell-Yan measurements can be interpreted as a measurement of  $\sigma_{tot}^{DY}$ . This measurement is as significant as the experimental measurement of the order  $\alpha_s$  correction to  $\sigma_{tot}^{e^+e^-}$  in (5.5.38). The Drell-Yan experimental results deviate from the naive parton models in the precise manner predicted by perturbative QCD.

As we have seen, the "little  $f$ " functions are process dependent. This means that the "K-factor" differs from process to process. Here we have only considered the Drell-Yan case. The "K-factor" must be recalculated for every process of interest. For example, the "K-factor" for quark-quark scattering (i.e., the subprocess  $q + q \rightarrow q + q$ ) has not yet been calculated. However, the exponential,  $\exp(2\pi\alpha_s/3)$ , in (5.5.37) arises from the  $\pi^2$  that came from the analytic continuation from the spacelike (deep inelastic scattering reference distributions) to the timelike (Drell-Yan) region of  $q^2$ . Hence, we might expect that whenever we try to describe a timelike (TL) process in terms of the deep inelastic (spacelike) structure functions we will have a correction term of the form

$$\sigma_{tot}^{TL}/\sigma_0 = \exp\left(\frac{2\pi}{3}\alpha_s(Q^2)\right)(1 + B\alpha_s(Q^2) + \dots), \quad (5.5.39)$$

where the coefficient  $B$  must be calculated for each process under consideration and it will depend on the choice of variable  $Q$ .

## 5.6 Large Transverse Momentum Muon Pairs

In QCD, transverse momentum of partons can arise in two ways. Firstly, in, for example, a proton beam, quarks are confined in the transverse direction to within the proton radius. Therefore, from the uncertainty principle, they must have some transverse momentum. This momentum called primordial, is intrinsic to the basic proton wave function. It involves small  $Q^2$  values and cannot be calculated from perturbation theory. It must be considered unknown by bounded, falling off like an exponential or Gaussian in transverse momentum,  $k_T$ . This primordial parton transverse momentum "smears" the parton model Born term in (5.1.22) causing the muon pairs to have a non-zero but bounded transverse momentum.

Secondly, in QCD, one expects an "effective"  $k_T$  of partons in protons due to the hard Bremsstrahlung of gluons which can be calculated perturbatively if the momentum transfers are large. For example, the perturbative component of the transverse momentum of muon pairs is generated by the 2-to-2 constituent subprocess  $q + \bar{q} \rightarrow \gamma^* + q$  ("annihilation") in Fig. 5.2 and  $q + g \rightarrow \gamma^* + q$  ("Compton") in Fig. 5.3. The cross sections for these processes

are given in (5.2.9) and (5.2.18). Namely,

$$\frac{d\hat{\sigma}_A}{dM^2 dt}(\hat{s}, \hat{t}) = \frac{8}{27} \frac{\alpha^2 \alpha_s e_q^2}{M^2 \hat{s}^2} \left( \frac{2M^2 \hat{s} + \hat{u}^2 + \hat{t}^2}{\hat{t} \hat{u}} \right), \quad (5.6.1)$$

$$\frac{d\hat{\sigma}_C}{dM^2 dt}(\hat{s}, \hat{t}) = \frac{1}{9} \frac{\alpha^2 \alpha_s e_q^2}{M^2 \hat{s}^2} \left( \frac{2M^2 \hat{u} + \hat{s}^2 + \hat{t}^2}{-\hat{s} \hat{t}} \right), \quad (5.6.2)$$

where I have used (5.3.13) and where the subscripts  $A$  and  $C$  refer to the “annihilation” and “Compton” subprocesses, respectively. These subprocesses must be embedded in the proton-proton collision reaction as in (5.3.8). For example, for the annihilation contribution we have

$$\frac{d\sigma}{dM^2}(s, M^2) = G_{p \rightarrow q}^{(0)}(x_a) dx_a G_{p \rightarrow \bar{q}}^{(0)}(x_b) dx_b \left( \frac{d\hat{\sigma}_A}{dM^2 dt} \right) d\hat{t}, \quad (5.6.3)$$

where

$$p_q = x_a P_A, \quad (5.6.4)$$

$$p_{\bar{q}} = x_b P_B, \quad (5.6.5)$$

and

$$s = (P_A + P_B)^2, \quad (5.6.6)$$

$$t = (P_{\mu\mu} - P_A)^2, \quad (5.6.7)$$

$$u = (P_{\mu\mu} - P_B)^2, \quad (5.6.8)$$

which together with (5.2.5), (5.2.6), and (5.2.7) give

$$\hat{s} = x_a x_b s, \quad (5.6.9)$$

$$\hat{t} = M^2 = x_a(t - M^2), \quad (5.6.10)$$

$$\hat{u} = M^2 = x_b(u - M^2). \quad (5.6.11)$$

The condition

$$\hat{s} + \hat{t} + \hat{u} = M^2, \quad (5.6.12)$$

implies that

$$x_b = \frac{x_a x_b - \tau}{x_a - x_1}, \quad (5.6.13)$$

$$x_a = \frac{x_b x_1 - \tau}{x_b - x_2}, \quad (5.6.14)$$

with

$$x_1 = -(u - M^2)/s = \frac{1}{2}(x_T^2 + 4\tau)^{\frac{1}{2}} e^y, \quad (5.6.15)$$

$$x_2 = -(t - M^2)/s = \frac{1}{2}(x_T^2 + 4\tau)^{\frac{1}{2}} e^{-y}, \quad (5.6.16)$$

where

$$x_T = 2p_T/\sqrt{s}, \quad (5.6.17)$$

where  $p_T$  is the transverse momentum of the muon pair and  $y$  is their rapidity

as defined in (5.1.26). In this case, however,

$$x_E^2 = x_T^2 + x_L^2 + 4\tau, \quad (5.6.18)$$

replaces (5.1.15) and

$$y = \frac{1}{2} \log(x_1/x_2), \quad (5.6.19)$$

replaces (5.1.27) and

$$x_1 - x_2 = x_L, \quad (5.6.20)$$

replaces (5.1.13). Equations (5.6.10) and (5.6.11) become

$$\hat{t} = -x_a s x_2 + M^2, \quad (5.6.21)$$

$$\hat{u} = -x_b s x_1 + M^2, \quad (5.6.22)$$

and the cross section for producing muon pairs of mass  $M$ , rapidity  $y$ , and transverse momentum  $p_T$  at center-of-mass energy squared  $s$  is given by

$$\frac{d\sigma_{DY}}{dM^2 dy dp_T^2}(s, M^2, y, p_T) = \int_{x_a^{\min}}^1 dx_a G_{p \rightarrow q}^{(0)}(x_a) G_{p \rightarrow \bar{q}}^{(0)}(x_b) \left( \frac{x_a x_b}{x_a - x_1} \right) \left( \frac{1}{\pi} \frac{d\hat{\sigma}_A}{dM^2 dt}(\hat{s}, \hat{t}) \right), \quad (5.6.23)$$

where

$$x_a^{\min} = \frac{x_1 - \tau}{1 - x_2}, \quad (5.6.24)$$

is determined from (5.6.14) by setting  $x_b = 1$  and  $x_b$  is related to  $x_a$  as given in (5.6.13). Summing leading log corrections converts  $G^{(0)}(x)$  into  $G(x, M^2)$  so that (5.6.23) becomes

$$\begin{aligned} \sigma_P(s, M^2, y, p_T) &\equiv \frac{d\sigma}{dM^2 dy dp_T^2} = \\ &\int_{x_a^{\min}}^1 dx_a \left( \frac{x_a x_b}{x_a - x_1} \right) P_{q\bar{q}}^{DIS}(x_a, x_b, M^2) \left( \frac{1}{\pi} \frac{d\hat{\sigma}_A}{dM^2 dt}(\hat{s}, \hat{t}) \right) \\ &+ \int_{x_a^{\min}}^1 dx_a \left( \frac{x_a x_b}{x_a - x_1} \right) [P_{qg}^{DIS}(x_a, x_b, M^2) + P_{\bar{q}g}^{DIS}(x_a, x_b, M^2)] \\ &\quad \left( \frac{1}{\pi} \frac{d\hat{\sigma}_C}{dM^2 dt}(\hat{s}, \hat{t}) \right), \end{aligned} \quad (5.6.25)$$

where I have included both “annihilation” and “Compton” contributions and interchanged beam and target partons. The label “ $P$ ” refers to the perturbative contribution and  $x_a^{\min}$  and  $x_b$  are given by (5.6.24) and (5.6.13), respectively.

At large  $p_T$  the perturbative cross section in (5.6.25) behaves like  $1/p_T^2$ . For example, the annihilation contribution can be expressed in the form

$$\frac{d\sigma_A}{dM^2 dy dp_T^2}(s, M^2, y, p_T) = \frac{8}{27} \frac{\alpha^2 \alpha_s}{M^2} \left( \frac{1}{p_T^2} \right)$$

$$\int_{x_a^{\min}}^1 dx_a P_{q\bar{q}}^{DIS}(x_a, x_b, M^2) \frac{1}{(x_a - x_1)} \left( 1 + \frac{\tau^2}{(x_a x_b)^2} - \frac{x_T^2}{2x_a x_b} \right), \quad (5.6.26)$$

where  $x_a^{\min}$  is given in (5.6.24) and

$$x_b = \frac{x_a x_2 - \tau}{x_a - x_1}, \quad (5.6.27)$$

with  $x_1$  and  $x_2$  given in (5.6.15) and (5.6.16), respectively, and  $x_T$  given by (5.6.17). In constructing (5.6.26) from (5.6.1) I have used the fact that

$$\frac{\hat{t}\hat{u}}{\hat{s}} = p_T^2, \quad (5.6.28)$$

so that

$$\hat{t} = -\frac{\hat{s}}{2} \left\{ (1 - \hat{\tau}) - [(1 - \hat{\tau})^2 - 4p_T^2/\hat{s}]^{\frac{1}{2}} \right\}, \quad (5.6.29)$$

$$\hat{u} = -\frac{\hat{s}}{2} \left\{ (1 - \hat{\tau}) + [(1 - \hat{\tau})^2 - 4p_T^2/\hat{s}]^{\frac{1}{2}} \right\}. \quad (5.6.30)$$

If we ignore the scale breaking of the structure functions in (5.6.26) (*i.e.*, neglect the  $M^2$  dependence of  $P(x_a, x_b, M^2)$ ) then,

$$M^2 p_T^2 \frac{d\sigma_A}{d\tau dy dp_T^2}(x, M^2, y, p_T) = \alpha_s F_A(\tau, y, x_T), \quad (5.6.31)$$

where  $F_A(\tau, y, x_T)$  is a function of the dimensionless variables  $\tau$ ,  $y$ , and  $x_T$ . Similarly, the "Compton" contribution can be written in the form

$$M^2 p_T^2 \frac{d\sigma_C}{d\tau dy dp_T^2}(x, M^2, y, p_T) = \alpha_s F_C(\tau, y, x_T), \quad (5.6.32)$$

The perturbative contributions in (5.6.25) are shown in Fig. 5.8 together with data on  $pp \rightarrow \mu^+ \mu^- + x$  at  $M = 8.4$  GeV and  $W = \sqrt{s} = 27.4$  GeV<sup>9</sup>. The perturbative contributions are absolutely normalized and agree roughly with the data at large transverse momenta. They, however, have the wrong shape and diverge at  $p_T = 0$ . We will see in the next section that this divergence occurs at every order of perturbation theory but disappears in the sum. In addition, nonperturbative effects at small  $p_T$  regularize this singularity leaving a smooth transverse momentum distribution<sup>10</sup>.

The soft, nonperturbative, primordial transverse momentum of the partons within the initial protons produce a net transverse momentum,  $k_T$ , of, for example, the initial  $q\bar{q}$  system that can be parameterized by a gaussian

$$f(k_T^2) = \frac{1}{4\pi\sigma_q^2} \exp\left(-\frac{k_T^2}{4\sigma_q^2}\right), \quad (5.6.33)$$

where for a single constituent in a proton, one has

$$\langle k_T^2 \rangle_{\text{primordial}} = 2\sigma_q^2. \quad (5.6.34)$$

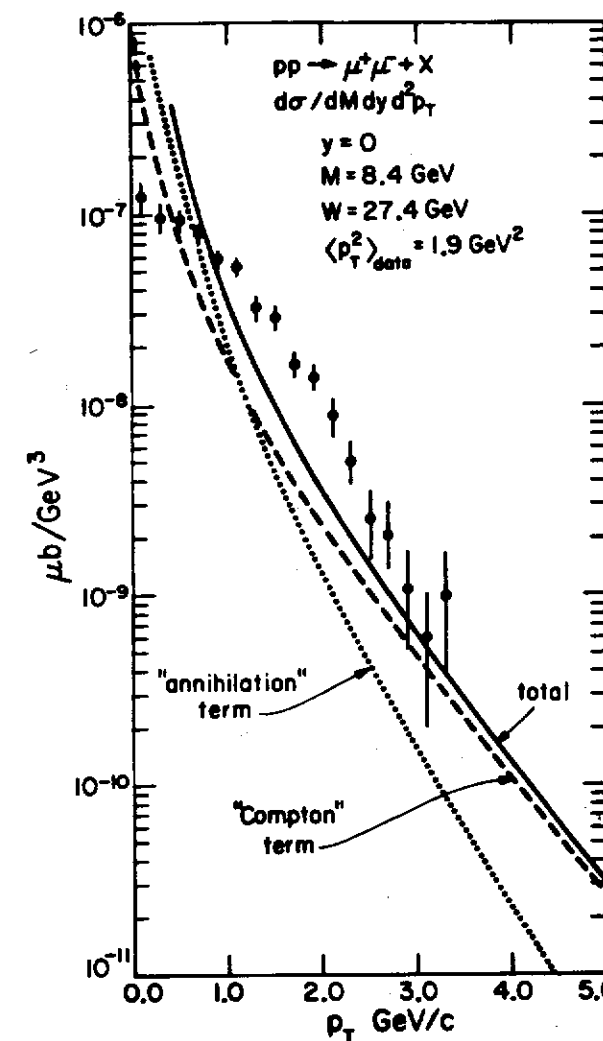


**Figure 5.8** The distribution in transverse momentum,  $p_T$ , of muon pairs,  $\mu^+ \mu^-$  produced in  $pp$  collisions at  $W = \sqrt{s} = 27.4$  GeV compared with the leading order perturbative QCD result. The "Compton" and "annihilation" contributions are given by the dashed and dotted curves, respectively (*taken from Ref. 9*).

This primordial transverse momentum "smears" the perturbative contribution in (5.6.25) as follows:

$$\sigma_S(s, M^2, y, p_T^2) = \int f(k_T^2)$$

$$\left[ \sigma_P(s, M^2, (\tilde{p}_T - \tilde{k}_T)^2) + \sigma_V(s, M^2) \delta((\tilde{p}_T - \tilde{k}_T)^2) \right] d^2 k_T, \quad (5.6.35)$$

where the subscript  $S$  refers to "smeared" and where I have included the virtual corrections  $\sigma_V(s, M^2)$  that contribute only at the point where  $\tilde{k}_T = \tilde{p}_T$ . Equation (5.6.35) can be rewritten in the form

$$\begin{aligned} \sigma_S(s, M^2, y, p_T^2) &= \int \sigma_P(s, M^2, (p_T - k_T)^2) [f(k_T^2) - f(p_T^2)] d^2 k_T \\ &+ f(p_T^2) \int \left[ \sigma_P(s, M^2, y, (\tilde{p}_T - \tilde{k}_T)^2) + \sigma_V(s, M^2) \delta((\tilde{p}_T - \tilde{k}_T)^2) \right] d^2 k_T, \end{aligned} \quad (5.6.36)$$

where the second term has been subtracted and then added and the  $\delta$ -function drops out of the first term since  $[f(k_T^2) - f(p_T^2)]\delta(k_T^2)$  vanishes. Both terms in (5.6.36) are now finite and the smeared cross section becomes

$$\begin{aligned} \sigma_S(s, M^2, y, p_T^2) &= \int \sigma_P(s, M^2, y, q_T^2) [f((\tilde{p}_T - \tilde{q}_T)^2) - f(p_T^2)] d^2 q_T \\ &+ f(p_T^2) \sigma_{\text{tot}}^{DY}(s, M^2, y), \end{aligned} \quad (5.6.37)$$

where

$$\sigma_{\text{tot}}^{DY}(s, M^2, y) \equiv \frac{d\sigma_{\text{tot}}^{DY}}{dy}(s, M^2, y), \quad (5.6.38)$$

as given in (5.1.29) and

$$\tilde{q}_T = \tilde{p}_T - \tilde{k}_T. \quad (5.6.39)$$

Equation (5.6.37) is well behaved at all values of  $p_T^2$  and we are left with one parameter  $\sigma_q$ , in (5.6.34). The fit to the data in Fig. 5.9 yields  $\sigma_q = 0.48 \text{ GeV}$  or

$$\langle k_T \rangle_{\text{primordial}} = \sqrt{\frac{\pi}{2}} \sigma_q \approx 600 \text{ MeV}. \quad (5.6.40)$$

This is a rather large value for the primordial transverse momentum of partons within the proton. It means that at the energy in Fig. 5.9 about  $0.9 \text{ GeV}^2$  of the muon pair mean  $p_T^2$  is due to the primordial motion and about  $1.0 \text{ GeV}^2$  arises from the hard QCD subprocesses. We shall find out in the next section, however, that summing all the leading double logarithmic terms causes the perturbative contributions to vanish at  $p_T = 0$  and it is this corrected perturbative cross section that should be "smeared." Doing so results in a slightly smaller value of the primordial  $k_T$ .

Actually the fit in Fig. 5.9 cannot by itself be viewed as a success of perturbative QCD. One could have fit the same data with just the Gaussian in (5.6.33) provided  $\sigma_q = 0.677 \text{ GeV}$ . The test of the presence of the perturbative component to the transverse momentum of muon pairs comes from examining the energy or mass dependence of the muon pair  $p_T$  spectrum. Figure 5.10 shows that as the energy increases (at fixed  $M$ ) the spectrum becomes flatter. This change in the muon pair transverse momentum spectrum is a general

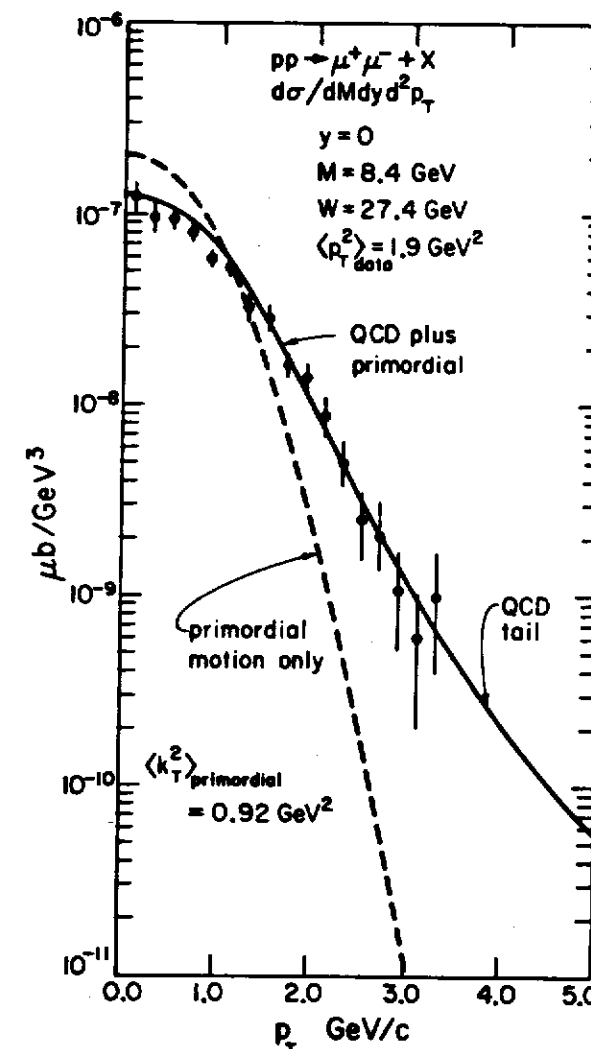
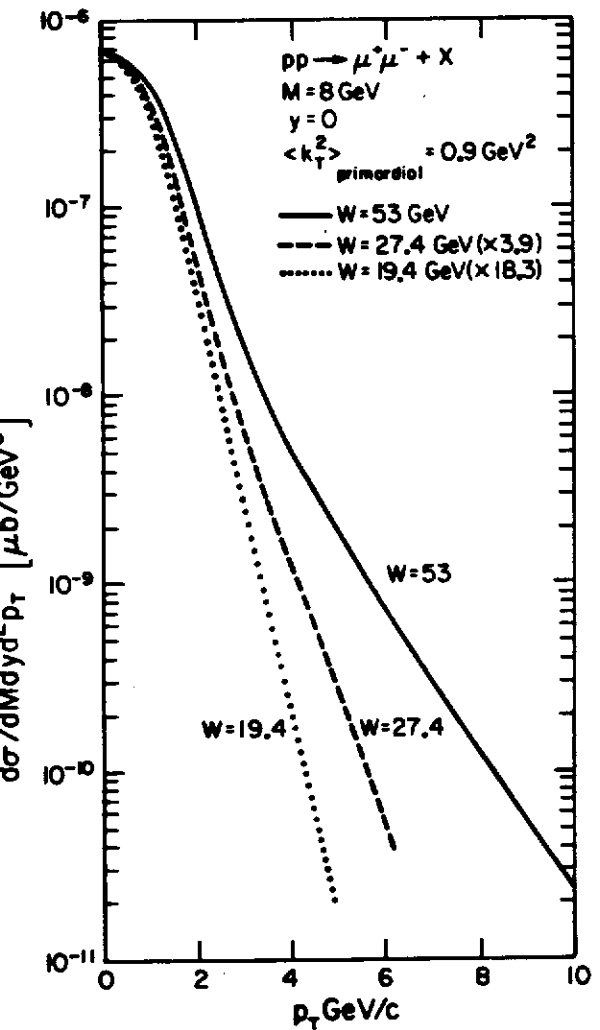


Figure 5.9 The distribution in transverse momentum,  $p_T$ , of muon pairs,  $\mu^+ \mu^-$  produced in  $pp$  collisions at  $W = \sqrt{s} = 27.4 \text{ GeV}$  compared with the leading order perturbative QCD result "smeared" with a Gaussian primordial transverse momentum spectrum with  $\langle k_T \rangle_{p \rightarrow q} = 600 \text{ MeV}$  (solid curve). The dashed curve is the primordial transverse momentum spectrum with no perturbative QCD terms (taken from Ref. 9).

feature of QCD resulting from the  $1/p_T^2$  behavior of the perturbative contributions. As we will see in more detail later, the mean value of  $p_T^2$  has the form



**Figure 5.10** Energy dependence of the large transverse momentum “tail” predicted for the production of muon pairs in  $pp$  collisions from the leading order QCD subprocesses. The leading order perturbative QCD result has been “smeared” with a Gaussian primordial transverse momentum spectrum with  $\langle k_T^2 \rangle_{p \rightarrow q} = 600$  MeV.

(neglecting logarithms),

$$\langle p_T^2 \rangle_P \propto \alpha_s(M^2) (p_T^2)_{\max}, \quad (5.6.41)$$

where

$$\begin{aligned} (p_T^2)_{\max} &= \frac{s}{4} [(1 - \tau)^2 - x_L^2] \\ &= \frac{s}{4} \left[ \frac{(1 - \tau)^2 - 4\tau \sinh^2(y)}{\cosh^2(y)} \right], \end{aligned} \quad (5.6.43)$$

is the maximum transverse momentum squared of the muon pair and the subscript  $P$  again refers to the perturbative contribution. These equations imply that (neglecting logarithms),

$$\langle p_T^2 \rangle_P \propto \alpha_s(M^2) s, \quad (5.6.42)$$

or

$$\langle p_T^2 \rangle_P \propto \alpha_s(M^2) M^2, \quad (5.6.43)$$

at fixed values of the dimensionless variables  $\tau$  and  $y$  or  $\tau$  and  $x_L$ . Presumably the primordial component is independent of the energy and the mass of the muon pair so that the resulting mean  $p_T^2$  of the muon pairs has the form

$$\langle p_T^2 \rangle \approx \langle p_T^2 \rangle_{\text{primordial}} + C_1 \alpha_s(M^2) s, \quad (5.6.44)$$

or

$$\langle p_T^2 \rangle \approx \langle p_T^2 \rangle_{\text{primordial}} + C_2 \alpha_s(M^2) M^2, \quad (5.6.45)$$

at fixed  $\tau$  and  $y$ , and  $C_1$  and  $C_2$  are approximately constant and can be calculated from (5.6.25).

## 5.7 Small Transverse Momentum Muon Pairs

Let us examine more closely the divergences that occur at  $p_T = 0$  in the perturbative contributions to the muon pair cross section. For example, the “annihilation” contribution in (5.6.23) is given by

$$\begin{aligned} \frac{d\sigma_A}{d\tau dy dp_T^2}(s, M^2, y, p_T) &= \frac{8}{27} \frac{\alpha^2 \alpha_s}{M^2} \left( \frac{1}{p_T^2} \right) \\ &\int_{x_a^{\min}}^1 dx_a P_{q\bar{q}}^{DIS}(x_a, x_b, M^2) \frac{1}{(x_a - x_1)} \left( 1 + \frac{\tau^2}{(x_a x_b)^2} - \frac{x_T^2}{2x_a x_b} \right), \end{aligned} \quad (5.7.1)$$

where  $P_{q\bar{q}}^{DIS}(x_a, x_b, M^2)$  is given in (5.5.15) and

$$x_a^{\min} = \frac{x_1 - \tau}{1 - x_2}, \quad (5.7.2)$$

$$x_b = \frac{x_a x_2 - \tau}{(x_a - x_1)}, \quad (5.7.3)$$

with  $x_1$  and  $x_2$  defined in (5.6.15) and (5.6.16), respectively, and  $x_T$  given by

(5.6.17). It would appear that the cross section (5.7.1) diverges like  $1/p_T^2$  as  $p_T \rightarrow 0$ . However, this is not quite correct since

$$x_a^{\min} - x_1 = \frac{1}{4} \frac{x_T^2}{1 - x_2}, \quad (5.7.4)$$

and

$$x_a^{\min} x_2 - \tau = \frac{1}{4} \frac{x_T^2}{1 - x_2}, \quad (5.7.5)$$

so that the integral over  $x_a$  gives a logarithmic divergence as  $x_T \rightarrow 0$ . In particular,

$$\int_{x_a^{\min}}^1 dx_a \frac{1}{(x_a - x_1)} \left( 1 + \frac{\tau^2}{(x_a x_b)^2} \right) \approx -2 \log(x_T^2/4), \quad (5.7.6)$$

where I have dropped terms that vanish as  $x_T \rightarrow 0$ . Also as  $x_T \rightarrow 0$

$$x_1 \xrightarrow[x_T \rightarrow 0]{} \sqrt{\tau} e^y, \quad (5.7.7)$$

$$x_2 \xrightarrow[x_T \rightarrow 0]{} \sqrt{\tau} e^{-y}, \quad (5.7.8)$$

so that keeping only the leading terms as  $p_T \rightarrow 0$  gives

$$\frac{d\sigma_A}{dr dy dp_T^2}(s, M^2, y, p_T) \approx \frac{8}{27} \frac{\alpha^2 \alpha_s}{M^2} P_{q\bar{q}}^{DIS}(x_a, x_b, M^2) \frac{2}{p_T^2} \log(s/p_T^2), \quad (5.7.9)$$

where

$$x_a = \sqrt{\tau} e^y, \quad (5.7.10)$$

$$x_b = \sqrt{\tau} e^{-y}. \quad (5.7.11)$$

Equation (5.7.9) can be rewritten in the form

$$\frac{d\sigma_{DY}}{dr dy dp_T^2}(s, M^2, y, p_T) = \left( \frac{d\sigma_{DY}}{d\tau dy}(s, M^2, y) \right)_{\text{Born}} \left\{ \frac{4\alpha_s}{3\pi} \frac{1}{p_T^2} \log(s/p_T^2) \right\}, \quad (5.7.12)$$

where

$$\left( \frac{d\sigma_{DY}}{d\tau dy}(s, M^2, y) \right)_{\text{Born}} = \frac{4\pi\alpha^2}{9M^2} P_{q\bar{q}}^{DIS}(x_a, x_b, M^2), \quad (5.7.13)$$

is the cross section in (5.1.29). The divergence in (5.7.12) as  $p_T \rightarrow 0$  has precisely the same form as that observed in (3.8.18) since in both cases the divergence arises from the region of phase space in which the gluon is both soft and nearly collinear to the quark and the antiquark. Both here and in (3.8.18) the quark and antiquark are nearly back-to-back. As we saw in Chapter 3 this is the region where one must sum the double logarithms in order to arrive at the correct perturbative result. To correct (5.7.12) we must multiply it by the

"Sudakov form factor" in (3.8.23) giving

$$\frac{d\sigma_{DY}}{dr dy dp_T^2}(s, M^2, y, p_T) = \left( \frac{d\sigma_{DY}}{d\tau dy}(s, M^2, y) \right)_{\text{Born}} \left\{ \frac{4\alpha_s}{3\pi} \frac{1}{p_T^2} \log(s/p_T^2) \exp \left[ -\frac{2\alpha_s}{3\pi} \log^2(p_T^2/s) \right] \right\}, \quad (5.7.14)$$

which instead of diverging at  $p_T = 0$  vanishes as  $p_T \rightarrow 0$ . Once you allow for an infinite number of soft gluon emissions, it becomes impossible for the initial quark and antiquark to remain precisely back-to-back. At modest  $p_T$  (5.7.14) exhibits the  $1/p_T^2$  behavior found at order  $\alpha_s$ , but for  $p_T \leq (p_T)_{\text{peak}}$ , where

$$(p_T^2)_{\text{peak}} \approx \frac{s}{2} \exp \left( \frac{-3\pi}{4\alpha_s} \right), \quad (5.7.15)$$

radiation damping occurs and the spectrum goes rapidly to zero. Unfortunately at center-of-mass energies less than 200 GeV this perturbative peak is washed out by the primordial transverse momentum smearing as in (5.6.37). However, the peak should become evident at very high energy.

## 5.8 Vector Boson Production

In the naive parton model the weak intermediate  $W^\pm$  bosons are produced in proton-proton collisions via the subprocess  $q_i + \bar{q}_j \rightarrow W^\pm$ . The experimental cross section is expressed in terms of the parton subprocess as in (5.1.1). Namely,

$$\sigma(p+p \rightarrow W^\pm + X) = G_{p \rightarrow q_i}(x_a) dx_a G_{p \rightarrow \bar{q}_j}(x_b) dx_b \hat{\sigma}(q_i + \bar{q}_j \rightarrow W^\pm), \quad (5.8.1)$$

where  $G_{p \rightarrow q}(x_a) dx_a$  is the probability of finding a quark with momentum

$$p_q = x_a P_A, \quad (5.8.2)$$

and  $G_{p \rightarrow \bar{q}}(x_b) dx_b$  is the probability of finding an antiquark with momentum

$$p_{\bar{q}} = x_b P_B, \quad (5.8.3)$$

where  $P_A$  and  $P_B$  are the momentums, respectively, of the initial two protons. From (A.3.1) we see the the 2-to-1 cross section is given by

$$\hat{\sigma}(q_i + \bar{q}_j \rightarrow W^\pm; \hat{s}) = \frac{\pi}{\hat{s}} |\overline{\mathcal{M}}(q_i + \bar{q}_j \rightarrow W^\pm)|^2 \delta(\hat{s} - M_W^2), \quad (5.8.4)$$

where  $|\overline{\mathcal{M}}|^2$  is the spin averaged matrix element squared and  $M_W$  is the mass of the vector boson. The Feynman rules for the couplings of  $W$  bosons to quarks given in Appendix C yields

$$|\overline{\mathcal{M}}(u + \bar{d}_\theta \rightarrow W^+)|^2 = \frac{1}{3} \frac{1}{4} 8g_W^2 \hat{s}, \quad (5.8.5)$$

where  $g_W$  is the dimensionless weak coupling

$$g_W^2 = \frac{G_F M_W^2}{\sqrt{2}} = \frac{\pi \alpha}{2 x_W}, \quad (5.8.6)$$

and  $x_W$  is the square of the sine of the Weinberg angle,  $x_W = \sin^2(\theta_W)$  and  $G_F$  is the Fermi constant. Here we sum over the three allowed helicity states of the  $W^\pm$  boson ( $\lambda = 0, \pm 1$ ) by using (2.2.18). The factor of  $1/3$  is the color factor that arises from our convention of averaging over the initial color states and summing over the final color states and the factor of  $1/4$  comes from averaging over the quark spins. Furthermore,  $\bar{d}_\theta$  is the rotated state

$$\bar{d}_\theta = d \cos(\theta_C) + s \sin(\theta_C), \quad (5.8.7)$$

where  $\theta_C$  is the Cabibbo angle. Combining (5.8.4) and (5.8.5) gives

$$\hat{\sigma}(u + \bar{d} \rightarrow W^+; \hat{s}) = \frac{2}{3} \pi g_W^2 \delta(\hat{s} - M_W^2), \quad (5.8.8)$$

or

$$\hat{\sigma}(u + \bar{d} \rightarrow W^+; \hat{s}) = \frac{2}{3} \pi g_W^2 \cos^2(\theta_C) \delta(\hat{s} - M_W^2), \quad (5.8.9)$$

and

$$\hat{\sigma}(u + \bar{s} \rightarrow W^+; \hat{s}) = \frac{2}{3} \pi g_W^2 \sin^2(\theta_C) \delta(\hat{s} - M_W^2). \quad (5.8.10)$$

The  $W^-$  cross sections are similar but with all particles replaced by their respective antiparticles. The experimentally observable cross section in (5.8.1) becomes

$$\begin{aligned} \sigma(p + p \rightarrow W^\pm + X; s) &= \int dx_a \int dx_b \\ &G_{p \rightarrow q_i}(x_a) G_{p \rightarrow \bar{q}_j}(x_b) \hat{\sigma}(q_i + \bar{q}_j \rightarrow W^\pm; \hat{s}), \end{aligned} \quad (5.8.11)$$

where  $\hat{s} = x_a x_b s$ . Inserting the subprocess cross sections gives the naive parton model prediction<sup>11</sup>

$$\begin{aligned} \sigma(p + p \rightarrow W^\pm + X; s) &= \frac{2\pi g_W^2}{3s} \int_{\tau_W}^1 \frac{dx_a}{x_a} P_{qqW^\pm}(x_a, \tau_W/x_b) \\ &= \sqrt{2}\pi G_F \tau_W \frac{1}{3} \int_{\tau_W}^1 \frac{dx_a}{x_a} P_{qqW^\pm}(x_a, \tau_W/x_b), \end{aligned} \quad (5.8.12)$$

where  $\tau_W$  is defined according to

$$\tau_W = M_W^2/s. \quad (5.8.13)$$

The joint probabilities  $P_{qqW^\pm}$  are given by

$$\begin{aligned} P_{qqW^+}(x_a, x_b) &= [G_{p \rightarrow u}(x_a) G_{p \rightarrow \bar{d}}(x_b) + G_{p \rightarrow \bar{d}}(x_a) G_{p \rightarrow u}(x_b)] \cos^2(\theta_C) \\ &+ [G_{p \rightarrow u}(x_a) G_{p \rightarrow \bar{s}}(x_b) + G_{p \rightarrow \bar{s}}(x_a) G_{p \rightarrow u}(x_b)] \sin^2(\theta_C), \end{aligned} \quad (5.8.14)$$

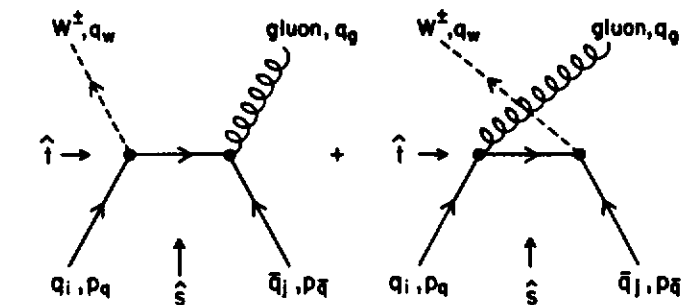


Figure 5.11 Leading order diagrams for the quark-antiquark “annihilation” subprocess  $q_i + \bar{q}_j \rightarrow W^\pm + g$ .

for  $W^+$  production and

$$\begin{aligned} P_{qqW^-}(x_a, x_b) &= [G_{p \rightarrow u}(x_a) G_{p \rightarrow \bar{d}}(x_b) + G_{p \rightarrow \bar{d}}(x_a) G_{p \rightarrow u}(x_b)] \cos^2(\theta_C) \\ &+ [G_{p \rightarrow u}(x_a) G_{p \rightarrow \bar{s}}(x_b) + G_{p \rightarrow \bar{s}}(x_a) G_{p \rightarrow u}(x_b)] \sin^2(\theta_C), \end{aligned} \quad (5.8.15)$$

for  $W^-$  production where only the first two weak isospin doublets of quarks has been included.

The total cross section for producing  $Z^0$  bosons in proton-proton collisions is arrived at in a similar manner with the parton model result given by

$$\sigma(p + p \rightarrow Z^0 + X; s) = 2\sqrt{2}\pi G_F \tau_Z \frac{1}{3} \int_{\tau_Z}^1 \frac{dx_a}{x_a} P_{q\bar{q}Z}(x_a, \tau_Z/x_a), \quad (5.8.16)$$

where

$$\tau_Z = M_Z^2/s, \quad (5.8.17)$$

and where the joint probability  $P_{q\bar{q}Z}$  is given by

$$\begin{aligned} P_{q\bar{q}Z}(x_a, x_b) &= [G_{p \rightarrow u}(x_a) G_{p \rightarrow \bar{d}}(x_b) + G_{p \rightarrow \bar{d}}(x_a) G_{p \rightarrow u}(x_b)] [\frac{1}{4} - \frac{2}{3}x_W + \frac{8}{9}x_W^2] \\ &+ [G_{p \rightarrow u}(x_a) G_{p \rightarrow \bar{s}}(x_b) + G_{p \rightarrow \bar{s}}(x_a) G_{p \rightarrow u}(x_b)] \\ &+ [G_{p \rightarrow u}(x_a) G_{p \rightarrow \bar{t}}(x_b) + G_{p \rightarrow \bar{t}}(x_a) G_{p \rightarrow u}(x_b)] [\frac{1}{4} - \frac{1}{3}x_W + \frac{2}{9}x_W^2]. \end{aligned} \quad (5.8.18)$$

In QCD we must also consider the possibility that the initial quark or antiquark can radiate a gluon before combining to form a  $W^\pm$  or  $Z^0$  boson as shown in Fig. 5.11. For massless partons the differential cross section for the

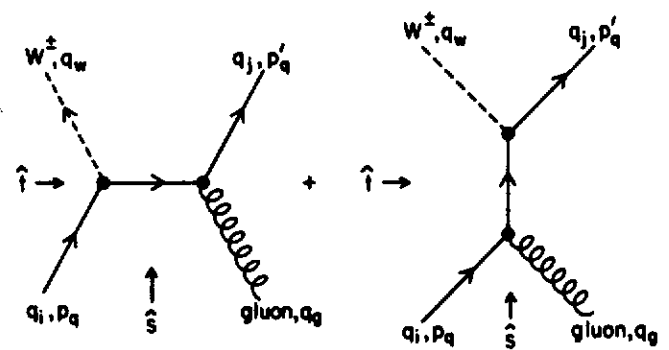


Figure 5.12 Leading order diagrams for the “Compton” subprocess  $q_i + g \rightarrow W^\pm + q_j$ .

“annihilation” subprocess  $q + \bar{q} \rightarrow W^\pm + g$  is given by

$$\frac{d\hat{\sigma}_A}{dt}(\hat{s}, \hat{t}) = \frac{2\pi\alpha_s}{\hat{s}^2} \frac{g_W^2}{4\pi} \frac{8}{3} \left\{ \frac{\hat{t}^2 + \hat{u}^2 + 2M_W^2\hat{s}}{\hat{t}\hat{u}} \right\}, \quad (5.8.19)$$

which is the same as differential cross section  $q + \bar{q} \rightarrow \gamma^* + g$  in (5.2.9) with the replacement

$$M \rightarrow M_W, \quad (5.8.20)$$

and

$$\alpha \rightarrow 2 \frac{g_W^2}{4\pi}. \quad (5.8.21)$$

Similarly, the differential cross section for the “Compton” subprocess  $q + g \rightarrow W^\pm + q$  shown in Fig. 5.12 is given by

$$\frac{d\hat{\sigma}_C}{dt}(\hat{s}, \hat{t}) = \frac{2\pi\alpha_s}{\hat{s}^2} \frac{g_W^2}{4\pi} \frac{1}{3} \left\{ \frac{\hat{t}^2 + \hat{s}^2 + 2M_W^2\hat{u}}{-\hat{s}\hat{t}} \right\}, \quad (5.8.22)$$

which again is the same as the differential cross section  $q + g \rightarrow \gamma^* + q$  in (5.2.18) with the replacements given in (5.8.20) and (5.8.21). Thus, to order  $\alpha_s$ , QCD corrections to the productions of  $W^\pm$  bosons in hadron-hadron collisions differ from their counterparts in the Drell-Yan process only by a constant factor. Because of this we can simply carry over the leading and order  $\alpha_s$  results that we computed for the Drell-Yan process and apply them to  $W^\pm$  and  $Z^0$  production. For example, in leading order QCD the naive

parton model formula in (5.8.12) becomes

$$\begin{aligned} \sigma(p + p \rightarrow W^\pm + X; s)_{\text{leading order}} = \\ \sqrt{2\pi} G_F \tau_W \frac{1}{3} \int_{\tau_W}^1 \frac{dx_a}{x_a} P_{q\bar{q}W^\pm}^{DIS}(x_a, \tau_W/x_b, M_W^2), \end{aligned} \quad (5.8.23)$$

where  $\tau_W = M_W^2/s$  and the joint probabilities are given in terms of the deep inelastic scattering reference distributions evaluated at the scale  $Q^2 = M_W^2$ . Namely,

$$\begin{aligned} P_{q\bar{q}W^+}^{DIS}(x_a, x_b, Q^2) = & [G_{p\rightarrow u}(x_a, Q^2)G_{p\rightarrow d}(x_b, Q^2) \\ & + G_{p\rightarrow d}(x_a, Q^2)G_{p\rightarrow u}(x_b, Q^2)] \cos^2(\theta_C) \\ & + [G_{p\rightarrow u}(x_a, Q^2)G_{p\rightarrow \bar{u}}(x_b, Q^2) \\ & + G_{p\rightarrow \bar{u}}(x_a, Q^2)G_{p\rightarrow u}(x_b, Q^2)] \sin^2(\theta_C), \end{aligned} \quad (5.8.24)$$

and

$$\begin{aligned} P_{q\bar{q}W^-}^{DIS}(x_a, x_b, Q^2) = & [G_{p\rightarrow u}(x_a, Q^2)G_{p\rightarrow d}(x_b, Q^2) \\ & + G_{p\rightarrow d}(x_a, Q^2)G_{p\rightarrow u}(x_b, Q^2)] \cos^2(\theta_C) \\ & + [G_{p\rightarrow \bar{u}}(x_a, Q^2)G_{p\rightarrow s}(x_b, Q^2) \\ & + G_{p\rightarrow s}(x_a, Q^2)G_{p\rightarrow \bar{u}}(x_b, Q^2)] \sin^2(\theta_C). \end{aligned} \quad (5.8.25)$$

Just as was the case in Fig. 5.5 for the Drell-Yan process, the leading logarithm QCD corrections from subprocesses such as  $q + \bar{q} \rightarrow W^\pm + g$  and  $q + g \rightarrow W^\pm + q$  sum to give the “renormalization group improved” parton distributions  $G_{p\rightarrow q}(x, Q^2)$  and  $G_{p\rightarrow \bar{q}}(x, Q^2)$ .

At order  $\alpha_s$ , the  $W^\pm$  cross section becomes

$$\begin{aligned} \sigma(p + p \rightarrow W^\pm + X; s)_{\text{order } \alpha_s} = & \frac{\sigma_{\text{tot}}^W}{\sigma_0} \sigma(p + p \rightarrow W^\pm + X, s)_{\text{leading order}} \\ & + \sqrt{2\pi} G_F \frac{1}{3} \int_{\tau_W}^1 \frac{dx_a}{x_a} \int_{\tau_W/x_a}^1 \frac{dx_b}{x_b} P_{q\bar{q}W^\pm}^{DIS}(x_a, x_b, M_W^2) 2\alpha_s \Delta f_q^{DY}(\hat{\tau}_W) \\ & + \sqrt{2\pi} G_F \frac{1}{3} \int_{\tau_W}^1 \frac{dx_a}{x_a} \int_{\tau_W/x_a}^1 \frac{dx_b}{x_b} P_{q\bar{q}W^\pm}^{DIS}(x_a, x_b, M_W^2) \alpha_s \Delta f_g^{DY}(\hat{\tau}_W) \\ & + \sqrt{2\pi} G_F \frac{1}{3} \int_{\tau_W}^1 \frac{dx_a}{x_a} \int_{\tau_W/x_a}^1 \frac{dx_b}{x_b} P_{q\bar{q}W^\pm}^{DIS}(x_a, x_b, M_W^2) \alpha_s \Delta f_g^{DY}(\hat{\tau}_W), \end{aligned} \quad (5.8.26)$$

where  $\hat{\tau}_W = \tau_W/(x_a x_b)$ ,  $\tau_W = M_W^2/s$ , and where  $\Delta f_q^{DY}$  and  $\Delta f_g^{DY}$  are the same functions that appear in the Drell-Yan case, (5.5.11) and (5.5.12), respectively. The joint probabilities  $q\bar{q}W^\pm$  are given in (5.8.24) and (5.8.25) and the new joint probabilities  $qgW^\pm$  and  $\bar{q}gW^\pm$  are given in terms of the

deep inelastic scattering reference distributions as follows:

$$\begin{aligned} P_{q\bar{q}W^+}^{DIS}(x_a, x_b, Q^2) = & [G_{p \rightarrow u}(x_a, Q^2) G_{p \rightarrow g}(x_b, Q^2) \\ & + G_{p \rightarrow g}(x_a, Q^2) G_{p \rightarrow u}(x_b, Q^2)] \\ & [G_{p \rightarrow c}(x_a, Q^2) G_{p \rightarrow g}(x_b, Q^2) \\ & + G_{p \rightarrow g}(x_a, Q^2) G_{p \rightarrow c}(x_b, Q^2)], \end{aligned} \quad (5.8.27)$$

and

$$\begin{aligned} P_{q\bar{q}W^+}^{DIS}(x_a, x_b, Q^2) = & [G_{p \rightarrow d}(x_a, Q^2) G_{p \rightarrow g}(x_b, Q^2) \\ & + G_{p \rightarrow g}(x_a, Q^2) G_{p \rightarrow d}(x_b, Q^2)] \\ & [G_{p \rightarrow s}(x_a, Q^2) G_{p \rightarrow g}(x_b, Q^2) \\ & + G_{p \rightarrow g}(x_a, Q^2) G_{p \rightarrow s}(x_b, Q^2)], \end{aligned} \quad (5.8.28)$$

for  $W^+$  production and

$$\begin{aligned} P_{q\bar{q}W^-}^{DIS}(x_a, x_b, Q^2) = & [G_{p \rightarrow d}(x_a, Q^2) G_{p \rightarrow g}(x_b, Q^2) \\ & + G_{p \rightarrow g}(x_a, Q^2) G_{p \rightarrow d}(x_b, Q^2)] \\ & [G_{p \rightarrow s}(x_a, Q^2) G_{p \rightarrow g}(x_b, Q^2) \\ & + G_{p \rightarrow g}(x_a, Q^2) G_{p \rightarrow s}(x_b, Q^2)], \end{aligned} \quad (5.8.29)$$

and

$$\begin{aligned} P_{q\bar{q}W^-}^{DIS}(x_a, x_b, Q^2) = & [G_{p \rightarrow u}(x_a, Q^2) G_{p \rightarrow g}(x_b, Q^2) \\ & + G_{p \rightarrow g}(x_a, Q^2) G_{p \rightarrow u}(x_b, Q^2)] \\ & [G_{p \rightarrow c}(x_a, Q^2) G_{p \rightarrow g}(x_b, Q^2) \\ & + G_{p \rightarrow g}(x_a, Q^2) G_{p \rightarrow c}(x_b, Q^2)], \end{aligned} \quad (5.8.30)$$

for  $W^-$  production, where again only the first two quark doublets have been included. The total cross section ratio,  $\sigma_{tot}^W/\sigma_0$ , is the same as the Drell-Yan case. Namely,

$$\begin{aligned} \sigma_{tot}^W = & \sigma_0 (1 + \alpha_s I_q^{DY} + \dots) \\ = & \sigma_0 \left\{ 1 + \left( \frac{2\pi}{9} - \frac{7}{3\pi} \right) \alpha_s + \dots \right\}, \end{aligned} \quad (5.8.31)$$

in the unexponentiated form and

$$\sigma_{tot}^W = \sigma_0 \exp \left( \frac{2\pi}{3} \alpha_s \right) \left\{ 1 + \left( \frac{2\pi}{9} - \frac{7}{3\pi} \right) \alpha_s + \dots \right\}, \quad (5.8.32)$$

in the exponentiated form.

The "K-factor" for  $W^\pm$  production is defined by

$$K_{W^\pm}(s) = \frac{\sigma(p + p \rightarrow W^\pm + X; s)_{\text{order } \alpha_s}}{\sigma(p + p \rightarrow W^\pm + X; s)_{\text{leading order}}}, \quad (5.8.33)$$

and as in the Drell-Yan case consists of three terms,

$$K_{W^\pm}(s) = K_{W^\pm}^\delta + K_{W^\pm}^q(s) + K_{W^\pm}^g(s). \quad (5.8.34)$$

The  $\delta$ -function term is identical to the Drell-Yan case and is given by

$$\begin{aligned} K_{W^\pm}^\delta &= \frac{\sigma_{tot}^{W^\pm}}{\sigma_0} + \frac{9}{3\pi} \alpha_s + \dots \\ &= 1 + \alpha_s I_q^{DY} + \frac{9}{3\pi} \alpha_s + \dots \\ &= 1 + \left( \frac{8\pi}{9} + \frac{2}{3\pi} \right) \alpha_s (M_W^2) + \dots, \end{aligned} \quad (5.8.35)$$

in the unexponentiated form or

$$K_{W^\pm}^\delta = \exp \left( \frac{2\pi}{3} \alpha_s (M_W^2) \right) \left\{ 1 + \left( \frac{2\pi}{9} + \frac{2}{3\pi} \right) \alpha_s (M_W^2) + \dots \right\}, \quad (5.8.36)$$

in the exponentiated form. At the scale of  $M_W^2$   $\alpha_s \approx 0.10$  so that

$$K_{W^\pm}^\delta \approx 1.35. \quad (5.8.37)$$

The quark and gluon terms in (5.8.34) are similar to the Drell-Yan case except the structure functions are slightly different. In particular

$$\begin{aligned} K_{W^\pm}^q(s) = & \left\{ \int_{\tau_W}^1 \frac{dx_a}{x_a} \int_{\tau_W/x_a}^1 \frac{dx_b}{x_b} P_{q\bar{q}W^\pm}^{DIS}(x_a, x_b, M_W^2) 2\alpha_s \Delta \tilde{f}_q^{DY}(\hat{\tau}_W) \right\} \\ & / \left\{ \int_{\tau_W}^1 \frac{dx_a}{x_a} P_{q\bar{q}W^\pm}^{DIS}(x_a, \tau_W/x_a, M^2) \right\}, \end{aligned} \quad (5.8.38)$$

and

$$\begin{aligned} K_{W^\pm}^g(s) = & \left\{ \int_{\tau_W}^1 \frac{dx_a}{x_a} \int_{\tau_W/x_a}^1 \frac{dx_b}{x_b} P_{q\bar{q}W^\pm}^{DIS}(x_a, x_b, M_W^2) \alpha_s \Delta f_g^{DY}(\hat{\tau}_W) \right. \\ & + \left. \int_{\tau_W}^1 \frac{dx_a}{x_a} \int_{\tau_W/x_a}^1 \frac{dx_b}{x_b} P_{q\bar{q}W^\pm}^{DIS}(x_a, x_b, M_W^2) \alpha_s \Delta f_g^{DY}(\hat{\tau}_W) \right\} \\ & / \left\{ \int_{\tau_W}^1 \frac{dx_a}{x_a} P_{q\bar{q}W^\pm}^{DIS}(x_a, \tau/x_a, M_W^2) \right\}, \end{aligned} \quad (5.8.39)$$

where  $\Delta \tilde{f}_q^{DY}$  and  $\Delta f_g^{DY}$  are given by (5.5.29) and (5.5.12), respectively.

As in the Drell-Yan case the "annihilation" and "Compton" differential cross sections in (5.8.19) and (5.8.22), respectively, are responsible for the transverse momentum of the produced  $W^\pm$  bosons. Everything stated in Sections 5.6 and 5.7 about the transverse momentum of large mass muon pairs is also true for the production of  $W^\pm$  and  $Z^0$  bosons in hadron-hadron collisions. For example, at order  $\alpha_s$ , the transverse momentum spectrum of  $W^\pm$

mesons produced at pseudorapidity,  $y$ , is given by

$$\begin{aligned} \frac{d\sigma^{W^\pm}}{dydp_T^2}(s, y, p_T) &= \int_{x_a^{\min}}^1 dx_a \left( \frac{x_a x_b}{x_a - x_1} \right) P_{q\bar{q}W^\pm}^{DIS}(x_a, x_b, M_W^2) \left( \frac{1}{\pi} \frac{d\hat{\sigma}_A}{dt}(\hat{s}, \hat{t}) \right) \\ &+ \int_{x_a^{\min}}^1 dx_a \left( \frac{x_a x_b}{x_a - x_1} \right) \left[ P_{qgW^\pm}^{DIS}(x_a, x_b, M_W^2) + P_{\bar{q}gW^\pm}^{DIS}(x_a, x_b, M_W^2) \right] \\ &\quad \left( \frac{1}{\pi} \frac{d\hat{\sigma}_C}{dt}(\hat{s}, \hat{t}) \right), \end{aligned} \quad (5.8.40)$$

where the “annihilation” and “Compton” differential cross sections are given in (5.8.19) and (5.8.22), respectively, and

$$x_a^{\min} = \frac{x_1 - \tau_W}{1 - x_2}, \quad (5.8.41)$$

and

$$x_b = \frac{x_a x_2 - \tau_W}{x_a - x_1}, \quad (5.8.42)$$

with  $x_1$  and  $x_2$  given by (5.6.15) and (5.6.16), respectively, with  $M = M_W$ . Neglecting logarithms, the transverse momentum spectrum of the produced vector bosons behaves like  $1/p_T^2$  resulting in a perturbative contribution to the mean square transverse momentum behaving as in (5.6.41). For example for  $W^\pm$  production

$$\begin{aligned} \langle p_T^2 \rangle_W &\propto \alpha_s(M_W^2) \langle p_T^2 \rangle_{\max} \\ &\propto \alpha_s(M_W^2) s. \end{aligned} \quad (5.8.43)$$

At small transverse momentum the  $1/p_T^2$  spectrum arising from the order  $\alpha_s$  diagrams is modified by the “Sudakov form factor” as in (5.7.14). For example, for  $W^\pm$  production

$$\begin{aligned} \frac{d\sigma^{W^\pm}}{dydp_T^2}(s, y, p_T) &= \left( \frac{d\sigma^{W^\pm}}{dy}(s, y) \right)_{\text{Born}} \\ &\quad \left\{ \frac{4\alpha_s}{3\pi} \frac{1}{p_T^2} \log(s/p_T^2) \exp\left[-\frac{2\alpha_s}{3\pi} \log^2(p_T^2/s)\right] \right\}, \end{aligned} \quad (5.8.44)$$

where

$$\left( \frac{d\sigma^{W^\pm}}{dy}(s, y) \right)_{\text{Born}} = \sqrt{2}\pi G_F \frac{1}{3} P_{q\bar{q}W^\pm}^{DIS}(x_a, x_b, M_W^2), \quad (5.8.45)$$

with

$$\begin{aligned} x_a &= \sqrt{\tau_W} e^y, \\ x_b &= \sqrt{\tau_W} e^{-y}. \end{aligned} \quad (5.8.46)$$

### Problems

#### 5.1. Starting from

$d\sigma = G_{p\rightarrow q}(x_a) dx_a G_{p\rightarrow \bar{q}}(x_b) dx_b \hat{\sigma}(q + \bar{q} \rightarrow \mu^+ \mu^-)$ ,  
with  $\hat{\sigma}(q + \bar{q} \rightarrow \mu^+ \mu^-)$  given in (5.1.17) and assuming that the incoming partons are parallel to the initial hadrons verify that

$$\frac{d\sigma}{d\tau dx_L}(s, M^2, x_L) = \frac{4\pi\alpha^2}{9M^2} \frac{1}{(x_a + x_b)} P_{q\bar{q}}(x_a, x_b),$$

where the joint probability  $P_{q\bar{q}}(x_a, x_b)$  is given by (5.1.23) and

$$\begin{aligned} x_a x_b &= \tau, \\ x_a - x_b &= x_L, \end{aligned}$$

where  $\tau = M^2/s$  and  $x_L$  is the longitudinal momentum fraction of the muon pair given in (5.1.13). Show that

$$\begin{aligned} x_a &= \sqrt{\tau} e^y, \\ x_b &= \sqrt{\tau} e^{-y}, \end{aligned}$$

where

$$y = \frac{1}{2} \log \left( \frac{E + p_L}{E - p_L} \right)$$

is the rapidity of the muon pair. Also verify that

$$\frac{d\sigma}{dy} = x_E \frac{d\sigma}{dx_E} = (x_a + x_b) \frac{d\sigma}{dx_L},$$

where  $x_E$  is the muon pair fractional energy defined in (5.1.15). Integrate  $d\sigma/d\tau dx_L$  over  $x_L$  and show that

$$\frac{d\sigma}{d\tau}(s, M^2) = \frac{4\pi\alpha^2}{9M^2} \int_\tau^1 \frac{dx_a}{x_a} P_{q\bar{q}}(x_a, \tau/x_a).$$

#### 5.2. Show that the differential cross section for the “annihilation” subprocess $q + \bar{q} \rightarrow \gamma^* + g$ in Fig. 5.2 is given by

$$\frac{d\hat{\sigma}}{dt}(\hat{s}, \hat{t}) = \frac{\pi\alpha\alpha_s e_q^2}{\hat{s}^2} \frac{8}{9} \left\{ \frac{\hat{t}^2 + \hat{u}^2 + 2M^2\hat{s}}{\hat{t}\hat{u}} \right\},$$

where  $M^2$  is the mass of the virtual photon,  $\gamma^*$ , and the partons are taken to be massless.

#### 5.3. Show that the differential cross section for the “Compton” subprocess $q + g \rightarrow \gamma^* + q$ in Fig. 5.3 is given by

$$\frac{d\hat{\sigma}}{dt}(\hat{s}, \hat{t}) = \frac{\pi\alpha\alpha_s e_q^2}{\hat{s}^2} \frac{1}{3} \left\{ \frac{\hat{t}^2 + \hat{s}^2 + 2M^2\hat{u}}{-\hat{s}\hat{t}} \right\},$$

where  $M^2$  is the mass of the virtual photon,  $\gamma^*$ , and the partons are taken to be massless.

- 5.4. Show that the differential cross section for the "annihilation" subprocess  $q + \bar{q} \rightarrow \gamma_\Sigma^* + g$  in Fig. 5.2 is given by

$$\frac{d\hat{\sigma}}{d\hat{t}}(\hat{s}, \hat{t}) = \frac{\pi\alpha\alpha_s e_q^2}{\hat{s}^2} \frac{8}{9} \left\{ \frac{\hat{u}}{\hat{t}} + \frac{\hat{t}}{\hat{u}} \right. \\ + \frac{2(M^2 + m_g^2)(M^2 + m_g^2 - \hat{u} - \hat{t})}{\hat{u}\hat{t}} \\ \left. - M^2 M_g^2 \left( \frac{1}{\hat{t}^2} + \frac{1}{\hat{u}^2} \right) \right\},$$

where  $M$  and  $m_g$  are the masses of the virtual photon,  $\gamma^*$ , and gluon, respectively, and the quarks are taken to be massless. Use (A.3.10) to verify that in this case the maximum and minimum values of  $\hat{t}$  are given by

$$\hat{t}_{\min, \max} = -\frac{M^2}{2\hat{r}} \left\{ (1 - \hat{r} - \beta\hat{r}) \right. \\ \left. \mp [(1 - \hat{r})^2 + \beta\hat{r}(\beta\hat{r} - 2\hat{r} - 2)]^{\frac{1}{2}} \right\},$$

where  $\hat{r} = M^2/\hat{s}$  and  $\beta = m_g^2/M^2$ .

- 5.5. Verify that

$$\int_0^{1-2\sqrt{\beta}} \frac{\log(\hat{t}_{\max}/\hat{t}_{\min})}{1-\hat{r}} d\hat{r} = \frac{\pi^2}{12} - \log^2(2) \\ + \int_0^{1-2\sqrt{\beta}} \frac{\log(\beta\hat{r}^2/(1-\hat{r})^2)}{1-\hat{r}} d\hat{r},$$

where  $\hat{t}_{\max}$  and  $\hat{t}_{\min}$  are given in (5.3.2).

- 5.6. Using (5.3.14) verify that

$$\left( \frac{1}{\sigma_0} \frac{d\hat{\sigma}_{MG}^q}{d\hat{r}} \right)_{DY} = 2 \frac{2\alpha_s}{3\pi} \left\{ \frac{1+\hat{r}^2}{1-\hat{r}} \log \left( \frac{(1-\hat{r})^2 M^2}{\hat{r}^2 m_g^2} \right) - 2(1-\hat{r}) \right. \\ \left. + \left( 2\log^2(2) - \frac{\pi^2}{6} \right) \delta(1-\hat{r}) \right\}.$$

Integrate this from  $\hat{r}_{\min} = 0$  to  $\hat{r}_{\max} = 1/(1+\sqrt{\beta})^2 \approx 1 - 2\sqrt{\beta}$  and show that

$$(\sigma_{MG}(\text{real}))_{DY} = \frac{2\alpha_s}{3\pi} \sigma_0 \{ \log^2(\beta) + 3\log(\beta) + \pi^2 \},$$

where  $\beta = m_g^2/M^2$ .

- 5.7. Verify that

$$\frac{1}{\sigma_0} \left( \frac{d\hat{\sigma}_{MG,DY}^q}{d\hat{r}} \right)_+ = 2 \frac{\alpha_s}{2\pi} P_{q \rightarrow qg}(\hat{r}) \log(M^2/m_g^2) + 2\alpha_s f_{MG}^{q,DY}(\hat{r}),$$

where

$$P_{q \rightarrow qg}(\hat{r}) = \frac{4}{3} \left( \frac{1+\hat{r}^2}{1-\hat{r}} \right)_+,$$

and

$$\alpha_s f_{MG}^{q,DY}(\hat{r}) = \frac{2\alpha_s}{3\pi} \left\{ 2(1+\hat{r}^2) \left( \frac{\log(1-\hat{r})}{1-\hat{r}} \right)_+ \right. \\ \left. - 2 \left( \frac{1+\hat{r}^2}{1-\hat{r}} \right) \log(\hat{r}) - 2(1-\hat{r}) - \frac{2\pi^2}{3} \delta(1-\hat{r}) \right\}.$$

Show that

$$\int_0^1 \alpha_s f_{MG}^{q,DY}(\hat{r}) d\hat{r} = 0.$$

- 5.8. Show that the differential cross section for the "Compton" subprocess  $q + g \rightarrow \gamma_\Sigma^* + q$  in Fig. 5.3 is given by

$$\frac{d\hat{\sigma}}{d\hat{t}}(\hat{s}, \hat{t}) = \frac{\pi\alpha\alpha_s e_q^2}{\hat{s}^2} \frac{1}{3} \left\{ -\frac{\hat{t}}{\hat{s}} - \frac{\hat{s}}{\hat{t}} \right. \\ + \frac{2(M^2 - m_g^2)(\hat{s} + \hat{t} - M^2 + m_g^2)}{\hat{s}\hat{t}} \\ \left. - M^2 M_g^2 \left( \frac{1}{\hat{s}^2} + \frac{1}{\hat{t}^2} \right) \right\},$$

where  $M$  is the mass of the virtual photon,  $\gamma^*$ , and the gluon is off mass-shell by an amount  $q_g^2 = -m_g^2$ , and the quarks are taken to be massless. Show that in this case the maximum and minimum values of  $\hat{t}$  are given by

$$\hat{t}_{\min} = -\hat{r}m_g^2, \\ \hat{t}_{\max} = -M^2(1-\hat{r})/\hat{r},$$

where  $\hat{r} = M^2/\hat{s}$ .

- 5.9. Verify that

$$\left( \frac{1}{\sigma_0} \frac{d\hat{\sigma}_{MG}^g}{d\hat{r}} \right)_{DY} = \frac{\alpha_s}{2\pi} P_{g \rightarrow gg}(\hat{r}) \log(M^2/m_g^2) + \alpha_s f_{MG}^{g,DY}(\hat{r}),$$

where

$$P_{g \rightarrow gg}(\hat{r}) = \frac{1}{2}(\hat{r}^2 + (1-\hat{r})^2),$$

and

$$\alpha_s f_{MG}^{q,DY}(\hat{\tau}) = \frac{\alpha_s}{2\pi} \frac{1}{2} \left\{ (\hat{\tau}^2 + (1-\hat{\tau})^2) \log\left(\frac{1-\hat{\tau}}{\hat{\tau}^2}\right) - \frac{1}{2} + \hat{\tau} - \frac{3}{2}\hat{\tau}^2 \right\}.$$

5.10. Using (E.1.12) show that

$$\begin{aligned} \int_0^1 (1-\hat{\tau})^\epsilon \hat{\tau}^{-\frac{1}{2}} \frac{1}{1-\hat{\tau}} d\hat{\tau} &= \frac{1}{\epsilon} f_\tau, \\ \int_0^1 (1-\hat{\tau})^\epsilon \hat{\tau}^{-\frac{1}{2}} \frac{\hat{\tau}}{1-\hat{\tau}} d\hat{\tau} &= \frac{1}{\epsilon} \frac{1-\frac{1}{2}\epsilon}{1+\frac{1}{2}\epsilon} f_\tau \\ &= \left( \frac{1}{\epsilon} - 1 + \frac{1}{4}\epsilon + \dots \right) f_\tau, \\ \int_0^1 (1-\hat{\tau})^\epsilon \hat{\tau}^{-\frac{1}{2}} \frac{\hat{\tau}^2}{1-\hat{\tau}} d\hat{\tau} &= \frac{1}{\epsilon} \frac{1-\frac{3}{4}\epsilon + \frac{1}{8}\epsilon^2}{1+\frac{3}{4}\epsilon + \frac{1}{8}\epsilon^2} f_\tau \\ &= \left( \frac{1}{\epsilon} - \frac{3}{2} + \frac{9}{8}\epsilon + \dots \right) f_\tau, \end{aligned}$$

where

$$f_\tau = \frac{\Gamma(1+\epsilon)\Gamma(1-\frac{\epsilon}{2})}{\Gamma(1+\frac{\epsilon}{2})}.$$

5.11. Show that in  $N$  spacetime dimensions the matrix element squared for the "annihilation" subprocess  $q + \bar{q} \rightarrow \gamma_\Sigma^* + g$  is given by

$$|\overline{\mathcal{M}}(q + \bar{q} \rightarrow \gamma_\Sigma^* + g)|^2 = 16\pi^2 \alpha_N^{QED} \alpha_N^{QCD} e_q^2 \frac{8}{9} \left(1 + \frac{\epsilon}{2}\right) \left\{ \frac{2(\hat{\tau}^2 y^2 - 2\hat{\tau}y^2 + y^2 + \hat{\tau}^2 + 2\hat{\tau} + 1)}{(1-\hat{\tau})^2(1-y^2)} + \frac{2}{(1-y^2)} \epsilon \right\},$$

where  $N = 4 + \epsilon$ ,  $\hat{\tau} = M^2/\hat{s}$ ,  $\hat{t} = -\hat{s}(1-\hat{\tau})(1-y)/2$ , and  $\hat{u} = -\hat{s}(1-\hat{\tau})(1+y)/2$ . Verify that

$$I = \int_{-1}^1 dy (1-y^2)^{\epsilon/2} |\overline{\mathcal{M}}|^2 = 16\pi^2 \alpha_N^{QED} \alpha_N^{QCD} e_q^2 \frac{8}{9} \left(1 + \frac{\epsilon}{2}\right) 2^\epsilon \frac{\Gamma^2(1+\frac{\epsilon}{2})}{\Gamma(1+\epsilon)} \left\{ \frac{1+\hat{\tau}^2}{(1-\hat{\tau})^2} \frac{8}{\epsilon} + \frac{4\epsilon}{1+\epsilon} \right\}.$$

Using (5.4.3) and (5.4.9) show that

$$\left( \frac{1}{\sigma_0} \frac{d\hat{\sigma}_{DR}^q}{d\hat{\tau}} \right)_{dy} = 2 \frac{2\alpha_s}{3\pi} \left( \frac{M^2(1-\hat{\tau})^2}{\hat{\tau}^4 \pi m_D^2} \right)^{\epsilon/2} \frac{\Gamma(1+\frac{\epsilon}{2})}{\Gamma(1+\epsilon)} \left\{ \frac{1+\hat{\tau}^2}{1-\hat{\tau}} \frac{2}{\epsilon} + \frac{\epsilon(1-\hat{\tau})}{1+\epsilon} \right\}.$$

Integrate this over  $\hat{\tau}$  and show that

$$\begin{aligned} (\hat{\sigma}_{DR}(\text{real}))_{DY} &= \int_0^1 \frac{d\hat{\sigma}_q}{d\hat{\tau}} d\hat{\tau} = \\ &\frac{2\alpha_s}{3\pi} \sigma_0 \left( \frac{M^2}{4\pi m_D^2} \right)^{\epsilon/2} \Gamma\left(1 - \frac{\epsilon}{2}\right) \\ &\left\{ \frac{8}{\epsilon^2} - \frac{6}{\epsilon} + \frac{9}{2} + \dots \right\}. \end{aligned}$$

5.12. Expand (5.4.11) in powers of  $\epsilon$  and verify that

$$\frac{1}{\sigma_0} \left( \frac{d\hat{\sigma}_{DR,DY}^q}{d\hat{\tau}} \right)_+ = 2 \frac{\alpha_s}{2\pi} P_{q \rightarrow gg}(\hat{\tau}) \log(M^2/m_D^2) + 2\alpha_s f_{DR}^{q,DY}(\hat{\tau}),$$

where

$$P_{q \rightarrow gg}(\hat{\tau}) = \frac{4}{3} \left( \frac{1+\hat{\tau}^2}{1-\hat{\tau}} \right)_+,$$

and

$$\begin{aligned} \alpha_s f_{DR}^{q,DY}(\hat{\tau}) &= \frac{2\alpha_s}{3\pi} \left\{ 2(1+\hat{\tau}^2) \left( \frac{\log(1-\hat{\tau})}{1-\hat{\tau}} \right)_+ \right. \\ &- \frac{1+\hat{\tau}^2}{1-\hat{\tau}} \log(\hat{\tau}) - \left( \frac{\pi^2}{3} + \frac{9}{4} \right) \delta(1-\hat{\tau}) \Big\} \\ &+ \frac{\alpha_s}{2\pi} P_{q \rightarrow gg}(\hat{\tau}) \left\{ \frac{2}{\epsilon} + \gamma_E - \log(4\pi) \right\}. \end{aligned}$$

5.13. Show that in  $N$  spacetime dimensions the matrix element squared for the "Compton" subprocess  $q + g \rightarrow \gamma_\Sigma^* + q$  is given by

$$\begin{aligned} |\overline{\mathcal{M}}(q + g \rightarrow \gamma_\Sigma^* + q)|^2 &= 16\pi^2 \alpha_N^{QED} \alpha_N^{QCD} e_q^2 \frac{1}{3} \left(1 + \frac{\epsilon}{2}\right) \left\{ \frac{2 + \frac{1}{2}(1-\hat{\tau})^2(1-y)^2 - 2\hat{\tau}(1-\hat{\tau})(1+y)}{(1-\hat{\tau})(1-y)} \right. \\ &\quad \left. + \frac{(\hat{\tau} + \frac{1}{2}(1-\hat{\tau})(1+y))^2}{(1-\hat{\tau})(1-y)} \epsilon \right\}, \end{aligned}$$

where  $N = 4 + \epsilon$ ,  $\hat{\tau} = M^2/\hat{s}$ ,  $\hat{t} = -\hat{s}(1-\hat{\tau})(1-y)/2$ , and  $\hat{u} = -\hat{s}(1-\hat{\tau})(1+y)/2$ . Verify that

$$I = \int_{-1}^1 dy (1-y^2)^{\epsilon/2} |\overline{\mathcal{M}}|^2 = 16\pi^2 \alpha_N^{QED} \alpha_N^{QCD} e_q^2 \frac{1}{3} \left(1 + \frac{\epsilon}{2}\right) \frac{2^\epsilon}{(1-\hat{\tau})} \frac{\Gamma^2(1+\frac{\epsilon}{2})}{\Gamma(1+\epsilon)} \left\{ 2(\hat{\tau}^2 + (1-\hat{\tau})^2) \frac{2}{\epsilon} + 2\left(\frac{3}{2} + \hat{\tau} - \frac{3}{2}\hat{\tau}^2\right) \right\}.$$

Using (5.4.3) and (5.4.9) show that

$$\left( \frac{1}{\sigma_0} \frac{d\hat{\sigma}_{DR}^g}{d\hat{\tau}} \right)_{DY} = \frac{\alpha_s}{2\pi} \left( \frac{M^2(1-\hat{\tau})^2}{\hat{\tau}4\pi m_D^2} \right)^{\epsilon/2} \frac{\Gamma(1+\frac{\epsilon}{2})}{\Gamma(1+\epsilon)} \left\{ \frac{1}{2}(\hat{\tau}^2 + (1-\hat{\tau})^2) \frac{2}{\epsilon} + \frac{1}{2} \left( \frac{3}{2} + \hat{\tau} - \frac{3}{2}\hat{\tau}^2 \right) \right\}.$$

Expand this in powers of  $\epsilon$  and verify that

$$\frac{1}{\sigma_0} \left( \frac{d\hat{\sigma}_{DR}^g}{d\hat{\tau}} \right)_{DY} = \frac{\alpha_s}{2\pi} P_{g \rightarrow q\bar{q}}(\hat{\tau}) \log(M^2/m_D^2) + \alpha_s f_{DR}^{g,DY}(\hat{\tau}),$$

where

$$P_{g \rightarrow q\bar{q}}(\hat{\tau}) = \frac{1}{2}(\hat{\tau}^2 + (1-\hat{\tau})^2),$$

and

$$\begin{aligned} \alpha_s f_{DR}^{g,DY}(\hat{\tau}) = & \frac{\alpha_s}{2\pi} \frac{1}{2} \left\{ (\hat{\tau}^2 + (1-\hat{\tau})^2) \log \left( \frac{(1-\hat{\tau})^2}{\hat{\tau}} \right) \right. \\ & \left. - \frac{3}{2}\hat{\tau}^2 + \hat{\tau} + \frac{3}{2} \right\} \\ & + \frac{\alpha_s}{2\pi} P_{g \rightarrow q\bar{q}}(\hat{\tau}) \left\{ \frac{2}{\epsilon} + \gamma_E - \log(4\pi) \right\}. \end{aligned}$$

- 5.14. Substitute  $G_{p \rightarrow q}^{DY}(x, M^2)$  and  $G_{p \rightarrow \bar{q}}^{DY}(x, M^2)$  defined in (5.5.5) and (5.5.6), respectively, into (5.5.3) and show that to order  $\alpha_s$ , (5.5.3) is the same as (5.5.1) provided

$$\sigma_{tot}^{DY}/\sigma_0 = 1 + \alpha_s I_q^{DY} + \dots,$$

where

$$\alpha_s I_q^{DY} = \alpha_s \left( \frac{8\pi}{9} - \frac{7}{3\pi} \right).$$

- 5.15. Show that the term

$$\frac{2\alpha_s}{3\pi} (1 + \hat{\tau}^2) \left( \frac{\log(1-\hat{\tau})}{1-\hat{\tau}} \right)_+$$

that appears in the expression for  $\Delta f_q^{DY}$  given in (5.5.29) results in the behavior

$$\frac{G_{p \rightarrow q}^{DY}(x, Q^2)}{G_{p \rightarrow q}(x, Q^2)} \xrightarrow{x \rightarrow 1} 1 + \frac{\alpha_s(Q^2)}{3\pi} \log^2(1-x),$$

where  $G_{p \rightarrow q}^{DY}(x, Q^2)$  are defined in (5.5.9) and  $G_{p \rightarrow q}(x, Q^2)$  are the reference distributions defined in deep inelastic scattering.

- 5.16. Show that the term

$$\frac{2\alpha_s}{3\pi} \frac{3}{2} \frac{1}{(1-\hat{\tau})_+}$$

that appears in the expression for  $\Delta f_q^{DY}$  given in (5.5.29) results in the behavior

$$\frac{G_{p \rightarrow q}^{DY}(x, Q^2)}{G_{p \rightarrow q}(x, Q^2)} \xrightarrow{x \rightarrow 1} 1 + \frac{\alpha_s(Q^2)}{\pi} \log(1-x),$$

where  $G_{p \rightarrow q}^{DY}(x, Q^2)$  are defined in (5.5.9) and  $G_{p \rightarrow q}(x, Q^2)$  are the reference distributions defined in deep inelastic scattering.

- 5.17. Substitute  $\hat{G}_{p \rightarrow q}^{DY}(x, M^2)$  and  $\hat{G}_{p \rightarrow \bar{q}}^{DY}(x, M^2)$  defined in (5.5.33) and (5.5.34), respectively, into (5.5.32) and show that to order  $\alpha_s$ , (5.5.31) is the same as (5.5.1) provided

$$\sigma_{tot}^{DY}/\sigma_0 = 1 + \alpha_s I_q^{DY} + \dots,$$

where

$$\alpha_s I_q^{DY} = \alpha_s \left( \frac{8\pi}{9} - \frac{7}{3\pi} \right).$$

Show that with this definition of "Drell-Yan" parton distribution functions that

$$\begin{aligned} \int_0^1 (\hat{G}_{p \rightarrow q_i}^{DY}(x, M^2) - \hat{G}_{p \rightarrow \bar{q}_i}^{DY}(x, M^2)) dx = \\ \int_0^1 (G_{p \rightarrow q_i}(x, M^2) - G_{p \rightarrow \bar{q}_i}(x, M^2)) dx, \end{aligned}$$

so that (to order  $\alpha_s$ ) the net number of quarks in the proton is the same for the "Drell-Yan" distributions as for the reference distributions.

- 5.18. Starting from

$$\frac{d\sigma}{dM^2}(s, M^2) = G_{p \rightarrow q}^{(0)}(x_a) dx_a G_{p \rightarrow \bar{q}}^{(0)}(x_b) dx_b \left( \frac{d\hat{\sigma}}{dM^2 dt} \right) dt$$

in (5.6.3) show that

$$\begin{aligned} \frac{d\sigma}{dM^2 dy d^2 p_T}(s, M^2, y, p_T) = & \int_{x_a^{\min}}^1 dx_a G_{p \rightarrow q}^{(0)}(x_a) G_{p \rightarrow \bar{q}}^{(0)}(x_b) \\ & \left( \frac{x_a x_b}{x_a - x_1} \right) \left( \frac{1}{\pi} \frac{d\hat{\sigma}}{dM^2 dt}(\hat{s}, \hat{t}) \right), \end{aligned}$$

where

$$\begin{aligned}x_a^{\min} &= \frac{x_1 - \tau}{1 - x_1}, \\x_b &= \frac{x_a x_b - \tau}{x_a - x_1}, \\s &= x_a x_b s, \\t &= -x_a s x_2 + M^2, \\u &= -x_b s x_1 + M^2, \\x_1 &= \frac{1}{2}(x_T^2 + 4\tau)^{\frac{1}{2}} e^y, \\x_2 &= \frac{1}{2}(x_T^2 + 4\tau)^{\frac{1}{2}} e^{-y}, \\x_T &= 2p_T/\sqrt{s}.\end{aligned}$$

- 5.19. Show that if one neglects the  $M^2$  dependence of the structure functions so that

$$\begin{aligned}G_{p \rightarrow q_i}(x, M^2) &= G_{p \rightarrow q_i}(x), \\G_{p \rightarrow g}(x, M^2) &= G_{p \rightarrow g}(x),\end{aligned}$$

then the contributions from the "annihilation" and "Compton" subprocess in Fig. 5.2 and Fig. 5.3, respectively, can be written in the form

$$\begin{aligned}M^2 p_T^2 \frac{d\sigma_A}{d\tau dy dp_T^2}(s, M^2, y, p_T) &= \alpha_s F_A(\tau, y, x_T), \\M^2 p_T^2 \frac{d\sigma_C}{d\tau dy dp_T^2}(s, M^2, y, p_T) &= \alpha_s F_C(\tau, y, x_T),\end{aligned}$$

where  $F_A(\tau, y, x_T)$  and  $F_C(\tau, y, x_T)$  are functions of the dimensionless variables  $\tau$ ,  $y$ , and  $x_T$ . Determine  $F_A(\tau, y, x_T)$  and  $F_C(\tau, y, x_T)$ .

- 5.20. Show that the contribution from the "annihilation" subprocess  $q + \bar{q} \rightarrow \mu^+ \mu^- + g$  to the muon pair invariant cross section is given by

$$\begin{aligned}\frac{d\sigma_{DY}}{dM^2 dp_T^2}(s, M^2, p_T) &= \int_{\tau_+}^1 dx_a \int_{\tau_+/x_a}^1 dx_b P_{q\bar{q}}^{DIS}(x_a, x_b, M^2) \\&\quad \left( \frac{x_a x_b}{V} \right) \frac{d\hat{\sigma}}{dM^2 d\hat{t}}(q + \bar{q} \rightarrow \mu^+ \mu^- + g; \hat{s}, \hat{t}),\end{aligned}$$

where the joint  $q\bar{q}$  probability is given in (5.5.15) and

$$\begin{aligned}\tau &= M^2/s, \\x_T &= 2p_T/\sqrt{s}, \\s &= x_a x_b s, \\t &= \frac{1}{2}s(\tau - x_a x_b + V), \\u &= \frac{1}{2}s(\tau - x_a x_b - V), \\V^2 &= (\tau - x_a x_b)^2 - x_T^2 x_a x_b = (x_a x_b - \tau_+)(x_a x_b - \tau_-), \\\tau_{\pm} &= \frac{1}{4}(x_T \pm \bar{x}_T)^2, \\bar{x}_T^2 &= x_T^2 + 4\tau.\end{aligned}$$

Verify that the "annihilation" differential cross section is given by

$$\frac{d\hat{\sigma}_A}{dM^2 d\hat{t}} = \frac{8\alpha^2 \alpha_s e_q^2}{27 M^2 \hat{s}^2} \left\{ \frac{(\hat{t} - M^2)^2 + (\hat{u} - M^2)^2}{\hat{t} \hat{u}} \right\}.$$

Show that if one neglects the  $M^2$  dependence of the parton distribution functions so that

$$P_{q\bar{q}}(x_a, x_b, M^2) = P_{q\bar{q}}(x_a, x_b),$$

then

$$M^4 \frac{d\sigma_{DY}}{dM^2 dp_T^2} = \frac{\alpha_s}{p_T^2} F_A(\tau, x_T),$$

where

$$\begin{aligned}F_A(\tau, x_T) &= \frac{8\alpha^2}{27} \tau \int_{\tau_+}^1 dx_a \int_{\tau_+/x_a}^1 dx_b \frac{P_{q\bar{q}}(x_a, x_b)}{V} \\&\quad \left( 1 + \frac{\tau^2}{x_a^2 x_b^2} - \frac{x_T^2}{2x_a x_b} \right).\end{aligned}$$

Show that in the limit  $x_T \rightarrow 0$  that

$$\frac{d\sigma_{DY}}{dM^2 dp_T^2} \Big|_{p_T \rightarrow 0} \approx \left( \frac{d\sigma_{DY}}{dM^2} \right)_{\text{Born}} \frac{4\alpha_s}{3\pi} \frac{1}{p_T^2} \log \left( \frac{2(1-\tau)}{x_T^2 \sqrt{\tau}} \right),$$

where

$$\left( \frac{d\sigma_{DY}}{dM^2} \right)_{\text{Born}} = \frac{4\pi\alpha^2}{9M^2 s} \int_{\tau}^1 \frac{dx_a}{x_a} P_{q\bar{q}}(x_a, \tau/x_a).$$

- 5.21. Show that the transverse momentum spectrum in (5.7.14) vanishes at  $p_T = 0$  and behaves like  $1/p_T^2$  at large  $p_T$ . Also show that the distribution peaks

roughly at the point

$$(p_T^2)_{\text{peak}} \approx \frac{s}{2} \exp\left(-\frac{3\pi}{4\alpha_s}\right).$$

Determine  $(p_T^2)_{\text{peak}}$  for the data in Fig. 5.9 and consider whether or not it would be washed out by the intrinsic transverse momentum of the partons within the incident protons.

- 5.22. Using the Feynman rules given in Appendix C verify that

$$|\bar{\mathcal{M}}(u + \bar{d}_s \rightarrow W^+)|^2 = \frac{1}{3} \frac{1}{4} 8 g_W^2 \hat{s},$$

where  $g_W$  is the dimensionless weak coupling

$$g_W^2 = \frac{G_F M_W^2}{\sqrt{2}} = \frac{\pi \alpha}{2 x_W},$$

and  $x_W$  is the square of the sine of the Weinberg angle,  $x_W = \sin^2(\theta_W)$  and  $G_F$  is the Fermi constant. Show that in the naive parton model

$$\sigma(p + p \rightarrow W^\pm + X; s) = \frac{2\pi g_W^2}{3s} \int_{\tau_W}^1 \frac{dx_a}{x_a} P_{q\bar{q}W^\pm}(x_a, \tau_W/x_b),$$

where  $\tau_W = M_W/s$  and the joint probabilities  $P_{q\bar{q}W^\pm}$  are given in (5.8.14) and (5.8.15).

- 5.23. Show that in the naive parton model the total cross section for producing  $Z^0$  bosons in proton-proton collisions is given by

$$\sigma(p + p \rightarrow Z^0 + X; s) = 2\sqrt{2}\pi G_F \tau_Z \frac{1}{3} \int_{\tau_Z}^1 \frac{dx_a}{x_a} P_{q\bar{q}Z}(x_a, \tau_Z/x_b),$$

where  $\tau_Z = M_Z^2/s$  and where the joint probability  $P_{q\bar{q}Z}$  is given by

$$\begin{aligned} P_{q\bar{q}Z}(x_a, x_b) &= [G_{p \rightarrow u}(x_a)G_{p \rightarrow \bar{u}}(x_b) + G_{p \rightarrow \bar{u}}(x_a)G_{p \rightarrow u}(x_b)] \\ &\quad [\frac{1}{4} - \frac{2}{3}x_W + \frac{8}{9}x_W^2] \\ &+ [G_{p \rightarrow d}(x_a)G_{p \rightarrow \bar{d}}(x_b) + G_{p \rightarrow \bar{d}}(x_a)G_{p \rightarrow d}(x_b)] \\ &+ [G_{p \rightarrow s}(x_a)G_{p \rightarrow \bar{s}}(x_b) + G_{p \rightarrow \bar{s}}(x_a)G_{p \rightarrow s}(x_b)] [\frac{1}{4} - \frac{1}{3}x_W + \frac{2}{9}x_W^2], \end{aligned}$$

where  $x_W = \sin^2(\theta_W)$  is the square of the sine of the Weinberg angle.

- 5.24. Verify that for massless partons the differential cross section for the “annihilation” subprocess  $q + \bar{q} \rightarrow W^\pm + g$  is given by

$$\frac{d\hat{\sigma}_A}{dt}(\hat{s}, \hat{t}) = \frac{2\pi\alpha_s}{\hat{s}^2} \frac{g_W^2}{4\pi} \frac{8}{9} \left\{ \frac{\hat{t}^2 + \hat{u}^2 + 2M_W^2 \hat{s}}{\hat{t}\hat{u}} \right\},$$

which is the same as differential cross section  $q + \bar{q} \rightarrow \gamma_\Sigma^* + g$  and the differential cross section for the “Compton” subprocess  $q + g \rightarrow W^\pm + q$  is

given by

$$\frac{d\hat{\sigma}_C}{dt}(\hat{s}, \hat{t}) = \frac{2\pi\alpha_s}{\hat{s}^2} \frac{g_W^2}{4\pi} \frac{1}{3} \left\{ \frac{\hat{t}^2 + \hat{s}^2 + 2M_W^2 \hat{u}}{-\hat{s}\hat{t}} \right\}.$$

- 5.25. Show that at order  $\alpha_s$ , the  $W^\pm$  cross section becomes

$$\begin{aligned} \sigma(p + p \rightarrow W^\pm + X; s)_{\text{order } \alpha_s} &= \frac{\sigma_{\text{tot}}^W}{\sigma_0} \sigma(p + p \rightarrow W^\pm + X, s)_{\text{leading order}} \\ &+ \sqrt{2}\pi G_F \frac{1}{3} \int_{\tau_W}^1 \frac{dx_a}{x_a} \int_{\tau_W/x_a}^1 \frac{dx_b}{x_b} P_{q\bar{q}W^\pm}^{DIS}(x_a, x_b, M_W^2) 2\alpha_s \Delta f_q^{DY}(\hat{\tau}_W) \\ &+ \sqrt{2}\pi G_F \frac{1}{3} \int_{\tau_W}^1 \frac{dx_a}{x_a} \int_{\tau_W/x_a}^1 \frac{dx_b}{x_b} P_{q\bar{q}W^\pm}^{DIS}(x_a, x_b, M_W^2) \alpha_s \Delta f_g^{DY}(\hat{\tau}_W) \\ &+ \sqrt{2}\pi G_F \frac{1}{3} \int_{\tau_W}^1 \frac{dx_a}{x_a} \int_{\tau_W/x_a}^1 \frac{dx_b}{x_b} P_{q\bar{q}W^\pm}^{DIS}(x_a, x_b, M_W^2) \alpha_s \Delta f_g^{DY}(\hat{\tau}_W), \end{aligned}$$

where  $\hat{\tau}_W = \tau_W/(x_a x_b)$ ,  $\tau_W = M_W^2/s$ , and where  $\Delta f_q^{DY}$  and  $\Delta f_g^{DY}$  are the same functions that appear in the Drell-Yan case, (5.5.11) and (5.5.12), respectively, and the joint probabilities  $q\bar{q}W^\pm$ ,  $qgW^\pm$ , and  $\bar{q}gW^\pm$  are given in terms of the deep inelastic scattering reference distributions according to (5.8.24), (5.8.25), and (5.8.27)-(5.8.30), and where

$$\begin{aligned} \sigma_{\text{tot}}^W &= \sigma_0 (1 + \alpha_s I_q^{DY} + \dots) \\ &= \sigma_0 \left\{ 1 + \left( \frac{8\pi}{9} - \frac{7}{3\pi} \right) \alpha_s + \dots \right\}. \end{aligned}$$

#### Further Reading

G. Altarelli, “Partons in Quantum Chromodynamics,” *Physics Reports* 81, 1 (1982).

R. K. Ellis, “An Introduction to the QCD Parton Model”, Fermilab preprint, FNAL-CONF-88/60-T, 1988.

#### References

1. S.D. Drell and T.M. Yan, *Phys. Rev. Lett.* 25, 316 (1970).
2. J. Kubar-Andre and F. Paige, *Phys. Rev. D* 19, 221 (1979).
3. G. Altarelli, R.K. Ellis, and G. Martinelli, *Nucl. Phys.* B143, 521 (1978). *Erratum* B146, 544 (1978).

4. G. Parisi, *Phys. Lett.* **90B**, 295 (1980).
5. G. Curci and M. Greco, *Phys. Lett.* **92B**, 175 (1980).
6. H.D. Politzer, *Nucl. Phys.* **B129**, 301 (1977).
7. C.T. Sachrada, *Phys. Lett.* **73B**, 185 (1978).
8. F. Khalafi and W.J. Stirling, *Z. Phys.* **C18**, 315 (1983).
9. D. Antreasyan *et al.*, *Phys. Rev. Lett.* **48**, 302 (1982).
10. G. Altarelli, G. Parisi, and R. Petronzio, *Phys. Lett.* **76B**, 351 (1978).  
*ibid* **76B**, 356 (1978).
11. C. Quigg, *Rev. Mod. Phys.* **49**, 297 (1977).

## CHAPTER 6

## Renormalization and the Running Coupling Constant in QCD



In this chapter we will compute the effective coupling in QCD,  $\alpha_s(Q^2)$ , using the same dimensional regularization techniques developed in the previous chapters. An infinite set of ultraviolet divergent terms will be chosen and used to define an effective coupling. Normally renormalization is presented as a procedure in which one introduces counter terms to the Lagrangian thereby removing the ultraviolet divergences. There is a very nice discussion of the field theoretic approach to renormalization in the book by Pierre Ramond.<sup>1</sup> I will be less formal here and simply consider renormalization as a procedure in which one expresses experimental observables in terms of other experimental observables. Once this is done the theory should be finite and independent of any cut-offs used during the intermediate stages.

## 6.1 The Gluon Propagator – $Z_3$

First we consider the quark loop corrections to the gluon propagator shown in Fig. 6.1,

$$\Pi_{\mu\nu;ab}^q(q) = -g_N^2 n_f \text{tr}(\mathbf{T}_a \mathbf{T}_b) \int \frac{d^N k}{(2\pi)^N} \frac{\text{tr}[\gamma_\mu \not{k} \gamma_\nu (\not{k} - \not{q})]}{(k - q)^2 k^2}, \quad (6.1.1)$$

where I have summed over  $n_f$  quark flavors and the integral over the loop momentum,  $k$ , is performed in  $N$  spacetime dimensions and  $g_N$  is the  $N$ -dimensional coupling in (2.8.25). The color factor

$$\text{tr}(\mathbf{T}_a \mathbf{T}_b) = \frac{1}{2} \delta_{ab}, \quad (6.1.2)$$

is discussed in Appendix D and it is traditional to define

$$C_f = \frac{1}{2} n_f. \quad (6.1.3)$$

The trace is performed using (B.5.8) giving

$$\text{tr}[\gamma_\mu \not{k} \gamma_\nu (\not{k} - \not{q})] = 4 [g_{\mu\nu}(k \cdot q - k^2) - (k_\mu q_\nu + k_\nu q_\mu) + 2k_\mu k_\nu]. \quad (6.1.4)$$

We use the Feynman parameterization

$$\frac{1}{ab} = \int_0^1 dx \frac{1}{[ax + b(1-x)]^2}, \quad (6.1.5)$$

with

$$a = (k - q)^2 = k^2 - 2k \cdot q + q^2, \quad (6.1.6)$$

$$b = k^2, \quad (6.1.7)$$

giving

$$ax + b(1-x) = K^2 - C, \quad (6.1.8)$$

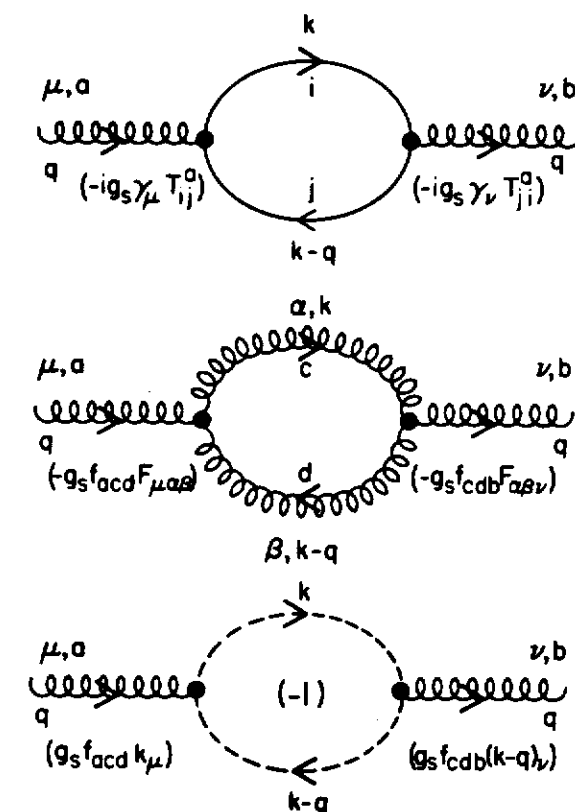


Figure 6.1 Order  $g_s^2$  corrections to the gluon propagator.

with

$$K = k - xq, \quad (6.1.9)$$

$$C = Q^2 x(1-x), \quad (6.1.10)$$

and

$$Q^2 = -q^2 > 0. \quad (6.1.11)$$

We now shift the integration from  $k \rightarrow K + xq$  arriving at

$$\Pi_{\mu\nu;ab}^q(q) = -g_N^2 C_f \delta_{ab} \int dx \int \frac{d^N K}{(2\pi)^N} \frac{N(k - K + xq)}{[K^2 - C]^2}, \quad (6.1.12)$$

where the shifted numerator is given by

$$\begin{aligned} N(k \rightarrow K + xq) = & -4g_{\mu\nu} \left[ x(1-x)Q^2 + \left( \frac{N-2}{N} \right) K^2 \right] \\ & - 8q_\mu q_\nu x(1-x), \end{aligned} \quad (6.1.13)$$

and where terms linear in  $K$  have been dropped since they do not contribute to the integral and the substitution

$$K_\mu K_\nu \rightarrow \frac{1}{N} g_{\mu\nu} K^2, \quad (6.1.14)$$

has been made. The integration over  $K$  is performed using (C.2.6) with the result

$$g_N^2 \int \frac{d^N K}{(2\pi)^N} \frac{1}{[K^2 - C]^2} = \frac{-ig_s^2}{16\pi^2} \frac{2}{\epsilon} f_K [x(1-x)]^{\epsilon/2}, \quad (6.1.15)$$

where

$$f_K = \Gamma \left( 1 - \frac{\epsilon}{2} \right) \left( \frac{Q^2}{4\pi m_D^2} \right)^{\epsilon/2}, \quad (6.1.16)$$

and

$$N = 4 + \epsilon. \quad (6.1.17)$$

The mass  $m_D$  comes from replacing the  $N$ -dimensional coupling  $g_N$  with the dimensionless coupling  $g_s$  defined in (2.8.25). Similarly,

$$g_N^2 \int \frac{d^N K}{(2\pi)^N} \frac{K^2}{[K^2 - C]^2} = \frac{-ig_s^2}{16\pi^2} \frac{2}{\epsilon} \left( \frac{4+\epsilon}{2+\epsilon} \right) f_K Q^2 [x(1-x)]^{1+\epsilon/2}. \quad (6.1.18)$$

So the complete integration over  $K$  is given by

$$\begin{aligned} \Pi_{\mu\nu;ab}^q(q) = & \frac{-ig_s^2}{16\pi^2} (C_f \delta_{ab}) \frac{16}{\epsilon} f_K \\ & (g_{\mu\nu} Q^2 + q_\mu q_\nu) \int_0^1 [x(1-x)]^{1+\epsilon/2} dx. \end{aligned} \quad (6.1.19)$$

The integration over  $x$  is easy,

$$\int_0^1 [x(1-x)]^{1+\epsilon/2} dx = \frac{\Gamma^2(2+\frac{\epsilon}{2})}{\Gamma(4+\epsilon)} = \frac{(2+\epsilon)}{4(1+\epsilon)(3+\epsilon)} f_x, \quad (6.1.20)$$

where

$$f_x = \frac{\Gamma^2(1+\frac{\epsilon}{2})}{\Gamma(1+\epsilon)}, \quad (6.1.21)$$

and (6.1.19) becomes

$$\Pi_{\mu\nu;ab}^q(q) = \frac{-ig_s^2}{16\pi^2} \delta_{ab} (g_{\mu\nu} Q^2 + q_\mu q_\nu) f_x f_K f_q, \quad (6.1.22)$$

where

$$f_q = C_f \frac{4(2+\epsilon)}{\epsilon(1+\epsilon)(3+\epsilon)} \rightarrow C_f \left\{ \frac{4}{3} \frac{2}{\epsilon} + \dots \right\}, \quad (6.1.23)$$

and  $f_K$  and  $f_x$  are given by (6.1.16) and (6.1.21), respectively. It is important that  $\Pi_{\mu\nu;ab}^q$  is proportional to  $\delta_{ab}$  as this is the same color factor appearing in the Born term expression for the gluon propagator. Also the factor  $(g_{\mu\nu} Q^2 + q_\mu q_\nu)$  insures that  $\Pi_{\mu\nu;ab}^q$  conserves current. Namely,

$$q_\mu \Pi_{\mu\nu;ab}^q = 0, \quad (6.1.24)$$

and

$$\Pi_{\mu\nu;ab}^q q_\nu = 0. \quad (6.1.25)$$

I have arranged factors so that  $f_K$  and  $f_x$  approach 1 as  $\epsilon \rightarrow 0$  so that the behavior of  $\Pi_{\mu\nu;ab}^q$  at the pole is governed by  $f_q$  and

$$f_q^{\text{pole}} = \frac{4}{3} C_f \left( \frac{2}{\epsilon_{\text{UV}}} \right). \quad (6.1.26)$$

Here I have labeled the  $1/\epsilon$  singularity by the subscript UV to remind us that it is an ultraviolet divergence. It arises from the integrations over  $K$  in (6.1.15) and (6.1.18).

The gluon loop in Fig. 6.1 gives a contribution of the form

$$\begin{aligned} \Pi_{\mu\nu;ab}^{g^0}(q) = & -g_N^2 \text{tr}(\mathbf{F}_a \mathbf{F}_b) \frac{1}{2} \\ & \int \frac{d^N K}{(2\pi)^N} \frac{F_{\mu\alpha\beta}(-q, k, (q-k)) F_{\alpha\beta\nu}(-k, -(q-k), q)}{(k-q)^2 k^2}, \end{aligned} \quad (6.1.27)$$

where I have used the Feynman gauge for the gluon propagator and where

$F_{\lambda\mu\nu}(p_1, p_2, p_3) = (p_1 - p_2)_\nu g_{\lambda\mu} + (p_2 - p_3)_\lambda g_{\mu\nu} + (p_3 - p_1)_\mu g_{\nu\lambda}$ , (6.1.28) comes from the triple-gluon coupling in Appendix C. The color factor arises from

$$\begin{aligned} f_{acd} f_{cdb} &= (\mathbf{F}_a)_{cd} (\mathbf{F}_a)_{dc} \\ &= \text{tr}(\mathbf{F}_a \mathbf{F}_b) = C_A \delta_{ab}, \end{aligned} \quad (6.1.29)$$

as can be deduced from Appendix D and  $C_A$  is the number of colors (i.e.,  $C_A = 3$ ). The factor of  $1/2$  the combinatorial factor arising from two identical bosons in a closed loop. With the same Feynman parameterization in (6.1.5) we have

$$\Pi_{\mu\nu;ab}^{g^0}(q) = -g_N^2 \frac{1}{2} C_A \delta_{ab} \int dx \int \frac{d^N K}{(2\pi)^N} \frac{N(k \rightarrow K + xq)}{[K^2 - C]^2}, \quad (6.1.30)$$

but in this case the shifted numerator is given by

$$N(k \rightarrow K + xq) = g_{\mu\nu} \left[ -2x(1-x)Q^2 + 5Q^2 - 6 \left( \frac{N-1}{N} \right) K^2 \right]$$

$$+ q_\mu q_\nu [2x(1-x)(2N-3) + (6-N)]. \quad (6.1.31)$$

If we now perform the  $K$  integrations using (6.1.15) and (6.1.18) and the  $x$  integration using (6.1.20) and

$$\int [x(1-x)]^{\epsilon/2} dx = \frac{1}{1+\epsilon} f_x, \quad (6.1.32)$$

we arrive at

$$\begin{aligned} \Pi_{\mu\nu;ab}^{g^0}(q) &= -\frac{ig_s^2}{16\pi^2} \delta_{ab} (g_{\mu\nu} Q^2 + q_\mu q_\nu) f_K f_x f_g^+ \\ &\quad - \frac{ig_s^2}{16\pi^2} \delta_{ab} (g_{\mu\nu} Q^2 - q_\mu q_\nu) f_K f_x f_g^-, \end{aligned} \quad (6.1.33)$$

with

$$f_g^+ = -C_A \left[ \frac{2(2+\epsilon)^2}{4\epsilon(1+\epsilon)(3+\epsilon)} + \frac{(11-2\epsilon)}{4\epsilon(1+\epsilon)} \right], \quad (6.1.34)$$

and

$$f_g^- = \frac{C_A}{4\epsilon(1+\epsilon)}. \quad (6.1.35)$$

Clearly something is wrong since  $\Pi_{\mu\nu;ab}^{g^0}$  does not conserve current. It contains a term proportional to  $(g_{\mu\nu} Q^2 - q_\mu q_\nu)$  as well as a current conserving term proportional to  $(g_{\mu\nu} Q^2 + q_\mu q_\nu)$ . This is the first time we have had to deal with this situation, but because of our choice to use a covariant gauge (rather than, for example, an axial gauge) we have introduced spurious gluon polarization states. These spurious states must be removed by computing a “ghost” contribution using the ghost- ghost-gluon couplings in Appendix C. Alternatively, we could have computed with an axial or “ghost free” gauge but it is usually much easier to use the simple Feynman gauge and add in the ghost contribution. The ghost loop contribution in Fig. 6.1 has the form of (6.1.30),

$$\Pi_{\mu\nu;ab}^0(q) = -g_N^2 C_A \delta_{ab} \int dx \int \frac{d^N K}{(2\pi)^N} \frac{N(k \rightarrow K+xq)}{[K^2 - C]^2}, \quad (6.1.36)$$

but the shifted numerator for the ghost contribution is

$$N(k \rightarrow K+xq) = g_{\mu\nu} \frac{K^2}{N} - q_\mu q_\nu x(1-x). \quad (6.1.37)$$

Remember to insert a  $(-1)$  for the ghost loop. Integrating over  $K$  and  $x$  gives

$$\begin{aligned} \Pi_{\mu\nu;ab}^0(q) &= -\frac{ig_s^2}{16\pi^2} \delta_{ab} (g_{\mu\nu} Q^2 + q_\mu q_\nu) f_K f_x f_0^+ \\ &\quad - \frac{ig_s^2}{16\pi^2} \delta_{ab} (g_{\mu\nu} Q^2 - q_\mu q_\nu) f_K f_x f_0^-, \end{aligned} \quad (6.1.38)$$

with

$$f_0^+ = \frac{C_A}{4\epsilon(3+\epsilon)}, \quad (6.1.39)$$

$$f_0^- = \frac{-C_A}{4\epsilon(1+\epsilon)}. \quad (6.1.40)$$

The ghost contribution also has both a current conserving and a current non-conserving term and the non-conserving term exactly cancels the non-conserving term in (6.1.35). The final result for the true gluon contribution is the sum

$$\begin{aligned} \Pi_{\mu\nu;ab}^g(q) &= \Pi_{\mu\nu;ab}^{g^0} + \Pi_{\mu\nu;ab}^0(q) \\ &= \frac{-ig_s^2}{16\pi^2} \delta_{ab} (g_{\mu\nu} Q^2 + q_\mu q_\nu) f_K f_x f_g, \end{aligned} \quad (6.1.41)$$

where

$$f_g = f_g^+ + f_0^+ = -C_A \frac{10+3\epsilon}{\epsilon(1+\epsilon)(3+\epsilon)} \rightarrow -C_A \left\{ \frac{5}{3} \frac{2}{\epsilon} + \dots \right\}, \quad (6.1.42)$$

and

$$f_g^{\text{pole}} = -\frac{5}{3} C_A \left( \frac{2}{\epsilon_{\text{UV}}} \right). \quad (6.1.43)$$

The “tadpole” diagram involving the four-gluon coupling vanishes in dimensional regularization<sup>2</sup> so the complete order  $g_s^2$  correction to the gluon propagator is the sum of the quark and gluon loops in (6.1.22) and (6.1.41). Namely,

$$\begin{aligned} \Pi_{\mu\nu;ab}(q) &= \Pi_{\mu\nu}^q(q) + \Pi_{\mu\nu}^g(q) \\ &= \frac{-ig_s^2}{16\pi^2} \delta_{ab} (g_{\mu\nu} Q^2 + q_\mu q_\nu) f_K f_x f_3, \end{aligned} \quad (6.1.44)$$

where

$$f_3 = f_q + f_g = \frac{C_f 4(2+\epsilon) - C_A(10+3\epsilon)}{\epsilon(1+\epsilon)(3+\epsilon)} \rightarrow (\frac{4}{3} C_f - \frac{5}{3} C_A) \frac{2}{\epsilon} + \dots, \quad (6.1.45)$$

and

$$f_3^{\text{pole}} = (\frac{4}{3} C_f - \frac{5}{3} C_A) \left( \frac{2}{\epsilon_{\text{UV}}} \right). \quad (6.1.46)$$

Again I have labeled the singularity by UV to remind us that it is an ultraviolet divergence. The renormalization factor  $Z_3$  is defined as the multiplicative factor correcting the gluon propagator so that

$$\begin{aligned} \left( \frac{-i\delta_{ab} g_{\mu\nu}}{q^2} \right) Z_3 &= \left( \frac{-i\delta_{ab} g_{\mu\nu}}{q^2} \right) + \left( \frac{-i\delta_{ac} g_{\mu\alpha}}{q^2} \right) \Pi_{\alpha\beta;cd}(q) \left( \frac{-i\delta_{db} g_{\beta\nu}}{q^2} \right) \\ &= \left( \frac{-i\delta_{ab} g_{\mu\nu}}{q^2} \right) \left( 1 + \frac{g_s^2}{16\pi^2} f_K f_x f_3 \right). \end{aligned} \quad (6.1.47)$$

Thus, to this order of perturbation theory

$$\begin{aligned} Z_3 &= 1 + \frac{g_s^2}{16\pi^2} f_K f_x f_3 \\ &= 1 + \frac{g_s^2}{16\pi^2} f_3 \frac{\Gamma(1 - \frac{\epsilon}{2}) \Gamma^2(1 + \frac{\epsilon}{2})}{\Gamma(1 + \epsilon)} \left( \frac{Q^2}{4\pi m_D^2} \right)^{\epsilon/2}, \end{aligned} \quad (6.1.48)$$

with  $f_3$  and  $f_3^{\text{pole}}$  given by (6.1.45) and (6.1.46), respectively.

## 6.2 Quark Self-Energy Corrections – $Z_2$

We have already computed the quark self-energy corrections in Chapter 2. Defining

$$\Sigma(p) = -ip \bar{\Sigma}, \quad (6.2.1)$$

as in (2.4.37) and shown in Fig. 2.8, (2.9.7) gives for a single quark color

$$\bar{\Sigma} = \frac{g_s^2}{16\pi^2} (\mathbf{T}_b \mathbf{T}_b) \left( \frac{-p^2}{4\pi m_D^2} \right)^{\epsilon/2} \frac{\Gamma(1 - \frac{\epsilon}{2}) \Gamma^2(1 + \frac{\epsilon}{2})}{\Gamma(1 + \epsilon)} \frac{(2 + \epsilon)}{\epsilon(1 + \epsilon)}, \quad (6.2.2)$$

where I have chosen the Feynman gauge ( $\eta = 0$ ). The renormalization factor  $Z_2$  is defined by

$$-(Z_2^{-1} - 1) = \bar{\Sigma}, \quad (6.2.3)$$

or

$$Z_2 = \frac{1}{1 - \bar{\Sigma}}, \quad (6.2.4)$$

so that to order  $g_s^2$

$$Z_2 = 1 + \frac{g_s^2}{16\pi^2} f_2 \left( \frac{-p^2}{4\pi m_D^2} \right)^{\epsilon/2} \frac{\Gamma(1 - \frac{\epsilon}{2}) \Gamma^2(1 + \frac{\epsilon}{2})}{\Gamma(1 + \epsilon)}, \quad (6.2.5)$$

where

$$f_2 = (\mathbf{T}_b \mathbf{T}_b) \frac{(2 + \epsilon)}{\epsilon(1 + \epsilon)} \rightarrow (\mathbf{T}_b \mathbf{T}_b) \left\{ \frac{2}{\epsilon} + \dots \right\}, \quad (6.2.6)$$

and

$$f_2^{\text{pole}} = (\mathbf{T}_b \mathbf{T}_b) \left( \frac{2}{\epsilon_{UV}} \right). \quad (6.2.7)$$

I have labeled the singularity by UV to remind ourselves that it is an ultraviolet divergence.

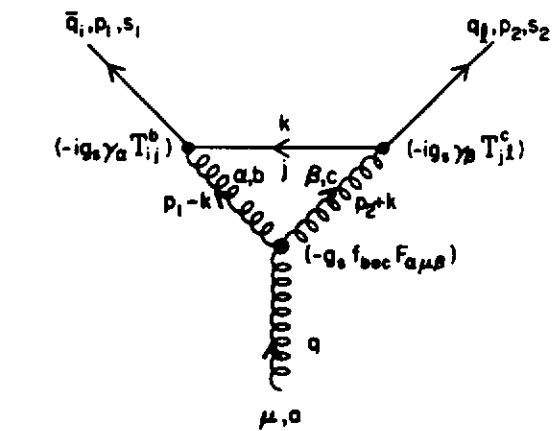
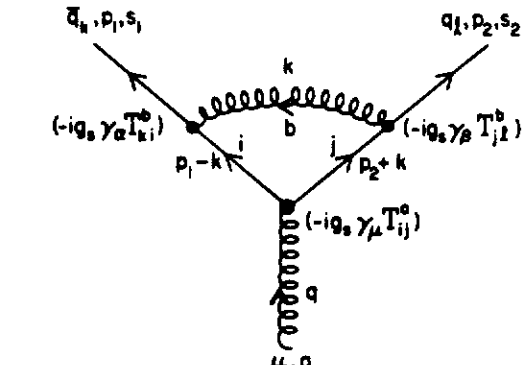


Figure 6.2 Order  $g_s^2$  corrections to the  $q\bar{q}g$  vertex.

## 6.3 Vertex Corrections – $Z_1$

The Born term vertex

$$-ig_s \mathbf{T}_a \gamma_\mu, \quad (6.3.1)$$

in Appendix C is modified by two corrections at order  $g_s^2$  as shown in Fig. 6.2. The first term does not involve the triple-gluon coupling and is given by

$$\bar{\Gamma}_\mu^{(1)} = ig_N^2 \left( -\frac{1}{2} C_A + \mathbf{T}_b \mathbf{T}_b \right) \int \frac{d^N k}{(2\pi)^N} \frac{\gamma_\alpha (\not{p}_1 - \not{k}) \gamma_\mu (\not{p}_2 + \not{k}) \gamma_\alpha}{(p_1 - k)^2 (p_2 + k)^2 k^2}, \quad (6.3.2)$$

where  $g_N$  is the  $N$ -dimensional coupling in (2.8.25) and where again I have chosen the Feynman gauge. The complete vertex to this order is given by

$$-ig_s \mathbf{T}_a \Gamma_\mu = -ig_s \mathbf{T}_a (\gamma_\mu + \bar{\Gamma}_\mu) = -ig_s \mathbf{T}_a \gamma_\mu (1 + \bar{\Gamma}). \quad (6.3.3)$$

The color factor is very important and arises from

$$\begin{aligned} \mathbf{T}_b \mathbf{T}_a \mathbf{T}_b &= [\mathbf{T}_b, \mathbf{T}_a] \mathbf{T}_b + \mathbf{T}_a \mathbf{T}_b \mathbf{T}_b \\ &= if_{bac} \mathbf{T}_c \mathbf{T}_b + \mathbf{T}_a \mathbf{T}_b \mathbf{T}_b, \end{aligned} \quad (6.3.4)$$

and

$$\begin{aligned} f_{bac} \mathbf{T}_c \mathbf{T}_b &= f_{bac} \frac{1}{2} (\frac{1}{3} \delta_{cb} + (d_{cbd} + if_{cbd}) \mathbf{T}_d) \\ &= \frac{i}{2} f_{bac} f_{cbd} \mathbf{T}_d \\ &= \frac{i}{2} (\mathbf{F}_a)_{bc} (\mathbf{F}_d)_{cb} \mathbf{T}_d \\ &= \frac{i}{2} \text{tr}(\mathbf{F}_a \mathbf{F}_d) \mathbf{T}_d \\ &= \frac{i}{2} C_A \mathbf{T}_a, \end{aligned} \quad (6.3.5)$$

so that

$$\mathbf{T}_b \mathbf{T}_a \mathbf{T}_b = \mathbf{T}_a (-\frac{1}{2} C_A + \mathbf{T}_b \mathbf{T}_b), \quad (6.3.6)$$

where  $C_A$  is defined in (6.1.29). Except for the color factor this is the same calculation we did in Chapter 2. Nevertheless, it is instructive to repeat the calculation in a slightly different manner. This time let's try the Feynman parameterization in (C.2.2). Namely,

$$\frac{1}{k^2(p_1-k)^2(p_2+k)^2} = 2 \int dz_1 \int dz_2 \int dz_3 \frac{\delta(1-z_1-z_2-z_3)}{[k^2 z_1 + (p_1-k)^2 z_2 + (p_2+k)^2 z_3]^3}, \quad (6.3.7)$$

so that (6.3.2) becomes

$$\begin{aligned} \bar{\Gamma}_\mu^{(1)} &= ig_N^2 (-\frac{1}{2} C_A + \mathbf{T}_b \mathbf{T}_b) 2 \int_0^1 dz_2 \int_0^{1-z_2} dz_1 \\ &\quad \int \frac{d^N K}{(2\pi)^N} \frac{N_\mu(k \rightarrow K + p_1 z_2 - p_2 z_3)}{[K^2 - C]^3}, \end{aligned} \quad (6.3.8)$$

where

$$z_3 = 1 - z_1 - z_2, \quad (6.3.9)$$

and

$$K = k - p_1 z_2 + p_2 z_3, \quad (6.3.10)$$

$$C = Q^2 z_2 z_3, \quad (6.3.11)$$

with

$$Q^2 = -q^2 = -(p_1 + p_2)^2 > 0, \quad (6.3.12)$$

and  $q^2$  is the virtual gluon 4-momentum squared which we take as spacelike. The shifted numerator has the form

$$\begin{aligned} N_\mu(k \rightarrow K + p_1 z_2 - p_2 z_3) &= A_1 \not{p}_1 \gamma_\mu \not{p}_1 + A_2 \not{p}_2 \gamma_\mu \not{p}_2 + A_3 \not{p}_1 \gamma_\mu \not{p}_2 \\ &\quad + A_4 \not{p}_2 \gamma_\mu \not{p}_1 + A_5 K^2 \gamma_\mu, \end{aligned} \quad (6.3.13)$$

where I have used

$$K \gamma_\mu K = K_\alpha K_\beta \gamma_\alpha \gamma_\mu \gamma_\beta \rightarrow \frac{K^2}{N} \gamma_\alpha \gamma_\mu \gamma_\alpha = \frac{(2-N)}{N} K^2 \gamma_\mu. \quad (6.3.14)$$

The Dirac equation for massless quarks guarantees that

$$\bar{u}(p_1, s_1) \not{p}_1 = 0, \quad (6.3.15)$$

and

$$\not{p}_2 v(p_2, s_2) = 0, \quad (6.3.16)$$

so that the surviving terms in the shifted numerator are

$$N_\mu(k \rightarrow K + p_1 z_2 - p_2 z_3) = (A_4 Q^2 + A_5 K^2) \gamma_\mu, \quad (6.3.17)$$

where

$$A_4 = (2 + \epsilon)(z_2^2 + z_1 z_2 - z_2) - 2z_1, \quad (6.3.18)$$

$$A_5 = -\frac{(2 + \epsilon)^2}{(4 + \epsilon)}. \quad (6.3.19)$$

In arriving at (6.3.17) I have used the fact that in the numerator of the integral over  $K$ ,

$$\not{p}_2 \gamma_\mu \not{p}_1 \rightarrow -2p_1 \cdot p_2 \gamma_\mu = Q^2 \gamma_\mu. \quad (6.3.20)$$

For the  $A_4$  term the integration over  $K$  is performed using

$$g_N^2 \int \frac{d^N K}{(2\pi)^N} \frac{1}{[K^2 - C]^3} = \frac{-ig_s^2}{16\pi^2 Q^2} \frac{1}{2} (z_2 z_3)^{\frac{1}{2}-1} f_K, \quad (6.3.21)$$

with  $f_K$  given by (6.1.16). There are no ultraviolet (UV) divergences in the  $A_4$  term, only infrared divergences that arise from the integrals over  $z_1$  and  $z_2$ . For example,

$$\begin{aligned} &\int_0^1 dz_2 \int_0^{1-z_2} dz_1 z_1 (z_2 z_3)^{\frac{1}{2}-1} \\ &= \int_0^1 dz_2 \int_0^{1-z_2} dz_1 z_1 z_2^{\frac{1}{2}-1} (1 - z_1 - z_2)^{\frac{1}{2}-1} \\ &= \int_0^1 dz_2 z_2^{\frac{1}{2}-1} (1 - z_2)^{\frac{1}{2}+1} \int_0^1 dv v (1 - v)^{\frac{1}{2}-1} \end{aligned}$$

$$= \frac{4}{\epsilon^2(1+\epsilon)} f_x, \quad (6.3.22)$$

where  $f_x$  is given in (6.1.21) and where I removed the nested integrals by the change of variable  $z_1 = v(1-z_2)$ . The  $A_4$  term gives

$$2 \int_0^1 dz_2 \int_0^{1-z_2} dz_1 \int \frac{d^N K}{(2\pi)^N} \frac{A_4 Q^2}{[K^2 - C]^3} = \frac{-i}{16\pi^2} f_x f_K f_4^{(1)}, \quad (6.3.23)$$

with

$$f_4^{(1)} = -\frac{8 + \epsilon^2}{\epsilon^2(1+\epsilon)} \rightarrow -\frac{8}{\epsilon_{IR}^2} + \frac{8}{\epsilon_{IR}} - 9 + \dots \quad (6.3.24)$$

The final form of  $f_4^{(1)}$  comes from expanding in powers of  $\epsilon$  and dropping terms that vanish as  $\epsilon \rightarrow 0$ . Furthermore, the  $1/\epsilon^2$  and  $1/\epsilon$  singularities are labeled with an IR to remind us that they are infrared singularities.

The  $A_5$  term in (6.3.17) produces an ultraviolet singularity. The integral over  $K$  is given by

$$g_N^2 \int \frac{d^N K}{(2\pi)^N} \frac{K^2}{[K^2 - C]^3} = \frac{-ig_s^2}{16\pi^2} \frac{1}{2} (z_2 z_3)^{\epsilon/2} \left( \frac{4}{\epsilon_{UV}} + 1 \right) f_K, \quad (6.3.25)$$

where  $f_K$  is given in (6.1.16) and I have labeled the  $1/\epsilon$  singularity by a UV to signify an ultraviolet divergence. The complete  $A_5$  term becomes

$$2g_N^2 \int_0^1 dz_2 \int_0^{1-z_2} dz_1 \int \frac{d^N K}{(2\pi)^N} \frac{A_5 K^2}{[K^2 - C]^3} = \frac{-ig_s^2}{16\pi^2} f_x f_K f_5^{(1)}, \quad (6.3.26)$$

where

$$f_5^{(1)} = \frac{-(2+\epsilon)}{\epsilon(1+\epsilon)} \rightarrow -\frac{2}{\epsilon_{UV}} + 1 + \dots \quad (6.3.27)$$

The complete result for  $\bar{\Gamma}_\mu^{(1)}$  in (6.3.2) can thus be written as

$$\bar{\Gamma}_\mu^{(1)} = \frac{g_s^2}{16\pi^2} \left( -\frac{1}{2} C_A + T_b T_b \right) \gamma_\mu f_x f_K \left( f_{UV}^{(1)} + f_{IR}^{(1)} \right), \quad (6.3.28)$$

where

$$f_{UV}^{(1)} = -\frac{2}{\epsilon_{UV}}, \quad (6.3.29)$$

and

$$f_{IR}^{(1)} = -\frac{8}{\epsilon_{IR}^2} + \frac{8}{\epsilon_{IR}} - 8. \quad (6.3.30)$$

Here I have arbitrarily decided to associate all the constant parts of  $f_4^{(1)}$  and  $f_5^{(1)}$  (i.e., terms that are finite as  $\epsilon \rightarrow 0$ ) with  $f_{IR}^{(1)}$ . With this choice we see that except for color factors the IR part of (6.3.28) is identical to (2.9.14).

The triple-gluon coupling vertex correction shown in Fig. 6.2 is given by

$$\bar{\Gamma}_\mu^{(2)} = -g_N^2 \left( -\frac{i}{2} C_A \right) \int \frac{d^N K}{(2\pi)^N} \frac{F_{\alpha\mu\beta}(p_1 - k, -q, p_2 + k) \gamma_\alpha \not{k} \gamma_\beta}{(p_1 - k)^2 (p_2 + k)^2 k^2}, \quad (6.3.31)$$

where the Feynman gauge has been used and the triple-gluon vertex factor  $F_{\alpha\mu\beta}(p_1, p_2, p_3)$  is given in (6.1.28). The color factor arises from

$$\begin{aligned} f_{bac} T_b T_c &= \frac{i}{2} f_{abc} f_{bcd} T_d \\ &= -\frac{i}{2} (\mathbf{F}_a)_{cb} (\mathbf{F}_d)_{bc} T_d \\ &= -\frac{i}{2} \text{tr}(\mathbf{F}_a \mathbf{F}_d) T_d \\ &= -\frac{i}{2} C_A T_a. \end{aligned} \quad (6.3.32)$$

Proceeding as before we arrive at

$$\begin{aligned} \bar{\Gamma}_\mu^{(2)} &= -g_N^2 \left( -\frac{i}{2} C_A \right) 2 \int_0^1 dz_2 \int_0^{1-z_2} dz_1 \\ &\quad \int \frac{d^N K}{(2\pi)^N} \frac{N_\mu(k \rightarrow K + p_1 z_2 - p_2 z_3)}{[K^2 - C]^3}, \end{aligned} \quad (6.3.33)$$

where the shifted numerator in this case has the same form

$$N_\mu(k \rightarrow K + p_1 z_2 - p_2 z_3) = (A_4 Q^2 + A_5 K^2) \gamma_\mu, \quad (6.3.34)$$

with

$$A_4 = 2(z_2^2 - z_2 - z_1 + z_1 z_2 + 1), \quad (6.3.35)$$

$$A_5 = -\frac{4(3+\epsilon)}{(4+\epsilon)}. \quad (6.3.36)$$

As was the case for  $\bar{\Gamma}_\mu^{(1)}$ , the  $A_4$  term produces no ultraviolet divergences. In particular,

$$2g_N^2 \int_0^1 dz_2 \int_0^{1-z_2} dz_1 \int \frac{d^N K}{(2\pi)^N} \frac{A_4 Q^2}{[K^2 - C]^3} = \frac{-ig_s^2}{16\pi^2} f_x f_K f_4^{(2)}, \quad (6.3.37)$$

with

$$f_4^{(2)} = \frac{2(3\epsilon+8)}{\epsilon(1+\epsilon)(2+\epsilon)} \rightarrow \frac{8}{\epsilon_{IR}} - 9 + \dots \quad (6.3.38)$$

The  $A_5$  term contains an ultraviolet divergence and is given by

$$2g_N^2 \int_0^1 dz_2 \int_0^{1-z_2} dz_1 \int \frac{d^N K}{(2\pi)^N} \frac{A_5 K^2}{[K^2 - C]^3} = \frac{-ig_s^2}{16\pi^2} f_x f_K f_5^{(2)}, \quad (6.3.39)$$

where

$$f_5^{(2)} = \frac{-4(3+\epsilon)}{\epsilon(1+\epsilon)(2+\epsilon)} \rightarrow \frac{-6}{\epsilon_{UV}} + 7 + \dots \quad (6.3.40)$$

The complete result for  $\bar{\Gamma}_\mu^{(2)}$  becomes

$$\bar{\Gamma}_\mu^{(2)} = \frac{g_s^2}{16\pi^2} \left( \frac{1}{2} C_A \right) \gamma_\mu f_K f_x \left( f_{UV}^{(2)} + f_{IR}^{(2)} \right), \quad (6.3.41)$$

with

$$f_{UV}^{(2)} = -\frac{6}{\epsilon_{UV}}, \quad (6.3.42)$$

and

$$f_{IR}^{(2)} = \frac{8}{\epsilon_{IR}} - 2. \quad (6.3.43)$$

Again I have arbitrarily absorbed all the constant terms in  $f_4^{(2)}$  and  $f_5^{(2)}$  into  $f_{IR}^{(2)}$ .

Combining (6.3.28) and (6.3.41) we see that the complete order  $g_s^2$  vertex correction is given by

$$\begin{aligned} \bar{\Gamma} &= \bar{\Gamma}^{(1)} + \bar{\Gamma}^{(2)} \\ &= \frac{g_s^2}{16\pi^2} f_K f_x \left\{ \left( -\frac{1}{2} C_A + T_b T_b \right) f_{UV}^{(1)} + \frac{1}{2} C_A f_{UV}^{(2)} \right\} \\ &\quad + \frac{g_s^2}{16\pi^2} f_K f_x \left\{ \left( -\frac{1}{2} C_A + T_b T_b \right) f_{IR}^{(1)} + \frac{1}{2} C_A f_{IR}^{(2)} \right\}. \end{aligned} \quad (6.3.44)$$

The renormalization factor  $Z_1$  is defined by

$$-ig_s T_a \gamma_\mu (Z_1^{-1} - 1) \equiv -ig_s T_a \Gamma_\mu, \quad (6.3.45)$$

or from (6.3.3)

$$Z_1^{-1} = 1 + \bar{\Gamma}, \quad (6.3.46)$$

so that to order  $g_s^2$

$$\begin{aligned} Z_1 &= 1 + \frac{g_s^2}{16\pi^2} f_K f_x f_1 \\ &= 1 + \frac{g_s^2}{16\pi^2} f_1 \frac{\Gamma(1 - \frac{\epsilon}{2}) \Gamma^2(1 + \frac{\epsilon}{2})}{\Gamma(1 + \epsilon)} \left( \frac{Q^2}{4\pi m_D^2} \right)^{\epsilon/2}, \end{aligned} \quad (6.3.47)$$

where

$$f_1 = -\left( -\frac{1}{2} C_A + T_b T_b \right) f_{UV}^{(1)} - \frac{1}{2} C_A f_{UV}^{(2)}, \quad (6.3.48)$$

and

$$f_1^{\text{pole}} = (C_A + T_b T_b) \left( \frac{2}{\epsilon_{UV}} \right). \quad (6.3.49)$$

Only the ultraviolet divergences are included into  $Z_1$ . One could, however, also choose to include some of the constant terms.

The quantity  $\bar{\Gamma}$  in (6.3.44) contains both IR and UV poles. It is not obvious that one can handle simultaneously both IR and UV poles with dimensional regularization. Increasing the number of space-time dimensions,  $N = 4 + \epsilon$ , above four ( $\epsilon > 0$ ) improves the convergence of, for example, (6.3.2) at low

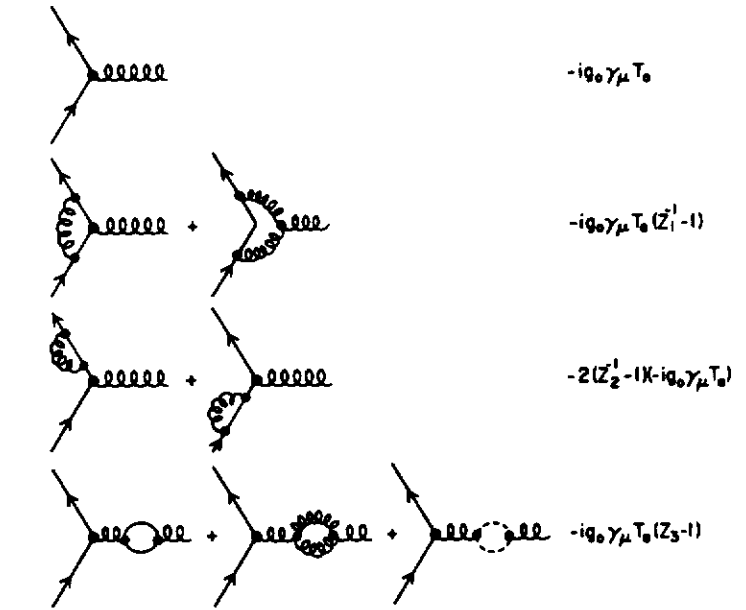


**Figure 6.3** Shows the bare  $q\bar{q}g$  vertex together with the leading order vertex corrections,  $Z_1$ , the leading order quark self-energy corrections,  $Z_2$ , and the leading order corrections to the gluon propagator,  $Z_3$ .

momentum,  $k$ , but worsens the large  $k$  behavior. Conversely, reducing  $N$  below four ( $\epsilon < 0$ ) improves the large  $k$  region but worsens the low  $k$  behavior. Fortunately, we never encounter mixed poles of the form  $1/(\epsilon_{UV}\epsilon_{IR})$ . The pole structure always breaks apart into a sum of  $1/\epsilon_{IR}$ ,  $1/\epsilon_{IR}^2$ , and  $1/\epsilon_{UV}$  terms and one can imagine that  $\epsilon > 0$  for the IR terms and  $\epsilon < 0$  for the UV pieces, respectively, without encountering a problem. This is one of the magical and nice features of dimensional regularization.

## 6.4 The Running Coupling Constant

We have computed, to order  $g_0^2$ , all three corrections to the “bare” coupling

$g_0$  shown in Fig. 6.3. From (6.1.48), (6.2.5), and (6.3.47) we see that

$$Z_1 = 1 + \frac{g_0^2}{16\pi^2} f_\Gamma \left( \frac{-q^2}{4\pi m_D^2} \right)^{\epsilon/2} f_1, \quad (6.4.1)$$

$$Z_2 = 1 + \frac{g_0^2}{16\pi^2} f_\Gamma \left( \frac{-p^2}{4\pi m_D^2} \right)^{\epsilon/2} f_2, \quad (6.4.2)$$

$$Z_3 = 1 + \frac{g_0^2}{16\pi^2} f_\Gamma \left( \frac{-q^2}{4\pi m_D^2} \right)^{\epsilon/2} f_3, \quad (6.4.3)$$

where

$$f_\Gamma = \frac{\Gamma(1 - \frac{\epsilon}{2}) \Gamma^2(1 + \frac{\epsilon}{2})}{\Gamma(1 + \epsilon)}, \quad (6.4.4)$$

and

$$f_i = f_i^{\text{pole}} + h_i, \quad (6.4.5)$$

where

$$f_1^{\text{pole}} = (C_A + T_b T_b) \frac{2}{\epsilon_{\text{UV}}}, \quad (6.4.6)$$

$$f_2^{\text{pole}} = (T_b T_b) \frac{2}{\epsilon_{\text{UV}}}, \quad (6.4.7)$$

$$f_3^{\text{pole}} = (\frac{4}{3} C_f - \frac{5}{3} C_A) \frac{2}{\epsilon_{\text{UV}}}. \quad (6.4.8)$$

The  $h_i$  in (6.4.5) are arbitrary constant terms (finite as  $\epsilon \rightarrow 0$ ). We are free to choose how much of the non-divergent parts of  $Z_1$ ,  $Z_2$  and  $Z_3$  are absorbed into our definition of the “effective coupling constant”  $\alpha_s(Q^2)$  with the remaining constant terms resulting in ordinary order  $\alpha_s^2$  corrections.

In forming the effective coupling  $\alpha_s(Q^2)$  we must be careful not to correct external lines twice. For example, an external fermion line represents a field amplitude and hence it is renormalized by the factor  $\sqrt{Z_2}$ . If we include all graphs giving corrections to the external lines, the result must be divided by  $\sqrt{Z_2}$  for each external quark line. In addition  $\sqrt{Z_3}$  is associated with the renormalization of the gluon source and the other factor of  $\sqrt{Z_3}$  the process of interest. Adding all the corrections to the bare coupling shown in Fig. 6.3 and dividing by  $\sqrt{Z_2}$  for each of the two external quark line and  $\sqrt{Z_3}$  for the external gluon line results in

$$\begin{aligned} -ig_s \gamma_\mu T_a &= \frac{-ig_0 \gamma_\mu T_a}{Z_2 \sqrt{Z_3}} [1 + (Z_1^{-1} - 1) - 2(Z_2^{-1} - 1) + (Z_3 - 1)] \\ &= \frac{-ig_0 \gamma_\mu T_a}{Z_2 \sqrt{Z_3}} \frac{[1 + (Z_1^{-1} - 1)][1 + (Z_3 - 1)]}{[1 + (Z_2^{-1} - 1)]^2} \\ &= \frac{Z_2 \sqrt{Z_3}}{Z_1} (-ig_0 \gamma_\mu T_a), \end{aligned} \quad (6.4.9)$$

or

$$g_s = \frac{Z_2 \sqrt{Z_3}}{Z_1} g_0. \quad (6.4.10)$$

From (6.4.1), (6.4.2) and (6.4.3) we see that, to order  $g_0^2$ ,

$$\frac{Z_2 \sqrt{Z_3}}{Z_1} = 1 + \frac{g_0^2}{16\pi^2} f_\Gamma \left( \frac{Q^2}{4\pi m_D^2} \right)^{\epsilon/2} \left( f_2 + \frac{1}{2} f_3 - f_1 \right), \quad (6.4.11)$$

where I have chosen the symmetric point

$$Q^2 = -p^2 = -q^2 > 0, \quad (6.4.12)$$

to do the evaluation. The effective coupling can thus be expressed as a power series in the bare coupling,  $\alpha_0$ . Namely,

$$\alpha_{\text{eff}}(Q^2) \equiv \alpha_s(Q^2) = \alpha_0 (1 + \alpha_0 B_{QCD}(Q^2)), \quad (6.4.13)$$

where

$$\alpha_0 = \frac{g_0^2}{4\pi}, \quad (6.4.14)$$

and

$$\alpha_0 B_{QCD}(Q^2) = -\frac{\alpha_0}{4\pi} f_\Gamma \left( \frac{Q^2}{4\pi m_D^2} \right)^{\epsilon/2} (2f_1 - 2f_2 - f_3). \quad (6.4.15)$$

Expanding in powers of  $\epsilon$  gives

$$f_\Gamma \left( \frac{Q^2}{4\pi m_D^2} \right)^{\epsilon/2} = 1 + \frac{\epsilon}{2} \left[ \log \left( \frac{Q^2}{4\pi m_D^2} \right) + \gamma_E \right] + \dots, \quad (6.4.16)$$

and

$$\begin{aligned} (2f_1 - 2f_2 - f_3) &= \frac{2}{\epsilon} \left( \frac{11}{3} C_A - \frac{4}{3} C_f \right) + (2h_1 - 2h_2 - h_3) + \dots \\ &= \frac{2}{\epsilon} \beta_0 + h + \dots, \end{aligned} \quad (6.4.17)$$

where

$$\beta_0 = \frac{11}{3} C_A - \frac{4}{3} C_f = 11 - \frac{2}{3} n_f, \quad (6.4.18)$$

since  $C_f = n_f/2$  and for three colors  $C_A = 3$  and

$$h = 2h_1 - 2h_2 - h_3, \quad (6.4.19)$$

are the constant terms of our choice. Equation (6.4.15) now becomes

$$\begin{aligned} \alpha_0 B_{QCD}(Q^2) &= -\frac{\alpha_0}{4\pi} \left\{ 1 + \frac{\epsilon}{2} [\log(Q^2/m_D^2) + \gamma_E - \log(4\pi)] + \dots \right\} \\ &\quad \left\{ \frac{2}{\epsilon} \beta_0 + h + \dots \right\} \\ &= -\frac{\alpha_0}{4\pi} \left\{ \beta_0 \left[ \frac{2}{\epsilon} + \log(Q^2/m_D^2) + \gamma_E - \log(4\pi) \right] + h + \dots \right\}, \end{aligned} \quad (6.4.20)$$

where terms that vanish as  $\epsilon \rightarrow 0$  have been dropped. These corrections form a geometric series of the form

$$\begin{aligned}\alpha_s(Q^2) &= \alpha_0 (1 + \alpha_0 B_{QCD}(Q^2) + \alpha_0 B_{QCD}(Q^2)\alpha_0 B_{QCD}(Q^2) + \dots) \\ &= \frac{\alpha_0}{1 - \alpha_0 B_{QCD}(Q^2)},\end{aligned}\quad (6.4.21)$$

so that

$$\frac{1}{\alpha_s(Q^2)} = \frac{1}{\alpha_0} - B_{QCD}(Q^2). \quad (6.4.22)$$

The function  $B_{QCD}(Q^2)$  diverges as  $\epsilon \rightarrow 0$ , however, the bare coupling  $\alpha_0$  is not an experimental observable. The idea behind renormalization is to express experimental observables in terms of other experimental observables. We must decide on what we mean by the “experimental QCD coupling,”  $\alpha_s$ , and then express the effective coupling,  $\alpha_s(Q^2)$ , in terms of it. In QED the effective coupling is expressed in terms of the fine structure constant  $\alpha \approx 1/137$ . The fine structure constant, on the other hand, is defined as the value of the effective coupling in the Thompson limit ( $Q^2 \rightarrow 0$ ).

In QCD  $B_{QCD}(Q^2)$  diverges as  $Q^2 \rightarrow 0$  so we cannot define  $\alpha_{\text{eff}}(Q^2)$  in terms of its value at  $Q^2 = 0$ . Instead we choose some value of  $Q^2$ , say  $Q^2 = \mu^2$ , and define the “experimental QCD coupling” to be

$$\alpha_s \equiv \alpha_s(\mu^2). \quad (6.4.23)$$

We then express all observables in terms of  $\alpha_s(\mu^2)$ . From (6.4.22) we see that when we express the effective coupling in terms of  $\alpha_s(\mu^2)$  we get

$$\frac{1}{\alpha_s(Q^2)} = \frac{1}{\alpha_s(\mu^2)} - (B_{QCD}(Q^2) - B_{QCD}(\mu^2)), \quad (6.4.24)$$

where the quantity

$$B_{QCD}(Q^2) - B_{QCD}(\mu^2) = -\frac{\beta_0}{4\pi} \log(Q^2/\mu^2), \quad (6.4.25)$$

is finite in the limit  $\epsilon \rightarrow 0$  and independent of dimensional regularization mass,  $m_D$ . Inserting (6.4.25) into (6.4.24) yields

$$\alpha_{\text{eff}}(Q^2) = \alpha_s(Q^2) = \frac{\alpha_s(\mu^2)}{1 + \alpha_s(\mu^2) \frac{\beta_0}{4\pi} \log(Q^2/\mu^2)}. \quad (6.4.26)$$

This equation expresses the effective QCD coupling in terms of the experimental observable  $\alpha_s(\mu^2)$ . The “renormalization point,”  $\mu$ , is, of course, arbitrary. Had we instead chosen the point  $\bar{\mu}$  then the two couplings would be related by

$$\frac{1}{\alpha_s(\bar{\mu}^2)} = \frac{1}{\alpha_s(\mu^2)} + \frac{\beta_0}{4\pi} \log(\bar{\mu}^2/\mu^2), \quad (6.4.27)$$

or

$$-\frac{4\pi}{\beta_0 \alpha_s(\bar{\mu}^2)} + \log(\bar{\mu}^2) = -\frac{4\pi}{\beta_0 \alpha_s(\mu^2)} + \log(\mu^2). \quad (6.4.28)$$

This means that  $\alpha_s(Q^2)$  is not a separate function of  $\alpha_s(\mu^2)$  and  $\mu^2$ , but instead can be written as a function of a single parameter,  $\Lambda$ , that is independent of  $\mu^2$  and given by

$$\log(\Lambda^2) = -\frac{4\pi}{\beta_0 \alpha_s(\mu^2)} + \log(\mu^2). \quad (6.4.29)$$

Inserting this into (6.4.26) gives<sup>3,4</sup>

$$\alpha_s(Q^2) = \frac{4\pi}{\beta_0 \log(Q^2/\Lambda^2)}, \quad (6.4.30)$$

where the mass scale  $\Lambda$  is a parameter that must be determined experimentally. It is the one parameter of perturbative QCD.

The choice of constant terms,  $h$ , to include in  $B_{QCD}(Q^2)$  in (6.4.20) is arbitrary and a matter of convention. The choice does not effect the  $Q^2$  dependence of the effective coupling  $\alpha_s(Q^2)$ , but it affects the value of the QCD parameter  $\Lambda$  as determined experimentally. In the “minimal subtraction” scheme (MS) no constant terms are absorbed into the effective coupling. On the other hand, in the “modified minimal subtraction” scheme ( $\overline{\text{MS}}$ ) one absorbs the constant terms

$$\gamma_E - \log(4\pi), \quad (6.4.31)$$

that arise from dimensional regularization into the effective coupling. In practice, at order  $\alpha_0^2$ , this corresponds to making the replacement

$$\alpha_0 - \frac{\alpha_0^2}{4\pi} \beta_0 \left( \frac{2}{\epsilon_{\text{UV}}} + \log(Q^2/m_D^2) + \gamma_E - \log(4\pi) \right) \longrightarrow \alpha_s(Q^2), \quad (6.4.32)$$

where  $\alpha_0$  is the bare QCD coupling and  $\alpha_s(Q^2)$  is the running coupling in (6.4.30).

## 6.5 The Beta Function

In (6.4.13) we expressed the effective coupling  $\alpha_s(Q^2)$  as a power series in the bare coupling  $\alpha_0$ . We could equally well have expanded the bare coupling as a power series in the effective coupling,

$$\alpha_0 = \alpha_s(Q^2) (1 - \alpha_s(Q^2) B_{QCD}(Q^2) + \dots). \quad (6.5.1)$$

Although  $B_{QCD}(Q^2)$  diverges as  $\epsilon \rightarrow 0$ , its derivative with respect to  $\log(Q^2)$  does not. From (6.4.15) we see that

$$\begin{aligned}\frac{dB_{QCD}(Q^2)}{d\tau} &= -\frac{1}{4\pi} \left( \frac{\epsilon}{2} \right) f \Gamma \left( \frac{Q^2}{4\pi m_D^2} \right)^{\epsilon/2} (2f_1 - 2f_2 - f_3) \\ &\xrightarrow{\epsilon \rightarrow 0} -\frac{\beta_0}{4\pi},\end{aligned}\quad (6.5.2)$$

where

$$\tau = \log(Q^2/\mu^2). \quad (6.5.3)$$

Differentiating (6.4.13) with respect to  $\tau$  gives

$$\frac{d\alpha_s(Q^2)}{d\tau} = \alpha_0^2 \frac{dB_{QCD}(Q^2)}{d\tau}. \quad (6.5.4)$$

Inserting (6.5.1) and (6.5.2) into this equation results in

$$\frac{d\alpha_s(Q^2)}{d\tau} = -\frac{\beta_0}{4\pi} \alpha_s^2(Q^2) + O(\alpha_s^3). \quad (6.5.5)$$

Thus, to leading order,

$$\int_{\alpha_s(\mu^2)}^{\alpha_s(Q^2)} \frac{d\alpha_s}{\alpha_s^2} = -\frac{\beta_0}{4\pi} \int_0^\tau d\tau, \quad (6.5.6)$$

yielding

$$\frac{1}{\alpha_s(Q^2)} = \frac{1}{\alpha_s(\mu^2)} + \frac{\beta_0}{4\pi} \log(Q^2/\mu^2), \quad (6.5.7)$$

or

$$\alpha_s(Q^2) = \frac{\alpha_s(\mu^2)}{1 + \alpha_s(\mu^2) \frac{\beta_0}{4\pi} \log(Q^2/\mu^2)}, \quad (6.5.8)$$

which is the same as (6.4.26). Equation (6.5.5) is traditionally written in the form

$$\frac{d\alpha_s(\tau)}{d\tau} = \beta(\alpha_s(\tau)), \quad (6.5.9)$$

with the condition

$$\alpha_s(\tau = 0) = \alpha_s(\mu^2) = \alpha_s. \quad (6.5.10)$$

The “beta function”  $\beta(\alpha_s(\tau))$  governs how the effective coupling  $\alpha_s(\tau)$  depends on  $\tau$ . It can be expanded in a power series in  $\alpha_s(\tau)$  as follows:

$$-\beta(\alpha_s(\tau)) = b_0 \alpha_s^2(\tau) + b_1 \alpha_s^3(\tau) + b_2 \alpha_s^4(\tau) + \dots, \quad (6.5.11)$$

where the first term is given in (6.5.5),

$$b_0 = \frac{\beta_0}{4\pi}. \quad (6.5.12)$$

The second coefficient has been computed<sup>5</sup> and is given by

$$b_1 = \frac{\beta_1}{16\pi^2}, \quad (6.5.13)$$

where

$$\beta_1 = (306 - 38 n_f)/3. \quad (6.5.14)$$

The third coefficient,  $b_2$ , and higher coefficients are renormalization scheme dependent.

One way to define the higher-order effective coupling is to write (6.5.9)

and (6.5.11) in the form

$$-\frac{d\alpha_s(Q^2)}{d\tau} = b_0 \alpha_s^2(Q^2) \left( 1 + \frac{b_1}{b_0} \alpha_s(Q^2) + \frac{b_2}{b_0} \alpha_s^2(Q^2) + \dots \right), \quad (6.5.15)$$

and rather than truncating the series ( $b_n = 0$   $n \geq 2$ ) we set

$$b_n = b_0 \left( \frac{b_1}{b_0} \right)^n, \quad (6.5.16)$$

so that (6.5.15) forms a geometric series and

$$\begin{aligned} -\frac{d\alpha_s(Q^2)}{d\tau} &= b_0 \alpha_s^2(Q^2) \sum_{n=0}^{\infty} \left( \frac{b_1}{b_0} \alpha_s(Q^2) \right)^n \\ &= \frac{b_0 \alpha_s^2(Q^2)}{1 - \frac{b_1}{b_0} \alpha_s(Q^2)}. \end{aligned} \quad (6.5.17)$$

To order  $\alpha_s^3(Q^2)$  equation (6.5.17) and (6.5.15) are equivalent, but the later expression provides a very nice “definition” of the QCD effective coupling. Solving for  $\alpha_s(Q^2)$  we get

$$-\int_{\alpha_s(\mu^2)}^{\alpha_s(Q^2)} \left( \frac{1}{b_0 \alpha_s^2} - \frac{b_1}{b_0^2} \frac{1}{\alpha_s} \right) d\alpha_s = \tau, \quad (6.5.18)$$

or

$$\frac{1}{b_0 \alpha_s(Q^2)} - \frac{1}{b_0 \alpha_s(\mu^2)} + \frac{b_1}{b_0^2} \log(\alpha_s(Q^2)/\alpha_s(\mu^2)) = \log(Q^2/\mu^2), \quad (6.5.19)$$

and we see that

$$\begin{aligned} -\frac{1}{b_0 \alpha_s(Q^2)} - \frac{b_1}{b_0^2} \log(\alpha_s(Q^2)) + \log(Q^2) &= \\ -\frac{1}{b_0 \alpha_s(\mu^2)} - \frac{b_1}{b_0^2} \log(\alpha_s(\mu^2)) + \log(\mu^2). \end{aligned} \quad (6.5.20)$$

This equation replaces (6.4.28) and thus

$$-\frac{1}{b_0 \alpha_s(\mu^2)} - \frac{b_1}{b_0^2} \log(\alpha_s(\mu^2)) + \log(\mu^2) = C, \quad (6.5.21)$$

where  $C$  is a constant and is related to the perturbative parameter of the theory. Taking

$$C = \log(\Lambda^2) + \frac{b_1}{b_0^2} \log(b_0), \quad (6.5.22)$$

gives

$$\alpha_s(Q^2) = \frac{1}{b_0 \left[ \log(Q^2/\Lambda^2) + \frac{b_1}{b_0^2} \log \left( \frac{1}{b_0 \alpha_s(Q^2)} \right) \right]}, \quad (6.5.23)$$

where  $b_0$  and  $b_1$  are given by (6.5.12) and (6.5.13), respectively. Unfortunately,

(6.5.23) cannot be solved explicitly for  $\alpha_s(Q^2)$ . Given the value of  $Q/\Lambda$  it can be solved numerically for the effective coupling  $\alpha_s(Q^2)$ . However, this is not what is usually done. Instead, we expand  $\alpha_s(Q^2)$  in terms of the leading order coupling in (6.4.30),

$$\alpha_{LO}(Q^2) = \frac{1}{b_0 \log(Q^2/\Lambda^2)}, \quad (6.5.24)$$

and we drop terms higher than order  $\alpha_{LO}^2$ . In this case (6.5.23) becomes

$$\begin{aligned} \alpha_s(Q^2) &= \alpha_{LO}(Q^2) \left[ 1 - \frac{\beta_1}{4\pi b_0} \alpha_{LO}(Q^2) \log \log(Q^2/\Lambda^2) \right] \\ &= \frac{4\pi}{b_0 \log(Q^2/\Lambda^2)} \left[ 1 - \frac{\beta_1}{\beta_0^2} \frac{\log \log(Q^2/\Lambda^2)}{\log(Q^2/\Lambda^2)} \right], \end{aligned} \quad (6.5.25)$$

where  $\beta_0$  and  $\beta_1$  are given by (6.4.18) and (6.5.14), respectively.

The mass scale,  $\Lambda$ , is the one parameter of perturbative QCD, however, its definition is not unique. The precise definition of  $\Lambda$  is a matter of convention. For example, the  $\Lambda$  appearing in the leading order expression for  $\alpha_s(Q^2)$  in (6.5.24) is not the same as the  $\Lambda$  in the higher order expression in (6.5.23). Formally  $\Lambda$  is defined by

$$\Lambda = \mu \exp \left\{ \frac{1}{2} \int_{\alpha_s(\mu^2)}^A \frac{d\alpha}{\beta(\alpha)} \right\}, \quad (6.5.26)$$

where the choice of the upper limit  $A$  is arbitrary (i.e., a matter of convention). It is easy to see that for any constant  $A$ ,  $\Lambda$  as defined in (6.5.26) is independent of  $\mu$  (the total derivative of (6.5.26) with respect to  $\mu$  vanishes). In the leading order formula in (6.5.24) we choose  $A \rightarrow \infty$ , while in the higher order formula in (6.6.21) we choose  $A$  to be the solution of

$$A \exp \left( \frac{b_0}{b_1 A} \right) = b_0. \quad (6.5.27)$$

## 6.6 The Renormalization Group Equation

Since QCD is a theory of massless quarks and gluons we were forced to introduce the scale  $\mu$ . The QCD coupling was defined to be the effective coupling at the scale  $\mu$ ,

$$\alpha_s \equiv \alpha_s(\mu^2) = \frac{g_s^2}{4\pi}. \quad (6.6.1)$$

Since physical observables cannot depend on our choice of  $\mu$ , a change in  $\mu$  must be compensated by a change in the coupling  $\alpha_s$ . Consider the case of a dimensionless quantity such as  $R^{e^+ e^-}$  in (2.1.16). In general the observable

depends on

$$\tau = \log(Q^2/\mu^2), \quad (6.6.2)$$

and the coupling  $\alpha_s$  in (6.6.1) but not on the renormalization point  $\mu$ ,

$$R(\tau, \alpha_s, \mu) = R(\tau, \alpha_s). \quad (6.6.3)$$

The independence of  $R$  on  $\mu$  strongly constrains its functional form and implies that the total derivative with respect to  $\mu$  is zero. Namely,

$$\mu^2 \frac{dR(\tau, \alpha_s)}{d\mu^2} = \left( \mu^2 \frac{\partial}{\partial \mu^2} + \mu^2 \frac{\partial \alpha_s}{\partial \mu^2} \frac{\partial}{\partial \alpha_s} \right) R(\tau, \alpha_s) = 0, \quad (6.6.4)$$

where the first term accounts for the  $\mu$  dependence through  $\tau$  and the second term accounts for the dependence on  $\alpha_s$ . If we define the “beta function” according to

$$\beta(\alpha_s) \equiv \mu^2 \frac{\partial \alpha_s}{\partial \mu^2} = \frac{\partial \alpha_s}{\partial \log(\mu^2)}, \quad (6.6.5)$$

then (6.6.4) becomes

$$\left( -\frac{\partial}{\partial \tau} + \beta(\alpha_s) \frac{\partial}{\partial \alpha_s} \right) R(\tau, \alpha_s) = 0, \quad (6.6.6)$$

and is referred to as a renormalization group equation (RGE)<sup>6,7</sup> since it tells us how a change in  $\mu$  (or  $\tau$ ) is compensated by a change in the coupling  $\alpha_s$ .

The solution of (6.6.6) is arrived at by introducing a function  $\alpha_s(\tau)$  such that

$$\tau = \int_{\alpha_s}^{\alpha_s(\tau)} \frac{d\alpha}{\beta(\alpha)}, \quad (6.6.7)$$

with the condition that

$$\alpha_s(\tau = 0) = \alpha_s(\mu^2) = \alpha_s, \quad (6.6.8)$$

as in (6.6.1). Differentiating (6.6.7) with respect  $\tau$  and  $\alpha_s$  yields

$$\frac{d\alpha_s(\tau)}{d\tau} = \beta(\alpha_s(\tau)), \quad (6.6.9)$$

and

$$\frac{d\alpha_s(\tau)}{d\alpha_s} = \frac{\beta(\alpha_s(\tau))}{\beta(\alpha_s)}, \quad (6.6.10)$$

respectively. The general solution of the RGE in (6.6.6) with the boundary condition given by (6.6.8) is

$$R(\tau, \alpha_s) = R(0, \alpha_s(\tau)). \quad (6.6.11)$$

Therefore, the RGE implies that the entire  $Q^2$  dependence of  $R$  arises from the running coupling  $\alpha_s(\tau)$  which in turn is a solution of (6.6.9). Furthermore the dependence of  $R$  on  $\alpha_s(\tau)$  is determined if one knows  $R(0, \alpha_s)$ . Thus, given

where  $\gamma_n(\alpha_s(\tau))$  given by (6.6.23) with

$$a_0 = -\frac{1}{8\pi}\gamma_0^{(n)}, \quad (6.6.28)$$

$$a_1 = -\frac{1}{32\pi^2}\gamma_1^{(n)}, \quad (6.6.29)$$

and

$$C_n^{NS}(0, \alpha_s(\tau)) = 1 + B_n^{NS} \frac{\alpha_s(\tau)}{4\pi} + \dots \quad (6.6.30)$$

From (6.6.26) and (6.6.27) we see that the change in  $M_n^{NS}(Q^2)$  with respect to  $\alpha_s(\tau)$  is given by

$$\frac{dM_n^{NS}(Q^2)}{d\alpha_s(\tau)} = \left( \frac{\gamma_n(\alpha_s(\tau))}{\beta(\alpha_s(\tau))} + \frac{1}{C_n^{NS}(0, \alpha_s(\tau))} \frac{dC_n^{NS}(0, \alpha_s(\tau))}{d\alpha_s(\tau)} \right) M_n^{NS}(Q^2). \quad (6.6.31)$$

Inserting the leading order expressions for  $\gamma_n(\alpha_s(\tau))$ , and  $C_n^{NS}(0, \alpha_s(\tau))$  into (6.6.31) results in

$$\alpha_s(\tau) \frac{dM_n^{NS}(Q^2)}{d\alpha_s(\tau)} = \frac{\gamma_0^{(n)}}{2\beta_0} M_n^{NS}(Q^2), \quad (6.6.32)$$

or

$$\frac{dM_n^{NS}(Q^2)}{d\kappa} = -\frac{\gamma_0^{(n)}}{4} M_n^{NS}(Q^2), \quad (6.6.33)$$

where

$$\kappa = \frac{2}{\beta_0} \log\{\alpha_s(Q_0^2)/\alpha_s(Q^2)\}. \quad (6.6.34)$$

Equation (6.6.33) is identical to (4.7.1) provided

$$\gamma_0^{(n)} = -4A_n^{NS}, \quad (6.6.35)$$

with  $A_n^{NS}$  given in (4.7.6). The solution is given in (4.7.10). Namely,

$$\begin{aligned} M_n^{NS}(Q^2) &= \exp(\kappa A_n^{NS}) M_n^{NS}(Q_0^2) \\ &= M_n^{NS}(Q_0^2) [\alpha_s(Q^2)/\alpha_s(Q_0^2)]^{d_n} \\ &= M_n^{NS}(Q_0^2) [\log(Q^2/\Lambda^2)/\log(Q_0^2/\Lambda^2)]^{-d_n}, \end{aligned} \quad (6.6.36)$$

with

$$d_n = -\frac{2A_n^{NS}}{\beta_0}, \quad (6.6.37)$$

as in (4.7.55). Notice that

$$\begin{aligned} [\alpha_s(Q^2)/\alpha_s(Q_0^2)]^{d_n} &= \left[ 1 - \frac{\beta_0}{4\pi} \alpha_s(Q^2) \log(Q^2/Q_0^2) \right]^{d_n} \\ &= 1 + \frac{\alpha_s(Q^2)}{2\pi} A_n^{NS} \log(Q^2/Q_0^2) + \dots, \end{aligned} \quad (6.6.38)$$

so that the RGE has in effect summed the infinite series of terms  $[\alpha_s \log(Q^2)]^n$  that we explicitly summed in Chapter 3 for the fragmentation functions and in Chapter 4 for the parton distributions.

Including the next order in (6.6.31) results in

$$\alpha_s(Q^2) \frac{dM_n^{NS}(Q^2)}{d\alpha_s(Q^2)} = \left( \frac{\gamma_0^{(n)}}{2\beta_0} + (h_n + B_n^{NS}) \frac{\alpha_s(Q^2)}{4\pi} \right) M_n^{NS}(Q^2), \quad (6.6.39)$$

where

$$h_n = \frac{\gamma_1^{(n)}}{2\beta_0} - \frac{\beta_1 \gamma_0^{(n)}}{2\beta_0^2}. \quad (6.6.40)$$

The solution of (6.6.39) is given by

$$\begin{aligned} M_n^{NS}(Q^2) &= M_n^{NS}(Q_0^2) [\alpha_s(Q^2)/\alpha_s(Q_0^2)]^{d_n} \\ &\quad \exp[(h_n + B_n^{NS}) (\alpha_s(Q^2) - \alpha_s(Q_0^2))/4\pi], \end{aligned} \quad (6.6.41)$$

where  $\alpha_s(Q^2)$  is given by (6.5.23) or (6.5.25). Here  $h_n$  and  $B_n^{NS}$  are, in general, regularization scheme dependent, however, the sum  $(h_n + B_n^{NS})$  is unique. If we expand (6.6.41) as a series in the leading order coupling,  $\alpha_{LO}(Q^2)$ , we arrive at

$$\begin{aligned} M_n^{NS}(Q^2) &= M_n^{NS}(Q_0^2) [\alpha_{LO}(Q^2)/\alpha_{LO}(Q_0^2)]^{d_n} \\ &\quad \{1 + (h_n + B_n + L_n) (\alpha_{LO}(Q^2) - \alpha_{LO}(Q_0^2))/4\pi\}, \end{aligned} \quad (6.6.42)$$

with

$$L_n = -\frac{\beta_1 \gamma_n^{(n)}}{2\beta_0^2} \log \log(Q^2/\Lambda^2), \quad (6.6.43)$$

and  $\alpha_{LO}(Q^2)$  given in (6.5.24).

Since  $\alpha_s(Q^2) - \alpha_s(Q_0^2)$  is of order  $\alpha_{LO}(Q^2)$ , the corrections in (6.6.41) due to  $h_n$  and  $B_n$  are of order  $\alpha_{LO}^2(Q^2)$ . Suppose, however, we are interested in comparing distributions determined in process  $A$ ,  $M_n^{NS,A}(Q^2)$ , with those determined in process  $B$ ,  $M_n^{NS,B}(Q^2)$ . For example, in Chapter 5 we compared the “Drell-Yan” parton distributions with the deep inelastic scattering distributions. We see from (6.6.41) that the difference of the two distributions is given to order  $\alpha_s(Q^2)$  by

$$M_n^{NS,B}(Q^2) - M_n^{NS,A}(Q^2) = M_n^{NS,A}(Q^2) \Delta B_n^{NS} \frac{\alpha_s(Q^2)}{4\pi}, \quad (6.6.44)$$

where

$$\Delta B_n^{NS} \equiv B_n^{NS,B} - B_n^{NS,A}. \quad (6.6.45)$$

Since  $d_n$  and  $h_n$  are independent of the process, only the  $B_n^{NS}$  corrections remain and are of order  $\alpha_s(Q^2)$  when comparing one process with another. The coefficients  $\Delta B_n^{NS}$  are simply related to the “little  $f$ ” functions we have

encountered previously. For instance,

$$G_{NS}^B(x, Q^2) = \int_x^1 \frac{dy}{y} G_{NS}^A(x, Q^2) \{ \delta(1-z) + \alpha_s(Q^2) \Delta f(z) \}, \quad (6.6.46)$$

where  $z = x/y$  and

$$\Delta B_n = 4\pi \int_0^1 z^{n-1} \Delta f(z) dz. \quad (6.6.47)$$

The coefficients  $\Delta B_n$  are simply the moments of the “little  $f$ ” functions. In leading order both  $M_n^{NS,A}(Q^2)$  and  $M_n^{NS,B}(Q^2)$  satisfy (6.6.36).

### Problems

#### 6.1. Show that

$$\text{tr} [\gamma_\mu \not{d} \gamma_\nu \not{d}] = 4(a_\mu b_\nu + a_\nu b_\mu - g_{\mu\nu} a \cdot b).$$

#### 6.2. Verify (6.1.15) and (6.1.18).

#### 6.3. Show that the quark loop corrections to the gluon propagator shown in Fig. 6.1 are given by

$$\Pi_{\mu\nu;ab}^q(q) = -\frac{ig_s^2}{16\pi^2} \delta_{ab} (g_{\mu\nu} Q^2 + q_\mu q_\nu) f_x f_K f_q,$$

where

$$f_x f_K = \frac{\Gamma(1-\frac{\epsilon}{2}) \Gamma^2(1+\frac{\epsilon}{2})}{\Gamma(1+\epsilon)} \left( \frac{Q^2}{4\pi m_D^2} \right)^{\epsilon/2},$$

and

$$f_q = C_f \frac{4(2+\epsilon)}{\epsilon(1+\epsilon)(3+\epsilon)} \rightarrow C_f \left\{ \frac{4}{3} \frac{2}{\epsilon} + \dots \right\}.$$

#### 6.4. Show that

$$\begin{aligned} f_{acd} f_{cdb} &= C_A \delta_{ab}, \\ T_b T_a T_b &= T_a (-\frac{1}{2} C_A + T_b T_b), \end{aligned}$$

and

$$f_{bac} T_b T_c = -\frac{i}{2} C_A T_a,$$

where

$$\text{tr}(F_a F_b) = C_A \delta_{ab},$$

and  $C_A$  is the number of colors.

#### 6.5. Show that in $N$ spacetime dimensions

$$\begin{aligned} F_{\mu\alpha\beta}(q_1, q_2, q_3) F_{\alpha\beta\nu}(-q_2, -q_3, -q_1) = & \\ & 2(q_1 - q_2)_\mu (q_1 - q_2)_\nu \\ & + 2(q_1 - q_3)_\mu (q_2 - q_3)_\nu \\ & - N(q_2 - q_3)_\mu (q_2 - q_3)_\nu \\ & - g_{\mu\nu} [(q_1 - q_2)^2 + (q_1 - q_3)^2], \end{aligned}$$

where  $F_{\lambda\mu\nu}(p_1, p_2, p_3)$  is the triple-gluon coupling factor defined in (6.1.28). Using this result show that

$$\begin{aligned} F_{\mu\alpha\beta}(-q, k, q - k) F_{\alpha\beta\nu}(-k, k - q, q) = & \\ (6 - N) q_\mu q_\nu + (6 - 4N) k_\mu k_\nu & \\ + (2N - 6) q_\mu k_\nu + 2N k_\mu q_\nu & \\ - g_{\mu\nu} (2k^2 - 2k \cdot q + 5q^2), & \end{aligned}$$

and verify (6.1.31).

#### 6.6. Show that $\Pi_{\mu\nu;ab}^{g^0}(q)$ in (6.1.30) is given by

$$\Pi_{\mu\nu;ab}^{g^0}(q) = \frac{ig_s^2}{16\pi^2} \delta_{ab} (f_1 q_\mu q_\nu + f_2 g_{\mu\nu} Q^2) f_K f_x,$$

where

$$f_K f_x = \frac{\Gamma(1-\frac{\epsilon}{2}) \Gamma^2(1+\frac{\epsilon}{2})}{\Gamma(1+\epsilon)} \left( \frac{Q^2}{4\pi m_D^2} \right)^{\epsilon/2},$$

and

$$\begin{aligned} f_1 &= C_A \left[ \frac{(5+2\epsilon)(2+\epsilon)}{2(1+\epsilon)(3+\epsilon)} + \frac{2-\epsilon}{1+\epsilon} \right] \frac{1}{\epsilon}, \\ f_2 &= C_A \left[ \frac{-(2+\epsilon)}{2(1+\epsilon)(3+\epsilon)} + \frac{7}{2(1+\epsilon)} \right] \frac{1}{\epsilon}. \end{aligned}$$

#### 6.7. Show that $\Pi_{\mu\nu;ab}^0(q)$ in (6.1.36) is given by

$$\Pi_{\mu\nu;ab}^0(q) = \frac{ig_s^2}{16\pi^2} \delta_{ab} (f_1 q_\mu q_\nu + f_2 g_{\mu\nu} Q^2) f_K f_x,$$

where

$$f_K f_x = \frac{\Gamma(1-\frac{\epsilon}{2}) \Gamma^2(1+\frac{\epsilon}{2})}{\Gamma(1+\epsilon)} \left( \frac{Q^2}{4\pi m_D^2} \right)^{\epsilon/2},$$

and

$$\begin{aligned} f_1 &= -C_A \frac{2+\epsilon}{2\epsilon(1+\epsilon)(3+\epsilon)}, \\ f_2 &= C_A \frac{1}{2\epsilon(1+\epsilon)(3+\epsilon)}. \end{aligned}$$

6.8. Show that

$$\gamma_\alpha \not{p}_1 \gamma_\mu \not{p}_2 \gamma_\alpha = -2 \not{p}_2 \gamma_\mu \not{p}_1 - (N-4) \not{p}_1 \gamma_\mu \not{p}_2.$$

6.9. Using the Dirac equation for massless partons show that

$$\bar{u}(p_1, s_1) \not{p}_2 \gamma_\mu \not{p}_1 \bar{v}(p_2, s_2) = -2 p_1 \cdot p_2 \bar{u}(p_1, s_1) \gamma_\mu \bar{v}(p_2, s_2),$$

and that

$$\begin{aligned} \bar{u}(p_1, s_1) \gamma_\alpha (\not{p}_1 - \not{k}) \gamma_\mu (\not{p}_2 + \not{k}) \bar{v}(p_2, s_2) = \\ \bar{u}(p_1, s_1) [-2 \not{p}_2 \gamma_\mu \not{p}_1 - 2 \not{k} \gamma_\mu \not{p}_1 \\ + 2 \not{p}_2 \gamma_\mu \not{k} + (N-2) \not{k} \gamma_\mu \not{k}] \bar{v}(p_2, s_2). \end{aligned}$$

Use this to show that the integral in (6.3.2),

$$\int \frac{d^N k}{(2\pi)^N} \frac{\gamma_\alpha (\not{p}_1 - \not{k}) \gamma_\mu (\not{p}_2 + \not{k}) \gamma_\alpha}{(p_1 - k)^2 (p_2 + k)^2 k^2},$$

reduces to

$$\int_0^1 dz_2 \int_0^{1-z_2} dz_1 \int \frac{d^N K}{(2\pi)^N} \frac{(A_4 Q^2 + A_5 K^2) \gamma_\mu}{[K^2 - C]^3},$$

where

$$\begin{aligned} K &= k - p_1 z_2 + p_2 z_1, \\ q &= p_1 + p_2, \\ Q^2 &= -q^2, \\ C &= Q^2 z_2 z_3, \\ 1 &= z_1 + z_2 + z_3, \\ A_4 &= -(2+\epsilon) z_2 z_3 - 2 z_1, \\ A_5 &= -\frac{(2+\epsilon)^2}{(4+\epsilon)}, \end{aligned}$$

and  $N = 4 + \epsilon$ .

6.10. Show that

$$\begin{aligned} \int_0^1 dz_2 \int_0^{1-z_2} dz_1 (z_2 z_3)^{\frac{\epsilon}{2}} &= \frac{1}{(2+\epsilon)(1+\epsilon)} f_x, \\ \int_0^1 dz_2 \int_0^{1-z_2} dz_1 z_1 (z_2 z_3)^{\frac{\epsilon}{2}-1} &= \frac{4}{\epsilon^2(1+\epsilon)} f_x, \\ \int_0^1 dz_2 \int_0^{1-z_2} dz_1 (z_2 z_3)^{\frac{\epsilon}{2}-1} &= \frac{4}{\epsilon^2} f_x, \end{aligned}$$

where  $1 = z_1 + z_2 + z_3$  and

$$f_x = \frac{\Gamma^2(1 + \frac{\epsilon}{2})}{\Gamma(1 + \epsilon)}.$$

6.11. Perform the integral over  $k$  in (6.3.2) and verify that

$$\begin{aligned} \bar{\Gamma}_\mu^{(1)} = \frac{g_s^2}{16\pi^2} & (-\frac{1}{2} C_A + T_b T_b) \gamma_\mu \frac{\Gamma(1 - \frac{\epsilon}{2}) \Gamma^2(1 + \frac{\epsilon}{2})}{\Gamma(1 + \epsilon)} \\ & \left( \frac{Q^2}{4\pi m_D^2} \right)^{\epsilon/2} \left( -\frac{2}{\epsilon_{UV}} - \frac{8}{\epsilon_{IR}^2} + \frac{8}{\epsilon_{IR}} - 8 + \dots \right), \end{aligned}$$

where  $Q^2 = -q^2 > 0$ .

6.12. Using the Dirac equation for massless partons show that

$$\begin{aligned} \bar{u}(p_1, s_1) F_{\alpha\mu\beta}(p_1 - k, -q, p_2 + k) \gamma_\alpha \not{k} \gamma_\beta \bar{v}(p_2, s_2) = \\ \bar{u}(p_1, s_1) [2 \not{k} \gamma_\mu \not{k} - 2 \not{k} \gamma_\mu \\ + 2 \not{p}_2 \gamma_\mu \not{k} - 2 N k_\mu \not{k} + (2-N)(p_2 - p_1)_\mu \not{k}] \bar{v}(p_2, s_2). \end{aligned}$$

Use this to show that the integral in (6.3.31),

$$\int \frac{d^N k}{(2\pi)^N} \frac{F_{\alpha\mu\beta}(p_1 - k, -q, p_2 + k) \gamma_\alpha \not{k} \gamma_\beta}{(p_1 - k)^2 (p_2 + k)^2 k^2},$$

reduces to

$$\int_0^1 dz_2 \int_0^{1-z_2} dz_1 \int \frac{d^N K}{(2\pi)^N} \frac{(A_4 Q^2 + A_5 K^2) \gamma_\mu}{[K^2 - C]^3},$$

where

$$\begin{aligned} K &= k - p_1 z_2 + p_2 z_1, \\ q &= p_1 + p_2, \\ Q^2 &= -q^2, \\ C &= Q^2 z_2 z_3, \\ 1 &= z_1 + z_2 + z_3, \\ A_4 &= 2(z_2 + z_3 - z_2 z_3), \\ A_5 &= -\frac{4(3+\epsilon)}{(4+\epsilon)}, \end{aligned}$$

and  $N = 4 + \epsilon$ .

6.13. Perform the integral over  $k$  in (6.3.31) and verify that

$$\begin{aligned} \bar{\Gamma}_\mu^{(2)} = \frac{g_s^2}{16\pi^2} & (\frac{1}{2} C_A) \gamma_\mu \frac{\Gamma(1 - \frac{\epsilon}{2}) \Gamma^2(1 + \frac{\epsilon}{2})}{\Gamma(1 + \epsilon)} \\ & \left( \frac{Q^2}{4\pi m_D^2} \right)^{\epsilon/2} \left( -\frac{6}{\epsilon_{UV}} + \frac{8}{\epsilon_{IR}^2} - 2 + \dots \right), \end{aligned}$$

where  $Q^2 = -q^2 > 0$ .

- 6.14. Combine  $\bar{\Gamma}_\mu^{(1)}$  in (6.3.28) and  $\bar{\Gamma}_\mu^{(2)}$  in (6.3.41) and show that

$$\begin{aligned}\bar{\Gamma} = & \frac{g_s^2}{16\pi^2} \frac{\Gamma(1 - \frac{\epsilon}{2})\Gamma^2(1 + \frac{\epsilon}{2})}{\Gamma(1 + \epsilon)} \left( \frac{Q^2}{4\pi m_D^2} \right)^{\epsilon/2} \\ & \left\{ (C_A + T_b T_b) \left( -\frac{2}{\epsilon_{UV}} + \dots \right) \right. \\ & + \left( \frac{1}{2} C_A \right) \left( \frac{8}{\epsilon_{IR}^2} + 6 + \dots \right) \\ & \left. + T_b T_b \left( -\frac{8}{\epsilon_{IR}^2} + \frac{8}{\epsilon_{IR}} - 8 + \dots \right) \right\}.\end{aligned}$$

6.15. Using

$$Z_i = 1 + \frac{g_0^2}{16\pi^2} \frac{\Gamma(1 - \frac{\epsilon}{2})\Gamma^2(1 + \frac{\epsilon}{2})}{\Gamma(1 + \epsilon)} \left( \frac{Q^2}{4\pi m_D^2} \right)^{\epsilon/2} f_i,$$

with

$$f_i = f_i^{\text{pole}} + h_i,$$

and

$$\begin{aligned}f_1^{\text{pole}} &= (C_A + T_b T_b) \frac{2}{\epsilon_{UV}}, \\ f_2^{\text{pole}} &= (T_b T_b) \frac{2}{\epsilon_{UV}}, \\ f_3^{\text{pole}} &= (\frac{3}{4} C_f - \frac{5}{3} C_A) \frac{2}{\epsilon_{UV}},\end{aligned}$$

and using the relationship

$$g_s = \frac{Z_2 \sqrt{Z_3}}{Z_1} g_0,$$

show that to order  $\alpha_0^2$

$$\alpha_s(Q^2) = \alpha_0 - \frac{\alpha_0^2}{4\pi} \beta_0 \left[ \frac{2}{\epsilon_{UV}} + \log(Q^2/m_D^2) + \gamma_E - \log(4\pi) + H \right],$$

where  $H$  is an arbitrary (convention dependent) constant and  $\beta_0 = 11 - \frac{2}{3} n_f$  and  $\alpha_0 = g_0^2/(4\pi)$  is the bare QCD coupling.

- 6.16. Write a computer program to evaluate  $\alpha_s(Q^2)$  in (6.5.23) and compare the results with the tabulated values presented in Table 1.1 for the order  $\alpha_{LO}^2$  expression in (6.5.25).

- 6.17. Show that  $\Lambda$  defined according to

$$\Lambda = \mu \exp \left\{ \frac{1}{2} \int_{\alpha_s(\mu^2)}^A \frac{d\alpha}{\beta(\alpha)} \right\},$$

is independent of the renormalization point  $\mu$  for any choice of the upper limit  $A$ . Using this definition of  $\Lambda$ , show that the leading order expression for the QCD coupling,  $\alpha_s(Q^2)$ , in (6.4.30) corresponds to the choice  $A = \infty$ .

- 6.18. Show that the general solution of the RGE equation

$$\left( -\frac{\partial}{\partial \tau} + \beta(\alpha_s) \frac{\partial}{\partial \alpha_s} \right) R(\tau, \alpha_s) = 0,$$

with the boundary condition

$$\alpha_s(\tau = 0) = \alpha_s(\mu^2) = \alpha_s,$$

is

$$R(\tau, \alpha_s) = R(0, \alpha_s(\tau)).$$

- 6.19. Show that the general solution of the more general RGE equation

$$\left( -\frac{\partial}{\partial \tau} + \beta(\alpha_s) \frac{\partial}{\partial \alpha_s} + \gamma(\alpha_s) \right) F(\tau, \alpha_s) = 0,$$

with the boundary condition

$$\alpha_s(\tau = 0) = \alpha_s(\mu^2) = \alpha_s,$$

is

$$F(\tau, \alpha_s) = F(0, \alpha_s(\tau)) \exp \left\{ \int_{\alpha_s}^{\alpha_s(\tau)} \frac{\gamma(\alpha)}{\beta(\alpha)} d\alpha \right\}.$$

- 6.20. Show that if the non-singlet quark distributions are given by

$$M_n^{NS}(Q^2) = C_n^{NS}(Q^2/\mu^2, \alpha_s) \bar{M}_n^{(0)},$$

where  $\bar{M}_n^{(0)}$  represents the moments of the uncalculable non-perturbative distributions (*independent of  $Q^2$* ) and the “coefficient functions” satisfy the RGE equation

$$C_n^{NS}(\tau, \alpha_s) = C_n^{NS}(0, \alpha_s(\tau)) \exp \left\{ \int_{\alpha_s}^{\alpha_s(\tau)} \frac{\gamma_n(\alpha)}{\beta(\alpha)} d\alpha \right\},$$

then the change in  $M_n^{NS}(Q^2)$  with respect to  $\alpha_s(\tau)$  is given by

$$\begin{aligned}\frac{dM_n^{NS}(Q^2)}{d\alpha_s(\tau)} &= \left( \frac{\gamma_n(\alpha_s(\tau))}{\beta(\alpha_s(\tau))} \right. \\ &+ \left. \frac{1}{C_n^{NS}(0, \alpha_s(\tau))} \frac{dC_n^{NS}(0, \alpha_s(\tau))}{d\alpha_s(\tau)} \right) M_n^{NS}(Q^2).\end{aligned}$$

Using

$$\gamma_n(\alpha_s(\tau)) = -\frac{1}{8\pi}\gamma_0^{(n)}\alpha_s(\tau) - \frac{1}{32\pi^2}\gamma_1^{(n)}\alpha_s^2(\tau) + \dots,$$

$$C_n^{NS}(0, \alpha_s(\tau)) = 1 + B_n^{NS} \frac{\alpha_s(\tau)}{4\pi} + \dots,$$

$$-\beta(\alpha_s(\tau)) = \frac{1}{4\pi}\beta_0\alpha_s^2(\tau) + \frac{1}{16\pi^2}\beta_1\alpha_s^3(\tau) + \dots,$$

show that to leading order

$$M_n^{NS}(Q^2) = M_n^{NS}(Q_0^2) [\alpha_s(Q^2)/\alpha_s(Q_0^2)]^{d_n},$$

where

$$d_n = \frac{\gamma_0^{(n)}}{2\beta_0},$$

and that to order  $\alpha_s^2$  the solution is

$$M_n^{NS}(Q^2) = M_n^{NS}(Q_0^2) [\alpha_s(Q^2)/\alpha_s(Q_0^2)]^{d_n} \exp \left\{ \left( \frac{\gamma_1^{(n)}}{2\beta_0} - \frac{\beta_1\gamma_0^{(n)}}{2\beta_0^2} + B_n^{NS} \right) (\alpha_s(Q^2) - \alpha_s(Q_0^2)) / 4\pi \right\}.$$

- 6.21. Show that the  $B_n^{NS}$  terms in the expansion of the "coefficient function" in (6.6.30) correspond to corrections of order  $\alpha_s^2$  in the  $Q^2$  evolution of the non-singlet moments, but correspond to corrections of order  $\alpha_s$  when comparing quark or gluon distributions defined in two different processes as in (6.6.44).

#### Further Reading

- G. Altarelli, "Partons in Quantum Chromodynamics," *Physics Reports* 81,1 (1982).  
 J.D. Bjorken and S.D. Drell, *Relativistic Quantum Mechanics*, McGraw-Hill, New York, 1965.  
 A.J. Buras, *Rev. Mod. Phys.* 52, 199 (1980).  
 Chris Quigg, *Gauge Theories of the Strong, Weak, and Electromagnetic Interactions*, Frontiers in Physics, The Benjamin-Cummings Publishing Company, Inc., 1983.  
 P. Ramond, *Field Theory: A Modern Primer*, Frontiers in Physics, The Benjamin-Cummings Publishing Company, Inc., 1981.

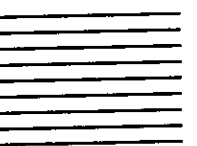
#### References

- P. Ramond, *Field Theory: A Modern Primer*, Frontiers in Physics, The Benjamin-Cummings Publishing Company, Inc., 1981.

- G. 't Hooft and M. Veltman, *Nucl. Phys.* B44, 189 (1972).
- D.J. Gross and F. Wilczek, *Phys. Rev. Lett.* 30, 1343 (1973).
- H.D. Politzer, *Phys. Rev. Lett.* 30, 1346 (1973).
- W. Caswell, *Phys. Rev. Lett.* 33, 244 (1974). D.R.T. Jones, *Nucl. Phys.* B75, 531 (1974).
- C. Callan, *Phys. Rev.* D2, 1541 (1970).
- K. Symanzik, *Comm. Math. Phys.* 18, 227 (1970).

CHAPTER 7

**The Production of  
Particles and Jets  
in Hadron-Hadron  
Collisions**



In the early days of the parton model many theorists believed that the only way to study the constituents within nucleons was by performing deep inelastic electron and neutrino scattering experiments. Hadron-hadron collisions were considered by many to be on a different footing. A famous theorist once remarked that, “you cannot learn about the insides of a watch by colliding two watches together.” On the contrary, however, history has shown that much can be learned about the constituent nature of nucleons from hadron-hadron collisions that involve a large momentum transfer or that produce a large mass object. In these cases short distances are being probed and the basic constituent subprocesses dominate. At least for that portion of the problem that involves short distances the parton approach is applicable and in addition we can employ QCD perturbation theory. In this chapter we will examine some perturbative QCD applications to hadron-hadron collisions.

### 7.1 Single and Double Photon Production

---

In Chapter 4 an incident virtual photon was used to probe the structure of the proton. In hadron-hadron collisions real photons at high transverse momentum can serve as a short distance probe of the incident hadrons<sup>1</sup>. In leading order real photons are produced, for example, by the “annihilation” subprocess  $q + \bar{q} \rightarrow \gamma + g$  and double photons by the purely electromagnetic annihilation  $q + \bar{q} \rightarrow \gamma + \gamma$ . These subprocesses are shown in Fig. 7.1.

In general the exclusive process  $A + B \rightarrow c + d + X$  shown in Fig. 7.2 is described by the following “external” (or experimentally observable) invariants

$$s \equiv (P_A + P_B)^2 = 2 P_A \cdot P_B, \quad (7.1.1)$$

$$t \equiv (p_c - P_A)^2 = -2 p_c \cdot P_A = -\frac{s}{2} x_T T_c \quad (7.1.2)$$

$$u \equiv (p_c - P_B)^2 = -2 p_c \cdot P_B = -\frac{s}{2} x_T \frac{1}{T_c}, \quad (7.1.3)$$

where

$$x_T = 2p_T/\sqrt{s}, \quad (7.1.4)$$

and

$$T_c \equiv \tan(\theta_c/2). \quad (7.1.5)$$

In arriving at these expressions the masses of all the constituents and the incident hadrons have been neglected and  $p_T$  is the transverse momentum of constituent  $c$  (and constituent  $d$  provided the incident partons are parallel to the incident hadrons). The invariants of the “internal” constituent 2-to-2 subprocess are defined by

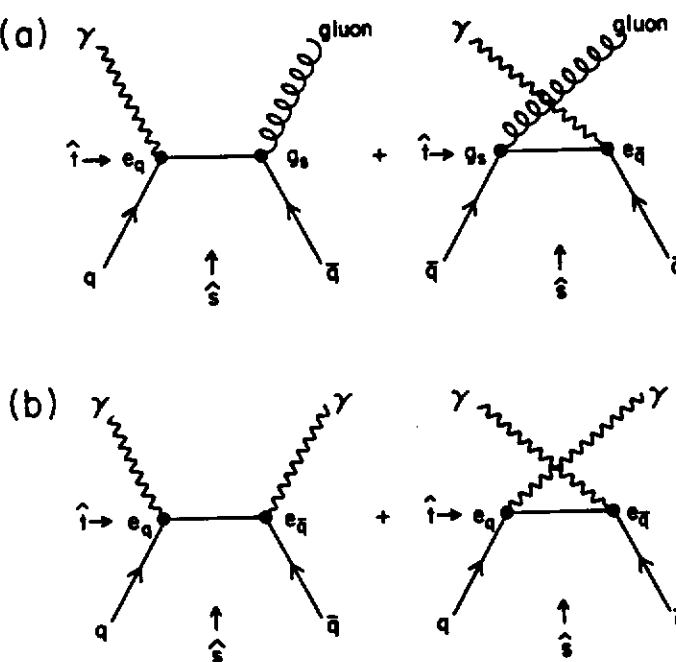


Figure 7.1 (a) Amplitudes for quark-antiquark annihilation into a photon and a gluon,  $q + \bar{q} \rightarrow \gamma + g$ . (b) Amplitudes for quark-antiquark annihilation into two photons,  $q + \bar{q} \rightarrow \gamma + \gamma$ .

$$\hat{s} \equiv (p_a + p_b)^2 = 2 p_a \cdot p_b = x_a x_b s, \quad (7.1.6)$$

$$\hat{t} \equiv (p_c - p_a)^2 = -2 p_c \cdot p_a = x_a t, \quad (7.1.7)$$

$$\hat{u} \equiv (p_c - p_b)^2 = -2 p_c \cdot p_b = x_b u, \quad (7.1.8)$$

where the momentum fractions  $x_a$  and  $x_b$  are given by

$$p_a = x_a P_A, \quad (7.1.9)$$

and

$$p_b = x_b P_B. \quad (7.1.10)$$

Momentum and energy conservation of the constituent 2-to-2 subprocess,

$$p_a + p_b = p_c + p_d, \quad (7.1.11)$$

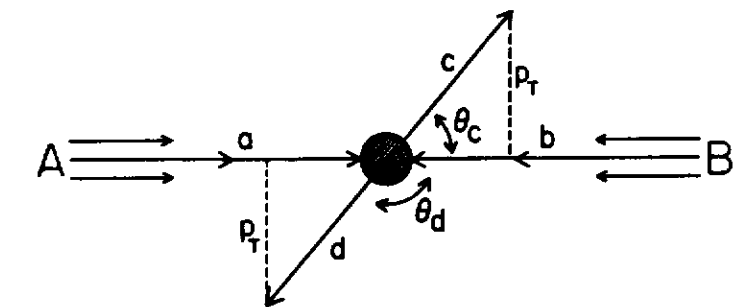


Figure 7.2 Illustration of the inclusive process  $A + B \rightarrow c + d + X$  resulting from the 2-to-2 hard scattering constituent subprocess,  $a + b \rightarrow c + d$ .

insures that

$$\hat{s} + \hat{t} + \hat{u} = 0, \quad (7.1.12)$$

which means that

$$x_a x_b s + x_a t + x_b u = 0, \quad (7.1.13)$$

or

$$x_a = \frac{x_b x_1}{x_b - x_2}, \quad (7.1.14)$$

and

$$x_b = \frac{x_a x_2}{x_a - x_1}, \quad (7.1.15)$$

with

$$x_1 = -\frac{u}{s} = \frac{1}{2} x_T \frac{1}{T_c}, \quad (7.1.16)$$

$$x_2 = -\frac{t}{s} = \frac{1}{2} x_T T_c. \quad (7.1.17)$$

Furthermore,

$$p_T^2 = \frac{tu}{s} = \frac{\hat{t}\hat{u}}{\hat{s}}. \quad (7.1.18)$$

The invariant  $\hat{t}$  can be expressed as

$$\hat{t} = (p_c - p_a)^2 = -2 p_c \cdot p_a = -\frac{s}{2} x_T x_a T_c, \quad (7.1.19)$$

or from (7.1.11) equivalently as

$$\hat{t} = (p_c - p_b)^2 = 2 p_d \cdot p_b = -\frac{s}{2} x_T x_b T_d \quad (7.1.20)$$

where  $T_d$  is defined by (7.1.5) and

$$T_d \equiv \tan(\theta_d/2). \quad (7.1.21)$$

Equation (7.1.19) and (7.1.20) together imply that

$$x_a T_c = x_b T_d. \quad (7.1.22)$$

Longitudinal momentum conservation gives

$$p_a - p_b = E_c \cos(\theta_c) + E_d \cos(\theta_d) \quad (7.1.23)$$

or

$$x_a - x_b = x_T [\cot(\theta_c) + \cot(\theta_d)]. \quad (7.1.24)$$

Combining (7.1.22) and (7.1.24) results in

$$x_a = \frac{1}{2} x_T \left( \frac{1}{T_c} + \frac{1}{T_d} \right) \quad (7.1.25)$$

$$x_b = \frac{1}{2} x_T (T_c + T_d) \quad (7.1.26)$$

and using (7.1.6), (7.1.7) and (7.1.8) gives

$$\hat{s} = \frac{s}{4} x_T^2 \left( 2 + \frac{T_c}{T_d} + \frac{T_d}{T_c} \right), \quad (7.1.27)$$

$$\hat{t} = -\frac{s}{4} x_T^2 \left( 1 + \frac{T_c}{T_d} \right), \quad (7.1.28)$$

$$\hat{u} = -\frac{s}{4} x_T^2 \left( 1 + \frac{T_d}{T_c} \right). \quad (7.1.29)$$

The external experimental cross section is given in terms of the constituent differential cross section,  $d\sigma/d\hat{t}$ , by

$$d\sigma = G_{A \rightarrow a}^{(0)}(x_a) dx_a G_{B \rightarrow b}^{(0)}(x_b) dx_b \left( \frac{d\hat{\sigma}}{d\hat{t}}(\hat{s}, \hat{t}) \right) d\hat{t}, \quad (7.1.30)$$

where  $G_{A \rightarrow a}^{(0)}(x_a) dx_a$  is the probability of finding constituent  $a$  within hadron  $A$  carrying fractional momentum  $x_a$  and similarly for  $G_{B \rightarrow b}^{(0)}(x_b)$ .

The single particle inclusive cross section  $A + B \rightarrow c + X$  is arrived at by integrating (7.1.30) over  $\theta_d$  (or equivalently over  $x_a$ ). From (7.1.14) and (7.1.19) it is easy to compute the Jacobian

$$\frac{\partial(x_b, \hat{t})}{\partial(\theta_c, x_T)} = \frac{s}{2} \frac{x_a x_b}{x_a - x_1} \frac{x_T}{\sin(\theta_c)}. \quad (7.1.31)$$

Furthermore, the invariant differential is given by

$$\frac{d^3 p}{E} = dy \, d^2 p_T = \frac{\pi}{2} \frac{s x_T}{\sin(\theta_c)} d\theta_c \, dx_T, \quad (7.1.32)$$

where  $y$  is the rapidity of particle  $c$  (rapidity is defined in (5.1.26)) and

$$dy = \frac{d\theta_c}{\sin(\theta_c)}. \quad (7.1.33)$$

Combining (7.1.32) and (7.1.31) gives

$$dx_b d\hat{t} = \frac{1}{\pi} \frac{x_a x_b}{(x_a - x_1)} \frac{d^3 p}{E}, \quad (7.1.34)$$

and (7.1.30) becomes

$$E \frac{d\sigma}{d^3 p}(A + B \rightarrow c + X; s, p_T, \theta_c) = \frac{1}{\pi} \int_{x_a^{\min}}^{1.0} dx_a G_{A \rightarrow a}^{(0)}(x_a) G_{B \rightarrow b}^{(0)}(x_b) \left( \frac{x_a x_b}{x_a - x_1} \right) \frac{d\hat{\sigma}}{d\hat{t}}(a + b \rightarrow c + d; \hat{s}, \hat{t}), \quad (7.1.35)$$

where

$$x_b = \frac{x_a x_2}{x_a - x_1}, \quad (7.1.36)$$

$$\hat{s} = x_a x_b s, \quad (7.1.37)$$

and

$$\hat{t} = -\frac{s}{2} x_a x_T T_c, \quad (7.1.38)$$

and  $x_a^{\min}$  is determined by setting  $x_b = 1$  in (7.1.14) giving

$$x_a^{\min} = \frac{x_1}{1 - x_2} = \frac{x_T/T_c}{2 - x_T T_c}. \quad (7.1.39)$$

If we do not integrate over the angle  $\theta_d$  then

$$dx_a = (x_a - x_1) dy_d, \quad (7.1.40)$$

where  $y_d$  is the rapidity of particle  $d$  and we arrive at the double differential cross section

$$E_c \frac{d\sigma}{d^3 p_c dy_d}(A + B \rightarrow c + d + X; s, p_T, \theta_c, \theta_d) = \\ x_a x_b G_{A \rightarrow a}^{(0)}(x_a) G_{B \rightarrow b}^{(0)}(x_b) \frac{1}{\pi} \frac{d\hat{\sigma}}{d\hat{t}}(a + b \rightarrow c + d; \hat{s}, \hat{t}), \quad (7.1.41)$$

where  $x_a$  and  $x_b$  are given by (7.1.25) and (7.1.26), respectively, and  $\hat{s}$  and  $\hat{t}$  by (7.1.27) and (7.1.28), respectively<sup>2</sup>.

Summing the leading logarithmic contributions from gluon Bremsstrahlung converts the “bare” structure functions in (7.1.35) and (7.1.40) into the  $Q^2$  dependent QCD structure functions  $G_{A \rightarrow a}(x, Q^2)$  and  $G_{B \rightarrow b}(x, Q^2)$ . These

"renormalization group" improved structure functions satisfy the  $Q^2$  evolution equations derived in Chapter 4 and, for example, (7.1.35) becomes

$$E \frac{d\sigma}{d^3 p} (A + B \rightarrow c + X; s, p_T, \theta_c) = \frac{1}{\pi} \int_{x_a^{\min}}^{1.0} dx_a G_{A \rightarrow a}(x_a, Q^2) G_{B \rightarrow b}(x_b, Q^2) \left( \frac{x_a x_b}{x_a - x_1} \right) \frac{d\hat{\sigma}}{dt} (a + b \rightarrow c + d; \hat{s}, \hat{t}). \quad (7.1.42)$$

Here it is not clear what to use for the variable,  $Q$ , that determines the scale at which the structure functions  $G(x, Q^2)$  are sampled and also sets the strength of the strong interaction coupling,  $\alpha_s$ . At leading order all choices for  $Q$  that increase with the parton-parton center-of-mass energy are equivalent. Different choices affect the beyond leading order terms. The best choice would be the one that minimized the higher order terms, thus providing us with an accurate approximation. However, this cannot be decided without knowing the beyond leading order terms which in most cases are beyond ones ability to calculate. Some guesses at the best choice include

$$Q^2 = 4p_T^2, \quad (7.1.43)$$

and

$$Q^2 = \frac{2\hat{s}\hat{t}\hat{u}}{\hat{s}^2 + \hat{t}^2 + \hat{u}^2}. \quad (7.1.44)$$

In most cases the choice of  $Q^2$  does not make much difference since it always appears in conjunction with the QCD parameter  $\Lambda$  (i.e.,  $Q^2/\Lambda$ ) and the value of  $\Lambda$  is still somewhat uncertain.

The differential cross section for the constituent subprocess  $q + \bar{q} \rightarrow \gamma + g$  shown in Fig. 7.1 is given by

$$\frac{d\hat{\sigma}}{dt}(\hat{s}, \hat{t}) = \frac{\pi\alpha\alpha_s e_q^2}{\hat{s}^2} \frac{4}{9} 2 \left( \frac{\hat{u}}{\hat{t}} + \frac{\hat{t}}{\hat{u}} \right), \quad (7.1.45)$$

which is the same as (5.2.9) except now  $M^2 = 0$ . The differential cross section for the purely electromagnetic subprocess  $q + \bar{q} \rightarrow \gamma + \gamma$  in Fig. 7.1b is given by

$$\frac{d\hat{\sigma}}{dt}(\hat{s}, \hat{t}) = \frac{\pi\alpha^2 e_q^4}{\hat{s}^2} \frac{1}{3} 2 \left( \frac{\hat{u}}{\hat{t}} + \frac{\hat{t}}{\hat{u}} \right), \quad (7.1.46)$$

and it identical to (7.1.45) except the former has a color factor of  $4/9$  and the latter a color factor of  $3/9 = 1/3$  and  $\alpha_s$  is replaced by  $\alpha e_q^2$ . The ratio of these two cross sections is thus given by

$$\frac{d\hat{\sigma}/dt(q\bar{q} \rightarrow \gamma\gamma)}{d\hat{\sigma}/dt(q\bar{q} \rightarrow \gamma g)} = \frac{3}{4} \frac{\alpha}{\alpha_s} e_q^2, \quad (7.1.47)$$

which leads to several interesting predictions for pion-proton collisions. If we naively assume that the dominant contributions to the production of single and double photons at high  $p_T$  are the annihilation terms  $\bar{u}u \rightarrow \gamma g$  and

$\bar{d}d \rightarrow \gamma g$ , respectively, for  $\pi^- p$  collisions and the annihilation terms  $\bar{d}d \rightarrow \gamma\gamma$  and  $\bar{d}d \rightarrow \gamma\gamma$ , respectively, for  $\pi^+ p$  collisions we conclude that

$$\frac{Ed\sigma/d^3 p(\pi^- p \rightarrow \gamma\gamma + X)}{Ed\sigma/d^3 p(\pi^- p \rightarrow \gamma + X)} = \frac{3}{4} \frac{\alpha}{\alpha_s} e_u^2 = \frac{1}{3} \frac{\alpha}{\alpha_s}, \quad (7.1.48)$$

and

$$\frac{Ed\sigma/d^3 p(\pi^+ p \rightarrow \gamma\gamma + X)}{Ed\sigma/d^3 p(\pi^+ p \rightarrow \gamma + X)} = \frac{3}{4} \frac{\alpha}{\alpha_s} e_d^2 = \frac{1}{12} \frac{\alpha}{\alpha_s}. \quad (7.1.49)$$

The added assumption that  $G_{p \rightarrow u}(x, Q^2) \approx 2G_{p \rightarrow d}(x, Q^2)$  yields

$$\frac{Ed\sigma/d^3 p(\pi^+ p \rightarrow \gamma + X)}{Ed\sigma/d^3 p(\pi^- p \rightarrow \gamma + X)} \approx \frac{1}{2} \left( \frac{e_d}{e_u} \right)^2 = \frac{1}{8}, \quad (7.1.50)$$

and

$$\frac{Ed\sigma/d^3 p(\pi^+ p \rightarrow \gamma\gamma + X)}{Ed\sigma/d^3 p(\pi^- p \rightarrow \gamma\gamma + X)} \approx \frac{1}{2} \left( \frac{e_d}{e_u} \right)^4 = \frac{1}{32}. \quad (7.1.51)$$

Thus, in the large  $p_T$  regime, a  $\pi^-$  beam should be 32 times more efficient at producing double photons and 8 times more efficient at producing single photons compared with a  $\pi^+$  beam. Furthermore, from (7.1.48) and (7.1.49) we have the exciting possibility of making a direct measurement of the ratio of the electromagnetic to the strong coupling,  $\alpha/\alpha_s$ . With  $\alpha_s = 0.25$ , these equations imply a double to single photon ratio of about 0.01 for  $\pi^- p$  collisions. On the average, one out of every 100 large  $p_T$  photon triggers would be balanced on the away-side by another photon of roughly the same transverse momentum.

Unfortunately, these simple estimates are altered by constituent subprocesses involving gluons. An important contribution to the single photon rate comes from "Compton" subprocess  $q + g \rightarrow \gamma + q$  and  $\bar{q} + g \rightarrow \gamma + \bar{q}$  shown in Fig. 7.3. The differential cross section for these subprocesses is given by

$$\frac{d\hat{\sigma}}{dt}(qg \rightarrow \gamma q) = \frac{\pi\alpha\alpha_s e_q^2}{\hat{s}^2} \frac{1}{6} 2 \left( -\frac{\hat{t}}{\hat{s}} - \frac{\hat{s}}{\hat{t}} \right), \quad (7.1.52)$$

which is the same as (5.2.18) but with  $M^2 = 0$ . When summed over quarks and antiquarks the Compton subprocess contribute equally to  $\pi^+ p$  and  $\pi^- p$  collisions.

An interesting source of double photons that contributes equally to  $\pi^+ p$  and  $\pi^- p$  collisions is gluon-gluon annihilation into two photons,  $gg \rightarrow \gamma\gamma$ . This process proceeds through a quark loop as shown in Fig. 7.4b. There are actually six amplitudes that must be summed. They correspond to the gluons and photons attaching at various points around the quark loop. The differential cross section can be arrived at from the light-light scattering cross section,  $\gamma\gamma \rightarrow \gamma\gamma$ , first computed by De Tollis in 1965<sup>3</sup>. The result is given by<sup>4</sup>

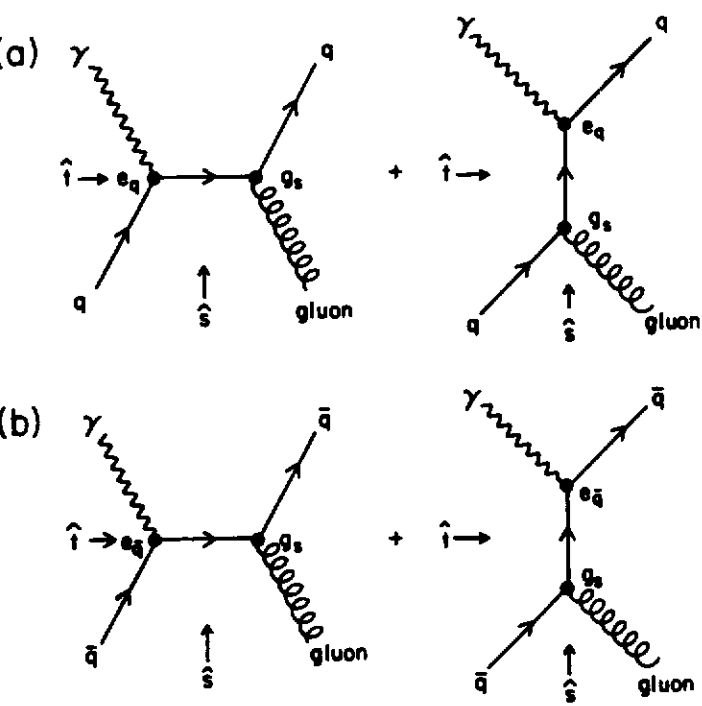


Figure 7.3 Amplitudes for the "Compton" production of a photon via the subprocess (a)  $q + g \rightarrow \gamma + q$  and (b)  $\bar{q} + g \rightarrow \gamma + \bar{q}$ .

$$\begin{aligned} \frac{d\hat{\sigma}}{dt}(gg \rightarrow \gamma\gamma; \hat{s}, \hat{t}) = & \frac{\alpha^2 \alpha_s^2}{8\pi \hat{s}^2} \left( \sum_{i=1}^{n_f} e_{q_i}^2 \right)^2 \\ & \left\{ \frac{1}{8} \left[ \left( \frac{(\hat{s}^2 + \hat{t}^2)}{\hat{u}^2} \log^2(-\hat{s}/\hat{t}) + 2 \frac{(\hat{s} - \hat{t})}{\hat{u}} \log(-\hat{s}/\hat{t}) \right)^2 \right. \right. \\ & + \left( \frac{(\hat{s}^2 + \hat{u}^2)}{\hat{t}^2} \log^2(-\hat{s}/\hat{u}) + 2 \frac{(\hat{s} - \hat{u})}{\hat{t}} \log(-\hat{s}/\hat{u}) \right)^2 \\ & + \left. \left. \left( \frac{(\hat{t}^2 + \hat{u}^2)}{\hat{s}^2} (\log^2(\hat{t}/\hat{u}) + \pi^2) + 2 \frac{(\hat{t} - \hat{u})}{\hat{s}} \log(\hat{t}/\hat{u}) \right)^2 \right] \right. \\ & \left. + \frac{1}{2} \left[ \frac{(\hat{s}^2 + \hat{t}^2)}{\hat{u}^2} \log^2(-\hat{s}/\hat{t}) + 2 \frac{(\hat{s} - \hat{t})}{\hat{u}} \log(-\hat{s}/\hat{t}) + \frac{(\hat{s}^2 + \hat{u}^2)}{\hat{t}^2} \log^2(-\hat{s}/\hat{u}) \right. \right. \end{aligned}$$

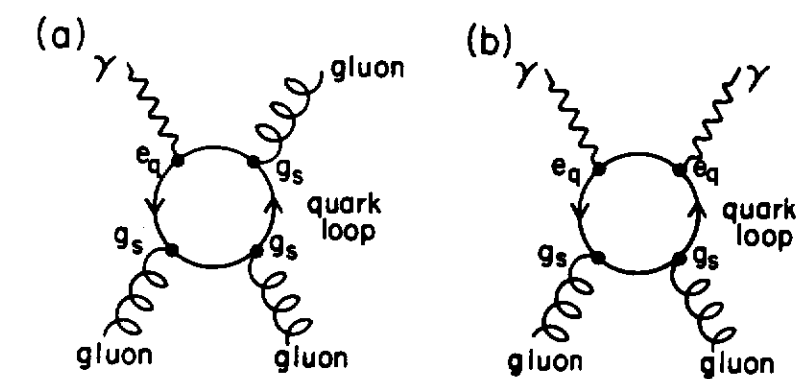


Figure 7.4 The production of a single photon (a) and two photons (b) via gluon-gluon annihilation which proceeds through a quark loop.

$$\begin{aligned} & + 2 \frac{(\hat{s} - \hat{t})}{\hat{t}} \log(-\hat{s}/\hat{u}) + \frac{(\hat{t}^2 + \hat{u}^2)}{\hat{s}^2} (\log^2(\hat{t}/\hat{u}) + \pi^2) + 2 \frac{(\hat{t} - \hat{u})}{\hat{s}} \log(\hat{t}/\hat{u}) \Big] \\ & + \frac{\pi^2}{2} \left[ \left( \frac{(\hat{s}^2 + \hat{t}^2)}{\hat{u}^2} \log(-\hat{s}/\hat{t}) + \frac{(\hat{s} - \hat{t})}{\hat{u}} \right)^2 \right. \\ & \left. + \left( \frac{(\hat{s}^2 + \hat{u}^2)}{\hat{t}^2} \log(-\hat{s}/\hat{u}) + \frac{(\hat{s} - \hat{u})}{\hat{t}} \right)^2 \right] + 4 \Big\}, \quad (7.1.53) \end{aligned}$$

where the color factor is equal to  $1/32$  and arises from

$$\frac{1}{8} \frac{1}{8} \sum_{a,b} (\text{tr}(\mathbf{T}_a \mathbf{T}_b))^2 = \frac{1}{8} \frac{1}{8} \frac{1}{4} 8 = \frac{1}{32}, \quad (7.1.54)$$

where I have used (D.1.8). The gluon-gluon fusion to a single photon,  $gg \rightarrow \gamma g$ , cross section is given by

$$\frac{d\hat{\sigma}}{dt}(gg \rightarrow \gamma g; \hat{s}, \hat{t}) = \frac{5\alpha_s}{12\alpha} \frac{\left( \sum_{i=1}^{n_f} e_{q_i} \right)^2}{\left( \sum_{i=1}^{n_f} e_{q_i}^2 \right)^2} \frac{d\hat{\sigma}}{dt}(gg \rightarrow \gamma\gamma; \hat{s}, \hat{t}). \quad (7.1.55)$$

In this case the color factor is

$$\frac{1}{8} \frac{1}{8} \sum_{a,b,c} \frac{d_{abc}}{4} \frac{d_{cba}}{4} = \frac{1}{8} \frac{1}{8} \frac{1}{16} \frac{5}{3} 8 = \frac{5}{384}, \quad (7.1.56)$$

where I have used (D.1.9). The antisymmetric structure constants  $f_{abc}$  do not contribute since the amplitude is symmetric under the interchange of any two of the gluons. Comparing (7.1.54) and (7.1.56) gives the factor of  $5/12$  in

(7.1.55). For  $n_f = 4$  the ratio is given by

$$\frac{d\hat{\sigma}/d\hat{t}(gg \rightarrow \gamma\gamma)}{d\hat{\sigma}/d\hat{t}(gg \rightarrow \gamma g)} = \frac{20}{3} \frac{\alpha}{\alpha_s} \approx \frac{1}{5}, \quad (7.1.57)$$

where the last figure comes from setting  $\alpha_s = 0.25$  and although  $gg \rightarrow \gamma g$  gives a negligible contribution to the single photon rate,  $gg \rightarrow \gamma\gamma$  does make a significant contribution to the double photon yield. The  $gg \rightarrow \gamma\gamma$  contribution is of order  $\alpha^2 \alpha_s^2$  and is down by two powers of  $\alpha_s$  from the pure electromagnetic quark-antiquark annihilation,  $q\bar{q} \rightarrow \gamma\gamma$ . Nevertheless, the large numbers of small  $x$  gluons within hadrons makes  $gg \rightarrow \gamma\gamma$  an important subprocess. For example, in  $\pi^+ p$  collisions at  $\sqrt{s} = 27.4$  GeV and  $p_T = 4$  GeV it is estimated that the  $gg \rightarrow \gamma\gamma$  term makes up about 40% of the double photon rate<sup>4</sup>.

If one includes all the contributions to single and double photon production one arrives at the ratios  $\pi^- p \rightarrow (\gamma\gamma/\gamma) + X$ ,  $\pi^+ p \rightarrow (\gamma\gamma/\gamma) + X$ ,  $(\pi^+/\pi^-)p \rightarrow \gamma + X$ , and  $(\pi^+/\pi^-)p \rightarrow \gamma\gamma + X$  shown in Fig. 7.5 at  $\sqrt{s} = 27.4$  GeV. The naive estimates in (7.1.46), (7.1.49), (7.1.50) and (7.1.51), respectively, are approached, but only at very large  $x_T$ .

## 7.2 Large Transverse Momentum Mesons

In the naive parton model, the large transverse momentum production of hadrons in the process  $A + B \rightarrow h + X$  is described by the diagram in Fig. 7.6. The process is assumed to occur as the result of a single large-angle scattering of constituents  $a + b \rightarrow c + d$  followed by the fragmentation of constituent  $c$  into the outgoing hadron  $h$  and constituent  $d$  into “away-side” hadron,  $h_2$ . The result is the four “jet” structure in Fig. 7.7.

The single particle cross section,  $A + B \rightarrow h + X$ , is given by

$$d\sigma(s, t) = G_{A \rightarrow a}^{(0)}(x_a) dx_a G_{B \rightarrow b}^{(0)}(x_b) \left( \frac{d\hat{\sigma}}{dt}(\hat{s}, \hat{t}) \right) d\hat{t} D_{0,c}^h(z_c) dz_c, \quad (7.2.1)$$

where  $G_{A \rightarrow a}^{(0)}(x) dx$  is the probability of finding a parton of type  $a$  carrying fractional momentum  $x$  of the hadron  $A$  and  $D_{0,c}^h(z) dz$  is the probability that constituent  $c$  fragments into hadron  $h$  giving it a fraction  $z$  of its initial momentum. The “external” (or experimentally observable) invariants are

$$s \equiv (P_A + P_B)^2 = 2 P_A \cdot P_B, \quad (7.2.2)$$

$$t \equiv (P_h - P_A)^2 = -2 P_h \cdot P_A, \quad (7.2.3)$$

$$u \equiv (P_h - P_B)^2 = -2 P_h \cdot P_B, \quad (7.2.4)$$

and the “internal” (or constituent) invariants are

$$\hat{s} \equiv (p_a + p_b)^2 = 2 p_a \cdot p_b = x_a x_b s, \quad (7.2.5)$$

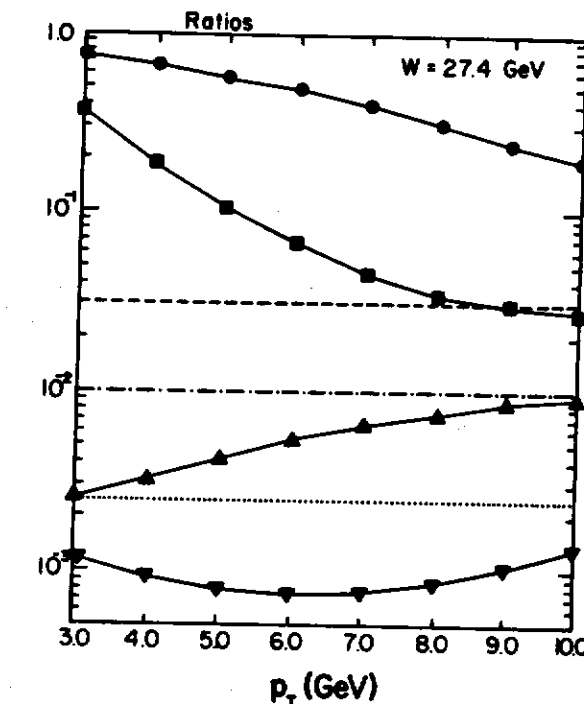


**Figure 7.5** Beam ratios and double to single photon ratios in  $\pi p$  collisions at  $W = \sqrt{s} = 27.4$  GeV and  $\theta = 90^\circ$ :  $(\pi^+/\pi^-)p \rightarrow \gamma + X$  (solid dots),  $(\pi^+/\pi^-)p \rightarrow \gamma\gamma + X$  (solid squares),  $\pi^- p \rightarrow (\gamma\gamma/\gamma) + X$  (up pointing triangles),  $\pi^+ p \rightarrow (\gamma\gamma/\gamma) + X$  (down pointing triangles). Also shown are the naive estimates:  $\frac{1}{2}(\epsilon_d/\epsilon_u)^2$  (dashed line),  $\frac{3}{4}(\alpha/\sigma_s)\epsilon_u^2$  (dot-dashed line),  $\frac{3}{4}(\alpha/\sigma_s)\epsilon_d^2$  (dotted line) (taken from Ref. 4).

$$\hat{t} \equiv (p_c - p_a)^2 = -2 p_c \cdot p_a = x_a t / z_c, \quad (7.2.6)$$

$$\hat{u} \equiv (p_c - p_b)^2 = -2 p_c \cdot p_b = x_b u / z_c. \quad (7.2.7)$$

The connection between the internal and external invariants comes from

$$p_a = x_a P_A, \quad (7.2.8)$$

$$p_b = x_b P_B, \quad (7.2.9)$$

$$P_h = z_c p_c, \quad (7.2.10)$$

where constituent and hadron masses are neglected. The 2-to-2 scattering constraint

$$\hat{s} + \hat{t} + \hat{u} = 0, \quad (7.2.11)$$

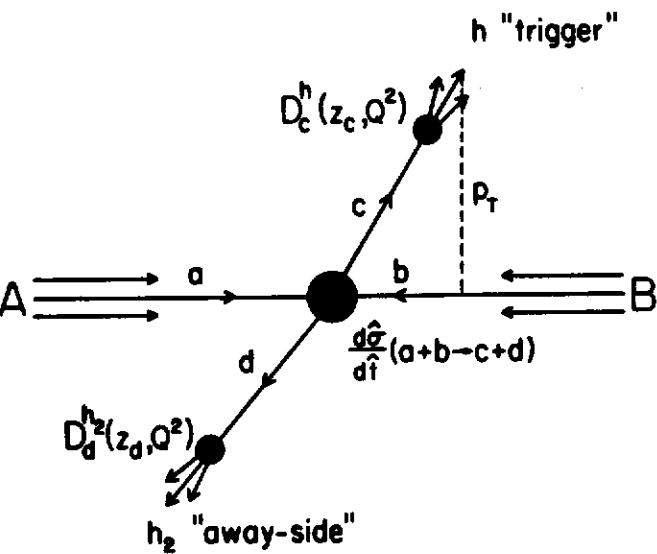


Figure 7.6 Illustration of the inclusive process  $A + B \rightarrow h + h_2 + X$  resulting from the 2-to-2 hard scattering constituent subprocess,  $a + b \rightarrow c + d$ .

implies that

$$z_c = \frac{x_2}{x_b} + \frac{x_1}{x_a}, \quad (7.2.12)$$

where

$$x_1 = -u/s = \frac{1}{2}x_T \frac{1}{T_h}, \quad (7.2.13)$$

$$x_2 = -t/s = \frac{1}{2}x_T T_h, \quad (7.2.14)$$

as in (7.1.16) and (7.1.17) with

$$x_T = 2p_T/\sqrt{s}, \quad (7.2.15)$$

and

$$T_h = \tan(\theta_{cm}/2), \quad (7.2.16)$$

where  $\theta_{cm}$  is the center-of-mass scattering angle of the hadron  $h$ .

From (7.2.6) and (7.2.12) it is easy to see that the Jacobian is given by

$$\frac{\partial(z_c, \hat{t})}{\partial(\theta_{cm}, x_T)} = \frac{s x_T}{2 z_c \sin(\theta_{cm})}, \quad (7.2.17)$$

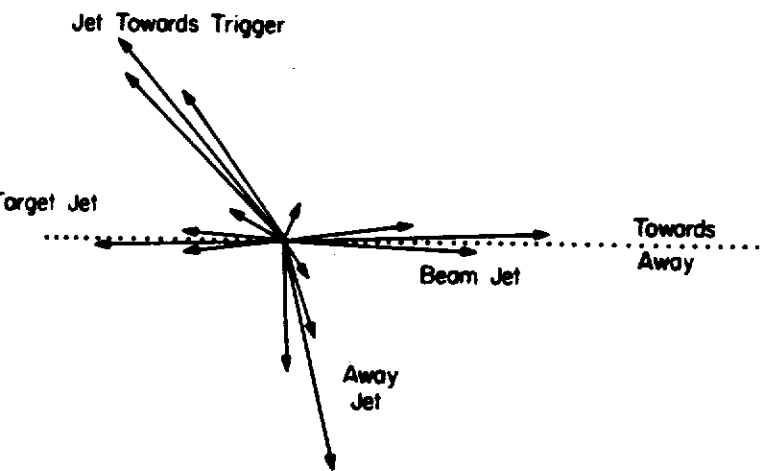


Figure 7.7 Illustration of the four jet structure resulting from a beam hadron (entering from the left along the dotted line) colliding with a target hadron (entering from the right along the dotted line) in the center-of-mass frame: two jets (collection of particles moving in roughly the same direction) with large transverse momentum,  $p_T$ , and two jets with small  $p_T$  that result from the break-up of the beam and target hadron.

which together with

$$d\theta_{cm} dx_T = \frac{2}{s\pi} \frac{\sin(\theta_{cm})}{x_T} \frac{d^3 p}{E}, \quad (7.2.18)$$

gives

$$dz_c d\hat{t} = \frac{1}{\pi z_c} \frac{d^3 p}{E}, \quad (7.2.19)$$

and (7.2.1) becomes

$$\begin{aligned} Ed\sigma/d^3 p(A + B \rightarrow h + X; s, p_T, \theta_{cm}) = & \\ \frac{1}{\pi} \int_{z_c^{\min}}^{1.0} dz_c \int_{x_b^{\min}}^{1.0} dx_b G_{A \rightarrow a}(x_a, Q^2) G_{B \rightarrow b}(x_b, Q^2) D_c^h(z_c, Q^2) \\ & \frac{1}{z_c} \frac{d\hat{\sigma}}{d\hat{t}}(ab \rightarrow cd; \hat{s}, \hat{t}), \end{aligned} \quad (7.2.20)$$

where  $z_c$  is given in (7.2.12). The limit of the integration over  $x_b$  is arrived at

by setting  $z_c = 1$  in (7.2.12) and solving for  $x_b$  which gives

$$x_b^{\min} = \frac{x_a x_2}{x_a - x_1}. \quad (7.2.21)$$

For the limit on  $x_a$  one sets both  $z_c = 1$  and  $x_b = 1$  and solves for  $x_a$  giving

$$x_a^{\min} = \frac{x_1}{1 - x_2}. \quad (7.2.22)$$

The invariant cross section for the production of a constituent parton can be arrived at from (7.2.20) by setting

$$D_c(z_c, Q^2) = \delta(1 - z_c), \quad (7.2.23)$$

and using

$$\delta(1 - z_c) \rightarrow \frac{x_b^2}{x_2} \delta\left(x_b - \frac{x_2 x_a}{x_a - x_1}\right). \quad (7.2.24)$$

In this case

$$E d\sigma/d^3 p(A + B \rightarrow c + X; s, p_T, \theta_{cm}) = \int_{x_a^{\min}}^{1.0} dx_a \frac{x_b^2}{x_2} G_{A \rightarrow a}(x_a, Q^2) G_{B \rightarrow b}(x_b, Q^2) \frac{d\hat{\sigma}}{dt}(ab \rightarrow cd; \hat{s}, \hat{t}), \quad (7.2.25)$$

with

$$x_b = \frac{x_2 x_a}{x_a - x_1}, \quad (7.2.26)$$

and  $x_a^{\min}$  given in (7.2.22). This is the same formula we arrived at in (7.1.42).

As illustrated in Fig. 7.8 the “bare” quark distributions,  $G^{(0)}(x)$ , in (7.2.1) have been replaced by the “renormalization group improved” distributions  $G(x, Q^2)$  that satisfy the  $Q^2$  evolution equations in Chapter 4. In so doing we have in effect summed a set of leading log contributions. Similarly, the “bare” fragmentation function,  $D^{(0)}(x)$ , have been replaced by the  $Q^2$  dependent functions,  $D(x, Q^2)$  and thus summing the leading log corrections to the fragmentation functions. If we compute the constituent differential cross section,  $d\hat{\sigma}/d\hat{t}$ , to order  $\alpha_s^2$  then (7.2.20) and (7.2.21) are correct to leading order. The seven parton-parton differential cross sections that contribute are given by<sup>5</sup>

$$\frac{d\hat{\sigma}}{d\hat{t}}(ab \rightarrow cd; \hat{s}, \hat{t}) = \frac{\pi \alpha_s^2}{\hat{s}^2} |\overline{\mathcal{M}}(ab \rightarrow cd)|^2, \quad (7.2.27)$$

where

$$|\overline{\mathcal{M}}(q_i q_j \rightarrow q_i q_j)|^2 = |\overline{\mathcal{M}}(q_i \bar{q}_j \rightarrow q_i \bar{q}_j)|^2 = \frac{4}{9} \frac{\hat{s}^2 + \hat{u}^2}{\hat{t}^2}, \quad (7.2.28)$$

$$|\overline{\mathcal{M}}(q_i q_i \rightarrow q_i q_i)|^2 = \frac{4}{9} \left( \frac{\hat{s}^2 + \hat{u}^2}{\hat{t}^2} + \frac{\hat{s}^2 + \hat{t}^2}{\hat{u}^2} \right) - \frac{8}{27} \frac{\hat{s}^2}{\hat{u}\hat{t}}, \quad (7.2.29)$$

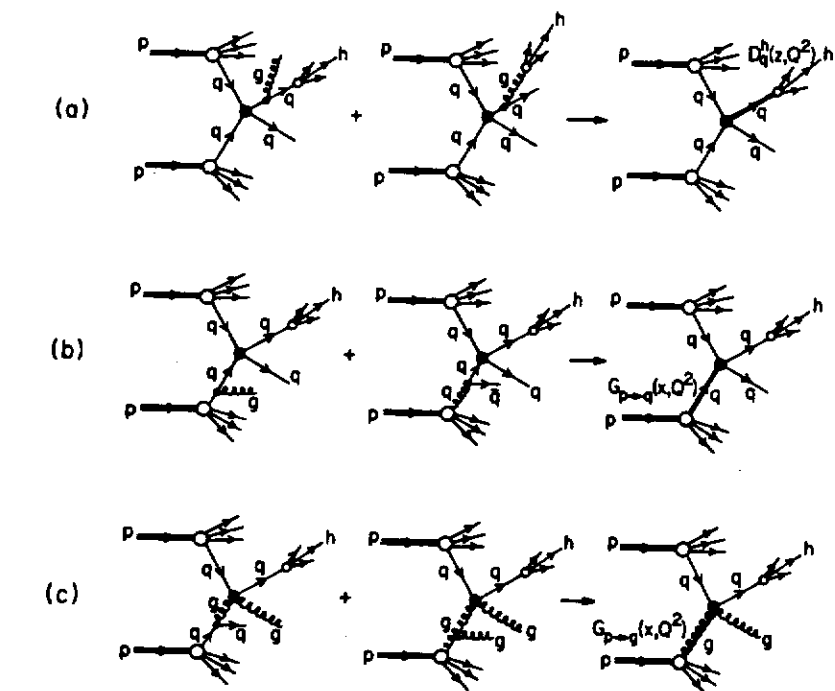


Figure 7.8 (a) Illustration of how the leading log parts of the subprocess  $q + q \rightarrow g + q + q$  sum to give the  $Q^2$  dependent fragmentation functions,  $D_q^h(z, Q^2)$ . (b) Illustration of how the leading log parts of the subprocesses  $q + q \rightarrow q + q + g$  and  $q + g \rightarrow q + q + g$  sum to give the  $Q^2$  dependent quark probability distributions,  $G_{p \rightarrow q}(x, Q^2)$ . (c) Illustration of how the leading log parts of the subprocesses  $q + g \rightarrow q + g + g$  and  $q + g \rightarrow q + g + g$  sum to give the  $Q^2$  dependent gluon probability distribution,  $G_{p \rightarrow g}(x, Q^2)$ .

$$|\overline{\mathcal{M}}(q_i \bar{q}_i \rightarrow q_i \bar{q}_i)|^2 = \frac{4}{9} \left( \frac{\hat{s}^2 + \hat{u}^2}{\hat{t}^2} + \frac{\hat{t}^2 + \hat{u}^2}{\hat{s}^2} \right) - \frac{8}{27} \frac{\hat{u}^2}{\hat{s}\hat{t}}, \quad (7.2.30)$$

$$|\overline{\mathcal{M}}(q_i \bar{q}_i \rightarrow gg)|^2 = \frac{32}{27} \left( \frac{\hat{u}^2 + \hat{t}^2}{\hat{u}\hat{t}} \right) - \frac{8}{3} \left( \frac{\hat{u}^2 + \hat{t}^2}{\hat{s}^2} \right), \quad (7.2.31)$$

$$|\overline{\mathcal{M}}(gg \rightarrow q_i \bar{q}_i)|^2 = \frac{1}{6} \left( \frac{\hat{u}^2 + \hat{t}^2}{\hat{u}\hat{t}} \right) - \frac{3}{8} \left( \frac{\hat{u}^2 + \hat{t}^2}{\hat{s}^2} \right), \quad (7.2.32)$$

$$|\bar{\mathcal{M}}(q;g \rightarrow q;g)|^2 = -\frac{4}{9} \left( \frac{\hat{u}^2 + \hat{s}^2}{\hat{u}\hat{s}} \right) + \left( \frac{\hat{u}^2 + \hat{s}^2}{\hat{t}^2} \right), \quad (7.2.33)$$

$$|\bar{\mathcal{M}}(gg \rightarrow gg)|^2 = \frac{9}{2} \left( 3 - \frac{\hat{u}\hat{t}}{\hat{s}^2} - \frac{\hat{u}\hat{s}}{\hat{t}^2} - \frac{\hat{s}\hat{t}}{\hat{u}^2} \right). \quad (7.2.34)$$

We will not compute all of these cross sections here, however, it is instructive to examine closely the subprocess  $gq \rightarrow gq$ . This is the first time we have dealt with two external gluons which causes some extra complications. The amplitudes for  $gq \rightarrow gq$  are shown in Fig. 7.9. We will first examine gauge invariance for the QED and QCD case.

In the QED process  $\gamma q \rightarrow \gamma q$  only the amplitudes  $A$  and  $B$  in Fig. 7.9 are present and

$$A + B = (A + B)_{\mu\nu} \epsilon_\mu(\lambda_1) \epsilon_\nu^*(\lambda_2), \quad (7.2.35)$$

where  $\epsilon_\mu(\lambda_1)$  and  $\epsilon_\nu(\lambda_2)$  are the polarization 4-vectors of the incoming and outgoing photons with helicities  $\lambda_1$  and  $\lambda_2$ , respectively, and

$$(A + B)_{\mu\nu} = -ie^2 e_q^2 \bar{u}(p_2, s_2) \left[ \frac{\gamma_\nu(p_1 + q_1)\gamma_\mu}{(p_1 + q_1)^2} + \frac{\gamma_\mu(p_2 - q_1)\gamma_\nu}{(p_2 - q_1)^2} \right] u(p_1, s_1). \quad (7.2.36)$$

Gauge invariance requires that if we make the replacement

$$\epsilon_\mu(\lambda_1) = (q_1)_\mu, \quad (7.2.37)$$

then

$$(A + B)_{\mu\nu} (q_1)_\mu \epsilon_\nu^*(\lambda_2) = 0. \quad (7.2.38)$$

With this replacement the factor in brackets in (7.2.36) becomes

$$\frac{\gamma_\nu(p_1 + q_1)q_1}{(p_1 + q_1)^2} + \frac{q_1(p_2 - q_1)\gamma_\nu}{(p_2 - q_1)^2} = -\frac{\gamma_\nu q_1 p_1}{2p_1 \cdot q_1} + \frac{p_2 q_1 \gamma_\nu}{2p_2 \cdot q_1}, \quad (7.2.39)$$

where quark masses have been neglected and  $q_1^2 = q_2^2 = 0$  and where I have used

$$p_1 q_1 = -q_1 p_1 + 2p_1 \cdot q_1, \quad (7.2.40)$$

$$q_1 p_2 = -p_2 q_1 + 2p_2 \cdot q_1. \quad (7.2.41)$$

These equations together with the Dirac equations

$$p_1 u(p_1, s_1) = 0, \quad (7.2.42)$$

$$\bar{u}(p_2, s_2) p_2 = 0, \quad (7.2.43)$$

insure that (7.2.38) holds. Similarly, it is easy to show that

$$(A + B)_{\mu\nu} \epsilon_\mu(\lambda_1)(q_2)_\nu = 0. \quad (7.2.44)$$

In the QCD case amplitudes  $A$  and  $B$  give

$$(A + B)_{\mu\nu} = -ig_s^2 \bar{u}(p_2, s_2) \left[ \frac{\mathbf{T}_b \mathbf{T}_a \gamma_\nu(p_1 + q_1)\gamma_\mu}{(p_1 + q_1)^2} \right.$$

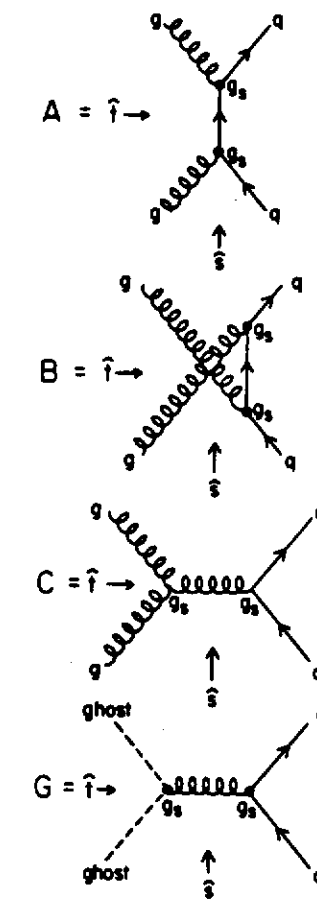


Figure 7.9 Amplitudes  $A$ ,  $B$  and  $C$  for elastic gluon-quark scattering,  $g+q \rightarrow g+q$ , and the amplitude  $G$  for elastic "ghost"-quark scattering.

$$+ \frac{\mathbf{T}_a \mathbf{T}_b \gamma_\mu(p_2 - q_1)\gamma_\nu}{(p_2 - q_1)^2} \left] u(p_1, s_1) \right. \quad (7.2.45)$$

where  $\mathbf{T}_a$  and  $\mathbf{T}_b$  are the  $SU(3)$  color matrices given in Appendix D which satisfy

$$\mathbf{T}_a \mathbf{T}_b = \mathbf{T}_b \mathbf{T}_a + i f_{abc} \mathbf{T}_c. \quad (7.2.46)$$

Inserting this into (7.2.45) yields

$$(A + B)_{\mu\nu} = -ig_s^2 \mathbf{T}_b \mathbf{T}_a \bar{u}(p_2, s_2) \left[ \frac{\gamma_\nu(p_1 + q_1)\gamma_\mu}{(p_1 + q_1)^2} + \frac{\gamma_\mu(p_2 - q_1)\gamma_\nu}{(p_2 - q_1)^2} \right] u(p_1, s_1) \\ + g_s^2 f_{abc} \mathbf{T}_c \bar{u}(p_2, s_2) \left[ \frac{\gamma_\mu(p_2 - q_1)\gamma_\nu}{(p_2 - q_1)^2} \right] u(p_1, s_1). \quad (7.2.47)$$

and

$$(A + B)_{\mu\nu} (q_1)_\mu = -g_s^2 f_{abc} \mathbf{T}_c \bar{u}(p_1, s_2) \gamma_\nu u(p_1, s_1). \quad (7.2.48)$$

The first term in (7.2.47) vanishes as in the QED case but the second term does not and gauge invariance does not hold. Of course this presents no problem since the third amplitude in Fig. 7.9 involving the triple-gluon coupling will restore the gauge invariance. From Appendix C we see that

$$C_{\mu\nu} = g_s^2 f_{bac} \mathbf{T}_c \bar{u}(p_2, s_2) \frac{F_{\nu\mu\lambda}(q_2, -q_1, q_3)\gamma_\lambda}{q_3^2} u(p_1, s_1), \quad (7.2.49)$$

where  $F_{\alpha\beta\gamma}$  is given in (6.1.28) and

$$q_3 = q_1 - q_2. \quad (7.2.50)$$

Contracting with  $(q_1)_\mu$  gives

$$F_{\nu\mu\lambda}(q_2, -q_1, q_3)(q_1)_\mu = (q_1)_\lambda (q_2)_\nu + (q_2)_\lambda (q_1)_\nu - (q_1)_\lambda (q_1)_\nu + q_3^2 g_{\lambda\nu}, \quad (7.2.51)$$

and we arrive at

$$C_{\mu\nu} (q_1)_\mu \epsilon_\nu^*(\lambda_2) = g_s^2 f_{abc} \mathbf{T}_c \bar{u}(p_2, s_2) \gamma_\nu u(p_1, s_1) \\ - g_s^2 f_{abc} \mathbf{T}_c \bar{u}(p_2) \not{q}_1 u(p_1, s_1) \frac{q_2 \cdot \epsilon_2^*}{2q_1 \cdot q_2}. \quad (7.2.52)$$

Combining this with (7.2.48) gives

$$(A + B + C)_{\mu\nu} (q_1)_\mu \epsilon_\nu^*(\lambda_2) = 0, \quad (7.2.53)$$

provided

$$q_2 \cdot \epsilon_2 = 0. \quad (7.2.54)$$

Similarly, one can show that

$$(A + B + C)_{\mu\nu} \epsilon_\mu(\lambda_1) (q_2)_\nu = 0, \quad (7.2.55)$$

provided

$$q_1 \cdot \epsilon_1 = 0. \quad (7.2.56)$$

Thus gauge invariance holds and the current is conserved provided the polarization 4-vectors  $\epsilon_\mu(\lambda_1)$  and  $\epsilon_\nu(\lambda_2)$  represent physical transverse states obeying (7.2.54) and (7.2.56). This is different from the QED case where (7.2.38) and (7.2.44) hold regardless of the choice of  $\epsilon_\mu(\lambda_1)$  and  $\epsilon_\nu(\lambda_2)$ . The additional conditions in (7.2.54) and (7.2.56) arise from the nature of QCD (*i.e.*, the presence of the triple-gluon coupling). They imply that we cannot use the

trick of replacing the sum over gluon polarization states by

$$\sum_\lambda \epsilon_\mu(\lambda) \epsilon_\nu^*(\lambda) \rightarrow -g_{\mu\nu}, \quad (7.2.57)$$

when there is more than one external gluon. For one external gluon we showed in Chapters 2 that this replacement (equivalent to the Feynman gauge) gives the correct sum over the two physical helicity states. The unphysical states cancel out. With two or more external gluons these unphysical polarization states do not cancel out and one does not arrive at the correct gauge invariant cross section by the use of (7.2.57).

One way to obtain the correct cross section is to insist that the polarization states  $\epsilon_\mu(\lambda_1)$  and  $\epsilon_\nu(\lambda_2)$  are physical (*i.e.*, transverse). This is accomplished by the projection

$$\sum_\lambda \epsilon_\mu(\lambda) \epsilon_\nu^*(\lambda) = - \left[ g_{\mu\nu} - \frac{n_\mu k_\nu + n_\nu k_\mu}{(n \cdot k)} + \frac{n^2 k_\mu k_\nu}{(n \cdot k)^2} \right], \quad (7.2.58)$$

where  $n$  is an arbitrary 4-vector and  $k$  is the gluon 4-momentum. This is analogous to using an axial (or physical) gauge. A convenient choice for the 4-vector  $n$  is

$$n = p_1, \quad (7.2.59)$$

for the incoming gluon and

$$n = p_2, \quad (7.2.60)$$

for the outgoing gluon. With this choice

$$\sum_{\lambda_1} \epsilon_\mu(\lambda_1) \epsilon_\nu^*(\lambda_1) = -g_{\mu\nu} + \frac{2}{\hat{s}} [(p_1)_\mu (q_1)_\nu + (p_1)_\nu (q_1)_\mu], \quad (7.2.61)$$

$$\sum_{\lambda_2} \epsilon_\mu(\lambda_2) \epsilon_\nu^*(\lambda_2) = -g_{\mu\nu} + \frac{2}{\hat{s}} [(p_2)_\mu (q_2)_\nu + (p_2)_\nu (q_2)_\mu], \quad (7.2.62)$$

yielding

$$\frac{d\hat{\sigma}}{dt}(g + q \rightarrow g + q; \hat{s}, \hat{t}) = \frac{\pi \alpha_s^2}{\hat{s}^2} |A + B + C|^2, \quad (7.2.63)$$

where

$$|A|^2 = \frac{2}{9} \frac{1}{4} 8 \left( -\frac{\hat{u}}{\hat{s}} \right), \quad (7.2.64)$$

$$|B|^2 = \frac{2}{9} \frac{1}{4} 8 \left( -\frac{\hat{s}}{\hat{u}} \right), \quad (7.2.65)$$

$$2AB^* = 0, \quad (7.2.66)$$

$$|C|^2 = \frac{1}{2} \frac{1}{4} 16 \left( 1 - \frac{\hat{s}\hat{u}}{\hat{t}^2} \right), \quad (7.2.67)$$

$$2AC^* = -\frac{i}{4} \frac{1}{4} 16 i \left( \frac{\hat{s}}{\hat{t}} \right), \quad (7.2.68)$$

$$2BC^* = \frac{i}{4} \frac{1}{4} 16i \left( \frac{-\hat{u}}{\hat{t}} \right), \quad V \quad (7.2.69)$$

giving

$$|A + B + C|^2 = -\frac{4}{9} \left( \frac{\hat{s}^2 + \hat{u}^2}{\hat{s}\hat{u}} \right) + 2 \left( 1 - \frac{\hat{s}\hat{u}}{\hat{t}^2} \right) - 1, \quad (7.2.70)$$

which is identical to (7.2.33). In (7.2.64)–(7.2.69) the first factor is the color factor and the second factor arises from spin averaging. For example, the color factor for  $|A|^2$  is given by

$$\begin{aligned} \frac{1}{8} \frac{1}{3} \text{tr}(\mathbf{T}_a \mathbf{T}_b \mathbf{T}_b \mathbf{T}_a) &= \frac{1}{24} [\text{tr}(\mathbf{T}_a \mathbf{T}_b \mathbf{T}_a \mathbf{T}_b) - i f_{abc} \text{tr}(\mathbf{T}_a \mathbf{T}_b \mathbf{T}_c)] \\ &= \frac{1}{24} \left( -\frac{1}{12} \delta_{bb} + \frac{1}{4} 3 \delta_{aa} \right) \\ &= \frac{8}{24} \left( -\frac{1}{12} + \frac{3}{4} \right) = \frac{2}{9}, \end{aligned} \quad (7.2.71)$$

and the color factor for  $|C|^2$  is given by

$$\begin{aligned} \frac{1}{8} \frac{1}{3} f_{abc} f_{abc} \text{tr}(\mathbf{T}_c \mathbf{T}_e) &= \frac{1}{24} \frac{1}{2} f_{abc} f_{abc} \\ &= -\frac{1}{24} \frac{1}{2} (\mathbf{F}_c)_{ab} (\mathbf{F}_c)_{ab} = \frac{1}{24} \frac{1}{2} \text{tr}(\mathbf{F}_c \mathbf{F}_c) \\ &= \frac{1}{24} \frac{3}{2} \delta_{cc} = \frac{1}{24} \frac{24}{2} = \frac{1}{2}. \end{aligned} \quad (7.2.72)$$

Alternatively, we could use the Feynman gauge projection in (7.2.57) together with the ghost-quark scattering diagram in Fig. 7.9. This gives

$$|C|_\Sigma^2 = \frac{1}{24} 16 \left( 1 - \frac{5}{4} \frac{\hat{s}\hat{u}}{\hat{t}^2} \right), \quad (7.2.73)$$

for the square of amplitude  $C$  where the subscript  $\Sigma$  signifies that (3.2.57) has been used to sum the gluon polarization states. Comparing with (7.2.67) we see that

$$|C|_\Sigma^2 = |C|^2 - \frac{1}{2} \frac{\hat{s}\hat{u}}{\hat{t}^2}. \quad (7.2.74)$$

The use of (7.2.57) has produced the spurious contribution

$$-\frac{1}{2} \frac{\hat{s}\hat{u}}{\hat{t}^2}. \quad (7.2.75)$$

This spurious contribution can be removed by including the ghost contribution in Fig. 7.9,

$$\begin{aligned} |G|^2 &= \frac{1}{2} \frac{1}{2} \frac{1}{\hat{t}^2} \text{tr}(\not{p}_2 \not{q}_2 \not{p}_1 \not{q}_1) \\ &= \frac{1}{2} \frac{(-\hat{u})\hat{s}}{\hat{t}^2}, \end{aligned} \quad (7.2.76)$$

where as before the first factor is the color factor (same as for  $|C|^2$ ) and the second factor arises from spin averaging (treating the ghost as a scalar). To arrive at the correct gauge invariant result we must subtract (7.2.76) from (7.2.73). Namely,

$$|C|_\Sigma^2 - |G|^2 = |C|^2, \quad (7.2.77)$$

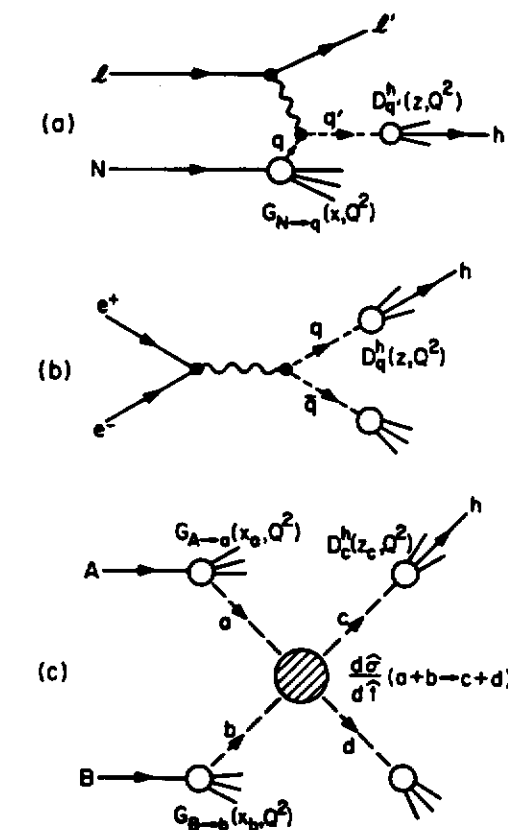


Figure 7.10 Illustration of the universal nature of the quark probability distributions,  $G_{N \rightarrow q}(x, Q^2)$ , and the fragmentation functions,  $D_q^h(z, Q^2)$ . At leading order in QCD the same functions describe: (a) deep inelastic lepton-nucleon scattering, (b) hadron production in  $e^+e^-$  annihilations, and (c) particle production at large transverse momentum in hadron-hadron collisions.

and the two methods are equivalent. The extra  $(-1)$  for the ghost contribution is analogous to the  $(-1)$  that one must insert for a ghost loop.

As illustrated in Fig. 7.10 (7.2.20) together with the seven cross sections (7.2.27)–(7.2.34) can be used to predict the rate of large transverse momentum meson production in hadron-hadron collisions from the structure functions,  $G(x, Q^2)$ , determined in deep inelastic lepton-hadron scattering and the

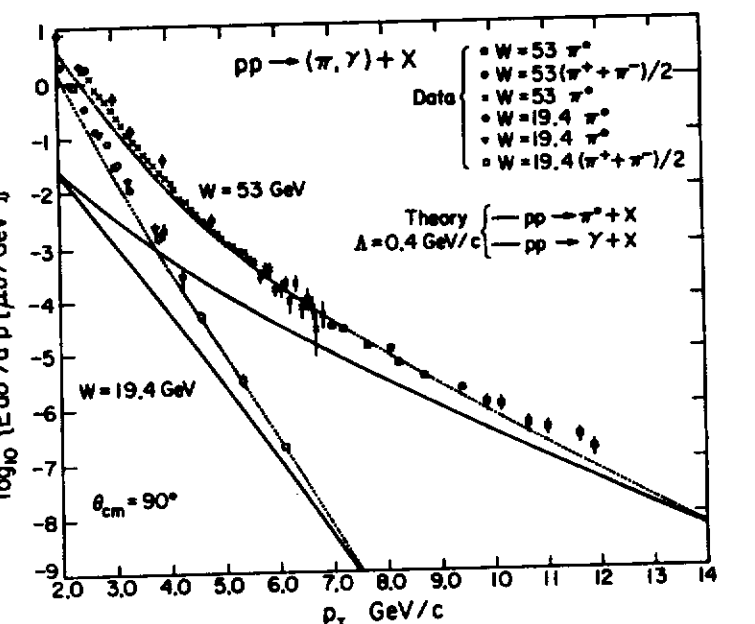


Figure 7.11 Predictions of leading order perturbative QCD for the production of large transverse momentum pions in proton-proton collisions,  $pp \rightarrow \pi + X$ , compared with data at  $W = \sqrt{s} = 19.4$  and  $53\text{ GeV}$ . Also shown are the corresponding predictions for large transverse momentum photons,  $pp \rightarrow \gamma + X$  (taken from Ref. 6).

fragmentation functions,  $D(z, Q^2)$ , determined in  $e^+e^-$  annihilations. As mentioned before it is not clear what to use for the variable  $Q$  that determines the scale at which the structure functions and fragmentation functions are sampled and also sets the strength of the strong interaction coupling,  $\alpha_s(Q^2)$ . At leading order all choices for  $Q$  that increase with the parton-parton center-of-mass energy are equivalent. Different choices affect beyond leading order terms. Some guesses at the best choice include

$$Q^2 = 4\hat{p}_T^2, \quad (7.2.78)$$

and

$$Q^2 = \frac{2\hat{s}\hat{t}\hat{u}}{\hat{s}^2 + \hat{t}^2 + \hat{u}^2}, \quad (7.2.79)$$

where  $\hat{p}_T$  is the parton transverse momentum. Fig. 7.11 shows a QCD prediction for  $pp \rightarrow \pi^0 + X$  at a center-of-mass energy of  $19.4$  and  $53\text{ GeV}$  and  $\theta_{CM} = 90^\circ$  using (7.2.20) and  $\Lambda = 0.4\text{ GeV}^6$ . To compare with data the leading order formula in (7.2.20) has been “smeared” over the intrinsic transverse momentum of the parton within the initial hadron,  $(k_T)_{h \rightarrow q}$ , and over the transverse momentum of the hadrons within the outgoing jets,  $(k_T)_{q \rightarrow h}$ . Smearing is an important effect in hadron-hadron collisions due to the “trigger bias” which selects configurations in which the initial partons are already moving toward the trigger<sup>7</sup>.

Another interesting application of the leading order formula in (7.2.20) is the prediction of large  $p_T$  particle ratios in  $\pi p$  and  $pp$  collisions. Fig. 7.12 shows the predictions for  $\pi^- p$  and  $pp$  interactions compared with data at  $200\text{ GeV}$  and  $\theta_{CM} = 90^\circ$ <sup>8</sup>. Although in some cases the agreement is not exact, the systematics of the data are described correctly. The proton contains more  $u$  than  $d$  quarks and since  $u$ -quark jets contain (at high  $z$ ) more  $\pi^+$  than  $\pi^-$ , one expects and sees a  $\pi^-/\pi^+$  ratio considerably less than one in  $pp$  collisions. For  $\pi^- p$  collisions, on the other hand, one predicts a  $\pi^-/\pi^+$  ratio slightly greater than one. This is because the  $d$  (and  $\bar{u}$ ) quark in the  $\pi^-$  has on the average a higher momentum than the  $u$ -quark within the proton which at  $90$  degrees results in a slight excess of  $\pi^-$  over  $\pi^+$  at large  $p_T$ . The data shows a  $\pi^-/\pi^+$  ratio that is slightly greater than one but not quite as large as the prediction.

In  $pp$  collisions one can only produce large  $p_T K^-$  mesons by scattering partons out of the proton “sea” or by producing them as non-leading particles in the quark jets. A very small  $K^-/K^+$  ratio for  $pp$  collisions is therefore predicted. On the other hand,  $K^-$  mesons can be produced directly in  $\pi^- p$  collisions through the scattering of the valence  $\bar{u}$  quark within the  $\pi^-$  so that the  $K^-/K^+$  ratio here should not be as small. This is indeed what is observed in Fig. 7.12b.

While the  $\pi^-/\pi^+$ ,  $K^-/K^+$  and  $K^-/\pi^-$  ratios are predicted to be quite different for  $\pi^-$  and proton beams, the  $K^+/\pi^+$  ratio is predicted to be essentially identical for the two beams. This is because neither the  $\pi^-$  or the proton contain any valence strange quarks. In both reactions large  $p_T K^+$  mesons arise from the fragmentation of  $u$ -quark jets. The  $K^+/\pi^+$  ratio for both reactions simply measures the extra difficulty of producing a  $s\bar{s}$  pair over a  $d\bar{d}$  pair during the fragmentation process and should be the same for both reactions. The data in Fig. 7.12d confirm this.

### 7.3 Jet Production

Theoretically it is easy to define the “jet” cross section. It is the cross section for producing a parton (quark or gluon) and is computed to leading order by (7.2.25) together with the parton-parton cross sections in (7.2.27)–(7.2.34). As

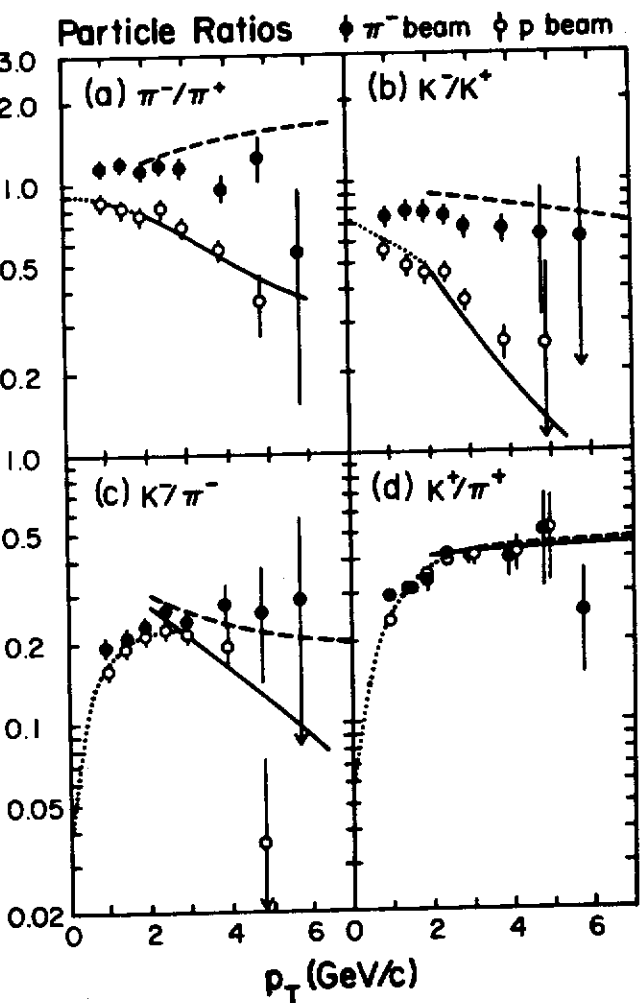


Figure 7.12 Comparison of data on the large transverse momentum,  $p_T$ , trigger particle ratios for  $\pi^-p$  and  $pp$  collisions at a laboratory beam momentum of  $200 \text{ GeV}/c$  and  $\theta_{cm} = 90^\circ$  with leading order QCD predictions. The solid and dashed curves are the predictions for  $pp$  and  $\pi^-p$ , respectively, and should only be compared with data above about  $3 \text{ GeV}/c$ . The dotted curves are extrapolations of the low  $p_T$   $pp$  data (taken from Ref. 8).

can be seen in Fig. 7.13 the “jet” cross section is predicted to be considerably larger than the single particle cross section<sup>9</sup>. The single particle trigger always comes from a parton carrying more momentum (typically 10–15% more) than

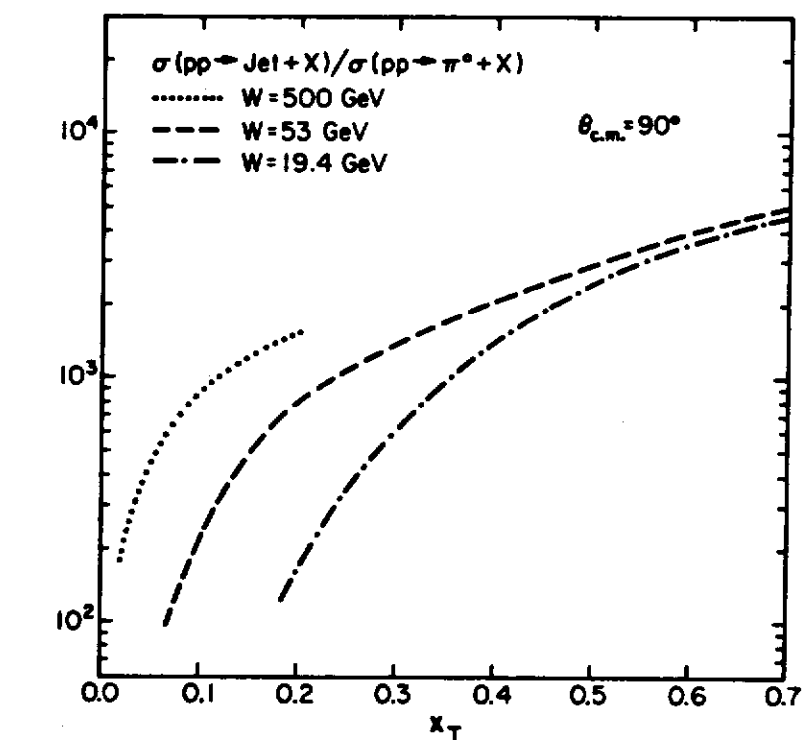


Figure 7.13 Leading order QCD predictions for the ratio of “jet” production (in this case parton production) at large transverse momentum,  $p_T$ , to the production of a single  $\pi^0$  at the same  $p_T$  in proton-proton collisions. The predictions at  $W = \sqrt{s} = 19.4, 53$ , and  $500 \text{ GeV}$  are plotted versus  $x_T = 2p_T/W$  (taken from Ref. 6).

the trigger particle. Furthermore, the probability that one particle carries almost all the momentum of the parent parton is quite small (only a few percent). These two effects combine to give the  $\sigma(pp \rightarrow \text{jet} + X)/\sigma(pp \rightarrow \pi^0 + X)$  ratio seen in Fig. 7.13. Experimentally it is difficult to define a “jet.” One can never be sure that one has included the desired hadrons and rejected to undesired ones. Nevertheless, as can be seen in Fig. 7.14, the early QCD predictions of a large jet cross section are in rough accord with data<sup>6</sup>.

It is an interesting consequence of the leading order formulas in (7.2.20) and (7.2.25) that the single particle and “jet” cross sections are not very sensitive to the QCD perturbative parameter  $\Lambda$ . One might think that since the parton-parton differential cross sections are proportional to  $\alpha_s^2(Q^2)$  that, for example, the jet rate would depend strongly on  $\Lambda$ . Fig. 7.15 shows that this is not the case. The reason is due to the compensating effect of the parton distributions,  $G(x, Q^2)$ . If  $\Lambda$  is small (i.e.,  $\alpha_s$  small) then  $d\sigma/dt$  is small but the

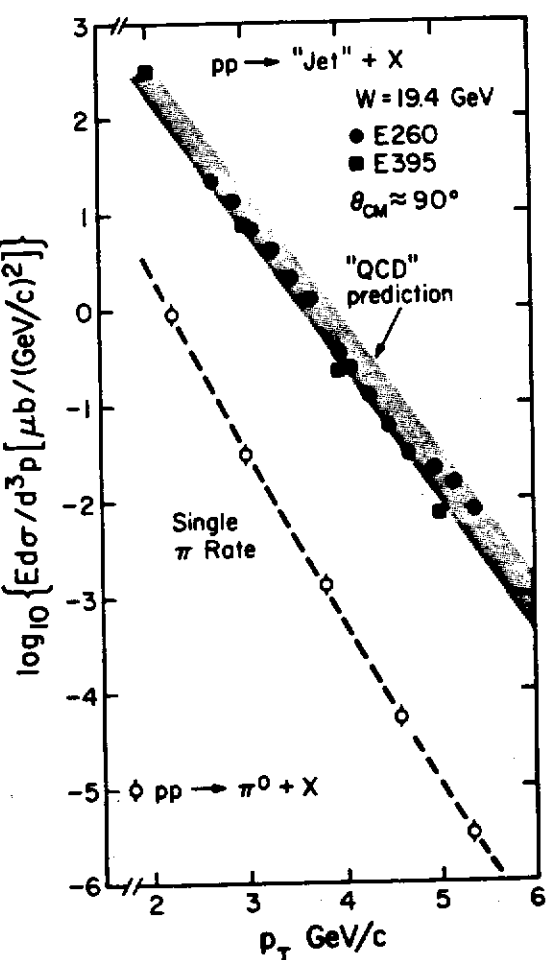


Figure 7.14 Data from the first Fermilab experiments to confirm the leading order prediction of perturbative QCD of a large "jet" cross section at high transverse momentum in proton-proton collisions (taken from Ref. 12).

probability of finding a large  $x$  partons within the initial hadrons is large since  $G(x, Q^2)$  has not changed much from its reference value,  $G(x, Q_0^2)$ . On the other hand, if  $\Lambda$  is large (i.e.,  $\alpha_s$  large) then  $d\hat{\sigma}/dx$  is large but the probability of finding partons at large  $x$  is small since  $G(x, Q^2)$  will now have evolved far away from its reference value. This means that data on the cross section for

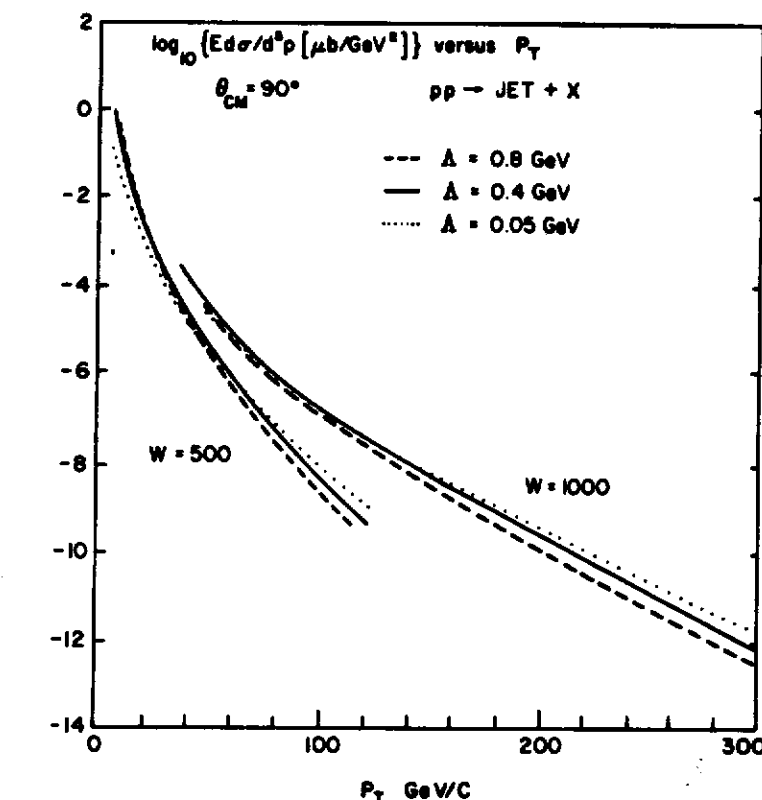
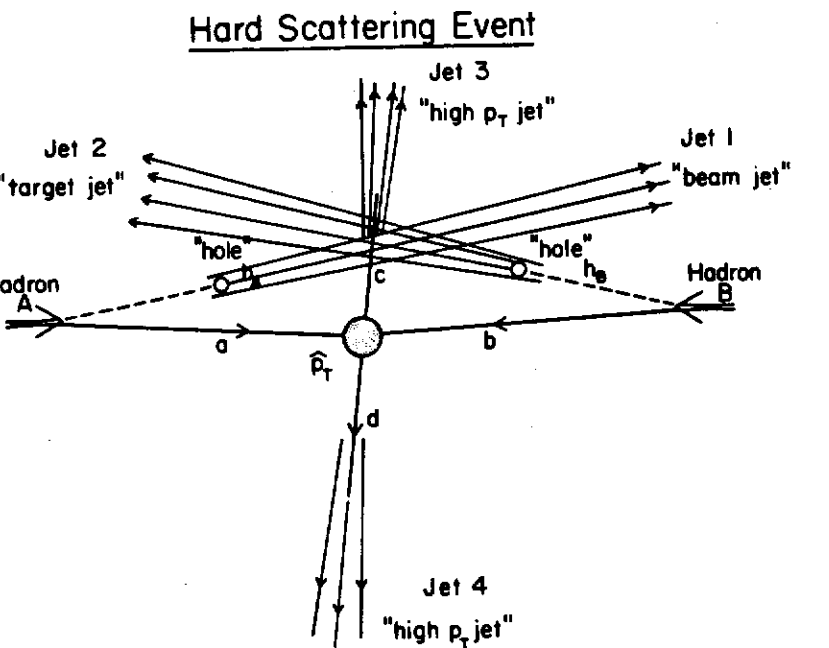


Figure 7.15 Shows the insensitivity of the leading order QCD predictions for the production of large transverse momentum "jets" (in this case partons) to the precise value of the perturbative parameter,  $\Lambda$ .

single hadrons and "jets" produced in hadron-hadron collisions cannot be used to determine the perturbative parameter  $\Lambda$ . However, it also means that the data *must* agree roughly with the QCD predictions something is very wrong.

## 7.4 Monte Carlo Models and Event Topologies

As we have seen in the previous sections in leading order QCD, mesons are produced at large transverse momentum in hadron-hadron collisions as the



**Figure 7.16** Illustration of the naive parton model in which high transverse momentum particles are produced by a single, hard, large-angle elastic scattering of partons; one from the beam hadron and one from the target hadron. The large- $p_T$  event consists of four jets; two with large transverse momentum resulting from the fragmentation of the outgoing partons and two with small transverse momentum resulting from the break-up of the beam and target hadron as illustrated in Fig. 7.7.

result of a hard parton-parton collision; one parton from the incoming beam hadron and one from the target hadron. The resulting elastic parton-parton scattering produces two outgoing partons which subsequently "fragment" into jets of hadrons producing the four "jet" event structure (two large  $p_T$  jets, a beam jet and a target jet) shown in Fig. 7.16. The invariant cross section  $A + B \rightarrow h + X$  has the form given in (7.2.20), where  $d\sigma/d\hat{s}$  is the hard scattering constituent differential cross section,  $a + b \rightarrow c + d$ , and where one must sum over all parton types (i.e.,  $qq \rightarrow qq$ ,  $qg \rightarrow qg$ ,  $gg \rightarrow gg$ , etc.). The variables  $\hat{s}$  and  $\hat{p}_T$  are the center-of-mass energy squared and transverse momentum, respectively, for the hard constituent subprocess.

The effects of soft and collinear gluon emissions off the incoming partons are treated by assigning the proper  $Q^2$  dependence to the parton structure

functions,  $G_{A \rightarrow a}(x, Q^2)$ . Similarly, soft and collinear gluon Bremsstrahlung off the outgoing partons results in a  $Q^2$  dependence of the fragmentation functions,  $D_c^h(z, Q^2)$ . The  $Q^2$  dependence of the structure and fragmentation functions is given by perturbation theory. Since, to leading order, one need consider only the case where the gluon radiation is soft or collinear, one is still left with an effective 2-to-2 subprocess and a four jet structure similar to that for the naive parton model shown in Fig. 7.16.

On the other hand, equation (7.2.20) is not completely satisfactory. A successful description of single particle production at high  $p_T$  requires that one include the effects of the "intrinsic" transverse momentum,  $k_T$ , of the partons within the initial hadrons. In hadron-hadron collisions the incoming partons cannot be taken to be parallel with the incoming hadrons. In fact, phenomenologically  $\langle k_T \rangle$  appears to be quite large. Feynman, Field, and Fox<sup>6</sup> found an effective  $\langle k_T \rangle$  of 0.85 GeV in hadron-hadron collisions. Because of the rapid fall with  $\hat{p}_T$  of the constituent parton-parton cross section, one has a "trigger bias" in single particle experiments. One preferentially selects events in which the incoming two partons are moving toward the trigger. Similarly, the outgoing hadrons are not produced precisely parallel to the outgoing partons. One way to include the effects of both the transverse momentum spread of the hadrons within the outgoing "jets" and the intrinsic  $k_T$  of the partons within the initial hadrons is by "smearing" the basic equation (7.2.20). The intrinsic transverse momentums are assumed to be distributed as a gaussian (or an exponential) independent of both  $Q^2$  and the process and one then integrates over these  $k_T$  values.

However, in QCD, a large effective intrinsic transverse momentum is understood in terms of noncollinear gluon Bremsstrahlung. As illustrated in Fig. 7.17a, single particle triggers tend to come from the fragmentation of a large  $p_T$  parton that is balanced on the "away-side" by several lower momentum partons. The same bias effect occurs for "small aperture" jet (calorimeter) triggers. By small aperture calorimeters I mean observations that sum the total transverse energy,  $E_T$ , in a small region ( $\sim 1$  steradian in the center-of-mass frame) of phase space. Such a calorimeter roughly contains all the hadrons from a single parton "jet." Clearly, the use of (7.2.20) plus smearing is a crude way to include the effects of noncollinear gluon emissions. The leading order formula does reasonably well in estimating the magnitude of the single particle cross section or the small aperture jet cross section, but is not very good if one is interested in more detailed questions as to the overall event structure. For one thing, (7.2.20) plus smearing still treats the problem as an effective 2-to-2 subprocess, whereas the subprocess in Fig. 7.17a is actually a 2-to-4 subprocess ( $qq \rightarrow qqqg$ ). In order to make further progress and to answer more detailed questions about high  $p_T$  events one needs a method of calculating (or approximating) the effects of 2  $\rightarrow N$  subprocesses. One must include the effects of the noncollinear emission of gluons off the initial and final partons.

One way to proceed is to extend the QCD "leading pole" Monte Carlo

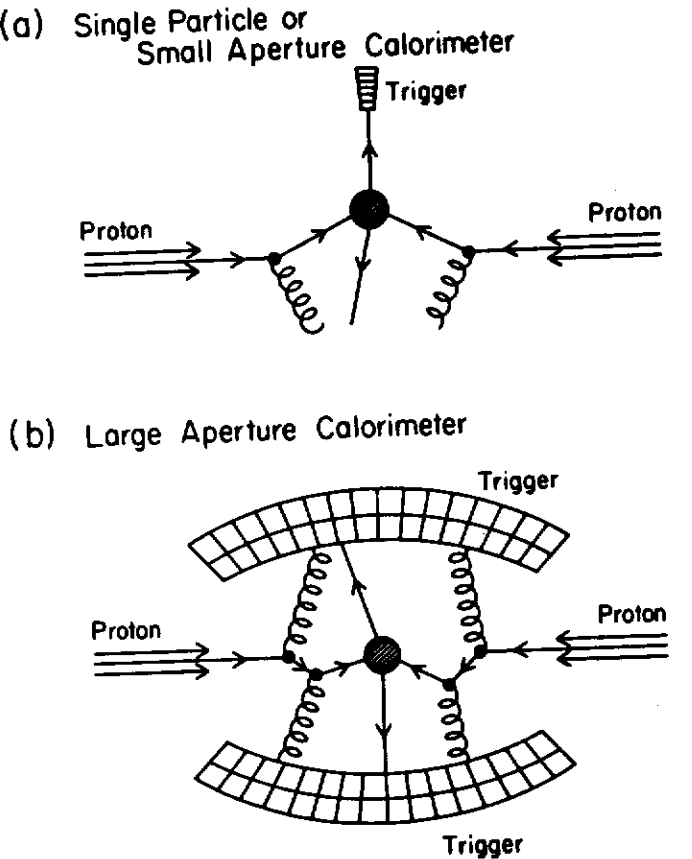


Figure 7.17 (a) Illustration of the trigger bias effect for a single particle or a small aperture calorimeter experiments in hadron-hadron collisions. The large transverse momentum,  $\hat{p}_T$ , trigger is obtained by combining a 2-to-2 hard scattering of smaller  $\hat{p}_T$  with additional transverse momentum gained by the incoming quarks through the emission (or *Bremsstrahlung*) of gluons. (b) Illustration of the trigger bias that occurs for large aperture calorimeter experiments. Large transverse energy,  $E_T$ , is produced by the *Bremsstrahlung* of many lower energy gluons in addition to the hard 2-to-2 scattering.

parton-shower approach discussed in Chapter 3 to hadron-hadron collisions<sup>10,11</sup>. The hard scattering 2-to-2 subprocesses,  $d\hat{\sigma}/d\hat{s}$ , are calculated to leading order exactly (the shaded circles in Fig. 7.17) with all remaining parton emissions estimated using the “leading pole” Monte-Carlo parton shower method. As

### Hard Scattering Event

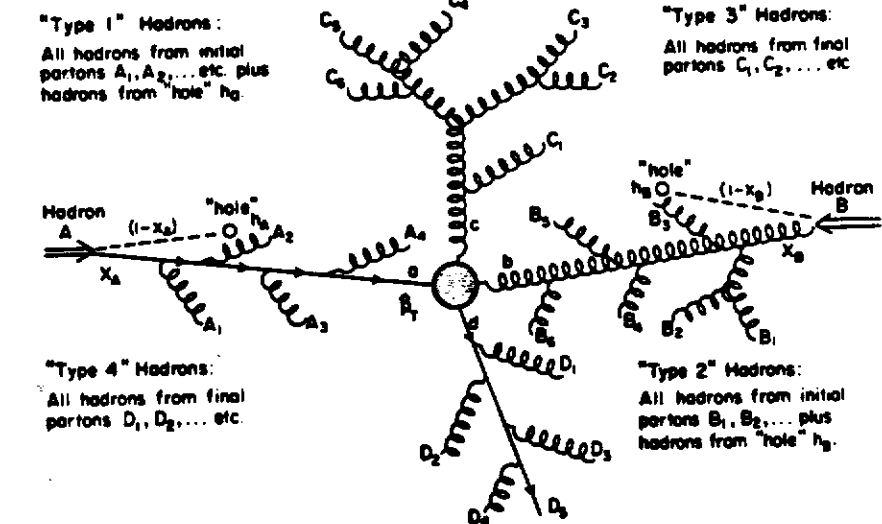


Figure 7.18 Illustration of a hard scattering QCD parton-shower Monte Carlo event which includes in an approximate manner the emission of gluons off both the initial and final state partons. Hadrons are labeled according to where they originate with type 1 hadrons arising from the fragmentation of the initial state partons  $A_1, A_2, \dots$  plus the fragmentation of the “hole”  $h_A$  (which is assumed to have momentum  $1 - x_A$ ). Similarly, type 2 hadrons arise from the fragmentation of initial state partons  $B_1, B_2, \dots$  plus “hole”  $h_B$ . Type 3 and 4 hadrons arise from the fragmentation of final state partons  $C_1, C_2, \dots$  and  $D_1, D_2, \dots$ , respectively, and  $\hat{p}_T$  is the transverse momentum of the hard 2-to-2 constituent subprocess,  $a + b \rightarrow c + d$ .

illustrated in Fig. 7.18 final state partons have timelike invariant masses and are allowed to radiate until their masses are below the cut-off  $t_c^A = (\mu_c^A)^2$ . Initial partons have spacelike invariant masses with maximum (negative) value taken to be  $t_{\min}^B = -Q^2$  (here one usually takes  $Q^2 = 4\hat{p}_T^2$ ). These partons are evolved from an initial value of  $t_c^B = -(\mu_c^B)^2$  up to this maximum. Multiparton cross sections are approximate but all gluon emissions are retained including the (infinite sum of) divergent soft and collinear configurations. One is, however, not restricted to the collinear case as exact kinematics are maintained at each emission<sup>12</sup>.

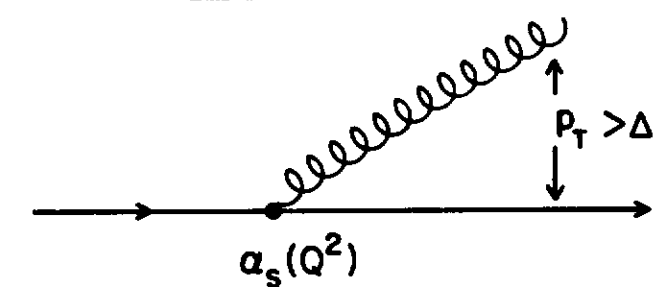
Present day QCD Monte-Carlo models for hadron-hadron collisions contain many approximations and should not be taken too seriously<sup>13</sup>. At the parton level the "leading pole" approximation can be off by a sizable amount for wide angle Bremsstrahlung plus there are other theoretical uncertainties. The most uncertain ingredient in the models, however, is the "hadronization" phase (the algorithm used to turn the outgoing partons into hadrons). At present we really do not know the correct way to fragment a collection of partons into hadrons. There are a variety of suggestions in the literature. The simplest is to fragment each parton independently in the hadron-hadron center-of-mass frame according to the Field-Feynman prescription discussed in Chapter 3. Clearly this method cannot be precisely correct. In hadron-hadron collisions there are many soft quanta for which the FF prescription is inadequate and inappropriate. Furthermore, when there are many nearby quarks and gluons, one cannot consider their fragmentation as independent. Presumably, it is color separation that is responsible for the fragmentation.

Nevertheless, with the FF hadronization scheme one can keep track of where the outgoing hadrons come from. As is illustrated in Fig. 7.18, type 1 hadrons are those arising from initial partons  $A_1, A_2, \dots$  etc., plus the 1 hadrons arising from the fragmentation of the "hole"  $h_A$ . Similarly, type 2 hadrons arise from the initial partons  $B_1, B_2, \dots$  etc., plus the "hole"  $h_B$ . Outgoing partons  $C_i$  and  $D_i$  fragment into hadron of type 3 and type 4, respectively. I have been careful not to call, for example, type 3 hadrons a "jet." Type 3 hadrons may form several "jets" or no "jets" or type 3 and type 1 hadrons may conspire to form one "jet." The precise definition of a "jet" is at the discretion of the experimenter.

Although the parton-shower Monte-Carlo models are a crude attempt to reproduce nature, they do contain in an approximate manner many of the features expected from QCD. As the momentum transfer of the hard parton-parton scattering subprocess,  $Q$ , increases the QCD parton-shower models deviates more and more from the naive parton model. This is due to the fact that the probability of radiating a hard gluon off an initial or final state parton increases logarithmically as  $Q$  increases (see Fig. 7.19). In addition, in the QCD parton-shower approach there are dynamical correlations between the outgoing high  $p_T$  jets (hadrons of type 3 and 4) and the low  $p_T$  "background" jets (hadrons of type 1 and 2). Large  $p_T$  outgoing jets means that a large  $Q^2$  subprocess occurred which in turn stimulates a large amount of gluon Bremsstrahlung in the initial state. In the QCD approach it is incorrect to consider a high  $p_T$  event as a superposition of two high  $p_T$  jets on top of a "minimum bias" background (i.e., ordinary low  $p_T$  event). The great majority of minimum bias events contain no hard scattering, whereas essentially all large  $p_T$  events occur as the result of a hard parton-parton scattering.

With the QCD parton-shower Monte-Carlo one can investigate many aspects of large  $p_T$  hadron-hadron collisions that could not be estimated by smearing the leading order equation in (7.2.20). One can, for example, examine more detailed questions as to the overall event shape and the manner

### Gluon Emission



$$\text{Prob } (p_T > \Delta) \propto \alpha_s(Q^2) \log^2(Q^2/\Delta^2) \propto \log(Q^2)$$

Figure 7.19 Illustration of gluon emission. The probability of emitting a hard gluon (one with  $p_T > \Delta$ ) is given by  $P(p_T > \Delta) \propto \alpha_s(Q^2) \log^2(Q^2/\Delta^2)$  and increases like  $\log(Q^2)$  which causes the QCD parton-shower Monte Carlo model (Fig. 7.18) to deviate more and more from the naive parton model (Fig. 7.16) as the transverse momentum,  $\hat{p}_T$ , of the constituent subprocess,  $a + b \rightarrow c + d$ , increases.

in which transverse momentum is balanced. It is quite interesting to compare the underlying parton substructure dominant for large aperture transverse energy triggers to that for single particle (or small aperture) triggers. These two types of triggers preferentially select different parton substructures.

Large aperture calorimeter triggers are biased in favor of parton subprocesses involving an anomalously large amount of gluon Bremsstrahlung as illustrated in Fig. 7.17b<sup>14</sup>. In the small aperture case (Fig. 7.17a), the Bremsstrahlung is opposite the trigger, whereas a large aperture calorimeter catches most of the gluon Bremsstrahlung. If one asks for a large amount of transverse energy,  $E_T$ , in a hadron-hadron collisions, nature gives this  $E_T$  in the way that is most efficient. Because of the rapid decrease in the hard parton-parton scattering cross section with increasing  $\hat{p}_T$ , one has, in effect, a source of outgoing partons whose intensity falls rapidly with increasing center-of-mass energy,  $\hat{s}$ . In contrast to this, in  $e^+e^-$  annihilations, one has a monoenergetic source of partons with center-of-mass energy  $\hat{s} = Q^2$  and for large  $Q^2$  the two jet structure is evident. In both  $e^+e^-$  annihilations and hadron-hadron collisions, wide angle gluon emission is only a few percent. However, the steep spectrum in the hadron case means that small corrections to larger cross section scatterings (smaller  $\hat{p}_T$ ) can dominate at a given large  $p_T$ . This

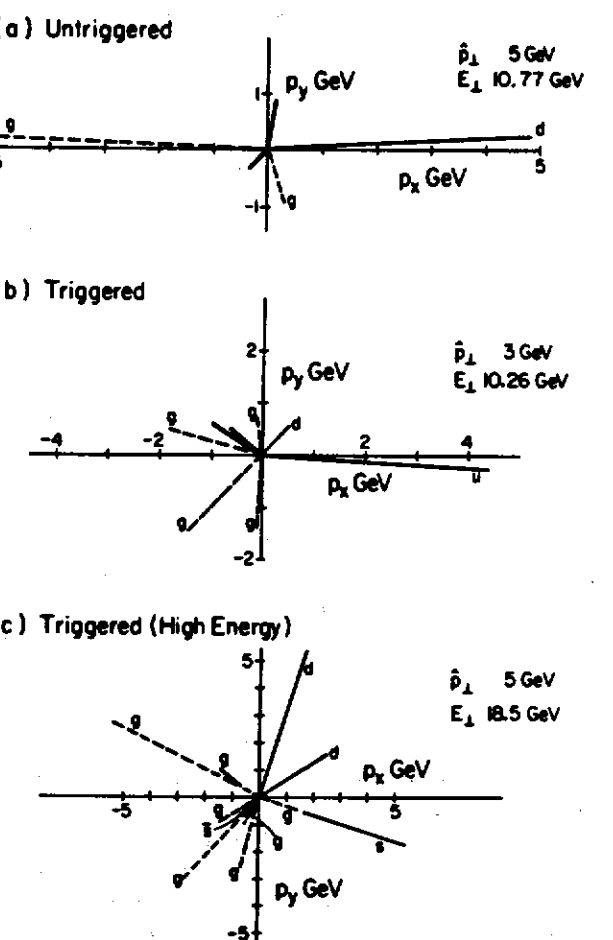


Figure 7.20 The transverse momentum projections for some typical events produced from a QCD parton-shower Monte Carlo model: (a) untriggered event at hadron-hadron center-of-mass energy  $W = 24 \text{ GeV}$ , (b) and (c) global transverse energy triggered events at  $W = 24$  and  $540 \text{ GeV}$ , respectively. Partons are denoted by dashed lines (gluons) and solid lines (quarks) (taken from Ref. 14).

is illustrated in Fig. 7.20. Fig. 7.20a shows a typical “untriggered” event in  $p\bar{p}$  collisions at  $\sqrt{s} = 24 \text{ GeV}$  in which one clearly sees a two jet structure in the transverse momentum plane with total transverse energy,  $E_T$ , approximately  $2\hat{p}_T$ . On the other hand, Fig. 7.20b shows a triggered event in which

$E_T > 10 \text{ GeV}$  was demanded. Here  $2\hat{p}_T$  is only about  $6 \text{ GeV}$  with gluon Bremsstrahlung making up the remaining  $E_T$ . Fig. 7.20c shows the profusion of partons generated at  $\sqrt{s} = 540 \text{ GeV}$  in an  $E_T$  triggered event.

One way to examine and quantify the event topology in hadron-hadron collisions is to define “clusters.” Events are analyzed by dividing the solid angle (for a given range in pseudorapidity,  $\eta = \log[\tan(\theta/2)]$ ), into cells. The global transverse energy of an event is the sum of the transverse energies of all the cells. Clusters of cells are formed by including in a “cluster” all cells with a common side, but where cells with transverse energy less than  $E_T(\min)$  are ignored. The transverse energy of a cell is computed, not by adding the transverse energy of each hadron in the cell, but by using  $E_T(\text{cell}) = \sin(\theta) E(\text{cell})$ , where  $\theta$  is computed from the knowledge of position of the center of the cell. A cell is considered as a massless “particle” of energy  $E(\text{cell})$  and with a direction given by the position of the center of the cell. Clusters have an energy given by the sum of the energies of all the cells in the cluster and a momentum,  $P_{cl}$ , given by the vector sum of the momenta of the cells. The invariant mass of a cluster is simply  $M_{cl} = \sqrt{E_{cl}^2 - P_{cl}^2}$ . Finally, clusters are ordered according to the total transverse energy of all the cells in the cluster with cluster #1 having the highest  $E_T$ .

Fig. 7.21 shows an important difference between QCD and the naive parton model<sup>16</sup>. The total number of clusters, on the average, with  $E_T(\text{each}) > 10 \text{ GeV}$  is plotted versus the global  $E_T$  for  $p\bar{p}$  collisions at  $\sqrt{s} = 540 \text{ GeV}$  as observed by the UA2 group at the CERN collider<sup>16</sup> ( $|\eta| < 1$ , cell size  $\Delta\theta\Delta\phi = 10^\circ \times 15^\circ$ , 240 cells). In the naive parton model illustrated in Fig. 7.16 the multiplicity of clusters with  $E_T(\text{each}) > 10 \text{ GeV}$  quickly becomes two and remains two as the global  $E_T$  increases. In the naive parton model there are only two large  $E_T$  jets! QCD, on the other hand, predicts that the average number of clusters will increase beyond two. As the global  $E_T$  is increased there becomes an increasing probability of finding 3, 4, etc., clusters each of which has  $E_T(\text{each}) > 10 \text{ GeV}$ . This is true no matter what one chooses for the value of  $E_T(\text{each})$ . The data show support for the QCD approach over the naive parton model.

The rich topological structure expected of QCD events cannot be seen by merely studying the average number of clusters as in Fig. 7.21. More information is contained in Fig. 7.22 which shows the probability of finding  $N_{cl}$  clusters in a given event each of which has  $E_T(\text{each}) > 10 \text{ GeV}$ . For example, for global  $E_T$  in the range  $100 < E_T < 120 \text{ GeV}$  the QCD parton-shower Monte Carlo model predicts a 35% probability of finding 3 clusters with  $E_T(\text{each}) > 10 \text{ GeV}$  and a 4% probability of finding 4. The naive parton model gives essentially a 100% chance of finding 2 clusters in every event. In this global  $E_T$  bin UA2 find 3 clusters 28% of the time and 4 clusters about 4% of the time.

Alternatively, one can interpret the data in terms of “jets” rather than clusters. Again phase space is divided into cells and “jets” are constructed from a jet algorithm. In the UA1 jet algorithm<sup>17</sup> one first considers the “hot” cells

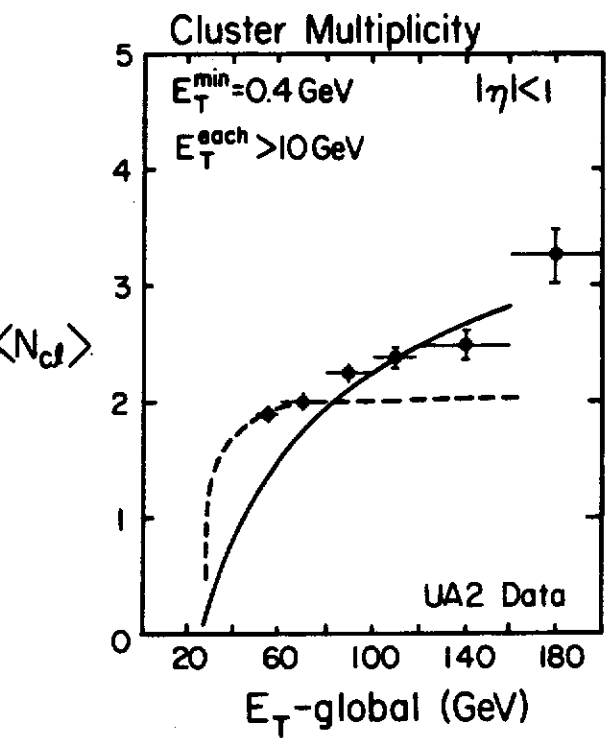


Figure 7.21 Average number of “clusters” having  $E_T(\text{each}) > 10 \text{ GeV}$  versus the global transverse energy,  $E_T$  resulting from a QCD parton-shower Monte Carlo model (solid curve) and the naive parton model (dashed curve) for  $p\bar{p}$  collisions at  $\sqrt{s} = 540 \text{ GeV}$ . The data are from UA2<sup>16</sup>. (Figure taken from Ref. 15)

(those with transverse energy greater than  $E_T(\text{hot})$ ). Hot cells are combined to form a “jet” if they lie within a “distance”  $d = \sqrt{\Delta\eta^2 + \Delta\phi^2} < d_0$  from each other, with the jet direction being the vector sum of the momenta of each cell in the jet. Cold cells (those with  $E_T < p_T(\text{hot})$ ) are added to a jet if  $d < d_0$  or if the angle of the cold cell relative to the jet is less than  $45^\circ$  and the relative  $p_T$  is less than 1 GeV.

In QCD, one encounters a multitude of event topologies and the choice of trigger (or even the manner in which one bins the data) preferentially selects certain topologies over others. Fig. 7.23 shows the percentage of events with  $N$  “UA1-jets” ( $d_0 = 1$ ,  $p_T(\text{hot}) = 2.5 \text{ GeV}$ ) with  $E_T(\text{each}) > 15 \text{ GeV}$  for cells of size  $\Delta\eta\Delta\phi = 0.2 \times 15^\circ$  with  $|\eta| < 2.5$  versus the transverse energy of the leading jet,  $E_T(\text{jet})$ . The data are from the UA1 group<sup>17</sup> and are in qualitative agreement with the Monte-Carlo.

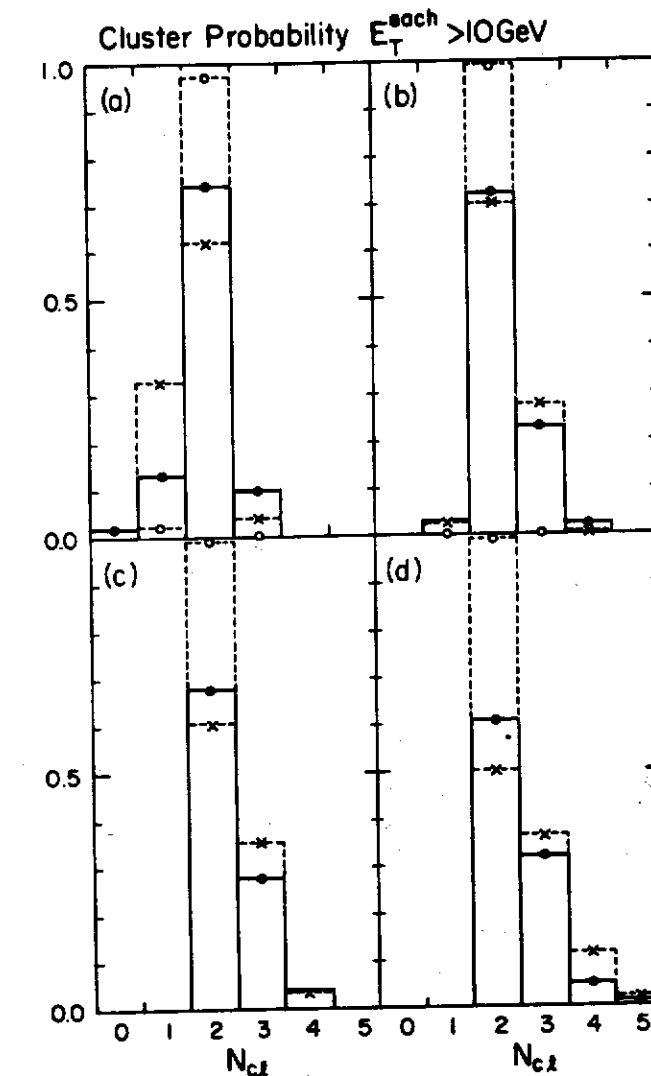


Figure 7.22 Probability of finding in a given event  $N_{cl}$  clusters having  $E_T(\text{each}) > 10 \text{ GeV}$  resulting from a QCD parton-shower Monte Carlo model (dashed lines and crosses) and the naive parton model (dashed lines and open circles) for  $p\bar{p}$  collisions at  $\sqrt{s} = 540 \text{ GeV}$  with global transverse energy in the range: (a)  $60 < E_T < 80 \text{ GeV}$ , (b)  $80 < E_T < 100 \text{ GeV}$ , (c)  $100 < E_T < 120 \text{ GeV}$ , and (d)  $120 < E_T < 160 \text{ GeV}$ . The data (solid lines and solid dots) are from UA2<sup>16</sup> (taken from Ref. 15).

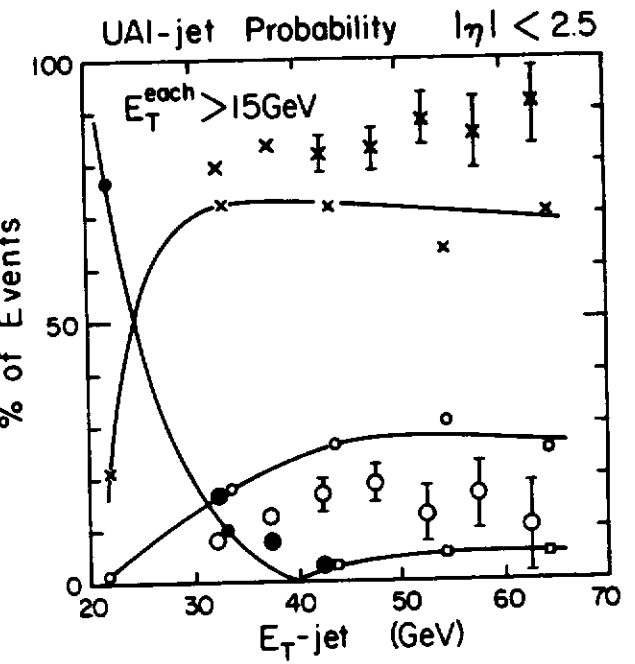


Figure 7.23 Percentage of events with  $N_{jet}$  "UA1-jets" with  $E_T(\text{each}) > 15 \text{ GeV}$  versus the transverse energy of the leading "UA1-jet",  $E_T(\text{jet})$ , resulting from a QCD parton-shower Monte Carlo model (solid curves) for  $\bar{p}p$  collisions at  $\sqrt{s} = 540 \text{ GeV}$ , with  $N_{jet} = 1$  solid dots,  $N_{jet} = 2$  crosses,  $N_{jet} = 3$  open circles, and  $N_{jet} = 4$  open squares. The data are from UA1<sup>17</sup> with  $N_{jet} = 1$  large solid dots,  $N_{jet} = 2$  large crosses, and  $N_{jet} = 3$  large open circles (taken from Ref. 15).

Extrapolations of the QCD parton-shower Monte Carlo model to  $p\bar{p}$  collisions at the Superconducting Super Collider (SSC) energy of 40 TeV are shown in Fig. 7.24 and Fig. 7.25. Fig. 7.24 shows the predicted average transverse energy flow relative to the direction of the highest  $E_T$  jet (with  $|\Delta\phi| \leq 90^\circ$ ). Multiple jet topologies are averaged over and one sees a narrow "hot" jet core rising above a plateau. Fig. 7.25 shows the predicted average multiplicity flow relative to the leading jet. For comparison the UA1 data<sup>17</sup> for  $\bar{p}p$  collisions at 540 GeV are also shown. As expected the hot jet cores for both the transverse energy and multiplicity flow rise markedly in going from 540 GeV and  $E_T$  values of around 100–150 GeV to 40 TeV and  $E_T$  of 2 TeV. However, the QCD parton-shower Monte-Carlo model predicts that the level of the plateaus will also increase significantly in going to the higher  $E_T$  values of the SSC due to the larger  $Q^2$  sampled.

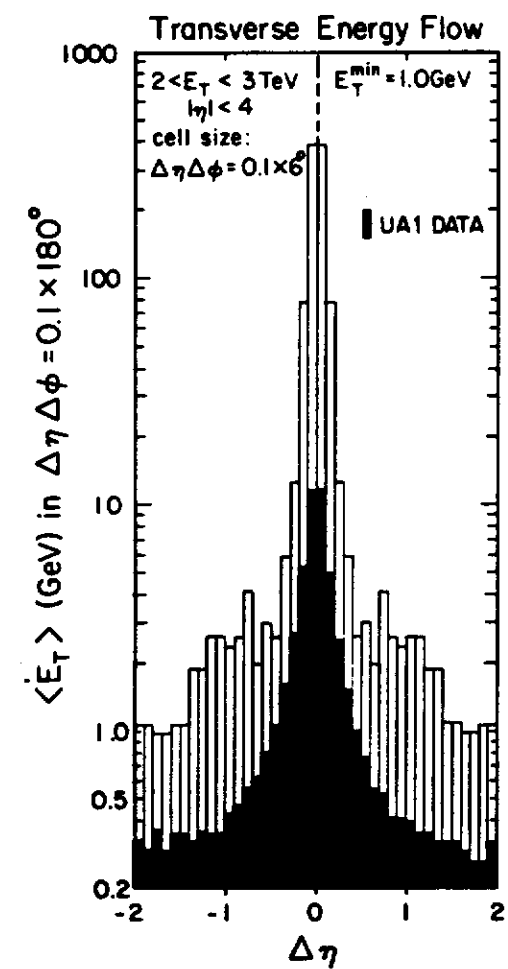


Figure 7.24 Average transverse energy flow relative to the leading (highest  $E_T$ ) cluster for global transverse energy in the range  $2,000 < E_T < 3,000 \text{ GeV}$  in  $p\bar{p}$  collisions at  $\sqrt{s} = 40,000 \text{ GeV}$  resulting from a QCD parton-shower Monte Carlo model. Each bin gives the average transverse energy in  $\Delta\eta\Delta\phi = 0.1 \times 180^\circ$  with  $|\Delta\phi| \leq 90^\circ$  relative to the leading cluster (i.e., toward side). The shaded region are data from UA1<sup>17</sup> at  $W = 540 \text{ GeV}$  and  $E_T(\text{jet}) > 35 \text{ GeV}$  (taken from Ref. 15).

About one half of the transverse energy and multiplicity flow plateau in Fig. 7.24 and Fig. 7.25 arises from initial state gluon Bremsstrahlung. The QCD parton-shower model predicts about 22.8 charged particles in  $\Delta\eta\Delta\phi =$

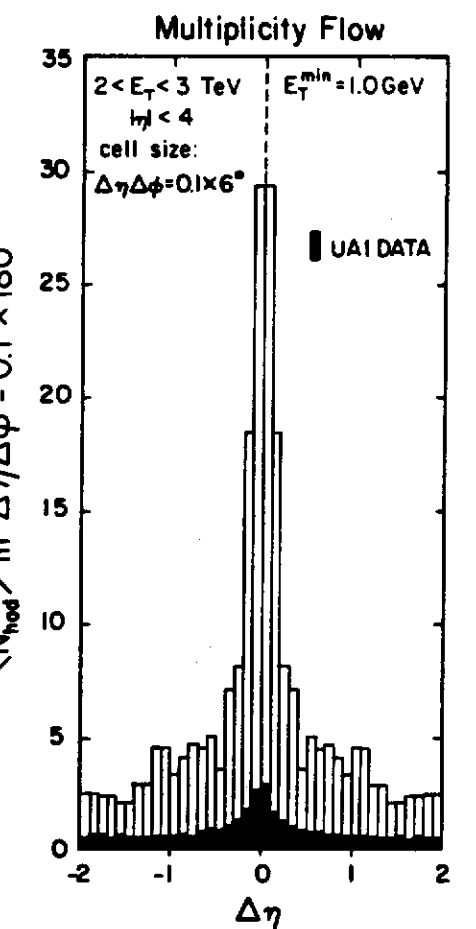


Figure 7.25 Average particle multiplicity flow relative to the leading (highest  $E_T$ ) cluster for global transverse energy in the range  $2,000 < E_T < 3,000 \text{ GeV}$  in  $p\bar{p}$  collisions at  $\sqrt{s} = 40,000 \text{ GeV}$  resulting from a QCD parton-shower Monte Carlo model. Each bin gives the average number of particles in  $\Delta\eta\Delta\phi = 0.1 \times 180^\circ$  with  $|\Delta\phi| \leq 90^\circ$  relative to the leading cluster (i.e., toward side). The shaded region are data from UA1<sup>17</sup> at  $W = 540 \text{ GeV}$  and  $E_T(\text{jet}) > 35 \text{ GeV}$  (multiplied by a factor of 1.75 to convert from charged particle multiplicity to the total multiplicity) (taken from Ref. 15).

$1 \times 360^\circ$ . This is about a factor of 3.5 times higher than the charged particle

density of about 6.5 expected from minimum bias events at this energy. This enhancement of the plateau over minimum bias is also observed by the UA1 group at 540 GeV, however, at the larger  $E_T$  values of the SSC the effect is predicted to be even greater. The large transverse energy and multiplicity plateaus arise because we are demanding large  $E_T$  and hence a large  $Q^2$ . The large  $Q^2$  induces a lot of initial and final gluon Bremsstrahlung and this produces a large number of "plateau" hadrons.

At this state QCD Monte-Carlo models are still quite crude and only qualitative comparisons with data are warranted. Nevertheless much has already been learned. Existing data on the production of multi-jets with large transverse energy are in good qualitative agreement with the expectations of QCD and deviate greatly from the predictions of the naive parton model. Overall the hadron collider data show strong qualitative evidence for QCD which strengthens the evidence from data on  $e^+e^-$  annihilations and deep inelastic lepton-hadron scattering.

### Problems

- 7.1. Show that the differential cross section for the "annihilation" subprocess  $q + \bar{q} \rightarrow \gamma + g$  in Fig. 7.1a is given by

$$\frac{d\hat{\sigma}}{dt}(\hat{s}, \hat{t}) = \frac{\pi\alpha\alpha_s e_q^2}{\hat{s}^2} \frac{4}{9} 2 \left( \frac{\hat{u}}{\hat{t}} + \frac{\hat{t}}{\hat{u}} \right),$$

and for the purely electromagnetic subprocess  $q + \bar{q} \rightarrow \gamma + \gamma$  in Fig. 7.1b is given by

$$\frac{d\hat{\sigma}}{dt}(\hat{s}, \hat{t}) = \frac{\pi\alpha^2 e_q^4}{\hat{s}^2} \frac{1}{3} 2 \left( \frac{\hat{u}}{\hat{t}} + \frac{\hat{t}}{\hat{u}} \right).$$

Also show that the differential cross section for the "Compton" subprocess  $q + g \rightarrow \gamma + q$  is given by

$$\frac{d\hat{\sigma}}{dt}(\hat{s}, \hat{t}) = \frac{\pi\alpha\alpha_s e_q^2}{\hat{s}^2} \frac{1}{6} 2 \left( -\frac{\hat{t}}{\hat{s}} - \frac{\hat{s}}{\hat{t}} \right).$$

- 7.2. Verify that

$$\frac{d\hat{\sigma}/d\hat{t}(gg \rightarrow \gamma\gamma)}{d\hat{\sigma}/d\hat{t}(gg \rightarrow \gamma g)} = \frac{12\alpha}{5\alpha_s} \frac{\left( \sum_{i=1}^{n_f} e_{q_i}^2 \right)^2}{\left( \sum_{i=1}^{n_f} e_{q_i} \right)^2} \xrightarrow{n_f=4} \frac{20}{3} \frac{\alpha}{\alpha_s}.$$

- 7.3. Consider the inclusive process  $A + B \rightarrow c + d + X$  shown in Fig. 7.2. Starting from

$$d\sigma = G_{A \rightarrow a}^{(0)}(x_a) dx_a G_{B \rightarrow b}^{(0)}(x_b) dx_b \left( \frac{d\hat{\sigma}}{dt}(\hat{s}, \hat{t}) \right) d\hat{t},$$

show that the double differential cross section is given by

$$E_c \frac{d\sigma}{d^3 p_c dy_d} (A + B \rightarrow c + d + X; s, p_T, \theta_c, \theta_d) = \\ x_a x_b G_{A \rightarrow a}^{(0)}(x_a) G_{B \rightarrow b}^{(0)}(x_b) \frac{1}{\pi} \frac{d\hat{\sigma}}{dt} (a + b \rightarrow c + d; \hat{s}, \hat{t}),$$

where

$$\begin{aligned} \hat{s} &= \frac{s}{4} x_T^2 \left( 2 + \frac{T_c}{T_d} + \frac{T_d}{T_c} \right), \\ \hat{t} &= -\frac{s}{4} x_T^2 \left( 1 + \frac{T_c}{T_d} \right), \\ \hat{u} &= -\frac{s}{4} x_T^2 \left( 1 + \frac{T_d}{T_c} \right). \\ x_a &= \frac{1}{2} x_T \left( \frac{1}{T_c} + \frac{1}{T_d} \right), \\ x_b &= \frac{1}{2} x_T (T_c + T_d), \end{aligned}$$

with  $T_i = \tan(\theta_i/2)$  and  $x_T = 2p_T/\sqrt{s}$ . Integrate this expression over  $\theta_d$  and show that the single particle inclusive cross section is given by

$$E \frac{d\sigma}{d^3 p} (A + B \rightarrow c + X; s, p_T, \theta_c) = \frac{1}{\pi} \int_{x_a^{\min}}^{1.0} dx_a \\ G_{A \rightarrow a}^{(0)}(x_a) G_{B \rightarrow b}^{(0)}(x_b) \frac{x_a x_b}{(x_a - x_1)} \frac{d\hat{\sigma}}{dt} (a + b \rightarrow c + d; \hat{s}, \hat{t}),$$

where

$$\begin{aligned} x_b &= \frac{x_a x_2}{(x_a - x_1)}, \\ x_a^{\min} &= \frac{x_1}{(1 - x_2)} = \frac{x_T/T_c}{2 - x_T T_c}, \\ \hat{s} &= x_a x_b s, \\ \hat{t} &= -\frac{s}{2} x_a x_T T_c, \\ \hat{u} &= -\frac{s}{2} x_a x_T \frac{1}{T_c}, \end{aligned}$$

and

$$\begin{aligned} x_1 &= \frac{1}{2} x_T \frac{1}{T_c}, \\ x_2 &= \frac{1}{2} x_T T_c. \end{aligned}$$

- 7.4. Consider the inclusive process  $A + B \rightarrow h + X$  shown in Fig. 7.6. Starting from

$$d\sigma(s, t) = G_{A \rightarrow a}^{(0)}(x_a) dx_a G_{B \rightarrow b}^{(0)}(x_b) \left( \frac{d\hat{\sigma}}{dt}(\hat{s}, \hat{t}) \right) d\hat{t} D_{0,c}^h(z_c) dz_c,$$

show that

$$E d\sigma/d^3 p(A + B \rightarrow h + X; s, p_T, \theta_{cm}) = \\ \frac{1}{\pi} \int_{z_c^{\min}}^{1.0} dz_c \int_{x_b^{\min}}^{1.0} dx_b G_{A \rightarrow a}^{(0)}(x_a) G_{B \rightarrow b}^{(0)}(x_b) D_{0,c}^h(z_c) \\ \frac{1}{z_c} \frac{d\hat{\sigma}}{dt}(ab \rightarrow cd; \hat{s}, \hat{t}),$$

where

$$\begin{aligned} z_c &= \frac{x_2}{x_b} + \frac{x_1}{x_a}, \\ x_b^{\min} &= \frac{x_a x_2}{x_a - x_1}, \\ x_a^{\min} &= \frac{x_1}{1 - x_2}, \\ \hat{s} &= x_a x_b s, \\ \hat{t} &= x_a t, \\ \hat{u} &= x_b u, \end{aligned}$$

where

$$\begin{aligned} x_1 &= -u/s = \frac{1}{2} x_T/T_h, \\ x_2 &= -t/s = \frac{1}{2} x_T T_h, \end{aligned}$$

and

$$\begin{aligned} x_T &= 2p_T/\sqrt{s}, \\ T_h &= \tan(\theta_{cm}/2). \end{aligned}$$

Let  $D_{0,c}^h(z_c) = \delta(1 - z_c)$  and show that the resulting formula is equivalent to (7.1.41).

- 7.5. Evaluate the seven parton-parton differential cross sections in (7.2.28)-(7.2.34) at  $\theta_{cm} = 90^\circ$ . Order them according to their size at  $90^\circ$ . Which is largest?

- 7.6. Repeat the calculation in (7.2.36), (7.2.38), and (7.2.39) for the case in which the quark in the subprocess  $\gamma q \rightarrow \gamma q$  is massive. Show that, as is true for massless quarks,

$$(A + B)_{\mu\nu} (q_1)_\mu \epsilon_\nu^*(\lambda_2) = 0,$$

and

$$(A + B)_{\mu\nu} \epsilon_\mu(\lambda_1)(q_2)_\nu = 0.$$

- 7.7. For the reaction  $g + q \rightarrow g + q$  in Fig. 7.9 show that for massless partons

$$(A + B + C)_{\mu\nu} (q_1)_\mu \epsilon_\nu^*(\lambda_2) = 0,$$

provided

$$q_2 \cdot \epsilon_2 = 0,$$

and

$$(A + B + C)_{\mu\nu} \epsilon_\mu(\lambda_1)(q_2)_\nu = 0,$$

provided

$$q_1 \cdot \epsilon_1 = 0.$$

7.8. Verify that

$$\begin{aligned}\frac{d\hat{\sigma}}{dt}(q_i q_j \rightarrow q_i q_j; \hat{s}, \hat{t}) &= \frac{\pi \alpha_s^2}{\hat{s}^2} \frac{4 \hat{s}^2 + \hat{u}^2}{9 \hat{t}^2}, \\ \frac{d\hat{\sigma}}{dt}(q_i q_i \rightarrow q_i q_i; \hat{s}, \hat{t}) &= \frac{\pi \alpha_s^2}{\hat{s}^2} \left\{ \frac{4}{9} \left( \frac{\hat{s}^2 + \hat{u}^2}{\hat{t}^2} + \frac{\hat{s}^2 + \hat{t}^2}{\hat{u}^2} \right) - \frac{8}{27} \frac{\hat{s}^2}{\hat{u}\hat{t}} \right\}, \\ \frac{d\hat{\sigma}}{dt}(q_i \bar{q}_i \rightarrow q_i \bar{q}_i; \hat{s}, \hat{t}) &= \frac{\pi \alpha_s^2}{\hat{s}^2} \left\{ \frac{4}{9} \left( \frac{\hat{s}^2 + \hat{u}^2}{\hat{t}^2} + \frac{\hat{t}^2 + \hat{u}^2}{\hat{s}^2} \right) - \frac{8}{27} \frac{\hat{u}^2}{\hat{s}\hat{t}} \right\}.\end{aligned}$$

7.9. Using the axial gauge projections in (7.2.61) and (7.2.62) compute the differential cross section for the "Compton" subprocess  $gq \rightarrow gq$  and for the "annihilation" subprocesses  $q + \bar{q} \rightarrow gg$  and  $gg \rightarrow q + \bar{q}$ . These latter two subprocesses differ only by spin and color factors.

#### Further Reading

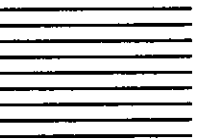
- G. Altarelli, "Partons in Quantum Chromodynamics," *Physics Reports* 81,1 (1982).  
 F. Halzen and A.D. Martin, *Quarks and Leptons. An Introductory Course in Modern Particle Physics*, John Wiley & Sons, Inc., 1984.  
 Donald Perkins, *Introduction to High Energy Physic*, The Advanced Book Program, Addison-Wesley Publishing Company, Inc., 1986.  
 R. K. Ellis, "An Introduction to the QCD Parton Model", Fermilab preprint, FNAL-CONF-88/60-T, 1988.  
 P. Bagnaia and S. D. Ellis, "CERN Collider Results and the Standard Model", University of Washington preprint, 1988.

#### References

1. H. Fritzsch and P. Minkowski, *Phys. Lett.* 73B, 80 (1978).
2. S.D. Ellis and M.B. Kislinger, *Phys. Rev.* D9, 207 (1974).
3. B. De Tollis, *Nuovo Cimento* 35, 1182 (1965).
4. E.L. Berger, E. Braaten and R.D. Field, *Nucl. Phys.* B239, 52 (1984).
5. R. Cutler and D. Sivers, *Phys. Rev.* D16, 679 (1977). *ibid* *Phys. Rev.* D17, 196 (1978).

6. R.P. Feynman, R.D. Field and G.C. Fox, *Phys. Rev.* D18, 3320 (1978).
7. R.D. Field, *Phys. Rev. Lett.* 40, 997 (1978).
8. R.D. Field, *Phys. Rev.* D27, 546 (1983).
9. S.D. Ellis, M. Jacob and P.V. Landshoff, *Nucl. Phys.* B108, 93 (1976).
10. G.C. Fox and R.L. Kelly, AIP Conference Procedures No. 85, "Proton-Antiproton Collider Physics" (1981).
11. G. Marchesini and B. R. Webber, "Monte Carlo Simulation of General Hard Processes with Coherent QCD Radiation", University of Cambridge preprint, Cavendish-HEP-87/8 (1987).
12. R.D. Field and G.C. Fox, "QCD Monte-Carlo Models for  $e^+e^-$  Annihilations and Hadron-Hadron Collisions," published in the Europhysics Study Conference on Jet Dynamics in Quark and Lepton Interactions, Erice, 1982.
13. J.C. Collins and T.O. Gottschalk, "Assessment of Perturbative Monte Carlos for Hadron-Hadron Scattering," Proceedings of the 1986 Summer Study on the Physics of Superconducting Supercollider, Snowmass (1986).
14. R.D. Field, G.C. Fox and R.L. Kelly, *Phys. Rev.* D27, 546 (1983).
15. R.D. Field, *Nucl. Phys.* B264, 687 (1986).
16. P. Bagnaia *et al.* (UA2 Collaboration), CERN preprint CERN-EP/84-12; J. Hansen, Proceedings of the First Aspen Winter Physics Conference on Collider Physics at Ultra-High Energies, Aspen (1985).
17. G. Arnison *et al.* (UA1 Collaboration), *Phys. Lett.* 122B, 103 (1983). *ibid* 126B, 398 (1983). *ibid* 134B, 469 (1984). *ibid* 147B, 241 (1984). J. Rolf, contribution to the 1984 DPF Snowmass Summer Study on the Design and Utilization of the Superconducting Super Collider.

# Other Applications of Perturbative QCD



In this chapter we will examine several other applications of perturbative QCD. I will not be able to include every important application. I have attempted to pick applications that cover a broad range but my choice is prejudiced somewhat by my own work.

## 8.1 Upsilon Decay

The decays of heavy quarkonium states provide many interesting tests of QCD. For sufficiently high quark mass the decay rates can be computed in terms of the wave function at (or near) the origin from perturbation theory. In the simplest approach one neglects spin dependence and relativistic effects and computes the decay amplitudes to order  $\alpha_s$ . The lowest order decay channel is determined from the fact that while both  $C$ -even and  $C$ -odd states can go into three gluons, only  $C$ -even states can couple to two gluons. In addition  $J = 1$  states cannot decay into two on-shell massless gluons. Thus the  $J^{pc} = 1^{--}$  ( $1s$ ) state should decay primarily into three gluons. It also decays into two gluons and a photon, but this mode is suppressed by  $\alpha/\alpha_s$ . To leading order

$$\frac{\Gamma(1s \rightarrow gg\gamma)}{\Gamma(1s \rightarrow ggg)} = \frac{36}{5} e_q^2 \frac{\alpha}{\alpha_s}, \quad (8.1.1)$$

and is independent of the wave function at the origin<sup>1</sup>. Computing the next order correction to (8.1.1) and comparing with data allows for a determination of  $\alpha_s$ <sup>2</sup>. Existing experiments can measure only high energy photons and the total rate  $\Gamma(1s \rightarrow gg\gamma)$  is estimated from the calculated photon spectrum.

The “Born term” matrix element for the decay of a  $1s$  quarkonium state into two massless gluons and a photon (Fig. 8.1a) yields a cross section (normalized to unity) given by<sup>1</sup>

$$\frac{1}{\sigma} \frac{d\sigma}{dz_\gamma dx_1} = \frac{1}{(\pi^2 - 9)} \left[ \frac{(1-x_1)^2}{(x_2 z_\gamma)^2} + \frac{(1-x_2)^2}{(x_1 z_\gamma)^2} + \frac{(1-z_\gamma)^2}{(x_1 x_2)^2} \right], \quad (8.1.2)$$

where  $x_{1,2} = 2E_{1,2}/W$  are the fractional energies of the two gluons and  $z_\gamma = 2E_\gamma/W$  is the fractional energy of the photon and  $W$  is the total center-of-mass energy (i.e., the mass of the quarkonium state). For massless gluons the range of values of  $x_1$  and  $z_\gamma$  are

$$0 \leq z_\gamma \leq 1, \quad (8.1.3)$$

$$1 - z_\gamma \leq x_1 \leq 1, \quad (8.1.4)$$

with

$$x_1 + x_2 + z_\gamma = 2, \quad (8.1.5)$$

resulting in the familiar triangular Dalitz plot shown in Fig. 8.2a. To high accuracy (8.1.2) can be approximated by a constant,

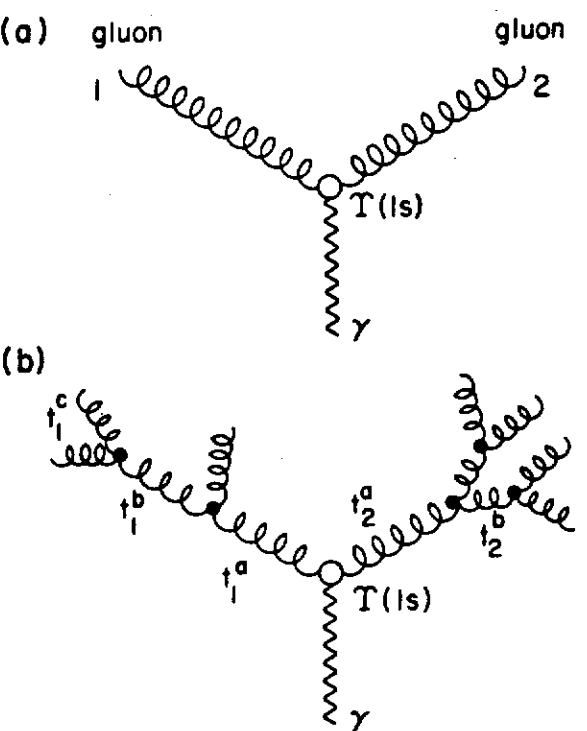


Figure 8.1 (a) Born term diagram for the decay of the upsilon into two massless gluons and a photon,  $\Upsilon(1s) \rightarrow gg\gamma$ . (b) Parton-shower diagram for the decay of the upsilon. The initial two gluons are allowed to radiate additional gluons which in turn can Bremsstrahlung more gluons producing two parton showers (or "jets").

$$\frac{1}{\sigma} \frac{d\sigma}{dz_\gamma dx_1} \approx 2, \quad (8.1.6)$$

which means that the decay is given primarily by phase-space alone. Integrating (8.1.6) over  $x_1$  yields a photon spectrum given by

$$\frac{1}{\sigma} \frac{d\sigma}{dz_\gamma} = \int_{1-z_\gamma}^1 2dx_1 = 2z_\gamma, \quad (8.1.7)$$

which is compared to the exact integral of (8.1.2),

$$\frac{1}{\sigma} \frac{d\sigma}{dz_\gamma} = \frac{1}{(\pi^2 - 9)} [4(1 - z_\gamma) \log(1 - z_\gamma)/z_\gamma^2$$

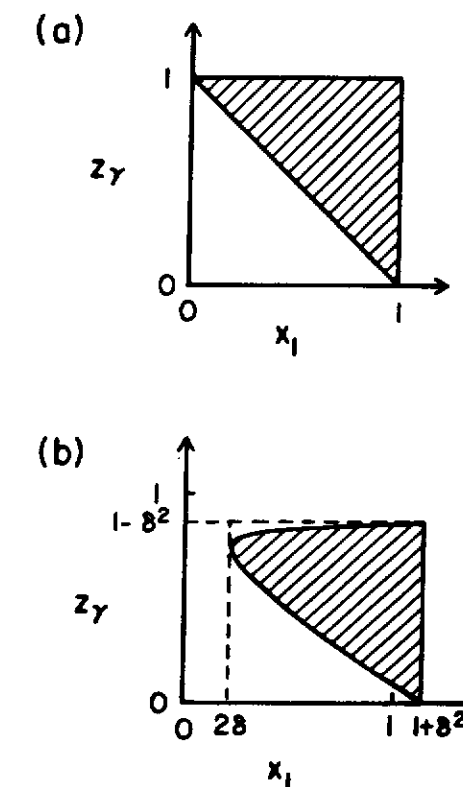


Figure 8.2 Allowed "Dalitz plot" decay regions for the decay of a 1s quarkonium state of mass  $W$  into two gluons of energies  $x_i = 2E_i/W$  and a photon of energy  $z_\gamma = 2E_\gamma/W$  for the case (a) where both gluons are massless and (b) where one gluon has a mass  $\delta = m_g/W$ .

$$- 4(1 - z_\gamma)^2 \log(1 - z_\gamma)/(2 - z_\gamma)^3 + 2z_\gamma(2 - z_\gamma)/z_\gamma^2 \\ + 2z_\gamma(1 - z_\gamma)/(2 - z_\gamma)^2], \quad (8.1.8)$$

in Fig. 8.3. Except for the slight deviation at high  $z$  the two curves agree.

On the other hand, if one (or both) of the outgoing gluons had a non-zero invariant mass then kinematically the photon could not obtain the value of  $z_\gamma = 1$ . Figure 8.2b shows the distortion of the triangular Dalitz region for the case where one gluon has an invariant mass  $m_g$ . In this case  $z_\gamma \leq 1 - \delta^2$ , where  $\delta = m_g/W$ . In QCD, the outgoing gluons will always radiate additional gluons thereby obtaining an invariant mass and this the naive " $2z_\gamma$ " photon spectrum cannot be correct.

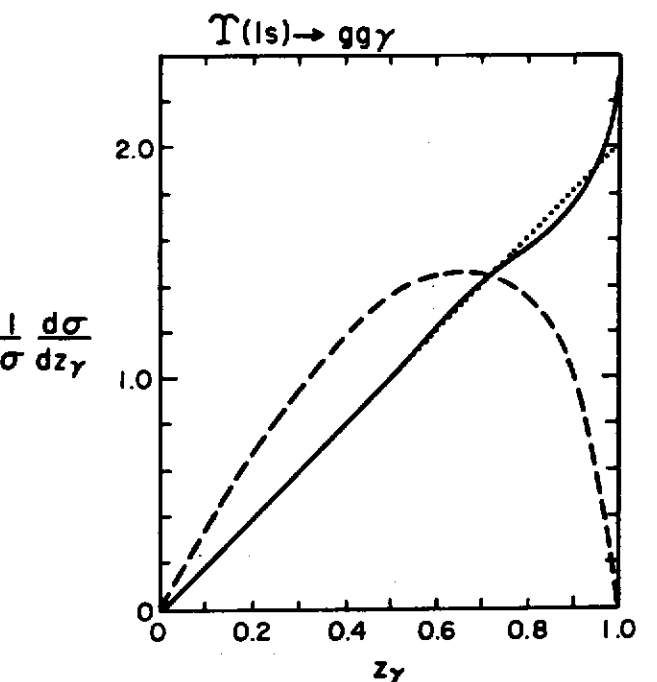


Figure 8.3 Spectrum of the direct photon energies  $z_\gamma = 2E_\gamma/W$  in the decay of a  $1s$  quarkonium state of mass  $W = 10$  GeV into a photon and two gluons. The solid curve is the “Born term” matrix element result for massless gluons and the dotted curve is the pure phase space (“ $2z_\gamma$ ”) approximation. The dashed curve is the prediction of a QCD parton-shower Monte Carlo model with  $\Lambda = 0.2$  GeV and  $\mu_c = 0.45$  GeV.

We can estimate the invariant mass of a gluon “jet” by the use of the parton-shower Monte Carlo approach discussed in Chapter 3. In this case, the initial gluons produced by the heavy quarkonium decay are allowed to Bremsstrahlung gluons until their invariant masses have been degraded to some cut-off mass  $\mu_c$ . The invariant masses of radiated partons are kinematically constrained to be less than those of their parents with the difference being converted into the transverse momentum of the emitted partons. The radiated gluons may themselves radiate more gluons or produce quark-antiquark pairs, producing a shower of partons as shown in Fig. 8.1b. The emission of the partons is treated independently using the simple “leading pole” approximation to QCD and exact kinematics are maintained. The invariant mass spectrum of one of the initiating gluons in the decay  $T(1s) \rightarrow gg\gamma$  resulting from the

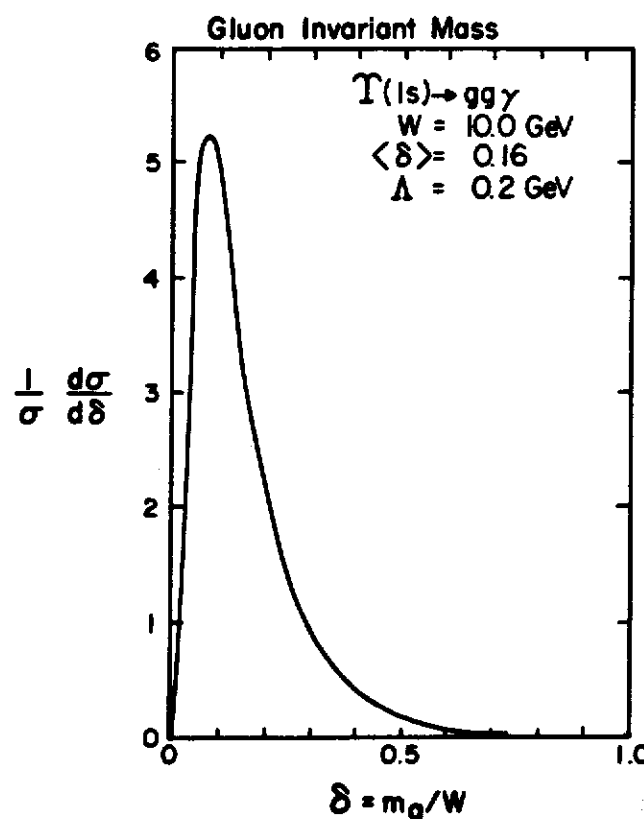


Figure 8.4 Invariant mass distribution of one of the two initiating gluons in the decay of a  $1s$  quarkonium state of mass  $W = 10$  GeV into two gluons and a photon resulting from a QCD parton-shower Monte Carlo model with  $\Lambda = 0.2$  GeV and  $\mu_c = 0.45$  GeV.

parton-shower Monte-Carlo approach with  $\Lambda = 0.2$  GeV and  $\mu_c = 0.45$  GeV is shown in Fig. 8.4. The first gluon can have an invariant mass as large as  $W$ , however, since correct kinematics are maintained the mass of gluon number 2 must be less than  $W$  minus the mass of gluon number 1. The resulting direct photon spectrum is shown by the dashed line in Fig. 8.3<sup>3</sup>. Since one of the initiating gluons always radiates at least one gluon the photon spectrum is predicted to vanishes at  $z_\gamma = 1$ .

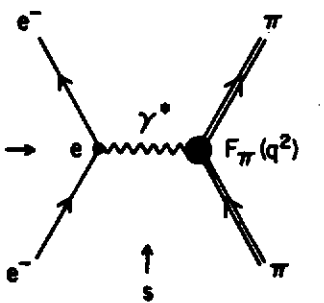


Figure 8.5 The pion form factor.

## 8.2 The Pion Form Factor

One of the most interesting applications of perturbative QCD is the prediction of the asymptotic behavior of hadron form factors. The situation concerning baryon form factors is complicated so I will consider here only meson form factors and, in particular, the pion form factor<sup>4</sup>.

The pion form factor measures the distribution of electric charge within the pion. For example, if pion beams did not decay so quickly, one could imagine scattering electrons off pions as shown in Fig. 8.5 and comparing the result with the known cross section for the scattering of electrons from a point charge,

$$\frac{d\sigma}{d\Omega}(e + \pi \rightarrow e + \pi) = \left( \frac{d\sigma}{d\Omega} \right)_{\text{point}} |F_\pi(Q^2)|^2, \quad (8.2.1)$$

where  $Q^2 = -q^2$  and  $q^2$  is the 4-momentum squared of the virtual photon. The point (or Mott) cross section for a structureless target is given by

$$\left( \frac{d\sigma}{d\Omega} \right)_{\text{point}} = \frac{\alpha^2}{2|\vec{q}|^4} (8E_i E_f - 4p_i \cdot p_f + 4m_e^2), \quad (8.2.2)$$

with

$$p_i \cdot p_f = m_e^2 + 2\beta^2 E^2 \sin^2(\theta/2), \quad (8.2.3)$$

and

$$|\vec{q}|^2 = 4p_{cm}^2 \sin^2(\theta/2), \quad (8.2.4)$$

where  $\theta$  is the center-of-mass scattering angle and

$$E_i = E_f = E_{cm}, \quad (8.2.5)$$

and

$$|\vec{p}_i| = |\vec{p}_f| = p_{cm}, \quad (8.2.6)$$

so that in the center-of-mass frame (8.2.2) becomes

$$\left( \frac{d\sigma}{d\Omega} \right)_{\text{point}} = \frac{\alpha^2}{4p_{cm}^2 \beta^2 \sin^4(\theta/2)} (1 - \beta^2 \sin^2(\theta/2)), \quad (8.2.7)$$

with

$$\beta = p_{cm}/E_{cm}. \quad (8.2.8)$$

For a static target the form factor is simply the Fourier transform of the charge distribution,  $\rho(r)$ ,

$$F_\pi(\vec{q}) = \int \rho(\vec{r}) e^{i\vec{q}\vec{r}} d^3r, \quad (8.2.9)$$

and the condition that

$$\int \rho(\vec{r}) d^3r = 1, \quad (8.2.10)$$

for a  $\pi^+$  implies the normalization

$$F_{\pi^+}(0) = 1. \quad (8.2.11)$$

In perturbative QCD the pion form factor has the form

$$F_\pi(Q^2) = \int_0^1 dx \int_0^1 dy \phi^\dagger(y, Q^2) T(x, y, Q^2) \phi(x, Q^2), \quad (8.2.12)$$

where terms of the order  $(\text{mass})^2/Q^2$  have been neglected. This equation is illustrated in Fig. 8.6 where  $x$  and  $(1-x)$  are the fraction of the pion momentum carried by the quark and antiquarks, respectively. The function  $\phi(x, Q^2)$  is related to the pion wave function and gives the amplitude for finding the quark carrying the fractional momentum  $x$  and the antiquark carrying the fractional momentum  $1-x$  within the pion. All the soft gluon contributions (divergent mass singularities) of the form  $[\alpha_s \log(Q^2/m^2)]^n$  have been absorbed (summed) into  $\phi(x, Q^2)$  and generate its  $Q^2$  dependence (see Fig. 8.6b). The function  $T(x, y, Q^2)$  can be considered as the “hard” scattering amplitude for a parallel  $q\bar{q}$  pair of total momentum  $P$  hit by a virtual photon,  $\gamma^*$ , of momentum  $q$  to end up as a parallel  $\bar{q}$  pair of momentum  $P' = P + q$ . The amplitude  $T(x, y, Q^2)$  has a well defined perturbation expansion of the form

$$T(x, y, Q^2) = \alpha_s(Q^2) T_B(x, y, Q^2) \{1 + \alpha_s(Q^2) T_2(x, y, Q^2) + \dots\}. \quad (8.2.13)$$

The amplitude  $\phi_0(u, P)$ , for finding a quark and antiquark with momentum  $uP$  and  $(1-u)P$ , respectively, within a pion of momentum  $P$  is related to the pion wave function and has 16 components,  $u_\lambda(uP)\bar{v}_\mu((1-u)P)$ , when

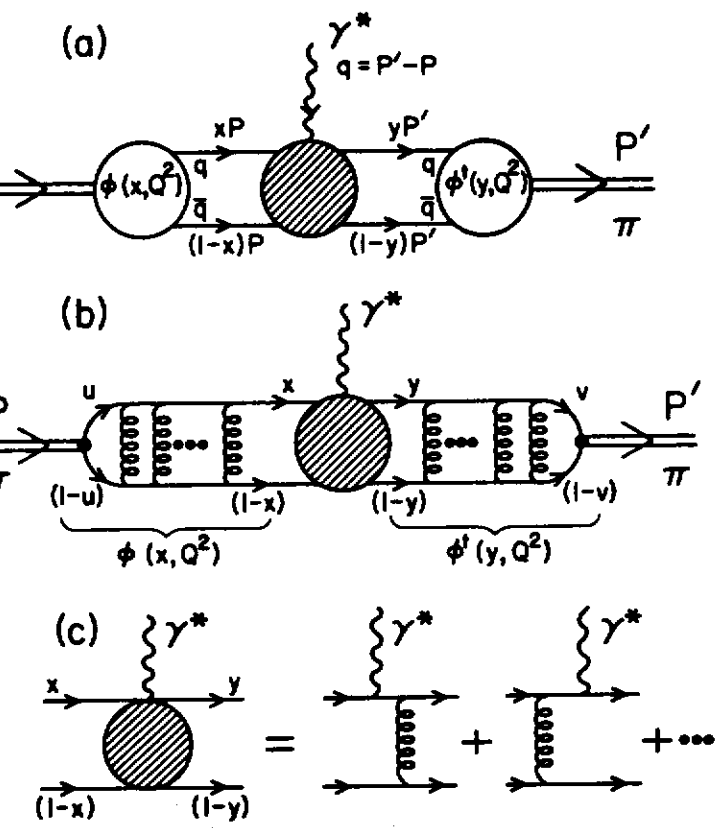


Figure 8.6 (a) Illustration of the calculation of the pion form factor. The "wave function",  $\phi(x, Q^2)$ , gives the amplitude for finding a quark of fractional momentum  $x$  and an antiquark with fractional momentum  $1-x$  within a pion, where  $Q^2 = -q^2$  is the 4-momentum squared transferred by the virtual photon,  $\gamma^*$ . The shaded region is the "hard scattering" amplitude. (b) illustrates how the soft gluon mass singularities are absorbed into  $\phi(x, Q^2)$  and generate its  $Q^2$  dependence. (c) illustrates the "hard scattering" part of diagram (b) which can be expanded in a perturbation series.

summed over the quark and antiquark helicities  $\lambda$  and  $\mu$ . This amplitude can be written as a four by four matrix as follows:

$$\phi_0(u, P) = \sum_{\lambda, \mu} u_\lambda(uP) \bar{v}_\mu((1-u)P) f_{\lambda\mu}$$

$$\begin{aligned}
 & \text{Top: } \text{virtual photon } \gamma^* \text{ with momentum } q = P' - P \text{ interacts with a pion } \pi. \\
 & \text{Middle: } = \sum_{\text{initial helicities}} \sum_{\text{final helicities}} \bar{V}_\lambda((1-u)P) U_\lambda(uP) \bar{V}_\mu((1-v)P') U_\mu(vP') \\
 & \text{Bottom: } = \text{trace} \left\{ \gamma_5 \phi_0(u) \frac{P}{\sqrt{2}} \bar{\phi}_0((1-u)P) + \gamma_5 \phi_0^1(v) \frac{P'}{\sqrt{2}} \bar{\phi}_0((1-v)P') \right\}
 \end{aligned}$$

Figure 8.7 Illustration of the construction of a spin  $0^-$  pion from a spin  $\frac{1}{2}^+$  quark and antiquark.

$$= \frac{\sqrt{(1-u)u}}{\sqrt{2}} \gamma_5 \bar{\phi}_0(u) P = \gamma_5 \phi_0(u) P / \sqrt{2}, \quad (8.2.14)$$

where the factor  $\sqrt{(1-u)u}$  coming from the normalization of the spinors has been absorbed into the function  $\phi_0(u)$ . Terms proportional to  $(\text{mass})/P$  and  $k_T/P$  have been ignored. In this limit isospin symmetry is exact giving  $\phi_0(u) = \phi_0(1-u)$ . The  $\gamma_5$  arises because the quark and antiquark have opposite intrinsic parity and we demand that  $f_{+-} = -f_{-+}$  to insure a  $0^-$  state. As illustrated in Fig. 8.7 (8.2.14) allows us to write the amplitude for the interaction of a virtual photon  $\gamma^*$ , with a pion,  $\gamma^* \pi \rightarrow \pi$ , in terms of a trace over a fermion loop. In particular we can write

$$\text{Amp}(\gamma^* \pi \rightarrow \pi) = \int_0^1 du \int_0^1 dv \phi_0^\dagger(v) A(u, v, Q^2) \phi_0(u), \quad (8.2.15)$$

with

$$A(u, v, Q^2) = \frac{1}{2} \text{tr}(\gamma_5 P B \gamma_5 P' B'), \quad (8.2.16)$$

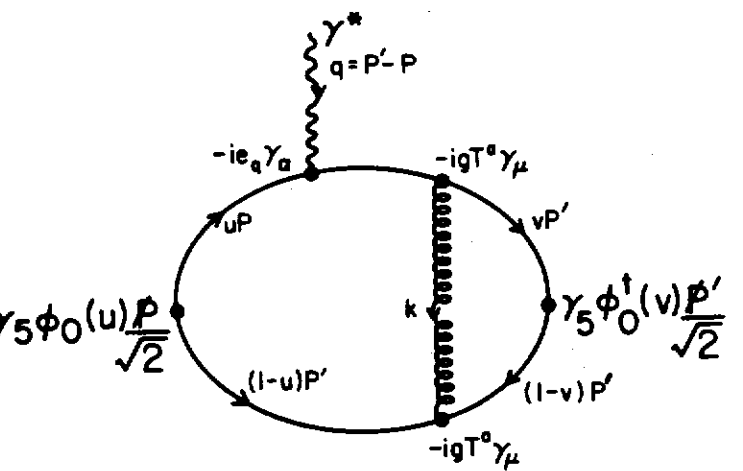


Figure 8.8 One of the four diagrams contributing to the Born amplitude for  $\gamma^* \pi \rightarrow \pi$ . The other diagrams correspond to allowing the gluon to interact at the left of the photon vertex and allowing the photon to also couple to the antiquark.

where  $B$  and  $B'$  depend, of course, on the details within the shaded blob shown in Fig. 8.7. The function  $\phi_0(u)$  is an unknown. However, the integral of  $\phi_0(u)$  over  $u$  is related to the pion decay constant,  $f_\pi$ .

In general, the coupling of a virtual photon to a pion is given by

$$\begin{aligned} \text{Amp}(\gamma^* \pi \rightarrow \pi) &= ie_\pi \langle P' | J_\alpha^{EM} | P \rangle \\ &= ie_\pi F_\pi(Q^2)(P_+)_\alpha + ie_\pi F_-(Q^2)(P_-)_\alpha, \end{aligned} \quad (8.2.17)$$

where

$$(P_+)_\alpha = (P + P')_\alpha, \quad (8.2.18)$$

and

$$(P_-)_\alpha = (P' - P)_\alpha = q_\alpha, \quad (8.2.19)$$

are the only two independent vectors that can be constructed from the initial pion momentum,  $P$ , and the final pion momentum,  $P'$ , and the 4-momentum transfer  $q$ . The quantity  $e_\pi$  is the electric charge of the pion. Conservation of the electromagnetic current,  $J_\alpha^{EM}$ , demands that  $F_-(Q^2)$  be identically zero and hermiticity of  $J_\alpha^{EM}$  means that the pion form factor,  $F_\pi(Q^2 = -q^2)$ , is real.

We define the Born contributions to the pion form factor as the sum of terms of order  $\alpha_s$ , not including any contributions of the form  $\alpha_s [\alpha_s \log(Q^2/m^2)]^n$ ,

which are, however, technically of the same order as  $\alpha_s$ . There are four terms of order  $\alpha_s$  contributing. One diagram is shown in Fig. 8.8 and its contribution to the  $\gamma^* \pi \rightarrow \pi$  amplitude is given by (8.2.15) with  $A(u, v, Q^2) = A_{B1}(u, v, Q^2)$ , where

$$A_{B1}(u, v, Q^2) = \frac{1}{2} \left[ \frac{1}{3} \text{tr}(\mathbf{T}_a \mathbf{T}_a) \right] ie_q g_s^2 \text{tr} [\gamma_5 P' \gamma_\mu (d + uP) \gamma_\alpha \gamma_5 P \gamma_\mu] / [(q + uP)^2 k^2], \quad (8.2.20)$$

where  $P' = P + q$  and  $k = (1 - v)P' - (1 - u)P$  and where  $e_q$  is the charge of the quark. The term in brackets is the familiar color factor

$$\frac{1}{3} \text{tr}(\mathbf{T}_a \mathbf{T}_a) = \frac{1}{3}. \quad (8.2.21)$$

Evaluating the trace yields

$$A_{B1}(u, v, Q^2) = \frac{4}{3} \frac{ie_q 16\pi\alpha_s}{Q^2(1-u)(1-v)} P_\alpha, \quad (8.2.22)$$

where the quarks, gluons and the  $\pi$  have been taken to be massless (i.e.,  $P^2 = P'^2 = 0$ ) and where the strong coupling constant,  $g_s$ , is related to  $\alpha_s$  as usual by  $\alpha_s = g_s^2/4\pi$ .

The diagram with the gluon interacting with the quark before it does with the virtual photon is given by (8.2.22) with  $P_\alpha$  replaced by  $P'_\alpha$  and the interchange of  $u$  and  $v$ . The remaining two Born graphs are arrived at by allowing the photon to couple to the antiquark. This means that one sums over quark charges  $e_q$  leaving  $e_\pi$ . Thus, the complete Born amplitude is given by (8.2.15) with  $A(u, v, Q^2) = A_B(u, v, Q^2)$  and

$$A_B(u, v, Q^2) = \frac{4}{3} \frac{ie_\pi 16\pi\alpha_s}{Q^2(1-u)(1-v)} (P + P')_\alpha. \quad (8.2.23)$$

The amplitude is proportional to  $(P + P')_\alpha$  as required by gauge invariance of the electromagnetic current and from (8.2.17) we see that the Born form factor is given by

$$F_\pi^{BORN}(Q^2) = \int_0^1 du \int_0^1 dv \phi_0^\dagger(v) \alpha_s T_B(u, v, Q^2) \phi_0(u), \quad (8.2.24)$$

where

$$T_B(u, v, Q^2) = \frac{4}{3} \frac{16\pi}{Q^2(1-u)(1-v)}. \quad (8.2.25)$$

The Born term result is not very significant since at the next order and in higher orders there are soft gluon divergences (mass singularities) of the form  $\alpha_s(Q^2)[\alpha_s(Q^2) \log(Q^2/m^2)]^n$ , where  $m$  is the mass used to regularize the divergence. All these terms are of the same order and must be summed to give the complete order  $\alpha_s(Q^2)$  result. These gluon mass singularities are summed and absorbed into the unknown function  $\phi_0(u)$  in (8.2.24) resulting in a "renormalization group improved" wave function,  $\phi(x, Q^2)$ , similar to the procedure used for the quark distributions,  $G(x, Q^2)$ , in Chapter 4.

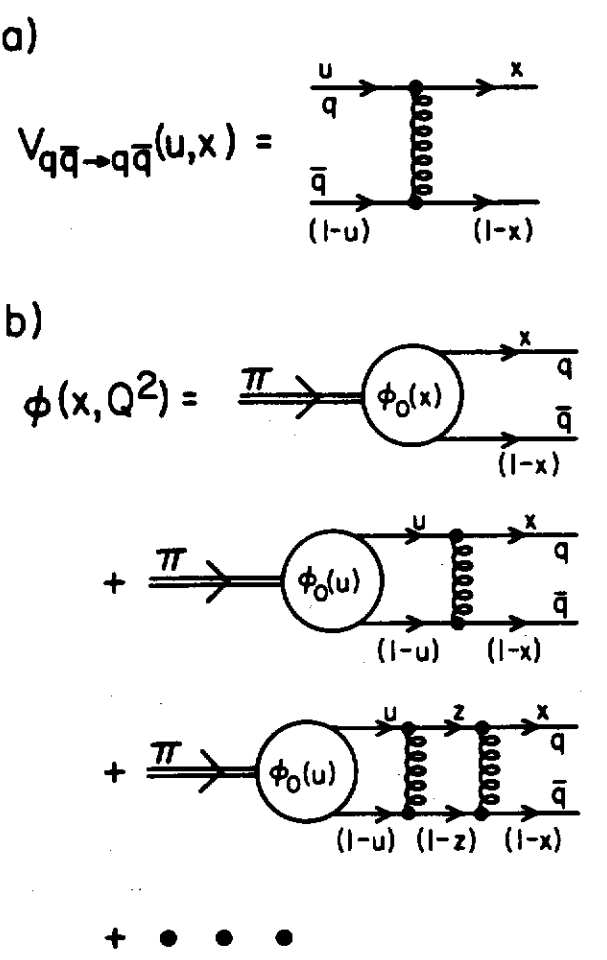


**Figure 8.9** (a) The quantity  $V_{q\bar{q} \rightarrow q\bar{q}}(u, x)$  represents the leading log forward amplitude for a quark and antiquark of fractional momentum  $u$  and  $1-u$ , respectively, to obtain fractional momentum  $x$  and  $1-x$  after interacting with a gluon. (b) Illustrates how the “wave function”  $\phi(x, Q^2)$  is built up from an infinite number of “soft” gluon exchanges.

The leading log sum is most easily performed in an axial gauge where the divergent terms take on the ladder structure as shown in Fig. 8.9. One can define a kernel,  $V_{q\bar{q} \rightarrow q\bar{q}}(u, x)$ , which represents the amplitude (leading log part) for a quark with fractional momentum  $u$  and antiquark with  $(1-u)$  to become a quark with fractional momentum  $x$  and antiquark with  $(1-x)$  by

the exchange of a gluon as shown in Fig. 8.9a. The complete sum,  $\phi(x, Q^2)$ , is arrived at in a manner similar to the method in Chapter 3 and is given by<sup>5</sup>

$$\begin{aligned} \phi(x, Q^2) &= \phi_0(x) + \kappa \int_0^1 du V_{q\bar{q} \rightarrow q\bar{q}}(u, x) \phi_0(u) \\ &+ \frac{\kappa^2}{2!} \int_0^1 du \int_0^1 dz V_{q\bar{q} \rightarrow q\bar{q}}(u, z) V_{q\bar{q} \rightarrow q\bar{q}}(z, x) \phi_0(u) + \dots, \\ &\equiv \exp[\kappa V_{q\bar{q} \rightarrow q\bar{q}}(u, x) *] \phi_0(u), \end{aligned} \quad (8.2.26)$$

where in this case I have defined the convolution symbol  $*$  to mean

$$A * B = \int_0^1 dz A(z) B(z), \quad (8.2.27)$$

and where the kernel  $V_{q\bar{q} \rightarrow q\bar{q}}(u, x)$  is given by

$$\begin{aligned} V_{q\bar{q} \rightarrow q\bar{q}}(u, x) &= \frac{2}{3} \left\{ \frac{1-u}{1-x} \left( 1 + \frac{1}{u-x} \right)_+ \theta(u-x) \right. \\ &\left. + \frac{u}{x} \left( 1 + \frac{1}{x-u} \right)_+ \theta(x-u) \right\}. \end{aligned} \quad (8.2.28)$$

The “+ functions” in (8.2.28) are analogous to those defined in Chapter 3 and discussed in Appendix E. Here they signify that the singularity at  $x = u$  in  $V_0(u, x)$  is canceled by a contribution arising from self-energy corrections to the quark propagator (which occur only at  $u = x$ ). In particular,

$$V_{q\bar{q} \rightarrow q\bar{q}}(u, x) = V_0(u, x) - \delta(x-u) \int_0^1 dz V_0(z, x). \quad (8.2.29)$$

The quantity  $\kappa$  in (8.2.26) arises from integrals over the loop momentum with the running coupling constant at the vertices as in Chapter 3 and is given by

$$\kappa = \frac{2}{\beta_0} \log\{\alpha_s(Q_0^2)/\alpha_s(Q^2)\} \quad (8.2.30)$$

with  $\beta_0$  defined in (1.2.19). From (8.2.26) we see that  $\phi(x, Q^2)$  satisfies the following differential equation,

$$\frac{d\phi(x, Q^2)}{d\kappa} = \int_0^1 du V_{q\bar{q} \rightarrow q\bar{q}}(u, x) \phi(u, Q^2). \quad (8.2.31)$$

The complete order  $\alpha_s^2$  expression for the pion form factor is then given by

$$F_\pi(Q^2) = \int_0^1 dx \int_0^1 dy \phi^\dagger(y, Q^2) \alpha_s(Q^2) T_B(x, y, Q^2) \phi(x, Q^2), \quad (8.2.32)$$

where  $T_B$  is the “hard scattering” Born amplitude given by (8.2.25) and  $\phi(x, Q^2)$  satisfies the differential equation in (8.2.31).

The differential equation for  $\phi(x, Q^2)$  can be solved quite easily if one

first notices that Gegenbauer polynomials of order  $3/2$ ,  $C_n^{(3/2)}(x)$ , satisfy the following eigenvalue equation

$$\int_0^1 dz C_n^{(3/2)}(2z-1) V_{q\bar{q} \rightarrow q\bar{q}}(z, x) = \frac{1}{2} A_n^{NS} C_n^{(3/2)}(x), \quad (8.2.33)$$

where  $A_n^{NS}$  turns out to be the same non-singlet anomalous dimensions given in (4.7.6),

$$A_n^{NS} = \frac{4}{3} \left[ -\frac{1}{2} + \frac{1}{(n+1)(n+2)} - 2 \sum_{j=2}^{n+1} \frac{1}{j} \right]. \quad (8.2.34)$$

Using the properties of the Gegenbauer polynomials given in Appendix E, we define Gegenbauer moments by

$$\phi_n(Q^2) = \frac{4(2n+3)}{(n+1)(n+2)} \int_0^1 dx C_n^{(3/2)}(2x-1) \phi(x, Q^2), \quad (8.2.35)$$

the inverse of which is

$$\phi(x, Q^2) = x(1-x) \sum_{n=0}^{\infty} \phi_n(Q^2) C_n^{(3/2)}(2x-1). \quad (8.2.36)$$

In terms of Gegenbauer moments the differential equation (8.2.31) becomes

$$\frac{d\phi_n(Q^2)}{dk} = A_n^{NS} \phi_n(Q^2), \quad (8.2.37)$$

where (8.2.33) has been used. This implies that

$$\begin{aligned} \phi_n(Q^2) &= \exp(A_n^{NS} k) \phi_n(Q_0^2) \\ &= [\alpha_s(Q^2)/\alpha_s(Q_0^2)]^{d_n} \phi_n(Q_0^2) \end{aligned} \quad (8.2.38)$$

where

$$d_n = -2A_n^{NS}/\beta_0, \quad (8.2.39)$$

or by the use of (8.2.36)

$$\phi(x, Q^2) = x(1-x) \sum_{n=0}^{\infty} [\alpha_s(Q^2)/\alpha_s(Q_0^2)]^{d_n} C_n^{(3/2)}(2x-1) \phi_n(Q_0^2). \quad (8.2.40)$$

Given the wave function,  $\phi(x, Q_0^2)$ , at some  $Q_0^2$  one can use (8.2.38) and (8.2.40) to compute it at any other  $Q^2$  provided one knows the perturbative parameter  $\Lambda$ .

One can make use of the simple factorizing form for  $T(x, y, Q^2)$  and write the order  $\alpha_s(Q^2)$  form factor as

$$F_\pi(Q^2) = 16\pi \frac{4}{3} \frac{\alpha_s(Q^2)}{Q^2} \left| \int_0^1 dx \frac{\phi(x, Q^2)}{(1-x)} \right|^2 \quad (8.2.41)$$

or by using E.4.6 cast it in the form

$$F_\pi(Q^2) = 4\pi \frac{4}{3} \frac{\alpha_s(Q^2)}{Q^2} \left| \sum_{n=0}^{\infty} \phi_n(Q_0^2) [\alpha_s(Q^2)/\alpha_s(Q_0^2)]^{d_n} \right|^2. \quad (8.2.42)$$

Keeping only the first few terms gives

$$\begin{aligned} F_\pi(Q^2) &= 4\pi \frac{4}{3} \frac{\alpha_s(Q^2)}{Q^2} \left\{ |\phi_0(Q_0^2)|^2 \right. \\ &\quad \left. + 2\text{Re}(\phi_0(Q_0^2)\phi_1^*(Q_0^2)) [\alpha_s(Q^2)/\alpha_s(Q_0^2)]^{d_1} + \dots \right\}. \end{aligned} \quad (8.2.43)$$

Except for  $n = 0$  all terms die off like fractional powers of  $\alpha_s(Q^2)/\alpha_s(Q_0^2) = \log(Q_0^2/\Lambda)/\log(Q^2/\Lambda^2)$  (e.g.  $d_1 = 0.0427$  with  $n_f = 4$ ). This means that as  $Q^2$  becomes large  $F_\pi(Q^2)$  approaches the first term in (8.2.43)

$$F_\pi(Q^2) \underset{Q^2 \rightarrow \infty}{\sim} 4\pi \frac{4}{3} \frac{\alpha_s(Q^2)}{Q^2} |\phi_0(Q_0^2)|^2. \quad (8.2.44)$$

The approach to this limiting value is, however, extremely slow and (8.2.44) is not very useful at existing  $Q^2$  values.

If the wave functions at  $Q_0^2$  has the particularly simple form

$$\phi(x, Q_0^2) = C_0 x(1-x), \quad (8.2.45)$$

then from (8.2.35) and (E.4.2) we see that

$$\phi_n(Q_0^2) = \begin{cases} C_0 & \text{for } n = 0 \\ 0 & \text{for } n > 0 \end{cases}. \quad (8.2.46)$$

For this choice  $\phi(x, Q^2)$  in (8.2.40) does not evolve with  $Q^2$  (remember  $A_0^{NS} = 0$ ) and is simply given by

$$\phi(x, Q^2) = C_0 x(1-x). \quad (8.2.47)$$

In this case  $F_\pi(Q^2)$  is equal to its asymptotic value at all  $Q^2$ . Namely,

$$F_\pi(Q^2) = 4\pi \frac{4}{3} \frac{\alpha_s(Q^2)}{Q^2} |C_0|^2, \quad (8.2.48)$$

for all  $Q^2$  provided  $\phi(x, Q_0^2)$  is given by (8.2.45).

In general, however,  $\phi(x, Q_0^2)$  is an unknown function. One cannot deduce it from perturbation theory. Nevertheless, it must satisfy one important constraint. Namely, the first Gegenbauer moment  $\phi_0(Q^2)$  in (8.2.35) is related to the pion wave function at the origin,

$$\phi_0 = \phi_0(Q^2) = 6 \int_0^1 dx \phi(x, Q^2). \quad (8.2.49)$$

For pions this constant can be determined from the weak decay amplitude

$\pi \rightarrow \mu\nu$ . Namely,

$$\phi_0 = \sqrt{3} f_\pi \quad (f_\pi \approx 93 \text{ MeV}). \quad (8.2.50)$$

For the case  $\phi(x, Q_0^2) = C_0 x(1-x)$  this implies that

$$C_0 = \sqrt{3} f_\pi, \quad (8.2.51)$$

and

$$F_\pi(Q^2) = 16\pi \frac{\alpha_s(Q^2)}{Q^2} f_\pi^2. \quad (8.2.52)$$

For other choices of  $\phi(x, Q_0^2)$  this value is approached (very slowly) as  $Q^2 \rightarrow \infty$ . If  $\phi(x, Q^2)$  is more peaked at  $x = 1/2$  than (8.2.45) than the limit is approached from below. If, on the other hand,  $\phi(x, Q_0^2)$  is less peaked at  $x = 1/2$  than (8.2.45), then the limit is approached from above. In either case the approach is quite slow.

### Problems

- 8.1. Show that the "Born term" double differential cross section for the decay of a quarkonium  $1s$  state into two massless gluons and a photon is given by

$$\frac{1}{\sigma} \frac{d\sigma}{dz_\gamma dx_1} = \frac{1}{(\pi^2 - 9)} \left[ \frac{(1-x_1)^2}{(x_2 z_\gamma)^2} + \frac{(1-x_2)^2}{(x_1 z_\gamma)^2} + \frac{(1-z_\gamma)^2}{(x_1 x_2)^2} \right],$$

where  $x_{1,2} = 2E_{1,2}/W$  are the fractional energies of the two gluons and  $z_\gamma = 2E_\gamma/W$  is the fractional energy of the photon and  $W$  is the mass of the quarkonium state. Show that to a high degree of accuracy this differential cross section can be approximated by

$$\frac{1}{\sigma} \frac{d\sigma}{dz_\gamma dx_1} \approx 2.$$

- 8.2. Integrate the double differential cross section in (8.1.2) over the allowed range of  $x_1$  and verify (8.1.8).

- 8.3. Show that the point (or Mott) cross section for the scattering of electrons off a structureless target is given in the center-of-mass frame by

$$\left( \frac{d\sigma}{d\Omega} \right)_{\text{point}} = \frac{\alpha^2}{4p_{cm}^2 \beta^2 \sin^4(\theta/2)} (1 - \beta^2 \sin^2(\theta/2)),$$

where

$$\beta = p_{cm}/E_{cm}.$$

- 8.4. Show that, in general, the coupling of a virtual photon to a pion is given by

$$\begin{aligned} \text{Amp}(\gamma^* \pi \rightarrow \pi) &= ie_\pi \langle P' | J_\alpha^{EM} | P \rangle \\ &= ie_\pi F_\pi(Q^2)(P_+)_\alpha + ie_\pi F_-(Q^2)(P_-)_\alpha, \end{aligned}$$

where  $J_\alpha^{EM}$  is the electromagnetic current and  $(P_+)_\alpha = (P + P')_\alpha$  and  $(P_-)_\alpha = (P' - P)_\alpha = q_\alpha$  are the only two independent vectors that can be constructed from the initial pion momentum,  $P$ , and the final pion momentum,  $P'$ , and the 4-momentum transfer  $q$ . Verify that conservation of the electromagnetic current demands that  $F_-(Q^2)$  be identically zero and hermiticity implies that the pion form factor,  $F_\pi(Q^2 = -q^2)$ , is real.

- 8.5. Show that the diagram in Fig. 8.6 gives a contribution to the  $\gamma^* \pi \rightarrow \pi$  amplitude of the form given in (8.2.15) with

$$\begin{aligned} A_{B1}(u, v, Q^2) &= \frac{1}{2} \left[ \frac{1}{3} \text{tr}(T_a T_a) \right] ie_q g_s^2 \\ &\quad \text{tr} [\gamma_5 P' \gamma_\mu (1 + uP) \gamma_\alpha \gamma_5 P \gamma_\mu] / [(q + uP)^2 k^2], \end{aligned}$$

where  $P' = P + q$  and  $k = (1-v)P' - (1-u)P$  and where  $e_q$  is the charge of the quark. Evaluate this for massless partons and pions and verify that

$$A_{B1}(u, v, Q^2) = \frac{4}{3} \frac{ie_q 16\pi \alpha_s}{Q^2(1-u)(1-v)} P_\alpha.$$

- 8.6. Show that the complete  $\gamma^* \pi \rightarrow \pi$  Born amplitude is given by

$$A_B(u, v, Q^2) = \frac{4}{3} \frac{ie_\pi 16\pi \alpha_s}{Q^2(1-u)(1-v)} (P + P')_\alpha,$$

and verify that the Born pion form factor is given by

$$F_\pi^{BORN}(Q^2) = \int_0^1 du \int_0^1 dv \phi_0^\dagger(v) \alpha_s T_B(u, v, Q^2) \phi_0(u),$$

where

$$T_B(u, v, Q^2) = \frac{4}{3} \frac{16\pi}{Q^2(1-u)(1-v)}.$$

- 8.7. Show that the asymptotic behavior of the pion form factor is given by

$$F_\pi(Q^2) \xrightarrow{Q \rightarrow \infty} 16\pi \frac{\alpha_s(Q^2)}{Q^2} f_\pi^2,$$

with the pion weak decay amplitude given by  $f_\pi \approx 93 \text{ MeV}$ .

### Further Reading

G. Altarelli, "Partons in Quantum Chromodynamics," *Physics Reports* 81, 1 (1982).

F. Halzen and A.D. Martin, *Quarks and Leptons. An Introductory Course in Modern Particle Physics*, John Wiley & Sons, Inc., 1984.

References

1. P.B. MacKenzie and G.P. Lepage, *Phys. Rev. Lett.* **47**, 1244 (1981).
2. S.J. Brodsky, G.P. Lepage and P.B. MacKenzie, *Phys. Rev.* **D28**, 228 (1983).
3. R.D. Field, *Phys. Lett.* **133B**, 248 (1983).
4. S.J. Brodsky and G.P. Lepage, *Phys. Lett.* **87B**, 359 (1979). *ibid* *Phys. Rev. Lett.* **43**, 545 (1979). Erratum *ibid* **43**, 1625 (1979).
5. M.K. Chase, *Nucl. Phys.* **B167**, 125 (1980). *ibid* **B174**, 109 (1980).

## APPENDIX A

**S-Matrix Formulas**

In this book I follow closely the conventions of Quigg<sup>1</sup> which is the same as Bjorken and Drell<sup>2</sup> except for the normalization of Dirac spinors.

### A.1 Invariant Amplitude

The invariant amplitude  $\mathcal{M}$  is related to the  $S$ -matrix through the relation

$$S_{\beta\alpha} = \delta_{\beta\alpha} - i(2\pi)^4 \delta^4(p_\beta - p_\alpha) \frac{\mathcal{M}_{\beta\alpha}}{\sqrt{\prod_i (2E_i)}}, \quad (A.1.1)$$

where  $\alpha$  and  $\beta$  label the initial and final states and the product of factors  $(2E_i)$  is over both initial and final states.

### A.2 Decay Process $\alpha \rightarrow (1, 2, \dots, n)$

The transition probability for the decay process  $\alpha \rightarrow (1, 2, \dots, n)$  is given by

$$dW_{\beta\alpha} = \frac{(2\pi)^4}{2E_\alpha} |\mathcal{M}_{\beta\alpha}|^2 \prod_{i=1}^n \frac{d^3 p_i}{(2\pi)^3 (2E_i)} \delta^4(p_1 + p_2 + \dots + p_n - p_\alpha). \quad (A.2.1)$$

For a two-body final state (A.2.1) becomes

$$dW_{\beta\alpha} = \frac{1}{32\pi^2} |\mathcal{M}_{\beta\alpha}|^2 \frac{p_{cm} d\Omega_{cm}}{M_\alpha^2}, \quad (A.2.2)$$

where  $M_\alpha$  is the parent mass and

$$p_{cm}^2 = \frac{1}{4M_\alpha^2} [M_\alpha^2 - (m_1 + m_2)^2] [M_\alpha^2 - (m_1 - m_2)^2]. \quad (A.2.3)$$

### A.3 2-to-2 Differential Cross Section

For an initial state  $\alpha = (1, 2)$ , where particle number 1 is the projectile and number 2 is the target, and a final state  $\beta = (3, 4, \dots, n)$  the differential cross section is

$$d\sigma = \frac{(2\pi)^4 |\mathcal{M}_{\beta\alpha}|^2}{4\sqrt{(p_1 \cdot p_2)^2 - m_1^2 m_2^2}} \prod_{i=3}^n \frac{d^3 p_i}{(2\pi)^3 (2E_i)} \delta^4 \left( \sum_{i=3}^n p_i - p_\alpha \right). \quad (A.3.1)$$

The 2-to-2 collision differential cross section ( $m_1 + m_2 \rightarrow m_3 + m_4$ ) is given

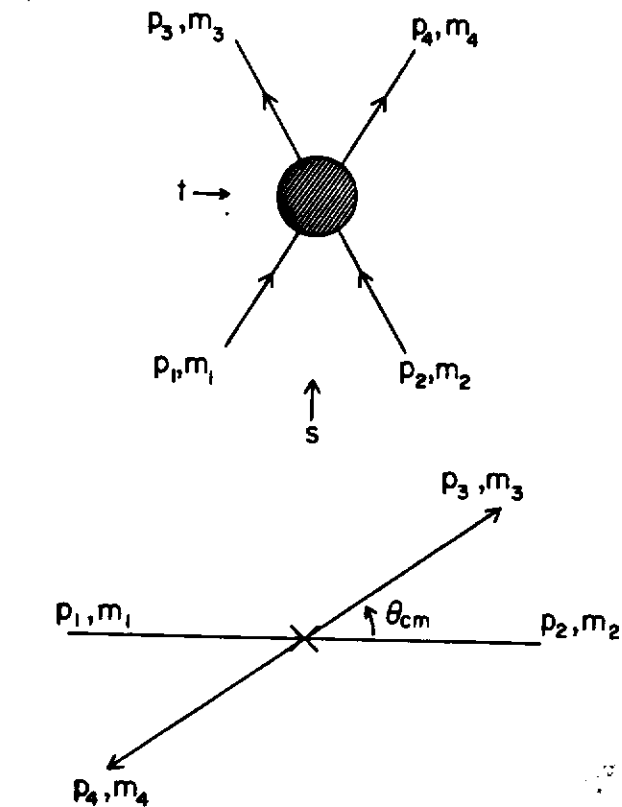


**Figure A.1** Illustration of a 2-to-2 scattering,  $1 + 2 \rightarrow 3 + 4$ , through a center-of-mass scattering angle,  $\theta_{cm}$ .

by

$$\frac{d\sigma}{d\Omega_{cm}}(s, \theta) = \frac{1}{64\pi^2 s} \frac{p'_{cm}}{p_{cm}} |\mathcal{M}_{\beta\alpha}|^2, \quad (A.3.2)$$

where  $d\Omega = d(\cos \theta_{cm}) d\phi_{cm}$ . The invariants  $s$ ,  $t$  and  $u$  are defined by

$$s = (p_1 + p_2)^2 = (p_2 + p_4)^2, \quad (A.3.3)$$

$$t = (p_3 - p_1)^2 = (p_2 - p_4)^2, \quad (A.3.4)$$

$$u = (p_4 - p_1)^2 = (p_2 - p_3)^2, \quad (A.3.5)$$

where  $p_i$  are the 4-momenta shown in Fig. A.1. Momentum and energy conservation implies

$$p_1 + p_2 = p_3 + p_4, \quad (A.3.6)$$

which guarantees that

$$s + t + u = \sum_{i=1}^4 m_i^2. \quad (A.3.7)$$

The invariant  $s$  is the square of the total energy in the center-of-mass frame and is also given by

$$s = m_1^2 + m_2^2 + 2m_2(E_1)_{\text{LAB}}. \quad (A.3.8)$$

The invariant  $t$  is the 4-momentum transfer squared and is given by

$$t = t_{\min} + 2p_{cm}p'_{cm}(\cos\theta_{cm} - 1), \quad (A.3.9)$$

where

$$t_{\min} = (E_1^{cm} - E_3^{cm})^2 - (p_{cm} - p'_{cm})^2, \quad (A.3.10)$$

where the initial and final center-of-mass momenta are given by

$$p_{cm}^2 = \frac{1}{4s} [s - (m_1 + m_2)^2] [s - (m_1 - m_2)^2], \quad (A.3.11)$$

$$(p'_{cm})^2 = \frac{1}{4s} [s - (m_3 + m_4)^2] [s - (m_3 - m_4)^2], \quad (A.3.12)$$

respectively, and the energies of particles 1 and 3 in the center-of-mass frame are

$$E_1^{cm} = \frac{(s + m_1^2 - m_2^2)}{2\sqrt{s}}, \quad (A.3.13)$$

$$E_2^{cm} = \frac{(s + m_3^2 - m_4^2)}{2\sqrt{s}}. \quad (A.3.14)$$

The flux factor in (A.3.1) is given by

$$[(p_1 \cdot p_2)^2 - m_1^2 m_2^2]^{1/2} \stackrel{\text{LAB}}{=} m_2 (p_1)_{\text{LAB}}, \quad (A.3.15)$$

$$[(p_1 \cdot p_2)^2 - m_1^2 m_2^2]^{1/2} \stackrel{cm}{=} p_{cm} \sqrt{s}, \quad (A.3.16)$$

in the laboratory and center-of-mass frame, respectively. Using (A.3.2), we have

$$\begin{aligned} \frac{d\sigma}{dt}(s, t) &= \frac{\pi}{p_{cm}p'_{cm}} \frac{d\sigma}{d\Omega_{cm}}(s, \theta) \\ &= \frac{1}{64\pi s p_{cm}^2} |\mathcal{M}_{\beta\alpha}|^2. \end{aligned} \quad (A.3.17)$$

The Kibble function is given by

$$\begin{aligned} \phi(s, t, u) &= stu - s(m_1^2 m_2^2 + m_3^2 m_4^2) \\ &\quad - t(m_1^2 m_3^2 + m_2^2 m_4^2) - u(m_1^2 m_4^2 + m_2^2 m_3^2) \\ &\quad + 2(m_1^2 m_2^2 m_3^2 + m_1^2 m_3^2 m_4^2 + m_2^2 m_3^2 m_4^2 + m_1^2 m_2^2 m_4^2). \end{aligned} \quad (A.3.18)$$

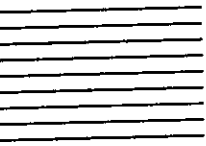
The solution of the implicit equation  $\varphi(s, t, u) = 0$  gives the boundaries of the physical phase space region for the reaction shown in Fig. A.1.

## References

1. C. Quigg, *Gauge Theories of the Strong, Weak, and Electromagnetic Interactions*, Frontiers in Physics, The Benjamin-Cummings Publishing Company, Inc., 1983.
2. J.D. Bjorken and S.D. Drell, *Relativistic Quantum Mechanics*, McGraw-Hill, New York, 1965.

## APPENDIX B

## Metric and Matrices



The metric

$$g_{\mu\nu} = \begin{pmatrix} 1 & 0 & 0 & 0 \\ 0 & -1 & 0 & 0 \\ 0 & 0 & -1 & 0 \\ 0 & 0 & 0 & -1 \end{pmatrix}, \quad (B.1.1)$$

or

$$g_{00} = 1, \quad g_{0i} = 0, \quad g_{ij} = -\delta_{ij} \quad (i, j = 1, 2, 3) \quad (B.1.2)$$

is chosen throughout the text. The space-time and energy-momentum four-vectors are taken to be

$$x_\mu = \begin{pmatrix} x_0 \\ x_1 \\ x_2 \\ x_3 \end{pmatrix} \quad (B.1.3)$$

$$p_\mu = \begin{pmatrix} E \\ p_x \\ p_y \\ p_z \end{pmatrix} \quad (B.1.4)$$

and the 4-vector dot product is given by

$$p^2 \equiv p \cdot p = g_{\mu\nu} p_\mu p_\nu = E^2 - \vec{p} \cdot \vec{p} = m^2 \quad (B.1.5)$$

and

$$p_1 \cdot p_2 \equiv g_{\mu\nu} (p_1)_\mu (p_2)_\nu = E_1 E_2 - \vec{p}_1 \cdot \vec{p}_2. \quad (B.1.6)$$

I will not distinguish between contravariant and covariant vectors and, unless specifically indicated to the contrary, repeated indices are summed.

B.2 Metric ( $N$  dimensions)

In  $N$  spacetime (one time,  $N - 1$  space) dimensions the metric is taken to be

$$g_{00} = 1, \quad g_{0i} = 0, \quad g_{ij} = -\delta_{ij} \quad (i, j = 1, 2, \dots, N - 1), \quad (B.2.1)$$

and the  $N$ -vector dot product is

$$k \cdot p \equiv g_{\mu\nu} k_\mu p_\nu = k_0 p_0 - k_1 p_1 - k_2 p_2 - \dots - k_{N-1} p_{N-1}. \quad (B.2.2)$$

### B.3 Dirac Algebra ( $N = 4$ dimensions)

The  $4 \times 4$  Dirac matrices satisfy

$$\gamma_\mu \gamma_\nu + \gamma_\nu \gamma_\mu = \{\gamma_\mu, \gamma_\nu\} = 2g_{\mu\nu} \mathbf{I}_4, \quad (B.3.1)$$

where  $\mathbf{I}_4$  is the  $4 \times 4$  unit matrix and  $\mu$  and  $\nu$  run over 0, 1, 2, 3. From (B.3.1) it is easy to show that

$$\gamma_\mu \gamma_\mu = 4 \mathbf{I}_4, \quad (B.3.2)$$

$$\gamma_\mu \gamma_\alpha \gamma_\mu = -2\gamma_\alpha, \quad (B.3.3)$$

$$\gamma_\mu \gamma_\alpha \gamma_\beta \gamma_\mu = 4g_{\alpha\beta} \mathbf{I}_4, \quad (B.3.4)$$

$$\gamma_\mu \gamma_\alpha \gamma_\beta \gamma_\lambda \gamma_\mu = -2\gamma_\lambda \gamma_\beta \gamma_\alpha. \quad (B.3.5)$$

Furthermore, the following trace relations are satisfied

$$\text{tr}(\mathbf{I}_4) = 4, \quad (B.3.6)$$

$$\text{tr}(\gamma_\alpha \gamma_\beta) = 4g_{\alpha\beta}, \quad (B.3.7)$$

$$\text{tr}(\text{odd } \# \text{ of } \gamma's) = 0, \quad (B.3.8)$$

$$\text{tr}(\gamma_\alpha \gamma_\beta \gamma_\lambda \gamma_\rho) = 4(g_{\alpha\beta} g_{\lambda\rho} - g_{\alpha\lambda} g_{\beta\rho} + g_{\alpha\rho} g_{\beta\lambda}). \quad (B.3.9)$$

In deriving the above relations one makes use of

$$\text{tr}(\mathbf{AB}) = \text{tr}(\mathbf{BA}), \quad (B.3.10)$$

$$\text{tr}(\mathbf{ABC}) = \text{tr}(\mathbf{CAB}) = \text{tr}(\mathbf{BCA}), \quad (B.3.11)$$

$$\text{tr}(c_1 \mathbf{A} + c_2 \mathbf{B}) = c_1 \text{tr}(\mathbf{A}) + c_2 \text{tr}(\mathbf{B}), \quad (B.3.12)$$

where  $\mathbf{A}$ ,  $\mathbf{B}$  and  $\mathbf{C}$  are matrices and  $c_1, c_2$  are constants.

The symbol  $\not{d}$  is defined by

$$\not{d} \equiv \mathbf{a} \cdot \boldsymbol{\gamma} = g_{\mu\nu} a_\mu \gamma_\nu = a_0 \gamma_0 - \vec{a} \cdot \vec{\gamma}, \quad (B.3.13)$$

where  $\mathbf{a}$  is an arbitrary 4-vector. From (B.3.7) and (B.3.9) we have

$$\text{tr}(\not{d} \not{d}) = 4a \cdot b, \quad (B.3.14)$$

$$\text{tr}(\not{d} \not{d} \not{d} \not{d}) = 4[a \cdot b \ c \cdot d - a \cdot c \ b \cdot d + a \cdot d \ b \cdot c], \quad (B.3.16)$$

respectively.

### B.4 Dirac Matrices ( $N = 4$ dimensions)

A convenient representation of the Dirac algebra in (B.3.1) is given by

$$\gamma_0 = \begin{pmatrix} \mathbf{I}_2 & 0 \\ 0 & -\mathbf{I}_2 \end{pmatrix} \quad (B.4.1)$$

$$\gamma_i = \begin{pmatrix} 0 & \sigma_i \\ -\sigma_i & 0 \end{pmatrix} \quad (i = 1, 3), \quad (B.4.2)$$

where  $\mathbf{I}_2$  is the  $2 \times 2$  unit matrix and the Pauli matrices,  $\sigma_i$ , satisfy

$$\{\sigma_i, \sigma_j\} = 2\delta_{ij}, \quad (B.4.3)$$

$$\sigma_i \sigma_j = i \epsilon_{ijk} \sigma_k, \quad (B.4.4)$$

and are represented by

$$\sigma_1 = \begin{pmatrix} 0 & 1 \\ 1 & 0 \end{pmatrix}, \quad \sigma_2 = \begin{pmatrix} 0 & -i \\ i & 0 \end{pmatrix}, \quad \sigma_3 = \begin{pmatrix} 1 & 0 \\ 0 & -1 \end{pmatrix}. \quad (B.4.5)$$

It is useful to define

$$\gamma_5 = i\gamma_0 \gamma_1 \gamma_2 \gamma_3 = \begin{pmatrix} 0 & \mathbf{I}_2 \\ \mathbf{I}_2 & 0 \end{pmatrix}, \quad (B.4.6)$$

and

$$\sigma_{\mu\nu} = \frac{1}{2}(\gamma_\mu \gamma_\nu - \gamma_\nu \gamma_\mu) = \frac{i}{2}[\gamma_\mu, \gamma_\nu], \quad (B.4.7)$$

where

$$\gamma_5^2 = \mathbf{I}_4, \quad (B.4.8)$$

and

$$\{\gamma_\mu, \gamma_5\} = 0. \quad (B.4.9)$$

It is easy to see that

$$\text{tr}(\gamma_\mu) = 0. \quad (B.4.10)$$

### B.5 Dirac Algebra ( $N$ dimensions)

In  $N$  space-time (one time,  $N - 1$  space) dimensions the Dirac matrices satisfy

$$\gamma_\mu \gamma_\nu + \gamma_\nu \gamma_\mu = 2g_{\mu\nu} \mathbf{I}_N, \quad (B.5.1)$$

where  $\mathbf{I}_N$  is the unit matrix in  $N$  dimensions and  $\mu$  and  $\nu$  run from 0 to  $N - 1$ . In addition,

$$\gamma_\mu \gamma_\mu = N \mathbf{I}_N, \quad (B.5.2)$$

$$\gamma_\mu \gamma_\alpha \gamma_\mu = (2 - N)\gamma_\alpha, \quad (B.5.3)$$

$$\gamma_\mu \gamma_\alpha \gamma_\beta \gamma_\mu = 4g_{\alpha\beta} \mathbf{I}_N + (N - 4)\gamma_\alpha \gamma_\beta, \quad (B.5.4)$$

$$\gamma_\mu \gamma_\alpha \gamma_\beta \gamma_\lambda \gamma_\mu = -2\gamma_\lambda \gamma_\beta \gamma_\alpha - (N - 4)\gamma_\alpha \gamma_\beta \gamma_\lambda. \quad (B.5.5)$$

Furthermore, the trace of  $\mathbf{I}_N$  is defined as follows<sup>1</sup>:

$$\text{tr}(\mathbf{I}_N) = 4, \quad (B.5.6)$$

resulting in

$$\text{tr}(\gamma_\alpha \gamma_\beta) = 4g_{\alpha\beta}, \quad (B.5.7)$$

$$\text{tr}(\gamma_\alpha \gamma_\beta \gamma_\lambda \gamma_\rho) = 4(g_{\alpha\beta}g_{\lambda\rho} - g_{\alpha\lambda}g_{\beta\rho} + g_{\alpha\rho}g_{\beta\lambda}), \quad (B.5.8)$$

which is the same as (B.3.7) and (B.3.9). Similarly,

$$\text{tr}(\text{odd } \# \text{ of } \gamma's) = 0. \quad (B.5.9)$$

Equations (B.5.7) and (B.5.8) imply

$$\text{tr}(\not{a}) = 4a \cdot b, \quad (B.5.10)$$

$$\text{tr}(\not{a}\not{b}\not{c}\not{d}) = 4[a \cdot b c \cdot d - a \cdot c b \cdot d + a \cdot d b \cdot c], \quad (B.5.11)$$

respectively, where the "slash" symbol is defined in  $N$  dimensions by

$$\not{a} = a \cdot \gamma = g_{\mu\nu} a_\mu \gamma_\nu = a_0 \gamma_0 - a_1 \gamma_1 - a_2 \gamma_2 - \cdots - a_{N-1} \gamma_{N-1}. \quad (B.5.12)$$

## B.6 Dirac Equation and Spinors

A free spin-1/2 particle of mass  $m$  and spin  $s$  is described by the spinor  $u(p, s)$  which satisfies the Dirac equation

$$(\not{p} - m)u(p, s) = 0, \quad (B.6.1)$$

while the adjoint spinor

$$\bar{u}(p, s) \equiv u^\dagger(p, s)\gamma_0, \quad (B.6.2)$$

satisfies

$$\bar{u}(p, s)(\not{p} - m) = 0. \quad (B.6.3)$$

The spin 4-vector  $s$  satisfies

$$s \cdot p = 0, \quad (B.6.4)$$

$$s^2 = -1, \quad (B.6.5)$$

and in the rest frame of the particle has the form

$$s_\mu = \begin{pmatrix} 0 \\ \vec{s} \end{pmatrix}, \quad (B.6.6)$$

where  $\vec{s}$  is the polarization vector and

$$\vec{s} \cdot \vec{s} = 1. \quad (B.6.7)$$

The antiparticle spinors satisfy

$$(\not{p} + m)v(p, s) = 0, \quad (B.6.8)$$

$$\bar{v}(p, s)(\not{p} + m) = 0, \quad (B.6.9)$$

where

$$\bar{v}(p, s) \equiv v^\dagger(p, s)\gamma_0. \quad (B.6.10)$$

The spinors and antispinors are normalized so that

$$\sum_{\text{spin}} \bar{u}(p, s)u(p, s) = 2m, \quad (B.6.11)$$

$$\sum_{\text{spin}} \bar{v}(p, s)v(p, s) = -2m, \quad (B.6.12)$$

and the projection operators  $\Lambda_\pm$  are given by

$$2m\Lambda_+ = \sum_{\text{spin}} u(p, s)\bar{u}(p, s) = \not{p} + m, \quad (B.6.13)$$

$$2m\Lambda_- = -\sum_{\text{spin}} v(p, s)\bar{v}(p, s) = -\not{p} + m. \quad (B.6.14)$$

In forming the absolute value squared of the scattering amplitude one encounters the Hermitian conjugate which can be expressed as

$$[\bar{u}(p', s')\Gamma u(p, s)]^\dagger = \bar{u}(p, s)\bar{\Gamma} u(p', s'), \quad (B.6.15)$$

where

$$\bar{\Gamma} = \gamma_0 \Gamma^\dagger \gamma_0. \quad (B.6.16)$$

Some examples are

$$\bar{\gamma}_\mu = \gamma_\mu, \quad (B.6.17)$$

$$\bar{\sigma}_{\mu\nu} = \sigma_{\mu\nu}, \quad (B.6.18)$$

$$\overline{(i\gamma_5)} = i\gamma_5, \quad (B.6.19)$$

$$\overline{\not{p}_1 \not{p}_2 \cdots \not{p}_n} = \not{p}_n \not{p}_{n-1} \cdots \not{p}_1, \quad (B.6.20)$$

where  $\sigma_{\mu\nu}$  is defined by (B.4.7).

A convenient basis for spin is the helicity basis in which  $u_\lambda(p)$  are eigenstates of the operator  $\frac{1}{2}\gamma_5 s$ , with eigenvectors  $\lambda = \pm\frac{1}{2}$  corresponding to spin aligned parallel or antiparallel to the direction of motion. In this case (B.6.11) and (B.6.12) imply

$$\bar{u}_\lambda(p)u_{\lambda'}(p) = 2m \delta_{\lambda\lambda'}, \quad (B.6.21)$$

$$\bar{v}_\lambda(p)v_{\lambda'}(p) = -2m \delta_{\lambda\lambda'}, \quad (B.6.22)$$

respectively. An explicit form for the spinor representation of a fermion with momentum  $\vec{p}$  along the positive  $\hat{z}$ -axis and with helicity  $\lambda$  is given by

$$u_\lambda(p) = \sqrt{E + m} \begin{pmatrix} \chi_\lambda \\ \frac{2\lambda|\vec{p}|}{E+m} \chi_\lambda \end{pmatrix} \quad (B.6.23)$$

$$\bar{u}_\lambda(p) = \sqrt{E + m} \begin{pmatrix} \chi_\lambda^\dagger & \frac{-2\lambda|\vec{p}|}{E+m} \chi_\lambda^\dagger \end{pmatrix} \quad (B.6.24)$$

where

$$\chi_{\frac{1}{2}} = \begin{pmatrix} 1 \\ 0 \end{pmatrix}, \quad \chi_{-\frac{1}{2}} = \begin{pmatrix} 0 \\ 1 \end{pmatrix}, \quad (B.6.25)$$

and  $E^2 = p^2 + m^2$ . The corresponding antiparticle is computed using

$$v_\lambda(p) = (-1)^{\lambda - \frac{1}{2}} \gamma_5 u_\lambda(p). \quad (B.6.26)$$

## References

1. In general, spin-space has dimensions  $2^{N/2}$  ( $N$  even) and  $2^{(N-4)/2}$  ( $N$  odd) so that  $\text{tr}(\mathbf{I}_N) = F(N) = 4 + f(N)$ , where  $f(N)$  vanishes as  $N \rightarrow 4$ . One can show that the extra terms introduced by  $f(N)$  do not affect the  $N \rightarrow 4$  limit and thus we define  $f(N) \equiv 0$ . See, W. J. Marciano, *Nucl. Phys.* **B84**, 132 (1975).

## Feynman Rules and Integrals



## C.1 Feynman Rules – General Discussion

### External Lines:

For particles in the initial or final state one writes the following factor:

- (a) Spin Zero Boson ..... 1

- (b) Spin One Boson .....  $\epsilon_\mu(\lambda)$

Here  $\epsilon_\mu(\lambda)$  is the polarization 4-vector for a boson with helicity  $\lambda$ . For the case of a massless spin one boson propagating along the  $\hat{z}$ -axis with 4-momentum  $k_\mu$  given by

$$k_\mu = \begin{pmatrix} k_0 \\ 0 \\ 0 \\ k_3 \end{pmatrix}, \quad (C.1.1)$$

with  $k_0 = |\mathbf{k}_3|$ , the polarization 4-vectors are given by

$$\epsilon_\mu(\lambda = \pm 1) = \frac{1}{\sqrt{2}} \begin{pmatrix} 0 \\ 1 \\ \pm i \\ 0 \end{pmatrix}, \quad (C.1.2)$$

for helicity  $\pm 1$ . The polarization 4-vectors satisfy

$$\mathbf{k} \cdot \boldsymbol{\epsilon} = 0, \quad (C.1.3)$$

and

$$\epsilon^2 = -1. \quad (C.1.4)$$

For a massive spin 1 boson with 4-momentum given by (C.1.1) but with  $k_0^2 = k_3^2 + M^2$  one also has the longitudinal state

$$\epsilon_\mu(\lambda = 0) = \frac{1}{M} \begin{pmatrix} k_3 \\ 0 \\ 0 \\ k_0 \end{pmatrix}, \quad (C.1.5)$$

where  $M$  is the boson mass.

- (c) Spin 1/2 fermion of momentum  $p$  and spin  $s$   
in initial state .....  $u(p, s)$  on the right  
in final state .....  $\bar{u}(p, s)$  on the left
- (d) Spin 1/2 antifermion of momentum  $p$  and spin  $s$   
in initial state .....  $\bar{v}(p, s)$  on the left  
in final state .....  $v(p, s)$  on the right

### Internal Lines (Propagators):

Each internal line describes a particle of momentum  $q$  and mass  $m$ . Some examples are as follows:

- (a) Spin Zero Boson

$$\frac{i}{q^2 - m^2 + i\epsilon} \quad (C.1.6)$$

- (b) Photon (Feynman Gauge)

$$\frac{-ig_{\mu\nu}}{q^2 + i\epsilon} \quad (C.1.7)$$

- (c) Spin One Boson

$$\frac{-i(g_{\mu\nu} - q_\mu q_\nu/m^2)}{q^2 - m^2 + i\epsilon} \quad (C.1.8)$$

- (d) Spin 1/2 fermion

$$\frac{i(q + m)}{q^2 - m^2 + i\epsilon} \quad (C.1.9)$$

For antifermions one uses the same propagator, treating the antifermion as a fermion of opposite 4-momentum (*i.e.*,  $-q$ ).

### Vertex Factors:

For each intersection of three (or more) lines at one point there is a vertex factor which depends on the structure of the interaction Lagrangian. Some examples are shown in Fig. C.1.

- (a) Three scalar boson vertex

$$-ig \quad (C.1.10)$$

- (b)  $ee\gamma$  vertex

$$-ie\gamma_\mu \quad (C.1.11)$$

Here  $e$  is the charge of the electron and the fine structure constant  $\alpha = e^2/(4\pi)$ .

- (c) Charged spin zero boson-photon vertex

$$-iQ(p_1 + p_2)_\mu \quad (C.1.12)$$

- (d) Four point coupling for charged spin zero boson-photon

$$2iQ^2 g_{\mu\nu} \quad (C.1.13)$$

### Loops and Combinatorics:

- (a) For each loop with undetermined momentum  $k$  .....  $\int d^4k/(2\pi)^4$

Here the integral runs over all values of the momentum.

- (b) For each closed fermion loop .....  $-1$

- (c) For each closed loop containing  $n$  identical bosons .....  $1/n!$

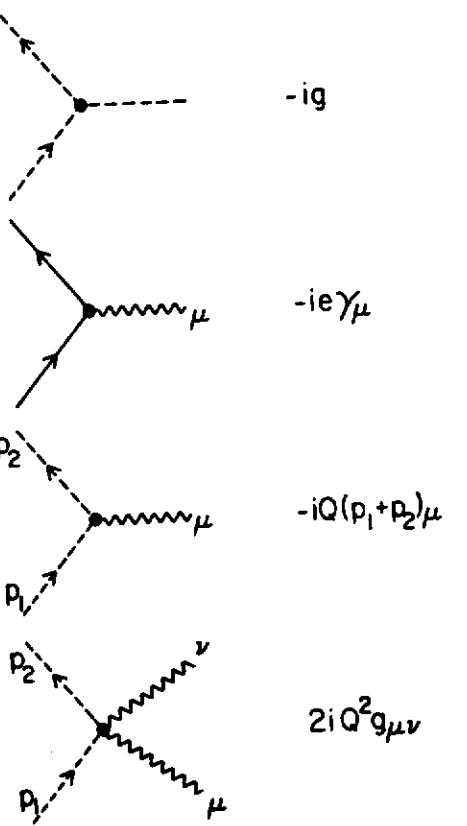


Figure C.1 Couplings for the triple-scalar-boson, electron-photon, charged spin zero boson-photon, and the four point charged spin zero boson-photon-photon vertices.

## C.2 Loop Integrations

Feynman Parameterizations:

$$\frac{1}{a_1 a_2 \dots a_n} = \Gamma(n) \int_0^1 dx_1 \int_0^1 dx_2 \dots \int_0^1 dx_n \frac{\delta(1 - \sum_{i=1}^n x_i)}{[\sum a_i x_i]^n}, \quad (C.2.1)$$

$$\frac{1}{abc} = 2 \int_0^1 dx \int_0^1 dy \int_0^1 dz \frac{\delta(1 - x - y - z)}{[ax + by + cz]^3}, \quad (C.2.2)$$

$$\frac{1}{a^R b^M} = \frac{\Gamma(R+M)}{\Gamma(R)\Gamma(M)} \int_0^1 dx \int_0^1 dy \frac{x^{R-1} y^{M-1} \delta(1-x-y)}{[ax+by]^{R+M}} \quad (C.2.3)$$

$$\frac{1}{a^R b^M} = \frac{\Gamma(R+M)}{\Gamma(R)\Gamma(M)} \int_0^1 dx \frac{x^{R-1} (1-x)^{M-1}}{[ax+b(1-x)]^{R+M}}, \quad (C.2.4)$$

Integral over  $d^4K$  ( $N = 4$  dimensions):

$$\int \frac{d^4K}{(2\pi)^4} \frac{(K^2)^R}{(K^2 - C)^M} = \frac{i(-1)^{R-M}}{16\pi^2} C^{R-M+2} \frac{\Gamma(R+2)\Gamma(M-R-2)}{\Gamma(M)}, \quad (C.2.5)$$

Integral over  $d^N K$  ( $N$  dimensions):

$$\int \frac{d^N K}{(2\pi)^N} \frac{(K^2)^R}{[K^2 - C]^M} = \frac{i(-1)^{R-M}}{(16\pi^2)^{N/4}} C^{R-M+N/2} \frac{\Gamma(R+\frac{1}{2}N)\Gamma(M-R-\frac{1}{2}N)}{\Gamma(\frac{1}{2}N)\Gamma(M)} \quad (C.2.6)$$

## C.3 Feynman Rules – QCD<sup>1–3</sup>

### External Lines

- (a) Gluons .....  $\epsilon_\mu(\lambda)$

Here  $\epsilon_\mu(\lambda)$  is the polarization 4-vector for a gluon with helicity  $\lambda$  as in (C.1.2). It satisfies the orthogonality condition

$$\epsilon_\mu(\lambda)\epsilon_\mu(\lambda') = -\delta_{\lambda\lambda}, \quad (C.3.1)$$

and

$$\epsilon \cdot k = 0 \quad (C.3.2)$$

where  $k_\mu$  is the 4-momentum of the gluon.

- (b) Quark of momentum  $p$  and spin  $s$   
in initial state .....  $u(p, s)$  on the right  
in final state .....  $\bar{u}(p, s)$  on the left  
(c) Antiquark of momentum  $p$  and spin  $s$   
in initial state .....  $\bar{v}(p, s)$  on the left  
in final state .....  $v(p, s)$  on the right

### Internal Lines (Propagators):

The QCD propagators shown in Fig. C.2 are the following:

quark		$i\delta_{ij}q/q^2$
gluon		$-i\delta_{ab}[g_{\mu\nu} + \eta \frac{q_\mu q_\nu}{q^2}]/q^2$
ghost		$-i\delta_{ab}/q^2$

Figure C.2 QCD propagators.

## (a) Quarks

$$\frac{i\delta_{ij}q}{q^2 + i\epsilon} \quad (C.3.3)$$

Here I have taken the quark mass to be zero. The indices  $i$  and  $j$  correspond to quark color and run from 1 to 3.

## (b) Gluons (covariant gauge)

$$\frac{-i\delta_{ab}[(g_{\mu\nu} - q_\mu q_\nu/q^2) + \beta q_\mu q_\nu/q^2]}{q^2 + i\epsilon}, \quad (C.3.4)$$

or

$$\frac{-i\delta_{ab}(g_{\mu\nu} + \eta q_\mu q_\nu/q^2)}{q^2 + i\epsilon}. \quad (C.3.5)$$

Here  $\eta \equiv \beta - 1$  is an arbitrary gauge parameter ( $\eta = 0$  is the Feynman gauge,  $\eta = -1$  is the Landau gauge). The indices  $a$  and  $b$  correspond to the gluon color and run from 1 to 8.

## (c) Ghost

$$\frac{-i\delta_{ab}}{q^2 + i\epsilon} \quad (C.3.6)$$

In a covariant gauge one must include internal ghost particles that couple to gluons as shown in Fig. C.3.

Fig. C.3.

## Vertex Factors:

The QCD vertex factors shown in Fig. C.3 are as follows:

## (a) Quark-quark-gluon

$$-i g_s \gamma_\mu T_{ij}^a \quad (C.3.7)$$

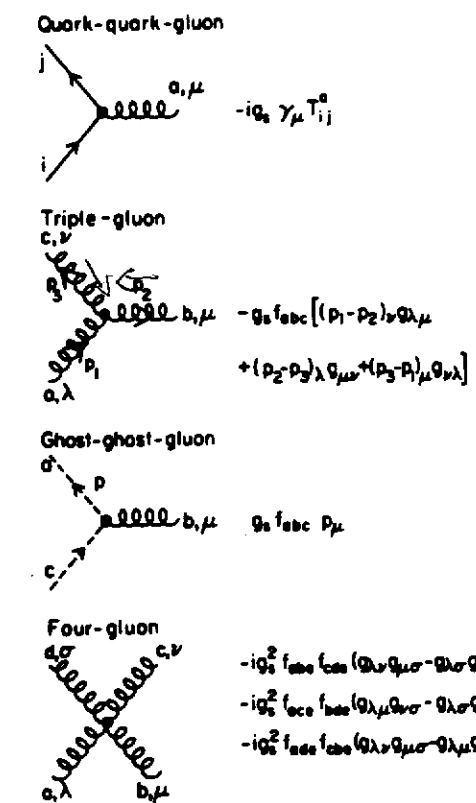


Figure C.3 QCD vertex factors.

The indices  $i$  and  $j$  correspond to the quark color and run from 1 to 3 and  $a$  corresponds to the gluon color and runs from 1 to 8. The eight  $3 \times 3$   $SU(3)$  matrices,  $T_a$ , handle the color and will be discussed in Appendix D. The QCD coupling constant is given by

$$\alpha = \frac{g_s^2}{4\pi} \quad (C.3.8)$$

## (b) Triple-gluon coupling

$$V_{λμν}(p_1, p_2, p_3) = -g_s f_{abc} F_{λμν}(p_1, p_2, p_3), \quad (C.3.9)$$

where

$$F_{\lambda\mu\nu}(p_1, p_2, p_3) = (p_1 - p_2)_\nu g_{\lambda\mu} + (p_2 - p_3)_\lambda g_{\mu\nu} + (p_3 - p_1)_\mu g_{\nu\lambda}. \quad (C.3.9)$$

The indices  $a, b, c$  correspond to the gluon color and run from 1 to 8 and  $f_{abc}$  are the  $SU(3)$  structure constants discussed in Appendix D. Energy-momentum conservation implies  $p_1 + p_2 + p_3 = 0$ .

(c) Ghost-ghost-gluon coupling

$$g_s f_{abc} p_\mu \quad (C.3.10)$$

The indices  $a, b, c$  correspond to color and run from 1 to 8 and  $f_{abc}$  are the  $SU(3)$  structure constants discussed in Appendix D.

(d) Four-gluon coupling

$$\begin{aligned} & -ig_s^2 f_{abc} f_{cde} (g_{\lambda\nu} g_{\mu\sigma} - g_{\lambda\sigma} g_{\mu\nu}) \\ & -ig_s^2 f_{ace} f_{bde} (g_{\lambda\nu} g_{\mu\sigma} - g_{\lambda\sigma} g_{\mu\nu}) \\ & -ig_s^2 f_{ade} f_{cbe} (g_{\lambda\nu} g_{\mu\sigma} - g_{\lambda\mu} g_{\sigma\nu}) \end{aligned} \quad (C.3.11)$$

The indices  $a, b, c, d$  correspond to color and run from 1 to 8 and  $f_{abc}$  are the  $SU(3)$  structure constants discussed in Appendix D.

**Loops and Combinatorics:**

Same as given in Appendix C.1 except that for ghost loops one must include a factor of  $-1$ .

## C.4 Feynman Rules – Weinberg-Salam Model

In the minimal or “standard” model<sup>4,5</sup> of the weak and electromagnetic interactions of leptons and quarks the leptons and the quarks are placed in left-handed “weak-isospin” doublets as follows:

$$\begin{aligned} L_e &= \begin{pmatrix} \nu_e \\ e^- \end{pmatrix}_L & L_\mu &= \begin{pmatrix} \nu_\mu \\ \mu^- \end{pmatrix}_L, \\ L_u &= \begin{pmatrix} u \\ d_\theta \end{pmatrix}_L & L_c &= \begin{pmatrix} c \\ s_\theta \end{pmatrix}_L, \end{aligned} \quad (C.4.1)$$

where

$$\begin{aligned} d_\theta &= d \cos(\theta_C) + s \sin(\theta_C), \\ s_\theta &= s \cos(\theta_C) - d \sin(\theta_C), \end{aligned} \quad (C.4.2)$$

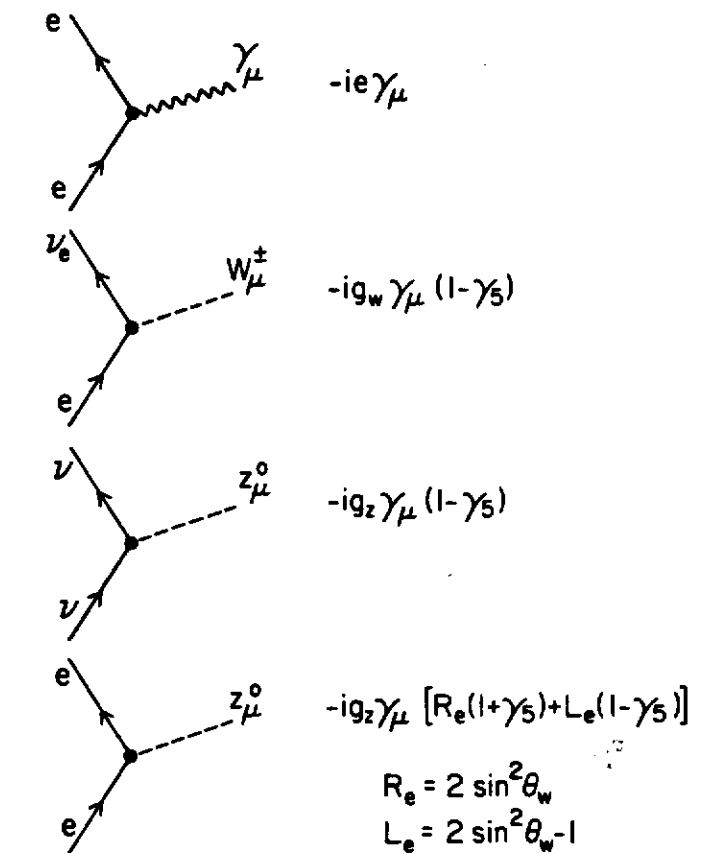


Figure C.4 Feynman rules for the coupling of leptons to photons and to  $W^\pm$  and  $Z^0$  Bosons in the Weinberg-Salam model.

where  $\theta_C$  is the Cabibbo angle, which has been determined as

$$\cos(\theta_C) = 0.9737 \pm 0.0025. \quad (C.4.3)$$

**Vertex Factors:**

The lepton-boson couplings shown in Fig. C.4 are as follows:

$$(a) ee\gamma \text{ vertex} \quad -ie\gamma_\mu \quad (C.4.4)$$

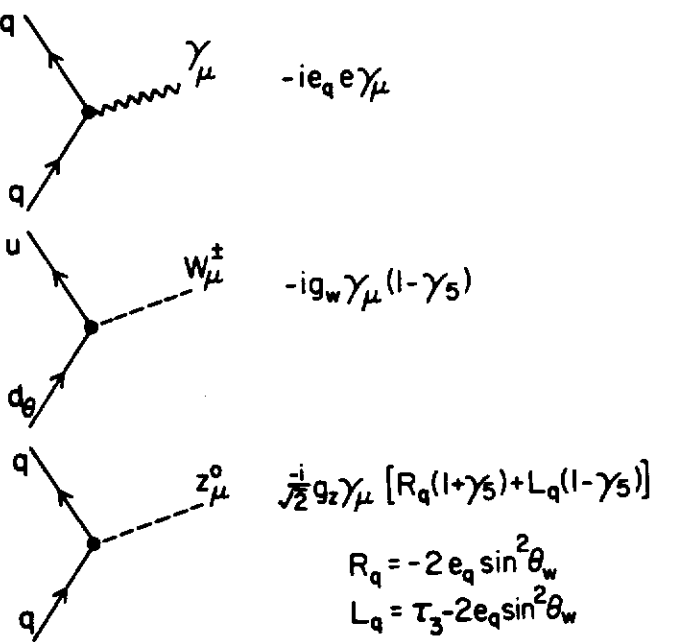


Figure C.5 Feynman rules for the coupling of quarks to photons and to  $W^\pm$  and  $Z^0$  Bosons in the Weinberg-Salam model.

(b)  $e\nu_e W$  vertex

$$-ig_w \gamma_\mu (1 - \gamma_5) \quad (C.4.5)$$

The dimensionless weak coupling,  $g_w$ , is given by

$$g_w^2 = \frac{1}{\sqrt{2}} G_F M_W^2 = \frac{\pi \alpha}{2x_w}, \quad (C.4.6)$$

where  $x_w$  is the square of the sine of the Weinberg angle

$$x_w = \sin^2(\theta_w), \quad (C.4.6)$$

and is constrained experimentally to be in the range<sup>5</sup>  $0.20 \leq x_w \leq 0.35$  and the Fermi constant is given by  $G_F = 1.15 \times 10^{-5} \text{ GeV}^{-2}$ .

(c)  $\nu\nu Z^0$  vertex

$$\frac{-i}{\sqrt{2}} g_z \gamma_\mu (1 - \gamma_5) \quad (C.4.7)$$

The dimensionless weak coupling,  $g_z$ , is given by

$$g_z^2 = \frac{1}{\sqrt{2}} G_F M_Z^2, \quad (C.4.8)$$

and

$$M_Z^2 = M_W^2 / (1 - x_w^2). \quad (C.4.9)$$

(d)  $eeZ^0$  vertex

$$\frac{-i}{\sqrt{2}} g_z \gamma_\mu [R_e (1 + \gamma_5) + L_e (1 - \gamma_5)], \quad (C.4.10)$$

with

$$R_e = 2 x_w, \\ L_e = 2 x_w - 1. \quad (C.4.11)$$

The quark-boson couplings shown in Fig. C.5 are as follows:

(e)  $qq\gamma$  vertex

$$-ie_q \gamma_\mu \quad (C.4.12)$$

(f)  $ud_\theta W$  or  $cs_\theta W$  vertex

$$-ig_w \gamma_\mu \quad (C.4.13)$$

where the dimensionless weak coupling  $g_w$  is given in (C.4.5).

(g)  $qqZ^0$  vertex

$$\frac{-i}{\sqrt{2}} g_z \gamma_\mu [R_q (1 + \gamma_5) + L_q (1 - \gamma_5)], \quad (C.4.14)$$

with

$$R_q = -2 e_q x_w, \\ L_q = \tau_3 - 2 e_q x_w, \quad (C.4.15)$$

where  $\tau_3$  is the third component of "weak-isospin" of the quark,  $q$ , and  $e_q$  is its electric charge (measured in units of the electron charge  $e$  and where  $x_w$  is the square of the sine of the Weinberg angle).

## References

1. D.J. Gross and F. Wilczek, *Phys. Rev.* **D8**, 3633 (1973). *ibid* **D9**, 980 (1974).
2. H.D. Politzer, *Physics Reports* **14C** (1974).
3. S. Weinberg, *Phys. Rev. Lett.* **31**, 494 (1973).
4. S. Weinberg, *Phys. Rev. Lett.* **19**, 1264 (1967).

5. C. Quigg, *Gauge Theories of the Strong, Weak, and Electromagnetic Interactions*, Frontiers in Physics, The Benjamin-Cummings Publishing Company, Inc., 1983.

APPENDIX D

**SU(3) of Color**



## D.1 Structure Constants and Color Matrices

The  $3 \times 3$   $SU(3)$  color matrices,  $\mathbf{T}_a$ , satisfy

$$[\mathbf{T}_a, \mathbf{T}_b] = i f_{abc} \mathbf{T}_c, \quad (D.1.1)$$

where  $f_{abc}$  are the antisymmetric  $SU(3)$  structure constants with non-zero values given by

<u>a</u>	<u>b</u>	<u>c</u>	<u><math>f_{abc}</math></u>
1	2	3	1
1	4	7	$\frac{1}{2}$
1	5	6	$-\frac{1}{2}$
2	4	6	$\frac{1}{2}$
2	5	7	$\frac{1}{2}$
3	4	5	$\frac{1}{2}$
3	6	7	$-\frac{1}{2}$
4	5	8	$\sqrt{3}/2$
6	7	8	$\sqrt{3}/2$

A convenient representation of the  $\mathbf{T}_a$  matrices is the one introduced by Gell-Mann<sup>1</sup> in which

$$\begin{aligned} \mathbf{T}_1 &= \frac{1}{2} \begin{pmatrix} 0 & 1 & 0 \\ 1 & 0 & 0 \\ 0 & 0 & 0 \end{pmatrix}, & \mathbf{T}_2 &= \frac{1}{2} \begin{pmatrix} 0 & -i & 0 \\ i & 0 & 0 \\ 0 & 0 & 0 \end{pmatrix}, \\ \mathbf{T}_3 &= \frac{1}{2} \begin{pmatrix} 1 & 0 & 0 \\ 0 & -1 & 0 \\ 0 & 0 & 0 \end{pmatrix}, & \mathbf{T}_4 &= \frac{1}{2} \begin{pmatrix} 0 & 0 & 1 \\ 0 & 0 & 0 \\ 1 & 0 & 0 \end{pmatrix}, \\ \mathbf{T}_5 &= \frac{1}{2} \begin{pmatrix} 0 & 0 & -i \\ 0 & 0 & 0 \\ i & 0 & 0 \end{pmatrix}, & \mathbf{T}_6 &= \frac{1}{2} \begin{pmatrix} 0 & 0 & 0 \\ 0 & 0 & 1 \\ 0 & 1 & 0 \end{pmatrix}, \\ \mathbf{T}_7 &= \frac{1}{2} \begin{pmatrix} 0 & 0 & 0 \\ 0 & 0 & -i \\ 0 & i & 0 \end{pmatrix}, & \mathbf{T}_8 &= \frac{1}{2\sqrt{3}} \begin{pmatrix} 1 & 0 & 0 \\ 0 & 1 & 0 \\ 0 & 0 & -2 \end{pmatrix}. \end{aligned} \quad (D.1.3)$$

The structure constants  $d_{abc}$  are defined according to

$$\{\mathbf{T}_a, \mathbf{T}_b\} = \frac{1}{3} \delta_{ab} + d_{abc} \mathbf{T}_c. \quad (D.1.4)$$

The  $\mathbf{T}_a$  matrices satisfy

$$\mathbf{T}_a \mathbf{T}_b = \frac{1}{2} [\frac{1}{3} \delta_{ab} + (d_{abc} + i f_{abc}) \mathbf{T}_c], \quad (D.1.5)$$

$$\mathbf{T}_{ij}^a \mathbf{T}_{kl}^a = \frac{1}{2} [\delta_{il} \delta_{jk} - \frac{1}{3} \delta_{ij} \delta_{kl}], \quad (D.1.6)$$

$$\text{tr}(\mathbf{T}_a) = 0, \quad (D.1.7)$$

$$\text{tr}(\mathbf{T}_a \mathbf{T}_b) = \frac{1}{2} \delta_{ab}, \quad (D.1.8)$$

$$\text{tr}(\mathbf{T}_a \mathbf{T}_b \mathbf{T}_c) = \frac{1}{4} (d_{abc} + i f_{abc}), \quad (D.1.9)$$

$$\text{tr}(\mathbf{T}_a \mathbf{T}_b \mathbf{T}_a \mathbf{T}_c) = -\frac{1}{12} \delta_{bc}. \quad (D.1.10)$$

The structure constants satisfy the following Jacobi identities:

$$f_{abe} f_{ecd} + f_{ebe} f_{acd} + f_{abe} f_{ace} = 0, \quad (D.1.11)$$

$$f_{abe} d_{ecd} + f_{cbe} d_{ced} + f_{abe} d_{ace} = 0. \quad (D.1.12)$$

In addition,

$$f_{abc} f_{cde} = \frac{2}{3} (\delta_{ac} \delta_{bd} - \delta_{ad} \delta_{bc}) + (d_{ace} d_{bde} - d_{bce} d_{ade}). \quad (D.1.13)$$

It is sometimes useful to define  $8 \times 8$  matrices  $\mathbf{F}_a$  and  $\mathbf{D}_a$  such that

$$(\mathbf{F}_a)_{bc} = -i f_{abc}, \quad (D.1.14)$$

$$(\mathbf{D}_a)_{bc} = d_{abc}, \quad (D.1.15)$$

in which case the Jacobi identities (D.1.11) and (D.1.12) become

$$[\mathbf{F}_a, \mathbf{F}_b] = i f_{abc} \mathbf{F}_c, \quad (D.1.16)$$

$$[\mathbf{F}_a, \mathbf{D}_b] = i f_{abc} \mathbf{D}_c. \quad (D.1.17)$$

In addition  $f_{abb} = 0$  and  $d_{abb} = 0$  implies

$$\text{tr}(\mathbf{F}_a) = 0, \quad (D.1.18)$$

$$\text{tr}(\mathbf{D}_a) = 0. \quad (D.1.19)$$

The following are some useful relationships

$$f_{acd} f_{bcd} = 3 \delta_{ab}, \quad (D.1.20)$$

$$\mathbf{F}_a \mathbf{F}_a = 3, \quad (D.1.21)$$

$$\text{tr}(\mathbf{F}_a \mathbf{F}_b) = 3 \delta_{ab}, \quad (D.1.22)$$

$$f_{acd} d_{bcd} = 0, \quad (D.1.23)$$

$$\mathbf{F}_a \mathbf{D}_a = 0, \quad (D.1.24)$$

$$\text{tr}(\mathbf{F}_a \mathbf{D}_b) = 0, \quad (D.1.25)$$

$$d_{acb} d_{bed} = \frac{5}{3} \delta_{ab}, \quad (D.1.26)$$

$$\mathbf{D}_a \mathbf{D}_a = \frac{5}{3}, \quad (D.1.27)$$

$$\text{tr}(\mathbf{D}_a \mathbf{D}_b) = \frac{5}{3} \delta_{ab}, \quad (D.1.28)$$

$$\text{tr}(\mathbf{F}_a \mathbf{F}_b \mathbf{F}_c) = i \frac{3}{2} f_{abc}, \quad (D.1.29)$$

$$\text{tr}(\mathbf{D}_a \mathbf{F}_b \mathbf{F}_c) = \frac{3}{2} d_{abc}, \quad (D.1.30)$$

$$\text{tr}(\mathbf{D}_a \mathbf{D}_b \mathbf{F}_c) = i \frac{5}{6} f_{abc}, \quad (D.1.31)$$

$$\text{tr}(\mathbf{D}_a \mathbf{D}_b \mathbf{D}_c) = -\frac{1}{2} d_{abc}, \quad (D.1.32)$$

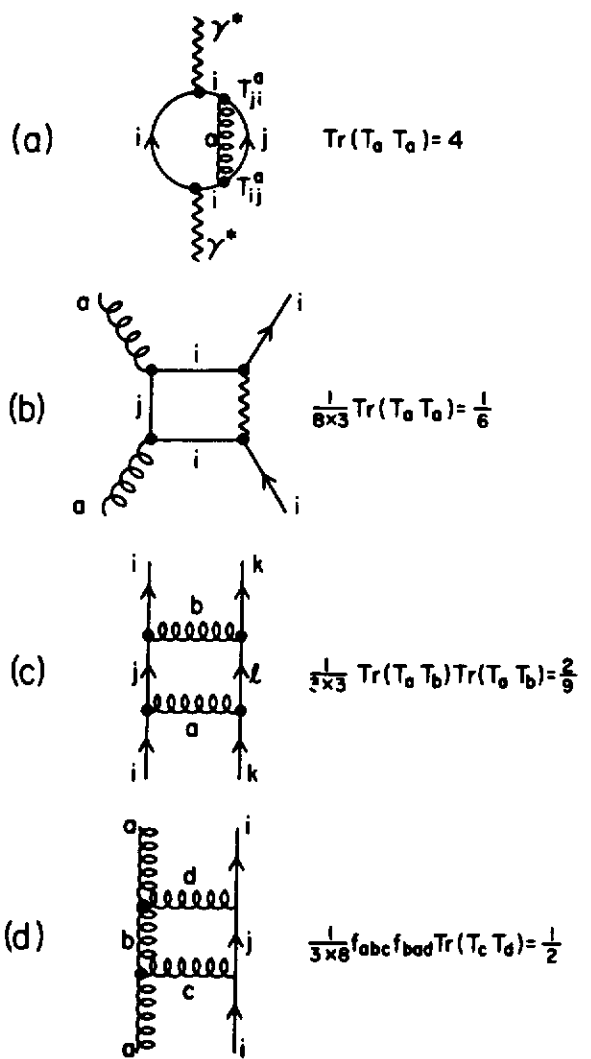


Figure D.1 Color factors for the square of the amplitudes (a)  $\gamma^* \rightarrow q + \bar{q}$ , (b)  $g + q \rightarrow q + \gamma$ , (c)  $q + q \rightarrow q + q$ , and (d)  $g + q \rightarrow g + q$ .

$$\text{tr}(F_a F_b F_c F_d) = \frac{9}{2} \delta_{bc}. \quad (D.1.33)$$

## D.2 Examples of Color Factors

As is the case with particle spins, we choose to sum over the final color states and average over initial color states. The color factor for the square of the  $\gamma^* \rightarrow q\bar{q}g$  amplitude shown in Fig. D.1a is given by

$$T_{ij}^a T_{ji}^a = \text{tr}(T_a T_a) = \frac{1}{2} \delta_{aa} = 4, \quad (D.2.1)$$

since

$$\delta_{aa} = 8. \quad (D.2.2)$$

Similarly, the color factor for the square of the  $gq \rightarrow \gamma^* q$  amplitude shown in Fig. D.1b is given by

$$\frac{1}{8} \frac{1}{3} T_{ij}^a T_{ji}^a = \frac{1}{24} \text{tr}(T_a T_a) = \frac{1}{6}, \quad (D.2.3)$$

where the factor of  $1/24$  arises from the initial state color averaging.

The color factor for the square of the  $qq \rightarrow qq$  amplitude shown in Fig. D.1c is given by

$$\begin{aligned} \frac{1}{3} \frac{1}{3} T_{ij}^a T_{ji}^b T_{kl}^a T_{lk}^b &= \frac{1}{9} \text{tr}(T_a T_b) \text{tr}(T_a T_b) \\ &= \frac{1}{9} \left(\frac{1}{2} \delta_{ab}\right) \left(\frac{1}{2} \delta_{ab}\right) \\ &= \frac{1}{9} \frac{1}{4} \delta_{aa} = \frac{2}{9}. \end{aligned} \quad (D.2.4)$$

The color factor for the square of the  $gq \rightarrow gq$  amplitude shown in Fig. D.1d is given by

$$\begin{aligned} \frac{1}{8} \frac{1}{3} f_{abc} f_{bad} T_{ij}^c T_{ji}^d &= \frac{1}{24} f_{abc} f_{bad} \text{tr}(T_c T_d) \\ &= \frac{1}{24} \frac{1}{2} \delta_{cd} f_{abc} f_{bad} \\ &= \frac{1}{48} f_{abc} f_{bac} = \frac{1}{48} \text{tr}(F_a F_a) \\ &= \frac{1}{48} 3 \delta_{aa} = \frac{1}{2}, \end{aligned} \quad (D.2.5)$$

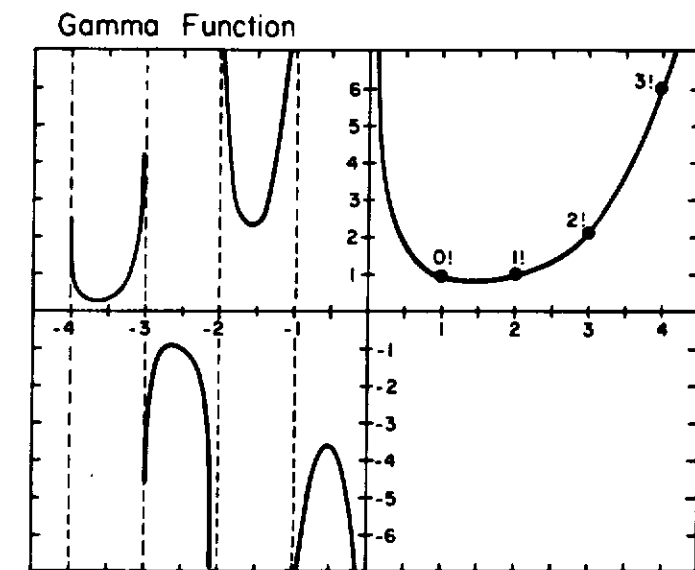
where (D.1.8) and (D.1.22) have been used.

## References

1. M. Gell-Mann, *Phys. Rev.* 125, 1067 (1962).

## APPENDIX E

## Special Functions

Figure E.1 Sketch of the behavior of  $\Gamma(x)$  versus  $x$ .**E.1 Gamma Function**

The gamma function  $\Gamma(x)$ , plotted in Fig. E.1 is defined by

$$\Gamma(x) = \int_0^1 e^{-y} y^{x-1} dy, \quad (x > 0) \quad (E.1.1)$$

and has the properties

$$\Gamma(n+1) = n! \quad (n = \text{integer}) \quad (E.1.2)$$

$$\Gamma(x+1) = x\Gamma(x) \quad (x > 0) \quad (E.1.3)$$

$$\Gamma(x)\Gamma(1-x) = \frac{\pi}{\sin(\pi x)} \quad (E.1.4)$$

$$\Gamma(2x) = \frac{2^{2x-1}}{\sqrt{\pi}} \Gamma(x)\Gamma\left(x + \frac{1}{2}\right) \quad (E.1.5)$$

$$\Gamma(1) = 1 \quad (E.1.6)$$

$$\Gamma(1/2) = \sqrt{\pi} \quad (E.1.7)$$

$$\lim_{x \rightarrow \infty} \Gamma(x+y+1) = \Gamma(x+1)x^y \quad (E.1.8)$$

$$\lim_{x \rightarrow \infty} \Gamma(x+1) = \sqrt{2\pi} x^{x+\frac{1}{2}} e^{-x} \quad (E.1.9)$$

$$\lim_{x \rightarrow \infty} \left( \frac{\Gamma(x+y)}{\Gamma(x)} \right) = x^y \quad (E.1.10)$$

$$\lim_{x \rightarrow \infty} \left( \frac{\Gamma(x+y)}{\Gamma(x+b)} \right) = x^{a-b} \quad (E.1.11)$$

In addition,

$$B(R, M) = \int_0^1 dx x^{R-1} (1-x)^{M-1} = \frac{\Gamma(R)\Gamma(M)}{\Gamma(R+M)}, \quad (E.1.12)$$

is the beta function and

$$\begin{aligned} & \int_0^1 dx x^{C-1} (1-x)^{M-1} \int_0^1 dy y^{B-1} (1-y)^{C-B-1} (1-xy)^{-A} \\ &= \frac{\Gamma(C)\Gamma(M)\Gamma(C-B)\Gamma(C+M-A-B)}{\Gamma(C+M-A)\Gamma(C+M-B)}, \end{aligned} \quad (E.1.13)$$

where the latter is valid provided  $\operatorname{Re}(C) > 0$ ,  $\operatorname{Re}(B) > 0$ , and  $\operatorname{Re}(C+M-A-B) > 0$ .

The first and second derivatives of the gamma function evaluated at  $x = 1$  are given by

$$\Gamma'(1) = -\gamma_E, \quad (E.1.14)$$

$$\Gamma''(1) = \gamma_E^2 + \frac{1}{6}\pi^2, \quad (E.1.15)$$

respectively, where  $\gamma_E$  is Eulers constant which satisfies

$$\gamma_E = \lim_{n \rightarrow \infty} \left[ -\log(n) + 1 + \frac{1}{2} + \frac{1}{3} + \cdots + \frac{1}{n} \right] = 0.5772157, \quad (E.1.16)$$

and

$$\gamma_E = - \int_0^\infty e^{-x} \log(x) dx. \quad (E.1.17)$$

From (E.1.14) and (E.1.15) we have the following Taylor series expansion of  $\Gamma(1+\epsilon)$ ,

$$\Gamma(1+\epsilon) = 1 - \gamma_E \epsilon + \frac{1}{2} \left( \gamma_E^2 + \frac{\pi^2}{6} \right) \epsilon^2 + \cdots \quad (E.1.18)$$

The Taylor expansion of the logarithm of the gamma function is

$$\log[\Gamma(1+\epsilon)] = -\gamma_E \epsilon + \frac{1}{2} \rho(2) \epsilon^2 - \frac{1}{3} \rho(3) \epsilon^3 + \cdots, \quad (E.1.19)$$

where

$$\rho(p) = 1 + \frac{1}{2^p} + \frac{1}{3^p} + \cdots \quad (E.1.20)$$

is the zeta function of order  $p$  with

$$\rho(2) = \frac{1}{6}\pi^2. \quad (E.1.21)$$

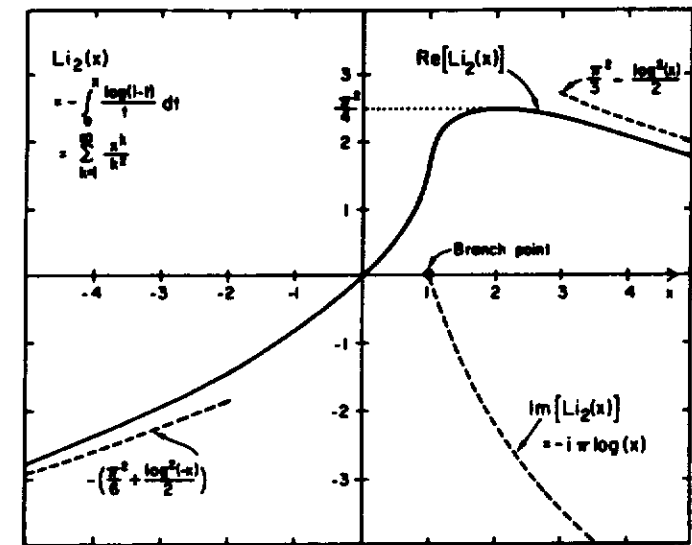


Figure E.2 Sketch of the behavior of  $\operatorname{Li}_2(x)$  versus  $x$ .

## E.2 Dilogarithm

A function that appears in many QCD perturbative calculations is the dilogarithm,  $\operatorname{Li}_2(x)$ . It is defined by

$$\operatorname{Li}_2(x) = \sum_{n=1}^{\infty} \frac{x^n}{n^2}, \quad (|x| < 1) \quad (E.2.1)$$

or

$$\operatorname{Li}_2(x) = - \int_0^x \frac{\log(1-t)}{t} dt, \quad (E.2.2)$$

and is plotted in Fig. E.2. Equivalent definitions are given by

$$\operatorname{Li}_2(x) = - \int_0^1 \frac{\log(1-xt)}{t} dt, \quad (E.2.3)$$

$$\operatorname{Li}_2(x) = - \int_{1-x}^1 \frac{\log(t)}{1-t} dt \quad (E.2.4)$$

$$\operatorname{Li}_2(x) = \int_0^1 \frac{\log(t)}{t - \frac{1}{x}} dt. \quad (E.2.5)$$

The dilogarithm has the following properties

$$\text{Li}_2(0) = 0 \quad (E.2.6)$$

$$\text{Li}_2(1) = \rho(2) = \frac{\pi^2}{6} \quad (E.2.7)$$

$$\text{Li}_2(-1) = -\frac{\pi^2}{12} \quad (E.2.8)$$

$$\text{Li}_2\left(\frac{1}{2}\right) = \frac{\pi^2}{12} - \frac{1}{2} \log^2(2) \quad (E.2.9)$$

$$\text{Li}_2(-x) + \text{Li}_2\left(-\frac{1}{x}\right) = -\frac{\pi^2}{6} - \frac{1}{2} \log^2(x) \quad (x > 0) \quad (E.2.10)$$

$$\text{Li}_2(x) + \text{Li}_2\left(\frac{1}{x}\right) = \frac{\pi^2}{3} - \frac{1}{2} \log^2(x) - i\pi \log(x) \quad (x > 1) \quad (E.2.11)$$

$$\text{Li}_2(x) + \text{Li}_2(1-x) = \frac{\pi^2}{6} - \log(x) \log(1-x). \quad (E.2.12)$$

### E.3 “+ Functions”

Strictly speaking “+ functions” are distributions that are well behaved only when convoluted with a smooth function that vanishes sufficiently rapidly as  $x \rightarrow 1$ . They have the property that

$$\int_0^1 (F(x))_+ dx = 0 \quad (E.3.1)$$

and are defined by the following limiting procedure

$$(F(x))_+ \equiv \lim_{\beta \rightarrow 0} \left\{ F(x) \theta(1-x-\beta) - \delta(1-x-\beta) \int_0^{1-\beta} F(y) dy \right\}. \quad (E.3.2)$$

where

$$\theta(y) = 0 \quad \text{for } y \leq 0 \quad (E.3.3)$$

$$\theta(y) = 1 \quad \text{for } y > 0. \quad (E.3.4)$$

Two important “+ functions” are

$$\frac{1}{(1-x)_+} \equiv \lim_{\beta \rightarrow 0} \left\{ \frac{1}{1-x} \theta(1-x-\beta) + \log(\beta) \delta(1-x-\beta) \right\} \quad (E.3.5)$$

and

$$\left( \frac{\log(1-x)}{1-x} \right)_+ \equiv \lim_{\beta \rightarrow 0} \left\{ \frac{\log(1-x)}{1-x} \theta(1-x-\beta) + \frac{1}{2} \log^2(\beta) \delta(1-x-\beta) \right\} \quad (E.3.6)$$

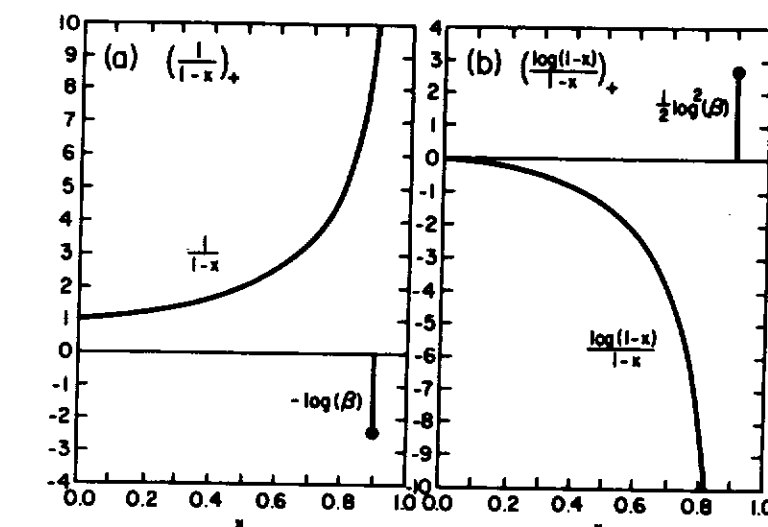


Figure E.3 Sketch of the behavior of “+ functions”  $1/(1-x)_+$  and  $(\log(1-x)/(1-x))_+$  versus  $x$ .

which are illustrated in Fig. E.3. When convoluted with a well behaved function  $G(y)$  one arrives at

$$\int_z^1 \frac{dy}{y} \frac{G(z/y)}{(1-y)_+} = G(z) \log(1-z) + \int_z^1 \frac{dy}{y} \frac{[G(z/y) - yG(z)]}{(1-y)} \quad (E.3.7)$$

and

$$\begin{aligned} \int_z^1 \frac{dy}{y} G(z/y) \left( \frac{\log(1-y)}{1-y} \right)_+ &= \frac{1}{2} G(z) \log^2(1-z) \\ &+ \int_z^1 \frac{dy}{y} \frac{[G(z/y) - yG(z)]}{(1-y)} \log(1-y). \end{aligned} \quad (E.3.8)$$

### E.4 Gegenbauer Polynomials

The Gegenbauer polynomials,  $C_n^{(\frac{1}{2})}(z)$ , are orthogonal on the interval  $-1$  to  $1$

1 with respect to the weight  $(1 - z^2)$ . In particular

$$\int_{-1}^1 dz (1 - z^2) C_n^{(\frac{1}{2})}(z) C_m^{(\frac{1}{2})}(z) = \begin{cases} 0 & n \neq m \\ \frac{(n+2)(n+1)}{2(2n+3)} & n = m. \end{cases} \quad (E.4.1)$$

This can be expressed on the interval 0 to 1 by the change of variable  $z = 2x - 1$  and (E.4.1) becomes

$$\int_0^1 dx x(1-x) C_n^{(\frac{1}{2})}(2x-1) C_m^{(\frac{1}{2})}(2x-1) = \begin{cases} 0 & n \neq m \\ \frac{(n+2)(n+1)}{4(2n+3)} & n = m. \end{cases} \quad (E.4.2)$$

The Gegenbauer polynomials can be deduced from the following recursive relation:

$$(n+1)C_{n+1}^{(\frac{1}{2})}(z) = (2n+3)zC_n^{(\frac{1}{2})}(z) - (n-2)C_{n-1}^{(\frac{1}{2})}(z), \quad (E.4.3)$$

where

$$C_0^{(\frac{1}{2})}(z) = 1, \quad (E.4.4)$$

$$C_1^{(\frac{1}{2})}(z) = 3z. \quad (E.4.5)$$

It is useful to note that  $1/(1-x)$  can be expanded in terms of Gegenbauer polynomials as follows:

$$\frac{1}{1-x} = \sum_{n=0}^{\infty} \frac{2(2n+3)}{(n+1)(n+2)} C_n^{(\frac{1}{2})}(2x-1). \quad (E.4.6)$$

- Additive quantum number, 63
- Adjoint spinor, 334
- Altarelli-Parisi, 78
- Analytic continuation, 181
- Analytically continue, 40-41, 49
- Angular distribution, 179
- Anomalous dimensions, 143, 148, 249, 320
- Antiparticle spinors, 334
- Antiparticle, 336
- Antisymmetric structure constants, 269
- Asymptotic freedom, 9, 57
- Asymptotic momentum fractions, 146
- Average quark flavor, 62
- Away-side hadrons, 270, 289
- Axial gauge, 75, 318
- Back-to-back, 204
- Bare coupling, 7, 240
- Baryon form factors, 312
- Beta function, 244, 247, 356
- Born term, 120, 134
- Bremsstrahlung, 195, 265, 289, 293, 310
- Cabibbo angle, 206, 345
- Calorimeter, 289
- Chain decay ansatz, 59
- Dalitz plot, 307
- Decay amplitudes, 307
- Deep inelastic scattering, 108
- Charge distribution, 313
- Closed loop, 229
- Clusters, 295
- Color factor, 3, 122, 124, 173, 175, 177, 206, 226, 229, 234, 266, 269, 280, 317, 353
- Color field, 59
- Color matrices, 5, 277, 350
- Color singlet, 4, 127
- Color symmetry, 2
- Combinatorial factor, 229
- Commute, 84
- Conservation of probability, 98
- Constant terms, 81, 240, 243
- Constituents, 261
- Contravariant, 331
- Convergence factor, 39
- Convolution method, 148
- Convolution notation, 70, 77, 138, 150, 155-156, 187
- Convolution symbol, 319
- Coulomb gauge, 8
- Counter terms, 226
- Coupled differential equations, 80
- Coupled equations, 140
- Covariant, 331
- Current conservation, 114

Deep inelastic scattering, 126, 176, 187, 190, 209, 251  
 Delta function contribution, 191  
 Diagonalizing, 144  
 Differential cross section, 326  
 Dilogarithm, 31, 357  
 Dimensional regularization mass, 43, 67, 71, 242  
 Dimensional regularization, 37, 42, 66  
 Dimensional regularization, 132  
 Dimensional regularization, 138, 184, 186, 226, 238  
 Dimensionless coupling, 43, 45  
 Dimensionless variable, 174  
 Dimensionless weak coupling, 206, 346  
 Dirac algebra, 332  
 Dirac equation, 235, 276  
 Dirac matrices, 332 -333  
 Dirac spinors, 326  
 Double logarithmic divergences, 97  
 Double logarithms, 204  
 Double photons, 266  
 Drell-Yan Model, 171, 176  
 DY distributions, 251  
 DY structure functions, 191  
 Effective coupling, 6-8, 226, 240, 244  
 Eigenvalues, 144  
 Eisenstates, 335  
 Eigenvectors, 335  
 Electromagnetic current, 316  
 Eulers constant, 46, 84, 356  
 Event shapes, 292  
 Event topology, 295  
 Evolution equations, 151  
 Experimental charge, 8  
 Exponential series, 101, 181  
 External lines, 240  
 Factorization of the mass singularities, 71  
 Fermi constant, 154, 206, 346  
 Fermion loop, 315  
 Feynman diagrams, 248  
 Feynman gauge, 23, 33, 39, 75, 229, 232, 279, 342  
 Feynman parameterization, 33, 226, 234

FF parameterization, 59  
 Field amplitude, 240  
 Final state, 57, 76  
 Fine structure constant, 242  
 Flavor dependence, 61  
 Flux factor, 115  
 Fourier transform, 60, 313  
 Fragmentation function, 58, 61, 63, 69-70, 78, 80-82, 84, 86, 138, 140-141, 148-149, 186, 248, 251, 274, 282, 289  
 Fragmentation, 16  
 Fragmentation, 58  
 Gamma function, 43, 355  
 Gauge dependent, 75  
 Gauge invariance, 23  
 Gauge invariance, 276  
 Gauge invariance, 276  
 Gauge invariance, 317  
 Gauge parameter, 33  
 Gegenbauer moments, 320  
 Gegenbauer polynomials, 320, 359  
 Geometric series, 242, 245  
 Ghost contribution, 230  
 Ghost loop, 230, 281  
 Ghost particles, 24  
 Ghost particles, 342  
 Ghost-quark scattering, 280  
 Gluon distributions, 140, 142, 149-150, 152  
 Gluon fragmentation function, 69, 87  
 Gluon jet, 96  
 Gluon jet, 97  
 Gluon loop, 229  
 Gluon polarization states, 279  
 Gluon propagator, 8, 226  
 Gluon-gluon fusion, 269  
 Gluons, 2  
 Hadronic tensor, 114  
 Hadronic vertex, 154  
 Hadronization, 292  
 Helicity basis, 335  
 Hermitian conjugate, 335  
 Hierarchy, 59  
 Higher twist, 12, 121  
 Higher-order effective coupling, 244  
 Hole, 292  
 Hot jet core, 298  
 Hypercharge, 63

Inclusive single hadron cross section, 69  
 Independent emission, 74, 92  
 Infrared divergence, 29, 97, 235  
 Infrared singularities, 57, 124  
 Initial state color, 173  
 Initial state quark spins, 122  
 Interference term, 75  
 Intrinsic parity, 315  
 Intrinsic transverse momentum, 283, 289  
 Invariant amplitude, 326  
 Invariant differential, 265  
 Invariants, 327  
 Isoscalar target, 110, 157  
 Isospin symmetry, 63, 109, 315  
 Jacobi identities, 351  
 Jacobian, 264, 272  
 Jet cross section, 283  
 Jets, 57, 270  
 Jets, 295  
 Jets, 310  
 Joint probabilities, 206  
 Joint probability function, 174  
 K factor, 190, 195, 210  
 Kernel, 319  
 Kibble function, 328  
 KLN theorem, 16  
 Laboratory frame, 114  
 Ladder structure, 76, 318  
 Landau gauge, 23, 33, 48, 342  
 Large x behavior, 150  
 Leading double log approximations, 100  
 Leading double logarithm summation, 101  
 Leading double logarithm, 99, 181  
 Leading log corrections, 197  
 Leading log sum, 318  
 Leading log, 73, 76  
 Leading order coupling, 12, 251  
 Leading pole approximation, 73, 76, 310  
 Leading pole formula, 87, 93  
 Lepton-boson couplings, 345  
 Leptonic tensor, 113  
 Light cone variables, 73  
 Light-light scattering, 267  
 Little f functions, 67-70, 78-80, 128-129, 136, 138-139, 150-151, 155, 186-187, 195, 251  
 Longitudinal cross section, 116  
 Longitudinal momentum conservation, 264  
 Longitudinal photons, 128, 131  
 Longitudinal state, 338  
 Longitudinal structure function, 118  
 Longitudinal structure function, 129, 132, 136, 152, 157-158  
 Mass scale, 71  
 Mass singularities, 30, 71, 79, 248, 313, 317  
 Massive gluon scheme, 37, 68, 70, 125, 138, 155, 186  
 Massive spin 1 boson, 338  
 Mean square transverse momentum, 212  
 Metric, 331  
 Minimal subtraction, 243  
 Minimum bias background, 292  
 Modified Bessel functions, 96  
 Modified minimal subtraction scheme, 12, 243  
 Moments, 61, 143-144, 248  
 Momentum fractions, 144  
 Monte Carlo, 87, 93  
 Monte-Carlo scheme, 90  
 Multiplicity flow, 299  
 N dimensional coupling, 134, 226  
 Nested integrals, 77, 89, 236  
 Neutrino nucleon scattering, 154  
 Neutrino nucleon scattering, 156  
 Non-perturbative phenomena, 72  
 Non-relativistic quark model, 108, 147  
 Non-singlet distribution, 138  
 Non-singlet fragmentation function, 76, 81  
 Non-singlet fragmentation functions, 70

- Non-singlet, 78, 249  
 Noncollinear gluon Bremsstrahlung, 289  
 Normalization condition, 70  
  
 Off-shell, 130  
  
 Parallel divergence, 29  
 Parity-violating, 154  
 Parton distributions, 251  
 Parton shower, 92  
 Parton shower, 290, 310  
 Parton-parton 2-to-2 differential cross sections, 274  
 Pauli matrices, 333  
 Perturbative parameter  $\Lambda$ , 11-12, 243  
 Photon spectrum, 308  
 Physical gauge, 279  
 Pion decay constant, 316  
 Pion form factor, 312  
 Pion wave function, 313  
 Pion-proton collisions, 266  
 Plateau, 298  
 Plus (+) functions, 65-66, 68, 73, 83, 128, 135, 182, 185, 191, 319, 358  
 Point (or Mott) cross section, 312  
 Polarization 4-vector, 115  
 Polarization 4-vectors, 338  
 Polarization states, 22, 75, 115, 122, 124, 230  
 Polarization vector, 334  
 Pole structure, 239  
 Primordial transverse momentum, 153  
 Primordial transverse momentum, 195, 198, 205  
 Projection operators, 335  
 Projection, 116, 128, 279  
 Proton substructure, 108  
 Proton wave function, 195  
  
 QCD parton-shower Monte Carlo Model, 92  
 QCD, 2  
 QED, 2  
 Quark confinement, 10  
 Quark distributions, 108, 121, 137, 142, 149-150, 248, 317

- Quark jet, 96 -97  
 Quark loop, 226, 267  
 Quark transverse momentum spectrum, 100  
 Quark-boson couplings, 347  
 Quarkonium, 307

Radiation damping occurs, 205  
 Rank, 59  
 Rapidity, 174, 196, 265  
 Reactions, 17  
 $e^+e^- \rightarrow$  hadrons, 17, 57, 68  
 $\gamma q \rightarrow q$ , 120, 132  
 $\gamma + q \rightarrow q + g$ , 121-122, 124, 128-129, 132-133, 155  
 $\gamma + g \rightarrow q + \bar{q}$ , 123, 130-132, 136, 155  
 $\gamma + N \rightarrow X$ , 125  
 $\sigma_{tot}(DIS)$ , 127 -128  
 $R(DIS)$ , 152  
 $W + q \rightarrow q + g$ , 155  
 $W + g \rightarrow q + \bar{q}$ , 155  
 $q\bar{q} \rightarrow \mu^+\mu^-$ , 171, 173  
 $pp \rightarrow \mu^+\mu^- + X$ , 174, 178  
 $e^+e^- \rightarrow \mu^+\mu^-$ , 18-19, 173  
 $q + \bar{q} \rightarrow \gamma + g$ , 175-177, 182, 195, 208, 261, 266  
 $q + g \rightarrow \gamma + q$ , 176, 182, 186, 195, 208, 267  
 $\sigma_{tot}(DY)$ , 180, 193  
 $q + q \rightarrow q + q$ , 195, 274  
 $q + \bar{q} \rightarrow W$ , 205  
 $q + \bar{q} \rightarrow W + g$ , 208  
 $q + g \rightarrow W + q$ , 208  
 $\sigma_{tot}(W)$ , 210  
 $\Upsilon \rightarrow gg\gamma$ , 307  
 $e^+e^- \rightarrow q\bar{q}$ , 19  
 $q + \bar{q} \rightarrow \gamma + \gamma$ , 261, 266  
 $A + B \rightarrow c + d + X$ , 261  
 $A + B \rightarrow c + X$ , 264  
 $g + g \rightarrow \gamma + \gamma$ , 267  
 $\gamma + \gamma \rightarrow \gamma + \gamma$ , 267  
 $g + g \rightarrow \gamma + g$ , 269  
 $A + B \rightarrow h + X$ , 270  
 $g + q \rightarrow g + q$ , 276  
 $\gamma + q \rightarrow \gamma + q$ , 276  
 $R(e^+e^-)$ , 20, 58, 248  
 $\gamma + \mu^+\mu^-$ , 21

$\gamma \rightarrow q\bar{q}$ , 22, 43  
 $\gamma \rightarrow q\bar{q}g$ , 24, 28, 45, 64, 68, 73, 98  
 $\sigma_{tot}(e^+e^-)$ , 42, 58, 65, 70, 97, 100, 127  
 $e + p \rightarrow e + X$ , 108  
 Real gluon corrections, 41  
 Real photons, 261  
 Recursive principle, 59  
 Reference distributions, 151  
 Reference distributions, 155, 194  
 Reference momentum, 84  
 Reference point, 78  
 Reference structure functions, 194  
 Regularization scheme dependence, 67, 136, 251  
 Regularization scheme, 81, 123, 128-129, 176 -177  
 Renormalization factor, 232, 238, 249  
 $Z_1$ , 238  
 $Z_2$ , 232  
 $Z_3$ , 232  
 Renormalization group equation, 72, 81, 247  
 Renormalization group improved, 209, 266  
 Renormalization group improved, 274, 317  
 Renormalization point, 8, 71, 242, 247  
 Renormalization, 7-8, 226  
 Resolvable radiation, 89  
 Running coupling constant, 6, 249, 319

S-matrix, 326  
 Scale breaking, 198  
 Scaling variable, 110, 118, 125  
 Scheme dependent, 81  
 Self-energy corrections, 36, 47, 232, 319  
 Shielding, 8  
 Single particle distribution, 60  
 Single particle inclusive cross section, 58  
 Single photons, 267  
 Singlet distribution, 140  
 Singlet fragmentation function, 80  
 Singularity structure, 83  
 Smearing, 199-200, 283, 289  
 Soft and collinear gluon emissions, 288  
 Soft divergence, 29

Spacelike, 40, 130, 171, 175, 195, 235  
 Spin, 335  
 Spinor, 334  
 Splitting functions, 76  
 $P_{q \rightarrow qq}(x)$ , 65, 67, 69, 73, 76, 81-83, 128, 136, 139, 182, 185  
 $P_{q \rightarrow gg}(x)$ , 68, 140, 149  
 $P_{g \rightarrow q\bar{q}}(x)$ , 76, 131-132, 140, 149, 183, 186  
 $P_{g \rightarrow gg}(x)$ , 76, 140  
 Spurious states, 230  
 Standard model, 344  
 Structure constants, 5, 344, 350  
 Structure function, 109, 114, 117, 126, 128, 148, 151, 154, 156, 186, 198, 281  
 $SU(3)$ , 2  
 Subtraction point, 8  
 Sudakov form factor, 101, 205, 212  
 Summing polarization states, 22  
 Superconducting Super Collider, 298  
 Symmetric point, 241

Tadpole, 231  
 Taylor series, 356  
 Thompson limit, 7, 10, 242  
 Three-body phase space, 25  
 Three-body phase-space, 44  
 Timelike, 41, 171, 175, 195  
 Transition probability, 326  
 Transverse cross section, 116  
 Transverse energy flow, 298  
 Transverse energy, 295  
 Transverse momentum spectrum, 171, 211  
 Transverse structure functions, 118  
 Trigger bias, 283, 289  
 Triple-gluon coupling, 229, 233, 236, 278  
 Triple-gluon vertex factor, 237  
 Triple-gluon vertex, 38  
 Two-body phase-space factor, 133  
 Two-body phase-space, 20, 42,

UA1 jet algorithm, 295  
 Ultraviolet cutoff, 7, 41, 81  
 Ultraviolet divergence, 6-8, 37, 39, 42, 226, 229, 232, 236

- Inphysical states, 279
  - Unrenormalized observable, 248
  - Unresolvably soft gluons, 88
  
  - /acuum polarization, 7, 11
  - /acuum, 16
  - /vector boson, 205
  - Vertex correction, 33, 48, 233, 238
  - Virtual corrections, 31, 41, 49, 65, 73, 97, 100, 179, 185
  - Virtual gluon contributions, 135
  - Virtual pairs, 16
  - Virtual photon nucleon total cross section, 115, 119
  - Virtual photon parton total cross section, 119
  
  - Virtual photon quark cross section, 122
  
  - Wave function renormalization, 36
  - Weak decay amplitude, 321
  - Weak intermediate bosons, 205
  - Weak-isospin doublets, 207, 344
  - Weinberg angle, 206, 346
  
  - Yang-Mills, 2
  
  - Zeta function, 356

The Addison-Wesley Advanced Book Program would like to offer you the opportunity to learn about our new physics and scientific computing titles in advance. To be placed on our mailing list and receive pre-publication notices and special offers, just **fill out this card completely** and return to us, postage paid. Thank you.

**Title and Author of this book:**

**Date purchased:**

Name \_\_\_\_\_  
Title \_\_\_\_\_  
School/Company \_\_\_\_\_  
Department \_\_\_\_\_  
Street Address \_\_\_\_\_  
City \_\_\_\_\_ State \_\_\_\_\_ Zip \_\_\_\_\_  
Telephone/s(      ) \_\_\_\_\_ (      ) \_\_\_\_\_

**Where did you buy/obtain this book?**

- Bookstore       Mail Order       School (Required for Class)  
 Campus Bookstore       Toll Free # to Publisher       Professional Meeting  
 Other \_\_\_\_\_  Publisher's Representative

**What professional scientific and engineering associations are you an active member of?**



**Check your areas of interest.**

10 Physics

- Physics  
11  Quantum Mechanics      18  Materials Science      25  Geophysics  
12  Particle/Astro Physics      19  Biological Physics      26  Medical Physics  
13  Condensed Matter      20  High Polymer Physics      27  Optics  
14  Mathematical Physics      21  Chemical Physics      28  Vacuum Physics  
15  Nuclear Physics      22  Fluid Dynamics  
16  Electron/Atomic Physics      23  History of Physics  
17  Plasma/Fusion Physics      24  Statistical Physics  
29  Other \_\_\_\_\_

**Are you more interested in:  theory  experimentation?**

**Are you currently writing, or planning to write a textbook, research monograph, reference work, or create software in any of the above areas?**

Yes  No

**(If Yes) Are you interested in discussing your project with us?**

Physics